

# Development of a Solar House Design Methodology and its Implementation into a Design Tool

William O'Brien

A Thesis  
In the Department  
of  
Building, Civil, and Environmental Engineering

Presented in partial fulfillment of the requirements  
for the degree of  
Doctor of Philosophy (Building Engineering) at  
Concordia University  
Montreal, Quebec, Canada

June 2011

© William O'Brien, 2011

**CONCORDIA UNIVERSITY  
SCHOOL OF GRADUATE STUDIES**

This is to certify that the thesis prepared

By: William O'Brien

Entitled: Development of a Solar House Design Methodology and its Implementation into a Design Tool

and submitted in partial fulfillment of the requirements for the degree of

PhD

complies with the regulations of the University and meets the accepted standards with respect to originality and quality.

Signed by the final examining committee:

<u>Sheldon Williamson</u>	Chair
<u>Alan Fung</u>	External Examiner
<u>Marius Paraschivoiu</u>	External to Program
<u>Paul Fazio</u>	Examiner
<u>Radu Zmeureanu</u>	Examiner
<u>Andreas Athientis and Ted Kesik</u>	Thesis Supervisor

Approved by

Chair of Department or Graduate Program Director

Dean of Faculty

## **Abstract**

Buildings consume on the order of 40% of energy in Canada and the developed world. It has been demonstrated that buildings can supplement a large fraction (or all) of their energy use by collecting solar energy. In order to design such buildings, an integrated design process should be used, in which they are designed as a system rather than as discrete subsystems. Otherwise, opportunities for cost-savings are missed. Energy-conserving and energy-collecting upgrades should be considered early in the design process when costs can be minimized and disruptions to construction avoided. The optimal solution to solar buildings typically balances energy efficiency measures and energy generation, since they both have diminishing returns.

Houses that offset their energy use with solar energy generation cannot justify the formality of the use of multiple designers because of the associated costs and potential cost savings. Therefore there is a need for a design methodology for solar houses and a corresponding design tool that can be used to support the process. It should enable the energy modeling of all relevant subsystems and provide guidance towards the near-optimal design space. The tool – called *Ecos* - will focus on early stage design and should enable the design of a near-optimal house within about an hour.

This thesis covers both a solar house design tool and the prerequisite work. There are four major interconnected parts of the work, including; a detailed energy model of a

solar house; innovative ways of graphically representing performance data, a detailed design methodology, and finally the design tool itself.

Ecos provides two main types of graphical feedback: 1) visualization of the design space and 2) visualization of key performance metrics during solar design days. One of the methods to support efficient design is to provide quasi real-time feedback to the user. In order to provide real-time feedback to support an efficient design process, a combination of shortened simulation periods and regression models are used.

The final part of this thesis discusses recently built solar house and applies the current model in a re-design study to examine potential further reductions in energy use.



## Acknowledgements and Personal Motivation

In my adolescence, I aspired to work on extraterrestrial projects because my perception was that any terrestrial projects were merely management, in that our work is done here and nothing exciting could happen anymore. However, during my undergraduate and master's degrees in aerospace engineering, I found myself repeatedly turning back to issues of sustainability on Earth. I can identify two experiences that sparked this interest: 1) going for long bike rides outside of Toronto and witnessing the rapid rate at which scenic hills were being devoured by low-density, car-centric developments and 2) observing the (successful) strategy that my parents used to keep our cottage cool in the summer by closing all the shades on the (predominantly west-facing) windows. During my masters, I took a course titled "Evaluating the sustainability of engineering activities". During research for the course project, I discovered the wealth of building performance analysis tools on the US DOE website. However, on further inspection, I couldn't even find a tool that simultaneously modelled a simple square office with daylighting, heating and cooling, and shade control. Thus, again, an area that on first inspection appeared to be largely addressed was actually seriously lacking in research. Between this opportunity and the ease at which complex buildings can be designed by examining many different solutions, I knew that this was the field I wanted to get into.

I would not have been able to complete this work without the support of many wonderful people in my life. First, I would like to thank my supervisors Drs. Andreas Athienitis and Ted Kesik. Andreas accepted me after only a brief meeting in Toronto, and for that, I am extremely grateful. During the past four years, he has provided a lot of encouragement, valuable knowledge, and a good understanding of managing projects. Ted has provided invaluable mentorship about practical issues of buildings, business skills, proposal writing, and research. With Ted's support, I was able to double the length of the work section of my CV to include many neat projects for a variety of clients. I'll never forget the meals at Einstein's and the trips to Fergus, ON and to Manitoulin Island. The financial support from both supervisors meant that I could focus on work without stress. Had it not been for them, I would not have had the opportunity to travel to Calgary, Quebec City, Fredericton, Ottawa, Halifax, Scotland, Germany, Reunion Island, Vancouver, Winnipeg, New York City, Austria, Halifax again, Las Vegas, Denver, Ottawa again, Berkeley, Denver again, and of course Toronto (many times!). I am particularly appreciative that both supervisors allowed (and encouraged) me to deviate from my core research to explore other topics of interest including urban planning, high-level analysis of urban energy, transportation, shade control and daylighting in commercial buildings, and optimization. It is these side projects that allowed me to develop a broad understanding of the field and that kept me motivated.

Thank you to the ‘Fab Five’ for your never-ending support and for making Montreal a second home. The out-of-town adventures, coffee breaks, dinners, and drinks we had together helped make this process painless and will not be soon forgotten. Thank you to Brad for being an excellent housemate, friend, and running partner.

Thank you to all other labmates who were in the ‘solar lab’ during my studies. Thank you to all of the people I collaborated with in research and publications, including Dr. Chris Kennedy (U of Toronto), Matt Doiron, Luis Candanedo, Jose Candanedo, Xiang Chen, Costa Kapsis, and Scott Bucking. I hope to continue collaborative research with all of you. Costa: your enthusiasm, support, and encouragement will be missed and never forgotten.

Thank you to the researchers in IEA Task 40 for providing valuable insight and international perspectives. Special thanks to Adam Hirsch for being so easy to work with. Thank you to Josef Ayoub for your support and recognition of my efforts.

Thank you to Lyne Dee and Meli Stylianou for your administrative and managerial support over the past four years. You’ve provided me with valuable skills and knowledge about organizing events and other logistics. Thank you Meli for granting me several government contracts and a part-time position at Natural Resources Canada during my studies.

Financial support from the NSERC Solar Buildings Research Network and the ASHRAE Grant-in-Aid is acknowledged.

Thank you Simren for being so very supportive and always being there for me.

Thank you Nina for being contributing to a very enjoyable last year and for your loving support.

Finally, without the support – emotional and financial - of my loving parents, it’s unlikely that I would have made it this far in my education. So, I would like to extend my extreme gratitude to you. My sister, Katie, has always been very supportive and a great person to talk to during the past four years. She is a best friend and made visiting Toronto a pleasure. I know that Meg would be very proud of me and is here in spirit. She helped me proofread important papers early on in my grad studies and taught me to be a better writer. My family has been there for me during the best and worst of times.

## Contents

Figures.....	x
Tables.....	xvi
Nomenclature.....	xviii
Definitions.....	xxvi
<b>1 Introduction.....</b>	<b>1</b>
1.1 Problem Statement .....	7
1.2 Research Objectives .....	7
1.3 Thesis Overview.....	9
<b>2 Literature Review .....</b>	<b>13</b>
2.1 Solar & Energy Efficient Houses.....	13
2.2 Household Energy Use and Efficiency Measures.....	17
2.2.1 Building Envelope .....	19
2.2.2 HVAC .....	22
2.2.3 Non-HVAC Energy Use.....	29
2.2.4 Passive Solar Heating .....	33
2.2.5 Direct Gain Systems .....	36
2.2.6 Indirect Gain Systems.....	37
2.2.7 Glazing.....	38
2.2.8 Shading: Static and Dynamic.....	43
2.2.9 Thermal Storage.....	44
2.2.10 Thermal Comfort.....	47
2.2.11 Energy Modelling of Passive Solar Houses .....	49
2.2.12 Design and Simulation of Passive Solar Homes .....	66
2.3 Active Solar.....	77
2.3.1 Solar Thermal Collectors .....	79
2.4 Building Code .....	88
2.5 Design Practice/Methodology .....	89
2.6 Building Simulation Software in the Design Process .....	96
2.7 Quantifying Performance and Objectives .....	101
2.8 Optimization.....	102
2.9 Existing Software Survey.....	106
2.10 Conclusion.....	106
<b>3 Passive solar houses and modelling.....</b>	<b>107</b>
3.1 Simulation Engines .....	110
3.2 Major model components.....	117
3.2.1 Major Geometry.....	125
3.2.2 Thermal and Control Zoning .....	127
3.2.3 Opaque Envelope.....	131
3.2.4 Windows .....	134
3.2.5 Fixed Shading .....	147

3.2.6	Moveable Shading Devices.....	149
3.2.7	External Shading.....	151
3.2.8	Thermal Mass.....	152
3.2.9	Infiltration.....	155
3.2.10	Basement/ground coupling.....	158
3.2.11	Weather.....	164
3.2.12	Internal Heat Gains.....	165
3.2.13	Ventilation, circulation, mechanical equipment and controls.....	172
3.2.14	Intermediate Metrics.....	179
3.2.15	Energy, power, and metrics.....	182
3.2.16	Thermal comfort metrics.....	186
3.3	Conclusions.....	188
<b>4</b>	<b>Active Solar Systems and Modelling.....</b>	<b>189</b>
4.1	Roof and collector geometry.....	190
4.1.1	Geometrical considerations.....	192
4.1.2	Self-shading.....	193
4.1.3	Shading from external obstructions.....	195
4.1.4	BIPV/T design considerations.....	196
4.2	PV System Model.....	197
4.2.1	Detailed PV calculation methodology.....	202
4.2.2	Other practical considerations of BIPV design.....	203
4.3	Solar Thermal System Model.....	205
4.3.1	SDHW system controls.....	213
4.3.2	Sample Performance.....	215
4.4	High-level outputs.....	215
4.5	Conclusion.....	216
<b>5</b>	<b>Integrated Design and Interactions.....</b>	<b>217</b>
5.1	Parameter Interactions.....	219
5.2	Model Coupling and Decoupling.....	227
<b>6</b>	<b>Use of the Design Tool and Model: Design Methodology.....</b>	<b>231</b>
6.1	Prioritizing house upgrades.....	231
6.2	Solar house design methodology.....	235
6.3	High-level solar house design methodology.....	236
6.4	Passive solar design: solar design day approach.....	238
6.5	Passive solar design: parametric analysis approach.....	243
6.6	Active solar system design.....	245
6.7	Passive solar design: hybrid SDD-parametric approach.....	250
6.8	Example design exercise.....	250
6.9	Conclusion.....	251
<b>7</b>	<b>Design Tool: Methodology and Implementation.....</b>	<b>252</b>
7.1	Design Tool Requirements.....	252
7.2	Scripting EnergyPlus Input File.....	253
7.3	Ecos Prototype.....	254
7.4	User Inputs.....	256

7.5	Development of Graphical Feedback Methods.....	258
7.5.1	House and component diagrams.....	262
7.5.2	Solar Design Days.....	264
7.5.3	Lines of Influence (LoI).....	266
7.5.4	Wheel of Interactions (WoI).....	268
7.5.5	Multi-Parameter Design Support Charts (MPDSC).....	269
7.5.6	Design Management System (DMS).....	271
7.5.7	GUI event sequences.....	273
7.5.8	Implementation of Real-Time Feedback.....	276
<b>8</b>	<b>Case Study: ÉcoTerra Redesign.....</b>	<b>283</b>
8.1	Performance model.....	284
8.1.1	Boundary conditions.....	285
8.1.2	Form and fabric.....	285
8.1.3	Operations.....	290
8.1.4	Renewable energy systems.....	290
8.1.5	Simulation results.....	292
8.2	Redesign Study.....	294
8.3	Conclusions.....	303
<b>9</b>	<b>Conclusions.....</b>	<b>305</b>
9.1	Major Contributions.....	307
9.2	Future work.....	309
<b>10</b>	<b>References.....</b>	<b>316</b>
<b>11</b>	<b>Appendix B: Design Exercise.....</b>	<b>351</b>
<b>12</b>	<b>Appendix C: Window Heat Balance Study.....</b>	<b>373</b>
<b>13</b>	<b>Appendix D: Extended calculations and code.....</b>	<b>380</b>
13.1	Detailed PV model calculations.....	380
13.2	Whole envelope conductance.....	388
13.3	Sample MATLAB Code.....	389
13.4	Solar domestic hot water system modeling.....	390
13.5	ANN Results.....	393
<b>14</b>	<b>Appendix E: ÉcoTerra Background information.....</b>	<b>395</b>
14.1	The Design and Construction.....	395
14.2	The Design Process.....	399
14.2.1	Design Objectives.....	399
14.2.2	Design team and design process.....	400
14.2.3	Use of design and analysis tools.....	402
14.2.4	Assessment of the design process.....	407
14.3	Measured performance.....	407
14.4	Lessons learned.....	411

## Figures

Figure 1-1: Thesis structural diagram .....	12
Figure 2-1: Attribution of energy use in residential buildings in Canada ( <a href="http://www.nrcan.gc.ca/eneene/effeff/resuse-eng.php">http://www.nrcan.gc.ca/eneene/effeff/resuse-eng.php</a> ) .....	14
Figure 2-2: Comparison of R-2000 house performance with conventional houses (Charron et al., 2006a) .....	16
Figure 2-3: Measured infiltration rates (in ach) for the seven built Equilibrium houses (Charron, 2010) .....	21
Figure 2-4: Cost to abate greenhouse gas emissions (McKinsey and Company, 2007) ...	22
Figure 2-5: Prevalence of plant types (left) and fuel type (right) in the existing Canadian housing stock .....	23
Figure 2-6: Prevalence of air-conditioners .....	24
Figure 2-7: Comparison between a 94% efficiency gas-fired furnace (base) and GSHP of unreported COP (taken from Kikuchi et al., 2009) .....	28
Figure 2-8: Comparison between predicted and measured (where available) non-HVAC electricity use (kWh/year) .....	30
Figure 2-9: Seasonal solar paths for the northern hemisphere ( <a href="http://www.knowledgepublications.com/heat/images/Solar_Air_Solar_Exposure.gif">http://www.knowledgepublications.com/heat/images/Solar_Air_Solar_Exposure.gif</a> ) ..	35
Figure 2-10: Total incident solar radiation on vertical surfaces by orientation and season. .....	36
Figure 2-11: A variety of common glazing types and their thermal and optical properties. .....	40
Figure 2-12: Window U-value as a function of gap thickness (in mm) (ASHRAE, 2001) .....	41
Figure 2-13: A simple example of how a one-dimensional wall responds to an a pulse temperature, based on the response function method (Clarke, 2001) .....	49
Figure 2-14: A simple wall showing temperatures and heat added .....	50
Figure 2-15: The magnitude of self admittance for different thicknesses of thermal mass .....	52
Figure 2-16: The magnitude of self admittance for different thicknesses of thermal mass. The volume of the mass is kept at $1\text{m}^3$ . Thus, the area is $1\text{m}^3$ divided by the thickness..	53
Figure 2-17: Numerical solution to some function $f(\gamma)$ (Clarke, 2001) .....	55
Figure 2-18: Nodal layout for a rectangular zone with multilayered walls (Clarke, 2001)	61
Figure 2-19: The matrix (A or B) that corresponds to the single zone model (Clarke, 2001) .....	62
Figure 2-20: The response of a wall surface based on a 3 and 15 node model (Clarke, 2001) .....	63
Figure 2-21: Discretization of thermal mass .....	64
Figure 2-22: The response of a wall surface based on a 3 and 15 node model (Clarke, 2001) .....	65
Figure 2-23: The energy performance of a house depending on temperature setpoints and the window to wall ratio (O'Brien et al., 2008a) .....	67

Figure 2-24: Results from the study, showing variation in floor surface temperature (Athienitis and Chen, 2000). It is clear that the warmest part of the floor follows the path of the beam radiation (with some lag).....	70
Figure 2-25: Typical solar thermal collector efficiency as a function of ambient conditions ( <a href="http://energytech.at/solar/portrait_kapitel-4.html">http://energytech.at/solar/portrait_kapitel-4.html</a> ).....	88
Figure 2-26: The opportunity for life-cycle cost reduction as a function of the design stage (Reed and Gordon, 2000) .....	91
Figure 2-27: Shading analysis of a building site ( <a href="http://sql1.org/wiki/Shading_Mask_Calculations">http://sql1.org/wiki/Shading_Mask_Calculations</a> ) .....	93
Figure 2-28: Parametric analysis results (Hayter et al., 2001).....	94
Figure 2-29: One version of a low-energy building design process .....	95
Figure 2-30: Star diagram for multi-criteria design (Andresen, 2008).....	102
Figure 2-31: Results of multi-criteria optimization using a genetic algorithm (Wright et al., 2002). The scattered points are possible solutions, while the Pareto front is marked as “Final Generation”.....	105
Figure 3-1: Relationship between model resolution and model accuracy .....	109
Figure 3-2: A 3D space upon which different modelling tools can be placed (taken from Athienitis et al (2010)).....	115
Figure 3-3: Flowchart summarizing the structure of the model .....	121
Figure 3-4: Energy use ranges for 30 parameters. The dashed horizontal line is the energy use when all parameters are at their nominal values.....	123
Figure 3-5: Major house geometry .....	126
Figure 3-6: Four different zoning configurations that were considered(taken from (O'Brien et al., 2010b)) .....	130
Figure 3-7: The effect of thermal zoning configuration on energy performance of a passive solar house (taken from (O'Brien et al., 2010b)).....	130
Figure 3-8: Magnitude of overheating as a function of zonal configuration and window size (taken from (O'Brien et al., 2010b)) .....	131
Figure 3-9: Influence of the four opaque envelope thermal resistance parameters .....	133
Figure 3-10: Three heat flow paths for windows (EnergyPlus, 2009b).....	135
Figure 3-11: Radiative phenomena for multiple glazing layer (left) and example of how window components can affect shading (right) (EnergyPlus, 2009b).....	136
Figure 3-12: Major window components and geometry .....	140
Figure 3-13: Three possible window modelling methods.....	143
Figure 3-14: Effect of window modeling resolution.....	145
Figure 3-15: Effect of WWR1 through WWR4 on energy use .....	147
Figure 3-16: Overhang geometrical specifications (left) and the “ideal overhang” geometry right) (taken from O'Brien et all (2010b)).....	149
Figure 3-17: Cross section of fenestration showing glass layers and a shading layer (EnergyPlus, 2009b) .....	150
Figure 3-18: Side view of ÉcoTerra house showing potential solar obstructions and the extreme seasonal solar altitudes.....	152
Figure 3-19: Section view of house showing locations of concrete slabs. ....	153

Figure 3-20: Representation of a thin material layer in EnergyPlus' implicit finite difference scheme (EnergyPlus, 2009b) .....	154
Figure 3-21: Schematic of basement configuration .....	160
Figure 3-22: Sample results from BASECALC.....	162
Figure 3-23: Ground temperatures - effective and approximated - under the nominal design conditions .....	163
Figure 3-25: Hourly profile for total electrical draw per house (taken from Armstrong et al., 2009) .....	167
Figure 3-26: Normalized daily internal gain profiles .....	168
Figure 3-27: Sample annual internal gains (all but lost portion; left and electricity consumption (right)).....	171
Figure 3-28: The forced-air HVAC system as conceived (left) and as modelled (right) (taken from O'Brien (2010b)).....	173
Figure 3-29: Combined heating and cooling energy for the temperature control setpoints over their ranges.....	176
Figure 3-30: Total heating and cooling energy (left) and overheating (right) as a function of WWR1 and CI (taken from O'Brien et al (2011a)).....	179
Figure 4-1: Schematic of equivalent four-parameter circuit for one-diode PV model (taken from EnergyPlus Engineering Reference (EnergyPlus, 2009b)) .....	199
Figure 4-2: Solar domestic hot water system configuration (Note that the exact position of the source and use-side heat exchangers is not critical because a mixed tank is modelled, as described in the following section.).....	206
Figure 4-3: Comparative test for different storage tank models and for different numbers of nodes.....	209
Figure 4-4: Solar fraction for the SDHW system under the nominal design conditions except for different tank volumes .....	210
Figure 4-5: Solar fraction for the SDHW system under the nominal design conditions but with different numbers of panels in parallel. ....	212
Figure 4-6: Daily DHW draw profile; fraction of daily total.....	213
Figure 5-1: Cost and benefit trends for the degree of integration (coupling) of models	217
Figure 5-2: Generic representation of responses and interactions .....	221
Figure 5-3: Example interactions plots showing a strong interaction (a) and a weak interaction (b).....	222
Figure 5-4: Visualization of the interactions with WWR1. Each line connecting two parameters indicates a strong interaction. The line thickness is proportional to the strength of the interaction. ....	223
Figure 5-5. Venn diagram of the potential for decoupling the subsystems. (BIPV = building-integrated photovoltaics; DHW = domestic hot water; BIPV/T = building-integrated photovoltaics with thermal energy recovery) (taken from (O'Brien et al., 2011b)).....	228
Figure 6-1: Design space according to two scales: passive-active and robustness. For convenience, the parameter acronyms are repeated in the next table. ....	232
Figure 6-2: High-level design methodology for solar houses.....	237
Figure 6-3: Auxiliary procedures for defining IN and IG.....	238



Figure 6-4: Solar design day approach procedure (left) and cold sunny day procedure (right) .....	239
Figure 6-5: Cold cloudy day procedure (left) and warm sunny day procedure (right)...	240
Figure 6-6: Auxiliary procedures 3 through 7. ....	241
Figure 6-7: Auxiliary procedures 8 through 10. ....	242
Figure 6-8: Flow charts for parametric path .....	244
Figure 6-9: Flow charts for parametric path .....	245
Figure 6-10: Flow charts for active solar system design .....	247
Figure 6-11: Flow charts for active solar system design .....	248
Figure 6-12: Flow charts for active solar system design .....	249
Figure 6-13: Flow chart for hybrid path procedure .....	250
Figure 7-1: High-level flow chart for data flow in Ecos and underlying model.....	255
Figure 7-2: Sample of typical tool inputs: text fields (HOT3000).....	256
Figure 7-3: Screenshot of user interface inputs in Ecos .....	256
Figure 7-4: Screenshot #1 of Ecos; showing LoI, SDD, and DMS .....	260
Figure 7-5: Screenshot #2 of Ecos; showing MPDSC and WoI.....	261
Figure 7-6: Representations of the house: Ecos (left) and SketchUp (right).....	263
Figure 7-7: Screen shots of house wireframe (left) and normal view of roof with collectors (right).....	263
Figure 7-8: Sample SDD graphs (cold sunny day) showing how the design of a house was improved. The design represented on the left has no significant thermal mass and had 15% glazing on the south façade. The design on the right has an 8” concrete slab on the ground floor and 45% glazing on the south façade (O’Brien, 2008a).....	264
Figure 7-9: Sample LoI overhang depth (near-linear) and house orientation (parabolic); the total annual heating and cooling energy are shown; the left LoI is for a small south-facing window; the right is for a large south-facing window .....	267
Figure 7-10: Wheel of interactions showing the relative magnitude of interaction between window-to-wall ratio for the near-south facing window and all other parameters. The labels around the outside of the wheel correspond to the abbreviations in the table of parameters. ....	269
Figure 7-11: Example LoI for heating energy .....	270
Figure 7-12: Sample screenshot of design management system in use. Like everywhere else in this work, the sign convention is energy consumption is positive and energy generation is negative. ....	272
Figure 7-13: Data structure of DMS .....	273
Figure 7-14: GUI events sequence for when the user changes a parameter value. ....	275
Figure 7-15: ANN structure, showing inputs, the hidden layer, and outputs (taken from Graupe (2007)).....	280
Figure 7-16: Training process for ANNs (Mathworks Inc., 2008).....	280
Figure 7-17: Results of the MRA and ANN models.....	282
Figure 8-1: A photograph of ÉcoTerra house as seen from the south-west.....	283
Figure 8-2: a) ÉcoTerra; b) timeline of significant events (taken from (O'Brien et al., 2010c)) .....	284

Figure 8-3: Map of area around ÉcoTerra (marked “A”), including nearest EPW format weather file locations: Montreal and Sherbrooke, QC.....	285
Figure 8-4: Section view of thermal model with zoning scheme .....	287
Figure 8-5: Views of model clockwise from top-left: south elevation, east elevation, west elevation, isometric, plan, and north elevation. ....	289
Figure 8-6: Schematic (left) and thermal network of a control volume in the BIPV/T system model (right) (taken from Candanedo L., O’Brien, W., et al (2009)) .....	292
Figure 8-7: Comparison between measured heat pump electricity and modelled values. ....	294
Figure 8-8: Distribution of heat losses.....	298
Figure 8-9: Electricity use for successive upgrades.....	299
Figure 8-10: Modelled and measured PV performance (for the current design with a 30-degree slope).....	301
Figure 8-11: Comparison of thermal loads and BIPV/T useful energy output.....	302
Figure 8-12: Comparison of thermal loads and BIPV/T useful energy output.....	303
Figure 9-1: Example of Sankey diagram for a house (source: <a href="http://blog.airscapfans.com/wp-content/uploads//2010/08/arron-energy-flow1.jpg">http://blog.airscapfans.com/wp-content/uploads//2010/08/arron-energy-flow1.jpg</a> ).....	313
Figure 10-1: The evaluated tools in the resolution-design stage space .....	326
Figure 12-1: heating and cooling degree-hours for Toronto with a balance point of 12°C .....	374
Figure 12-2: Monthly incident solar radiation on vertical surfaces in 30-degree increments .....	375
Figure 12-3: Total solar radiation incident on surfaces during the heating and cooling seasons .....	375
Figure 12-4: Net heat gain during heating season for South-facing windows.....	377
Figure 12-5: Net heat gain during heating season for S30E .....	378
Figure 12-6: Net heat gain during heating season for S60E .....	378
Figure 12-7: Net heat gain during heating season for East.....	379
Figure 12-8: Net heat gain during heating season for North-facing windows.....	379
Figure 13-1: Modeling the effect of snow on annual performance (left); a photograph of ÉcoTerra after snowfall (right). ....	385
Figure 13-2: Example heat loss values for (clockwise, starting with left): the above-grade envelope, below-grade envelope, and air exchange. Note that “Worst parameter values” refers to all parameters being set to the values that cause the highest heat loss. Similarly, “Best parameter values” refers to all parameters being set to the values that cause the lowest heat loss. ....	388
Figure 13-3: Sample MATLAB script to create the building surface objects in the idf file .....	389
Figure 13-4: Hierarchy of EnergyPlus components/objects that are part of the SDHW system. Arrows indicate the direction of referencing of components (e.g., the water use connections object references the water use equipment object) .....	390

Figure 13-5: EnergyPlus schematic of SDHW system (note: purpose of this figure is merely to show the limitations of EnergyPlus output; not to see individual components)	391
Figure 13-6: SHDW system sample performance	392
Figure 13-7: Validation plot for annual heating energy	393
Figure 13-8: Validation plot for annual cooling energy	393
Figure 13-9: Validation plot for annual DHW energy	394
Figure 14-1: Photographs of the underside of the BIPV/T roof (left) and the ventilated slab before the concrete is poured on the decking (right)	396
Figure 14-2: ÉcoTerra system schematic (Chen et al. 2010)	397
Figure 14-3: Design process outline (taken from (Doiron et al., 2011))	402
Figure 14-4: Results of parametric analysis that was used to decide on the optimal insulation level in the walls	404
Figure 14-5: Sample results from parametric analysis for roof, wall, and basement slab insulation	404
Figure 14-6: Construction details of the ÉcoTerra house	406
Figure 14-7: ÉcoTerra's monthly energy use in 2010 (values in kWh)	409
Figure 14-8: Annual breakdown of electricity use in ÉcoTerra house (values in kWh)	409
Figure 14-9: Daily power draw, generation, and indoor temperature profiles (taken from Doiron et al (2011))	411

## Tables

Table 2-1: Equilibrium home heating and ventilation systems (Canada Mortgage and Housing Corporation (CMHC), 2010).....	24
Table 2-2: Conversion ratios from purchased energy to heating energy (NRCan: OEE, 2010b).....	26
Table 2-3: Primary energy to electricity conversion ratios for major US regions (Deru et al., 2007). .....	27
Table 2-4: Electricity supply system for Canada’s four most populous provinces (taken from Kikuchi et al., 2009).....	28
Table 2-5: Select code requirements.....	89
Table 2-6: Example decision matrix.....	101
Table 3-1: Summary of model inputs.....	120
Table 3-2: Summary of Sensitivity Analysis for 30 Parameters.....	124
Table 3-3: Material properties of the wall construction.....	132
Table 3-4: Material properties of the ceiling construction.....	132
Table 3-5: Material properties of the roof construction.....	133
Table 3-6: Summary of glazing types available in the Ecos. Thick cell borders indicate the surface that the low-e coating is on. The naming convention is: first two letters indicate the number of glass layers, second two letters indicate whether all of the glass is clear or if one of them has a low-e coating, and the last two letters indicate whether the gas fill is air or argon. ....	138
Table 3-7: Glass properties (from Window 6 software).....	139
Table 3-8: Window frame properties.....	139
Table 3-9: Whole window U-values for all glazing and frame combinations.....	141
Table 3-10: Whole window SHGCs for all glazing and frame combinations.....	141
Table 3-11: Properties of explicitly defined windows (per window); also applies to multiplier option.....	144
Table 3-12: Properties of grouped windows.....	144
Table 3-13: Shade properties.....	150
Table 3-14: Modelled concrete properties.....	153
Table 3-15: Results from infiltration model (taken from O’Brien et al (2011b)).....	157
Table 3-16: Material properties of basement wall and floor construction.....	160
Table 3-17: Basement model parameter; *parameters that are fixed in the model.....	161
Table 3-18: Summary of internal gains and coefficients.....	170
Table 3-19: Heating and cooling control schedules.....	175
Table 4-1: Summary of active solar system parameters.....	190
Table 4-2: Roof geometry for solar collectors.....	194
Table 4-3: Three common roof types and their geometrical and solar implications. The panel layout is based on two standard sizes of Uni-Solar panels. Climate Data is based on Toronto conditions. All active area slopes are 45 degrees (12/12) and South-facing. (Figure taken from (O’Brien et al., 2009b)).....	195
Table 4-4: PV performance results for different models.....	200
Table 4-5: Solar thermal collector specifications.....	210
Table 4-6: All allowed collector configurations.....	212

Table 5-1: Normalized strength of interactions between all pairs of the 30 house model parameters. The strength of the interactions is formulated in Equation 5-3. ....	224
Table 5-2. Top ten interacting pairs of parameters .....	226
Table 5-3. Top ten interacting pairs of design parameters.....	226
Table 6-1: Robustness table for all parameters. The heating and cooling season columns refer to the sign of the slope of the LoI for total space conditioning energy for the first 28 (passive) parameters. Notes: (1) south-facing is optimal for both the heating and cooling season, (2) when used in conjunction, BLT and BLS become robust; individually, they are not (3) parameter was tested for robustness using BIPV, (4) for parameters 29 through 36, a positive value indicates higher net energy as the parameter is increased. ....	234
Table 8-1: heat transfer characteristics of ÉcoTerra house: opaque constructions, fenestration, infiltration, and ventilation.....	288
Table 8-2: Annual performance results.....	294
Table 13-1: Toronto Weather data from RETScreen.....	380
Table 13-2: Summary of sensitivity analysis.....	387

## Nomenclature

A	area of a partition wall [m <sup>2</sup> ]
a	coefficient
A <sub>BG</sub>	below-grade surface area [m <sup>2</sup> ]
A <sub>cog</sub>	centre of glass area [m <sup>2</sup> ]
AE	PV module nominal efficiency
A <sub>envsurf</sub>	area of an envelope surface [m <sup>2</sup> ]
A <sub>envsurf,BG</sub>	below-grade surface area [m <sup>2</sup> ]
A <sub>eog</sub>	edge of glass area [m <sup>2</sup> ]
A <sub>f</sub>	Projected window frame area [m <sup>2</sup> ]
A <sub>i</sub>	area of a surface i [m <sup>2</sup> ]
A <sub>L</sub>	effective leakage area [m <sup>2</sup> ]
A <sub>PV</sub> /A <sub>roof</sub>	fraction of roof covered by PV modules
AR	aspect ratio
A <sub>surf</sub>	surface area [m <sup>2</sup> ]
b	coefficient
BLS	blind/shade solar threshold [W/m <sup>2</sup> ]
BLT	blind/shade outdoor temperature threshold [°C]
BS	basement slab resistance [m <sup>2</sup> K/W]
BW	basement wall resistance [m <sup>2</sup> K/W]
c	specific heat of a substance [J/kgK]
C <sub>1</sub> through C <sub>11</sub>	coefficients
CA	total PV cell area [m <sup>2</sup> ]
CI	air circulation rate [m <sup>3</sup> /s]
COP <sub>c</sub>	coefficient of performance in cooling mode
COP <sub>h</sub>	coefficient of performance in heating mode
C <sub>p</sub>	specific heat capacity of air [J/kgK]
C <sub>p,water</sub>	specific heat capacity of water [J/kgK]
CR	ceiling resistance [W/m <sup>2</sup> ]
CS	cooling setpoint [°C]
C <sub>s</sub>	stack coefficient
C <sub>z</sub>	heat capacity of zone air [J/K]
days_per_month	vector containing the number of days in each month (31, 28, 31,...,31)
d <sub>OH</sub>	depth of overhang [m]
E <sub>A,B</sub>	effect of parameter value change
E <sub>conditioning</sub>	total heating and cooling energy [kWh]
E <sub>conditioning no_solar</sub>	total heating and cooling energy when all window are shades [kWh]
E <sub>conditioning no_windows</sub>	total heating and cooling energy when the house has no windows [kWh]

$E_{cooling}$	total cooling energy [kWh]
$E_{DHW}$	domestic hot water energy [kWh]
$E_{fans}$	fan energy [kWh]
$E_{generation}$	total useful collected energy [kWh]
$E_{grid}$	energy exported to the electrical grid [kWh]
$E_{heating}$	total heating energy [kWh]
$E_{lighting}$	electric lighting energy [kWh]
$E_{major\_appliances}$	major appliance energy [kWh]
$E_{minor\_appliances}$	minor appliance energy [kWh]
$E_{net}$	net energy use (positive is net consumption) [kWh]
envsurf	index for envelope surface number
envsurf,BG	index for below-grade envelope surface number
$E_p$	energy produced by the PV array [kWh]
$f(x)$	ANN function
$F$	Fourier number
$FA$	floor area [ $m^2$ ]
$F_s$	view factor
$FT$	window frame type
$G$	incident solar radiation on surface [ $W/m^2$ ]
$GA_i$	glazing area for window $i$ [ $m^2$ ]
$g_i(x)$	ANN function
$G_{sc}$	solar constant (1367 $W/m^2$ )
GT1	glazing type 1
GT2	glazing type 2
GT3	glazing type 3
GT4	glazing type 4
$h$	hour index
$H_b$	monthly average daily beam solar radiation [kWh]
$\bar{H}$	monthly average daily solar radiation [kWh]
$h_c$	convective heat transfer coefficient [ $W/m^2K$ ]
$H_d$	monthly average daily global solar radiation [kWh]
$H_{d\_bar}$	monthly average daily diffuse solar radiation [kWh]
$h_f$	film coefficient for surface [ $W/m^2K$ ]
$h_g$	height of glazing [m]
$h_i$	film coefficient for surface $i$ [ $W/m^2K$ ]
$H_o$	extra terrestrial solar radiation [ $W/m^2$ ]
$\bar{H}_o$	monthly average daily extraterrestrial solar radiation [kWh]
$h_{OH}$	overhang height above top of glazing [m]

$h_r$	radiative heat transfer coefficient [W/m <sup>2</sup> K]
HS	heating setpoint (daytime) [°C]
HSN	heating setpoint (nighttime) [°C]
$H_w$	height of window [m]
$i$	index for node, surface, or zone, or month of interest
$I_{A,B}$	interaction between A and B
IE	inverter efficiency
IG	internal gains scheme
$i_{\text{gain}}$	type of internal gain: convective, radiative, latent, or lost (to outside)
$I_{\text{inv,max}}$	maximum allowable inverter input current (DC) [A]
IN	infiltration [ach]
Inf	infiltration rate (m <sup>3</sup> /s)
IP	mean parameter input value [same units as parameter]
$I_{\text{solar}}$	incident solar radiation on surface [W/m <sup>2</sup> ]
$I_{\text{string}}$	PV string current [A]
K	function for each node in ANN
k	material conductivity [W/mK]
$K_{\tau\alpha}$	incident angle modifier
$\overline{K_t}$	month average clearness index
L	length (of house) [m]
$L_i$	thermal mass thickness [m]
$m_n$	mass of control volume in stratified tank, node n [kg]
$M_A$ through $M_z$	arrays or vectors for solving system of Equations
$\dot{m}_{\text{use}}$	DHW mass supply rate [kg/s]
$\dot{m}_{\text{vent}}$	mass flow rate from infiltration [kg/s]
$\dot{m}_{12}$	interzonal mass flow rate [kg/s]
$\dot{m}_{\text{inf}}$	mass flow rate from infiltration [kg/s]
$\dot{m}_i$	mass flow rate from zone i [kg/s]
$\dot{m}_{\text{sys}}$	supply mass flow rate [kg/s]
$n_{\text{surfaces}}$	number of surfaces in the zone
$N_{\text{envsurf}}$	number of envelope surfaces
NOCT	nominal operating cell temperature [°C]
$n_{\text{panels/string}}$	number of PV panels per string
$N_{\text{sl}}$	number of convective sources of internal gains
$N_{\text{strings}}$	number of PV module strings
$N_{\text{surfaces}}$	number of surfaces in the zone
$N_{\text{zones}}$	number of zones in the model
OH	overhang depth ratio



OP	mean model output value [kWh]
OR	orientation [degrees]
P	generic parameter value
PL	parallel solar thermal collectors
$q_{net,n}$	net heat flow into node n in stratified tank [kg]
$Q_{af}$	specific power associated with the airflow; units: W/K
$Q_{AG}$	basement above-grade heat loss from BASECALC [GJ]
$Q_{AG,calc}$	basement above-grade heat loss calculated [GJ]
$Q_{BG}$	basement below-grade heat loss from BASECALC [GJ]
$Q_{BG,eff}$	basement below-grade effective heat loss [GJ]
$Q_{fan}$	flow rate through fan [ $m^3/s$ ]
$q_{heater}$	heat output of heater [W]
$q_{i \rightarrow j}$	airflow rate between zones I and j [L/s]
$Q_{inside}$	heat flow on inside surface of wall [W]
$q_{loss}$	heat loss [W]
$Q_{outside}$	heat flow on outside surface of wall [W]
$q_{source}$	tank heat gain from source (solar thermal collector array) [W]
$q_{use}$	tank heat loss to demand side (supply for DHW) [W]
$Q_{vent}$	ventilation flow rate [L/s]
R	thermal resistance of the partition wall between zones [ $m^2k/W$ ]
$R(\phi)$	window reflectance as a function of incident angle
$R_{A(-1)B(-1)}$	response of model at low values of parameters A and B
$r_d$	hourly fraction of daily diffuse solar radiation
$R_{envsurf}$	thermal resistance of an envelope surface [ $W/m^2k$ ]
$R_{envsurf,BG}$	below-grade surface thermal resistance
$RH_{amb}$	outdoor relative humidity
ROR	rotation matrix
$r_t$	hourly fraction of daily total solar radiation
RT	roof type
s	index for surface number
S	surface area [ $m^2$ ]
SHGC	solar heat gain coefficient
$SHGC_w$	solar heat gain coefficient of the window
$SHGC_{cog}$	solar heat gain coefficient of the glazing
$SHGC_f$	solar heat gain coefficient of the frame or other opaque constructions
SL	roof slope [degrees]
ST	number of stories
T	temperature [C]

$t$	time [s]
$T(\phi)$	transmittance as a function of incidence angle
$T_a$	ambient temperature [°C]
$T_{air,z}$	zone air temperature [°C]
$T_{amb}$	ambient temperature [°C]
$T_{attic}$	attic air temperature [°C]
$T_{back}$	back surface temperature in BIPV/T [°C]
$T_c$	PV cell temperature [°C]
$TC$	PV temperature coefficient [1/K]
$T_{ground,amp}$	ground temperature amplitude [°C]
$T_{ground,calc}$	calculated ground temperature [°C]
$T_{ground,mean}$	mean ground temperature [°C]
$T_{i,air}$	temperature of air node in current control volume [°C]
$T_{i,new}$	node i temperature at the current timestep [°C]
$T_{i,old}$	node i temperature at the previous timestep [°C]
$T_{i+1,new}$	node i+1 temperature at the current timestep [°C]
$T_{i-1,air}$	temperature of air node in the upstream control volume [°C]
$T_{i-1,new}$	node i-1 temperature at the current timestep [°C]
$T_{in}$	inlet temperature [°C]
$T_{inside}$	inside surface temperature [°C]
$T_{MRT}$	mean radiant temperature [°C]
$TMS$	thermal mass on south floor [m]
$TMV$	thermal mass on dividing wall [m]
$T_n$	current node temperature [°C]
$T_{n,old}$	Previous timestep node temperature [°C]
$T_o$	outdoor air temperature [°C]
$T_{op}$	operative temperature [°C]
$T_{PV}$	PV cell temperature [°C]
$T_s$	surface temperature [°C]
$T_{si}$	surface i temperature [°C]
$T_{supply}$	system supply air temperature [°C]
$T_{use}$	temperature of DHW supply [°C]
$TV$	collector storage tank volume [L]
$TV$	tank volume [m <sup>3</sup> ]
$T_z$	current zone air node temperature [°C]
$T_{zi}$	zone i air temperature [°C]

$T_z^t$	current zone air node temperature at time t [°C]
$u$	insulation conductance [W/m <sup>2</sup> K]
$U_{12,air}$	rate of heat transfer between adjacent zones through air exchange [W/K]
$U_{12,wall}$	rate of heat transfer between air nodes in adjacent zones [W/K]
$U_a$	total heat transfer between the back and the attic (BIPV/T) [W/m <sup>2</sup> K]
$UA_{AG,ENV}$	UA-value for above grade surfaces normalized by envelope area [W/m <sup>2</sup> K]
$UA_{AG,FA}$	UA-value for above grade surfaces normalized by floor area [W/m <sup>2</sup> K]
$UA_{BG}$	UA-value for below grade surfaces [W/K]
$U_{air,exchange}$	energy exchange with outside through ventilation and infiltration [W/K]
$U_{c,back}$	convective heat transfer to between the PV and back (BIPV/T) [W/m <sup>2</sup> K]
$U_{c,PV}$	convective heat transfer to between the PV and bulk air (BIPV/T) [W/m <sup>2</sup> K]
$U_{cog}$	conductance at the centre of glass (W/m <sup>2</sup> K)
$U_{eog}$	conductance at the edge of glass (W/m <sup>2</sup> K)
$U_f$	conductance of the frame [W/m <sup>2</sup> K]
$U_{ij}$	thermal conductance between nodes i and j [W/m <sup>2</sup> K]
$U_{o,PV}$	heat transfer to between the PV and outside
$U_r$	radiative heat transfer between PV and back (in BIPV/T) [W/m <sup>2</sup> K]
$V$	volume [m <sup>3</sup> ]
$V$	volume of substance [m <sup>3</sup> ]
$V_i$	zone I volume [m <sup>3</sup> ]
$V_{inv,max}$	maximum inverter voltage [V]
$V_{inv,min}$	minimum inverter voltage [V]
$V_{mpp,panel T=70^\circ C}$	PV module voltage at maximum power point [V]
$V_{oc,panel T=10^\circ C}$	maximum PV module voltage [V]
$V_{wind}$	windspeed [m/s]
$W$	width of house [m]
$W_f$	window frame width [m]
$w_i$	ANN weight
$WR$	wall resistance [m <sup>2</sup> K/W]
$W_w$	width of window [m]
$WWR1$	window-to-wall ratio 1
$WWR2$	window-to-wall ratio 2
$WWR3$	window-to-wall ratio 3
$WWR4$	window-to-wall ratio 4
$x_1$	input to regression model
$\hat{y}$	approximation of y
$Y_s$	self admittance [W/K]
$Y_t$	transfer admittance [W/K]

$\Delta C$	change in heat capacity [J/K]
$\Delta IP$	difference in input values
$\Delta OP$	difference in output values [kWh]
$\Delta T$	temperature change [K]
$\Delta t$	timestep duration [s]
$\Delta x$	Control volume thickness (i.e., node-to-node distance) [m]

### Greek symbols

$\alpha$	thermal diffusivity
$\alpha$	absorptance
$\alpha_{\max}$	maximum annual solar altitude (Summer solstice) [degrees]
$\alpha_{\min}$	minimum annual solar altitude (Winter solstice) [degrees]
$\alpha_s^f$	window frame absorptance
$\beta$	coefficient
$\gamma$	variable to measure time or space [s or m]
$\delta$	solar declination [degrees]
$\delta t$	timestep duration [s]
$\delta x$	control volume thickness [m]
$\varepsilon$	error term
$\varepsilon_{HRV}$	HRV effectiveness
$\varepsilon_{\text{source}}$	heat exchanger effectiveness in tank on supply side
$\varepsilon_{\text{use}}$	heat exchanger effectiveness in tank on use/demand side
$h$	system efficiency
$\lambda_{\text{losses}}$	PV system miscellaneous losses
$\pi$	Pi (3.14159...)
$r$	material mass density [kg/m <sup>3</sup> ]
$r(\phi)$	spectral reflectivity as a function of incident angle
$\tau$	transmittance [degrees]
$\phi$	incident angle [degrees]
$\phi'$	relative azimuth angle (between sun and window surface normal) [degrees]
$\phi_{\text{ground}}$	phase angle between air temperature and ground temperature [degrees]
$\psi$	site latitude [degrees]

## Acronyms

ach	Air changes per hour; variation ach <sub>50</sub> : air changes per hour with a 50 Pa pressure difference
AHU	Air handling unit
AC	alternating current
ASHRAE	American Society for Heating, Refrigeration, and Air Conditioning Engineers
BACnet	Building control and automation protocol
BPS	Building performance simulation
BIPV	Building-integrated photovoltaics
BIPV/T	Building-integrated photovoltaics with thermal energy recovery
CMHC	Canada Mortgage and Housing Corporation
COP	Coefficient of Performance; variations: subscripts <i>h</i> and <i>c</i> refer to heating and cooling
CSV	Comma-separate value file format
CFD	computational fluid dynamics
DMS	Design management system
DC	direct current
DHW	Domestic hot water
EEM	Energy efficiency measure
ERV	Energy recovery ventilation/ventilator
GA	Genetic algorithm
GHG	Greenhouse gas
GSHP	Ground-source heat pump
HRV	Heat recovery ventilation/ventilator
HVAC	Heating, ventilation, and air conditioning
IEA	International Energy Agency
LoI	Line(s) of Influence
MNECH	Model National Energy Code for Houses
NZEB/NZEH	Net-zero energy building/house
PCM	Phase change materials
PV	photovoltaics
RSI-value	R-value in SI units
SDD	Solar Design Day
SDHW	Solar domestic hot water
SHGC	Solar heat gain coefficient
R-value	Thermal resistance of a building material (English units)
Wol	Wheel of interactions

## Definitions

Active Solar: The act of collecting solar energy and storing it within a building to displace purchased energy with the use of an energy transfer medium that carries energy from the collector to the site of use or storage.

Base case building: a building that barely meets local building codes and that has windows distributed such that they face all directions equally.

Building-Integrated: a descriptor used to distinguish a component that is designed to be part of a façade or roof. In this work, it primarily refers to solar collectors.

Designers: architects, engineers, or building owners that have a role in the design of a building. In this thesis, the term “designers” is used synonymously with “users” (of the design tool).

Full factorial design: a systematic process of evaluating all possible combinations of a design. The number of combinations is  $m^n$ , where  $m$  is the number of settings for each variable, and  $n$  is the number of variables.

Net-zero energy homes (NZEH): houses which, on an annual basis, use as much energy as they produce, including purchased energy. (*Collected energy – purchased energy – used energy = 0*). A number of different net-zero energy definitions are being examined by IEA SCH Task 40.

Passive solar: The act of collecting solar energy and storing it within a building’s structure to displace purchased energy without the use of a working fluid. Passive solar can also refer to the act of preventing solar gains during the cooling season.

Purchased Energy: Energy, including, but not limited to fuel and electricity, that is brought on-site from an exterior source and that has a monetary cost.

Solar buildings/houses: buildings that are designed to displace some of their purchased energy by using on-site solar energy collection. Buildings that merely happen to collect some solar energy through their glazing, but are not designed to do so, are excluded from this definition.

Solar Fraction: the percent of a system’s total energy demand that is covered by solar energy.

# 1 INTRODUCTION

With the current environmental crises that humans and the rest of the world's inhabitants face, there is a need to fundamentally change the way we live. Assuming we want to at the very least maintain our quality of life, the only solution available to us is to do more with less (energy, materials, and other resources).

Building energy use represents nearly 40% of the total energy use in Canada, and is associated with a similar percentage for greenhouse gas emissions (GHG) . These figures are representative of other developed countries. For this reason, buildings represent one of the single largest opportunities to decrease energy use and GHG emissions.

Despite this fact, many buildings are designed and built to barely meet building codes or with cost, aesthetics, and overall marketability being given top priority. Undoubtedly, this short-sighted attitude routes from a combination of the builder not being the owner (i.e., not responsible for operating costs) or simply a lack of life-cycle cost analysis.

However, it also stems from the fact that good design tools are not widely available to building designers (Ellis et al., 2002). Usually models take so much effort to build that designers have little patience or time to actually vary parameters to determine their optimal values (Wetter, 2001). During design, designers need tools that allow them to efficiently explore the design space and apply different energy-saving measures to guide them towards the simplest and most cost-effective solutions that meet their requirements. In reality even the software that is labeled as a design tool is more often

than not merely an evaluation tool. Balcomb (1992) wrote that all design tools can be categorized as evaluation tools or guidance tools. The former category is akin to a specialized calculator in that it takes inputs, performs some computations, and provides outputs without explanation or validation. In contrast, guidance tools point designers in the direction of better design space.

In the past few decades, much of the emphasis in creating new building energy simulation tools has been on accuracy, speed of computation, and features (Augenbroe, 2002). Such features include modelling capabilities for different technologies and equipment, daylighting, and computational fluid dynamics (CFD) for studying airflow in and around buildings. Far fewer resources have been devoted to adapting the software for the use of design. Design tools include building simulation capabilities, but more importantly, provide guidance towards improvement (or at least valuable output) or facilities to control the level of detail such that it is appropriate for the design stage. Many graphically-oriented front-ends for simulation programs call themselves design tools. However, these are not true design tools, as they do not assist the user in making decisions; they merely provide an output resulting from inputs (Ellis and Mathews, 2001).

The potential for energy use reduction in houses is very impressive. It has been shown that it is possible to reduce the net annual energy consumption of houses to zero in Canada and in other similar climates where heating dominates energy demand



(Charron, 2005; Noguchi et al., 2008). Similarly, it has been shown that low-rise commercial buildings can achieve a similar status (Torcellini et al., 2006). One of the most effective ways to achieve this is to use building-integrated solar energy collection. Solar energy is reliable, cyclical, distributed, and its seasonal variation can be exploited to enhance passive solar performance.

Many solar buildings have been built in the past few decades. These have typically been designed by passionate and patient designers who were willing to spend considerable time using a variety of simulation tools in attempt to achieve an effective design. This level of research is necessary in the early stages of any new implementation of a group of integrated technologies. However, widespread design and construction of solar buildings will depend on design tools to shorten this process to an economical level. For instance, a typical house with annual energy bills on the order of a few thousand dollars cannot justify a design process that takes longer than several days and that requires multiple designers. It is desirable to determine the optimal form of the house and other high-level specifications in a matter of minutes rather than days. Thus, an obstacle to overcome in bringing such houses to the mainstream is to provide a tool that is aimed at designers who may have little experience in solar buildings.

Design tools should be useful at the early design stages when the most impact at the least cost can be had (Reed et al., 2000). The IEA SHC Task 40/ECBCS Annex 52 (“Towards Net-Zero Energy Solar Buildings”) website states as one of its objectives that:

“The development and testing of simplified net-zero energy building (NZEB) tools or interfaces (e.g. spreadsheet or web-based method) linked to a national/international database of building archetypes and technologies including a tool for architects to support architectural integration at the early design stage” (IEA SHC Task 40 - ECBCS Annex 52, 2009). Likewise, the Solar Buildings Research Network (SBRN) website states: “...there is a need for the development of methodologies for the systematic analysis of design options at the early design stage so that form is optimized to maximize the collection of solar energy” (SBRN, 2009). The motivation for a design tool is also extensively described by Athienitis et al (2006).

The most likely reason for the domination of building performance simulation (BPS) software without the design-oriented features is that creating a design tool is challenging. BPS software need only characterize physical processes with mathematical Equations. A second reason for the lack of design tools is the nature of common design practice, which typically leaves out energy performance analysis until most major design details have been established (Reed and Gordon, 2000). In contrast, design tools must be smart and the developers must foresee how their users will interact with them and perform design. That is, they must consider multiple disciplines including human factors, design methods, and building science. This is the basis for the motivation of the current research.

This work will establish a solar house design methodology and apply it to a prototype design tool (“Ecos”). The word Ecos means home in Greek. Ecos will allow designers to efficiently and systematically explore the design space, while being guided towards the near-optimal design space. In order to facilitate this, quasi real-time feedback is proposed, such that the effect of every design input is immediately displayed (O'Brien et al., 2008b).

Solar houses were chosen as the target of Ecos for several reasons. First, they have the potential to drastically reduce energy demand and greenhouse gas (GHG) emissions. This is because of their large area of solar-exposed surfaces to occupant and volume (and hence, energy demand) ratio. Next, their potential for absolute (as opposed to relative) reduction in energy does not justify hundreds of people-hours associated with formal BPS-based design. An exception to this would be the development of a large subdivision of identical houses. Thus, a tool that can be used to quickly arrive at a good solution by designers other than experienced simulationists is in demand. As an example for the need for a design tool, the designers of ÉcoTerra, an innovative solar house near Montreal, used a whole suite of tools to design a single house (O'Brien et al., 2010c). These tools were not necessarily compatible and some of them had to be custom-built from first principles to properly predict the house’s performance after construction.

The target audience is fundamentally ingrained in any product. For Ecos, the target audience includes designers, building owners, and architects<sup>1</sup>. It is intended to be used at the beginning of the design process, with the purpose of establishing major house characteristics. Based on the extensive literature review provided in this thesis, it seems that the greatest contribution to the field would be to create a user-friendly, efficient design tool, rather than a detailed design tool. Detailed design tools, such as TRNSYS, exist; however, there becomes a point in the design process where in-depth knowledge of the subject matter is imperative in order to use any software tool at all. For instance, the detailed design of a solar thermal system in TRNSYS requires the explicit implementation of controls and plumbing. In contrast, Ecos is not intended for such low-level design.

Upon determining the optimal<sup>2</sup> design, the Ecos user can proceed with detailed design or pass the specifications to an expert or to a more detailed tool. For instance, the model developed by Ecos can be readily imported by EnergyPlus.

This thesis is premised on the fact that occupant-based energy use can be approximated and HVAC-based energy can be calculated with much greater certainty. It follows that expecting a house to perform to a certain level within several percent in absolute terms

---

<sup>1</sup> It has since been pointed out that the product of this research is also an excellent educational tool to communicate basic solar building concepts.

<sup>2</sup> Throughout this work, “optimal” is used to define the best solution as seen by the designer, and not necessarily the mathematically-optimal solution.

is absurd<sup>3</sup> and that the objective should be to focus on designing aspects of a house that can be controlled during design (namely the envelope, HVAC system, and renewable energy systems).

## 1.1 Problem Statement

There is a need for an integrated solar building design methodology and design tool that allows designers to quickly design near-optimal buildings given a set of hard constraints (e.g., building code, site limitations, financial, geometrical constraints, net energy use) and soft constraints (e.g., aesthetics, personal preferences). The tool should help designers to balance and optimize different energy efficiency and energy collection measures. It should enable the consideration of many different low-energy strategies including the assessment of passive features and active solar systems. It should result in a good design on the order of an hour or less and should be usable by designers who do not have sophisticated energy modelling knowledge.

## 1.2 Research Objectives

The research objectives of this thesis are:

1. To develop an **integrated and accurate model** that is specialized for designing and characterizing solar homes (both passive and active elements). This work should

---

<sup>3</sup> This especially applies to individual houses. Certainty increases if: the building is multi-unit and there are a greater number of occupants, if the house is owner-built, or for buildings that are strictly-managed such as retirement homes, hospitals, or space stations!

- answer the question: what is the appropriate level of model resolution for each major aspect of the model?
2. To develop a means for **quantifying and understanding the affect of design parameters** – both individually and in subsets of the design space; determine the **significance of interactions** between parameters and the importance of integrated design. This work should answer the question: how effective is it to perform optimization on one parameter at a time?
  3. Development of **graphical design feedback** methods. Vast quantities of information are available from building simulation. Key metrics, graphs, figures will be developed to isolate the most pertinent information, based on the first objective. This work should answer the question: what are the most effective ways of visualizing and understanding the tremendous volumes of building performance simulation data?
  4. A **design methodology** for solar homes with specific guidelines and strategies to design effective low-energy solar houses using the solar house design tool.
  5. A **prototype design tool** demonstrating the results of the first three research objectives. This will address the limitations of other simulation/design tools that were previously mentioned.

### 1.3 Thesis Overview

The scope of the **literature review** covers four main topics: low-energy and solar house features and technologies, modelling solar houses, solar house design processes, and design tools suitable for solar houses.

The **passive solar modelling** chapter describes the detailed model that was used in the current research including the envelope and heat transfer, basement model, windows and shading, thermal mass, thermal and control zoning, thermal comfort, daylighting, controls, and internal heat gains. Major topics include modelling techniques, parameterization of the design space, model resolution, and performance metrics. This chapter's scope is the form and the fabric of houses.

The **active solar system** modelling chapter describes the photovoltaic and solar thermal systems that were used in the current research, including technologies, modelling techniques, and building-integration of solar collectors. The models and the corresponding parameters used to define are described in detail. The scope of this chapter includes photovoltaic and solar domestic hot water systems.

The **integrated design and interactions** chapter explores the importance of simultaneously considering multiple aspects of the house design or parameters to describe the house. The design space was studied in detail to gain a mathematical and practical understanding of which parameters need to be designed or considered simultaneously, and which can be independently optimized. One of the major

components of this research – parameter interactions – is explored in detail. This concept is expanded to the subsystem level and the design space is qualitatively assessed for opportunities to decouple models. Decoupling models provides the dual benefits of reducing the design space and simplifying the model.

The **solar house design methodology** chapter presents a methodology for designing solar houses and references how Ecos should be used to support this. The concepts of robustness and passiveness are introduced as a means for prioritizing design aspects. Detailed flow charts are presented as a means to suggest ideal design methods. Three different design methods are explored, including: parametric, solar design day, and a hybrid of the two. Finally, an example exercise is demonstrated using the hybrid approach.

The **design tool and interface** chapter discusses how the concepts of the previous four chapters are implemented into Ecos. Topics covered include: interfacing with EnergyPlus, Ecos inputs, performance simulations and calculations, Ecos outputs, and the forms of graphical feedback.

The **case study** chapter first describes ÉcoTerra and reports its performance. The design process and design tools used are critically assessed. Finally, this chapter describes how the model was used to further optimize its design.



The **conclusion** chapter briefly summarizes the work that was accomplished, lists the major contributions of the work, and finally discusses the limitations and future directions of the research.

A flow chart of the structure of this thesis is shown in Figure 1-1. Chapters 3 through 9 are original work, with the exception of brief references to some existing work by other researchers. Furthermore, the current author's previous publications are frequently referenced. As the flowchart indicates, this work is methodology-heavy.

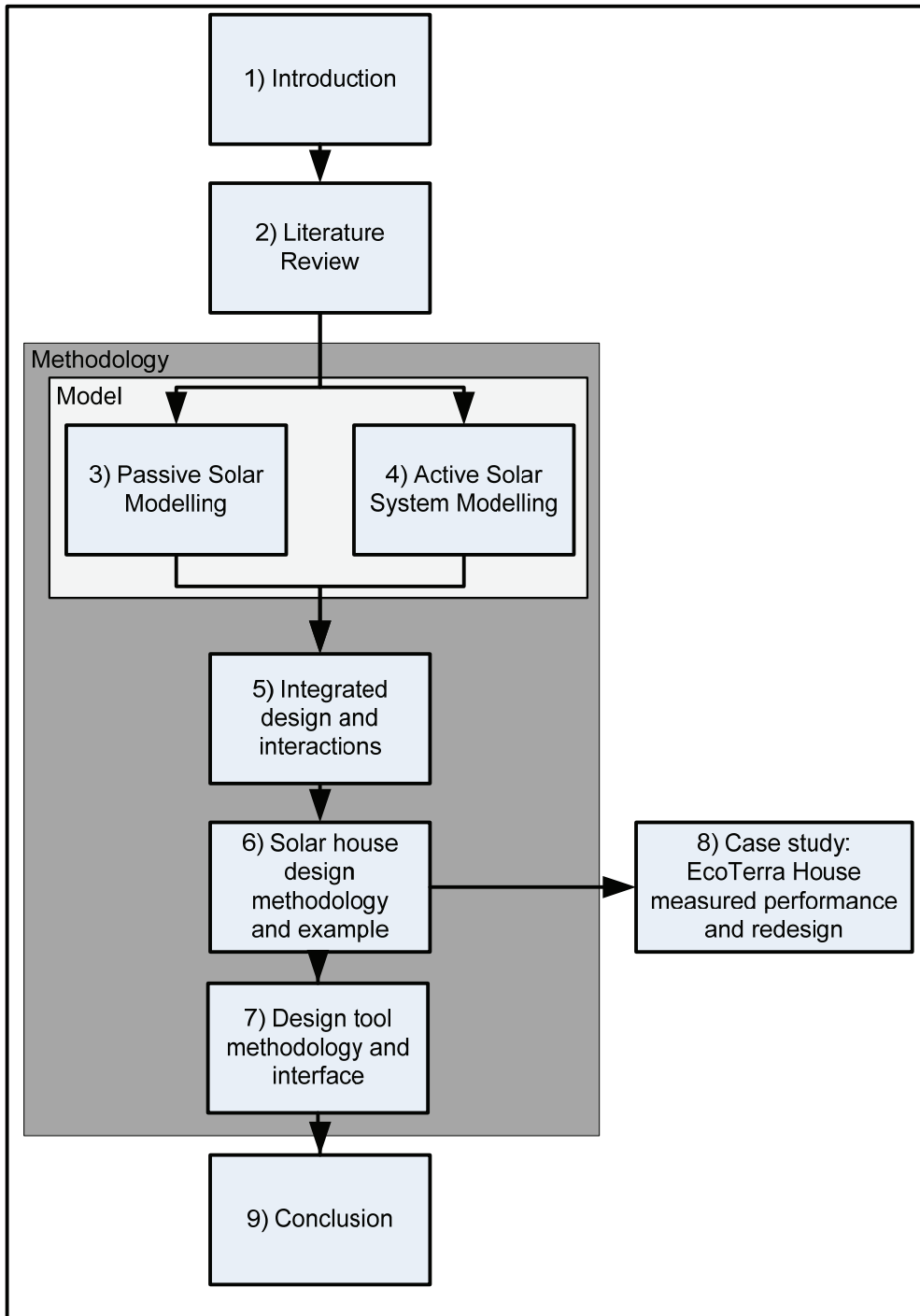


Figure 1-1: Thesis structural diagram

## **2 LITERATURE REVIEW**

Because of the multidisciplinary nature of this thesis, a variety of topics are covered in the literature review, including a summary of notable existing energy efficiency measures, solar collector technologies, solar homes, design practice, and finally building performance simulation (BPS) software.

### **2.1 Solar & Energy Efficient Houses**

In considering the overall impact of the housing stock, the first obvious step is to examine the break-down of energy use. Figure 2-1 shows the primary energy use in all Canadian residential buildings. The good news is that about 80% of it is low-grade thermal energy and offers the potential of nearly 100% primary to useful energy conversion<sup>4</sup>. However, this data represents the average for the existing Canadian housing stock. As envelopes become increasingly well-insulated and airtight, the other portions gain in proportion. For instance, the portion of total energy (electricity) use devoted to space heating in ÉcoTerra is a mere 20%. One might argue that there is little point in attempting to address heating energy since its share is decreasing; however, there are several reasons why this is fallacious, including: 1) it is only after the envelope, ventilation, and heating equipment are improved that this occurs, and 2) there is greater certainty that a high-performance envelope will translate to lower energy use

---

<sup>4</sup> Either fossil fuels are combusted on-site with conversion efficiencies of approximately 90% or the central electrical grid, with a conversion efficiency of about 30% is coupled with a heat pump coefficient of performance (COP of about 3.5), yielding a primary energy to thermal energy conversion of about 105%.

than high-efficiency appliances and lighting (which are most subject to occupant behaviour) and, 3) an envelope has more permanence than lights and appliances, since the envelope's life cycle is 2-10 times longer (Keoleian et al., 2000).

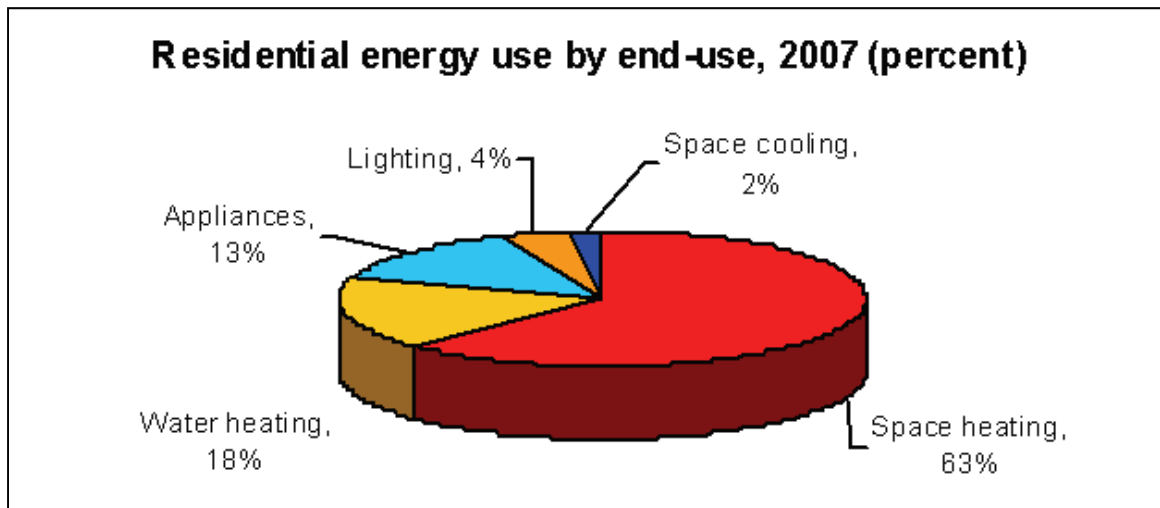


Figure 2-1: Attribution of energy use in residential buildings in Canada (<http://www.nrcan.gc.ca/eneene/effeff/resuse-eng.php>)

The first solar home discussed throughout the literature is the (Massachusetts Institute of Technology) MIT's Solar One, built in 1939 in Boston, Massachusetts (MIT, 2008). Its designers claimed that it was the first North American house to intentionally use solar radiation as a heat source. It used a very large roof-integrated solar thermal collector. Its water-based thermal storage was "swimming pool-sized" and bridged the gap between sunny winter periods (US DOE: EERE, 2008). A lack of south-facing glazing to take advantage of passive solar heating is likely an artefact of the poorly performing windows of the time. That is, the heating season's net-heat gain through the windows would have likely been negative. It was noted that night time heat loss through the glazing was high despite aluminum shutters (Grossman, 1948). In fact, it wasn't until MIT's Solar Five,

which was built in 1978, that passive solar elements were included as a major design aspect.

While photovoltaic cells were first developed in 1954, they were intended for extraterrestrial applications (Goetzberger et al., 2003). They were 6% efficient and cost about \$300 per Watt (approximately 60 times the current cost; all in current dollars).

The first mention of houses with integrated PV modules in the literature is in the early 1970s (Elliott, 1960; Boer, 1974). The catalysts for the surge in investment were the Oil Crises of the 1970s (Wittwer et al., 1994). Since then, many efforts towards more energy efficient houses have emerged, from single implementations to government programs and standards.

One successful implementation of low-energy standards in Canada is the R-2000 program (NRCan, 2008a). It covers energy efficiency measures, alone, including envelope and ventilation upgrades. The program claims to result in a 30% energy reduction by having requirements that are 40% above building code, as illustrated by Figure 2-2.

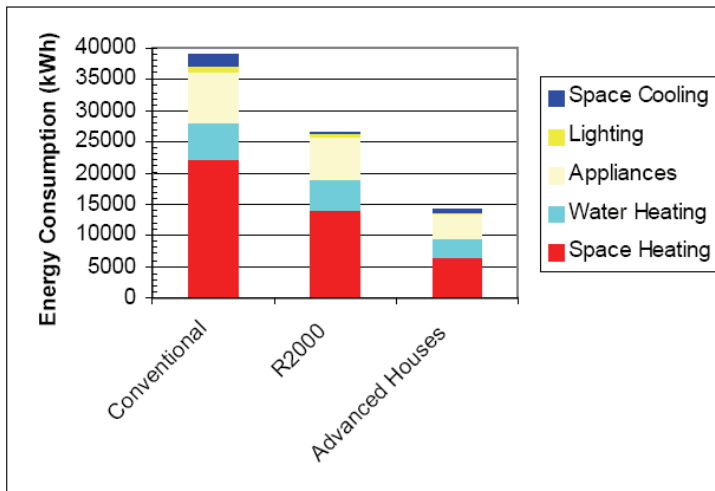


Figure 2-2: Comparison of R-2000 house performance with conventional houses (Charron et al., 2006a)

The Passivhaus standard is far more aggressive, though less successful (if measured by houses built to date), than the R-2000 program (Schnieders, 2003). It requires a combination of “superinsulation”, passive solar heating, and a reduction in ventilation heat loss. Wall and ceiling insulation are reported to be as thick as 13 and 20 inches, respectively. Houses that adhere to the standards typically achieve an 85% reduction in space heating energy. Interestingly, peak heating loads are so low that the need for a heat distribution is eliminated, thus saving equipment costs. This is a fundamental example of how an integrated design process yields cost savings.

Canada’s Advanced House program yielded 10 low-energy houses (Charron et al., 2006a). The objective was to supplement energy efficiency measures used in the R-2000 program with active solar energy collection; resulting in a further 50% decrease in annual energy use, as shown in Figure 2-2.

The latest generation of energy efficiency houses is net-zero energy houses, which are predicted (or preferably measured) to produce as much energy as they consume over the course of a year (Charron, 2005). While having a slightly arbitrary<sup>5</sup> objective, such houses do, nevertheless, push the envelope in terms of being state-of-the-art. Typically, the houses use a cost-optimal balance of energy efficient measures and solar energy collection. Net-zero energy houses that collect solar energy usually do not meet energy demands in the winter, but make up for this deficit in the summer when they produce more electricity than they require. The EQuilibrium program, a recent incentive program by Canada Housing and Mortgage Corporation (CMHC) yielded 15 net (or near net) zero energy house designs (Noguchi et al., 2008). To date, six of the houses been constructed.

## **2.2 Household Energy Use and Efficiency Measures**

Efficiency measures are commonly considered to be the most logical starting point to upgrade a design (or retrofit) (Parker, 2009). They are distinguished as upgrades that make better use of energy inputs while providing the same services. Parker reports that the use of efficiency measures yields energy savings at a lower incremental cost than active technologies. However, he cautions that the Passivhaus standard risks over-investing in efficiency measures relative to active technologies because of the former's

---

<sup>5</sup> Presumably, the net-zero energy concept was created to imply self-sufficiency. However, net-zero energy buildings are typically still reliant on a central utility for electricity when they are not producing their own (e.g., night and winter months).

diminishing returns. Though, based on a study of 12 Passivhaus houses, Schnieders (2003) found that the energy use reduction cost an average of 5.1¢/kWh compared to 10-15¢/kWh for the cost of solar thermal systems. To support this, Rob Dumont, a Canadian pioneer in low-energy housing stated “insulate, then insolate”, referring to the wise strategy to insulate a house well before implementing solar energy collection (Dumont, 2005). A further consideration to support this is that most passive energy efficient measures are essentially fail-proof since they usually do not require moving parts. Results from the National Renewable Energy Laboratory’s (NREL’s) BEopt software suggests that on the scale from minimum building code to net-zero energy status, the economically-optimal limit of energy efficiency measures is between 40 and 60% (NREL, 2009). Beyond that, active solar systems become more economical.

In general the biggest end-use energy consumers present the greatest opportunity for reduction. As seen in Figure 2-1, space and water heating account for nearly 80% of energy use in Canadian houses. It should be noted that, if emissions are the concern, the graph slightly misrepresents reality since the specific energy input for heating could be on the order of a third of that for electricity consumers (for regions that obtain their electricity from the combustion of fossil fuels). Regardless, the graph demonstrates the significance of energy use for heating. Common measures for energy efficiency are reviewed in this section.



### **2.2.1 Building Envelope**

Heat loss from conduction through the envelope accounts for a large portion of heating loads. The main solutions are to increase opaque wall effective insulation levels (including reducing thermal bridging), use windows with lower U-values (including frames), and increase air tightness. Though insulation offers diminishing returns with thickness, it is among the simplest upgrades (for new homes). The R-2000 and Passivhaus standards have proven that space heating energy use can be reduced by between 30 and 85% from envelope improvements alone. The cost of adding insulation tends to increase at a greater rate than linearly with thickness because the walls' structural elements must increase in size. Thermal bridging caused by framing members can be reduced by using a continuous layer of insulation that divides the indoors from the outdoors (Hutcheon et al., 1995).

Thermal bridging through window frames is a significant source of heat loss. 10 to 20% of the heat loss through a window is through the framing, despite the fact that the frame typically represents only 3 to 5% of the window area (Winkelmann, 2001). Frame conductivity (U-values) range from 2.0 for vinyl frames to 10.8 W/m<sup>2</sup>K for aluminum frames with no thermal break (Athienitis et al., 2002). The higher extreme of this range is on the order of 100 times greater than a Passivhaus' walls. Interestingly, heat loss through windows accounts for 3% of all energy use in the United States (Arasteh et al., 1989). Glazing should be selected to be as insulating as possible, with the exception that

for near-south orientations, the U-value of glazing should be balanced with the solar heat gain coefficient to maximize net energy gains during the heating season.

Heat loss from infiltration is significant. Purdy and Beausoleil-Morrison (2001) found that a drop from 3.0 ach to 1.5 ach (in normal conditions) resulted in a heating load reduction of 27%. A house's airtightness is typically characterized by air changes per hour (ach) at a 50 Pa pressure difference across the envelope. Values can be as high as 8 ach, but a more reasonable value today, for high-performance houses, is closer to 0.5 ach (Zmeureanu et al., 1999; Schnieders, 2003). The 6700 Canadian house energy audits that were performed between 2005 and 2010, inclusive, measured an average infiltration rate of 3.11 ach at 50 Pa (NRCan: OEE, 2010a). In contrast, the built EQUilibrium houses were measured to have significantly lower rates, as shown in Figure 2-3. The NOW House has a higher rate because it is a retrofit and there were fewer opportunities to seal it. The other houses achieved between about 0.5 and 1.5 ach. Interestingly, most predicted a rate of 0.5 ach during design; suggesting that accurately predicting infiltration is not realistic. Reducing infiltration is dependent on a high-quality construction methods and is assisted by the use of an air barrier, caulking, and weather stripping (US DOE: EERE, 2009).

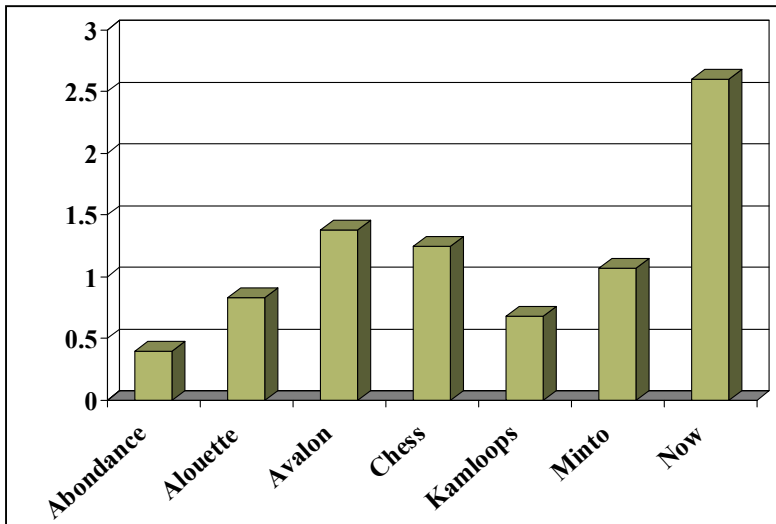


Figure 2-3: Measured infiltration rates (in ach) for the seven built Equilibrium houses (Charron, 2010)

To contrast the uncertainty of non-HVAC energy use (discussed later), heating and cooling energy tend to be more predictable because their magnitude is primarily a function of envelope U-value and solar aperture, HVAC equipment, and controls (all of which are associated with relatively high certainty). Major sources of uncertainty route from workmanship (e.g., insulation installation and air-sealing), external shading of windows, and the temperature control setpoints. Assuming occupants have control over setpoints, a designer cannot be sure of their value until after a house is occupied. Differences in electricity usage can route from culture, socio-economic status, age, and use of space.

Figure 2-4 shows the life-cycle GHG abatement costs of a large range of strategies. Among the least expensive are high-performance envelopes for new buildings. In stark contrast, the cost of retrofitting the envelopes of existing buildings is considerably higher and has a positive abatement life-cycle cost. It is not necessarily the case that



(again, gas, oil, or electrically fueled), heat pumps (ground, air or water-source; electrically-powered), or electric resistance. Other less common types include wood-burning (or other biomass) stoves or fireplaces. Active solar-based space heating systems are described in Section 2.3.

To distribute the heat or coolness from the plant to the space, the most common systems are forced-air or hydronic systems that are coupled with radiant floor systems or wall-mounted radiators. Homes with electric baseboard heaters have the plant (the resistive element) and distribution (primarily natural convection) in each room. The prevalence of heating systems is shown in Figure 2-5 and was obtained from NRCan (2006).

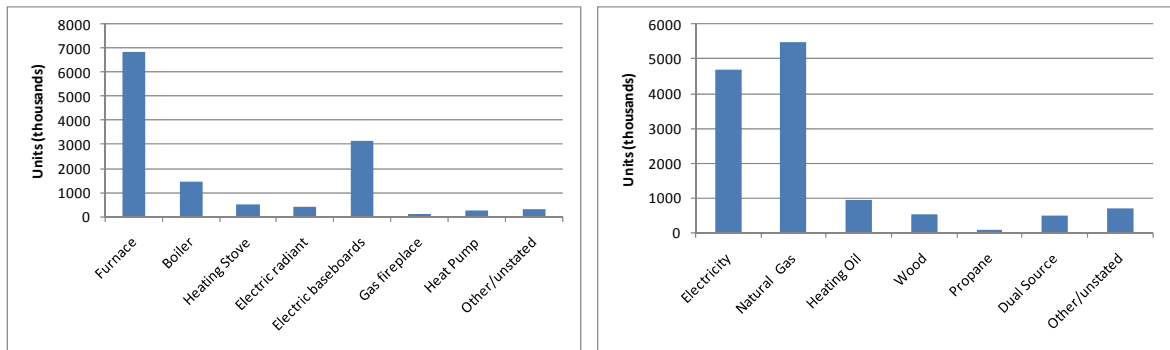


Figure 2-5: Prevalence of plant types (left) and fuel type (right) in the existing Canadian housing stock

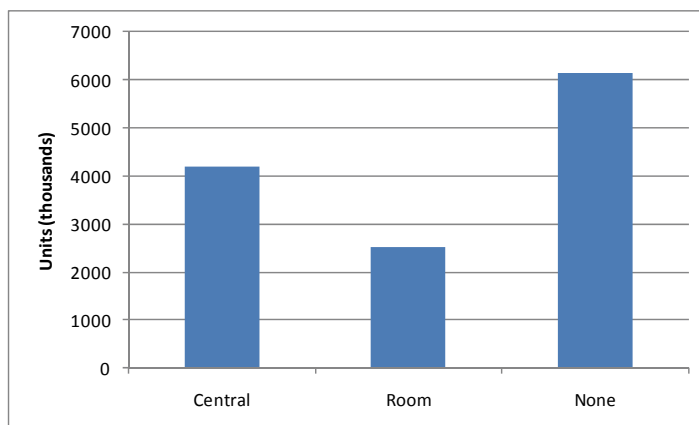
In stark contrast to the Canadian average for heating systems, the EQUilibrium homes tended to overwhelmingly favour ground-source heat pumps and active solar thermal systems (see Table 2-1). Though, somewhat surprisingly, three of the ten that are reported using electric resistance heaters as back-up. The common justification for baseboard electric heaters is that for high-performance envelopes, their lower capital

cost and scalability (i.e., they are available in smaller sizes and do not suffer from part load efficiency decreases) outweigh higher efficiency.

As shown in Figure 2-6, only about half of Canadian households have air-conditioners (NRCan, 2006).

*Table 2-1: Equilibrium home heating and ventilation systems (Canada Mortgage and Housing Corporation (CMHC), 2010)*

House Name	Mechanical Heating System	Ventilation
Abundance le Soleil	GSHP with forced-air for each apartment unit	HRV units for each apartment
Alstonvale Net Zero House	BIPV/T with heat pump, active thermal storage, and hydronic floor heating; GSHP back-up	HRV
Avalon Discovery 3	Solar thermal (evacuated tube; hydronic radiant floor heating) with electric boiler backup	HRV
ÉcoTerra™	BIPV/T with GSHP/forced-air	HRV integrated into forced-air system
EchoHaven	Radiant electrical panels with individual room controls	HRV with CO2 sensors
The Green Dream Home	unstated	unstated
Harmony House	unstated	unstated
Inspiration – the Minto ecohome	Solar thermal with gas furnace back-up; forced-air distribution	HRV
The Laebon CHESS Project	unstated	HRV
The Moncton VISION Home	unstated	unstated
Now House®	Tank-less gas boiler with forced-air distribution	HRV
Riverdale NetZero Project	Solar thermal with electric-resistance back-up; forced air distribution	HRV
Top of the Annex TownHomes	GSHP distributed with forced-air and in-floor heating	HRV with CO2 and RH sensors
Urban Ecology	Solar thermal with in-line electric resistance back-up; hydronic floor distribution	2 HRV units installed in series



*Figure 2-6: Prevalence of air-conditioners*

The controls used for heating systems consist of one or more sensors in the house that sense the temperature (essentially air temperature; not mean radiant or operative<sup>6</sup>) and inform the plant to begin producing heat (or coolness). While traditional houses often have a single control zone<sup>7</sup>, the literature reports that advanced houses have had between two and eight (O'Brien et al., 2010b). Such systems allow finer control of temperatures in different spaces in the house and are particularly useful under the following conditions: the occupants prefer cooler temperatures in certain zones (e.g., bedrooms, cold storage, and bathrooms) or certain zones experience significantly greater heat gains than others. This is particularly crucial in passive solar houses and has been found to be critical for predictions of both energy use and thermal comfort (O'Brien et al., 2010b). For the single zone configuration in passive solar houses, care must be taken to properly position the thermostat. If it is positioned near the south side of the house, it will tend to sense higher temperatures caused by solar gains and not trigger heating. Conversely, if it is positioned in a cool part of the house, it may trigger heating when the south side of the house is already amply warm from passive solar gains. Both hydronic and forced-air systems can be configured with valves and dampers, respectively, to control whether heat (or coolness) is delivered to a particular zone.

---

<sup>6</sup> Most thermostats are enclosed in a semi-open casing such that they are not directly exposed to the room surfaces; just the air that naturally passes through.

<sup>7</sup> About 40% of homes with a thermostat have two or more (NRCan, 2006)

All system configurations can be considered to provide essentially the same function of contributing heat to the space to elevate its operative temperature (defined in Section 2.2.10) of the space, but can differ in the resulting thermal comfort, primary to heat energy conversion, cost, and controllability.

Given the theme of this work, a major design objective is to achieve some optimal balance of minimizing life-cycle cost and GHG emissions of heating systems. Particular attention should be given to primary energy to heating and cooling energy conversion ratios. Heating (and cooling) system conversion ratios on the supply side (i.e., what the homeowner is interested in) are summarized in Table 2-2. The conversion from primary energy to purchased energy is equally important and is summarized in Table 2-3. The product of the two gives the heating energy to primary energy ratio, as shown in Equation 2-1.

*Table 2-2: Conversion ratios from purchased energy to heating energy (NRCan: OEE, 2010b)*

<b>Plant type</b>	<b>Heating energy/ purchased energy</b>
Furnace (natural gas)	0.90 to 0.97
Furnace (electric resistance)	1.0
Electric Baseboard	1.0
Heat Pump (air, water, ground-source)	2.5 to 4.0



Table 2-3: Primary energy to electricity conversion ratios for major US regions (Deru et al., 2007).

	National	Eastern	Western	ERCOT	Alaska	Hawaii
T&D Losses	9.9%	9.6%	8.4%	16.1%	12.9 %	8.9 %
Fossil Fuel Energy *	2.500	2.528	2.074	3.168	3.368	3.611
Nonrenewable Energy **	3.188	3.321	2.415	3.630	3.386	3.653
Renewable Energy ***	0.177	0.122	0.480	0.029	0.264	0.368
Total Energy	3.365	3.443	2.894	3.658	3.650	4.022

\* Fossil Fuel Energy includes all coal, natural gas, petroleum fuels, and other fossil fuel

\*\* Nonrenewable Energy includes Fossil Fuel Energy and nuclear

\*\*\* Renewable Energy includes hydro, renewable fuels, geothermal, wind, and solar PV

An interesting rule-of-thumb to note is that GSHPs that are supplied by electricity with a predominantly fossil-fuel or nuclear-powered grid have approximately the same primary energy inputs as gas-fired furnaces. However, GSHPs that are powered by PV are an exception to this rule-of-thumb because their primary energy input is minimal (only the embodied energy for manufacturing the systems).

Of particular interest for global warming potential, the amount of heating energy delivered per unit of GHG emissions can be found by Equation 1-2. Table 2-3 shows the huge geographical variability of GHG emissions per unit of electricity delivered by Canadian provinces. Kikuchi et al (2009) found the GHG emissions from generating electricity in Alberta to be so high that heating a home with a GSHP caused marginally more emissions than using a gas-fired furnace (summarized in Figure 2-7). A counter-argument to this is that electricity is a more versatile form of energy and that the situation will improve as (if) the electricity supply becomes more efficient; however, installed gas-fired furnaces are fixed to using natural gas and cannot increase in efficiency unless they are replaced.

Table 2-4: Electricity supply system for Canada's four most populous provinces (taken from Kikuchi et al., 2009)

	Ontario	Quebec	Alberta	British Columbia
Main electricity generation	Nuclear (42.4%) Coal (24.6%) Hydro (23.8%) Gas (7.4%)	Hydro (93.1%)	Coal (83.1%) Gas (12.7%)	Hydro (94.9%)
Emission factor			0.0598	
Natural gas (kg-CO <sub>2</sub> eq./MJ)		41		43
Electricity (g-CO <sub>2</sub> eq./kWh)	301		909	

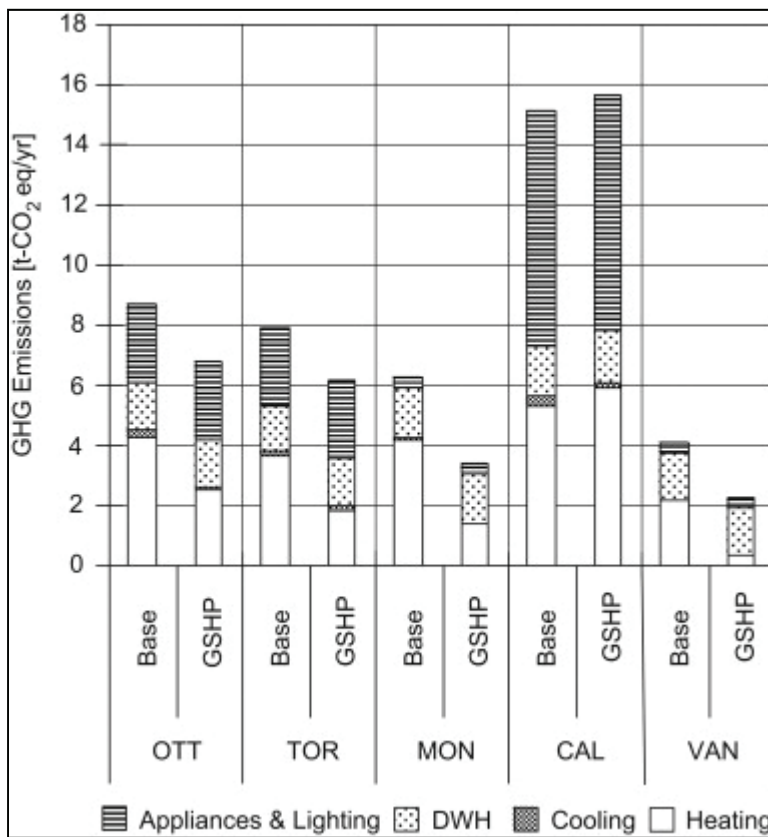


Figure 2-7: Comparison between a 94% efficiency gas-fired furnace (base) and GSHP of unreported COP (taken from Kikuchi et al., 2009)

Heat recovery ventilators (HRV) can be used to minimize the heating or cooling of incoming fresh air. HRVs are heat exchangers that heat incoming fresh air with outgoing

exhaust air (NRCan: OEE, 2009a). They can assist in the transfer of as much as 80% of the heat. HRVs should be considered standard installations in low-energy homes; this point is made in the survey of EQUilibrium homes (Table 2-1). However, HRVs do come at the expense of additional fan energy and the need for filter cleaning. To put HRV fan energy use into perspective, the ÉcoTerra HRV fan consumes about 500 kWh/year; or about one-fifth of that of the heat pump. An advantage to forced-air distribution systems is that the ducting can be used redundantly to distribute fresh-air and remove exhaust air; whereas, houses with hydronic and baseboard systems require their own ductwork for distributing fresh air.

### **2.2.3 Non-HVAC Energy Use**

Non-HVAC (also referred to as occupant-based or discretionary) energy use represents significant fraction of the total energy use. Typically it ranges between 20% (for the existing housing stock) and 50% for new low-energy solar houses, such as the ÉcoTerra House.

Unlike building envelope and HVAC performance, building simulation cannot be used to accurately predict discretionary loads because of the high degree of uncertainty. Three examples illustrate the significance of relative certainty. Saldahna (2010) measured non-HVAC electricity consumption for a wide variety of houses (in accordance with (Armstrong et al., 2009)) in the Ottawa region and obtained an annual range of 2641 to 11257 kWh/year. To further quantify human variability, a study by Seryak and Kissock (2003) at a university residence examined non-heating electricity use during the

academic year and found that the coefficients for variation ranged between 17 and 33% (when units were segregated by number of occupants). For example, of the four-student units, electricity use varied from 353 to 2100 kWh per academic year. Naturally, the pricing scheme plays a role in variability, in that higher electricity prices and paying for what you use (rather than fixed monthly rates) would tend to drive the average energy use downwards. As a final example, Charron (2010) presented the large variability in predicted non-HVAC energy use for ten Equilibrium™ homes. The three occupied and monitored house used 15 to 60% more energy than anticipated (see Figure 2-8). Since the design teams for the houses were motivated to achieve low total energy use, there is some undeniable bias in the predictions.

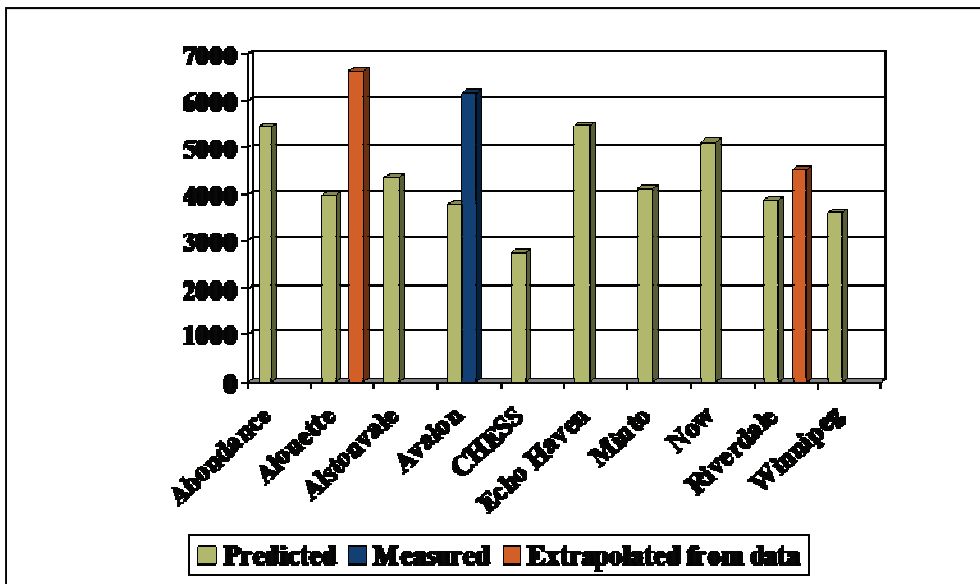


Figure 2-8: Comparison between predicted and measured (where available) non-HVAC electricity use (kWh/year)

The relationship between occupant-based energy use and HVAC-related energy use is that much of the heat gains from the former are usually produced within the house and

either immediately warm the space (convective portion of gains) or heat the surrounding surfaces (radiative portion of the gains). It is reasonable to assume that all heat gains be added to the space with the exception of those that vent directly outdoors (e.g., dryers and vented stovetops) and domestic hot water (which is usually assumed to mostly drain before the heat gains occur). While it can be argued that heat gains from appliances reduce the heating load, they do so under unfavourable circumstances: converting electricity to heat (COP of 1) and in an uncontrolled fashion (i.e., the heat may not be needed, especially in the cooling season).

#### **2.2.3.1 Domestic Hot Water (DHW)**

DHW heating represents about 18% of household energy use in Canada (NRCan, 2008b). Typically, water is heated by combusting fuel or using electricity and stored in a tank for future use. This is associated with storage losses, though tank-less heaters that heat water on demand eliminate these losses (NRCan: OEE, 2009b). For hot water heaters with tanks, the tank should be insulated to reduce the energy input required to maintain the water at the desired temperature. A drain water heat recovery unit can be installed that transfers outgoing waste heat to incoming mains water, much the way a HRV recovers heat from exhaust air (NRCan: OEE, 2009b). Another promising method for reducing DHW energy use is through the use of active solar collectors, as reviewed later.

#### **2.2.3.2 Major Appliances**

Given that appliances use 14% of household energy use in the existing housing stock, they represent a substantial opportunity for overall energy use reduction. Furthermore,

a large fraction of that is electricity, which can be considered a valuable form of secondary energy, given that the input of primary energy can be several times the amount of electrical energy output, as previously discussed. Low-energy appliances, such as those with the EnergyStar rating, should be used. Though it is important to consider that efficient appliances and lighting do not necessarily decrease the absolute amount of energy use – merely the value of the service provided. Jevons' Paradox (York, 2006) states that as energy consuming devices become more efficient, the market adapts by demanding more of it. For instance, the author has witnessed the transition in behaviour that his mother has made from a 30 year-old dishwasher to a modern one: she often runs the new one at half the capacity of the old one. On the house-level, houses that were once shack-sized because the cost to heat them would have been unmanageable are now mansions (in relative terms) because it takes much less energy per unit of floor area to heat. From 1990 to 2007, Canada's heating intensity ( $\text{GJ}/\text{m}^2$ ) decreased by 21.2% but the floor space per person increased by 20.8% (NRCan, 2010b)- resulting in nearly the same energy use per person. Meanwhile, Canada's population grew by 20% - resulting in approximately a 20% increase in environmental impact.

### **2.2.3.3 Lighting**

Lighting represents about 5% of energy use in the existing housing stock. Energy reductions can be achieved by installing energy efficient lamps and advanced controls (e.g., motion sensors and dimmers). The use of daylighting must be carefully assessed because it may increase heating and cooling energy use since windows are usually more

thermally conductive than walls and may also admit unwanted solar gains. Furthermore, the temporal pattern of daylight availability is often incongruent with household occupancy (i.e., the occupants are at home in morning before sunrise and the evening after sunset). BPS should be used to quantify the optimal window area; though the unquantifiable benefits (e.g., productivity, views, and the house's economic value) of daylight cannot be overlooked.

#### **2.2.4 Passive Solar Heating**

Passive solar heating is the act of collecting and storing heat with building-integrated components that do not require an active heat transfer medium. The principle of passive solar heating is fairly simple: some of the solar radiation that is incident on the glazing of a building is transmitted (or absorbed by the glazing and later radiated or convected inwards), where it is converted to long-wave (infrared) radiation (Athienitis and Santamouris, 2002; Arasteh et al., 2007). This incoming radiation is either reflected or absorbed by opaque interior surfaces. The radiation that is absorbed causes the temperature of these surfaces to increase, and in turn, warm the indoor air. This is accomplished by direct convection to the air or by re-radiation to other surfaces. The rate at which heat is released from the surface is dependent on its heat capacity and its heat exchange with the air.

The two undesirable effects of large glazing areas are nighttime heat losses and cooling season solar gains and overheating. The challenge is that glazing tends to be a poorer insulator than opaque walls. Thus, the added solar gains come at the cost of increased

thermal losses. The fundamental design challenge is to select glazing types that maximize solar gains and minimize heat loss. Furthermore, glazing should be oriented such that solar gains are maximized during the heating season and minimized during the cooling season. Glazing is best oriented southwards (or more generally, towards the equator) where the seasonal magnitude of incident solar radiation and the heating loads are congruent (CMHC, 1998). Conveniently, this orientation minimizes unwanted solar gains in the cooling season. Glazing within 15 degrees of south is nearly as effective, while even 25 to 30 degrees off can experience a positive heat balance (CMHC, 1998). An in-depth study of this is reported in Appendix C.

Figure 2-9 shows how the seasonal solar variation. The results of a more detailed study show the total incident solar radiation on all orientations for vertical surfaces (in Toronto) (see Figure 2-10).

The benefits of daylighting and view aside, windows should only be located where the net gain in the heating season is positive.



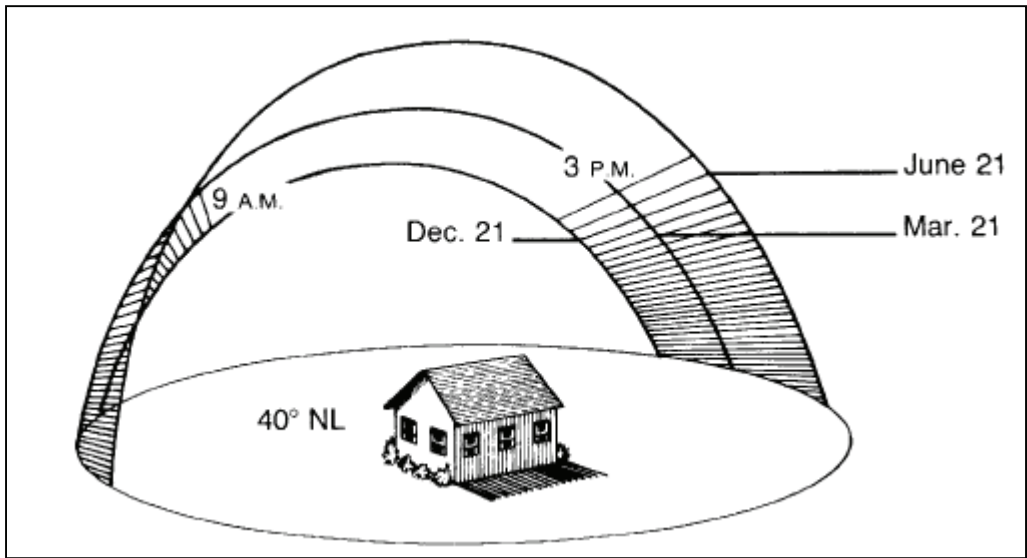


Figure 2-9: Seasonal solar paths for the northern hemisphere  
 ([http://www.knowledgepublications.com/heat/images/Solar\\_Air\\_Solar\\_Exposure.gif](http://www.knowledgepublications.com/heat/images/Solar_Air_Solar_Exposure.gif))

The nature of solar energy is that it is available in spurts: too much sometimes and not enough at others. To buffer this availability pattern, thermal mass is used to absorb daytime solar gains and release them at night (Athienitis and Santamouris, 2002).

Thermal mass also helps maintain comfort by reducing the magnitude of temperature swings. The principle can be explained by considering the units of heat capacity: J/kgK.

For a given amount of solar energy entering a house (in J), the corresponding temperature rise is inversely proportional the heat capacity. This is slightly complicated by the fact that the effectiveness of thermal mass depends on its ability to absorb and re-release the energy. Thus, thermal mass is usually implemented using large, relatively thin concrete (or other materials of high heat capacity and conduction) that are placed in the path of the sun. This is later quantified. There are two main categories of passive solar heating configurations: direct gain and indirect gain.

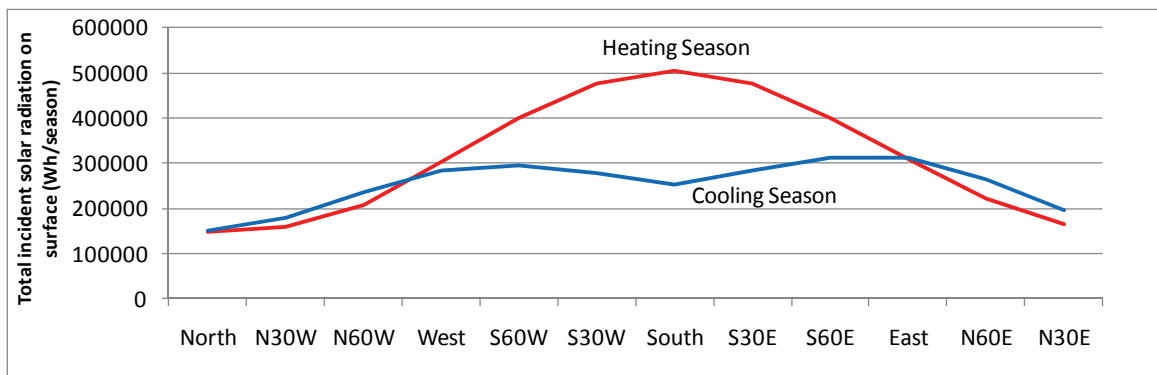


Figure 2-10: Total incident solar radiation on vertical surfaces by orientation and season.

### 2.2.5 Direct Gain Systems

Direct gain houses most resemble the technique described above. The glazing of the house represents the solar collectors, while the interior mass (e.g., concrete, gypsum, furnishings, etc.) of the house represents thermal storage (Sander et al., 1985; Givoni, 1991; Athienitis and Santamouris, 2002). Direct gain systems are distinguished by the fact that both the glazing and thermal mass are part of the conditioned space in the house. This type of passive solar heating is arguably the simplest to implement, but at the cost of a lesser degree of control over gains and thermal comfort (Fernández-González, 2007). Direct gain systems require relatively high-performance windows and/or nighttime insulation to maintain a positive heat balance (Hastings, 1995; Wall, 2006). O'Brien et al (2009d) estimated that the efficiency of passive solar heating is on the order of 10%. This is the fraction of incident solar radiation on glazing that contributes to reducing purchased energy. It is based on a typical solar aperture with substantial thermal mass.

In general, passive solar heating should be considered a major element to solar houses. It is simple, cost-effective, and permits large windows (Athienitis and Santamouris, 2002). However, the size of the passive solar collectors (windows) is limited by thermal comfort and construction constraints. With these constraints, the maximum advisable solar aperture is 12.5% or about 40% of the south-facing glazing area for Southern Canada (CMHC, 1998). Solar aperture is defined as the south-facing glazing area to conditioned floor area. This upper limit in glazing area can achieve space heating reductions of about 15 to 20%, but depends on the window performance and climate. Larger glazing areas causes the solar gains to be delivered in bursts that are too large to be passively buffered, while causing significant nighttime heat losses.

### **2.2.6 Indirect Gain Systems**

Indirect gain systems are characterized by houses in which the glazing is isolated from the conditioned space by a wall. Common types include sunspaces and Trombe walls. Sunspaces are glazed extensions of houses that share at least one wall with the main part of the house, but that are usually not conditioned (Kesik et al., 2002; Mottard et al., 2007). This provides the ability to control the interaction between the sunspace and house. For instance, solar gains can be included or excluded from the house passively using operable openings and convective loops or actively using a fan. During cold periods with minimal solar gains, the space can be isolated to reduce heat loss to the sunspace. Through a simulation study, Kesik and Simpson (2007) found that direct gain

systems are usually more efficient than sunspaces and that sunspaces can experience significant overheating unless proper shading is implemented.

Storage-collector (Trombe) walls can be seen as a special case of sunspaces. But, instead of being a living space, they are merely a thin air gap (typically, on the order of centimeters), sandwiched between glazing on the outside and a thermally massive wall on the inside. The space can be isolated or ventilated through natural or forced convection to the interior space (Duffie et al., 2006). The principle is similar to the other two passive solar heating techniques, but introduces some degree of control and reduces the nighttime heat loss of direct gain configurations. Givoni (1991) stated that Trombe walls are ineffective in climates with long cloudy periods (several days) because the feature acts as a heat sink, causing substantial heat loss. Similarly, CMHC (1998) advises against them for the Canadian climate.

Both of the latter types of passive solar systems can be considered to be decreasing in relevance as window thermal resistance increases with advancing technology. Heat losses aside, direct gain systems provide the advantage of simpler architectural integration, copious daylight, and views. Although, sunspaces provide additional living space and could act as a greenhouse.

### **2.2.7 Glazing**

High-performance glazing is crucial to successful passive solar heating. The perfect window (for heating-dominated buildings) would have high transmittance (visible and

short-wave radiation) and low heat transfer. All three types of heat transfer occur in windows, including: radiation between glazing layers, convection in gaps, and conduction through window frames and spacers. Unfortunately, heat transfer and transmittance in windows tend to be inversely related, to some extent, as Figure 2-11 illustrates. The optimal glazing types for passive solar heating are in the lower right corner of the graph. O'Brien et al (2008a) found that, under certain circumstances, double-glazed windows can actually result in lower purchased heating than triple-glazed because the additional transmittance is more beneficial than the negative effects of the poorer thermal properties. It is standard to characterize glazing's ability to transmit solar gains as the solar heat gain coefficient (SHGC). This includes not only the transmitted radiation, but also that which is absorbed by the glazing and eventually convected and radiated inwards. Figure 2-11 shows the performance of a large number of glazing types. SHGC values are angularly dependent, but it is standard to rate glazing by its normal SHGC value (the maximum).

A variety of glazing types were created in Window5 software, by the author, and plotted in Figure 2-11. It shows that a clear Pareto front (as described in the optimization section) emerges.

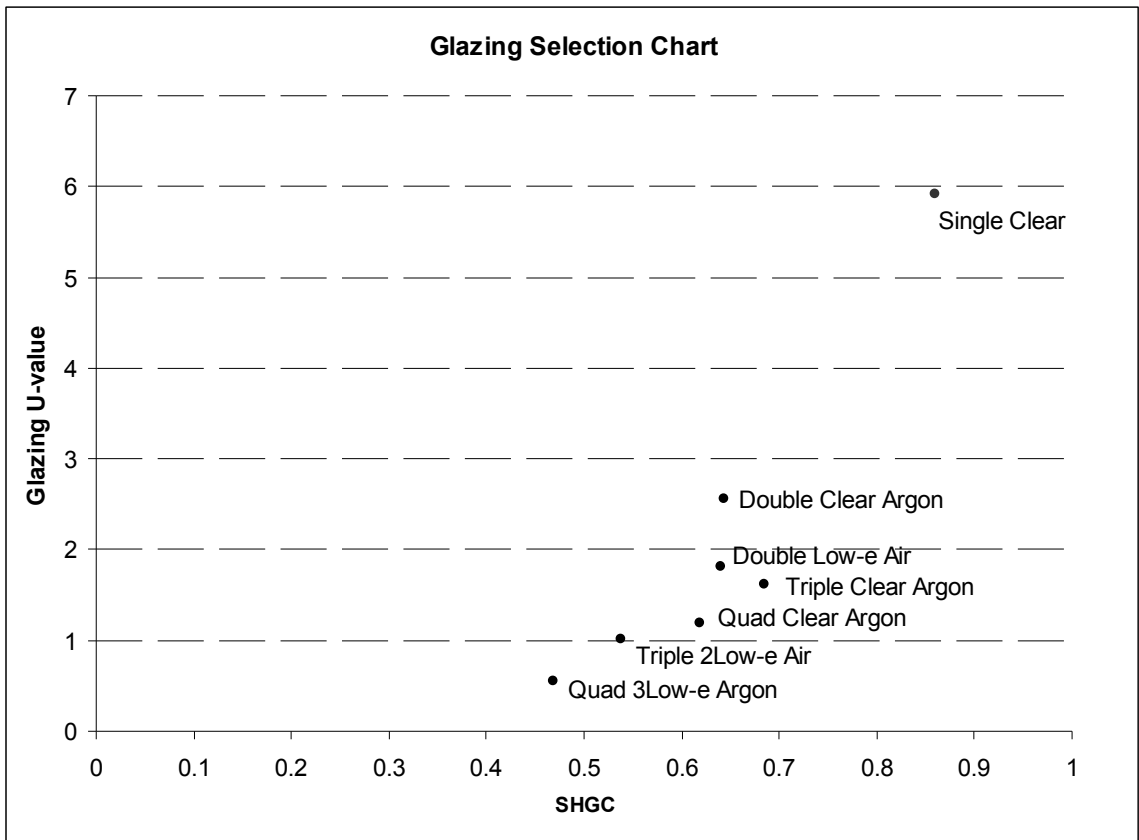


Figure 2-11: A variety of common glazing types and their thermal and optical properties.

Current glazing technology has advanced to the point where two to four layers of glazing are used. Often the gaps between glass layers are filled with inert, heavy gases such as argon or krypton (Hutcheon and Handegord, 1995). Glass has little thermal resistance; and thus, the majority of the thermal resistance of a window results from the gas-filled cavity or cavities. Unfortunately, as shown in Figure 2-12, the benefit of the cavity is limited to about 13mm, at which point an increase has minimal effect on thermal resistance and convective loops begin to occur (Athienitis and Santamouris, 2002). Low-emissivity coatings can reduce the emissivity of glazing from about 0.9 to 0.1. Usually, the coatings are used on one of each pair of cavity-facing glazing surfaces.

For example, the addition of a low-e coating to a double-clear window can reduce the U-value by about 25% and the SHGC by 5% - a worthwhile trade-off (Arasteh et al., 2007).

If there is flexibility, surface coatings should be applied on glazing layers that are towards the inside, since they absorb more heat than clear glazing, and this absorbed heat is less likely to return outside.

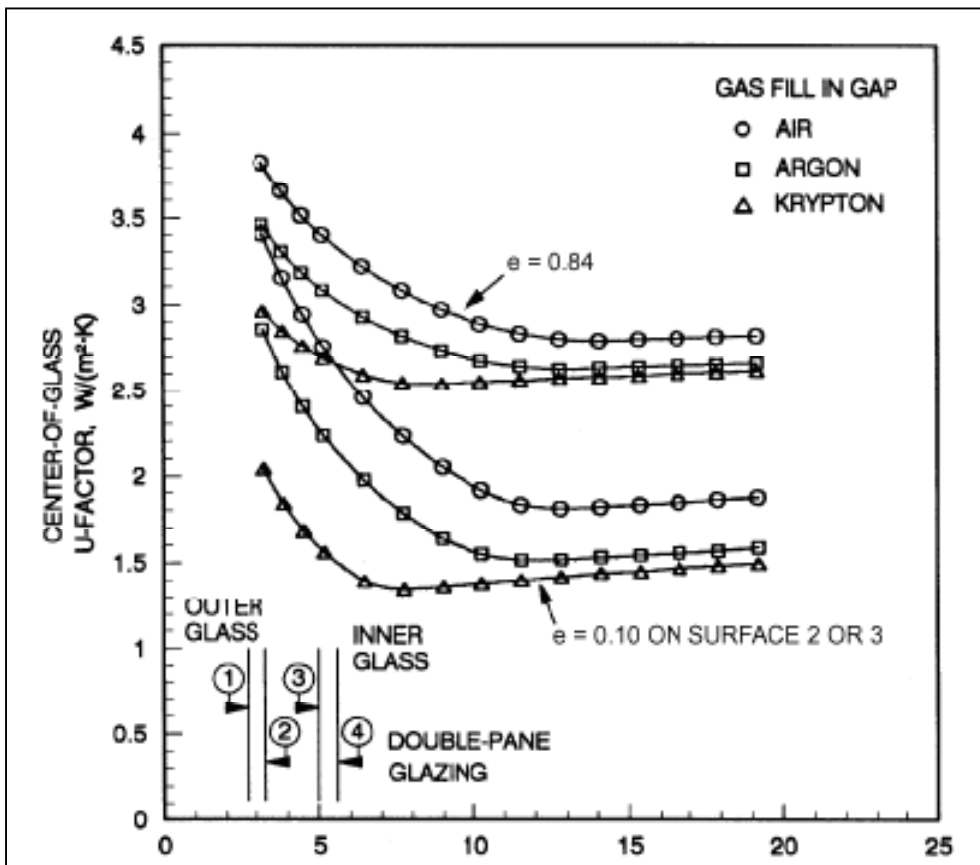


Figure 2-12: Window U-value as a function of gap thickness (in mm) (ASHRAE, 2001)

Tinted and heat-absorbing glass is not appropriate for passive solar heating of residential buildings in cold climates, since it reduces the amount of solar radiation that eventually enters the indoors. However, it could be used in non-south facing windows where higher levels of solar gains occur during the cooling season.

Several emerging glazing technologies show potential for passive solar heating, including Aerogel and honeycombs (Carmody et al., 2004). While eliminating views because of their opacity, these products drastically reduce heat loss by suppressing convective heat transfer in the cavity. The addition of Aerogel – a silica-based foam-like substance – has been shown to reduce the center of glass U-value to 0.05 W/m<sup>2</sup>K. The evacuation of gas to create a vacuum between layers of glass can virtually eliminate convective heat transfer while still allowing a view. However, this has technical challenges such as the inward bowing of panes and “leakage” (Carmody et al., 2004).

Removable glazing insulation can play an important role in energy savings (Hastings, 1995). Unless mechanized, this requires the active daily participation of occupants – something that is unlikely for the typical homeowner. The risk of insulating windows is that the probability of condensation increases because the inner glazing surface temperature can descend well below the dew point. The next section discusses shading, some types of which can have some positive effect on nighttime heat losses. Through experiments, Fang (2000) found that internal Venetian blinds can reduce the U-value of double clear glazing by 20%; though this would be a lower proportion for high performance glazing. Also, the isolation of the space immediately adjacent to the glazing could lead to chronic condensation, since the space is liable to get very cold. Thus, blinds should mainly be considered a solution to prevent unwanted solar gains.



### **2.2.8 Shading: Static and Dynamic**

To reduce unwanted solar gains, shading devices can be used. While they are also effective at controlling glare, this is beyond the scope of this work, which is primarily focused on energy and thermal comfort; not visual comfort. The commonly cited strategy of using deciduous trees for shading of passive solar houses can be ineffective. Given that the net energy gains, even from south-facing windows, can be marginal for average quality glazing in the winter, this shading could unintentionally push the net energy to negative.

There are two categories of shading devices: static and dynamic. Static shading devices include overhangs, sidefins, and light shelves. Dynamic devices include Venetian and roller blinds (both interior and exterior), louvers, and retractable awnings.

Static shading devices have the advantage of simplicity. However, their fixed nature means that their geometry must be carefully planned to maximize solar gains in the heating season and minimize them in the cooling season. Overhangs have been shown to have the potential to reduce cooling loads by 13% - a significant amount for an inexpensive, passive component (Raeissi et al., 1998). Nevertheless, since there is a seasonal lag between peak solar altitude and peak temperatures, fixed shading devices have two limitations: they can block late-spring solar gains when heating is still required and they are not effective at preventing late summer/early fall overheating (O'Brien et al., 2008b). Thus, a more flexible/controllable solution would be beneficial to performance.

For external shading devices, absorbed and reflected solar radiation (for external shading devices) is almost completely rejected, making them more effective at preventing solar gains because the shading devices are not contained by glazing (La Roche et al., 2004).

Extensive studies have examined the potential in energy savings through controlled (manually or automatically) internal blinds (Lee et al., 1998; Foster et al., 2001; Tzempelikos et al., 2007). Retractable awnings have the potential to reduce summertime solar gains by up to 80%, though at the cost of reduced daylight (Athienitis and Santamouris, 2002). Fragile external dynamic shading devices such as Venetian blinds are not currently appropriate for Canada's climate because of the harsh winter conditions. Internal blinds, which are protected from the elements, have the potential to reduce cooling loads, but their position allows some solar gains to enter the room (i.e., not all reflected solar gains are ultimately rejected to the outdoors). Furthermore, the solar radiation that is absorbed by the shades is nearly immediately convected to the space, unlike that this is absorbed by thermally massive surfaces.

### **2.2.9 Thermal Storage**

There are two main purposes of thermal storage for passive solar heating applications. The first is to reduce the magnitude of air temperature swings. The second is to create a thermal lag in the building; absorbing heat during the day (when there is ample solar energy) and releasing it at night (when there is no solar energy available). Thermal storage systems can be approximately categorized as passive and active, though there

are systems that could straddle the line. For instance, it is possible to actively charge a concrete slab, and passively discharge it.

### **2.2.9.1 Passive Storage**

Passive storage, which is typically positioned to absorb direct (beam) solar radiation, is made of materials with a high thermal capacity and high conductance, such as concrete, masonry, or contained water (Athienitis and Santamouris, 2002). The purpose of the first property was previously explained. The second property ensures that absorbed solar radiation is conducted depth-wise to allow the deeper thermal mass to be used (i.e., store energy). Although, the limit in depth of useful thermal concrete or masonry is about 15 to 20 cm (Athienitis and Santamouris, 2002; O'Brien et al., 2009c). Concrete and masonry floors or walls can double as structural elements of the building. For instance, ÉcoTerra contains concrete floors in both the basement and first floor, on its southern half (Noguchi et al., 2008). It also has a three-foot high concrete wall at the back of the direct gain zone.

A more advanced type of passive thermal storage uses phase change materials (PCMs). PCMs are substances with a high heat of fusion (Xu et al., 2005). To be useful in buildings, PCMs should change state (e.g., liquid-solid, solid-solid) at a temperature near room temperature (Johnson, 1977). Such a PCM would effectively resist temperature from increasing beyond room temperature, unless considerable energy is added. The name “phase change material” is a bit of a misnomer since it is generally used to describe materials that change phases at a convenient temperature, unlike water, for

instance, which changes from solid to liquid at 0°C, under standard atmospheric conditions. PCMs can be combined with structural components such as concrete or with gypsum to form a compound to be used in walls, floors, or ceilings (Tyagi et al., 2007). The advantage of PCMs over traditional thermal storage media is that it can absorb considerably more energy per unit of temperature change. Thus it is more effective and takes up less living space (Streicher, 2007). In fact, delVall et al (2007) reported that wax (a common PCM) has 20 times greater heat capacity than concrete, and changes state at about 25°C. Though there has been concern over degradation in performance of PCMs (MIT, 2008), delVall et al (2007) showed that there was only a 2% decrease in performance after 1,600 cycles. The use of PCMs is not common in homes, yet, but they appear to be promising.

### **2.2.9.2 Active Storage**

Active storage functions as passive storage, except that thermal energy is delivered to, taken from, or both, using a heat transfer fluid, such as air or refrigerant. While circulating the fluid consumes electrical energy for pumps or fans, it enables better use of the thermal mass by promoting heat transfer (both between the mass and the fluid and within the mass itself). Furthermore, there is an element of control, in that heat can be removed from the thermal storage as needed. Several common types of active storage systems in passive solar houses are Trombe walls, rockbeds, and ventilated slabs (Beasley et al., 1983; Fraisse et al., 2006; Noguchi et al., 2008). The latter has the advantage of consuming less volume and acting as radiant floor heating, but cannot be

used for long-term (multiple day) storage because of its large surface area to volume ratio. Rock beds or other forms of compact storage can be insulated, but consume valuable space, since they cannot be integrated into the building as easily.

### **2.2.10 Thermal Comfort**

Thermal comfort is an integral part of passive solar design – particularly for direct gain zones, which can be equated to “live-in solar collectors”. Large glazing areas, which can enable a significant reduction in energy use, transmit large quantities of solar radiation during clear days, which can result in discomfort from elevated air and surface temperatures. A study by Athienitis and Haghghat (1992) found that the sensed temperature from beam radiation increases by about  $0.025 \text{ K/Wm}^{-2}$ . For instance,  $500 \text{ W/m}^2$  of beam radiation would result in a  $12.5^\circ\text{C}$  increase in sensed temperature. Furthermore, the operative temperature (the temperature sensed by occupants) is roughly two-thirds influenced by the temperature of the surrounding surfaces (Athienitis and Santamouris, 2002). This is dependent on the respective values of the convective and radiative heat transfer coefficients. ASHRAE (2001) simplifies the calculation by assuming equal weighting. For large glazing areas, the view factor between an occupant and glazing can approach 50%. Thus, a cold window, say  $10^\circ\text{C}$ , could lower the temperature sensed temperature by at least 3 to  $4^\circ\text{C}$ , requiring a higher air temperature to compensate. However, even with this compensation, asymmetric radiation can cause discomfort (ASHRAE, 2004b). Similarly, hot or cold floors and

ceilings can lead to discomfort. This fact plays a role in radiant floor heating systems and floors in direct gain zones, which should not exceed 29°C.

Problems associated with large windows can be mitigated with the use of blinds, glazing with a low U-value, or, as a last resort, smaller glazing areas. However, these design choices can lead to higher energy use. One fundamental trade-off in passive solar houses is that between thermal comfort and energy performance. If occupants can tolerate a greater temperature swing, more solar gains can be stored for later release. Energy savings of 10% or more can be achieved by broadening the thermostat's deadband by a few degrees (O'Brien et al., 2008a). The corresponding optimal glazing area also increases. Nicol and Humphreys (2002) report that Europe could save as much as 18% of cooling energy through more flexible thermal controls.

Determining the operative temperature if the air and indoor surface temperatures are known is relatively straightforward, though dependent on an assumption about the location of the occupant(s). A reasonable assumption is to assume the occupant is in the center of the room, though a conservative assumption would be to place them adjacent to the glazing. One commonly used metric for thermal comfort is the predicted mean vote (PMV), which is a -3 (cold) to +3 (hot) scale, in which 0 is neutral (ASHRAE, 2004b). Several simulation programs have the ability to report PMV in the post-processing stage, but cannot control conditions based on it (ESRU, 2007; EnergyPlus, 2009a).

### 2.2.11 Energy Modelling of Passive Solar Houses

While in the past, the energy use of buildings has been estimated using simplified methods such as the bin method, the characterization of passive solar buildings should be performed using dynamic simulations. A literature review of the dynamic modelling of passive solar houses reveals a history of at least 40 years. Modelling can be categorized as using either response function methods or numerical methods (Athienitis, 1985; Clarke, 2001). While being both capable of dynamic modelling, response function methods are mathematically elegant though somewhat less flexible. Response function methods allow the flux and temperature resulting from an excitation to be studied, as shown in Figure 2-13.

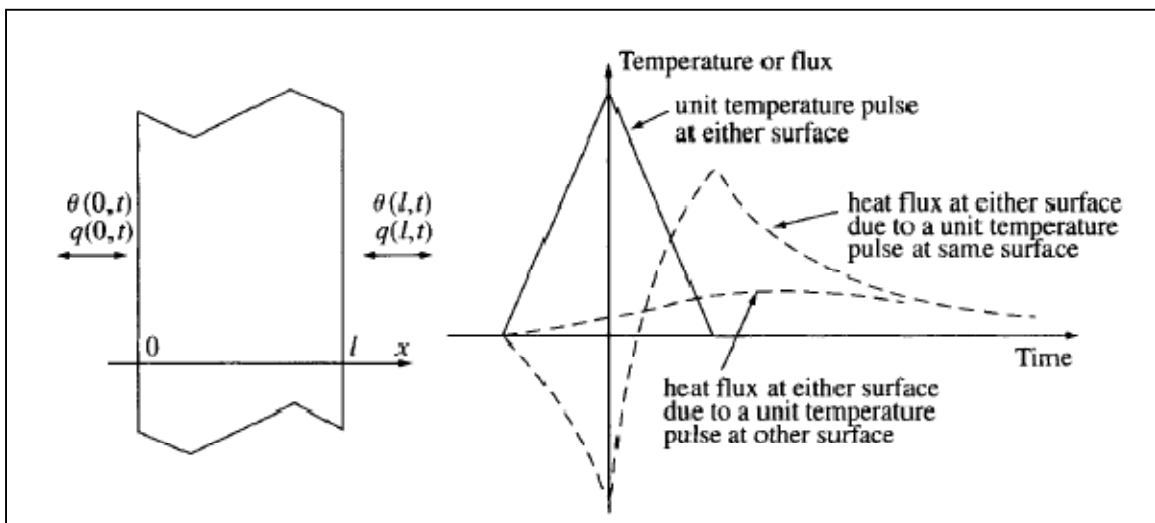


Figure 2-13: A simple example of how a one-dimensional wall responds to an a pulse temperature, based on the response function method (Clarke, 2001)

While a simple wall is shown, the response function method can be extended to more complex systems such as single or multi-zoned buildings, using network theory (Athienitis, 1985). The Fourier heat transfer Equation (2-5) can be solved in both the

time-domain and the frequency domain. Athienitis and Santamouris (2002) showed some valuable results by examining the response of a direct gain zone using the frequency domain. They define two transfer functions that are particularly useful: transfer admittance and self admittance. Transfer admittance ( $Y_t$ ), with units W/K, relates the heat source at a surface of a wall to the temperature at the other surface and is defined as:

$$Y_t = \frac{Q_{inside}}{T_{outside}} \quad (2-2)$$

Where  $Q$  is the heat added at the surface and  $T$  is surface temperature, as indicated by Figure 2-14. Self-admittance ( $Y_s$ ), also with units W/K, relates the heat source at a surface (e.g., massive floor) to its temperature. Thus, a high self admittance value would indicate that a lot of energy is required to increase the surface's temperature. It is defined as:

$$Y_s = \frac{Q_{inside}}{T_{inside}} \quad (2-3)$$

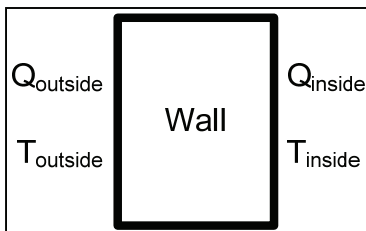


Figure 2-14: A simple wall showing temperatures and heat added

For an externally insulated massive wall, self admittance is given by:



$$Y_{S_{n,i}} = A \frac{u + k\gamma_n \tanh(\gamma_n L_i)}{\frac{u}{k\gamma_n} \tanh(\gamma_n L_i) + 1} \quad (2-4)$$

Where  $A$  is the surface area,  $u$  is the conductance of the insulation,  $k$  is the conductivity of the thermal mass material,  $\gamma_n$  is  $(j\omega/\alpha)^{1/2}$ ,  $L_i$  is the thickness of the mass,  $\alpha$  is the thermal diffusivity, which is equal to  $k/c\rho$ .

Using these concepts, Athienitis and Santamouris (2002) were able to find the optimal level of thermal mass (in terms of the ability to reduce the air temperature swing) – 20 cm in this case. This result is repeated in Figure 2-15. For the example, the following numerical values are used:

- $\omega$  is  $2\pi/\text{day}$ ,
- $u$  is  $0.4 \text{ W/m}^2\text{K}$ ,
- $c$  is  $800 \text{ J/kgK}$ ,
- $k$  is  $1.7 \text{ W/mK}$ , and;
- $\rho$  is  $2200 \text{ kg/m}^3$

In particular, the frequency of one cycle per day is very significant, as this is the main frequency representing solar gains. Higher frequencies can be used for effects such as scheduled temperature setpoints.

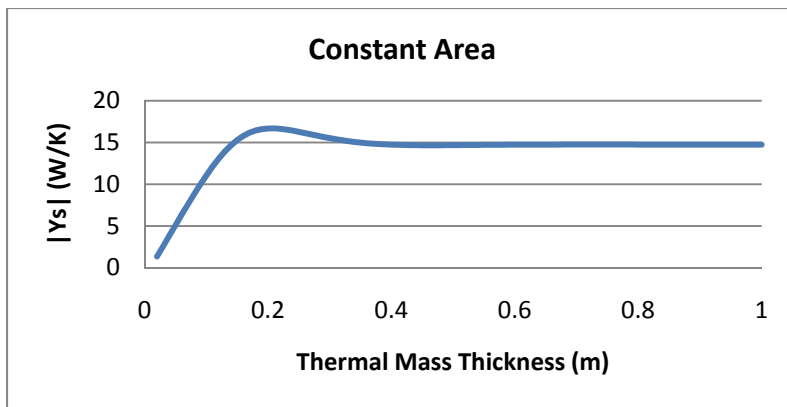


Figure 2-15: The magnitude of self admittance for different thicknesses of thermal mass

A second analysis was performed to examine the magnitude of self admittance for a constant volume ( $1 \text{ m}^3$ ). The results are shown in Figure 2-16. In this way, the effectiveness of having a very compact form of thermal mass can be compared to having one with a large surface area. The results show that beyond about 20 cm, the effectiveness of thermal mass, in terms of preventing large temperature swings, rapidly decreases. Thus, merely building a large volume of concrete into a house is not effective at reducing temperature swings unless it is somewhat distributed. The distribution allows a greater amount of solar energy collection and improved heat transfer to the air. The other conclusion that can be drawn from this analysis is that self-admittance is a good metric to quantify the effective level of thermal mass in a house. Self-admittance provides a means to quantitatively compare different thermal mass configurations.

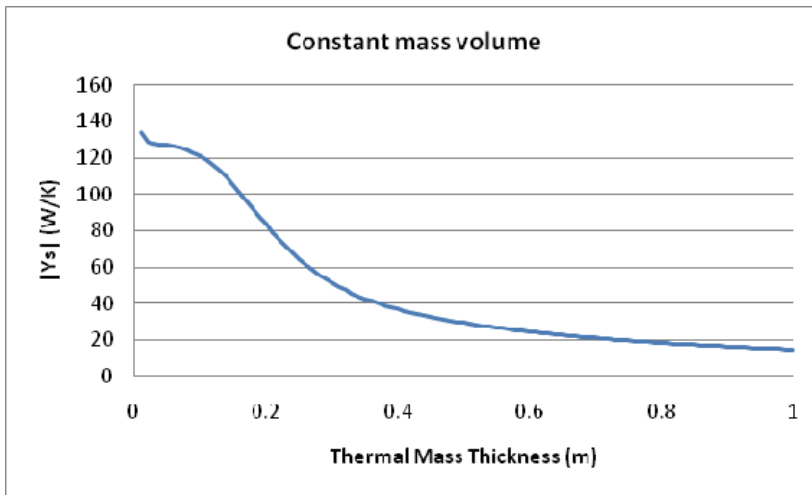


Figure 2-16: The magnitude of self admittance for different thicknesses of thermal mass. The volume of the mass is kept at  $1\text{m}^3$ . Thus, the area is  $1\text{m}^3$  divided by the thickness.

The phase angle of the self admittance corresponds to the time lag between the solar gains and peak surface temperature. For a frequency of one cycle per day, a phase angle of 30 degrees represents a two-hour lag.

Akander (2000) studied extensively on an optimized resistance-capacitance (ORC) method, which is similar to that presented by Athienitis (1985). Among the useful results, he demonstrated how the ORC method could be used to find the dynamic thermal resistance of a wall to minimize conduction through it. This is in contrast to simple R-values which does not properly characterize behaviour of a wall under dynamic boundary conditions.

It is interesting to note that response function methods do not require the discretization of thermal mass (Athienitis and Santamouris, 2002). This is in contrast to numerical methods (e.g., finite difference method), in which accuracy is positively related to the number control volumes. The response function method is limited to the modelling of

systems in which the components do not strongly interact (Clarke, 2001). It is based on the superposition principle, in which responses are summed and it usually assumes linearity (Athienitis, 1985).

Numerical techniques lend themselves to being applied to a wide variety of domains, such as HVAC, heat transfer, and renewable energy systems. Clarke (2001), who can be considered the founder of ESP-r, has extensively written on the development and application of the Equations it uses. The lumped parameter finite difference method is a commonly used method, within the numerical methods category. The basis for numerical methods is the approximation of a future state based on the present state at two or more discrete points. Figure 2-17 shows the approximation of the derivative of function  $f(\gamma)$  using the secant of any two of the three points, including  $f(\gamma-\delta\gamma)$ ,  $f(\gamma)$ ,  $f(\gamma+\delta\gamma)$ . For this application,  $\gamma$  could either measure time or space.  $f(\gamma)$  represents a state variable such as temperature or enthalpy.

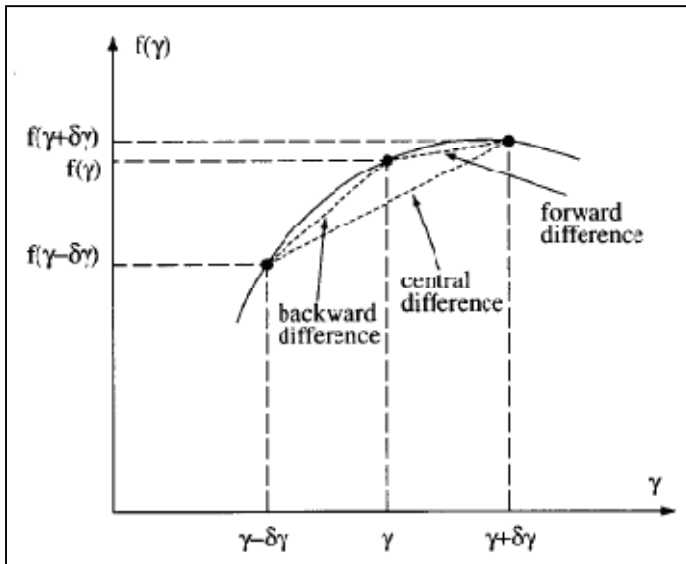


Figure 2-17: Numerical solution to some function  $f(\gamma)$  (Clarke, 2001)

The starting point for formulating the Equations used for the finite difference method is the Fourier heat Equation, which for a single dimension, is given by:

$$\frac{\partial^2 T(x,t)}{\partial x^2} = \frac{1}{\alpha} \frac{\partial T(x,t)}{\partial t} - \frac{q}{k} \quad (2-5)$$

Where  $T$  is the temperature of the substance at position  $x$  and time  $t$ ,  $\alpha$  is the thermal diffusivity, which is equal to  $k/c\rho$ , and  $q$  is the heat flux direction that the Equation pertains to.  $k$  is the thermal conductivity of the (homogeneous) substance,  $c$  is its specific heat capacity, and  $\rho$  is its mass density.

Since a numerical solution to the Fourier heat Equation is desired, the differential terms must be converted to finite differences. The second order derivative can be replaced with a truncated Taylor series (the central difference) and the first order derivative is replaced with the forward difference approximation, as indicated by Figure 2-17. The resulting Equation is given by:

$$\frac{T(i+1,t) - 2T(i,t) + T(i-1,t)}{(\delta x)^2} = \frac{1}{\alpha} \frac{T(i,t + \delta t) - T(i,t)}{\delta t} - \frac{q(i,t)}{k} \quad (2-6)$$

Where  $i$  is the node of interest,  $\delta x$  is the distance between adjacent nodes, and  $\delta t$  is the time between timesteps. Upon rearrangement, the fundamental Equation of the finite difference method is the energy balance at the node of interest  $i$ , and is given as

(Athienitis and Santamouris, 2002):

$$C_i \frac{dT_i}{dt} \approx C_i \frac{T_i^{p+1} - T_i^p}{\delta t} = Q_i + \sum_j U_{ij} (T_j - T_i) \quad (2-7)$$

Where  $C$  is the thermal capacity represented by the node,  $T_i$  is the temperature of node  $i$ ,  $Q$  is the equivalent heat generated at node  $i$ ,  $U$  is the thermal conductance between nodes  $i$  and  $j$  and  $T_j$  is the temperature of an adjacent node. Each node is used to represent the temperature of a control volume with homogeneous properties. Thus, the control volume is assumed to be isothermal. In layman terms, a node is affected by a weighted average of the temperatures in the surrounding zones and the heat injected or removed from that node. The node's rate of response to the conditions is dependent on its thermal capacity. A higher thermal capacity will cause it to react more slowly.

The results shown in Equation 2-6 are for the explicit finite difference, in which the next timestep's state is determined by the current state. While being simple to apply and good for controls, the method imposes limits on the discretization of both time and space. To ensure stability, a stability criterion must be obeyed, in which:

$$\frac{2k\delta t}{\rho C(\delta x)^2} \leq 1 \quad (2-8)$$

This condition effectively imposes limits on the maximum timestep length and distance between adjacent nodes. If it is violated, the explicit finite difference formula would indicate that heat is transferred from the colder node to the hotter node.

In contrast, the implicit finite difference method, in which a node's future temperature is determined by its current temperature and the future temperatures of the adjacent nodes, does not have such limits (Clarke, 2001). For the implicit formulation, the second order term of the Fourier heat Equation is replaced by the central difference Equation, but for the future (unknown) temperatures, while the first order term is based on the backwards difference Equation, as before. The result is:

$$\frac{T(i+1,t+\delta t) - 2T(i,t+\delta t) + T(i-1,t+\delta t)}{(\delta x)^2} = \frac{1}{\alpha} \frac{T(i,t+\delta t) - T(i,t)}{\delta t} - \frac{q(i,t+\delta t)}{k} \quad (2-9)$$

Rearranging this to group all future temperature terms at node  $i$ , yields the following Equation.

$$\left(1 + \frac{2k\delta t}{\rho C(\delta x)^2}\right) T(i,t+\delta t) = T(i,t) + \frac{2k\delta t}{\rho C(\delta x)^2} [T(i+1,t+\delta t) + T(i-1,t+\delta t)] + \frac{q(i,t+\delta t)\delta t}{\rho C} \quad (2-10)$$

The implicit finite difference is unconditionally stable, but attention should be given to maintaining reasonable accuracy. For example, when applied a to wall, the method

should not use timesteps of longer than 1 hour. Unlike the explicit method, the implicit method requires that the temperature of all nodal Equations be solved simultaneously. EnergyPlus – the primary simulation engine used in the current research – uses the implicit finite difference method.

In EnergyPlus, to determine each zone’s air temperature, an energy balance is performed on each zone’s air node at each time step and the amount of heat required to be added or removed to maintain the zone air temperature between the specified range is calculated (EnergyPlus, 2009b). Since an ideal system (with infinite capacity) was used, this amount of heat added or subtracted from each zone air node. Once this amount of heat is calculated, the current zone air temperature is calculated using Equation 2-11, in which the zone air energy balance is solved for the current temperature  $T_Z^t$  and the transient term (resulting from the thermal capacity of the air and non-surface zone contents) is approximated by a third-order Taylor series expansion of the Euler formula. The justification for this approach, and particularly the fact that the third order approximation is used, is thoroughly explored by Taylor et al. (1990).

$$T_Z^t = \frac{\sum_{i=1}^{N_{sl}} \dot{Q}_i + \sum_{i=1}^{N_{surfaces}} h_i A_i T_{si} + \sum_{i=1}^{N_{zones}} \dot{m}_i c_p T_{zi} + \dot{m}_{inf} c_p T_{\infty} + \dot{m}_{sys} c_p T_{supply} - A}{\left(\frac{11}{6}\right) \frac{C_z}{\delta t} \sum_{i=1}^{N_{surfaces}} h_i A_i + \sum_{i=1}^{N_{zones}} \dot{m}_i c_p + \dot{m}_{inf} c_p + \dot{m}_{sys} c_p} \quad (2-11)$$

$$A = \left(\frac{C_z}{\delta t}\right) \left(-3T_z^{t-\delta t} + \frac{3}{2}T_z^{t-2\delta t} - \frac{1}{3}T_z^{t-3\delta t}\right) \quad (2-12)$$



In Equation 2-10, all terms that contribute to the zone air energy balance are on the right side, including heat sources, heat exchange with the surfaces that enclose the zone, air exchange with other zones, air exchange with the outside (i.e., infiltration), and input from the HVAC. Furthermore, the right side contains the effect of the zone air energy storage from the previous three timesteps (Equation 2-12).

Another approach is to hybridize the implicit and explicit formulations. ESP-r uses the Crank-Nicholson formulation, which provides the benefits of both methods (Clarke, 2001). Essentially, the method bases the future temperature on a weighted average of that found by both methods. This provides a compromise between accuracy and computational efficiency. Furthermore, so long as the weighting is at least 50% implicit, the solution is unconditionally stable (Clarke, 2001). ESP-r uses a 50% weighting. It should be noted that while hourly timesteps do yield an unconditionally stable solution, it can oscillate.

For each node, in a uni-dimensional array of nodes in a solid surface, the following Crank-Nicholson Equation must be established.

$$\begin{aligned}
(1 + WF)T(i, t + \delta t) &= WF[T(i + 1, t + \delta t) + T(i - 1, t + \delta t)] \\
&+ [1 - 2F(1 - W)]T(i, t) + (1 - W)F[T(i + 1, t) + T(i - 1, t)] \\
&+ \frac{\delta t}{\rho C} [Wq(i, t + \delta t) + (1 - W)q(i, t)]
\end{aligned} \tag{2-13}$$

Where  $F$  is the Fourier number, defined as  $\alpha \delta t / (\delta x)^2$ , and  $W$  is the weighting between explicit and implicit. The resulting system of Equations can be rewritten in the form of arrays as:

$$\mathbf{M}_A \mathbf{T}(t + \delta t) = \mathbf{M}_B \mathbf{T}(t) + \mathbf{M}_C = \mathbf{M}_Z \tag{2-14}$$

Where  $\mathbf{M}_A$  is a matrix that stores the coefficients for the future timestep temperatures,  $\mathbf{M}_B$  is a matrix that stores the coefficients for the present timestep temperatures, and  $\mathbf{T}$  and  $\mathbf{M}_C$  are vectors.  $\mathbf{M}_A$  and  $\mathbf{M}_B$  (for this case) are of  $n$ -by- $n$ , where  $n$  is the number of nodes.  $\mathbf{M}_Z$  is an intermediate vector that stores the known information about the present timestep.

ESP-r uses Gaussian elimination to solve the system of Equations that are established at each timestep. The nodes involved in a simple rectangular zone are shown in Figure 2-18. It is important to note that nodes within each wall only see adjacent nodes, while interior surface nodes see all other interior nodes. This is reflected in the matrix representation (Figure 2-19), which shows that there are many off-diagonal terms.

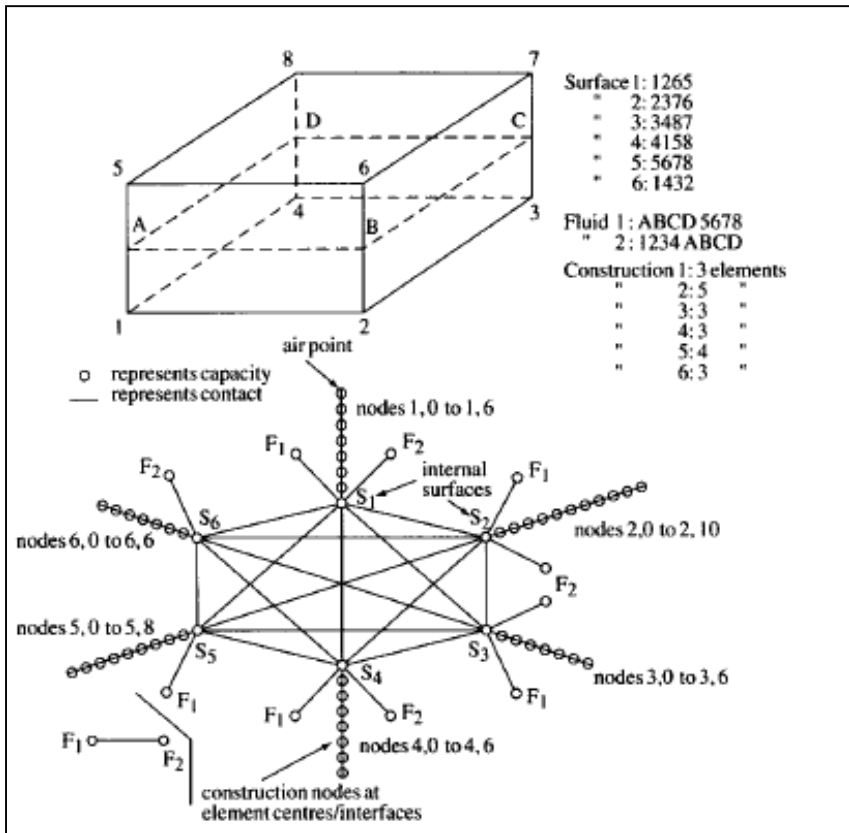


Figure 2-18: Nodal layout for a rectangular zone with multilayered walls (Clarke, 2001)

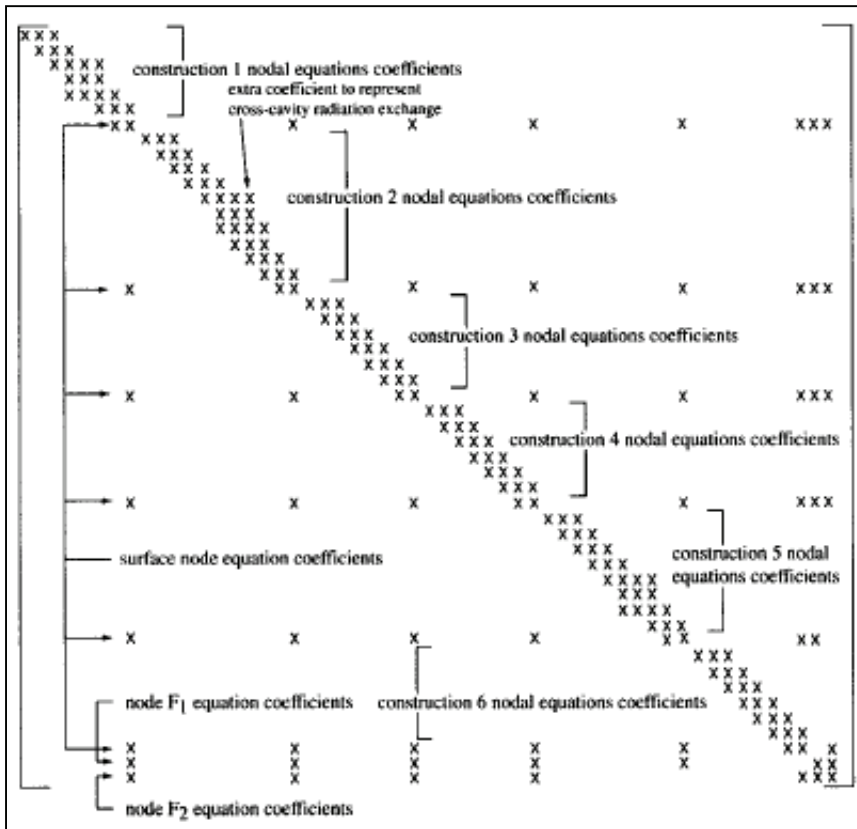


Figure 2-19: The matrix (A or B) that corresponds to the single zone model (Clarke, 2001)

As mentioned, one of the advantages to the finite difference method is that it can

handle nonlinear phenomena. However, the formulation described above would

suggest otherwise. In ESP-r, the modelling of simple zones with typical materials may

use the same coefficient matrices for subsequent timesteps. However, when system

properties (e.g., heat transfer coefficients, thermal capacity, and conductivity) change,

the coefficient matrices must reflect this. Two solutions present themselves:

1. Use present properties for the next timestep. This is the so-called “one timestep in arrears” principle, as stated by Clarke (2001). He states that there are few practical applications where this method fails.

- An iterative approach can be used, in which the arrays are updated until a reasonably good match is achieved.

### 2.2.11.1 Space and Time Discretization

Multiple nodes may represent a single material, such as a wall. As mentioned, a greater number of nodes yields higher accuracy. For instance, Figure 2-20 shows a comparison of temperature profiles for a massive wall represented by both 3 and 15 nodes. Clarke (2001), states that using fewer nodes is adequate for most wall constructions.

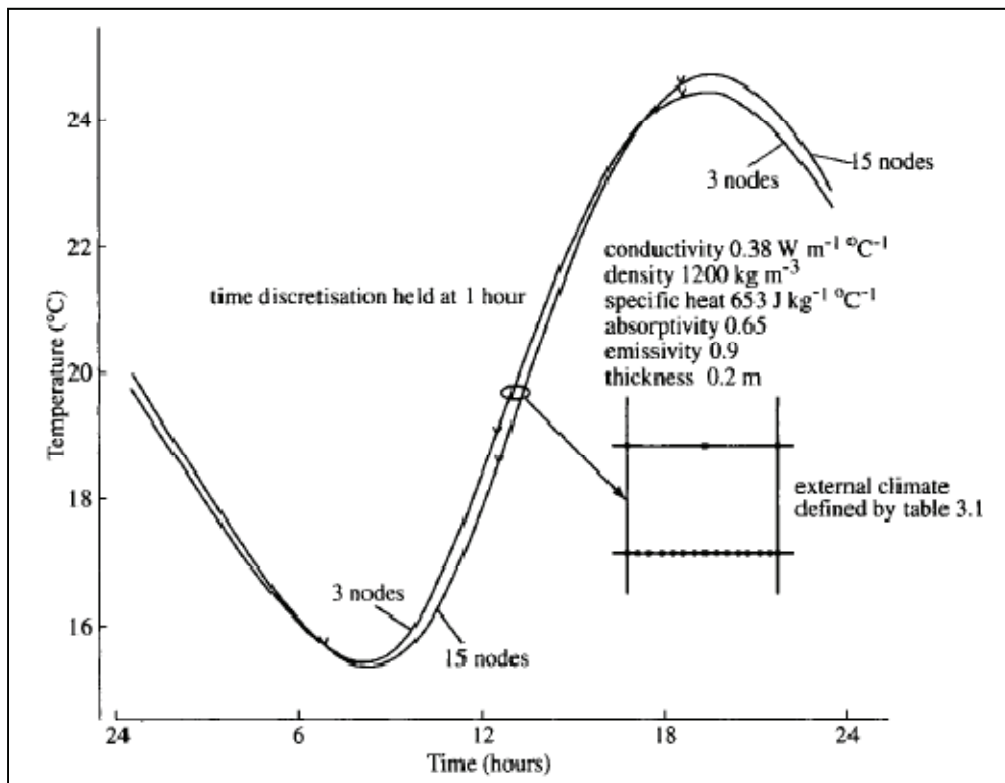


Figure 2-20: The response of a wall surface based on a 3 and 15 node model (Clarke, 2001)

Thermally massive walls or other substances should be assessed to determine the appropriate level of discretization, as a compromise between accuracy and simulation time. O'Brien (2008) simulated a three-zone passive solar house in ESP-r by representing

a 20-cm concrete floor with both one and four control volumes. The results showed that the annual energy use of the house was about 4% higher for the more finely-discretized slab, thus indicating the importance of examining this issue. Even if further discretization of a wall does not yield significantly better accuracy, additional nodes can be placed at locations of interest, such as the interface between two adjacent layers with different thermophysical properties.

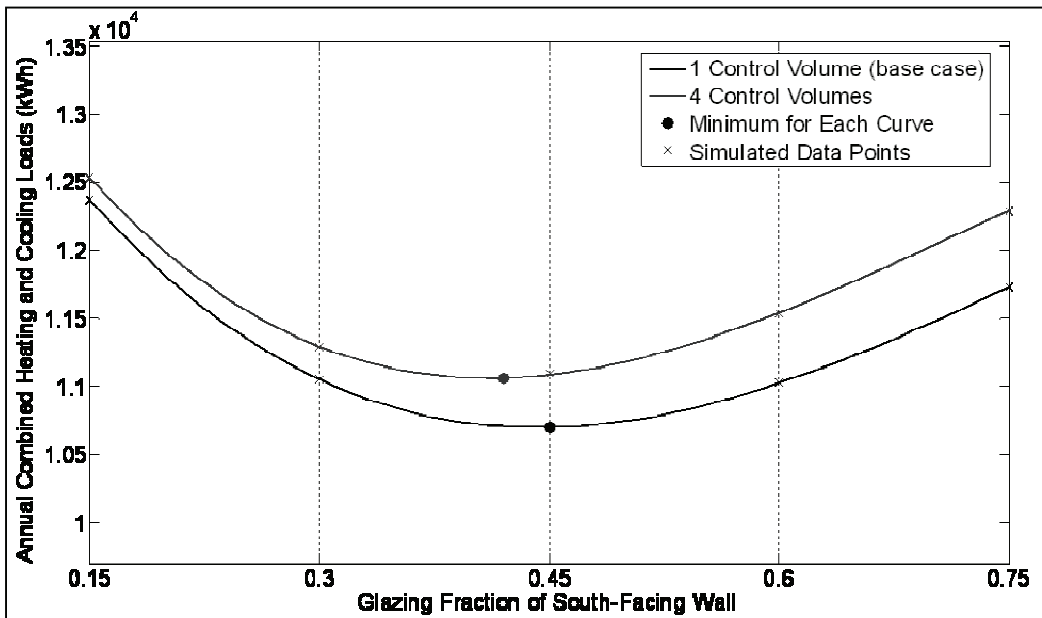


Figure 2-21: Discretization of thermal mass (top curve is 4 control volumes)

When studying the energy use of a building, walls are normally discretized in one dimension (the thickness direction) because they are usually much thinner than they are wide or tall. Thus, that is the predominant direction of flux (and hence temperature gradient). Furthermore, walls are typically layered in this direction. While, the layers

may not be homogeneous (e.g., there may be intermittent framing members), this can be usually accounted for using an equivalent conductance.

Similarly to space discretization, there is a trade-off between computational efficiency and model accuracy. As shown in Figure 2-22, longer timesteps can lead to greater predicted temperature swings. Furthermore, any lagged (i.e., “ping-pong”) solutions increase significantly in accuracy if shorter timesteps are used since current quantities are solved using past quantities. Clarke (2001) states that no universal rules exist regarding the relationship between model accuracy and timestep duration. Thus, the use of parametric analysis to select the appropriate compromise between accuracy and computational time is beneficial.

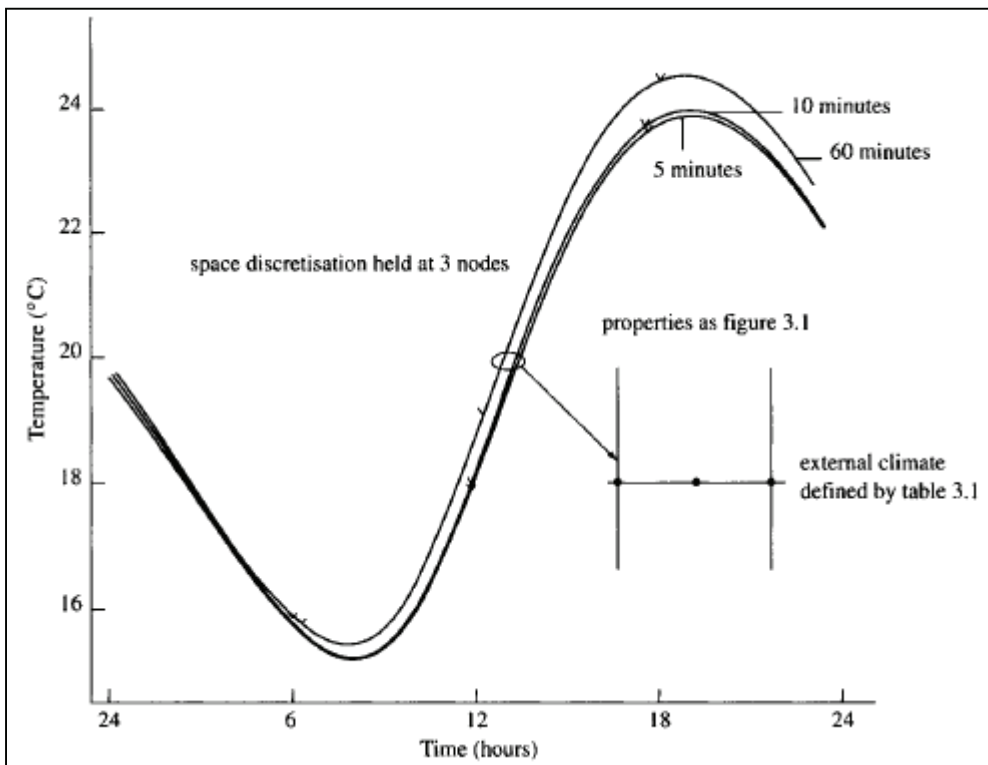


Figure 2-22: The response of a wall surface based on a 3 and 15 node model (Clarke, 2001)

### **2.2.12 Design and Simulation of Passive Solar Homes**

Rules of thumb for designing passive solar homes are expected to become decreasingly significant with the advancement of design tools as the product of this thesis will exemplify. Guidelines, such as those provided by CMHC (1998), are generalized and based on numerous assumptions – many of which are not stated. For instance, it is suggested that 40 m<sup>2</sup> of mass is required per additional square meter of south-facing glazing above 7%. Even more advanced design techniques such as the graphical method shown by Sander and Barakat (1985) omit many details and are based on a set of assumptions (e.g., temperature controls). It has been shown that, seemingly, minor assumptions such as those about ground reflectance, thermal zoning, and internal gains, can have an enormous effect on both predicted energy performance and optimal design (Lomas et al., 1992; Purdy and Beausoleil-Morrison, 2001; O'Brien et al., 2008a). An example of this is shown in Figure 2-23. The very nature of passive solar heating is based on thermal storage and the cyclical nature of solar gains. Therefore, it is concluded that proper modelling techniques consisting of transient simulations be used to assess performance and assist the design process.



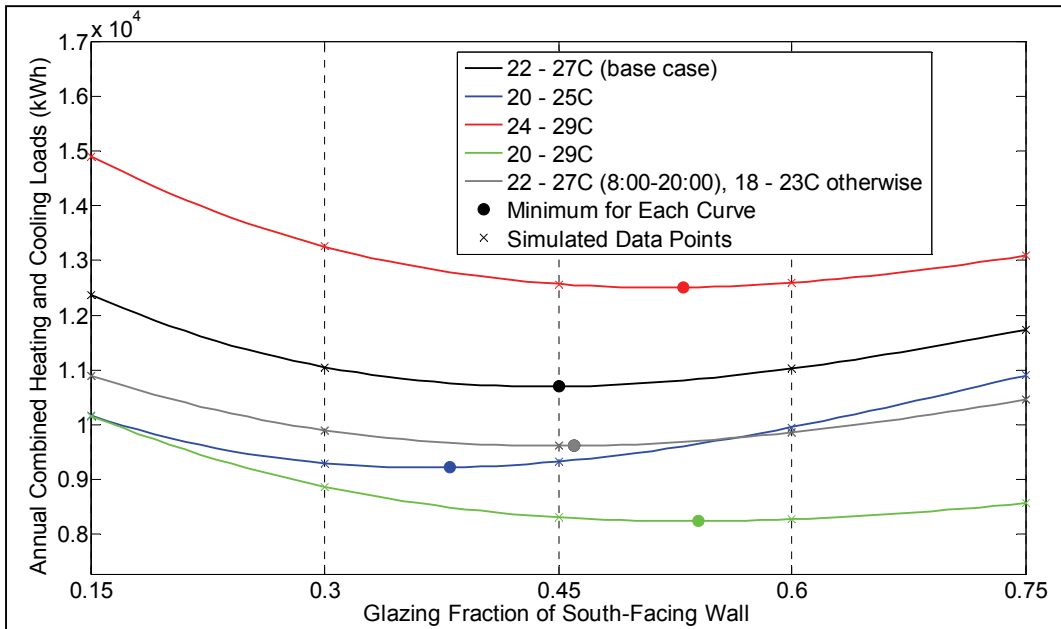


Figure 2-23: The energy performance of a house depending on temperature setpoints and the window to wall ratio (O'Brien et al., 2008a)

EnergyPlus-specific modelling details are provided in Chapter 3, where the model is described in great detail.

### 2.2.12.1 Thermal Bridging

Thermal bridging is a significant source of heat loss from the envelope and can affect energy use by about 5% (Déqué et al., 2001; Purdy and Beausoleil-Morrison, 2001). In typical Canadian houses, thermal bridging occurs through framing (e.g., corners and joints), door and window frames, window spacers, foundations, and any other high-conductivity material that connects regions of significantly different temperature (Hutcheon and Handegord, 1995).

For most energy modelling of houses, multi-dimensional conduction calculations is likely unnecessary. Most whole-building simulation tools use one-dimensional conduction,

since walls tend to be large relative to their thickness and they are uniform in the thickness direction. However, tools such as THERM allow heat transfer modelling on the component level, using the finite element method (FEM) (Huizenga et al., 1999). The results of such a tool can then be used to create a material with equivalent conduction, much the way ASHRAE (2001) recommends for finding the conduction through a wall. HOT3000 models thermal bridging from wall framing by using the equivalent conductance (Purdy and Beausoleil-Morrison, 2001).

#### **2.2.12.2 Window Size and Geometry Assumptions**

At the conceptual design stage of solar houses, the designer should choose the glazing type and window frame type, but they should not be concerned about exact layout and window sizing. WINDOW 5, a widely-used program for determining thermal and optical properties of windows, provides values for: center of glass, edge of glass, and framing conductivities (Mitchell et al., 2003).

In general, large windows have a greater glazing to frame ratio and should be used, from an energy standpoint. However, distributed windows give more flexibility in daylighting and help distribute beam radiation across any thermal mass that is present.

As mentioned, the size of windows plays a role in the thermal conductivity and heat loss of the envelope. Another important consideration is regarding the solar radiation transmittance. Often, during conceptual design, windows are lumped such that each zone has, at most, one window per zone and orientation. Essentially, this allows the

modeler to characterize the effect of solar gains and conduction. However, it ignores the fact that the position of incident solar radiation on the interior surfaces plays a role in performance. The explicit modelling of windows has been found to have little significance (0.2%, in this case) on energy performance (Purdy and Beausoleil-Morrison, 2001). Although, it should be noted that the large size of windows in passive solar homes would inflate the effect.

Many tools have multiple possible methods for determining the distribution of incoming short-wave radiation on interior surfaces (ESRU, 2007; EnergyPlus, 2009a). Among the simplest is to distribute it among all interior surfaces with an area weighting. This method is computationally fast, but neglects solar geometry and the fact that certain surfaces receive less (or no) direct solar radiation. A second method computes exactly where direct solar radiation is incident on interior surfaces. Though, for one-dimensional models the exact location of incident solar radiation on a surface has no impact, since each surface is represented by a single node. Athienitis and Chen (2000) used a detailed custom model with a discretized floor to examine such variations in the floor. The study was based on radiant floor heating, but the conclusions are expected to be similar for forced air heating. They found that the temperature range, at a given time, could reach 8°C, though thicker floors (they used 5 and 10 cm of concrete) would reduce this effect since conductivity between regions would increase. Despite the results, they stated that treating the floor as a single node (and temperature) was adequate for energy modelling purposes – the principal interest for this work. This result

can be extended to conclude that the exact position of windows is not critical for energy performance predictions. For design, windows and thermal mass should be positioned in relative positions to maximize the fraction of direct beam radiation that hits thermal mass. This discussion leads to the modelling of thermal mass.

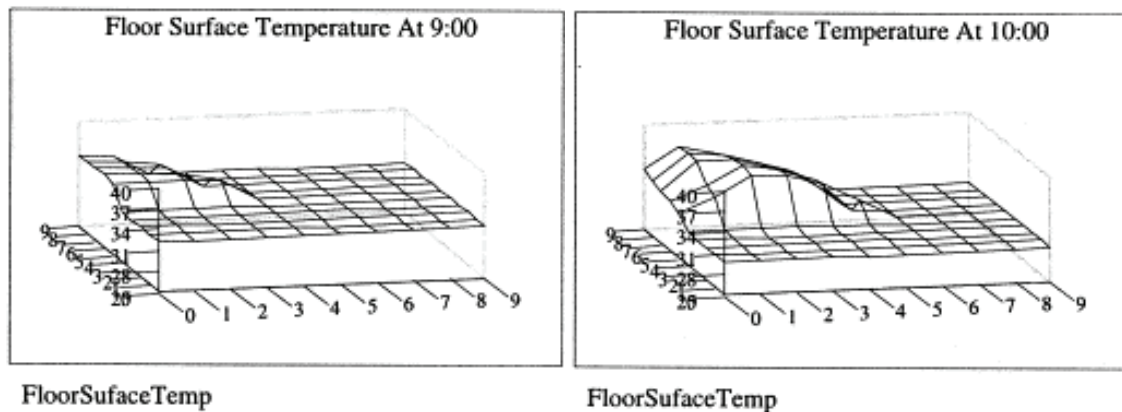


Figure 2-24: Results from the study, showing variation in floor surface temperature (Athienitis and Chen, 2000). It is clear that the warmest part of the floor follows the path of the beam radiation (with some lag).

### 2.2.12.3 Thermal Mass

As mentioned, thermal mass is important to thermal behaviour of passive solar houses because it reduces temperature swings and increases the lag between solar gains and the increase in indoor air temperature. While thermal mass is most easily modelled as a massive slab or wall, other considerations and complexities arise. First of all, significant mass can be found in furnishings (e.g., furniture, books, and aquariums) that may not be foreseen during design. Antonopoulos (2000) found the effect of furnishings in a house caused the time constant to increase by about 25%. (Purdy and Beausoleil-Morrison, 2001) found that the explicit modelling of internal walls affected heating loads by only 1.1%. However, the effect in a passive solar house would likely be up to several times

this. In many tools, non building-integrated thermal mass is modelled as a partition wall (which could float in the middle of the room) and for which nearly any thermophysical properties can be assigned. However, it should be noted that in order to be an accurate representation, the lumped mass should not only have the same heat capacity, but should also have similar heat transfer characteristics (to the surrounding air). A method for simplifying the mass of furnishings and partition walls is to use an “air capacity multiplier”. This implicitly models mass by increasing the thermal capacity of the air contained in a zone by some factor. Charron (2007) reports that values of 10 to 30 are suitable for houses.

The possibility of shading or insulation of thermal mass is a significant problem.

(Athienitis and Chen, 2000) showed that if thermal mass is completely covered by carpeting, energy use on a cold sunny day increased by about 50%. While carpeting can easily be modelled, the shading effect of furniture is significantly more complex.

Fortunately, the same study showed that a carpet that covered 20% of the floor surface increased energy use by only 6%. These results could be extended to conclude that moderate levels of furniture have a tolerable impact on performance.

Most simulation engines have some means for modelling the non-linearity of PCMs (Zhang et al., 2008; EnergyPlus, 2009b). In fact, the motivation for EnergyPlus developers to implement the finite difference model was for the sake of modelling PCMs.

#### **2.2.12.4 Zoning/Airflow**

Generally speaking, for modelling purposes, a thermal zone should be attributed to each part of a building that has a significantly unique set of boundary conditions and/or operating conditions. Increasing the number of zones would appear, at first, to be wise. However, it comes at two costs. First, it increases simulation time (Clarke, 2001). Second, it requires knowledge about the interaction between zones (particularly) regarding airflow, since thermal zones are rarely completely isolated (closed doors and void of openings).

For passive solar houses with basements, there are three main zones that should be modelled: the basement, a north zone, and a south zone (O'Brien et al., 2011a). The basement zone has significantly different boundary conditions than the other zones (namely, soil instead of air) and it may be operated at cooler temperatures. While one could model the above grade zones as one, this assumes that the air is completely mixed. In reality, the direct gain (normally south-facing) zone can get at least several degrees warmer than the other zones. O'Brien et al (2010b) showed that a single zone model resulted in as much as 20% less heating and cooling energy use than a four-zone model. Purdy and Beausoleil-Morrison's (2001) conclusions also reflect these results. However, their current HOT3000/ESP-r model uses a single zone for the above-grade living area. De Meulenaer et al (2005) disagreed with the practice of subdividing a house into zones, citing that multi-zone models take longer to create and zones rarely vary in

temperature by more than several degrees. However, the last point depends on the glazing area and thermal mass, in particular.

The house of interest almost certainly has partition walls that compartmentalize it. However, as mentioned, assigning a zone to each room merely increases computational efforts without improving the accuracy of the model. A remaining question is: how much airflow occurs between zones? This is obviously dependent on room layout, furnishings, the size and position of openings (e.g., doors), and the mechanical equipment. Only the behaviour of the mechanical equipment can be predicted to any accuracy during conceptual design before room layouts are established.

#### **2.2.12.5 External Obstructions**

As mentioned, the net energy gain from windows, unless they are high-performance, can be marginal. Therefore, external solar obstructions such as trees or buildings can have a significant influence on energy performance. Ideally, any intentional shading should be accomplished with building-integrated features, such they can be controlled. However, it is inevitable – particularly in an urban or forested environment – that solar obstructions, many of which cannot be controlled and may be dynamic, will be present. Though detailed models for shading patterns exist, the input of geometry can be complex; particularly if it changes on a seasonal basis (O'Brien et al., 2009b). Somewhat surprisingly, studies examining the effect of a nearby neighbouring building (on the order of 5 meters away) found annual energy use increases on the order of 5 to 7% (Purdy and Beausoleil-Morrison, 2001; O'Brien et al., 2008a). Though, the latter study

found that complete shading of a large window resulted in 50% greater annual energy use. These results suggest that some ability to model external solar obstructions would be beneficial, though it could be coarse (e.g., blocks) and require some judgment.

Often, glazing is modelled as being flush with walls. This slightly overestimates solar gains, since glazing is usually set back by several inches from the frame. ESP-r and EnergyPlus, among others, have the ability to model this characteristic, though such details are probably best specified later in design when specific products are selected. It should be noted that the explicit geometrical modelling of each window is required if the setback is considered, since square windows are less affected than oblong ones. From a design perspective, glazing should be positioned towards the outer wall surface. This is particularly important for super-insulated houses, which can have walls that are 30 cm or more in thickness.

#### **2.2.12.6 Infiltration**

As previously mentioned, infiltration can be the cause of on the order of 20% of total heat loss. One common modelling technique is to assume a constant rate of air exchange with the outdoors, though more detailed models exist such as AIM-2 (Alberta Infiltration Model - 2) (Wang et al., 2009). Purdy and Beausoleil-Morrison (2001) found that the difference in energy use between a constant infiltration rate and a the AIM-2 model was about 7%. The AIM-2 model, which has been used to model 350,000 houses via HOT2000 (the predecessor to HOT3000), was recently shown to underestimate infiltration rates by an average of 5%, based on the measurement of 16 different houses



(Wang et al., 2009). The AIM-2 model considers both wind effects and stack effects. Infiltration from wind occurs because the windward side of the house has higher pressure than the interior of downwind sides of the house. Thus, airflow occurs through any openings in the envelope to allow the pressure to equalize. The stack effect, though less significant in shorter buildings is caused by the fact that warmer interior air rises within the house and causes pressure differentials at both the top and bottom of the house (Hutcheon and Handegord, 1995). Inputs to the model are geometry (building height), distribution of openings (e.g., flue, cracks, among the ceiling, floor and walls, wind, and temperatures). The distribution of openings can be defined, through default values are available. Another input relates the surrounding environment and whether the house is sheltered or open. Despite the effort that has been put into accurately modelling infiltration, O'Brien et al (2011b) report that there is significant uncertainty with regards to infiltration rates until a building is built. Furthermore, the benefit of detailed models is relatively insignificant (~5%) over assuming a constant rate of infiltration.

#### **2.2.12.7 Foundation Heat Loss**

Foundation heat losses represent about a quarter of the total and have been poorly characterized in the past (Beausoleil-Morrison et al., 1997). Reflective of this significance, Purdy and Beausoleil-Morrison (2001) showed that the use of a simplified ground contact model resulted in a 10% difference in heating energy compared to the detailed model. Unlike above-grade surface boundary conditions which can be assumed

to be in contact with air of a uniform temperature, foundations that are submerged in soil, in which three-dimensional conduction plays a significant role. The most accurate modelling method is to use a three-dimensional finite difference model that extends in all directions (below grade) until the temperature difference between adjacent elements is negligible. However, such simulations can take an order of magnitude longer than whole-year energy simulations for a house with simpler boundary conditions (Beausoleil-Morrison and Mitalas, 1997). To minimize computational effort at simulation time, Beausoleil-Morrison and Mitalas pre-ran 33,000 simulations for 67 different foundation configurations and used regression techniques to determine the direct foundation boundary temperatures. The temperatures are a function of depth, area, configuration, and climate, among other things. The regression Equation was validated with an average error of about 4%. This is considered an acceptable trade-off. The resulting model is called BASESIMP and is currently used by HOT3000.

#### **2.2.12.8 Daylighting**

As mentioned, from a strictly energy standpoint, daylighting in houses has the potential to, lead to a reduction of, at most, several percent (assuming typical use profiles of being vacant during the day). Nevertheless, it tends to receive unprecedented attention because of the side psychological and aesthetic benefits. Reporting specific energy savings is likely premature for a house in which neither the electric lights nor the automatic controls (if any) have been defined. However, daylight autonomy provides a good sense of daylighting performance. It is defined as the fraction of occupied hours

during which daylight levels within the house are equal or greater to the prescribed level (Reinhart et al., 2006).

There is a wide range of daylighting calculation methods from daylight coefficients to radiosity and raytracing. ESP-r has two main methods of daylighting calculations, including a simple daylight coefficient method and the coupling of RADIANCE (an industry-leading illumination engine that uses ray-tracing) (Reinhart et al., 2000). The latter is computationally intensive and should be considered overkill if specific interior finishes and window positions are not defined. However, the former is more reasonable for the conceptual design stage, though assumptions must still be made about window positioning. The daylight coefficient method calculates the relationship between illumination on room surfaces and the illumination on the glazing, such that it is independent from the actual weather conditions. Thus, integrated energy and daylight simulations can be performed in a matter of minutes, rather than hours. EnergyPlus uses the split-flux method for daylight analysis; a method that has been shown to slightly overestimate daylight particularly far from windows, but at the benefit of simplicity (EnergyPlus, 2009b).

### **2.3 Active Solar**

Active solar systems are those that actively circulate an energy-carrying substance (e.g., fluid or electrons) between the site of collection and consumption. The systems are used to supplement some or all of the energy (thermal or electrical) demands of a

building. For this research, only building-integrated, fixed (i.e., not solar tracking) collectors are considered. Building-integrated solar collectors have several advantages over free-standing collectors including not needing a structure to support them, requiring less land, collecting energy close to the site of consumption, and doubling as cladding. The last point means that a roof with an integrated solar collector, can use the collector for weather protection or as an aesthetic finish (Keoleian et al., 2003).

Building-integration often means that building geometry and solar collectors are designed simultaneously. For instance, the ÉcoTerra house's roof was selected to exactly fit the selected photovoltaic modules. This ensured that there were no seams and irregularities. This had the dual purpose of aesthetics and preventing the penetration of water. Interestingly, the roof geometry was not solely designed to optimize solar energy collection, but also to enable geometric compatibility.

Active solar collectors can be divided into three main categories: electrical (PV), thermal (for space heating, DHW heating, cooling, or some combination of the above), and a hybrid of the two: PV/T.

Active solar collectors offer the advantages of design flexibility, efficiency, and do not directly impact thermal comfort (unlike passive solar heating). The energy they collect is usually transformed to a compact and transportable energy form. However, these advantages come at the expense of cost and complexity.

An important issue for active solar systems is the relative value of the energy they collect (assuming it is useful). Generally, electricity can be considered three to four times more valuable than low-temperature (20 - 40°C) fluid. There are two justifications for this ratio: 1) for electricity that is generated primarily by fossil fuel-fed power plants, the ratio of primary energy to electricity generated is about 3-3.5, as previously discussed, and 2) it is the approximate coefficient of performance (COP) for ground source heat pumps. Therefore, the efficiency of a solar collector should be only one of the deciding factors in selecting an active solar system. The useful solar fraction is a much more informative metric because it considers all system loss (e.g., storage, resistive) and the demand.

### **2.3.1 Solar Thermal Collectors**

There are two main categories of solar thermal collectors: flat-plate and evacuated tubes. They both have two elements in common: an absorbing surface to maximize absorbed solar radiation and a thermally-coupled passage for the transport fluid. Flat-plate collectors typically consist of a glazed box with a dark absorber plate that is thermally-bonded to tubes containing the heat transfer fluid (Duffie and Beckman, 2006). The fluid is usually water, a water-glycol mixture, or air. For cold climates, such as Canada's, the glycol mixture is necessary to prevent freezing (GSES, 2005). The underside of flat-plate collectors is often insulated to minimize heat loss.

Air-based flat-plate collectors use air channels instead of tubes to transport heat. Since air has a relatively low heat capacity, significantly higher flow rates are required than if a

liquid is used to transport heat. The advantages to air are that it is non-toxic and small leaks are relatively inconsequential. Also, if the energy is being used for space heating, the warmed air can be directly added to the space. If the heat is to be used for heating DHW, a heat exchanger must be included in the system, reducing the efficiency.

Evacuated tubes are similar to flat-plate collectors, but the absorbing surfaces are contained within tubes that contain a vacuum (typically around  $10^{-5}$  bar or 10 Pa (GSES, 2005)). The vacuum minimizes heat loss by suppressing convection which allows higher temperatures to be maintained. Unlike flat plate collectors, evacuated tubes contain heat pipes which contain a separate working fluid. Through a cycle of evaporation and condensation, the fluid transfers the collected solar energy to the tip of the tube, where it is transferred to another working fluid. Evacuated tubes are typically mounted with spaces between them, meaning that they cannot replace the roofing material, but rather, must be mounted overtop a roofing material (GSES, 2005). The construction of evacuated tube collectors allows them to perform well even in cold climates. However this can lead to overheating, though this problem is being mitigated in modern products (Frei, 2003).

### **2.3.1.1 Active Storage for Active Solar Systems**

Storage media are isolated and often insulated tanks that store thermal energy collected by solar collectors. They act as buffers; allowing energy to be stored and delivered between sunny periods. They are essential if a high solar fraction is to be achieved, since thermal demand and solar availability are often not necessarily

concurrent. In fact, if there is no thermal storage, the solar fraction for solar DHW systems approaches about 18% asymptotically as collector area increases (Duffie and Beckman, 2006). The capacity of thermal storage can range from less than a day's supply of energy to entire seasons' worth, in the case of seasonal storage (Lindenberger et al, 2000). Storage capacity of about 30 L of water per square meter of collector area is sufficiently large to smooth out diurnal solar variations (Duffie and Beckman, 2006). The Drake Landing Solar Community (DLSC) is a 52-house subdivision in Southern Alberta that uses seasonal storage in the form of borehole storage to achieve a predicted 90% solar fraction for heating (Sibbitt et al., 2007). Interestingly, the storage at DLSC is so thermally massive that it is expected to take five years before being fully charged. Until that point, it is using natural gas to supplement solar energy. Seasonal storage is most suitable for multi-house storage, for which storage losses are lower because of the greater volume to surface area ratio (Duffie and Beckman, 2006).

The recently completed IEA Task 32: "Advanced Storage Concepts for Solar and Low Energy Buildings" provides a vast amount of information on the current state of active storage technologies (Hadorn et al., 2007). Their reports covers three major categories of active thermal storage: water-based (sensible), PCM (latent), and chemical. Another storage media that has been used for air-based systems in the past is rocks, which are typically put in an insulated box with an inlet and outlet. The recently-built ÉcoTerra house uses a ventilated concrete slab has been used for thermal storage (Noguchi et al., 2008).

### **2.3.1.2 System Configurations**

While, nearly all solar thermal systems contain a collector, storage tank, and pipes or ducts to connect the two, there are numerous variations. For instance, many systems have multiple heat-exchangers, storage tanks, valves, and complex controls. Weiss (2003), alone, describes 20 different configurations, never mind different control algorithms. Numerous recent Canadian examples of solar thermal systems have indicated that complex systems are difficult to design, operate, and maintain. For instance, Gordon Howell of the Riverdale House in Edmonton, Alberta found that PV (a traditionally more expensive technology) was actually cheaper than his immensely complex solar combisystem, on a cost per unit energy basis. While the benefit of experimentation and innovation is undeniable, for solar thermal technologies to flourish and gain market share, simple, off-the-shelf, easily serviceable systems should be the focus. This may mean sacrificing some efficiency for the benefit of simplicity in installation, operation, and maintenance.

Solar DHW systems offer the advantage that demand is relatively constant throughout the year; offering some congruency between demand and solar energy availability. In contrast, the peak demand and solar availability are approximately out of phase by six months for solar thermal systems that only supplement space heating. This is an important design consideration.



### 2.3.1.3 Photovoltaics

While several types of solar collector can produce power (e.g., concentrator with Rankine engine), photovoltaics (PV) are arguably the most suitable for building-integration because of its simplicity, absence of moving parts, and relative insensitivity to solar position. PV cells convert solar radiation into electricity (Duffie and Beckman, 2006) with an efficiency of 5 to 25% (GSES, 2004). Most commercial products package multiple PV cells into modules. The modular nature of PV panels allows for relatively flexible design in terms of suiting the needs of a variety of building-surface geometries. However, in order to use PV power for grid-connection and to power most common household appliances, the direct current (DC) from the PV array must be converted to alternating current (AC) with an inverter. Since inverters have certain operating voltage and current ranges, the panel array does have some restrictions, as summarized below (GSES, 2004).

$$0.8P_{PV} < P_{inv,DC} < 1.2P_{PV} \quad (2-15)$$

$$\frac{V_{inv,min}}{V_{MPP,panel}|_{T=70^{\circ}C}} < n_{panels/string} < \frac{V_{inv,max}}{V_{OC,panel}|_{T=-10^{\circ}C}} \quad (2-16)$$

$$N_{strings} \leq \frac{I_{inv,max}}{I_{string}} \quad (2-17)$$

Where  $P_{PV}$  is the maximum output of the array,  $P_{inv,DC}$  and  $I_{inv,max}$  are the maximum power and current of the inverter, respectively,  $V_{inv,min}$  and  $V_{inv,max}$  are the minimum and maximum operating voltage of the inverter, respectively,  $V_{OC,panel}$  is the open circuit panel voltage,  $V_{MPP}$  is the maximum power point panel voltage,  $n_{panels/string}$  is the number of panels per string, and  $N_{strings}$  is the number of strings of panels in the array.

While the ranges allow for some flexibility, there are cases, such as in the ÉcoTerra house, in which house geometry was partially dictated by the PV module configuration. This supports the notion of integrated design and the current research.

Electrical storage is mainly important for isolated off-grid buildings, since without it, they can only supply electricity during hours of daylight. However, it may be desirable for some building owners to have some form of storage for a sense of energy security, much the way many buildings (such as hospitals) have back-up diesel generators.

Electrical storage is most commonly in the form of batteries (chemical), but could also be fuel cells or potential energy (i.e., pumping water into an elevated reservoir). The inclusion of energy storage causes some losses, which are on the order of 20% (GSES, 2004). Thus, combined with the fact that some regions offer lucrative subsidies for PV-produced electricity, remaining off-grid in electrified neighbourhoods is nonsensical.

#### **2.3.1.4 Design and Modelling of PV Systems**

The simulation of PV performance is perhaps the simplest of all types of solar collectors (at least for grid connected systems) because transient effects are minimal and performance is not energy demand-dependent. For grid-tied buildings, all electrical energy produced can be assumed to be dumped to the grid and shortages can be supplemented by the grid. In this way, household electrical demand or storage losses do not have to be considered. Transmission losses, which mainly occur in the electrical grid rather than on the building side of the electrical meter are usually not important in house-centric analyses because the electric meter does not incur these losses.

While PV cells are dependent on their temperature, this can be determined with an energy balance at each time step, though simpler methods can be applied with a reasonable degree of accuracy. O'Brien et al (2008c) used the RETScreen PV model to show that representing whole year performance with a typical day of each month predicts output to within about 4% compared to the results of hourly analysis. The model was compared to a TRNSYS model for a wide variety of Canadian climates and collector orientations. TRNSYS is popular software for the modelling of solar energy systems and allows the performance of virtually any system configuration to be analyzed. The computer processing time for the simplified model is amply fast for simultaneous analysis of different design options.

For systems that are off-grid and have electrical storage it is best to perform whole-year simulations, since demand and degree of discharge of the battery must be considered. However, simplified models have been developed to avoid this (RETScreen International, 2005; Duffie and Beckman, 2006).

#### **2.3.1.5 Photovoltaic/Thermal Collectors**

Photovoltaic/thermal (or building-integrated photovoltaic/thermal (BIPV/T)) collectors can produce both electrical current and thermal energy simultaneously. Their principle is that since the majority of solar radiation absorbed by PV cells is converted to heat (rather than electricity), this heat can be carried away by a fluid and used elsewhere. A secondary advantage to this type configuration is that the PV cells are cooled by the

fluid, allowing them to operate at a slightly cooler temperature, and therefore higher electrical efficiency.

One example of an air-based BIPV/T collector is on the roof of ÉcoTerra (Chen et al., 2010a). It uses a large air channel to mechanically ventilate the space under the PV panels. The warmed air can be used for one of three purposes: charging a ventilated slab, DHW heating (or pre-heating), and for a custom-built dryer. Though, in theory, the heat could be used for any purpose.

While PV performance can be determined in an isolated manner, its performance is partially tied to the rate of fluid that passes under the cells. Thus, as with solar thermal collectors, PV/T collectors should be considered as an integrated system with the house. Thus, design of BIPV/T – and any other solar thermal system - should, if possible, be accompanied by integrated simulations.

#### **2.3.1.6 Design and Modelling of Active Solar Systems**

Hottel and Woertz (1942) and Hottel and Whillier (1958) were among the first researchers to attempt detailed mathematical modelling of solar thermal systems. They recognized the need for time-step analyses, though their analyses were steady-state. Their computational resources limited the research to developing methodology, though they did create some generalized design curves (Hottel et al., 1953). Interestingly, many of their Equations and parameters are still commonly used in modern software tools, such as TRNSYS. Klein, one of the key developers of TRNSYS developed a graphical

design method (F-charts) to represent many design parameters on two-dimensional graphs (Duffie and Beckman, 2006). However, the method was based on the regression of hundreds of transient time-step simulations, thus limiting their usefulness to specific configurations. Currently, the use of TRNSYS allows new configurations or the integration into buildings. However, despite its modular approach, it is most appropriate for researchers, rather than designers, because of the need to implement every valve and pump, for example. Many other design tools or methodologies for solar energy system analysis are available, though they mostly route from the aforementioned researchers' work.

Except for isolated solar DHW systems, for which daily demand does not depend on the building design, most solar thermal systems must be assessed in a coupled fashion with the building. For instance, heating demand depends on passive solar heating performance. It is tempting to compare collectors in terms of a single efficiency value, as is indicative of PV performance. However, efficiency is highly-dependent on the temperature of the fluid in the collector, as illustrated by Figure 2-25. The temperature of the fluid in the collector depends on the state of the storage tank. This fact alone should convince the reader that dynamic simulations must be used to assess real performance.

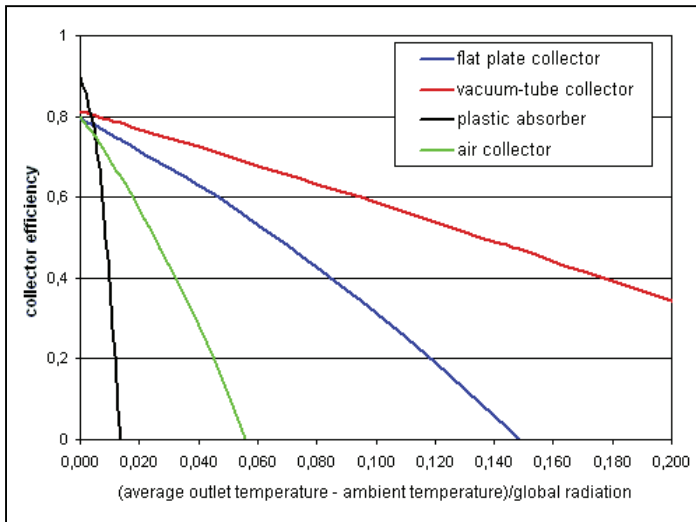


Figure 2-25: Typical solar thermal collector efficiency as a function of ambient conditions ([http://energytech.at/solar/portrait\\_kapitel-4.html](http://energytech.at/solar/portrait_kapitel-4.html))

## 2.4 Building Code

In order to reflect current regulations for solar houses, local buildings codes should be adhered to. The purpose of building codes within this work is to restrict designs to those that comply. Furthermore, there is an interest in establishing a benchmark for low-energy houses by comparing them to a base case house. The two most relevant building codes for this work are: the Model National Energy Code of Canada for Houses (MNECH) 1997 and ASHRAE Standard 90.2-2007 (“Energy efficient design for low-rise residential buildings”). MNECH 1997 is equivalent to ASHRAE Standard 90.2-1989, and is therefore often less demanding than Standard 90.2-2007. The most relevant aspects of the code for this work are the minimum thermal resistance values for the walls and windows.

Since Toronto is used in all examples throughout this work, the region selected was Ontario with less than 5000 degree days or ASHRAE Climate Zone 7. This region

represents Southern Ontario which houses about a quarter of the Canadian population. The code for this region is slightly more stringent than that of Southern Quebec. Key minimum requirements for thermal resistance are shown in Table 2-5.

*Table 2-5: Select code requirements*

Surface Type	Minimum RSI value (m <sup>2</sup> K/W)		
	MNECH-1997*	Std. 90.2-2007	Strictest
Roof - Type I (attic/roof space)	8.8	8.6	8.6
Walls	4.4	3.7	4.4
Windows	0.42	0.50	0.50
Below-grade walls	3.1	1.4	3.1
Below-grade floor	1.9	NR	1.9
*For electric resistance heating or other heating types, i.e., not gas, propane, oil, or a heat pump; NR=not-required			

Another relevant restriction is that total glazing area on the house should not exceed 20% of the floor area. However, south-facing (within 45 degrees of south) glazing that has a SHGC of 0.61 or greater only counts as 50% (i.e. 2 m<sup>2</sup> of south-facing glazing would count as 1 m<sup>2</sup>). This exception is added to allow for passive solar houses (which tend to use glazing with a high SHGC and low U-value), which actually benefit from high south-facing glazing areas.

## **2.5 Design Practice/Methodology**

The most fundamental concept of this section (and research) is integrated design. Integrated design is the act of designing a house (in this case) with recognition that it is a system, rather than individual parts that do not interact. It is a process that is being

pushed by academics but that has not been widely adopted in practice (Reed and Gordon, 2000; Matthiessen et al., 2004).

Traditional building design practice is a linear path from architectural team to mechanical engineer (Hayter et al., 2001). Thus, at best, each party of the design team can optimize their aspect of the building for energy use, though no common set of ecological objectives are established. Often times, the site and building form are laid out by non-design professionals, such as the owner, even before the architect even has a chance provide input (Reed and Gordon, 2000). This approach does not allow for life-cycle costs (or other goals) to be optimized because key aspects such as the envelope and HVAC systems are not designed (or even discussed) simultaneously. Figure 2-26 shows that this delay of design decisions ultimately affects the bottom line, since the opportunity for cost-effective energy reduction strategies quickly increases as the design process progresses.



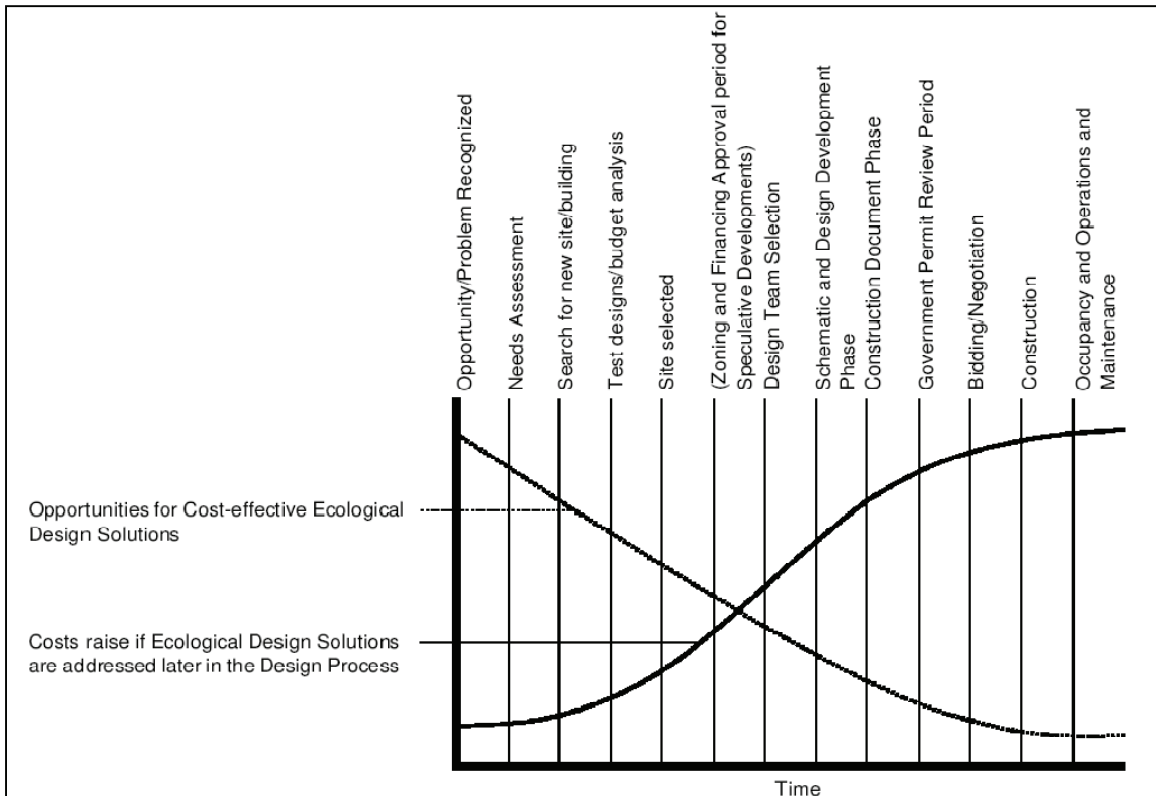


Figure 2-26: The opportunity for life-cycle cost reduction as a function of the design stage (Reed and Gordon, 2000)

One emerging practice is the use of design charrettes (CMHC, 2002). They are design meetings that last one or more days and involve all design team members, stakeholders, industry experts (e.g., equipment, materials), and even students. As a way to encourage their implementation, CMHC mandated their use in the 15 EQUilibrium projects that were previously mentioned. Between 18 and 32 people attended each one (Charron, 2008). Undoubtedly, the communication that occurs at charrettes is invaluable. However, the combined professional rates charged by design professionals for a day in comparison to the typical annual energy bill of a single detached house, does not justify the formality of design charrettes for houses. This notion is reinforced by Charron (2008). The exceptions to this would be mass manufactured houses (e.g., the ÉcoTerra

house) or large subdivisions of nearly identical houses. Also, the usefulness of design charrettes in large commercial buildings is justified by their cost and subsequent operating costs. As a side note, the author's experience of a design charrette was that many of the more influential participants had fixed ideas, and were not necessarily open to those of others. Furthermore, the sheer number of participants makes it difficult for everyone to be heard. All involved design professionals should be educated with some basic knowledge of the other fields, so that they have an understanding of the others' positions.

Design charrettes reinforce the need for a design tool – the product of the current research – in two ways. First, it illustrates the need for integrated design, in which all aspects are considered simultaneously. And second, it proves the need for having a tool that allows very fast turnaround, such that the user can quantify their concepts in a matter of minutes during design dialogue.

For the design of houses, there are likely to be just one or two main designers. A literature review reveals considerable work in the area of general low-energy building design methodology (Hayter et al., 2001; Andresen, 2008). Many of the more promising methodologies overlap and can be summarized by the following steps:

1. Pre-design: the site, climate, and functional building requirements are discussed and defined. Of particular importance for solar houses is the understanding of the site's solar obstructions. An excellent method for

visualizing shading is the use of a sky dome, in which the hemisphere (from the point of view of some point on the building) is projected onto the ground plane, as shown in Figure 2-27.

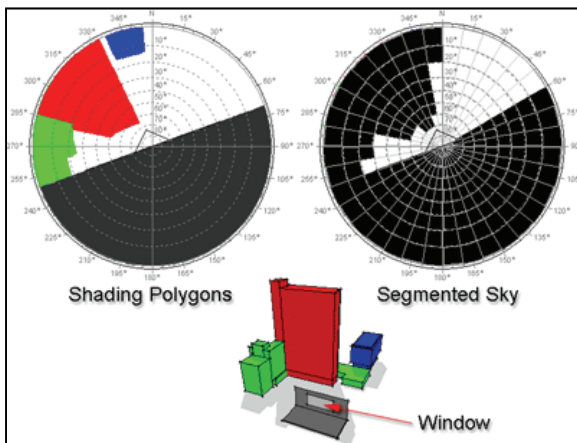


Figure 2-27: Shading analysis of a building site ([http://squ1.org/wiki/Shading\\_Mask\\_Calculations](http://squ1.org/wiki/Shading_Mask_Calculations))

2. A base case is established and simulated as a reference point. It meets all requirements and local building code and is often a solar-neutral, rectangular, and uses standard levels of electrical and occupancy loads (Hayter et al., 2001). “Solar neutral” means windows are distributed equally on all walls. A parametric analysis is performed. Using the base case as a starting point, performance is simulated by varying one parameter at a time (e.g. window type, insulation level). This provides a sense of the sensitivity of each of the main design parameters. It is often acceptable to use extreme values, as shown in Figure 2-28, as the results of this step are merely relative.

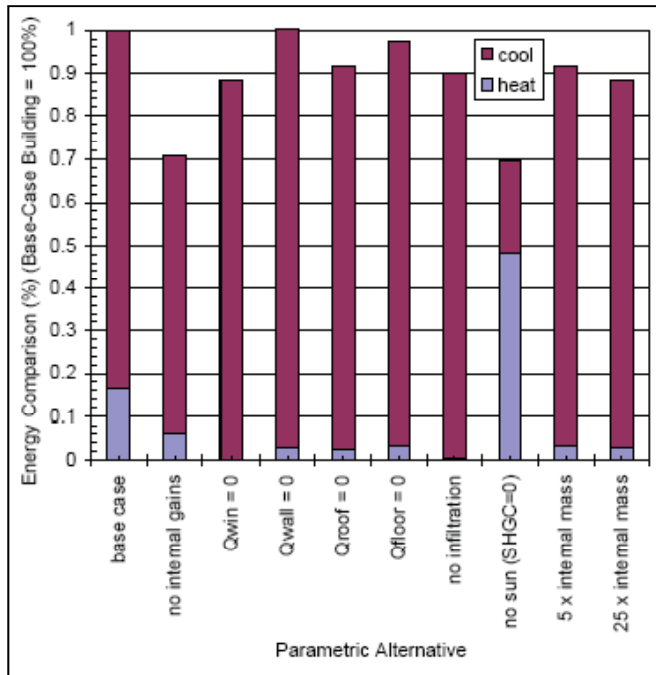


Figure 2-28: Parametric analysis results (Hayter et al., 2001)

3. Alternative designs, based on the information from the parametric analysis, are established and simulated, in turn.

While the above process appears to be linear and concise, many researchers suggest that the process is far from linear and involves a lot of iterations and backtracking. For example, Figure 2-29 shows the framework that Andresen (2008) developed.

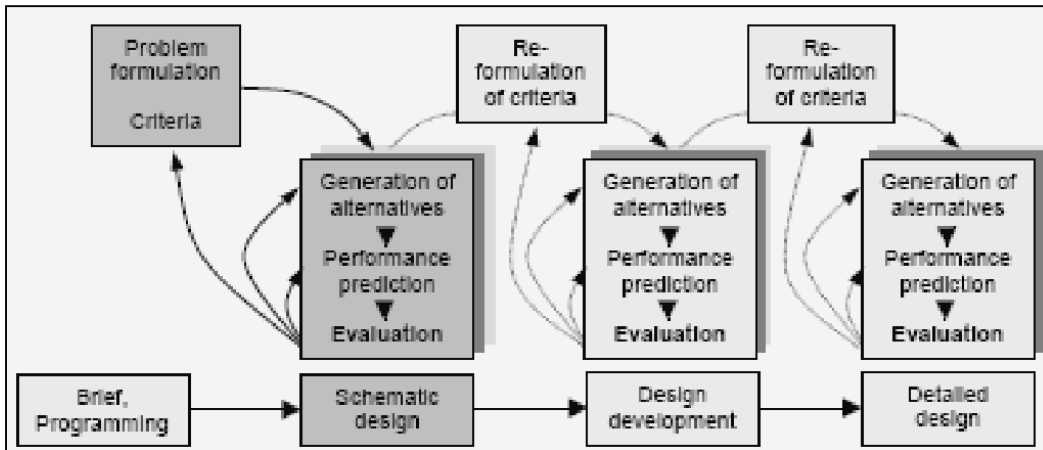


Figure 2-29: One version of a low-energy building design process

A more technology-specific approach, offered by IEA-SCH Task 23 (2002), suggests the following steps.

1. Establish performance goals.
2. Minimize heating and cooling loads, while maximizing daylight, by adjusting the form, fabric, and orientation of the building.
3. Meet loads using solar energy or other renewable energy sources. Supplement that with energy efficient HVAC systems.
4. Iterate steps 2 and 3 until objectives are met.

Arguably, the last step is the most important. It allows the compromise between energy efficiency measures and energy collection measures. The underlying reason for the iteration is step 4 is that steps 2 and 3 cannot easily be performed simultaneously. That is, while one can affect the other, it might not be possible to assess the exact effects during the design process. That being said, there are advantages to decoupling energy efficiency and energy collection measures. First, it is much more computationally

efficient. The second, and arguably more important, advantage to decoupling the system is that it simplifies the problem and allows the designer to focus on one thing at a time. This process is known as *problem decomposition* (Ulrich et al., 1995).

## **2.6 Building Simulation Software in the Design Process**

Although the purpose of investing in building energy simulation has generally been design, there is a considerable amount of discrepancy between simulation and design, and practice (Clarke, 2001). Only in about the past decade, have simulation tools begun to recognize their role in design, with programs such as: Energy-10 and Building Design Advisor. The majority of simulation tools focus on modelling capability, with little consideration of the designer. Ideally, there would be a tool, or set of tools that could be used at every stage of the design process, from pre-design to detailed design. If multiple tools are used, they should be interoperable, such that the same model can be carried through the design process, without requiring a new model to be built at each stage.

Several works, including Augenbroe (2002), Hong et al. (2000), Ellis and Mathews (2002), and Clarke (2001), examine some of the limitations of existing simulation software and the needs of the industry. These, along with several points encountered by the author, are listed below.

1. **Inputting design parameters is time-consuming** (Bazjanac, 2004). Many specifications must be made about building geometry, wall constructions, equipment, controls, and the site. Too often, these inputs are redundant (e.g.,

each the construction of each wall must be specified even though they will usually be the same). Also, many assumptions must be made early on, even though this information may not be known to the user. These assumptions may or may not have a big impact on the design.

2. Existing **simulation software is difficult to use**. An inherent trade-off exists. A program can be simple, allowing the most inexperienced user to obtain results relatively easily. However, such tools tend to remove most ability to input extensive model details, meaning that the user has little power over the calculations being performed. A complex, detailed program gives the user tremendous power, but requires the user to have a high level of technical knowledge. Furthermore, if the user does not have intimate knowledge of the inner workings of the software, they cannot be sure that their vision is represented by the model.
3. **The learning curve should be as short as possible**. For simplified tools, the time required to learn and use software should be reduced to minutes rather than hours (Ellis et al., 2001).
4. The design tool should **use a language familiar to designers** (Ellis and Mathews, 2001). In contrast, current tools tend to be use language familiar to simulationists and researchers.
5. **Use of multiple tools is almost certainly associated with incompatible assumptions**. If no single simulation tool is available to perform all required

functions, the designer is forced to use multiple tools with the hopes that the underlying assumptions are suitably compatible. For instance, the simultaneous simulation of daylighting, lighting controls, and thermal processes is particularly difficult with existing software. The majority of the best existing illumination software only handles issues related to illumination. So, if a combination of lighting and blind control is simulated, there is no way to properly explore the effect on solar gains. Likewise, in the ÉcoTerra House, where a basement concrete slab is used for storage of both direct solar gains and thermal energy from roof-integrated collectors, it is obvious that each source of heat will affect the behaviour of the other. If the floor is significantly heated by direct solar gains, the effectiveness of the roof-integrated collector is reduced. Thus, assessing them individually, would likely lead to an optimistic prediction.

6. **Little guidance is provided** to users about how to proceed towards a superior design, forcing them to rely on experience and luck in an iterative design process. This single feature has the potential to vastly improve the design process. Without it, a user can only be confident that they have reached a near-optimal design if they systematically explore the entire design space. Ellis and Mathews (2002) state “[current design tools] are consequently seen as decision support systems (DSS) rather than true design tools”.



7. Building design requires many **practical considerations**, but these are often not accounted for in simulation software. For instance, it is more economical to construct a house roof with a standard pitch, than at some arbitrary pitch.
8. **Extended simulation times** can prevent the proper exploration of the design space if the designer has limited time. When the author attempted to simulate daylighting and electric illumination of a classroom space, he found that the most suitable software, SPOT™ (Architectural Energy Corporation, 2008), took about one hour to perform a single whole-year simulation. Given that the study assessed the effect of many parameters (about 40), a full work week was required simply to obtain the results, never mind analyze them.
9. **Overwhelming amounts of data are produced** by the software (Prazeres et al., 2003). While this may be useful for the researcher or academic, it does not facilitate decision making. For instance, for each time-step ESP-r produces temperatures for each layer of a wall, flux through the layer, long-wave radiation exchanges, and conditioning energy, to name a few (ESRU, 2007). For a simple single-zone building with no equipment, ESP-r produces a spreadsheet that is too wide to fit in a standard spreadsheet program and 8760 rows long (for hourly time-steps).
10. **No context for performance data** is provided. Without benchmarks, only an experienced designer has knowledge of how their current design performs relative to other similar buildings. Standards do exist but typically do not allow

easy comparison within software. Such standards include R-2000, C-2000, and MNECH.

11. **Little insight to physical processes** is provided to the designer. Without understanding the behaviour of a system, it can be difficult for the designer to know how to improve it or diagnose problems. For instance, suppose a designer has a base case design (Case A) and changes two parameters for Case B. If the results are merely displayed as a single performance metric, say total heating energy, it is impossible to know what led to the improvement. It could be argued that this scenario could be improved by changing only one parameter at a time. However, it is entirely possible that the design change will result in similar energy use, but occurs for a different reason. It is preferable to offer the designer concise but detailed insight about the thermal processes of the building; particularly for passive solar buildings, in which daily temperature swings occur.
12. **Comparison of results** is typically a manual archiving process. If a designer would like to compare the results of several simulations, they might maintain a spreadsheet. Again, this is a time-consuming process that can reduce the patience of the designer. A built-in system to store several designs with the capability to compare them is desirable.

## 2.7 Quantifying Performance and Objectives

Builders and designers usually have many criteria for the successful design, whether they have explicitly defined them or not. The criteria can include: cost, energy performance, thermal comfort, aesthetics, environmental impact, resaleability, etc. The process is complicated when there are multiple stakeholders or design team members. Andresen (2008) created a tool called MDCM-23 (for Multi-criteria decision-making) that manages different criteria weightings for different stakeholders, though the tool does not actually perform any thermal analysis of the design.

A literature review reveals several common or popular formal methods for combining criteria into a single value, such that one design can be directly compared to another. Among the most common in engineering design theory is the decision (or Pugh) matrix, as depicted by Table 2-6. It simply compares two or more designs by summing the product of the weighted criteria and the rating of each design for each criterion. In the example, Option B scores slightly higher than Option A, thus it would be selected.

*Table 2-6: Example decision matrix*

	<b>Weighting</b>	<b>Option A</b>	<b>Option B</b>
Cost	10	7/10	6/10
Energy Use	5	4/10	9/10
Score		9	10.5

A more advanced version of the decision matrix is the “house of quality”, which has a similar purpose, but with more detail (Belhe et al., 1996). In particular, it requires that the interaction between criteria be defined.

One interesting method of displaying multi-criteria performance is to use a “star diagram”, as shown in Figure 2-30. The performance is proportional to the area of the gray polygon. The limitation of this implementation is that it only shows current performance, but no guidance towards better designs.

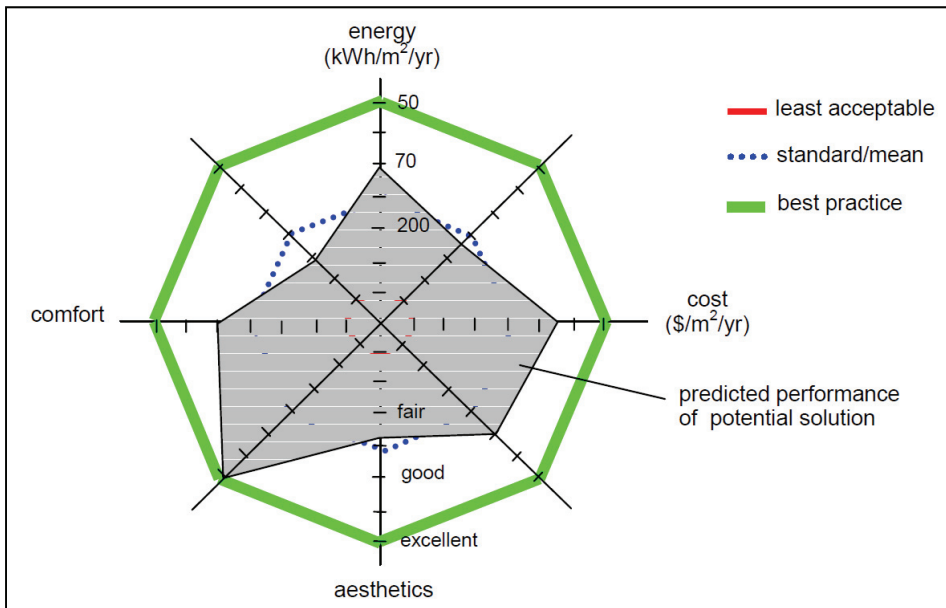


Figure 2-30: Star diagram for multi-criteria design (Andresen, 2008)

## 2.8 Optimization

While formal optimization differs from design in the process, the goal is essentially the same: the specification of a high (or optimum) performance system that satisfies all constraints. Formal optimization techniques are beginning to emerge as a practical solution to coming up with effective building designs. Because of the need to examine the interactions between design parameters and the large number of design options, a brute-force, full factorial approach is generally inappropriate. Thus, evolutionary

algorithms, such as genetic algorithms (GA) tend to dominate recent research (Coley et al., 2002; Wright et al., 2002; Wang et al., 2005; Charron et al., 2006b). However, such approaches tend to be hidden to the user, offering little information about the path to the optimal solution. Furthermore, optimization tends to be time consuming because of the number of simulations that must be performed. Arguably, the most relevant to the current research is one performed to determine optimal design parameters for solar houses in Canada using a GA coupled with TRNSYS (Charron, 2007). Charron optimized 17 different parameters of houses under a multitude of conditions and climates. If every combination (full factorial design) were explored, about 2.1 billion simulations would have to be performed. However, he showed that performing just 2,700 simulations that were driven by a GA was able to achieve a near-optimum solution. However, the optimization process still took about 13 hours per set of conditions (e.g., climate, lot constraint, etc.). This is an order of magnitude longer than the goal of the design tool. Essentially, the output of the GA was a single design that TRNSYS predicted to perform well. However, the user of the GA is provided with minimal insight into why that combination of parameters works well together. Magnier (2009) took a different approach in that he trained an artificial neural network (ANN) based on a database of 450 different simulation runs. This approach offered considerable flexibility as the GA was used to optimize the ANN rather than performing simulations during the optimization process.

While design ultimately allows the intervention of human judgment to determine if a design meets criteria, formal multi-criteria optimization requires that all criteria and their importance weighting be quantified. However, optimization can be used to find a set of optimal solutions, known as the Pareto set of solutions (Wright et al., 2002). The Pareto front marks the boundary of the optimal solution set in multi-criteria optimization. It allows the relationship between the criteria, which are often hard to combine into a single criterion, to be visualized. An example of a Pareto front in the optimization of thermal comfort and energy costs is shown in Figure 2-31. Clearly, these two metrics cannot be easily combined, without associating a monetary value to thermal comfort. The example shows that beyond a certain increase in energy costs, there is minimal potential to improve thermal comfort – a very valuable fact.

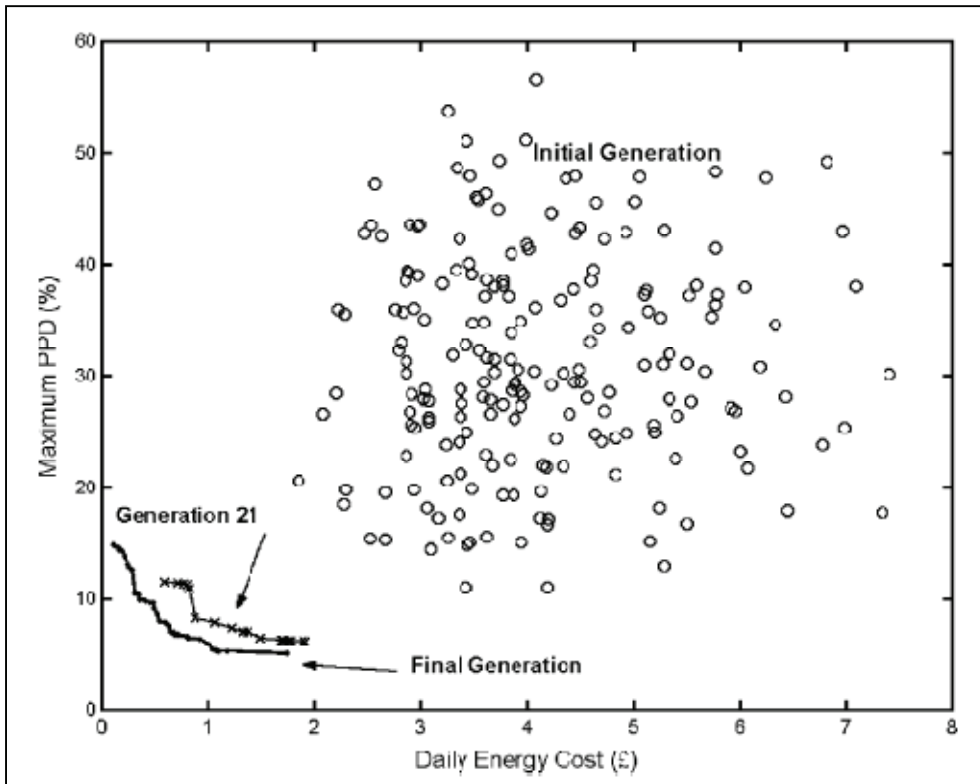


Figure 2-31: Results of multi-criteria optimization using a genetic algorithm (Wright et al., 2002). The scattered points are possible solutions, while the Pareto front is marked as “Final Generation”.

BEopt, a research-level optimization tool that optimizes the life cycle cost of net zero energy homes, offers a GUI with some control over the optimization (Christensen, 2006). Unfortunately it uses a one-dimensional sequential search which does not necessarily arrive at the optimum solution and ignores many interactions. Nevertheless, BEopt’s flexibility and recognition of user needs makes it a leader in research. Its features are explained in the Appendix A.

Regardless of optimization’s usefulness, several limitations of formal optimization in the design process have been identified, as follows:

- They make little use of user/designer knowledge and spend too much time optimizing design space that could likely be eliminated with common sense and experience.
- They offer little information on what makes a good design other than providing specifications for the optimal solution (or set of optimal solutions).
- They do not allow qualitative features to be valued.
- Once the solution is within the near-optimal design space, there is likely minimal room for improvement of the objective function, and thus practical issues and human factors should be given strong consideration. Formal optimization does not recognize this.

## **2.9 Existing Software Survey**

Several comprehensive surveys of available building energy simulation software have been performed (Haltrecht et al., 1999; Crawley et al., 2008). A survey of a subset of 13 of these that are either notably suitable for low-energy buildings, have unique GUIs or features, or are particularly good for building design, is provided in Appendix A.

## **2.10 Conclusion**

The purpose of this chapter was to provide a review of solar houses and their technologies, modelling techniques, and finally design processes and tools, to set the context of the chapters that follow; in which many of shortcomings are addressed.



### 3 PASSIVE SOLAR HOUSES AND MODELLING

This chapter describes the generic house model that was created excluding the active solar features (which are described in the next chapter). Each of the major components or features is discussed in terms of modelling methodology and when applicable, the relevant model (and design tool) inputs.

The generic house model was created in compliance with the following four principles, in no particular order.

1. **Flexibility.** Broadening the design space to include designs that are both weak and strong provides contextual information to the tool user. However, flexibility must be balanced while restricting designs that are below building code, absurd, impractical, or uncommon. Care was taken to reduce the size of the design space where possible because a larger design space means a much greater number of simulations has to be performed, as described in the Chapter 7.
2. **Simplicity.** Providing too many options (technologies, parameters, parameter ranges) to the user is unlikely to yield higher performance designs – beyond a certain point – but merely overwhelm them. Also, creating overly complex models necessarily has more inputs, many of which are unavailable during early stage design.

3. **Performance.** The typical user of the tool would be a designer who is interested in a high-performance house; not a house that barely meets building code. Thus, the parameter ranges and available technologies should be selected accordingly.
4. **Accuracy.** The objective of the tool is to guide designers toward the optimal design space (as defined by them). Therefore, the tool must accurately predict performance. Accuracy is defined as the model's ability to predict a house's performance relative to the measured performance. While there is some uncertainty regarding the effect that the occupants will have on a house, it is particularly critical that the tool diagnose any major design flaws (e.g., chronic overheating or high peak loads) and that the tool not misguide any of the corresponding major parameter settings such as window size, aspect ratio, or thermal insulation thicknesses.

A major issue and contribution of this thesis is selecting the **appropriate model resolution**. Accuracy must be balanced with complexity. Figure 3-1 shows the general relationship between accuracy and model resolution (detail and modelling effort). The diminishing returns mean that establishing the level of model resolution beyond which little benefit is gained is beneficial.

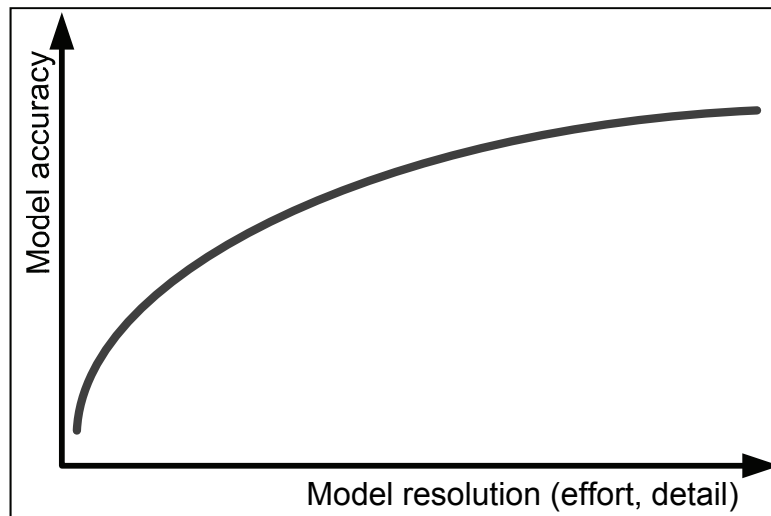


Figure 3-1: Relationship between model resolution and model accuracy

A building model should not necessarily have consistent model resolution throughout (i.e., for each aspect and subsystem) since if a particular component model of low resolution is good enough, there would be little benefit to using a high resolution model. High resolution models are usually associated with: more inputs (and hence, more uncertainty) and longer simulation times. Furthermore, for the detail-oriented simulationist, complex models are more difficult to debug.

Each of the model aspects and subsystems listed in this chapter underwent extensive analysis in order to select the most appropriate level of resolution. The above four points are major considerations for each model aspect; they are directly referenced where applicable.

Some of the original parameters were eliminated if they were found to be both insignificant and of little interest. For example East and West-facing overhangs are

ineffective at reducing unwanted solar gains. Similarly, of the five original glazing types, one was found to yield nearly identical properties to another; so the total number was reduced to four.

### **3.1 Simulation Engines**

There were two main options for modelling house performance in the current work: create a custom model and write code based on first principles or use an existing simulation and focus on advancing the state-of-the-art in modelling methodology and techniques for visualizing performance. The latter option was selected.

There are three main current simulation engines that dominate building performance simulation in research are: EnergyPlus, ESP-r, and TRNSYS. Several comprehensive review studies have been performed to compare these simulation engines along with many of the others (Crawley et al., 2008). Furthermore, they are all among the 13 tools that were critically assessed in Appendix A.

The tool of choice for this work – EnergyPlus – was selected by thoroughly using the simulation engines, reading their documentation, and reviewing the literature to determine prevalence of use. The criteria that were used to select EnergyPlus are described below in approximate order of importance.

1. **Accuracy of models.** The top priority is to accurately predict performance of the house and all its subsystems. Inaccurate models could mislead the tool's

user towards non-optimal designs. One of EnergyPlus' original disadvantages was that it only had a transfer function model available: a weakness for modelling high-mass buildings. However, it has since included an implicit finite difference method with the intent of accurately modelling non-linear material properties such as PCMs (EnergyPlus, 2009b). EnergyPlus, like the other listed simulation engines, has undergone BESTEST testing (Henninger et al., 2004) and proved to be accurate. BESTEST (ANSI/ASHRAE Std. 140) involves extensive comparison to 8 other tools. EnergyPlus was within the expected range for 58 of the 62 metrics and the remaining four results were within 5.6% of the range.

2. **Availability of features.** A priority of this work was to build an integrated model that contains all features and allows simultaneous modelling of all systems (if necessary). Therefore, an engine with as many of the intended features as possible is important. Of particular interest for this work are heat transfer through opaque envelopes, fenestration, thermal mass, multiple zone models, airflow networks, infiltration, scheduling of events, controls, equipment modelling, solar shading and shading devices, renewable energy technologies, and ground-basement thermal interaction. EnergyPlus is strong in its variety and depth of features; particularly those related to commercial buildings. Its strengths are form and fabric, scheduling, advanced fenestration systems, and detailed HVAC systems. Its weaknesses that are relevant to this work are a lack of typical residential-scale HVAC models, limited options for the

ground/foundation interface model, and a limited number of renewable energy technologies. For instance, TRNSYS has a vastly larger library of solar thermal collectors compared to EnergyPlus. ESP-r has among the most accurate basement/ground coupling modules, BASESIMP, integrated directly into the software.

3. **Ease of use and model implementation.** In selecting a program, it was important that the model and its features be relatively easy to implement. This saves time and more importantly reduces the risk of error. EnergyPlus' modular nature, strong documentation, intuitive text-based interface, consistency, and input file tagging format make it a strong candidate for this work. In particular, its centralized development means that it is consistent and intuitive across all features. While its main user interface – IDF Editor – is essentially text-based, add-ons such as the SketchUp OpenStudio plug-in means that certain aspects of the model can be easily visualized. A weakness is that high-resolution HVAC systems are difficult to model because the visualization feature is weak at this point. This requires a certain amount of trial-and-error debugging. However, most standard HVAC configurations can be modelled using built-in templates. Only if unusual systems, such as solar combisystems are modelled, does one have to build a custom model.
4. **Ability to interface with external software.** Since the current work, by definition, requires that data be inputted to and outputted from the simulation

engine, a strong ability to interface with it is essential. This means a common input structure, ideally text-based, with no redundancy of inputs and an equally-convenient output structure is valued. The tool must be able to be called and executed from a command prompt such that no human-involvement is necessary. EnergyPlus has a highly-favourable input file format: a single text file – the so-called “flat file” format. Each model object is represented by its own heading and is followed by a list of fields that are tagged and whose values are alphabetic or numeric. Objects are linked together by referring to other objects names, which can be long and descriptive. EnergyPlus’ output capabilities are expansive and very powerful. Practically any imaginable variable or metric can be output in any time-interval with a minimum of once per timestep and a maximum of annually. The output file format is comma-separated value (CSV), which makes it easily read by human and computer, alike. This differs from ESP-r, which, until recently, stored results in a binary file only. This was unreadable by programs other than ESP-r itself.

5. **Documentation.** In order to understand the exact implementation and algorithms being used in the simulation engine, proper documentation is essential. EnergyPlus has among the most thorough documentation of any simulation engine, at over 2000 pages. The Input/Output documentation (EnergyPlus, 2009a) describes how to use the models and the Engineering Reference (EnergyPlus, 2009b) explains the modelling methodology. Both of

these main documents include references to the literature such that further information can be obtained. Like for ESP-r and TRNSYS, EnergyPlus' source code is available to advanced users and to developers.

6. **Control of model resolution.** A objective of this work is the appropriate selection and justification of model resolution: a compromise between detail and accuracy. This is particularly important for the design tool, which is aimed at early stage design, and for which limited data may be available. Often simulation engines use a high level of model resolution to be “safe”. That is, the developers remove their liability for accuracy by forcing the user to input a large amount of information since it is perceived to be more accurate. EnergyPlus is a leader in providing significant freedom on model resolution. Most features allow two to three levels of model resolution and they can be mixed within a certain model. For instance, a simplified PV model can be mixed with a complex infiltration model for the same building. This is suitable either for situations when either the modeller is only interested in assessing the performance of one feature or when the modeller has determined that using the simpler models for a feature comes with no weakness. Figure 3-2 shows a conceptual space that was developed by IEA SHC Task 40/ECBCS Annex 52: “Towards Net-Zero Energy Solar Buildings”, as a means of classifying different building design/simulation tools.



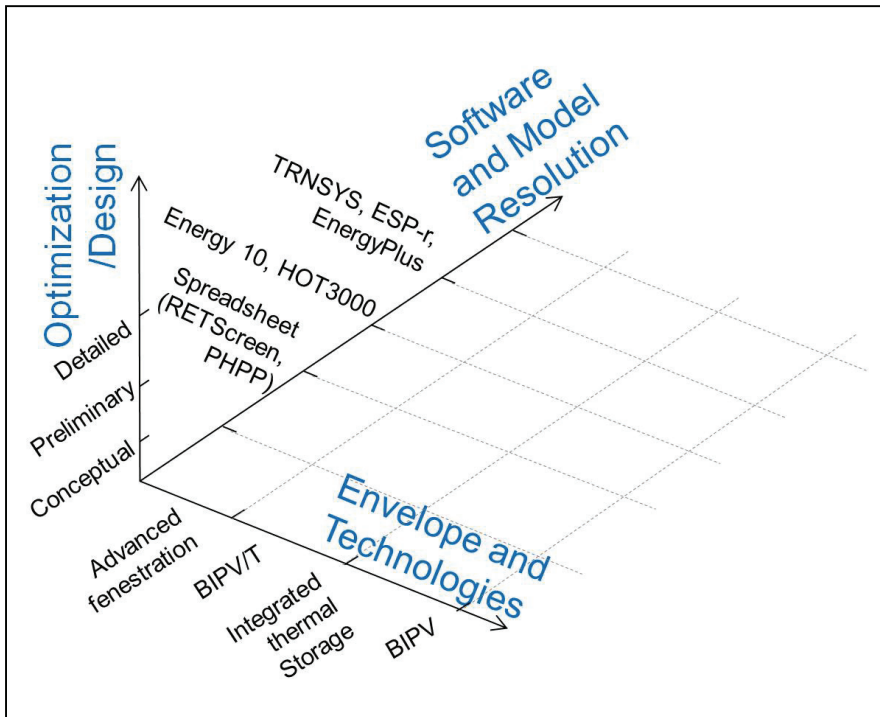


Figure 3-2: A 3D space upon which different modelling tools can be placed (taken from Athienitis et al (2010))

7. **Expandability.** In research, and even design practice, one often encounters a particular building feature or technology that cannot be modelled with the tool of choice. Therefore, having the ability to expand a simulation engine's capabilities is beneficial. All of the three main simulation engines can be expanded on by modifying source code. Arguably, this is most easily performed in TRNSYS, which is the most modularized of the three simulation engines. Anecdotes of the other two suggest that they are considerably more difficult to modify. EnergyPlus is unique in having a feature that allows basic programs to be written directly in its interface. This feature, called the Energy Management System (EMS) is particularly suitable for implementing more advanced controls, but could also be used to model new technologies or output aggregated or

modified simulation results (Ellis et al., 2008). A second feature that was recently developed for EnergyPlus is the Building Controls Virtual Test Bed (BCVTB). It allows run-time interfacing between EnergyPlus and a variety of high-level programming languages (e.g., Matlab and Modelica) and also with BACnet (Wetter et al., 2008).

Despite EnergyPlus' many strengths, there are some notable weaknesses. Particular to this work, its use of the implicit finite difference (as opposed to explicit or some hybrid, such as the Crank-Nicolson method) has a few drawbacks. Continuing from the discussion in the literature review, the implicit finite difference method is unconditionally stable for any discretization size in the space and time domains. However, excessively long time steps or small control volumes can lead to significant oscillations in solutions. Both of these situations were illustrated in the literature review. Of particular concern is underestimating temperature swings – a fundamental characteristic of passive solar houses. However, EnergyPlus recommends 3-minute timesteps, which is quite short and closely resembles what would be used for the less stable explicit formulation. Such short timesteps are important because, unlike more integrated tools like ESP-r, EnergyPlus uses a “ping-pong” solution for certain domains, including zone surface-air coupling, airflow networks, and HVAC. This means that zone air temperatures, for example, are calculated based on past zone surface temperatures. For rapidly changing conditions or excessively long timesteps, errors can begin to

propagate. For space discretization, EnergyPlus uses the Fourier criterion, as defined in Section 3.2.8.

A further potential limitation to the implicit finite difference method is that it is not tailored for controls (e.g., HVAC controls). In its formulation (shown in the literature review), current timestep node temperatures are simultaneously solved based on each other, the past node temperatures, and heat sources. However, the explicit formulation allows that heat source (or other control input) to be assigned a value based on past temperatures only. ESP-r's Crank-Nicolson implementation allows the calculation of the necessarily heat addition/extraction to maintain a zone's air temperature. However, EnergyPlus iterates between the zone solution and plant solution in order to determine the appropriate level of heat addition/extraction to achieve the temperature control setpoint.

## **3.2 Major model components**

The following sections describe the modelling methodology for each of the major features, except for the active solar systems which are described in the next chapter.

The entire model is parameterized such that it can be described with about 40 parameters. The model input parameters (passive elements only) are summarized in Table 3-1. The *Abr* heading refers to the short form version of each parameter and are referred to throughout this chapter and in the code. Each parameter can be classified as design or non-design. Here, non-design parameters (denoted with a *0*) are defined as

those that affect the service that the building provides, namely, shelter, space, and protection from the elements. Put differently, they are likely to be fixed at the beginning of the design process. Design parameters (denoted with a *1*) are defined as those that affect energy performance, but not the service to the occupants. As an example of each, the floor area (*FA*) is a non-design parameter because it is likely to be set at the beginning of design because the client has a certain budget and spatial needs; but overhang depth (*OH*) is a non-design parameter because it would be set later on in the design process and does not necessarily affect the service that the house provides other than reducing summertime solar gains. Two of the parameters – orientation (*OR*) and aspect ratio (*AR*) – could be considered either non-design or design parameters. Depending on the constraints posed by the site, the designer may or may not be able to vary them.

Continuous parameters (denoted as discrete = *0*) can be set to any value within the permissible range (though they may not all be convenient with regards to available building materials). Moreover, they can be modelled in EnergyPlus with a single value. Discrete parameters (discrete = *1*) can take on one of several distinct values. For instance the simplest way to define different glazing types is to explicitly model them, rather than having variable optical and thermal properties; some combinations of which would not be possible (e.g., high transmittance and low U-value).

The minimum and maximum parameter values are justified in the sections that follow. In general, they were selected to balance flexibility and simplicity, as previously defined. For parameters that are governed by building code, the minimum values were selected as to not violate the code. Discrete parameters are simply assigned an index number, with the maximum allowable value being equal to the number of discrete options.

The nominal parameter values were selected to represent typical values for good passive solar design. Unless otherwise noted, they are used for the sensitivity analyses throughout this chapter. They are also used as default values in Ecos. The last column of the table references the current chapter section describes the parameter in detail.

Table 3-1: Summary of model inputs

No.	Name	Abr.	Design?	Discrete?	Min	Max	Nominal	Units	Section
1	Infiltration	IN	0	0	0.025	0.15	0.05	ach	3.2.9
2	Internal gains	IG	0	1	1	3	1		3.2.12
3	Heating setpoint (daytime)	HS	0	0	17	22	22	°C	3.2.13
4	Heating setpoint (nighttime)	HSN	0	0	17	22	18	°C	3.2.13
5	Cooling setpoint	CS	0	0	22.5	27	26	°C	3.2.13
6	Floor area	FA	0	0	100	450	250	m <sup>2</sup>	3.2.1
7	Stories	ST	1	1	1	2	2		3.2.1
8	Aspect ratio	AR	1	0	0.5	2	1		3.2.1
9	Orientation	OR	1	0	-45	45	0	degrees	3.2.1
10	Wall resistance	WR	1	0	4.4	12	6	m <sup>2</sup> K/W	3.2.3
11	Ceiling resistance	CR	1	0	8.6	15	11	m <sup>2</sup> K/W	3.2.3
12	Basement slab resistance	BS	1	0	1.9	3	1.9	m <sup>2</sup> K/W	0
13	Basement wall resistance	BW	1	0	3.1	6	3.1	m <sup>2</sup> K/W	0
14	Glazing type 1	GT1	1	1	1	4	3		3.2.4
15	Glazing type 2	GT2	1	1	1	4	3		3.2.4
16	Glazing type 3	GT3	1	1	1	4	3		3.2.4
17	Glazing type 4	GT4	1	1	1	4	3		3.2.4
18	Window frame type	FT	1	1	1	3	2		3.2.4
19	Window-to-wall ratio 1	WWR1	1	0	0.05	0.6	0.4		3.2.4
20	Window-to-wall ratio 2	WWR2	1	0	0.05	0.3	0.1		3.2.4
21	Window-to-wall ratio 3	WWR3	1	0	0.05	0.3	0.1		3.2.4
22	Window-to-wall ratio 4	WWR4	1	0	0.05	0.3	0.1		3.2.4
23	Air circulation rate	CI	1	0	0	400	200	L/s	3.2.13
24	Overhang depth	OH	1	0	0.001	0.5	0.3	depth:glz. ht.	
25	Blind/shade solar threshold	BLS	1	0	0	1000	300	W/m <sup>2</sup>	3.2.13
26	Blind/shade outdoor temperature threshold	BLT	1	0	15	40	25	°C	3.2.13
27	Thermal mass thickness on south floor	TMS	1	0	0.001	0.2	0.1	m	3.2.7
28	Thermal mass thickness on dividing wall	TMV	1	0	0.001	0.2	0.1	m	3.2.7
29	Roof type	RT	1	1	1	2	1		3.2.1
30	Roof slope	SL	1	0	10	60	35	degrees	3.2.1

A flowchart of the model's structure is shown in Figure 3-3. This is only the house part of the complete flow chart. The full flow chart is shown in Figure 7-1.

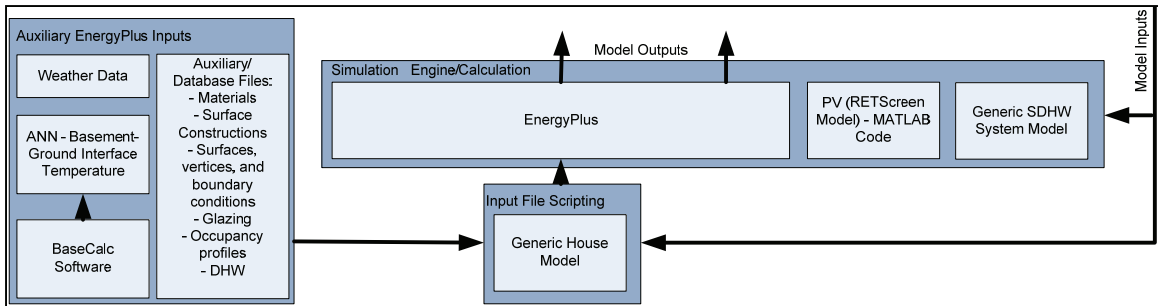


Figure 3-3: Flowchart summarizing the structure of the model

To introduce the parameters, the sensitivity of the 30 passive parameters is summarized in Figure 3-4 and Table 3-2. To quantify the relative significance of the parameters, a main effects plot was created. This has the purpose of identifying the effect of each parameter on energy consumption. All parameters were kept at their nominal values, as listed in Table 3-1, except for the parameter of interest, which was incrementally modified to determine the trends over the parameter range. It is important to note that the apparent sensitivity of a parameter is highly-dependent on the range, and must be taken into context when interpreting relative sensitivity (Hui, 1998). Figure 3-4 summarizes the results of the analysis and shows the complete range of simulated performance values for each parameter. Table 3-2 quantifies the minimum and maximum energy use values and the corresponding parameter values. Parameter value | Emin and value | Emax represent the parameter values at which the minimum heating and cooling energy occur. Table 3-2 also quantifies the sensitivity of each parameter according to the following Equation (Hui, 1998).

$$\left(\frac{\Delta OP}{\Delta IP}\right) \div \left(\frac{\overline{OP}}{\overline{IP}}\right) \tag{3-1}$$

where  $\Delta OP$  is the difference in output values (predicted energy use) for the extreme values of each parameter,  $\Delta IP$  is the difference in input values (extreme parameter values), and  $\overline{OP}$  and  $\overline{IP}$  are the mean output and input values, respectively.

Since, for many of the parameters, the energy consumption is non-linear over their range, their curves are shown throughout the following sections.



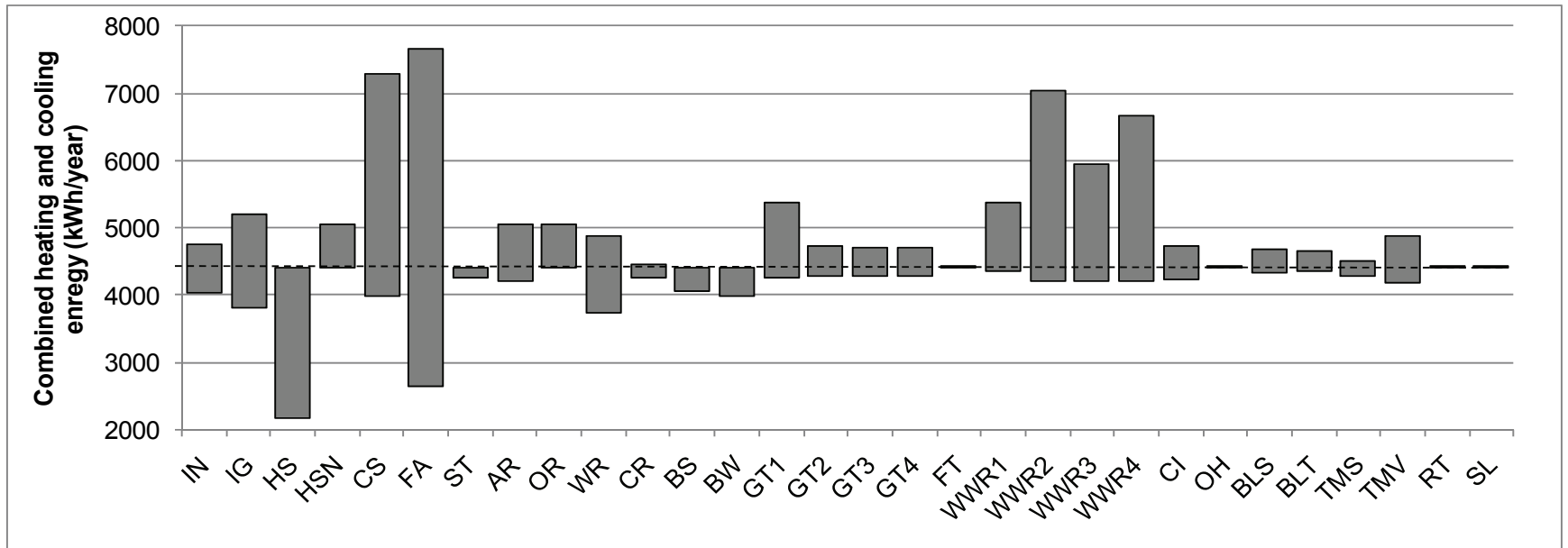


Figure 3-4: Energy use ranges for 30 parameters. The dashed horizontal line is the energy use when all parameters are at their nominal values.

Table 3-2: Summary of Sensitivity Analysis for 30 Parameters

	IN	IG	HS	HSN	CS	FA	ST	AR	OR	WR	CR	BS	BW	GT1	GT2
<b>Min. Energy (kWh/year)</b>	4042	3801	2172	4394	3991	2637	4251	4209	4403	3724	4253	4058	3972	4264	4288
<b>Max. Energy (kWh/year)</b>	4766	5203	4403	5059	7300	7660	4403	5045	5061	4874	4460	4403	4403	5377	4717
<b>Parameter value<sub>E<sub>min</sub></sub></b>	0.025	3	16	17	22.5	100	1	1.85	0	12	15	3	6	5	5
<b>Parameter value<sub>E<sub>max</sub></sub></b>	0.075	1	22	22	27	300	2	0.5	-45	4.4	8.8	1.6	3.1	1	1
<b>Parameter unit</b>	ach	-	°C	°C	°C	m <sup>2</sup>	m	-	degrees	m <sup>2</sup> K/W	m <sup>2</sup> K/W	m <sup>2</sup> K/W	m <sup>2</sup> K/W	-	-
<b>Sensitivity</b>	0.1646	-0.627	2.4601	0.5664	3.4494	1.0704	-0.052	0.1579	1E-07	0.3001	0.0915	0.135	0.1634	-0.698	-0.285
	GT3	GT4	FT	WWR1	WWR2	WWR3	WWR4	CI	OH	BLS	BLT	TMS	TMV	RT	SL
<b>Min. Energy (kWh/year)</b>	4292	4290	4403	4362	4216	4209	4199	4240	4399	4328	4367	4289	4170	4402	4397
<b>Max. Energy (kWh/year)</b>	4717	4717	4418	5381	7046	5959	6662	4721	4439	4667	4665	4507	4871	4403	4418
<b>Parameter value<sub>E<sub>min</sub></sub></b>	5	5	2	0.5	0.05	0.05	0.05	400	0.3503	0	19	0.2	0.2	2	50
<b>Parameter value<sub>E<sub>max</sub></sub></b>	1	1	1	0.05	0.5	0.5	0.5	0	0.001	1000	40	0.001	0.001	1	10
<b>Parameter unit</b>	-	-	-	-	-	-	-	L/s	-	W/m <sup>2</sup>	°C	m	m	-	degrees
<b>Sensitivity</b>	-0.283	-0.284	-0.007	0.1251	0.3162	0.2109	0.2824	0.0543	0.0045	0.037	0.0547	0.0252	0.0796	-4E-04	0.0032

### 3.2.1 Major Geometry

The model geometry was selected to compromise between flexibility and complexity and to cover the majority of expected Canadian house designs. House plan shape was limited to rectangular and detached; though, the current work could be easily extended to other forms of houses. The aspect ratio (*AR*) was given limits between 0.5 and 2.0; representing most common ones and including what is considered to be the optimal range for passive solar performance: 1.2 to 1.3 (Athienitis, 2007). All of the houses have a 2.5 meter high basement; 60% of which is below-grade. The house can either be one or two-storey (*ST*); each storey is 2.75 meters in height. The total heated floor (including basement) area (*FA*) is constrained to between 100 and 450 m<sup>2</sup>. The house orientation (*OR*) is allowed to vary within a 90-degree range with the normal vector of Wall 1 ranging from southeast to southwest. Extending the range beyond this would allow redundancy of designs since the house is essentially symmetrical (i.e., beyond 45 degrees from south, Window 2 or Window 4 becomes Window 1). Additionally, it would reduce the efficiency of the artificial neural network, as described in Chapter 7. Major geometry is shown in Figure 3-5. Note that the walls and corresponding windows are named 1 through 4 because they are not necessarily oriented with the cardinal directions.

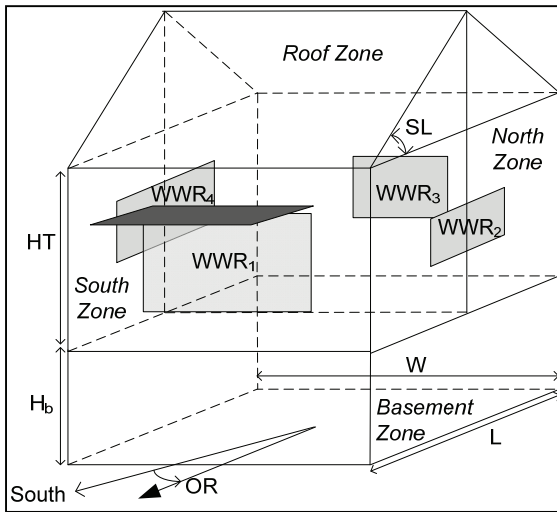


Figure 3-5: Major house geometry

The roof type (*RT*) is either gable or hip and covers a ventilated, unconditioned roof space. The eaves extend 30 cm outward from the exterior surface of all major exterior walls. The height of the roof is dependent on the roof slope (*SL*). The roof slope plays a significant role in predicted solar collector performance but has negligible effect on heating and cooling loads (O'Brien et al., 2010b). The length *L*, width *W* can be found with the following Equations.

$$W = [AR \cdot FA / (ST + 1)]^{1/2} \quad (3-2)$$

$$L = [FA / (ST + 1)] / W \quad (3-3)$$

A subtle though important detail is that the floor area, aspect ratio, and number of stories were selected as parameters to define major geometry rather than length and width. This is in recognition that the tool user is likely to fix the floor area at the beginning and then possibly manipulate aspect ratio.

### **3.2.2 Thermal and Control Zoning**

The house model, regardless of all parameter values, is comprised of a basement zone, two above-grade zones (north and south) and an unconditioned roof space zone, as shown by Figure 3-5. Three was selected in the interest of balancing accuracy and simplicity and is justified by extensive analysis that was first presented by O'Brien et al (2010b).

The following paragraphs are an excerpt from O'Brien et al (2010b):

“For modelling, a building should be subdivided into thermal zones such that a zone is attributed to each region with significantly different boundary conditions, loads, controls, and/or operating conditions. If higher resolution is required (e.g., knowledge of temperatures in a particular region of a building), further subdivision of zones is also appropriate. While early approaches for modelling houses used single-zone models, multizone models with interzonal airflow were developed to study individual heating and cooling loads and for the study of the distribution of air contaminants (Warren, 1996). Guides for energy modelling tools, such as that for EnergyPlus (US DOE 2009), suggest that the number of thermal zones represent the number of HVAC distribution units serving the building. Often, HVAC control zoning provides cues about thermal zoning (ASHRAE, 2005). In houses, using forced-air or hydronic distribution systems, it is possible to independently control zones with different needs (e.g., bedrooms, kitchen, living room) using thermostatically controlled dampers or valves (NRCan 2010a). For example, the Belgian PLEIADE row house described by Hestnes et al (2003), has four

independently-controlled zones. The literature indicates that there are instances of houses with between two and eight control zones being used in solar houses (e.g., see Athienitis (2007) and Galloway (2004)). The EnergyPlus manual (US DOE 2009) states that building modellers should avoid assigning a zone to each room of a building, though it admits that the task of zoning is an art form. Greater discretization of a space requires increased model input time, simulation time, and, more importantly, additional specification of interzonal heat transfer.

Many building energy simulation programs for houses (e.g., HOT3000 (CANMET CETC 2008) and BEopt (NREL 2009)) model the entire above-grade occupied space as a single zone, thus assuming that the air throughout the house is well-mixed. This may be suitable for typically-glazed, solar neutral homes (those with equal glazing area on all facades (Hayter et al., 2001)), but is less so when significant heat gains only occur in certain zones. Thus, the appropriate attribution of thermal zones to model buildings with passive solar features is an important area of research.

While the use of more control zones offers the advantage that thermal comfort can be maintained to a higher degree of resolution, it occurs at the expense of additional equipment and distribution costs. However, this can be, at least partially, offset with smaller ducts, equipment, and operating costs. For example, the Athienitis house (Athienitis, 2007) is programmed to operate only one of the two stages of the two-stage heat pump during periods when only one zone requires heating or cooling.

The specific results from this work suggest that for performance modelling of passive solar houses, the above-grade portion should be divided into at least two zones: direct gain and non-direct gain. The use of one zone should be limited to cases in which the house truly exists as a single space or CFD simulations have been performed to indicate that interzonal airflow approaches a level that is equivalent to perfect mixing. The use of multiple zones allows the potential for overheating to be better characterized. For HVAC design purposes, this allows heat to be added or removed from each zone, independently, as needed. If a conservative model is required, more zones should be modelled, such that the consequences of poorly distributed solar heat gains can be characterized.

Figure 3-7 shows the combined heating and cooling energy for the four different zonal configurations (shown in Figure 3-6). The results indicate that the models with more zones are consistently predicted to underperform relative to those with fewer zones. This is because heating is frequently used in the non-direct gain zones, even if the direct gain zone(s) is/are overheating. The configuration with just one or two zones implies that the solar-heated air is well-mixed throughout the house, thus using their heat capacity and making up for their heat losses in non-direct gain zones. The curves for the three and five-zone models are similar because both of them isolate the direct gain zone(s) from the rest of the house. Thus, the extra effort to discretize the south side of the house may not be justified. Similarly, the results suggest that the use of a single above-grade zone would be sufficient for houses with small glazing areas.”



Figure 3-6: Four different zoning configurations that were considered (taken from (O'Brien et al., 2010b))

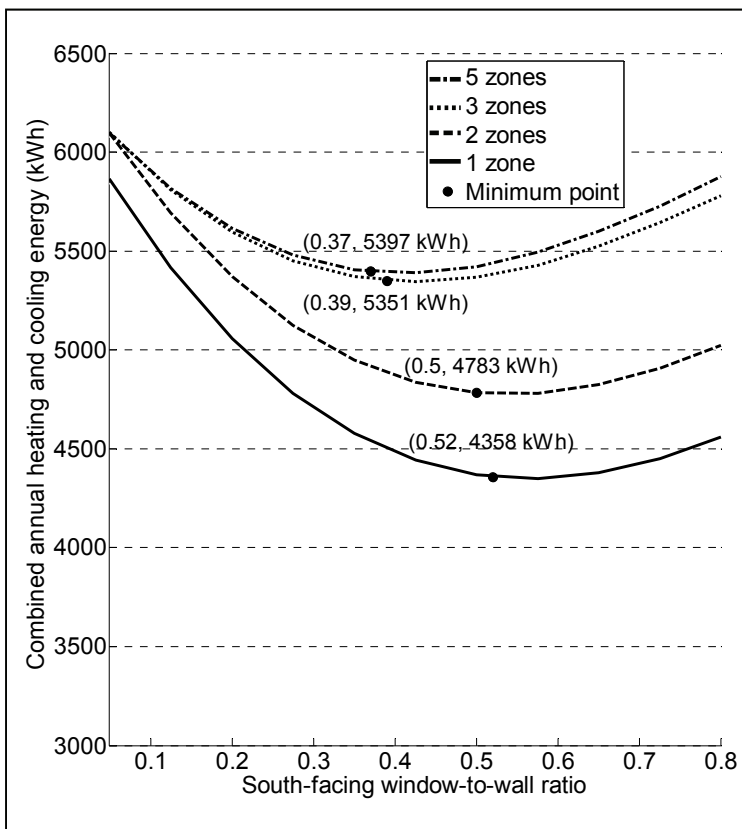


Figure 3-7: The effect of thermal zoning configuration on energy performance of a passive solar house (taken from (O'Brien et al., 2010b))

The results in Figure 3-8 show a similar result: there is little different in predicted overheating between the three and five-zone configurations. The definition of overheating that is used throughout this work is fully explained in Section 3.2.16.



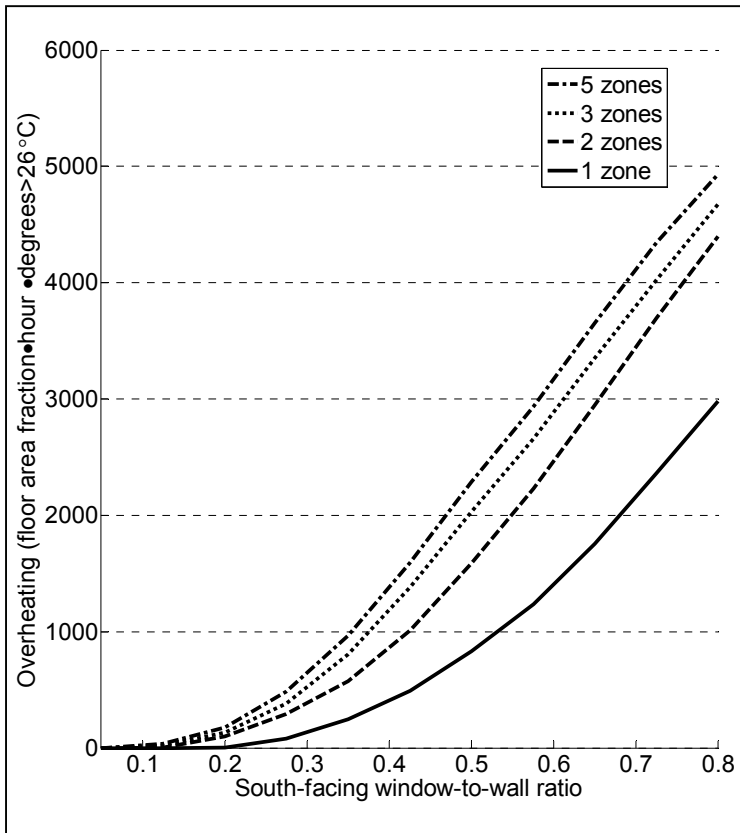


Figure 3-8: Magnitude of overheating as a function of zonal configuration and window size (taken from (O'Brien et al., 2010b))

In short, since Ecos is primarily intended to be used for houses with some passive solar features, the model should properly characterize the potential of overheating. Thus, the three-zone configuration, as shown in Figure 3-6, is used.

### 3.2.3 Opaque Envelope

The opaque envelope was modelled with reasonable materials to characterize their thermal behaviour. The purpose of Ecos is not to advise about exact wall constructions and how to prevent thermal bridging, but rather, how house performance is affected by certain R-values. It follows that upon selecting a certain R-value in Ecos, the designer would have to design a wall construction that exhibits the corresponding thermal

resistance. While EnergyPlus has the capability of modelling heat and moisture transfer simultaneously (EnergyPlus, 2009a), the focus of this work is on heat transfer; the material layers in the envelope constructions reflect this. The wall construction is summarized in Table 3-3. The only adjustable parameter for the exterior wall construction is the insulation thickness (WR).

*Table 3-3: Material properties of the wall construction*

	Thickness (m)	Conductivity (W/mK)	Density (kg/m <sup>3</sup> )	Heat capacity (J/kgK)	Solar absorptance	Emissivity
Outside finish – Wood siding	0.0254	0.09	592	1170	0.5	0.9
Core - Insulation	WR-k	0.03 (k)	19	960	0.4	0.9
Inside finish - Gypsum	0.0159	0.12	540	1210	0.4	0.9

Similarly, the ceiling construction is summarized in Table 3-4. As mentioned, the houses are limited to having a vented roof space, so all of the insulation is immediately outside the ceiling.

*Table 3-4: Material properties of the ceiling construction*

	Thickness (m)	Conductivity (W/mK)	Density (kg/m <sup>3</sup> )	Heat capacity (J/kgK)	Solar absorptance	Emissivity
Outside - Insulation	CR-k	0.03 (k)	19	960	0.4	0.9
Inside finish - Gypsum	0.0159	0.12	540	1210	0.4	0.9

The roof is modelled as having a layer of plywood topped with metal cladding. The properties of the roof are not critical because: A) the conditioned zones are isolated for the roofspace and B) the roof space is highly-ventilated. The modelled roof construction cannot be changed by parameters and is summarized in Table 3-5.

Table 3-5: Material properties of the roof construction

	Thickness (m)	Conductivity (W/mK)	Density (kg/m <sup>3</sup> )	Heat capacity (J/kgK)	Solar absorptance	Emissivity
Outside – metal cladding	0.008	45	7800	500	0.7	0.9
Inside - plywood	0.018	0.09	592	1170	0.4	0.9

The basement constructions are described in Section 3.2.10. Each of the two above-grade zones has a 2 m<sup>2</sup> door with a thermal resistance of 1.3 m<sup>2</sup>K/W.

The influence of the four opaque envelope insulation levels is shown in Figure 3-9 under the nominal design conditions. As expected, they all provide diminishing returns; at some level, other options become more practical and economical-attractive.

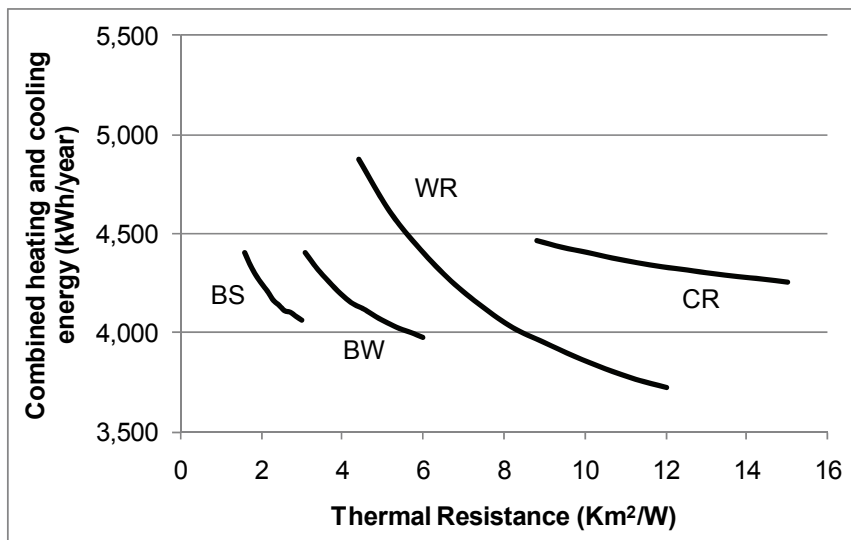


Figure 3-9: Influence of the four opaque envelope thermal resistance parameters

It is worth noting that the model is aimed at thermal analysis and not moisture transfer.

If moisture transfer were modelled, the surface constructions would have to contain vapour barriers and rain protection.

### **3.2.4 Windows**

Windows are a key element of passive solar houses and have been shown to have a significant effect on performance thus justifying their accurate modelling. There are two main physical phenomena to properly characterize in the model: transmitted solar radiation and thermal conductance.

The main heat flow paths related to windows are the glazing, the frame, the spacers, and the dividers (if present). Frames and spacers are often more conductive than the glazing section, which causes thermal bridging and results in 3D conduction. However, to simplify simulation, windows are modelled in three main regions: centre of glass, edge of glass, and frame; each assumed to have only 1D conduction (EnergyPlus, 2009b), as shown in Figure 3-10. The edge of glass forms a 6.5 cm perimeter around the outside of the glazing and its properties can be obtained from Window6 (LBNL 2010) among other programs. The optical properties of the edge of glass are the same as the centre of glass, while the thermal properties are dependent on both the frame and glass regions. Similarly, the frame and glazing section properties can be obtained from Window6 for a wide range of available products.

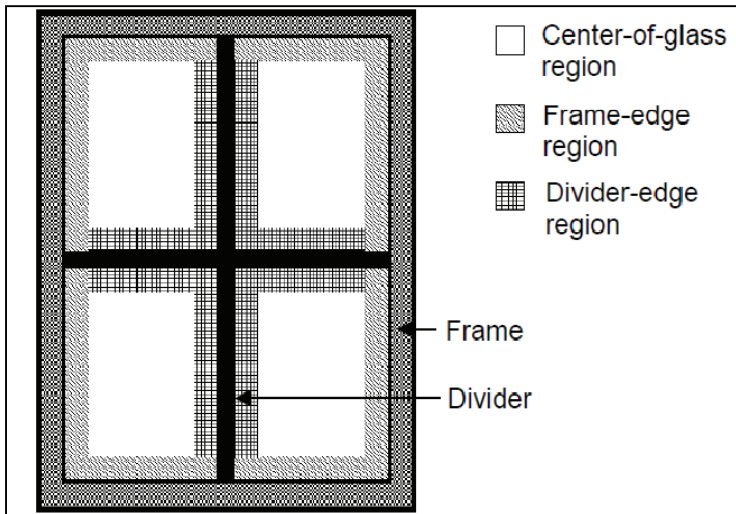


Figure 3-10: Three heat flow paths for windows (EnergyPlus, 2009b)

Once the effective 1D properties of the window sections are obtained, the total effective conductance and solar heat gain coefficient of the entire window are merely area-weighted averages as shown by Equations 3-4 and 3-5.

$$U_w = (A_f U_f + A_{eog} U_{eog} + A_{cog} U_{cog}) / (A_f + A_{eog} + A_{cog}) \quad (3-4)$$

$$SHGC_w = (A_f SHGC_f + A_{eog} SHGC_{eog} + A_{cog} SHGC_{cog}) / (A_f + A_{eog} + A_{cog}) \quad (3-5)$$

The quantification of windows' short-wave radiation transmittance is more complex than the thermal analysis the properties are dependent on the solar incidence angle. Frames, dividers, reveals, insect screens, movable shading devices, fixed shading devices, building surfaces, and external obstructions all affect the amount of short-wave radiation that is transmitted by windows.

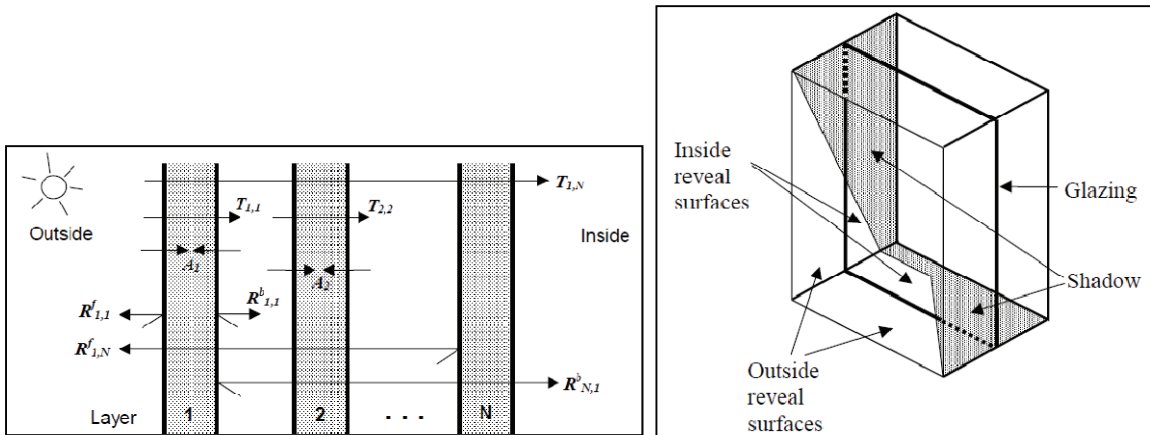


Figure 3-11: Radiative phenomena for multiple glazing layer (left) and example of how window components can affect shading (right) (EnergyPlus, 2009b)

EnergyPlus has the option of specifying customized spectral properties of glazing. This would be appropriate for spectrally selective glazing, such as those that have coatings with significantly different optical properties for different wavelengths.

Windows are one of EnergyPlus' more powerful and detailed elements. Their properties can be specified in terms of U-value and SHGC or they can be comprised of layers consisting of glass (coated or thermochromic), gas fills, insect screens, movable insulation, and shades or blinds (exterior, between pane, and interior), as indicated in Figure 3-11. Additional details can be provided about spectrally-selective glazing, frames, dividers, reveals, and sills. This modelling complexity must be supported with care to choose the most appropriate model resolution that offers accuracy without the burden of excessive complexity. Several extensive sensitivity analyses were performed and published. O'Brien et al (2010a) modelled ÉcoTerra with the intent of examining potential strategies to reduce energy consumption. They found that removing the

window dividers from the windows reduced predicted heating energy by a staggering 10%.

Typically, glazing is specified by its properties at normal incidence. However, transmittance decreases as the solar incident angle deviates from normal. EnergyPlus determines the properties for other incident angles using the following three relationships (EnergyPlus, 2009b):

$$T(\phi) = \frac{\tau(\phi)^2 e^{-\alpha d / \cos\phi'}}{1 - \rho(\phi)^2 e^{-2\alpha d / \cos\phi'}} \quad (3-6)$$

$$R(\phi) = \rho(\phi)(1 + T(\phi)e^{-\alpha d / \cos\phi'}) \quad (3-7)$$

$$\rho(\phi) = \left[ \left( \frac{n \cos\phi - \cos\phi'}{n \cos\phi + \cos\phi'} \right)^2 + \left( \frac{n \cos\phi' - \cos\phi}{n \cos\phi' + \cos\phi} \right)^2 \right] \quad (3-8)$$

The glazing types (*GT*) available in the model are listed in Table 3-6. The corresponding glass properties are shown in Table 3-7. The gas fill gaps are standard thicknesses and near-optimal for thermal resistance, as discussed in Section 2.2.7. The glazing types were selected to represent a wide range of commonly-available options. The performance data was obtained from Window 6 (LBNL 2010) and confirmed with EnergyPlus (which uses the same algorithms). It is important to note that window properties, despite appearing to be universally-constant (under different conditions) are calculated using the NFRC 100-2010 (National Fenestration Rating Council) conditions (LBNL 2010). Furthermore, optical properties are generally specified for normal incidence. Under these conditions, transmittance is normally at a maximum because the light has to penetrate the minimum thickness of glass. In reality, many windows never

experience normal incidence and the total incident solar radiation is combination of direct normal, ground reflected, and diffuse sky solar radiation. ASHRAE (2005) describes how to determine the hemispherical average for optical properties. Table 3-6 shows the SHGC at both normal incidence and the hemispherical average. The latter is about 0.1 lower for the glazing types shown – a significant amount. For heat balance studies (see Appendix C), the hemispherical average is more appropriate. However, the exact effective SHGC will depend on the window’s orientation. For instance, a North-facing window in Toronto will never experience normal direct solar radiation.

*Table 3-6: Summary of glazing types available in the Ecos. Thick cell borders indicate the surface that the low-e coating is on. The naming convention is: first two letters indicate the number of glass layers, second two letters indicate whether all of the glass is clear or if one of them has a low-e coating, and the last two letters indicate whether the gas fill is air or argon.*

<b>Name (<math>GT_i</math> index)</b>	<b>DGLEAR (1)</b>	<b>TGCLAR (2)</b>	<b>TGLEAR (3)</b>	<b>QGLEAR (4)</b>
<b>Outside Layer</b>	Clear 3mm	Clear 3mm	Clear 3mm	Clear 3mm
.	Argon 12.7 mm	Argon 12.7 mm	Argon 12.7 mm	Argon 12.7 mm
.	Low-e 3.8mm	Clear 3mm	Clear 3mm	Low-e 3.8mm
.		Argon 12.7 mm	Argon 12.7 mm	Argon 12.7 mm
<b>Inside Layer</b>		Clear 3mm	Low-e 3.8mm	Low-e 3.8mm
				Argon 12.7 mm
				Low-e 3.8mm
<b>Air space between inner glass layer and shade (if shade present)</b>	5 cm air space	5 cm air space	5 cm air space	5 cm air space
<b>Shade (if present)</b>	Reflective roller shade	Reflective roller shade	Reflective roller shade	Reflective roller shade
<b>U-value (<math>W/m^2K</math>)</b>	1.499	1.629	1.055	0.525
<b>Edge U-value (<math>W/m^2K</math>)</b>	2.625	2.680	2.473	2.363
<b>SHGC (normal incidence)</b>	0.690	0.685	0.612	0.533
<b>SHGC (hemispherical average)</b>	0.601	0.579	0.516	0.441



Table 3-7: Glass properties (from Window 6 software)

Name	Clear 3 mm	Low-e 3.8 mm
Window 6 Glass ID #	102	13008
Thickness	0.003 m	0.0038 m
Solar transmittance at normal incidence	0.837	0.729
Front side solar reflectance at normal incidence	0.075	0.177
Back side solar reflectance at normal incidence	0.075	0.155
Visible transmittance at normal incidence	0.898	0.890
Front side visible reflectance at normal incidence	0.081	0.066
Back side visible reflectance at normal incidence	0.081	0.073
Infrared transmittance at normal incidence	0	0
Front side infrared reflectance at normal incidence	0.84	0.093
Back side infrared reflectance at normal incidence	0.84	0.84
Conductivity	1.0 W/mK	1.0 W/mK

The model allows three different window frame types, as summarized in Table 3-8. They were obtained from the standard Window 6 and ASHRAE (2005) configurations. The window frame type (*FT*) parameter is one of those with discrete values.

Table 3-8: Window frame properties

Type ( <i>FT</i> index)	Aluminum with thermal break (1)	Wood (2)	Vinyl (3)
U-value (W/m <sup>2</sup> K)	5.68	2.27	1.70
Width (m)	0.0568	0.0695	0.0695

With properties for the three major window areas (centre of glass, edge of glass, and frame), the total window properties can be determined using Equations 3-4 and 3-5. The three areas corresponding to those shown in Figure 3-12 can be determined using the following Equations.

$$A_f = 4W_f^2 + 2(W_w + H_w)W_f \quad (3-9)$$

$$A_{eog} = 4(0.0635m)^2 + 2(0.0635m)[(W_w - 2W_f) + (H_w - W_f)] \quad (3-10)$$

$$A_{\text{cog}} = W_w \cdot H_w - A_f - A_{\text{eog}} \quad (3-11)$$

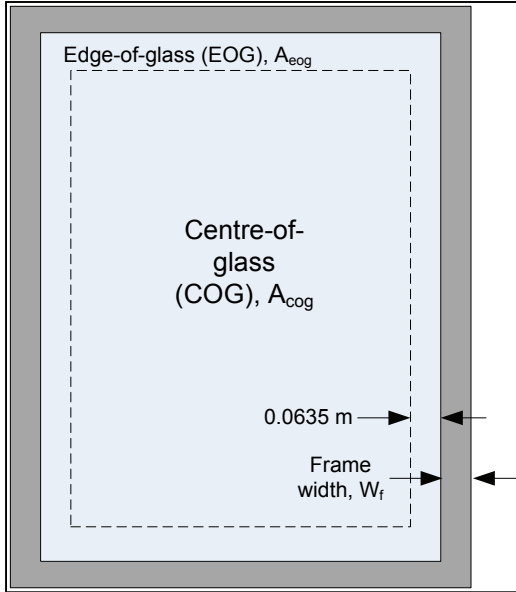


Figure 3-12: Major window components and geometry

The total window properties are merely area-weighted averages since the sectional properties were determined for this use (i.e., they are intended to be used as one-dimensional values). Note that the edge of glazing SHGC is equal to the centre of glass SHGC. Interestingly the SHGC for window frames and other opaque constructions is not zero, by definition, because some incident solar radiation is absorbed and conducted inwards. ASHRAE (2005) reports that SHGC for frames can be found using:

$$SHGC_f = \alpha_f^s \left( \frac{U_f}{h_f} \right) \left( \frac{A_f}{A_{\text{surf}}} \right) \quad (3-12)$$

Where  $\alpha_f^s$  is the absorptance of the frame,  $U_f$  is the conductance of the frame,  $h_f$  is the exterior heat transfer coefficient, and  $A_f/A_{\text{surf}}$  is the projected to surface area ratio. For

light-coloured window frames, the SHGC is likely to be on the order of 0.05 to 0.1. For well-insulated walls, it approaches zero because of the low U-value.

The U-values and SHGCs were calculated for every allowable glazing-frame combination for a 1.2 by 1.5 meter window (measured at outer edge of frame) and are shown in Table 3-9 and Table 3-10. The notable conclusions that can be drawn are that despite their proportionately-small area, the frame type has a significant (and negative) impact on thermal performance – particularly with the high-performance glazing; and frame type has minimal impact on SHGC since  $SHGC_f$  is relatively low for all frames.

*Table 3-9: Whole window U-values for all glazing and frame combinations*

	<b>Aluminum with thermal break (1)</b>	<b>Wood (2)</b>	<b>Vinyl (3)</b>
<b>DGLEAR</b>	2.45	1.94	1.83
<b>TGCLAR</b>	2.46	1.95	1.84
<b>TGLEAR</b>	2.10	1.59	1.48
<b>QGLEAR</b>	1.67	1.18	1.06

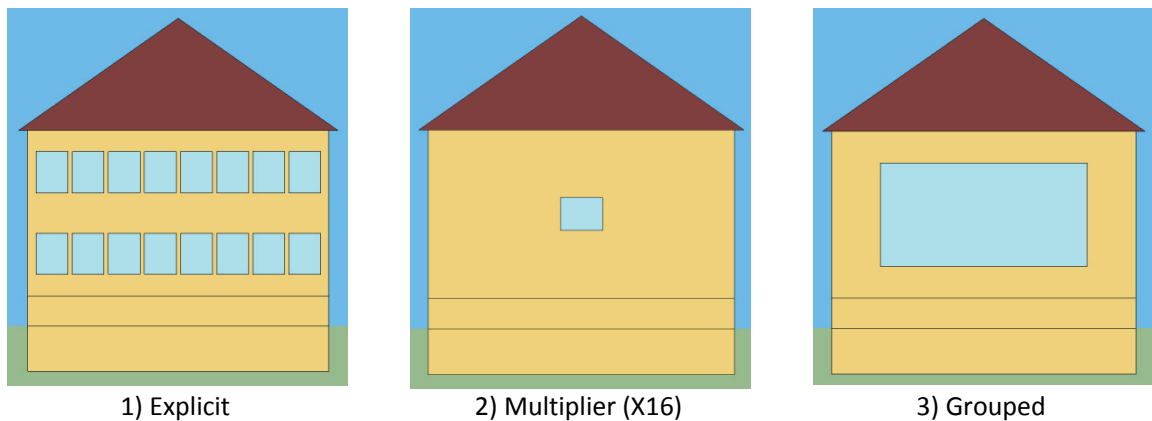
*Table 3-10: Whole window SHGCs for all glazing and frame combinations*

	<b>Aluminum with thermal break (1)</b>	<b>Wood (2)</b>	<b>Vinyl (3)</b>
<b>DGLEAR</b>	0.600	0.589	0.589
<b>TGCLAR</b>	0.573	0.563	0.563
<b>TGLEAR</b>	0.532	0.522	0.522
<b>QGLEAR</b>	0.369	0.362	0.362

With the window model implemented, consideration must be given to how they are integrated into the envelope. Three methods for modelling window geometry, in descending order of theoretical accuracy, are:

1. **Explicit:** each window is explicitly modelled as it would appear on the house. This is the most detailed and accurate, but also requires the most effort. Framing and frame-edge effects are accounted for with regards to both heat transfer and shading. Furthermore, this approach allows proper daylighting analysis, which is highly-dependent on window sizes and positions. Similarly, the effect of fixed external shading devices, such as overhangs, is better characterized if the windows are explicitly modelled. However, knowledge about window sizes and locations are required, yet unlikely to be available early in design.
2. **Multiplier:** a reasonably-sized window is modelled and its effects on house performance are multiplied by some integer. In EnergyPlus, the appropriate area of opaque envelope is removed as to not double-count surface area. This approach properly characterizes the effects of shading and conduction associated with a standard size of window. Its only limitation is that it is unsuitable for daylighting, since daylighting performance is sensitive to window location. The effect on passive solar performance is not expected to be significant since direct short-wave radiation is distributed over the entire surface or surfaces that it is incident on.
3. **Grouped:** windows are grouped as a single window with a frame that extends around its perimeter. This approach means that there is a direct translation from window-to-wall ratio (*WWR*) and window dimensions. However, it means

that the frame area is at a minimum relative to the glazing area, thus underestimating the effect of window frames. One approach to overcoming this is to separately model the frame as a rectangular region of equivalent area. However, this does not allow one to take advantage of EnergyPlus' built-in frame modelling capability and it neglects shading from frames.



*Figure 3-13: Three possible window modelling methods*

To compare the effect of grouping windows on optical and thermal properties of a window, a comparison was made between sixteen 1.2-by-1.5 meter windows and a single window with the same glazing area (see Table 3-11 and Table 3-12). Triple-glazed, low-e, argon-filled glazing was used with a vinyl frame, as previously defined. The total U-values and SHGCs clearly indicate that the explicitly defined windows are poorer performing for passive solar houses (in which low U-values and high SHGCs are desirable).

The three window modelling methods were simulated for a whole year under the nominal design conditions. The window properties for the cases are shown in Table 3-11 and Table 3-12. The equivalent window to wall ratio is 40%. But note that, as

throughout this work, “window area” is actually the glazing area. The results are summarized in Figure 3-14. The second and third measured quantities represent the total incident shortwave radiation that was absorbed by the floor and interior wall in the south zone, respectively.

*Table 3-11: Properties of explicitly defined windows (per window); also applies to multiplier option*

Explicit	Area		U-value	SHGC
	m <sup>2</sup>	%		
<b>COG</b>	1.15	64.0%	1.133	0.533
<b>EOG</b>	0.29	16.2%	2.473	0.533
<b>Frame</b>	0.36	19.8%	1.7	0
<b>Total</b>	1.8	100.0%	<b>1.46</b>	<b>0.43</b>

*Table 3-12: Properties of grouped windows*

Grouped	Area		U-value	SHGC
	m <sup>2</sup>	%		
<b>COG</b>	21.81	88.9%	1.133	0.533
<b>EOG</b>	1.29	5.3%	2.473	0.533
<b>Frame</b>	1.42	5.8%	1.700	0
<b>Total</b>	24.52	100.0%	<b>1.24</b>	<b>0.50</b>

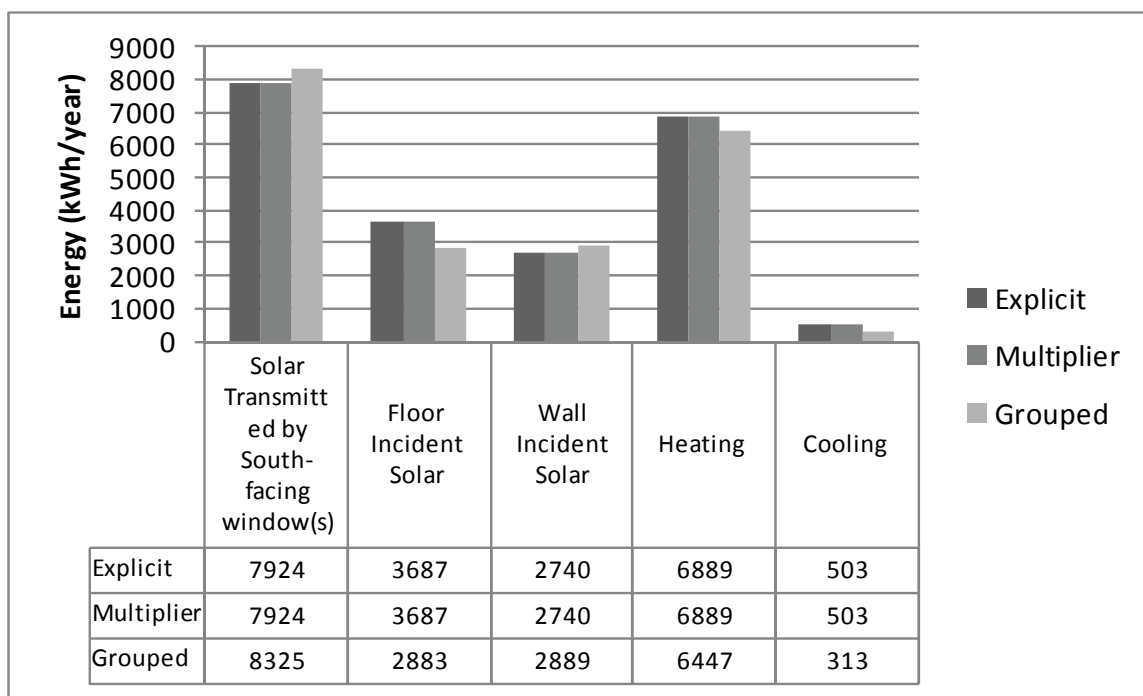


Figure 3-14: Effect of window modeling resolution.

The results indicate that the explicit and multiplier methods yield nearly identical results for all measured metrics, as expected. The results for the interior solar distribution suggest that exact positioning of windows is not critical to passive solar performance predictions. The grouped window model consistently over-performed over others. This is because of the reduced framing effect – both from shading and higher conductance. However, the effect is within about 5% for all measured quantities, except for cooling. While predicted cooling is 40% less for the “grouped” case, the absolute amount of cooling is relatively low. Interestingly, the explicit windows case took nearly twice as long to simulate (70.66 s) as the other cases (37.8 s).

The results from this study are most applicable to the combination of high-performance windows and frames. The accuracy would decrease further under any of the following conditions:

1. Frames that have a higher U-value.
2. Shading caused by frames is greater because of their geometry (e.g., deep reveal).
3. There is a greater number of small windows.

Despite the small amount of inaccuracy associated with grouping windows, this is the method that is used in the model. This is justified by the significantly greater simplicity over explicitly modelled windows. While the multiplier method is promising, its major limitation of not being able to calculate daylight means that the model cannot be extended in its capabilities in the future, as intended.

The glazing area is defined by the window-to-wall ratio for each of the four directions, as  $WWR_1$ ,  $WWR_2$ ,  $WWR_3$ , and  $WWR_4$  for nominally south, east, north, and west-facing windows, respectively. They are centered within the wall with an equal aspect ratio to the wall. The windows on the nominally east and west-facing windows are divided equally between the south and north zones. The effect of window-to-wall ratio on combined heating and cooling energy for the different orientations is shown in Figure 3-15. As expected, except for the south-facing window ( $WWR_1$ ), larger windows require more energy use.



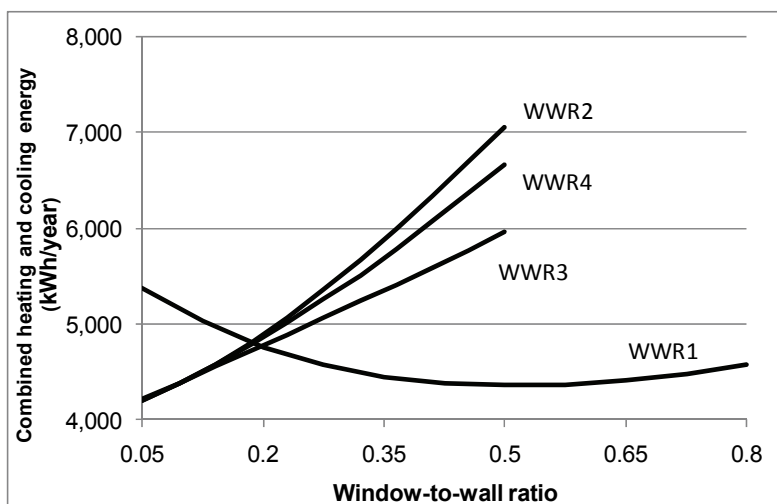


Figure 3-15: Effect of WWR1 through WWR4 on energy use

### 3.2.5 Fixed Shading

This section covers the shading of windows by fixed surfaces: overhangs. Since the generic model is rectangular, there are no instances of self-shading by walls – though EnergyPlus can account for it. A modest amount of shading occurs from the eaves on the roof, which extend out from the walls by 30 cm.

The fixed shading device in the model is an overhang over the window on Wall 1 (the wall that is nearest to south-facing). Overhangs have the advantage over moveable shading devices that they have no moving parts and exclude nearly all overhang-incident solar radiation from entering the house. However, their effectiveness is dependent on proper sizing and is premised on the fact that seasonal usefulness of solar gains is in phase with solar altitude. Overhangs have been found to be ineffective for East, West, and North-facing windows because incident solar radiation occurs on those windows at low solar altitudes when only very large overhangs could possibly obstruct the windows. Even overhangs for south-facing windows have limited benefit to the

Toronto climate because the solar altitude is low in the shoulder seasons (thus, avoiding standard overhangs) yet there are mild temperatures; the result is potential overheating. Nevertheless, overhangs have been included in the model because they are considered a standard element of passive solar design and have been found, through analysis, to be moderately effective at reducing energy use and discomfort.

The overhang geometry is defined by the ratio ( $OH$ ) of its depth to the glazing height. The range for  $OH$  is between 0 and 0.5. The script that creates the model input file automatically adjusts the height of the overhang above the top of the glazing ( $h_{OH}$  in Figure 3-16) to ensure that  $\alpha_{min}$  is the same as the solar altitude at solar noon at Winter Solstice (about  $21.5^\circ$  for Toronto). This ensures that the top of the glazing is never shaded from beam solar radiation in accordance with the EQUilibrium guidelines (Canada Mortgage and Housing Corporation (CMHC), 2009), among other overhang design guidelines (Balcomb, 1992). The entire glazing is shaded at solar noon on the Summer Solstice if  $\alpha_{max}$  is set to the solar altitude at solar noon at Summer solstice (about  $68.5^\circ$  for Toronto). The relevant geometrical relationships are defined by Equations 3-12 and 3-13. The side edges of the overhang are fixed to being directly above the edges of the glazing for simplicity. For the example shown in Figure 3-16, the south-facing wall is 10 meters wide and 5.5 meters high.

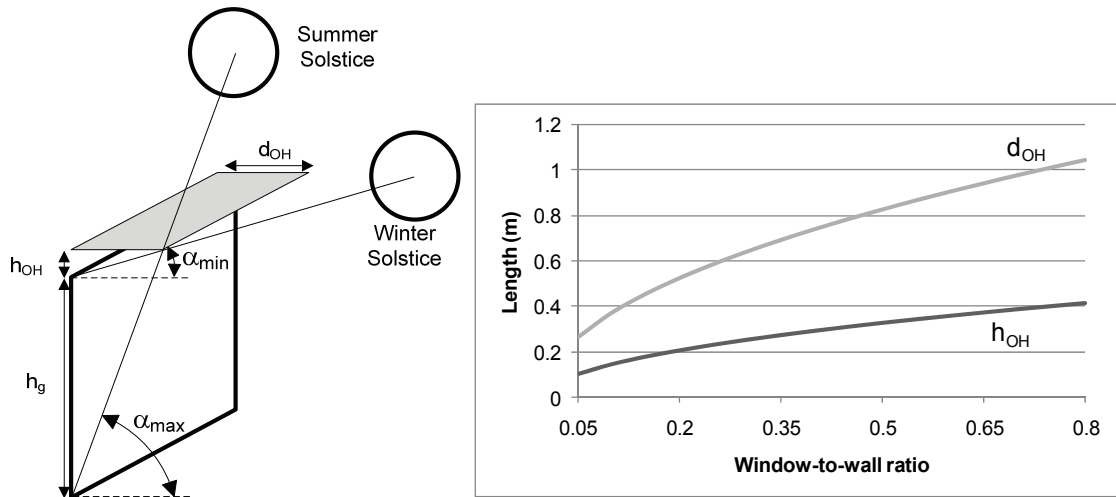


Figure 3-16: Overhang geometrical specifications (left) and the “ideal overhang” geometry right) (taken from O’Brien et al (2010b))

$$\tan(\alpha_{min}) = h_{OH} / d_{OH} \quad (3-12)$$

$$\tan(\alpha_{max}) = (h_{OH} + h_g) / d_{OH} \quad (3-13)$$

### 3.2.6 Moveable Shading Devices

One of the passive cooling techniques in the house model is controlled moveable shades. The model is limited to interior shades on all windows. These have previously shown to be very effective at reducing cooling loads if properly controlled (O'Brien et al., 2010b). They can also be used to reduce nighttime heat losses, though care must be taken to prevent condensation since isolating the window from indoors could cause them to cool down below the dew point.

EnergyPlus calculates the effect of shading devices using an energy balance for each layer of glass and the shading device, as illustrated by Figure 3-17, for each simulation timestep. The full derivation of the algorithm is presented in the EnergyPlus Engineering

Reference (EnergyPlus, 2009b). The modelled shade properties are summarized in Table 3-13.

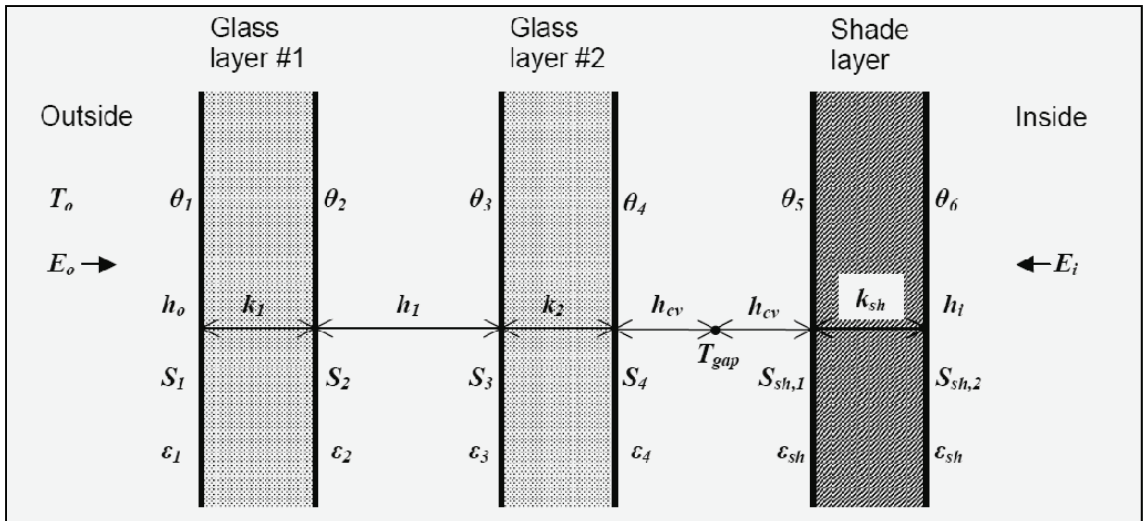


Figure 3-17: Cross section of fenestration showing glass layers and a shading layer (EnergyPlus, 2009b)

Table 3-13: Shade properties

Solar and visible reflectance	0.8
Solar and visible transmittance	0.0
Emissivity	0.9
Air permeability	0.2
Thickness	0.001 m
Conductivity	0.3 W/m2K

The parameters for the shades are control thresholds: incident solar radiation on exterior of window (*BLS*) and outdoor air temperature (*BLT*). The shades are controlled to close if both of these values are exceeded. Rather than have the option to have no controlled shades (as would be seen in a house with inactive occupants or merely without shades), the thresholds can be set to values such that the shades never close. The *and* control function eliminates the need for seasonal scheduling since a *BLT* value

of about 15°C is usually suitable for preventing significant summertime solar gains. *BLS* is limited to between 0 and 800 W/m<sup>2</sup>, representing the total expected range of values. *BLT* is limited to between 10 and 35°C, representing the range of outdoor temperatures when overheating can occur. If a designer finds values below 10°C to be beneficial, the house is likely over-glazed. The upper range of *BLT* can be used to effectively eliminate the presence of shades, since it does not occur in the Toronto weather file.

O'Brien et al (2010b) found optimal values of *BLS* and *BLT* to be 150 W/m<sup>2</sup> and 20°C, and reported that *BLS* values ranged from 150 to 250 W/m<sup>2</sup> in the literature.

EnergyPlus only allows shades to be fully up or fully down, as reported by O'Brien et al (2010d), but this is not a major limitation if daylighting performance is not being measured. Future work (both modelling and the technology) on exterior shades would be extremely beneficial since they are more effective at controlling solar gains.

### **3.2.7 External Shading**

One of the more complex issues of building performance modelling is characterizing external solar obstructions (e.g., neighbouring buildings, landscaping elements). Passive solar houses – with large windows – are particularly sensitive to shading. For instance, the ÉcoTerra house's trees underwent major trimming following a survey of the site and potential shading (see Figure 3-18).

The current work is premised on the fact that solar obstructions are not an issue because they are either designed around or modified. The choice to exclude solar

obstructions from the model is justified by the fact that geometries can be complex and cannot be easily defined by a small number of parameters, as many of the other aspects are. If it is expected to be an issue the designer should explicitly model solar obstructions immediately following the use of Ecos. The limitation to this approach is that the designer would have already optimized the window area assuming no unwanted shading.

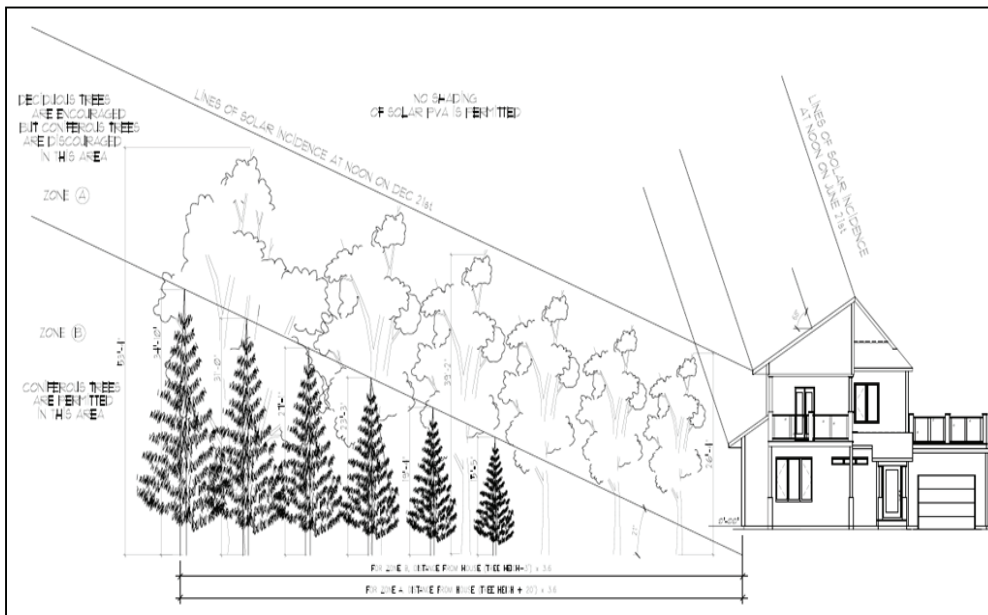


Figure 3-18: Side view of ÉcoTerra house showing potential solar obstructions and the extreme seasonal solar altitudes.

### 3.2.8 Thermal Mass

Thermal mass plays an important role in moderating the indoor air temperature in highly-glazed passive solar houses. The model allows a concrete slab on the floor of the South zone and a concrete wall dividing the South and North zones, as shown in Figure 3-19. The parameters used to define the thicknesses of these surfaces are TMS and TMV, respectively. They each have limits of between 0.001 m and 0.2 m. The lower end

of the range would be used for standard wood-frame construction without any added thermal mass. It is not 0 because that is more difficult to implement in the script. The upper range represents a near optimal value, as explained in Section 2.2.9.1.

Furthermore, from a practical perspective the high embodied energy of concrete and the required structural support of thick slabs favour thinner slabs. The modelled concrete thermophysical properties are fixed at the values shown in Table 3-14.

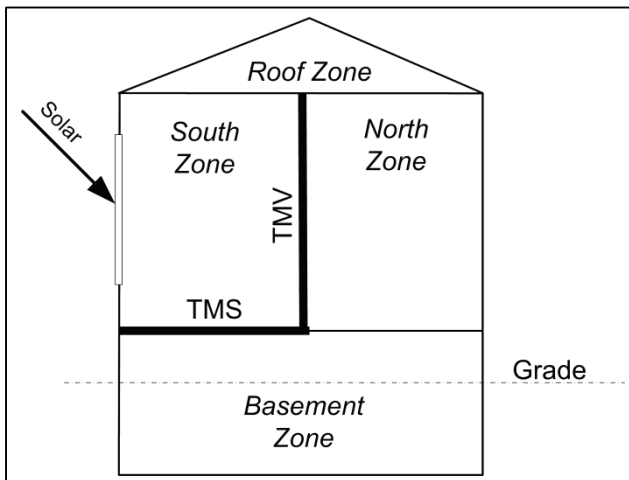


Figure 3-19: Section view of house showing locations of concrete slabs.

Table 3-14: Modelled concrete properties

Thickness (m)	TMS or TMV
Conductivity (W/mK)	1.95
Density ( $\text{kg/m}^3$ )	2240
Specific heat (J/kgK)	900
Reflectance	0.9
Absorptance	0.7
Emissivity	0.5

Since the EnergyPlus' finite difference algorithm is used, the concrete slabs (and other wall layers) are discretized into layers of equal thickness according to the Fourier stability criterion that was first introduced in Section 2.2.12. Although the implicit finite

difference method is used and is unconditionally stable for any control volume thickness, the criterion is used as a guideline. Solving for the control volume thickness yields the following relationship.

$$\delta x \geq \sqrt{\frac{2k\Delta t}{\rho C}} \quad (3-14)$$

The EnergyPlus formulation attempts to approach the explicit domain. For example, for a 50m<sup>2</sup> concrete slab with the above thermophysical properties and 180 second timesteps, EnergyPlus would use control volume thicknesses of  $[2 \cdot 1.95 \text{ W/mK} \cdot 180\text{s} / (2240 \text{ kg/m}^3 \cdot 900 \text{ J/kgK})]^{1/2} = 19 \text{ mm}$ . If the slab were 10 cm thick, EnergyPlus would use 6 control volumes in an attempt to approach the limit of stability. This can be overridden by manually discretizing a homogeneous layer into multiple layers in EnergyPlus. At the minimum, a particular material layer is represented by two surface nodes; each representing half of a control volume, as shown in Figure 3-20. For layers represented by more than 2 nodes, each additional inner control volume is represented by a node at its centre.

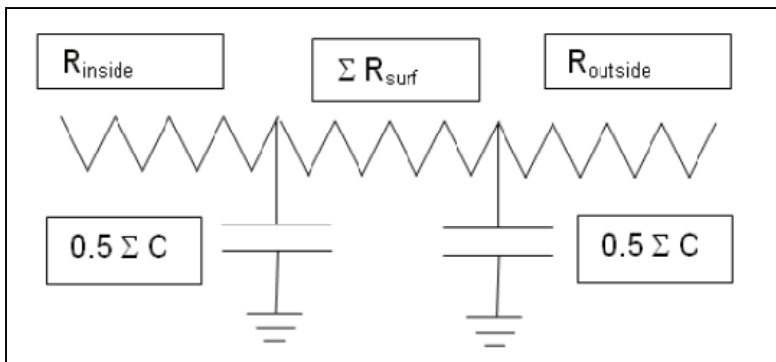


Figure 3-20: Representation of a thin material layer in EnergyPlus' implicit finite difference scheme (EnergyPlus, 2009b)



The thermal mass that was previously discussed is limited to that that is integrated into the building envelope or explicitly defined partition walls that define a zone. However, any occupied building is likely to have furnishings and equipment, all of which have some thermal capacity. There are two ways of defining these in EnergyPlus, as in most other simulation engines: implicitly defining them as a floating surface that does not affect radiation or with an air capacitance multiplier. The former method requires specific knowledge or assumptions of the positions of interior walls which is typically unknown early in design. Thus, the air capacitance multiplier approach was used for this model. A value of 20 was added to approximate the thermal mass effect of furnishings. Values of 10 to 30 are recommended for houses, as reported by Charron (2007). In practical terms, this causes the air contained by the zones to react more slowly to a given energy input.

### **3.2.9 Infiltration**

Infiltration is the measure of uncontrolled (and often unwanted) air exchange between a building and the outdoors. A building's airtightness can only be reasonably determined using a blower door test. Even post-construction visual inspection cannot accurately predict airtightness (American Society of Heating Refrigeration and Air Conditioning Engineers (ASHRAE), 2005). For early stage design, little is known about a house's infiltration characteristics, other than its major geometry and exposure to wind. Thus, this section focuses on two different infiltration modelling options, given that the mean air change rate is known.

EnergyPlus can either model infiltration as a fixed rate or have it dependent windspeed, outdoor temperature, house geometry, and exposure. The effective leakage area model is considered because it is suitable for small residential buildings (EnergyPlus, 2009a).

For it, infiltration is defined as follows.

$$\text{Inf} = \frac{A_L}{1000} \sqrt{C_S \Delta T + C_W V_{\text{wind}}^2} \quad (3-15)$$

where Inf is the instantaneous infiltration rate in m<sup>3</sup>/s, A<sub>L</sub> is the effective leakage area in cm<sup>2</sup>, C<sub>S</sub> is the stack coefficient, C<sub>W</sub> is the wind coefficient, ΔT is the temperature difference across the envelope, and V<sub>wind</sub> is the windspeed. The coefficients are based on empirical data and are typically provided for different building heights and general categories of wind exposure.

For the nominal house design, with “shelter conditions caused by other buildings across the street” and an effective leakage area of 120 cm<sup>2</sup> (selected as a typical value for high-performance homes) the mean annual infiltration for the model in the Toronto climate is 0.059 ach under normal conditions, or about 1.2 ach at 50 Pa. Sherman (1987) reported that in forty houses that were measured, the relationship between infiltration at 50 Pa and under actual conditions can be approximated with the following relationship. Though for certain geographic regions, the denominator could be as small as 13 or as large as 26.

$$\text{ACH} = \text{ACH}_{50}/18 \quad (3-16)$$

The effect of the infiltration rate varying with time can be determined by comparing the fixed rate model with the effective leakage area model. The reason that timing could have an effect - particular for passive solar houses – is that windspeed tends to be higher during the middle of the day when indoor temperatures are higher and thus, heat losses from infiltration could be higher.

*Table 3-15: Results from infiltration model (taken from O'Brien et al (2011b))*

Model	Mean annual Infiltration rate (ach)	Annual Heating Energy, kWh	Annual Cooling Energy, kWh
Fixed rate	0.0590	3,144	1,029
Effective Leakage Area	0.0590	2,964	1,010

The results of this analysis are shown in Table 3-15. They indicate that the temporal variation of infiltration rates is much less significant (about 6%) than the mean infiltration rate. Thus, the importance of identifying an appropriate infiltration rate is more important than the model, itself, for predicting the performance of un-built houses. The model uses a constant infiltration rate. The allowed range of infiltration rates in the model is between 0.025 and 0.15 ach under normal conditions, equivalent to between 0.45 and 1.35 ach at 50 Pa. These values represent the lowest portion of the spectrum of possible values in compliance for the model to focus on high-performance buildings. The literature review, Section 2.2.12.6, provides details on typical values. For the model, infiltration is assumed to be distributed evenly among all zones (relative to zonal volume).

### **3.2.10 Basement/ground coupling**

Basement heat losses have been reported to account for 10 to 40% of heating loads (Beausoleil-Morrison, 1996), and so, accurately modeling the basement-ground interface is important. Unlike above-grade surfaces for which the boundary is assumed to be air of a uniform temperature, below-grade surfaces interface with soil, which is thermally massive, and thus, slow to respond to weather conditions. The accepted assumption for the air boundary conditions in building simulation is that lost heat from the above-grade envelope is absorbed by the significantly vaster air space between buildings<sup>8</sup>. However, this is not a reasonable assumption for below-grade surfaces because the heat cannot quickly escape.

As reported in the literature review, ground temperatures are typically pre-processed based on basic foundation, soil, and climate characteristics and then input into the main building model. Because the ground temperature (below the surface) reacts very slowly (1-2°C/month) to outdoor air temperature, only monthly ground temperatures need be reported. The ground temperature model in EnergyPlus, which is based on a 3D finite difference method, is not well-suited for many typical basement configurations. For instance, it only allows exterior insulation on the basement walls and none above or below the basement floor.

---

<sup>8</sup> Recent research has found that this assumption is less valid for dense urban environments in which significant waste heat is generated and cannot be assumed to be completely dissipated to the ambient air as an infinite sink. The so-called “urban heat island” effect can cause the air temperatures to be up to 3°C warmer than in the surrounding regions, thus having adverse effects on cooling loads (Akbari, 2001).

Because basement models are normally decoupled from the main sub-hourly simulation of the house, there is no restriction on how the ground temperatures are determined. Thus, BASECALC (Beausoleil-Morrison, 1996), a comprehensive tool based on a 3D finite difference calculations was used. For ease of use, the process was scripted such that all parameters that describe basement geometry and thermal properties were varied and simulated. To limit the number of possible variations, only basement length, width, below-slab insulation, and the insulation outside the walls were examined. While having insulation on the inside of the concrete is another common configuration, this is unfavourable for passive solar houses because it isolates the thermal mass effect of the concrete, rendering it virtually useless. While windows in basements are typically small - and absent in the current model – the thermal mass in basements becomes useful if air is properly circulated from the direct gain zone to the other parts of the house (O'Brien et al., 2010b). The length and width of the basement are assumed to match that of the house. Insulation is assumed to be of uniform thickness for the entire basement floor or wall (below and above grade). Other inputs in the program include soil properties, basement depth, basement concrete thickness, insulation coverage, and basement air temperature. The default soil properties (by location) in BASECALC were used. As previously mentioned, the basement is assumed to be 2.5 meters high with 1 meter above grade. The basement walls and floor concrete thicknesses are assumed to be 0.2 meters and 0.1 meters thick, respectively. The basement configuration is shown in Figure 3-21 and the construction is tabulated in Table 3-16. The basement air

temperature is assumed to be a constant 20°C. This identifies a limitation of pre-processing the ground temperature: certain boundary conditions must be assumed. As shown in the sensitivity analysis, the model is quite sensitive to the assumed zone air temperature.

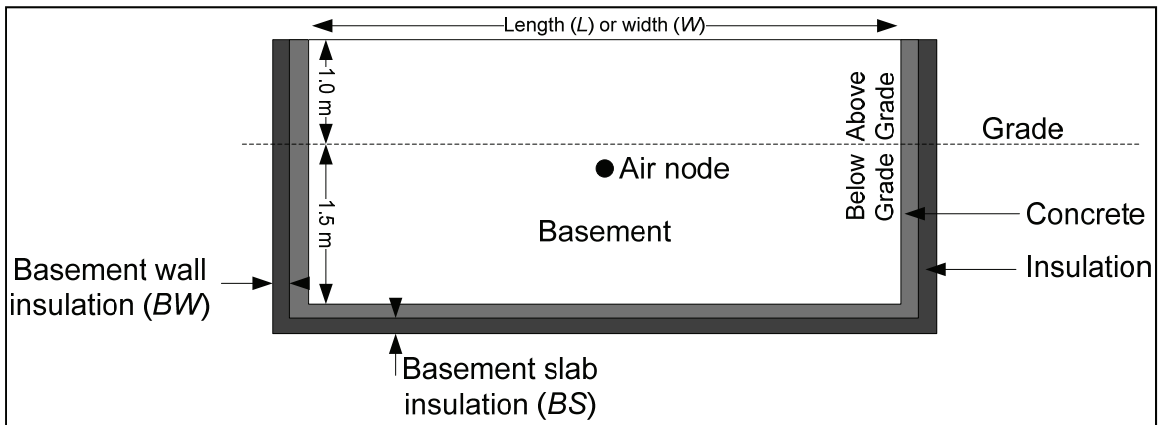


Figure 3-21: Schematic of basement configuration

Table 3-16: Material properties of basement wall and floor construction

	Thickness (m)	Conductivity (W/mK)	Density (kg/m <sup>3</sup> )	Heat capacity (J/kgK)	Solar absorptance	Emissivity
Outside - Insulation	Wall: BW·k Floor: BS·k	0.03 (k)	19	960	0.4	0.9
Inside finish - Concrete	Wall: 0.2 Floor: 0.1	1.95	2240	900	0.7	0.9

To test the assumptions made, so as to validate the approach taken, sensitivity analyses were performed. Results were compared to a nominal basement design with the following properties.

*Table 3-17: Basement model parameter; \*parameters that are fixed in the model*

Parameter	Nominal value	Low value	High value	Nominal annual heat loss (GJ)	Low value heat loss (GJ)	High value heat loss (GJ)
L = W	10 m	n/a	n/a	20.4	n/a	n/a
Basement wall insulation (BW)	3.1 m <sup>2</sup> K/W	n/a	n/a		n/a	n/a
Basement slab insulation (BS)	1.6 m <sup>2</sup> K/W	n/a	n/a		n/a	n/a
Basement wall concrete thickness*	0.2 m	0.1 m	0.3 m		20.0	20.4
Basement slab concrete thickness*	0.1 m	0.05 m	0.15 m		20.4	20.3
Above; Below slab soil conductivity*	0.8; 0.9 W/mK	-	1.2; 1.35 W/mW		n/a	22.9
Water table depth*	8 m	5 m	12 m		22.1	19.8
Basement mean air temperature*	20 °C	16 °C	24 °C		13.1	28.2

To establish the regression analysis, increments of one-fifths of the entire parameter range were used. Outputs of BASECALC are in the form of heat loss in GJ/month. These were converted to equivalent ground temperatures such that, assuming the basement air temperature remains at a constant 20°C and heat transfer is unidirectional in any given month, the heat loss was equivalent to that predicted by BASECALC. The BASECALC model uses 3D conduction, whereas the EnergyPlus model uses 1D conduction. To convert the BASECALC-predicted monthly heat loss (below and above grade), the following Equations were used for each month *i*. The objective was to determine the mean ground temperature that results is the same total basement heat loss as the BASECALC model predicts.

$$Q_{AG,calc}^i = (20^\circ\text{C} - T_{out}^i) \cdot \frac{1\text{m} \cdot 2(L + W)}{BW} \cdot \left( \text{days\_per\_month} \cdot 86400 \frac{\text{s}}{\text{day}} \right) \quad (3-17)$$

$$Q_{BG,eff}^i = Q_{BG}^i + (Q_{AG}^i - Q_{AG,calc}^i) \quad (3-18)$$

$$T_{ground,calc}^i = 20^\circ\text{C} \cdot \frac{Q_{BG,eff}^i}{\text{days\_per\_month} \cdot 86400 \text{ s/day}} \cdot \left( \frac{\frac{1.5\text{m} \cdot 2 \cdot (L + W)}{0.2\text{m}}}{1.73 \text{ W(mK)}^{-1} + BW} + \frac{L \cdot W}{\frac{0.1\text{m}}{1.73 \text{ W(mK)}^{-1} + BS}} \right) \quad (3-19)$$

An example of the temperature and heat loss profiles under the nominal design conditions are shown in Figure 3-22. Note that the ground temperature lags the air temperature by 1-2 months and that the amplitude is only about one-third of that of the air temperature.

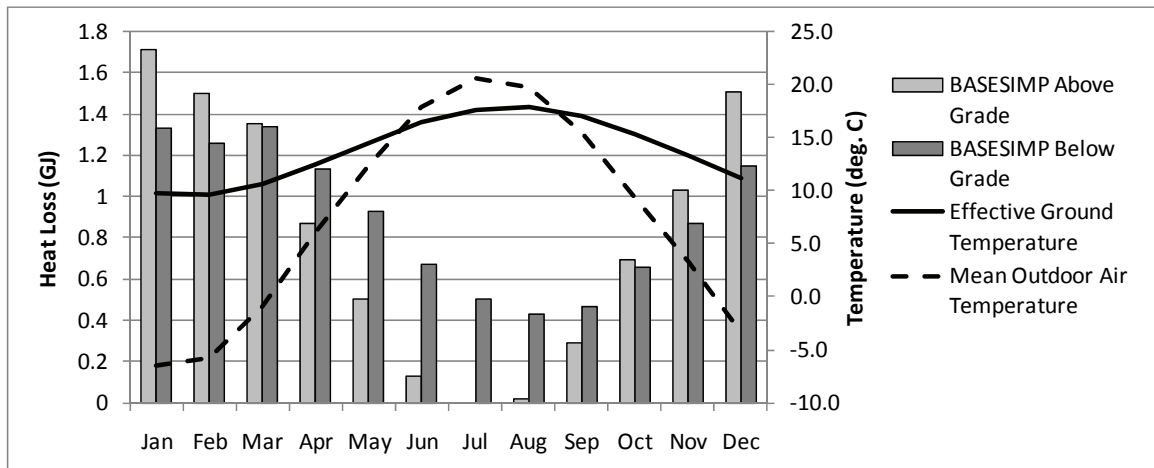


Figure 3-22: Sample results from BASECALC

The monthly temperatures are then fit to a sine wave with the following form.

$$T_{ground,calc}^i = T_{ground,mean} + T_{ground,amp} \sin\left(\frac{i - \phi_{ground}}{12} 2\pi\right) \quad (3-20)$$

The parameters are found using the following Equations.



$$T_{\text{ground,mean}} = \text{average}(T_{\text{ground,calc}}) \quad (3-21)$$

$$T_{\text{ground,amp}} = 0.5[\max(T_{\text{ground,calc}}) - \min(T_{\text{ground,calc}})] \quad (3-22)$$

$$\Phi_{\text{ground}} = 1 - i | T_{\text{ground,calc\_max}} \quad (3-23)$$

A sample for the nominal conditions is shown in Figure 3-23. The mean difference between the two curves is 0.41°C.

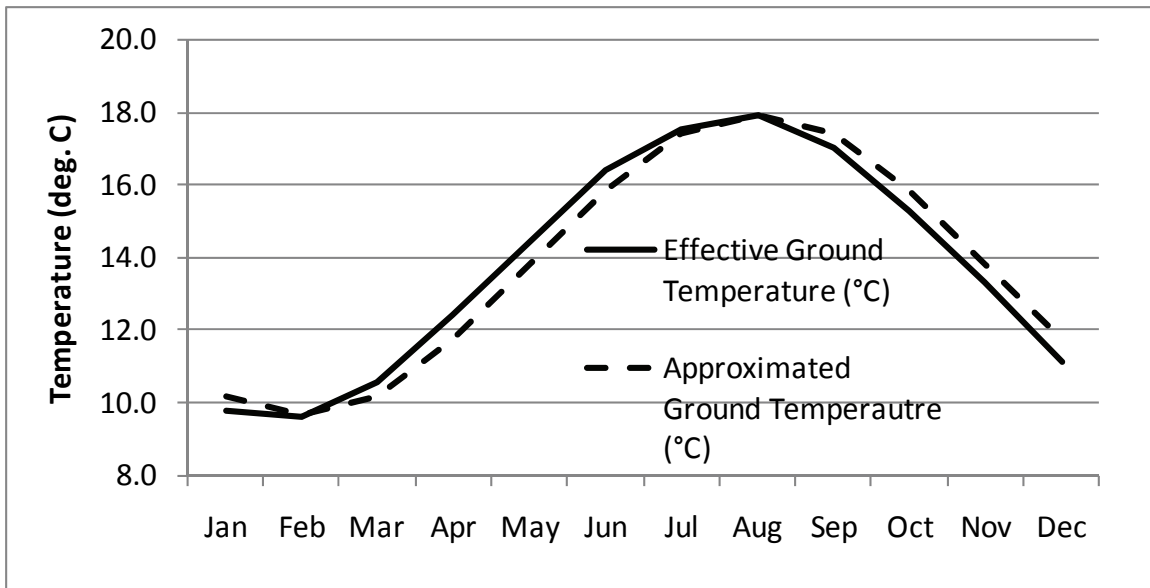


Figure 3-23: Ground temperatures - effective and approximated - under the nominal design conditions

After all of the basement configurations were run, a first-order polynomial regression Equation was used to predict each of these three parameters. The coefficients were determined using the Matlab non-linear fitting function. The form of the Equation for each parameter is:

$$P = a \cdot W + b \cdot L + c \cdot BW + d \cdot BS + e$$

1 (3-24)

Where P is  $T_{\text{ground,mean}}$ ,  $T_{\text{ground,amp}}$ , or  $\phi_{\text{ground}}$ .

### 3.2.11 Weather

The weather used as an input to the model is the EPW (EnergyPlus weather file format) for the city of interest – nominally Toronto. EPW is a file format that was created for EnergyPlus in about 1999 (Crawley et al., 1999). It contains the data of TMY2 (Typical Meteorological Year 2) files and two additional fields: “minute” and “infrared-sky”. The former allows weather data to be reported at intervals of less than one hour; the latter is used to calculate the sky temperature. TMY2 files, at the name suggests, consists of typical conditions experienced over a 30-year period (1961 to 1990). Specifically, the file contains weather conditions for a year and is concatenated by the data of individual months. The 8760 hourly values do not necessarily provide extreme conditions since they are intended to be typical; however, EPW files contain design conditions. The current work is not intended for sizing HVAC equipment and so this feature is not used.

The main inputs used by the current EnergyPlus model are outdoor air temperature, direct solar radiation, diffuse horizontal solar radiation, and the windspeed and wind direction. The weather file contains most relevant site information, such as coordinates, altitude, and time zone. While it contains ground temperatures for various depths, the EnergyPlus Input/Output Reference (EnergyPlus, 2009a) cautions that these are not to be used because they only apply to undisturbed ground that is far from building foundations.

Though the weather file for Toronto is used throughout this work, weather files for 71 other Canadian cities are available.

### **3.2.12 Internal Heat Gains**

As previously mentioned, discretionary energy use is playing an increasingly important role in total household energy use as envelopes become higher performance and consumer electronics become more numerous. It was previously shown this category of energy use is highly variable and unpredictable – particularly at the early design stage when the first owner(s), never mind subsequent ones, are unknown. This means there is significant uncertainty about appliances, other electronics, lighting, and the number of occupants. Therefore, the objective of this work is not to predict non-HVAC energy for the purpose of assessing total energy use, but rather to predict it for the purpose of providing it as an input to the model. The approach taken is to make a top-down estimate of non-HVAC energy use. That is, rather than attempt to predict the number of appliances and light fixtures in the house as was done by Charron (2007) for example, the aggregated data for all appliances and lighting is used to make reasonable estimates. To a certain extent, this removes some of the uncertainty about number of energy-consumers and their annual energy use; and it, at least, is representative of average existing homes. This approach is somewhat different than HOT3000, which allows a higher resolution of inputs such as number of occupants and some specifics about laundry and cooking equipment. However, HOT3000 is intended to be used for existing houses where these details are known.

The current model considers four categories of non-HVAC loads: major appliances (kitchen and laundry), minor appliances (computers, televisions, clocks, and radios), lights, and domestic hot water (DHW). Occupants contribute to internal heat gains but not directly to electricity consumption.

The approach taken is to sum all heat gains and then distribute them over an hourly schedule with a profile that is proportional to those proposed by Armstrong (2009) and shown in Figure 3-24. The exact profile has little bearing on the predicted performance of the house since the internal gains are relatively insignificant compared to solar gains. Also high-mass houses do not respond quickly to short-term changes in inputs. Finally, Ecos is not intended to examine highly time-sensitive phenomena such as time-of-use electricity pricing.

The house is assumed to be occupied from 18:00 to 8:00 daily and unoccupied otherwise, as shown in Figure 3-25. All other daily profiles were either obtained from Armstrong et al (2009) or estimated.

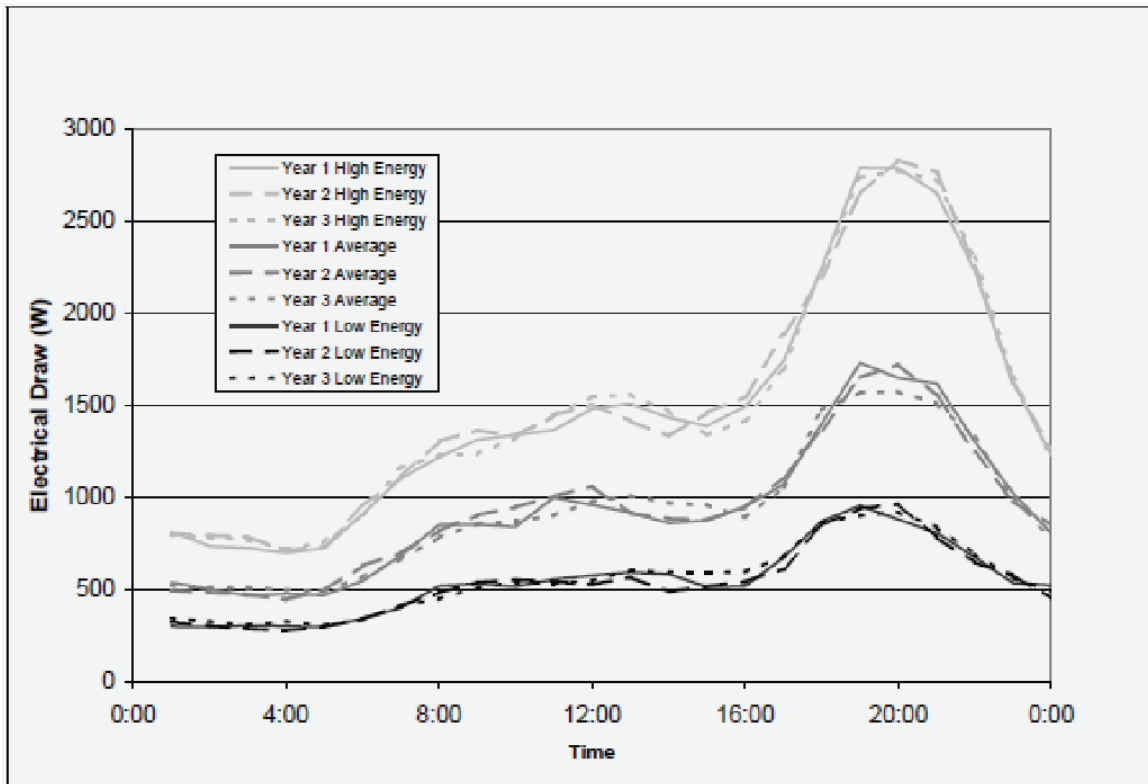


Figure 3-24: Hourly profile for total electrical draw per house (taken from Armstrong et al., 2009)

Three usage schemes were used referring to relative occupant energy-consciousness: low, medium, and high – corresponding to multipliers of 0.5, 1.0, and 1.5. *Medium* is intended to correspond to the average occupant reported by NRCan (2006). The multipliers are applied to the energy use for major and minor appliances, lighting, and DHW. The following paragraphs describe the assumptions made for each category of internal gains. A summary of the internal gains and electricity consumption is shown in Table 3-18.

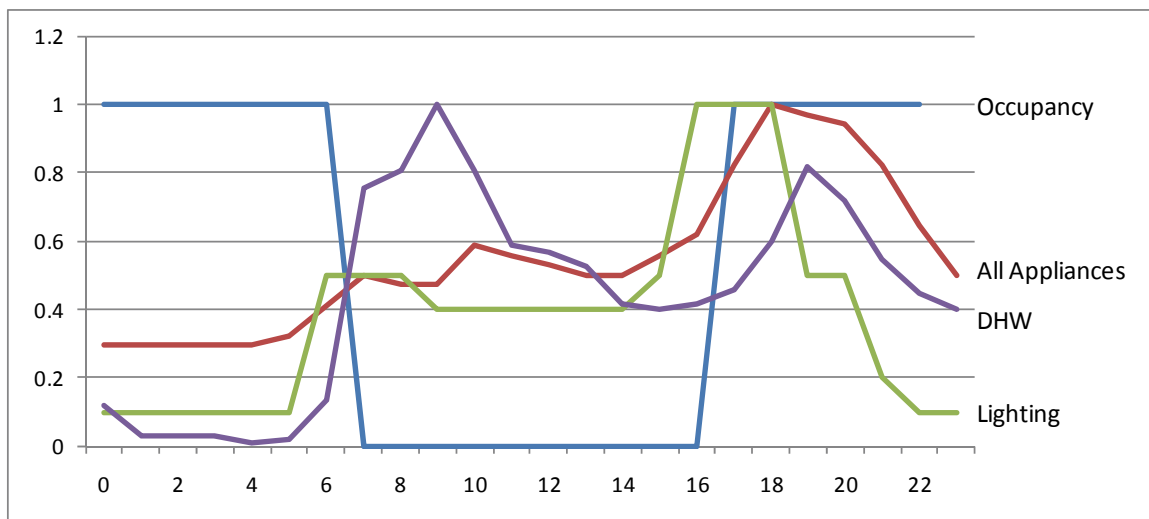


Figure 3-25: Normalized daily internal gain profiles

Major appliances were assumed to be independent of floor area and number of occupants because most houses have a standard set of appliances (range, oven, fridge, clothes washer and dryer). The annual consumption is based on the Canadian average.

Minor appliances, in contrast, were assumed to increase linearly with floor area to characterize the increasing numbers and use of computers, TVs, radios, clocks, etc.

Electric lighting energy use is assumed to increase linearly with floor area and is equal to Canada’s mean on a per m<sup>2</sup> basis. Daylighting was not included in the model as this is considered beyond the scope of this research. This is because daylighting performance is sensitive to window positioning and interior wall positioning and reflectance, whereas the model does not allow for detailed inputs of either. Furthermore, as previously explained energy savings potential from daylighting of houses is not very significant.

Domestic hot water consumption is predicted to be 85 L/day plus 35 L/day/person, in accordance with the scheme proposed by HOT3000 (2009). The monthly water mains

temperatures were obtained from RETScreen (2005). The water was assumed to be heated to 55°C at an efficiency of 90% with electricity. The water heater and distribution are explicitly modelled in order to compare this model to the solar domestic hot water system model that is discussed in the next chapter.

The number of occupants was estimated at 0.019/m<sup>2</sup> in accordance with the national average for detached houses NRCan (2008b), but is rounded to the nearest integer. The number of occupants affects both internal gains from occupants and the DHW usage. Each occupant was assumed produce 120 Watts of heat, representing an average of common household activities (e.g., sitting, standing, light work, and sleeping).

The average Canadian home was found to have 65 Watts from phantom loads (Armstrong et al., 2009); this was added to the other internal gains and assumed constant. These represent the standby electrical consumption of clocks, TVs, microwaves, and other minor and major appliances. A radiant fraction of 100% was used because most of these loads result from electronics (without fans).

Table 3-18: Summary of internal gains and coefficients

	Scheme	Constant (kWh/year)	Constant (W)	W/person	Per m <sup>2</sup> multiplier	kWh/person	kWh/m <sup>2</sup> /year	Convective Portion (%)	Radiant Portion (%)	Latent Portion (%)	Lost Portion (%)	Electrical Draw (yes/no)
Coef.	IG	C <sub>1</sub>	C <sub>2</sub>	C <sub>3</sub>	C <sub>4</sub>	C <sub>5</sub>	C <sub>6</sub>	C <sub>7</sub>	C <sub>8</sub>	C <sub>9</sub>	C <sub>10</sub>	C <sub>11</sub>
Major Appliances	0.5, 1, 1.5	3661						45	11	10	33	1
Minor Appliances							14.06	39	54	10		1
Lighting							9.75	21	79			1
Domestic Hot Water		1919				790					100	1
Phantom loads	1		65						100			1
Occupants	1			120	0.019			26	32	42		0

The total annual electric energy for each of the major categories of consumption can be found with Equation 3-25. The internal gains, by type and for each category of loads can be found with Equation 3-26.

$$E_{elec} = IG [C_1 + C_2 \cdot 8760 \text{ hrs} + \text{round}(C_4 \cdot FA) \cdot (C_3 \cdot 8760 \text{ h} + C_5) + C_6 \cdot C_{11}] \quad (3-25)$$

$$E_{thermal,i} = IG [C_1 + C_2 \cdot 8760 \text{ hrs} + \text{round}(C_4 \cdot FA) \cdot (C_3 \cdot 8760 \text{ h} + C_5) + C_6 \cdot C_{11}] \cdot i_{gain} \quad (3-26)$$

Where  $i_{gain}$  is either convective, radiative, latent, or lost, representing C<sub>7</sub>, C<sub>8</sub>, C<sub>9</sub>, or C<sub>10</sub>.

Equation 3-26 must be applied to each of the: radiant, convective, and latent portions.

Most electricity consumers also generate internal gains because every process that uses electricity results in some losses. If the electricity consumer is fully contained within a zone, all of the energy is ultimately converted to heat or stored. Neglecting stored



electricity (which is probably ultimately released later anyway) the sum of the convective, radiative, latent, and lost portions is one. The convective and radiant portions of the internal gains both contribute to warming the zone in which they occur. The difference is that convective gains are added to the air node of the zone, whereas the radiant gains are added to the surfaces that contain the zone. Latent gains contribute to humidity and are only relevant if cooling is used. The lost portion has no impact on the house's energy balance. The location of the internal gains among the zones is weighted by floor area.

The annual electricity consumption and internal gains for the extreme allowable floor areas and the three different internal gains schemes (IG) are shown in Figure 3-26.

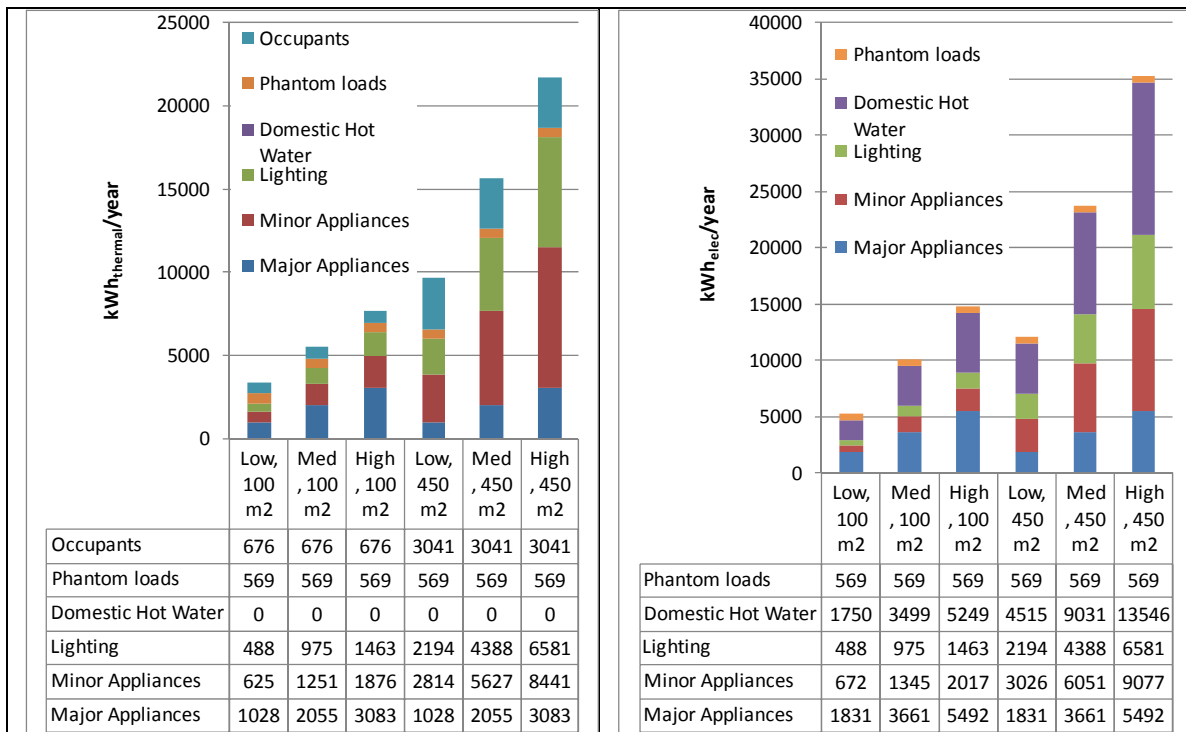


Figure 3-26: Sample annual internal gains (all but lost portion; left) and electricity consumption (right).

The appropriate portions of internal gains are summarized in Table 3-18 and were obtained from (Spitler et al., 2005). The major appliances portions of internal gains are based on a weighted average of all appliances. The electric range is assumed to lose 30% of its energy via a ventilation fan, while clothes dryers lose 80% via ventilation. Phantom loads were assumed to be completely radiant because they are typically not fan-cooled. Little research effort has been put into quantifying the heat gains from DHW; however, several sources (e.g., Swan (2010) and Spitler (2005)) estimate that the net heat gains are negligible because much of the heated water is drained, cold water is brought into the house, and the use of hot water is often associated with a ventilation fan which vents conditioned air to the outdoors.

The hourly electricity and internal gains schedules are such that they follow the aforementioned profiles and result in the totals calculated using Equations 3-25 and 3-26.

### **3.2.13 Ventilation, circulation, mechanical equipment and controls**

Fresh air, heating, and cooling requirements are all met by the same system – a forced-air system – and therefore all described together, in this section. A major objective of the Ecos is to assess heating and cooling loads resulting from different passive solar strategies rather than assessing specific HVAC technologies. As reported by the literature review, it is mainly the plant – not the distribution system – that has the most impact on performance.

The justification for using a forced-air system is: 1) it meets the requirement for a simple but accurate model intended for early stage design, 2) it also serves the purpose of distributing fresh air and circulating air among zones, and 3) such a system was successfully demonstrated in the low-energy houses, such as the ÉcoTerra house.

The conceived HVAC configuration used for this study is shown in Figure 3-27 (left). It uses a common set of ducts to supply conditioning and ventilation to each zone. Such a configuration saves in both equipment costs and in volume for ductwork. The airflow to each zone is controlled by a damper, such that heat can be added or removed, as required to maintain the desired temperature. Heat is added or removed from the air in the air handling unit (AHU), as needed. The exhaust air from each zone is partly exhausted to the outdoors, before which some of its heat is recovered by the HRV, and partly returned to the AHU.

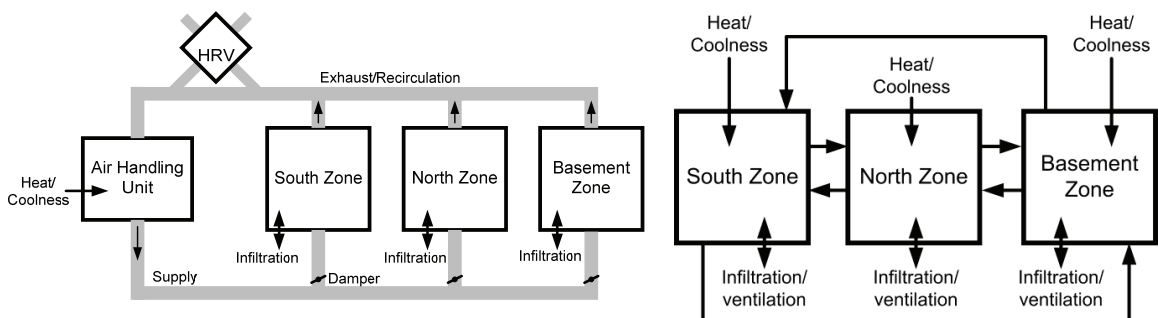


Figure 3-27: The forced-air HVAC system as conceived (left) and as modelled (right) (taken from O'Brien (2010b))

However, to simplify the model for the case study, ideal controls were used, such that heat and coolness were injected into the occupied zone(s) at the air node whenever needed. The “Ideal Loads Air System” in EnergyPlus was used. It is a variable air volume

(VAV) system that allows a variable airflow rate to satisfy the cooling or heating load. It should be noted that this airflow does not affect the interzonal airflow rates or mass balance in the model.

In contrast, the modelled configuration is shown in Figure 3-27 (right). While this approach is simpler to implement and provides considerable flexibility, its limitations should be noted. First, it neglects pressure drops, heat transfer, and leakage from ducts. Second, the modelled configuration assumes a constant rate of air mixing, whereas in reality, there are some occasions when not all of the zones require heating or cooling and their dampers would be closed. This modelling assumption is considered valid because the frequency at which this occurs is low and when it does occur, the benefit to increased airflow (described later) is insignificant because heating tends to be needed in all zones during periods of low solar gains (which is when interzonal airflow is less beneficial).

Specifically, the controls maintain the zonal air node temperature between *HS* and *CS*, except at night (10 PM to 7 AM) when there is the option of having a lower heating setpoint (*HSN*). This time is typically when occupants are sleeping and prefer cooler temperatures. The literature suggests nighttime setbacks passive solar houses of between 15°C and 20°C (Besant et al., 1979; Hestnes et al., 2003; Chen et al., 2010b; NRCan 2010a). The nighttime setback has two purposes: 1) delay the time at which

heating must be supplied at night, which ultimately reduces heating energy, and 2) provide a greater capacity to store solar gains before overheating occurs.

The temperature control setpoint schedules are shown in Table 3-19. The schedule was designed for Toronto’s climate and would have to be re-evaluated for significantly different climates.

*Table 3-19: Heating and cooling control schedules*

		Jan	Feb	Mar	Apr	Ma y	Jun	Jul	Aug	Sep	Oct	Nov	Dec
Purchased cooling setpoint		∞				CS			∞				
Purchased heating setpoint (7:00 – 22:00)		HS											
Purchased nighttime heating setpoint (22:00 – 7:00)		HSN											
Free cooling	Minimum indoor temperature	No free cooling				HS or HSN + 2°C			No free cooling				
	Minimum outdoor temperature					15°C							
	Maximum outdoor temperature					CS - 1°C							

The combined heating and cooling energy under the nominal design conditions but with setpoints that vary over their ranges, is shown in Figure 3-28. The results indicate that widening the gap between heating and cooling setpoints significantly reduces energy use. Since the nominal design has a large window, performance is sensitive to potential overheating and restricting the allowable temperature swings significantly increases energy use.

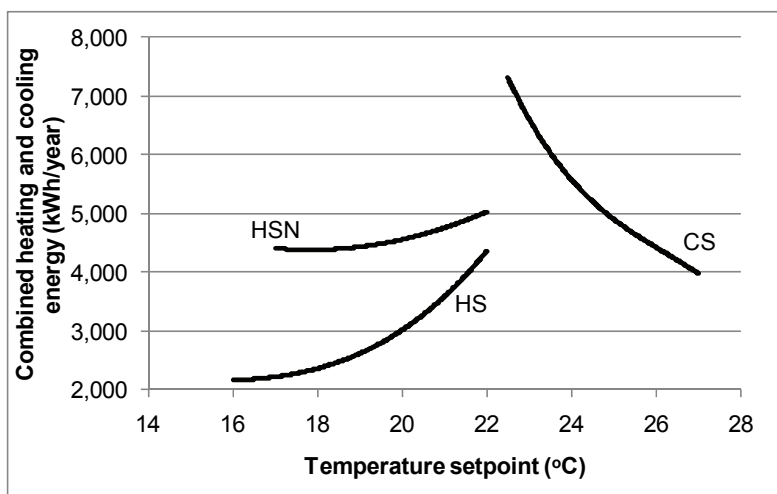


Figure 3-28: Combined heating and cooling energy for the temperature control setpoints over their ranges.

Free cooling was modelled by introducing outdoor air into each zone at a rate of 1.2 m<sup>3</sup>/s. Rates of 0.5 to 1.7 m<sup>3</sup>/s are typical for fans for the purpose of free cooling (Galloway, 2004). The conditions under which free cooling is enabled are outlined in Table 3-19.

Interzonal airflow rates are explicitly imposed by a forced air system fan. Such systems are efficient, low-cost, and enable a higher level of certainty than natural convection, as discussed in the literature review. Airflow rates (*CI*) can be between 0 and 1000 L/s representing typical values of low-energy houses discussed in the literature review. For all of them, air from each occupied zone is returned to the air handling unit (AHU), where it is assumed to be mixed, and re-supplied equally to each zone.

In order to properly represent the effective airflow rate, the real configuration (Figure 3-27 (left)) must be compared to the modelled configuration (Figure 3-27 (right)). A volume flow balance was used to calculate how much of the air leaving each zone

enters the other two. Consider a case where  $CI = 200$  L/s. Starting at the AHU, if 200 L/s is blown by the fan, one-third or 67 L/s enters each zone assuming the system is balanced, in re-circulation mode, and that the zones are of equal volume. Because of the conservation of mass, approximately the same amount of air leaves each zone, assuming that infiltration balances exfiltration for each zone. The exhaust air from each zone merges and is partly exhausted; 0.3 ach of ventilation is equivalent to 67 L/s for an  $800 \text{ m}^3$  house. Therefore, two-thirds of the air re-entering the AHU is exhaust air from the zones and the remaining third is fresh air. Assuming this air is perfectly mixed, the air entering each zone is one-third fresh air, and two-ninths is from each of the three zones. It is therefore concluded that the four-ninths of the mechanically-driven airflow actually causes effective interzonal airflow, while the remainder either distributes fresh air or merely returns exhaust air to the zone in which it originated. Thus, for the current model and the 200 L/s case, each pair of zones exchanges 44 L/s (two-ninths of 200 L/s). In general terms, the effective airflow rate from zone  $i$  to zone  $j$  can be determined with Equation 3-27. This applies to all permutations of the three conditioned zones.

$$q_{i \rightarrow j} = \left( \frac{V_i}{\sum V} Q_{\text{fan}} - \frac{q_{\text{vent}}}{3600 \text{ s/h}} \sum V \right) \cdot \frac{V_j}{\sum V} \quad (3-27)$$

For the range of airflow rates examined, the 0 L/s case could represent a house with radiant floor or baseboard heating, in which air is not the primary heat distribution medium, while the non-zero cases represent forced air systems. While the air is

constantly circulated for these simulations, a control system that limits fan use to periods of significant interzonal temperature differences is advisable to save fan energy.

This model is most applicable to houses with forced-air distribution systems, in which heat or coolness are delivered via ducts and returned to the system through returns, as previously described. The fan(s) could conceivably be used more effectively if the air were circulated directly between the direct gain and non-direct gain zones without mixing it first; thus eliminating the airflow that is merely returned to the zone from which it originated. Furthermore, the warm air should be taken from the top of the direct gain zone. Such advanced configurations are the subject of future research.

Under the nominal design conditions with different interzonal airflow rates explored, a similar though subtler trend to the number of zones exists, relative to the zoning configuration. Using airflow to distribute solar gains decreases loads and increases optimal glazing area. The results in Figure 3-29 indicate that increasing airflow provides diminishing returns for energy savings, since most of the benefit is achieved from 0 to 200 L/s, and that there is little benefit to increasing this to 400 L/s (see Figure 3-29). However, the designer should explore different airflow rates since features such as large windows increase the benefit of higher flow rates.



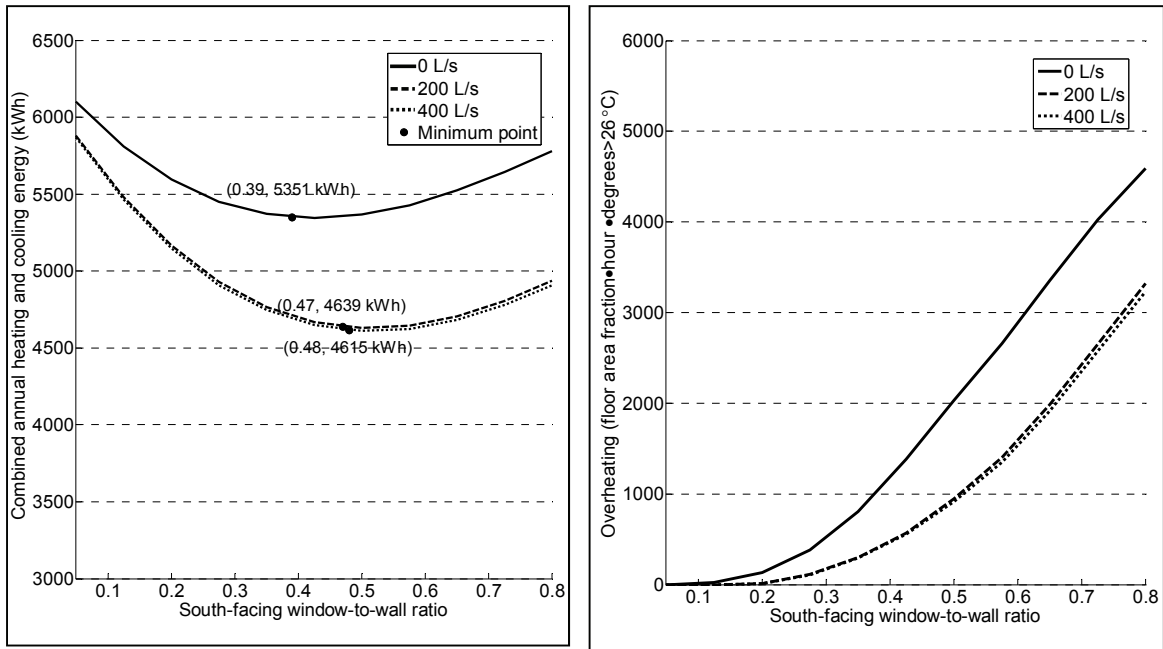


Figure 3-29: Total heating and cooling energy (left) and overheating (right) as a function of WWR1 and CI (taken from O'Brien et al (2011a))

Figure 3-29 reiterates the fact that increasing airflow provides diminishing returns. The temperature profiles indicate that increasing air circulation is most effective during times when the direct gain zone overheats and the other zones require heating. During periods of high solar gains and mild temperatures, if all of the zones begin to overheat, circulation offers little benefit, other than equalizing the temperatures, which may or may not be desirable.

### 3.2.14 Intermediate Metrics

There are several intermediate metrics (i.e., quantities that are derived directly from the parameter values before simulation) that are useful to design, including ones about overall envelope thermal resistance and house geometry.

Two useful intermediate metrics for assessing a house's thermal performance are summarized as follows and can be calculated using Equations 3-28 through 3-31.

1. Above-grade building heat loss coefficient (by floor area) ( $UA_{AG,FA}$ ): this metric provides an indication of heat loss resulting from the above-grade envelope. The normalization by total floor area gives credit to compactness.
2. Above-grade building heat loss coefficient (by above grade envelope area) ( $UA_{AG,ENV}$ ): this metric is similar to the one above but focuses on envelope quality rather than overall house compactness.
3. Below-grade building heat loss coefficient (by below grade envelope area) ( $UA_{BG,ENV}$ ): this metric is like the one above but for the below-grade envelope. This is kept separate because the boundary conditions for the below-grade portion of the house are significantly different than the above-grade portion; wind/sun-exposed and convective/radiative versus conductive only.
4. Building heat loss from air exchange ( $U_{air,exchange}$ ): this metric represents the heat loss associated with air exchange with the outdoors. It can be combined with the first two metrics for a better indication of total envelope quality.

These provide some indication of the total heat loss of the envelope. They are defined as follows.

$$UA_{AG,FA} = \frac{1}{FA} \left( \sum_{envsurf=1}^{N_{envsurf}} A_{envsurf}/R_{envsurf} \right) \quad (3-28)$$

$$UA_{AG,ENV} = \frac{1}{\sum A_{envsurf}} \left( \sum_{envsurf=1}^{N_{envsurf}} A_{envsurf}/R_{envsurf} \right) \quad (3-29)$$

$$UA_{BG} = \frac{1}{A_{BG}} \left( \sum_{envsurf,BG=1}^2 A_{envsurf,BG}/R_{envsurf,BG} \right) \quad (3-30)$$

$$U_{air,exchange} = c_{p,air} [(1 - \epsilon_{HRV})\dot{m}_{vent} + \dot{m}_{inf}] \quad (3-31)$$

It is important to note that none of these metrics can entirely replace the power of dynamic simulation because they are primarily for comparative purposes and could only reasonably predict house performance under steady-state conditions and for unglazed houses. A house with a higher UA-value resulting from larger windows could actually have lower heating energy use because of the solar gains. However, these metrics are useful in assessing the most effective means of reducing heat transfer of opaque envelope elements (e.g. window frames and walls).

Examples for extreme parameter settings and a 300 m<sup>2</sup> square, two-storey house are shown in Figure 13-2 in Appendix E. The above-grade quantities can be directly combined, indicating that for a house with the given geometry, the heat loss can range from 90 to 300 W/K. The below-grade heat loss must be put into the context that the ground temperature at the outside basement surfaces is typically much higher than

outdoor air temperatures in winter and that the mode of heat transfer is different (conductive versus convective and radiative).

Solar aperture is a traditional metric for relating south-facing (or near-south-facing) glazing area to the floor area, and specifically:

$$\text{Solar Aperture} = GA_1/FA = WWR_1 \cdot W \cdot H/FA \quad (3-32)$$

Its advantage over *WWR* is that it gives an indication glazing area to thermal mass ratio. Also, it is frequently presented in passive solar house guide books that give rules of thumb (see e.g., “Tap the Sun” (CMHC, 1998)). Under the nominal design conditions for *WWR1* values of 0.05 to 0.6, the equivalent solar apertures are about 0.01 to 0.12. The reason that *WWR* is favoured throughout this work is that it provides a better indication of what is practically possible. Values of *WWR* above 1 are impossible, and values above about 0.75 are impractical because of structural and framing limitations.

### **3.2.15 Energy, power, and metrics**

This section describes the outputs of the model that are of interest and are reported.

The main metric of interest is the combined heating and cooling energy (and active solar system performance, which is described in the next chapter) because that is what the model is best suited to predict. Throughout most of this chapter, the cost per unit of heating and cooling was assumed to be equal. This is most suitable for two common equipment configurations: 1) a heat pump with similar coefficients of performance (COPs) for heating and cooling, or 2) an electric air conditioner with a COP of about 3 for

cooling and a fossil fuel-based (e.g., natural gas) furnace for heating. In the latter case, the primary energy input per unit of heat added or removed to the space is approximately equal. For instance, North America’s primary energy input to secondary energy output ratio is approximately three (Deru and Torcellini, 2007) , but varies by region and time. But, if the per unit cost of cooling were less than heating, for instance, this would tend to increase optimal glazing areas. Ecos also allows the coefficient of performance (COP) for the heating ( $COP_h$ ) and cooling ( $COP_c$ ) systems to be individually specified so that their differential energy cost can be taken into account. Typical COPs were discussed in the literature review and can range from 0.8 to about 5 (anything less than 1.0 is really the “efficiency” and normally only applies to heating equipment).

These are applied post-simulation, as follows.

$$E_{\text{conditioning}} = E_{\text{heating}}/COP_h + E_{\text{cooling}}/COP_c \quad (3-33)$$

The total annual purchased electricity for conditioning is of interest for making economic decisions and estimating environmental impact. Furthermore, it is needed to determine total and net purchased electricity. The electricity use at each timestep is.

$$E_{\text{total}} = E_{\text{heating}}/COP_h + E_{\text{cooling}}/COP_c + E_{\text{lighting}} + E_{\text{major_appliances}} + E_{\text{minor_appliances}} + E_{\text{DHW}} + E_{\text{fans}} \quad (3-34)$$

Subtracting the renewable energy generation, as described in the next chapter, yields the net annual purchased energy, as follows.

$$E_{\text{net}} = E_{\text{total}} - E_{\text{generation}} \quad (3-35)$$

There is a major gap in the literature about the proper quantification of passive solar performance (as discussed in the literature review); likely because of the complexity of the issue. Duffie and Beckman (2006) stated that the solar fraction metric is not appropriate for passive solar heating. This area of research (performance metric definitions) is not trivial and should be addressed in detail. The definitions should reflect the bottom line and not optimistically represent reality, in such a way to persuade designers with any biases. The following paragraphs address this issue in detail.

First, it is worthwhile to recognize the energy balance for windows, as shown in Equation 3-36.

$$\begin{aligned} \text{Energy (electrical) benefits of windows} = & \\ & + (\text{displaced heating energy} - \text{additional heating energy}) \times \text{COP}_h \\ & + \text{displaced lighting energy from daylight} \\ & - (\text{added cooling energy} - \text{displaced cooling energy}) \times \text{COP}_c \end{aligned} \quad (3-36)$$

The complexity of the solar fraction issue arises from determining the usefulness of solar gains. In winter, they are generally all useful; while in summer, they are generally all adverse. However, in the spring and autumn periods, the need for heating or cooling is reduced and it is possible that some of the solar gains are useful (raising the temperature of the home up towards the desired temperature) while others are adverse (raising the temperature of the home up above the desired temperature and causing discomfort or the need for mechanical cooling). Also, solar gains are not used

immediately (especially for thermally massive homes), meaning that the criterion that instantaneous heating be required is not valid.

There are two possible methods for calculating solar fraction (i.e., the fraction of purchased energy that is displaced by solar energy):

1. Using a house with no windows as the baseline.

$$\text{SolarFraction1} = (E_{\text{conditioning}} |_{\text{no\_windows}} - E_{\text{conditioning}}) / E_{\text{conditioning}} \quad (3-37)$$

2. Using a house with no incident solar radiation as the baseline, as Balcomb suggests (Hestnes et al., 2003).

$$\text{SolarFraction2} = (E_{\text{conditioning}} |_{\text{no\_solar}} - E_{\text{conditioning}}) / E_{\text{conditioning}} \quad (3-38)$$

Where  $E_{\text{conditioning}}$  is the conditioning energy of the nominal design, modelled normally,  $E_{\text{conditioning}} |_{\text{no\_windows}}$  is the conditioning energy in a house with no windows, and  $E_{\text{conditioning}} |_{\text{no\_solar}}$  is the conditioning energy if the windows are completely shaded.

The first method is more appropriate and useful than the second method because it represents real situations. Ultimately, the solar fraction informs the designer of whether a bigger window (or any window at all) is advantageous. However, the second method uses a case for which windows are present but all of the adversities associated with windows (greater heat loss and discomfort) and none of the benefits (solar gains and daylight). Under the condition that the thermal resistance of the opaque walls is greater than that of the windows and the climate is heating-dominated,  $E_{\text{conditioning}} |_{\text{no\_solar}} >$

$E_{conditioning / no\_window}$ , the solar fraction is inflated if Equation 3-37 is used rather than Equation 3-38. For this reason, the more conservative and logical approach is taken for this work (Equation 3-38). The components of the Equation are obtained by simulating the house for the proposed design and re-simulating it with no windows.

### 3.2.16 Thermal comfort metrics

As mentioned in the literature review, thermal comfort is a major aspect of passive solar house and must be balanced with energy performance. The comfort metrics obtained from the model are air temperature and operative temperature. More complex models, such as the predicted mean vote (PMV), which are used to directly estimate occupant sensation (e.g., too hot or too cold), require significantly more information than is available during early stage design (e.g., clothing level, airspeed, metabolic activity) (ASHRAE, 2004a). The calculation of air temperature is straightforward since it is assumed constant throughout each zone. The operative temperature is a weighted average of the air temperature and mean radiant temperature in each zone and can be calculated using the following Equation.

$$T_{OP} = (h_r T_{MRT} + h_c T_{air}) / (h_r + h_c) \quad (3-39)$$

Under normal conditions (i.e., low airspeeds and typical indoor temperatures),  $h_r$  and  $h_c$  are usually assumed to be equal (Hutcheon and Handegord, 1995). Mean radiant temperature is a function of zone geometry, surface emissivity, location of the person, and surface temperatures. EnergyPlus has two main methods for dealing with the



location of the person relative to the surfaces: 1) assume the person is in the centre of the room, or 2) provide a specific location for the person. Since this model is intended to support early stage design and cues like furniture placement are unknown, the former method is used. The mean radiant temperature  $T_{MRT}$  in a zone is calculated with the following Equation.

$$T_{MRT} = \sum_{s=1}^{n\_surfaces} F_s T_s \quad (3-40)$$

All surfaces are assumed to have approximately the same emissivity – 0.9. The difference between the mean radiant temperature and the operative temperature is likely to be greater for passive solar houses than for typical houses because of the large windows, whose temperature could influence the mean radiant temperature by one-sixth or more.

Reporting frequency of the two comfort metrics is both hourly and for the entire year. For the entire year, preliminary simulation results were found to be particularly sensitive to the definition of overheating. Typically, overheating is quantified by the number of hours above 25°C or 28°C (e.g., see CMHC (1998) and Robinson and Haldi (2008)). However, this definition is not suitable for this research because it does not recognize temperature differences across zones, which can be 5°C or more.

Furthermore, merely measuring the number of hours above a certain temperature neglects the fact that higher temperatures are less comfortable than those just above

this threshold. Interestingly, it was found that merely measuring the hours above some threshold would indicate that circulating air is adverse, in some instances, because it leads to more zones being over the threshold – though barely. However, overall comfort conditions under these conditions would, in fact, be improved, by most standards. Thus, a new metric was devised to account for all of these considerations. It is hour-degrees (Celsius) above the cooling setpoint multiplied by the volume fraction of the house. More concisely, it can be calculated with the following Equation.

$$Overheating = \sum_{h=1}^{8760} \left( \sum_{z=1}^{n\_zones} \frac{V_{zone}}{V_{total}} \cdot (T_{air,z} - CS) \cdot (T_{air,z} > CS) \right) \quad (3-41)$$

Where *Overheating* is the severity of overheating and can be for either air temperature or operative temperature.

### 3.3 Conclusions

This chapter introduced the generic parameterized model and proposed the most suitable techniques for modelling all of its different aspects.

## **4 ACTIVE SOLAR SYSTEMS AND MODELLING**

This chapter parallels the previous one but describes the active solar components of the model in detail. As for the passive solar aspects, the models and parameter ranges were selected to balance flexibility, simplicity, performance, and accuracy for early stage design.

This chapter starts by examining practical issues related to roof-mounted solar collectors and is followed by a description of specific active solar systems. There are two active systems included in the model: building-integrated photovoltaics (BIPV) and solar domestic hot water (SDHW). As discussed in the literature review, these systems are among the most cost-effective – not necessarily because of their high efficiency – but rather because of the high value of energy they collect. The electricity generated by PV has the highest diversity of uses (e.g., heating, cooling, lighting, appliances, etc.) and excess can be exported with only modest transmission losses. Thermal energy collected by SDHW systems is valuable because the annual variation in demand is much less than that for space heating. This fact yields a much higher rate of utilization.

The parameters used to describe the active solar systems are shown in Table 4-1. The parameters are described in detail in the sections that follow.

Table 4-1: Summary of active solar system parameters

No.	Name	Abr.	Design?	Discrete?	Min	Max	Nominal	Units
31	Total PV cell area	CA	1	0	0	170	0	m <sup>2</sup>
32	PV module nominal efficiency	AE	1	0	0.05	0.2	0.1	
33	PV temperature coefficient	TC	1	0	0.0001	0.0004	0.0001	1/°C
34	Inverter efficiency	IE	1	0	0.8	0.95	0.95	
35	Parallel solar thermal collectors	PL	1	1	1	4	2	
36	Collector storage tank volume	TV	1	0	0.2	1	0.2	m <sup>3</sup>

## 4.1 Roof and collector geometry

Roof and collector geometry are common among the two types of solar collectors that are considered in this work: BIPV and SDHW. Roofs are arguably the best building surface upon which to mount solar collectors for the following reasons:

- Flexibility. Roof geometry (slope, shape) is flexible because it does not affect the living space. Within reasonable practical limits, it can be oriented to maximize solar exposure.
- Uninterrupted surfaces. Unlike vertical walls, roofs can be designed with few interruptions (windows, doors, vents, etc.), rendering them ideal for large expansive solar collector arrays and minimized wiring and plumbing. Exceptions to this are dormers and skylights; both of which complicate solar collector layout.
- Precipitation shedding. The pitch of a roof can be increased to effectively shed precipitation – particularly snow – so that accumulation is minimal and incident solar radiation is maximized.

- Height and minimized shading. Since shading from neighbouring houses and trees can be an issue, mounting solar collectors high up means that they are less likely to be shaded.

For these reasons, active solar collectors are constrained to roofs in the model. “Passive solar collectors” or windows are allowed (and limited to being) on the vertical walls of the house.

Roof geometry is defined by five previously-defined variables or parameters: house width ( $W$ ), house length ( $L$ ), roof slope ( $SL$ ), orientation ( $OR$ ), and roof type ( $RT$ ). Width and length are a function of floor area ( $FA$ ), the number of storeys ( $ST$ ) and the aspect ratio ( $AR$ ). The roof width and length are always 60 cm greater than that of the house in the model, to account for eaves, which were previously explained to protrude 30 cm in all directions. The depth of the eaves are denoted  $L_{eaves}$  in Table 4-2. The slope  $SL$  always refers to the slope of the active (collector-covered) roof surface. This allows the  $SL$  parameter to be used both for describing the roof shape and for an input to the active solar systems models.

The active roof surface is limited to the one that is oriented closest to south and is constrained to being between southwest and southeast because of the ranges of  $OR$ . This is in compliance with the requirement of the model to be high-performance and simple. Other orientations are significantly less favourable for performance.

The hip roof, because of practical constraints, must have its hips at 45-degree angles from the roof edges (see plan views in Table 4-2). Therefore, if the roof length is longer than the width, the active area changes from trapezoidal to triangular. In the unique case that the house is square with a hip roof, the roof is pyramid-shaped.

Complex roof shapes, though common in practice, are not part of the model. Although with care, their performance can be predicted with the simplified roofs in Ecos. These shapes are less suitable for solar energy collection because they usually result in poorer “packing efficiency” (the ratio of module area to gross roof area) and potential self-shading, as described in the sections that follow.

#### **4.1.1 Geometrical considerations**

In many active solar system modeling programs, the annual electricity production is based on collector area only. However, this is not an accurate representation of the system, since the number of modules in a real system is discrete. Also, most modules have a frame, meaning that not all of this area should be counted. Finally, for non-rectangular roof surfaces, a certain amount of area is wasted from geometric incompatibilities. Electrical and plumbing constraints can further restrict panel geometry. During detailed design, it is necessary to specify the module size such that the optimal arrangement can be determined and, if necessary, the roof geometry or panel type can be changed. For building-integrated PV, in which the PV panels serve the function of weather protection in addition to electricity production, it may be necessary

to match the two exactly. For modules that are merely mounted to an existing roof, this is less critical – functionally.

#### **4.1.2 Self-shading**

Self-shading includes shading of the collector array from architectural elements, including dormers, chimneys, antennas, or other roof sections. Like the effect of snow, the effect of a small shadow on a PV panel can have an effect which is much greater than its size would suggest (GSES, 2004). Furthermore, the shadow can sweep out an area that is several orders of magnitude larger than the footprint of the obstruction itself. Therefore, array shading should be avoided first by eliminating sources of shading, and secondly by not placing panels in the vicinity of the obstruction. Since Ecos will not allow the input of small obstructions, it will be up to the designer to avoid these elements. Shading from other roof sections can be avoided by excluding valleys, such that self-shading only occurs when the sun goes behind the surface. For example, gable and hip roofs are preferable to cross-gable roofs, simply because the former two do not experience self-shading. Table 4-3 provides examples of these roofs and their geometrical implications.

Table 4-2: Roof geometry for solar collectors

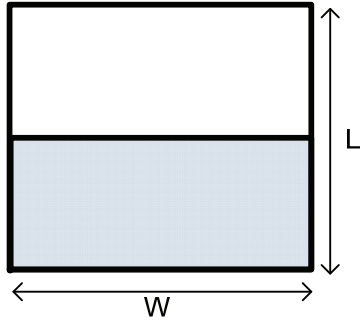
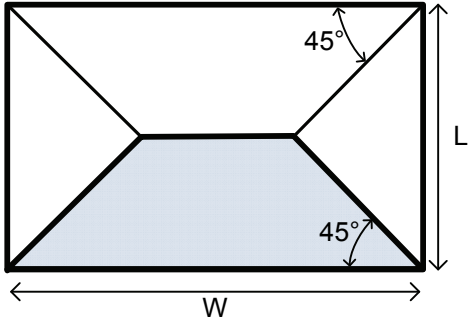
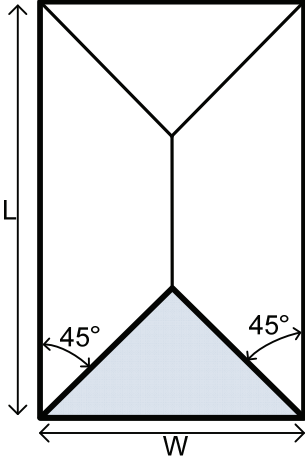
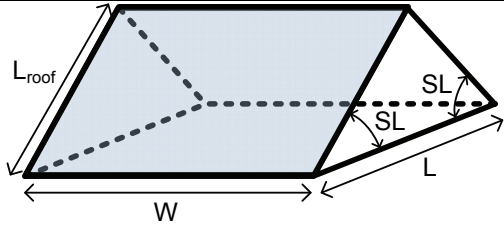
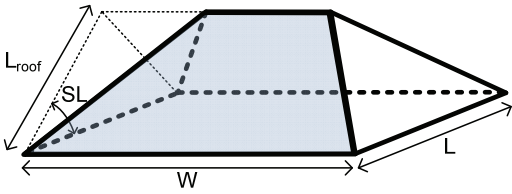
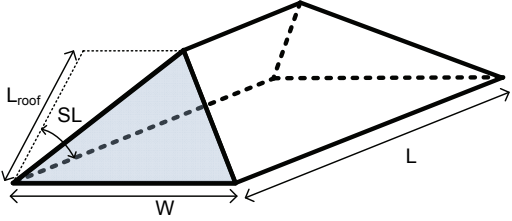
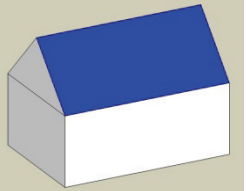
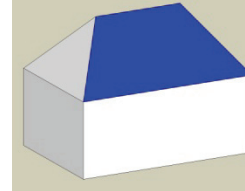
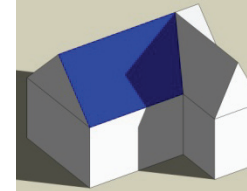
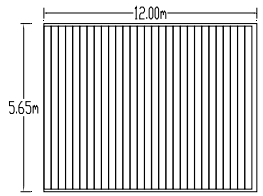
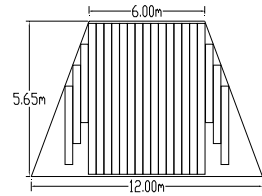
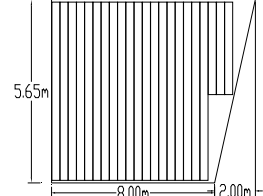
Name (RT)	Gable	Hip (W>L)	Hip (L>=W)
Plan View			
Isometric View			
Active area slope	SL		
Active Area	$(W+L_{eaves}) \cdot L_{roof}$ $= 0.5 \cdot (W+L_{eaves}) \cdot (L+L_{eaves}) \cdot \cos(SL)$	$[(W+L_{eaves}) - (L+L_{eaves})/2] \cdot (L+L_{eaves}) \cdot \cos(SL)$	$0.5 \cdot (W+L_{eaves}) \cdot L_{roof} = 0.5 \cdot (W+L_{eaves})^2 / \cos(SL)$



Table 4-3: Three common roof types and their geometrical and solar implications. The panel layout is based on two standard sizes of Uni-Solar panels. Climate Data is based on Toronto conditions. All active area slopes are 45 degrees (12/12) and South-facing. (Figure taken from (O'Brien et al., 2009b))

	Gable	Hip	Cross-Gable
Visualization			
Annual Solar Radiation on Roof (kWh/m <sup>2</sup> )	1481	1481	1214
% Shaded Annually	0	0	18 %
Optimal Panel Layout			
% Area Covered by Cells	80 %	66 %	76 %

#### 4.1.3 Shading from external obstructions

Designing around or avoiding external obstructions is often considerably more challenging than for self-shading for three reasons, as follows.

- The owner of the house of interest may not have control over the obstructions on neighbouring properties.
- The obstructions may change in shape over the long term, in the case of vegetation (e.g., tall trees or vines).
- Vegetation – in the case of deciduous shrubs and trees – varies seasonally.

Thus, a tree can transform from having little effect on PV performance to being

nearly opaque and allowing only some diffuse solar radiation to reach the panel.

While the models in use are capable of shading analysis, the limitation is that the measuring and input of obstructions is a very imprecise and time-consuming process; easily surpassing the time required to perform the conceptual design for the entire house. Like for the passive solar design aspects, Ecos is premised on the assumption that the designer eliminates the possibility of shading of solar collectors by properly positioning them.

#### **4.1.4 BIPV/T design considerations**

Additional design considerations occur for BIPV with thermal energy recovery systems, such as the one on EcoTerra, as described in Chapter 8. Not only should the total roof area be adequately large to accommodate enough PV modules to meet the energy objectives and the shape be designed to efficiently fit the modules, but the length (soffit to peak) should be selected to maximize performance. Since the air temperature increase rate decays with length of roof, the length should be carefully selected such that it is long enough to achieve a significant and useful increase, but not be too long to be practical. The analysis for EcoTerra showed that about 5 meters was optimal, however, other configurations (e.g., as glazed section) could yield other optima. Another important BIPV/T consideration – as for roofs with BIPV and SHDW systems – is compromising between electrical energy output and thermal energy output. The optima tend not to be the same because useful thermal energy collection tends to favour

steeper slopes to collect more thermal energy in the winter. Ideally, whole-year simulation is used to optimize roof geometry.

## **4.2 PV System Model**

This section describes the building-integrated PV (BIPV) model that was implemented in Ecos. BIPV represents a reasonable opportunity for decoupling from the rest of the model; this hypothesis is properly tested in this section and further discussed in Chapter 5. Ecos is primarily intended for grid-tied homes, for which electrical demand is supplemented by the grid when demand is higher than generation, and excess electricity generation is sold to the grid. This type of situation is simpler to analyze than off-grid applications because issues related to storage capacity and storage losses are avoided.

A number of methods to predict useful energy output of active solar systems have been established in the literature (Duffie and Beckman, 2006). While many of them are about 30 years old and their original motivation may have strongly influenced by computational demand (or allow hand calculations), they are very suitable for the early design stage. During this stage, performance simulations with hourly (or sub-hourly) time steps can be time-consuming and produce an overwhelming amount of data at an unnecessarily high level of complexity. Four PV models are considered, as follows, in increasing complexity.

1. EnergyPlus:Simple PV. This model merely multiplies incident solar radiation on the modules by their nominal efficiency). This ignores temperature effects and consequently does not attempt to predict cell temperature (which may also be of interest and an output).
2. The RETScreen model (RETScreen International, 2005). This model assumes that the array is freestanding and convectively cooled from both the front and the back surfaces. However, BIPV is typically only exposed on the front surface, causing it to operate at higher temperatures, unless the back is actively cooled (e.g., in BIPV/T system). Unlike the previous model, the RETScreen PV model does account for increased temperatures caused by incident solar radiation. Like all RETScreen models, weather data is provided by monthly averages, only; not hourly data. The method for properly making use of this data is described in detail later in this section.
3. EnergyPlus:One-diode, decoupled. This model is based on empirical PV performance and a simplified four-component circuit, as shown in Figure 4-1. The formulation of this model is described in detail in the EnergyPlus Engineering Reference (2009b). In order to estimate the cell temperature for this model, the nominal operating condition temperature (NOCT) is applied, which also assumes a windspeed of 1 m/s.

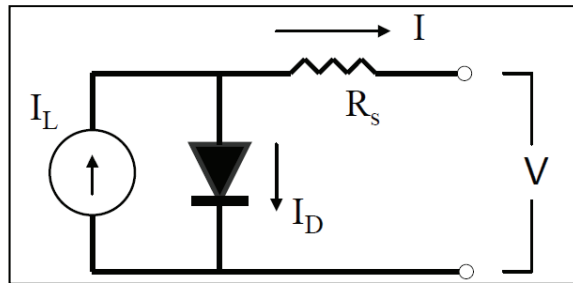


Figure 4-1: Schematic of equivalent four-parameter circuit for one-diode PV model (taken from EnergyPlus Engineering Reference (EnergyPlus, 2009b))

4. EnergyPlus:One-diode, roof-coupled. This model is identical to the previous one except that the PV performance calculation is coupled with the thermal calculation of the roof. This means that the back of the PV modules are protected from the wind and potentially high roofspace air temperatures and could thus increase the PV cell temperature. This will likely result in the highest cell temperature predictions of any of the models.

Each of the models was quantitatively compared, with the intention of using a model that yields a good compromise between the four aforementioned modelling criteria.

For the analysis, the Day 4 MC48 module (Day4 Energy, 2010), which has a nominal efficiency of about 14.9% and is composed of 48 multicrystalline silicon cells, was considered. It is necessary to model a real module in order to obtain realistic performance characteristics and inputs for the one-diode model. The roof was modelled with a slope of 35° and south-facing azimuth (the model's nominal parameter settings). Its outer material was dark-colored metal cladding. For the analysis, 42 - 1.3 m<sup>2</sup> modules were modelled as integrated in a spatially distributed fashion onto the roof, which is equivalent to having 80% of the roof covered in active solar cells.

The use of the simple model used an equivalent PV cell area with equal efficiency to that of the one-diode model under nominal conditions. The RETScreen model was used to estimate performance with and without snow cover modelled (details discussed later).

The one-diode model was explored as both decoupled and coupled to the roof.

Furthermore, for the roof-coupled model, the two cases were examined: roof vented at 1 ach and 10 ach (extreme values were chosen to determine magnitude of the effect).

All performance metrics assume that the system is grid-tied and that all generated electricity is useful. Only DC generation was considered to eliminate the effect of inverter losses (discussed later).

*Table 4-4: PV performance results for different models*

<b>Model</b>	<b>Thermally Coupled?</b>	<b>DC Generation (kWh/year)</b>	<b>Solar Radiation on Cells (kWh/year)</b>	<b>Mean Efficiency</b>	<b>Peak Annual PV Temperature (°C)</b>	<b>Mean Operating Temperature (°C)</b>
RETScreen no snow cover	Decoupled	11,576	78,944	14.66%	41*	-
RETScreen snow cover	Decoupled	11,356	77,460	14.66%	41*	-
Simple	Decoupled	11,034	74,053	14.90%	-	-
One-diode	Decoupled	10,419		14.07%	59.57	9.77
One-diode	Coupled Roof Unvented	9915		13.39%	72.65	12.26
One-diode	Coupled Roof Vented	9980		13.48%	69.95	11.85
<i>*Mean operating cell temperature in peak month (July)</i>						

The results in Table 4-4 indicate a general trend of modestly worse predicted performance as model complexity increases. In the case of the RETScreen models, this is because the predicted solar radiation is higher than calculated by EnergyPlus (and is no

fault of the PV model itself). For the simple EnergyPlus model, cell temperature is neglected and the PV cells are assumed to operate at nominal (favourable) conditions. However, the error associated with this simplification is only about 10%, which is the same order of magnitude as the effect of snow cover, for instance (O'Brien et al., 2009b).

Similarly, modest performance differences occur between the three cases using the one-diode model. This is because the PV cells in the more highly coupled models tend to operate at higher temperatures. However, perhaps more importantly, the predicted peak temperature for thermally coupled models is 13°C (23°F) hotter than that for the decoupled model. This is a concern, as high PV cell temperatures are damaging to their long-term performance (Chow et al., 2003). The mean operating temperature is defined as the time-averaged temperature when the PV has a positive electrical output.

Overall, BIPV represents a reasonable opportunity for the decoupling of subsystems. Clearly, the design of the roof, other than its orientation, has minimal impact on PV performance, as seen by the difference in performance for the last two cases explored. However, if it is decoupled, the PV model should properly account for reduced heat loss from the back surface to characterize higher operating temperatures and the associated performance.

To finalize the choice of the PV model to be used for the current model, it is worth revisiting the purpose of Ecos. Clearly, the simpler models slightly overestimate

performance (by as high as 10%). However, it is not the purpose of the tool to design the roof to any degree of detail, other than basic geometry. Therefore, reporting the exact peak temperature of the PV cells would be suggesting that the roof is modelled in more detail than it is. The Ecos user, in fact, has no control over the roof geometry and ventilation. The modified RETScreen model (with snow accounted for) offers the advantages that it is simple, relatively accurate, fast to compute, and most importantly, sufficiently open that it can be modified to for more advanced research purposes, such as investigating the effect of snow or sun-tracking systems (though this last option is not investigated in the current research).

#### **4.2.1 Detailed PV calculation methodology**

Typically, detailed modeling of PV performance is accomplished using hourly time steps, since both ambient temperature and incident solar radiation are dependent on time.

There would be little point in using a shorter timestep for PV simulation since the weather data is reported hourly and behaviour is not dynamic. To assess the solar radiation on the surface, diffuse, beam, and ground-reflected components are summed, and depend on surface orientation – surface slope and azimuth – as well as the site coordinates and climate. Cell temperature and electricity production are solved simultaneously since they are dependent on each other. Thus, a system of Equations must be solved about 5000 time steps (between sunrise and sunset, only); typically taking several seconds to process. However, to vastly reduce computational intensity, RETScreen (2005) presents a method in which solar angles and daily distribution can be



calculated for an average day each month – thus reducing computations by about 30 fold. This is permissible because for a given hour of the day, the sun is at roughly the same position in the sky for a given month. This approach is highly favourable because it is still based on first principles; allowing virtually any PV configuration or effect (e.g., shading, solar tracking, time-of-day electricity pricing) to be explored. The entire formulation is shown in Appendix D.

#### **4.2.2 Other practical considerations of BIPV design**

While reporting energy and thermal performance based on system design is standard for all building simulation software, informing the user of practical issues is uncommon.

Among all of the aspects, some can merely be included in numerical performance results, while it may be more appropriate for others to be displayed as warnings.

##### **4.2.2.1 Electrical considerations**

The electrical layout of the panels must be properly designed to ensure that they are compatible with the inverter. For instance, during the design process of the ÉcoTerra house, the designers realized that the width of the roof would only accommodate 20 of the selected PV panels, whereas, strings of 7 panels were optimal for the selected inverter. Therefore, the roof had to be widened by about 5% to accommodate an additional panel and allow 3 strings of 7 panels. A string is a group of PV panels that are connected in series. Strings are connected in parallel to the inverter.

There are a few guidelines that should be followed in selecting an appropriate number of panels per string and the number of strings for a given inverter. First, the inverter's

maximum power capacity should exceed – though minimally – the maximum possible output of the array. Also, each string’s voltage range should stay within the inverter’s operating voltage range and that the maximum current should not exceed the inverter capacity. Since voltage is largely dependent on cell operating temperature, the design voltage range should be based on extreme temperatures. James and James (2004) suggest -10°C and 70°C, respectively. Finally, the number of strings is limited to the maximum current of the inverter. Mathematically, these restrictions are as follows (GSES, 2004).

$$0.8P_{PV} < P_{inv,DC} < 1.2P_{PV} \quad (4-1)$$

$$\frac{V_{inv,min}}{V_{MPP,module}|_{T=70^{\circ}C}} < n_{modules/string} < \frac{V_{inv,max}}{V_{OC,module}|_{T=-10^{\circ}C}} \quad (4-2)$$

$$N_{strings} \leq \frac{I_{inv,max}}{I_{string}} \quad (4-3)$$

Where  $P_{PV}$  is the maximum output of the array,  $P_{inv,DC}$  and  $I_{inv,max}$  is the maximum power and current of the inverter, respectively,  $V_{inv,min}$  and  $V_{inv,max}$  is the minimum and maximum operating voltage of the inverter, respectively,  $V_{OC,panel}$  is the open circuit panel voltage,  $V_{MPP}$  is the maximum power point panel voltage,  $n_{modules/string}$  is the number of panels per string, and  $N_{strings}$  is the number of strings of panels in the array.

#### **4.2.2.2 Variable Electricity Rates**

For grid-connected houses that are situated in municipalities in which the retail price of electricity is not constant on an hourly or seasonal basis, it may be favourable to orient the array in a direction that does not yield the highest electricity production. For example, if afternoon rates were considerably higher than morning rates, it could be optimal to have a roof that faces west of south. The benefits of orienting the azimuth of the roof must also be balanced with passive solar heating performance (i.e. the roof orientation relative to the wall orientation is fixed). The current model has the capability of this economic analysis, though it is not implemented into Ecos.

### **4.3 Solar Thermal System Model**

The solar thermal system model is restricted to a single configuration (shown in Figure 4-2) and is for heating domestic hot water, only. The advantage of DHW heating is that it has a seasonally-consistent demand, usually resulting in higher annual performance than space heating applications, for which the thermal energy is only needed in the heating season. A modelling advantage to SDHW systems is that the system performance is not dependent on house performance, and thus the two models can be decoupled. A disadvantage of using solar energy to heat DHW is the high temperature requirement (about 55°C) means that the fraction of time when the solar collectors are outputting useful energy is reduced. However, normally solar energy can make some contribution to preheating the water, since water mains temperatures are relatively cold (e.g., between 2 and 12°C in Toronto (RETScreen International, 2005)).

Unlike PV for which transient effects can be largely ignored because of their lack of storage (for grid-tied systems), SDHW systems have significant transient effects and must be modelled accordingly. There are two main categories of SHDW system models: component-based dynamic or the F-chart (Duffie and Beckman, 2006). The former usually numerically solves a set of Equations representing the heat balances in the main components and is favourable for accuracy and flexibility, though at the cost of complexity and simulation time. The F-chart method is a popular correlation method that can be used to estimate the solar fraction of SDHW system for common configurations. F-charts are used in spreadsheet programs like RETScreen (RETScreen International, 2005). However, as component sizes, controls, and system configurations deviate from standard ones, the F-chart method becomes less accurate. For this work, a component-based dynamic model was created in EnergyPlus because of the cited advantages and control with regards to higher model resolution.

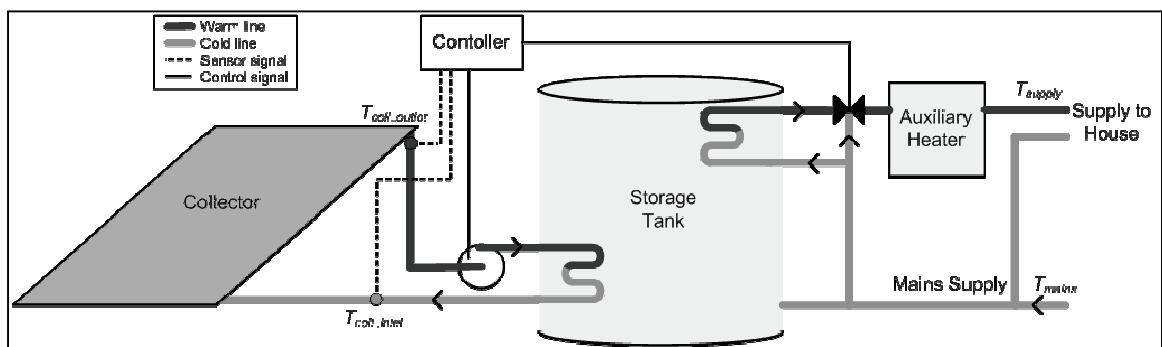


Figure 4-2: Solar domestic hot water system configuration (Note that the exact position of the source and use-side heat exchangers is not critical because a mixed tank is modelled, as described in the following section.)

The major system components, as shown in Figure 4-2, are the collector array, a collector storage tank, and an auxiliary instantaneous water heater. Secondary

components are pipes, a pump, a tempering valve, temperature sensors, and a controller. The collector-storage tank loop is activated by a pump when the conditions are favourable for raising the average tank temperature. If the hot water that is drawn from the storage tank is too cold, the instantaneous heater is used to bring it up to the desired temperature before delivering it to sinks, showers, and clothes washers. Since the main objective of this work is to predict the impact of having a solar thermal collector on energy use, the auxiliary heater is used. The only advantage to having a conventional secondary storage tank with an auxiliary heater is that loads can be shifted and the model could account for thermal losses from the tank. Instantaneous heaters are becoming a preferred method for water heating, though high peak current draws are a consideration for electrically-powered units.

For simplicity, the storage tank is assumed to have a height that is double its diameter and to be surrounded in insulation with thermal resistance of  $4 \text{ m}^2\text{K/W}$ . The heat exchangers in between the collector and use loops and the storage tank are assumed to have an effectiveness of 90%.

Storage tanks can be modelled using a single node or multiple nodes. Multiple nodes are used if stratification is to be characterized. The single-node (mixed) tank energy balance is described by the following Equation.

$$\rho V c_{p,water} \frac{dT}{dt} = q_{heater} + q_{loss} + q_{use} + q_{source} \quad (4-4)$$

Where, the right-hand side contains the heat gains and heat losses of the tank, as defined by:

$$q_{use} = \epsilon_{use} \dot{m}_{use} c_{p,water} (T_{use} - T) \quad (4-5)$$

$$q_{source} = \epsilon_{source} \dot{m}_{use} c_{p,water} (T_{source} - T) \quad (4-6)$$

and  $q_{heater}$  is the heat added by the heating element and  $q_{loss}$  is the heat lost by the tank to the environment.

For the stratified (multi-node) tank model, the nodes are defined by differential Equations that can be solved simultaneously. EnergyPlus uses the Forward-Euler numerical method to solve the temperature of each node based on the adjacent nodes' previous temperature (EnergyPlus, 2009b). The tank fluid is divided by  $n$  equal volume, vertically-stacked nodes. Each node has an energy balance that is equal to:

$$T_n = T_{n,old} + \frac{q_{net,n} \Delta t}{m_n c_{p,water}} \quad (4-7)$$

Comparative tests under the nominal design conditions show (see Figure 4-3) that the stratified tank model does predict modestly better performance but that there is little advantage to using more than two to three nodes, under the current conditions (nominal parameter values). Given that the stratified tank model is considerably more computationally-intensive than the mixed tank model and that the error is minimal (~5%), the mixed tank model shall be used. Furthermore, this approach is conservative, which, in general, is favoured over optimistic modelling assumptions. Note that the

mixed tank model was compared to the stratified tank model with 1 node. Ideally, they would have been identical, though they are only about 0.5% different. The difference occurs because the stratified tank model uses a shorter (hard-coded) timestep than the mixed model which uses the user-specified timestep. EnergyPlus arbitrarily set the maximum number of nodes at 10, though this does not appear to be a limitation to accuracy for typical storage tanks.

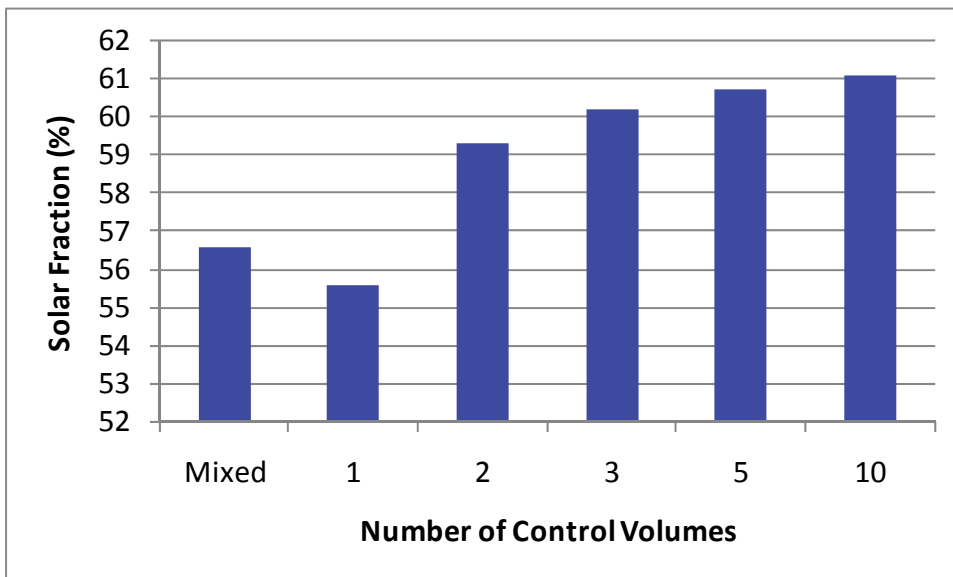


Figure 4-3: Comparative test for different storage tank models and for different numbers of nodes

The objective of this model is to size the collector and tank to achieve the desired solar fraction. The major design parameters are the number of collectors (PL) and the storage tank volume (TV). The size ranges are based on design rules of thumb. For collector area, usually a 2 m<sup>2</sup> collector is recommended for a two-person house with about 0.5 to 1 m<sup>2</sup> for each additional person. Similarly, tank volumes ranging from 320 to 480 liters are recommended. The maximum sizes in the range were increased to allow high solar fractions (as defined at the end of this chapter).

Predicted system performance for different tank volumes (mixed tank model) is shown in Figure 4-4, but will vary for different system designs and conditions.

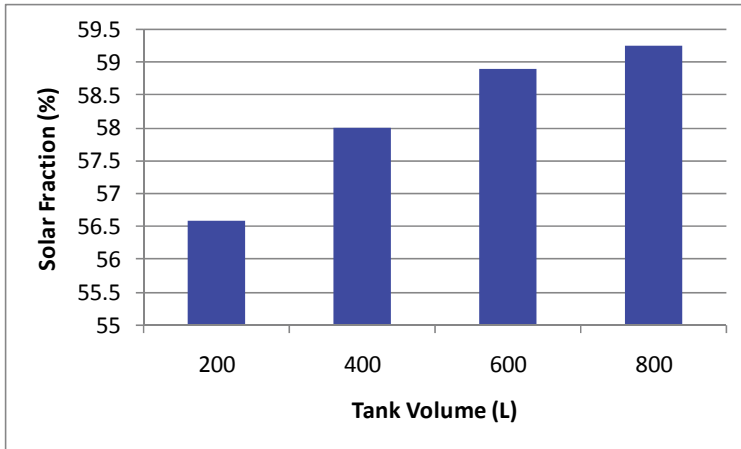


Figure 4-4: Solar fraction for the SDHW system under the nominal design conditions except for different tank volumes

The array is assumed to be flush-mounted to the active part of the roof (same surface as the PV array). The array performance is fixed with characteristics that match a prominent Canadian product (EnerWorks COL-4X8-NL-SG1). Its specifications (obtained from SRCC (2009)) are summarized in Table 4-5.

Table 4-5: Solar thermal collector specifications

Model Name	EnerWorks, Inc. COL-4x8-NL-SGI-SH10US
Net aperture area, gross area	2.691, 2.873 m <sup>2</sup>
Type	Single-glazed, copper tube, aluminum plate, mineral wool insulation
Efficiency curve	$\eta = 0.7622 - 3.2787 (T_{inlet} - T_{amb})/I - 0.129 (T_{inlet} - T_{amb})^2/I$
Incident angle correction	$K_{\alpha\tau} = 1 + 0.0566 \cdot (1/\cos\theta - 1) - 0.2167 \cdot (1/\cos\theta - 1)^2$
Test flow rate	53 ml/s

The EnergyPlus formulation (EnergyPlus, 2009b) for the flat-plate glazed solar collector consists of a heat balance of the system. Using empirically formulated coefficients, the collector efficiency is calculated using the following Equation.



$$\eta = c_0 + c_1 \frac{(T_{in} - T_{air})}{I_{solar}} + c_2 \frac{(T_{in} - T_{air})^2}{I_{solar}} \quad (4-8)$$

As the incident solar radiation deviates from being normal to the solar collector, the transmittance of the glazing decreases, as defined by the second-order incident angle modifier (IAM) as follows.


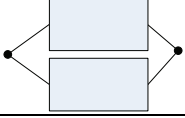
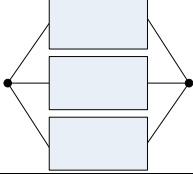
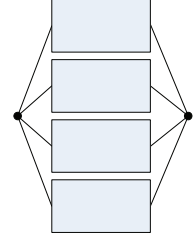
$$K_{\tau\alpha} = 1 + b_0 \left( \frac{1}{\cos\theta} - 1 \right) + b_1 \left( \frac{1}{\cos\theta} - 1 \right)^2 \quad (4-9)$$

The correlation is only valid for angles of 60° or less; EnergyPlus reduces incident solar radiation to zero for angles above this. Finally, the main value of interest is the outlet water temperature, which is found using the following Equation.

$$T_{out} = T_{in} + \frac{q}{\dot{m}c_p A} \quad (4-10)$$

In general, longer strings of collectors in series results in low system efficiency, but the outlet temperature is greater, thus increasing the period of time when the system can be used. Testing with this particular solar collector showed that there was very limited benefit to having more than one collector in series because under most weather conditions, the outlet fluid cannot be significantly increased.

Table 4-6: All allowed collector configurations

Parallel (PL)	Series	Configuration
1	1	
2	1	
3	1	
4	1	

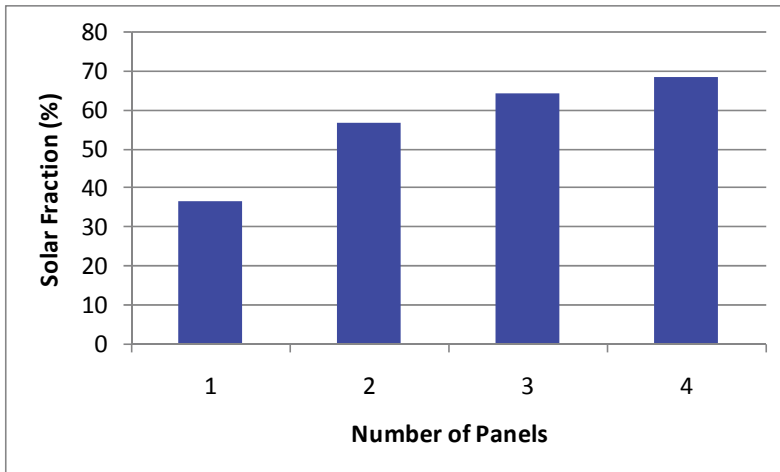


Figure 4-5: Solar fraction for the SDHW system under the nominal design conditions but with different numbers of panels in parallel.

The water draw profile is proportional to the one shown in Figure 4-6. The daily hot water use is dependent on the number of occupants, which in turn, is assumed to be solely dependent on the floor area (FA), as follows. This is consistent with the previous

chapter, which discusses the relationship between internal gains and the number of occupants.

$$V_{\text{DHW,daily}} = 85\text{L} + 35\text{L}\cdot\text{round}(\text{FA}\cdot 0.019/\text{m}^2) \quad (4-11)$$

Since the range of floor areas FA is 100 to 450 m<sup>2</sup>, the range of daily DHW draws is 155 to 400 L.

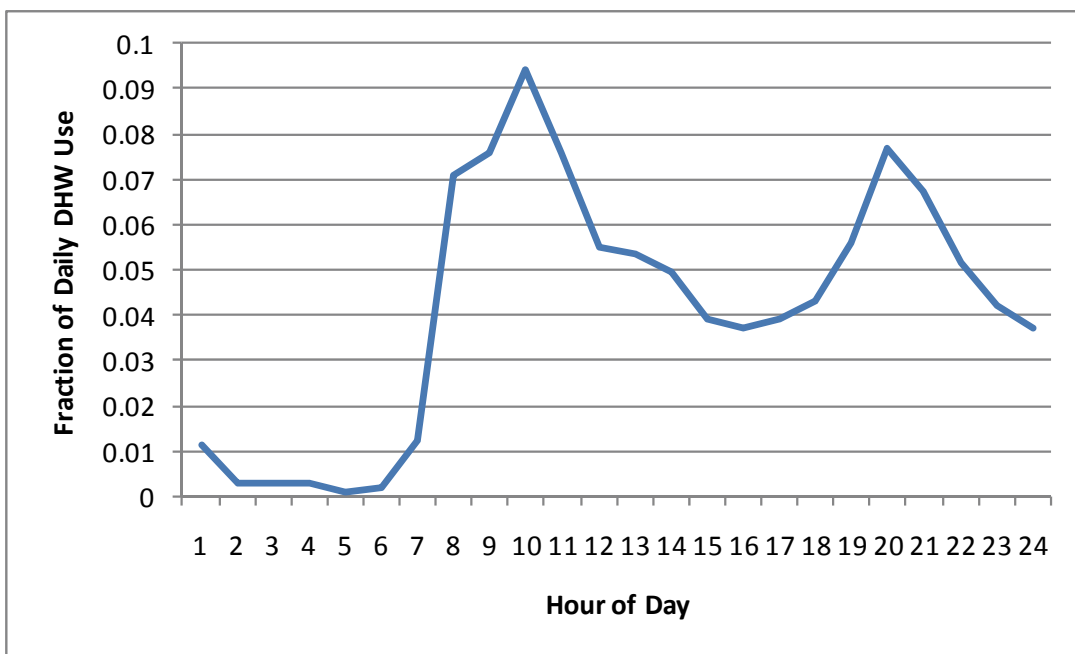


Figure 4-6: Daily DHW draw profile; fraction of daily total

### 4.3.1 SDHW system controls

Controls are implemented in the SDHW to optimize performance and protect the equipment from overheating or freezing. They are described below in detail.

1. *On if collector outlet temperature is warmer than the collector inlet temperature (approximately equal to the storage tank temperature).*

EnergyPlus recommends a dead band of 1 to 3°C; 2°C is used for the model.

The dead band accounts for inaccuracies in measurement and the fact that a sufficient rate of energy must be collected before electricity use for the pump can be justified.

2. Off if the collector outlet is below freezing (water is the modelled fluid, so 0°C).
3. Mix cold water with the hot water from the storage tank if it exceeds a safety threshold to prevent scalding of occupants; the model uses 55°C. This strategy has the advantage that the storage tank average temperature can reach higher temperatures and store even more energy.

As mentioned in the previous chapter when EnergyPlus was selected as the most suitable simulation engine for this work, a major drawback of the tool is the complexity of explicitly defining plant models. Figure 13-4 in Appendix E shows all of the objects required to build this relatively simple SHDW model. Furthermore, unlike TRNSYS which has an interactive flowchart-like interface that shows all components, EnergyPlus merely shows a simple flowchart with the major components (see Figure 13-5 in Appendix E). Because the modelling capabilities are intended for commercial building HVAC systems, many of the naming conventions are misleading for the SDHW system.

### **4.3.2 Sample Performance**

To illustrate typical performance of the system, key metrics for three summer days under the nominal design conditions are shown in Figure 13-6 in Appendix E.

## **4.4 High-level outputs**

One of the most useful metrics for active solar systems is the solar fraction, which is defined as the fraction of total energy demand that is provided by solar energy. The advantage to this metric is that it puts renewable energy generation in the context of the magnitude of energy use. For PV, it is the fraction of the total electrical demand that is met by PV generation. Note that it is the electrical energy output by the inverter (for houses with predominantly AC appliances); not the DC array output. This is because the quantities of interest are the potential energy cost savings and reduced environmental impact from reduced dependence of the utility grid.

For the SHDW system, solar fraction is not based on the energy collected by the solar collectors, but rather the displaced electricity use (for the instantaneous water heater).

For the baseline case (i.e., solar fraction = 0), the model can be simulated without the storage tank or solar collectors.

Since this work focuses on grid-tied houses, all inverter output is assumed to be useful in reducing costs and utility grid loads. However, for the SDHW systems, for which excess solar energy collection is not useful, high solar fractions almost certainly mean over-sizing the array in the summer.

For absolute system performance, monthly production of the PV and SDHW systems can be calculated. Similarly to the calculation for solar fraction, only the displaced purchased energy is of interest. Thus, for the SDHW, the solar contribution is calculated by subtracting the monthly purchased energy of the SDHW system from the standard (non-solar) system.

## **4.5 Conclusion**

This chapter carefully assesses active solar systems and assessed different methods for accurately modelling them. A simplified model was found to be adequate for modelling BIPV, but a dynamic EnergyPlus-based model was selected for the SDHW system. The six model inputs and the model outputs are also listed and discussed.

## 5 INTEGRATED DESIGN AND INTERACTIONS

Solar houses are complex systems that involve interacting subsystems and should be designed as such. However, as previously alluded to, a fully-integrated model comes with the cost of increased design/optimization and computational time. Depending on the model aspect, this is not necessarily associated with significantly greater accuracy (the ultimate measure of a model's success). Figure 5-1 shows the trends of accuracy and design/computational time versus the degree of model integration. As degree of model integration increases, time increases exponentially, while accuracy asymptotically approaches 1. These relationships indicate that a suitable level of model integration should be carefully selected for the application. Since the motivation of the model for this work is early stage design, there is pressure to reduce both computational and design time; though a reasonable level of accuracy is demanded.

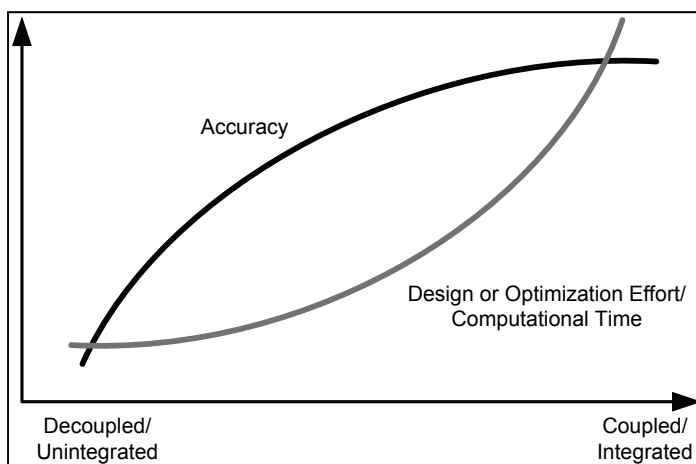


Figure 5-1: Cost and benefit trends for the degree of integration (coupling) of models

The examples that follow support the shape of the curves in Figure 5-1. Consider a system comprised of three subsystems, each with two design options. If the subsystems

are decoupled, the designer can select the best option for each subsystem: three decisions. If the systems are coupled, the designer must choose from as many as eight ( $2^3$ ) options. In general there are  $(\textit{number of options per subsystem})^{[\textit{number of subsystems}]}$  decisions; clearly indicating an exponential relationship.

In practical terms, a coupled model simultaneously determines each subsystem's boundary conditions, inputs, and outputs, while these things are merely estimated for each subsystem in a decoupled model. For example, suppose each subsystem is represented by two state variables (temperature, pressure, voltage, etc.). For the decoupled model, three sets of two differential Equations must be solved simultaneously. For the coupled model, six differential Equations must be solved simultaneously. If the solution is performed numerically, using matrix inversion, for which computational time is approximately proportional to the cube of the (square) matrix dimension, the computational cost of the coupled model is 27-fold ( $6^3/2^3$ ) relative to the decoupled model.

Accuracy cannot be so easily proven to provide diminishing returns because it varies by case. However, examples, such as the case of coupled versus decoupled BIPV, are found throughout this thesis.

This chapter addresses issues related to parameter and subsystem interactions. This work is fundamental to selecting appropriate model resolution, and ultimately, the way that Ecos is used to design houses.



## 5.1 Parameter Interactions

This section examines the potential for decoupling parameters during design. In many cases, it would be unwise to merely optimize each parameter independently since they all interact to some level. For instance, O'Brien et al (2008a) showed that the optimal south-facing glazing area for house with high internal gains was a third of the size of the optimal size with minimal internal gains. Therefore, one can conclude that certain parameters should be manipulated in subsets, rather than individually. Obviously, manipulating more than several parameters simultaneously is tedious and yields an exponentially expanding design space. To help solve this problem, batch simulations were run to identify the most significant interactions between pairs of parameters.

For a population of 30 parameters, there are 435 (30 choose 2) two-way interactions to consider. The focus of this work is on two-way interactions since high-order interactions are unusual (Shah et al., 2000). One common method to understand interactions is to create interactions plots, as is commonly performed in the field of design of experiments (DOE) (Mason et al., 2003). In all, 435 plots were created using MATLAB to drive EnergyPlus simulations with specific values of the 30 parameters. For the plots, all parameter settings were set to the nominal values (as previously defined), except for the pair of parameters being examined. For those two parameters, the extreme values were combined, to yield four ( $2^2$ ) different parameter combinations and corresponding performance values. Thus, for the 435 pairs of parameters, 1740 simulations were run.

Once the values (in this case combined annual heating and cooling energy) were obtained from the simulation results; they were plotted. The two parameters are denoted  $A$  and  $B$  herein. Each interactions plot contains two lines, each indicating a different value for parameter  $B$ , as shown in Figure 5-2. The endpoints of each line correspond to the low (left) and high (right) values of parameter  $A$ . It is important to note that these lines do not necessarily indicate a linear relationship between performance and the parameter value; they appear as linear because only the extreme parameters are evaluated (rather than the midpoints) for the interactions analysis. If the lines are parallel, this indicates that there is no interaction between the two parameters. In contrast, if they are nonparallel, an interaction exists. The relative slope of the lines indicates the magnitude of the interaction. The standard method for quantifying the interaction is using Equations 5-1 through 5-3 (Mason et al., 2003).

$$E_{A,B(-)} = R_{A(-)B(-)} - R_{A(+ )B(-)} \quad (5-1)$$

$$E_{A,B(+)} = R_{A(-)B(+)} - R_{A(+ )B(+)} \quad (5-2)$$

$$I_{A,B} = 0.5(E_{A,B(+)} - E_{A,B(-)}) \quad (5-3)$$

where  $A$  and  $B$  are the two parameters being examined for interactions,  $I_{A,B}$  is the magnitude of the interaction,  $E_{A,B(+)}$  is the effect of parameter  $A$  at the high level of parameter  $B$ , and  $E_{A,B(-)}$  is the effect of parameter  $A$  at the low level of parameter  $B$ , and the  $R_{AB}$  terms are the response (heating and cooling energy for this application) depending on the values of  $A$  and  $B$ . The responses ( $R_{AB}$ ) are shown in Figure 5-2.

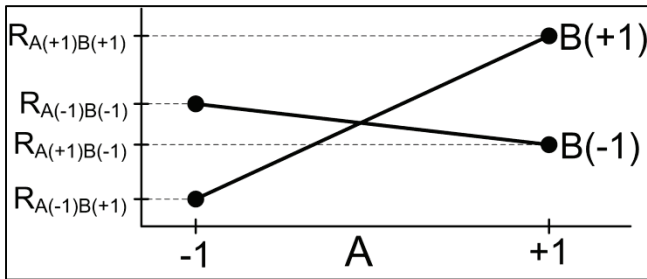


Figure 5-2: Generic representation of responses and interactions

The principle is best explained with two examples. Figure 5-3a shows the interaction between the south-facing glazing area (*WWR1*) and type (*GT1*); representing the single strongest interaction between two design parameters. In practical terms, this means the window area and type should not be selected independently because the optimal glazing area is dependent on the glazing type. The results show that a large glazing area is beneficial if it is triple-glazed, low-e, argon-filled. However, total energy use actually increases under the same range of glazing areas for clear, double-glazed, air-filled windows. Thus, clearly a designer who attempts to optimize one parameter at a time would oversee this critical interaction.

An important observation from Figure 5-3a is that the two points corresponding to low *WWR1* values are nearly coincident, despite the other parameter (*GT1*) being at its two extremes. While the results are intuitive in this case, it proves that one-dimensional parametric analyses can overlook the significance of parameters. In contrast, Figure 5-3b shows minimal interaction between the wall and ceiling thermal resistance (*WR* and *CR*). It indicates that if either of these quantities is increased individually, the energy

use decreases, and that, regardless of the value of  $WR$ , increasing  $CR$  is beneficial (for the range of values that were explored), and vice versa.

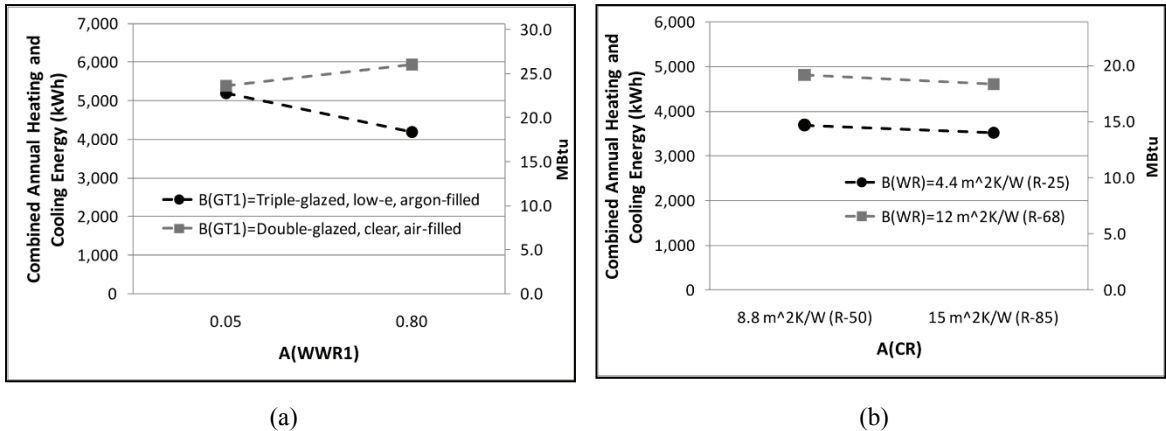


Figure 5-3: Example interactions plots showing a strong interaction (a) and a weak interaction (b).

The magnitudes of the strength of interactions are illustrated using a “wheel of interactions” (Wol) in which the parameters are plotted around a circle and those joined by a line indicate their strength. The thickness of the line is proportional to the strength of the interaction. Furthermore, they are shaded differently to indicate whether they are between design parameters, between non-design parameters, or between one of each (a design and a non-design parameter).

While some interactions are obvious, others are less so, such as that between  $GT1$  and  $AR$  or  $WR$  and  $WWR1$ . These stronger interactions, suggest that the design space should be assessed in a multi-dimensional fashion, where an array of practical combinations is explored. In contrast, parameters that show minimal interactions with any other parameters can be optimized individually; saving significant effort. For instance, as one would expect, the parameters defining the roof have minimal influence on the heating

and cooling energy of the house. This freedom means that the roof can be effectively decoupled from the rest of the house and that the roof can be optimized for active solar energy collection.

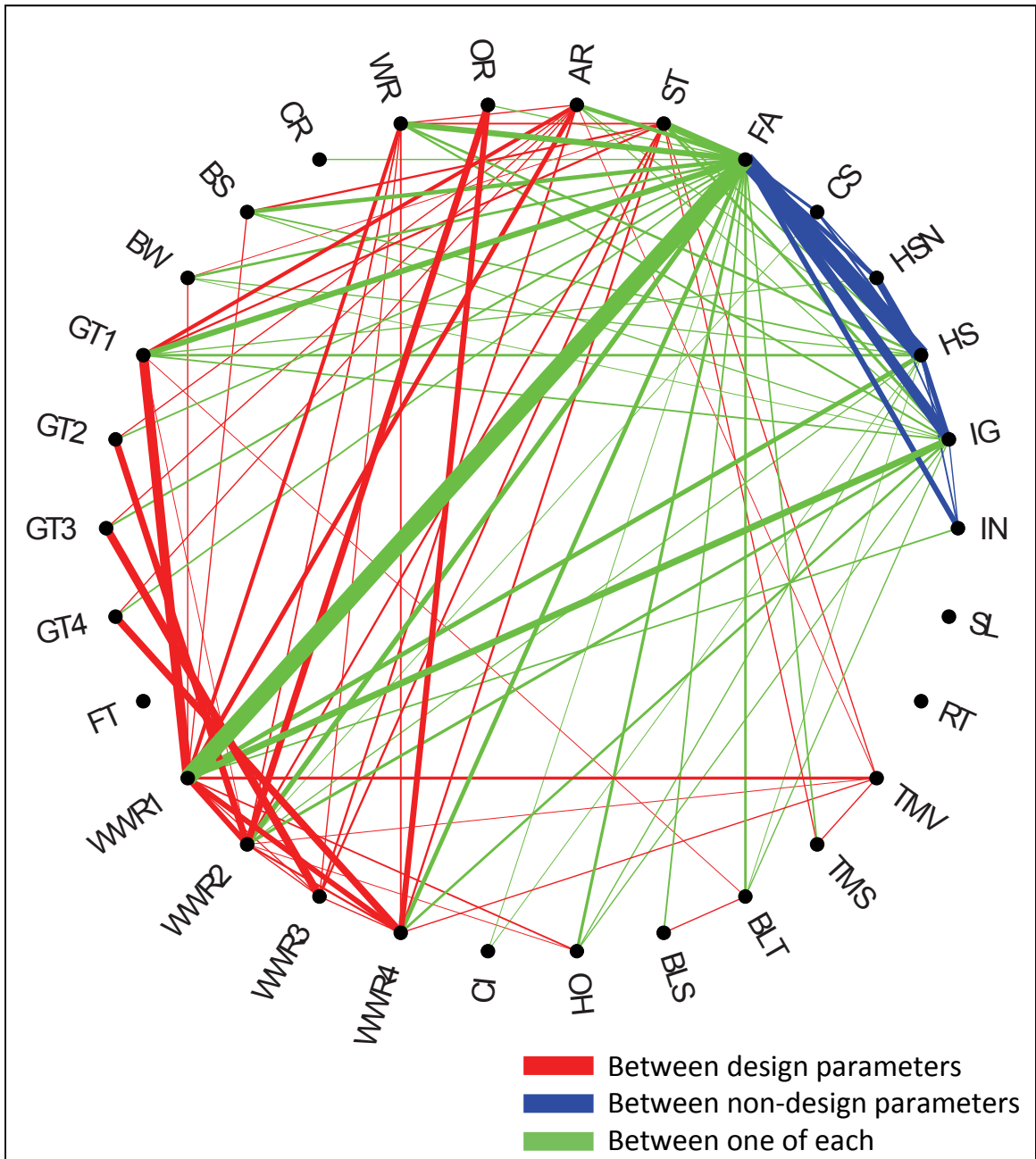


Figure 5-4: Visualization of the interactions with WWR1. Each line connecting two parameters indicates a strong interaction. The line thickness is proportional to the strength of the interaction.

Table 5-1: Normalized strength of interactions between all pairs of the 30 house model parameters. The strength of the interactions is formulated in Equation 5-3.

IN	0.075	0.089	0.032	0.003	0.324	0.034	0.033	0.010	0.031	0.000	0.019	0.015	0.018	0.004	0.009	0.005	0.000	0.094	0.036	0.005	0.032	0.004	0.018	0.007	0.011	0.007	0.003	0.000	0.001	
	IG	0.306	0.100	0.028	0.616	0.164	0.088	0.033	0.119	0.020	0.071	0.057	0.108	0.027	0.036	0.030	0.000	0.410	0.164	0.037	0.146	0.030	0.079	0.049	0.071	0.037	0.026	0.011	0.001	
		HS	0.440	0.139	0.982	0.113	0.066	0.035	0.141	0.026	0.092	0.072	0.163	0.047	0.054	0.048	0.000	0.275	0.066	0.040	0.048	0.057	0.065	0.038	0.057	0.007	0.039	0.010	0.002	
			HSN	0.101	0.274	0.023	0.036	0.007	0.052	0.011	0.024	0.019	0.068	0.017	0.017	0.016	0.001	0.011	0.031	0.050	0.010	0.001	0.010	0.017	0.014	0.022	0.005	0.003	0.000	
				CS	0.181	0.032	0.018	0.021	0.001	0.000	0.003	0.002	0.004	0.000	0.000	0.001	0.000	0.000	0.063	0.027	0.041	0.006	0.002	0.010	0.009	0.001	0.013	0.001	0.000	
					FA	0.424	0.254	0.070	0.362	0.081	0.263	0.163	0.349	0.093	0.117	0.097	0.000	1.000	0.298	0.023	0.259	0.060	0.171	0.107	0.147	0.098	0.033	0.014	0.001	
						ST'	0.039	0.011	0.096	0.034	0.115	0.061	0.129	0.043	0.041	0.042	0.000	0.024	0.136	0.126	0.128	0.004	0.004	0.000	0.002	0.080	0.067	0.000	0.009	
							AR	0.001	0.064	0.007	0.021	0.023	0.233	0.080	0.069	0.083	0.004	0.289	0.023	0.119	0.029	0.001	0.046	0.023	0.033	0.008	0.060	0.002	0.006	
								OR	0.015	0.001	0.009	0.006	0.035	0.014	0.004	0.026	0.000	0.012	0.401	0.027	0.364	0.006	0.011	0.022	0.024	0.003	0.012	0.004	0.002	
									WR	0.006	0.028	0.026	0.028	0.008	0.011	0.008	0.007	0.217	0.101	0.063	0.092	0.010	0.031	0.011	0.018	0.007	0.007	0.001	0.006	
										CR	0.007	0.003	0.004	0.001	0.003	0.003	0.000	0.021	0.012	0.003	0.006	0.000	0.008	0.000	0.001	0.000	0.001	0.006	0.001	
											BS	0.012	0.020	0.009	0.013	0.010	0.000	0.073	0.030	0.002	0.029	0.006	0.020	0.009	0.014	0.007	0.001	0.004	0.002	
												BW	0.014	0.006	0.009	0.006	0.000	0.066	0.025	0.000	0.021	0.007	0.015	0.006	0.009	0.007	0.003	0.001	0.002	
													GT1	0.004	0.008	0.006	0.003	0.584	0.057	0.017	0.044	0.003	0.033	0.041	0.060	0.001	0.011	0.001	0.006	
														GT2	0.004	0.003	0.003	0.002	0.400	0.000	0.010	0.001	0.004	0.003	0.002	0.001	0.003	0.002	0.004	
															GT3	0.004	0.001	0.037	0.023	0.469	0.017	0.003	0.009	0.005	0.006	0.003	0.002	0.000	0.002	0.004
																GT4	0.001	0.027	0.016	0.001	0.417	0.001	0.006	0.003	0.003	0.003	0.004	0.001	0.002	0.002
																	FT	0.000	0.002	0.002	0.001	0.000	0.000	0.000	0.000	0.000	0.000	0.000	0.000	
																		WWR1	0.322	0.077	0.316	0.039	0.098	0.030	0.047	0.047	0.188	0.002	0.002	
																			WWR2	0.080	0.121	0.002	0.054	0.038	0.053	0.030	0.062	0.001	0.005	
																			WWR3	0.079	0.006	0.015	0.014	0.017	0.016	0.052	0.001	0.001		
																			WWR4	0.009	0.047	0.035	0.047	0.032	0.080	0.006	0.008			
																					CI	0.001	0.004	0.005	0.012	0.031	0.000	0.003		
																						OH	0.003	0.001	0.011	0.015	0.003	0.002		
																							BLS	0.077	0.006	0.007	0.001	0.000		
																								BLT	0.011	0.016	0.001	0.001		
																									TMS	0.083	0.001	0.000		
																										TMV	0.002	0.008		
																											RT	0.002		

As previously explained, non-design parameters are those that would be set early in the design process as constraints or assumptions, and are unlikely to be modified later unless additional information is obtained. Thus, the designer may not be concerned with their values when attempting to optimize performance. However, strong interactions that involve non-design parameters are important, nonetheless. They emphasize the importance of accurately predicting them. For instance, the internal gains scheme (*IG*) exhibits strong interactions with the south-facing glazing areas (*WWR1*). This indicates that properly predicting the non-HVAC loads is critical to optimizing glazing area. In the context of *Ecos*, the non-design parameters that exhibit significant interactions with other parameters should be modelled and predicted with as much accuracy as reasonably possible. The use of the *Wol* is demonstrated in Chapter 7.

The implication of interactions in the design process is that once the strong interactions are identified, then the lesser interactions can be mostly overlooked. The top ten interactions are listed in Table 5-2 and the top ten interactions involving design parameters only are listed in Table 5-3. Note that  $|I_{A,B}| = |I_{B,A}|$ , and thus, absolute values are shown.

Table 5-2. Top ten interacting pairs of parameters

Rank	Interacting Parameters		$I_{A,B}/\max(I_{A,B})$
1	WWR1	FA	1
2	FA	HS	0.982
3	FA	IG	0.616
4	WWR1	GT1	0.584
5	WWR3	GT3	0.469
6	HSN	HS	0.440
7	ST	FA	0.424
8	WWR4	GT4	0.417
9	WWR1	IG	0.410
10	WWR2	OR	0.401

Table 5-3. Top ten interacting pairs of design parameters

Rank	Interacting Parameters		$I_{A,B}/\max(I_{A,B})$
1	WWR1	GT1	0.584
2	WWR3	GT3	0.469
3	WWR4	GT4	0.417
4	WWR2	OR	0.410
5	WWR2	GT2	0.401
6	WWR4	OR	0.364
7	WWR2	WWR1	0.322
8	WWR4	WWR1	0.316
9	WWR1	AR	0.289
10	GT1	AR	0.233

The results indicate that interactions involving window area and other major geometrical parameters are among the most significant. Additionally, operational-based parameters are involved in some very significant interactions. For example, the south-facing window-to-wall ratio (*WWR1*) is highly interacting with the floor area. This is because larger windows are more beneficial to larger houses, which have greater heat losses and a higher capacity to passively store solar gains. The relationship between the glazing types (*GT*) and (*WWR*) represent the strongest interactions among the design parameters because the benefit (or hindrance) of a window is highly-dependent on its



thermal and optimal properties. A large south-facing window is only beneficial if it has a sufficiently high solar transmittance and a sufficiently low conductance.

## **5.2 Model Coupling and Decoupling**

Interactions are not limited to occurring between parameters, but can also occur between entire subsystems (e.g., photovoltaic arrays, the house's envelope, solar thermal systems, etc.). Subsystems that do not interact at all can be designed independently. However, subsystems with substantial interactions should be designed in an integrated manner because the change of a one subsystem is likely to have a significant effect on the other(s). The importance of assessing the level of interaction is evident in reducing design efforts.

Figure 5-5 qualitatively describes the level of interaction between subsystems using a Venn diagram; with the central subsystem being the house's envelope and associated base loads. Interactions can be performance-based or practical in nature, and are noted in the diagram.

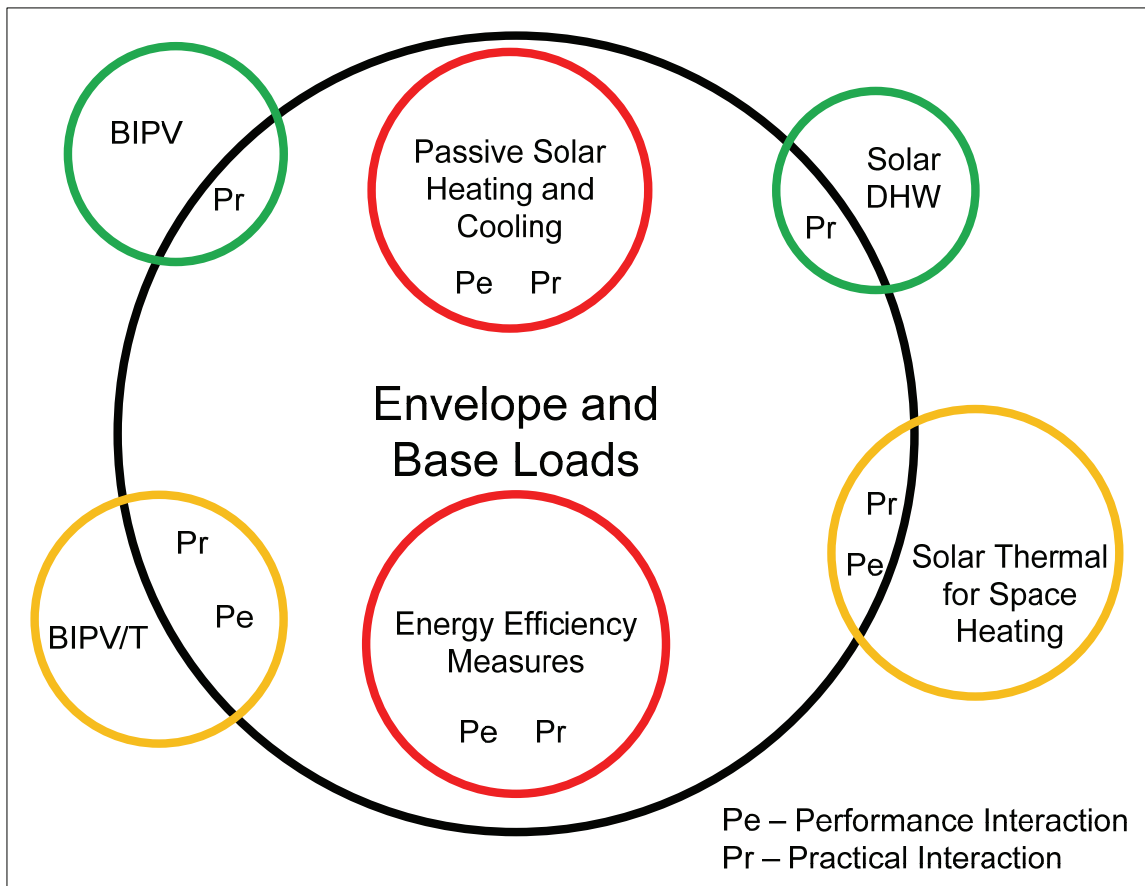


Figure 5-5. Venn diagram of the potential for decoupling the subsystems. (BIPV = building-integrated photovoltaics; DHW = domestic hot water; BIPV/T = building-integrated photovoltaics with thermal energy recovery) (taken from (O'Brien et al., 2011b))

Performance-based interactions are those for which the performance of two subsystems depend on each other. For instance, any solar thermal systems that supplements purchased heating depends on the design of the envelope. An energy efficient envelope will tend to be less dependent on the active solar collectors, and thus, the contribution of the active solar collectors is lessened. Therefore, the solar collectors and storage should be sized for the specific house. Similarly, the benefit of energy efficiency measures (EEMs) is highly-dependent on the performance of the other

systems. In general, EEMs provide diminishing returns, so assuming that they are additive is optimistic.

Practical interactions are those in which geometrical or other practical constraints must be considered. For instance, if BIPV roof is to be entirely covered in PV modules, the slope and dimensions of the roof must be selected to accommodate commercially available products. The ÉcoTerra roof's slope, at 30°, was partly selected so that the PV modules covered the entire distance from the eaves to the ridge (Noguchi et al., 2008). If only a practical interaction exists between two subsystems they may be modelled independently as long as the designer ensures compatibility between them. For instance, ÉcoTerra's BIPV was modelled separately (and with a different tool) from the thermal performance of the house to exploit the features of the different tools.

The best prospects for decoupling from the envelope and base loads are BIPV and solar DHW systems. BIPV's performance is not dependent on energy demands of the house (for grid-tied systems). While PV performance is a function of its operating temperature, this is unlikely to vary significantly between different house designs. Solar DHW systems' performance *is* dependent on demand. However, demand is not tied to the design of the house, per se, but rather occupant behavior. Both systems do share a geometric relationship with the house, but these relationships can be managed externally to the thermal models.

Solar thermal systems for space heating (including BIPV/T) have some traits in common with the other types of solar collector. However, their performance is tied to demand from the house. If no heat is needed because of passive solar gains, the system contributes nothing at that time, unless thermal storage is available. Similarly, collector performance may depend on the temperature of the storage medium (for closed-loop systems).

Decoupling models not only offers computational advantages, but more importantly, it helps the designer, by breaking the problem into more manageable problems and reduces the number of possible design combinations. Furthermore, it allows the use of multiple design tools in the case where the design tool of choice does not have a certain feature or technology. In the context of the design tool that is currently being developed, the identification of the models that can be decoupled offer advantages: (1) they can use separate models as simulation engines, and (2) they can be simulated independently, which often reduces model complexity and consequently, simulation time.

## **6 USE OF THE DESIGN TOOL AND MODEL: DESIGN**

### **METHODOLOGY**

The past three chapters explain the house performance model (passive and active solar elements) in detail and Ecos' implementation and user interface. This chapter explores a strategy for using the Ecos to design high-performance solar houses. The design methodology is intended for a cold climate, which is defined by Hutcheon and Handegord (1995) as having a winter design temperature of  $-7^{\circ}\text{C}$  or lower.

#### **6.1 Prioritizing house upgrades**

The priority in applying upgrades during the path from the current design to a design that meets the objectives is to select robust, passive, cost-effective measures. Figure 6-1 demonstrates positioning of the house model's parameters and the subsystems they represent within the space that defines two criteria: robustness and passivity.

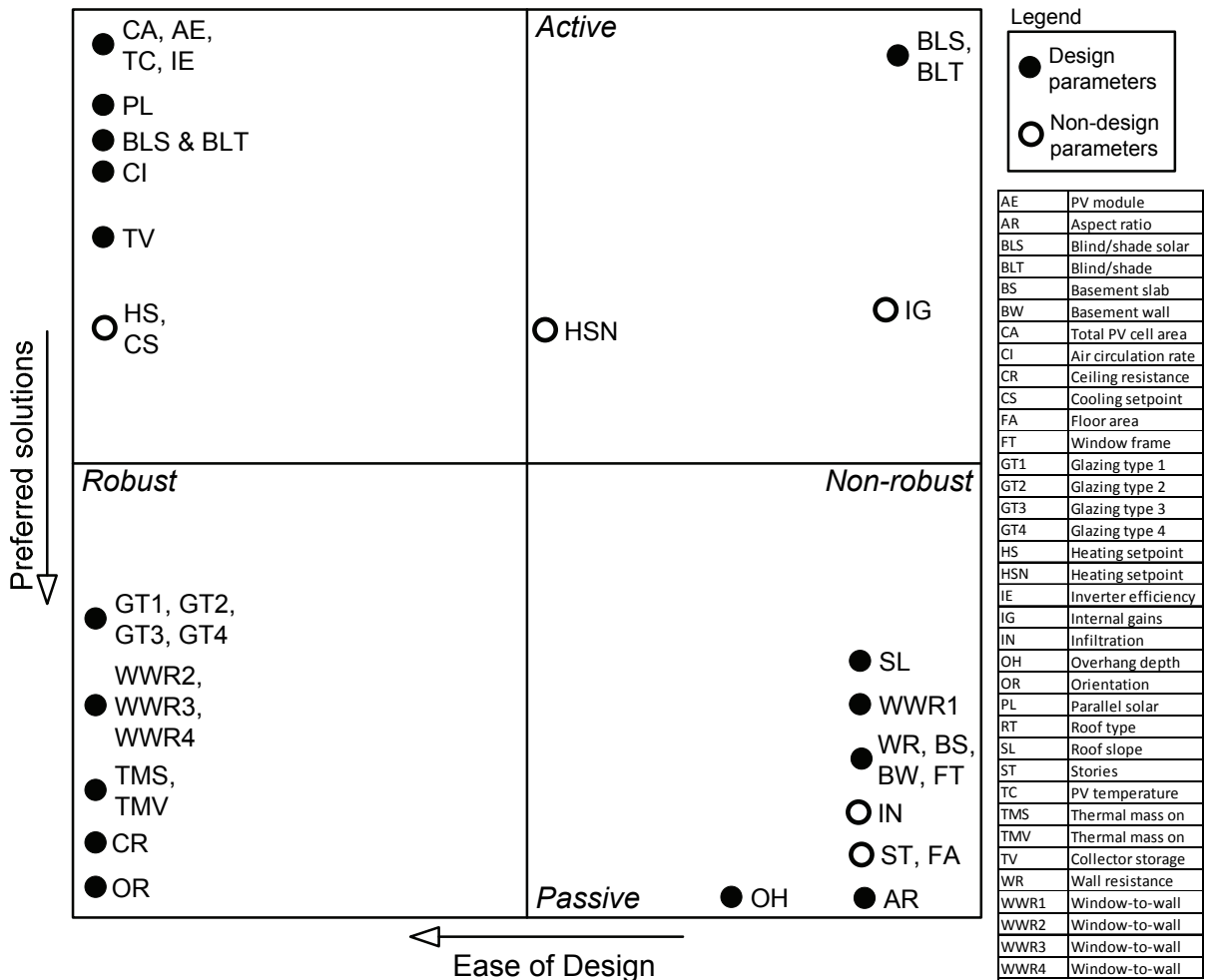


Figure 6-1: Design space according to two scales: passiveness and robustness. For convenience, the parameter acronyms are repeated in the next table.

Robustness is the measure of the parameter's (or subsystem's) ability to perform consistently under all expected boundary conditions (weather, internal gains). In this work, it is used in the statistical sense (performance is resistant to variability of inputs – weather conditions, in this case) as opposed to the durability of materials. For example, a large north-facing window (*WWR3*) is adverse under nearly all conditions: significant heat loss in the winter and some heat gain in the summer. Therefore, there are no conflicting strategies; a small north-facing glazing area is advantageous for thermal

performance. In contrast, a large south-facing window (WWR1) is beneficial in the heating season because of the significant solar gains, but adverse in the summer when such a large window can contribute to overheating. Therefore, WWR1 must be balanced to satisfy these conflicting conditions.

The 36 parameters that describe the house model were quantitatively tested for robustness, as follows. For each passive parameter (the first 28), the slope of the Lol (for the appropriate space conditioning metric) was obtained from Ecos for each parameter. A 1 indicates a positive slope from the lowest to highest parameter value; a -1 indicates the opposite. For example, increasing wall insulation (WR) leads to lower energy use and is therefore assigned a -1. In the rare case that the line is nearly flat, a 0 was used. In this way, a parameter is considered robust if the signs are equal in both the heating and cooling seasons. If they are opposite, the parameter is considered non-robust. Finally, if one of the slopes is zero and the other is non-zero, the parameter is considered neutral – neither robust nor non-robust. For the active parameters (parameters 29 through 36), the sign convention was reversed: a positive slope indicates greater energy collection potential for higher parameter values. The parameters that define active characteristics are all robust except for slope (SL), for which a higher values is preferable in the heating season, but not in the cooling season. Figure 6-1 summarizes the robustness of all parameters.

Table 6-1: Robustness table for all parameters. The heating and cooling season columns refer to the sign of the slope of the Lol for total space conditioning energy for the first 28 (passive) parameters. Notes: (1) south-facing is optimal for both the heating and cooling season, (2) when used in conjunction, BLT and BLS become robust; individually, they are not (3) parameter was tested for robustness using BIPV, (4) for parameters 29 through 36, a positive value indicates higher net energy as the parameter is increased.

No.	Name	Abr.	Heating Season	Cooling Season	Robust?	Note
1	Infiltration	IN	-1	1	No	
2	Internal gains	IG	-1	1	No	
3	Heating setpoint (daytime)	HS	1	1	Yes	
4	Heating setpoint (nighttime)	HSN	1	0	Neutral	
5	Cooling setpoint	CS	-1	-1	Yes	
6	Floor area	FA	1	-1	No	
7	Stories	ST	-1	1	No	
8	Aspect ratio	AR	-1	1	No	
9	Orientation	OR	U	U	Yes	1
10	Wall resistance	WR	-1	1	No	
11	Ceiling resistance	CR	-1	-1	Yes	
12	Basement slab resistance	BS	-1	1	No	
13	Basement wall resistance	BW	-1	1	No	
14	Glazing type 1	GT1	-1	-1	Yes	
15	Glazing type 2	GT2	-1	-1	Yes	
16	Glazing type 3	GT3	-1	-1	Yes	
17	Glazing type 4	GT4	-1	-1	Yes	
18	Window frame type	FT	-1	1	No	
19	Window-to-wall ratio 1	WWR1	-1	1	No	
20	Window-to-wall ratio 2	WWR2	1	1	Yes	
21	Window-to-wall ratio 3	WWR3	1	1	Yes	
22	Window-to-wall ratio 4	WWR4	1	1	Yes	
23	Air circulation rate	CI	-1	-1	Yes	
24	Overhang depth	OH	1	-1	No	
25	Blind/shade solar threshold	BLS	-1	1	No	2
26	Blind/shade outdoor temperature threshold	BLT	-1	1	No	2
27	Thermal mass on south floor	TMS	-1	-1	Yes	
28	Thermal mass on dividing wall	TMV	-1	-1	Yes	
29	Roof type	RT	-1	-1	Yes	3
30	Roof slope	SL	1	-1	No	3
31	Total PV cell area	CA	1	1	Yes	4
32	PV module nominal efficiency	AE	1	1	Yes	4
33	PV temperature coefficient	TC	-1	-1	Yes	4
34	Interver efficiency	IE	1	1	Yes	4
35	Parallel solar thermal collectors	PL	1	1	Yes	4
36	Collector storage tank volume	TV	1	1	Yes	4



The practical meaning of robustness during design is that robust parameters are the easiest to design for because their optimal value is consistent throughout the year. Non-robust parameters are more difficult to design for because the optimal value varies seasonally, yet (at least for hardware) must be fixed to a constant value. For this reason, in the construction materials industry, it is usually the non-robust subsystems that are adjustable, including: natural ventilation (via operable windows), retractable awnings, movable shading devices, and collector array orientation.

The passivity of a parameter or subsystem indicates the degree of inputs (controls, energy) for it to function properly. For instance, insulation, thermal mass, geometrical parameters, and windows do not need external inputs to function and are therefore considered passive. Controlled shading devices and the active solar systems are all considered active. As indicated by Figure 6-1, passive features are preferred over active ones because passive features are less prone to failure because of their lack of dependency on other systems; though they can deteriorate (e.g., leaky windows).

## **6.2 Solar house design methodology**

This section discusses an effective strategy for using Ecos to design high-performance solar houses. Ecos was designed to be flexible and provide quasi real-time feedback, thus suggested that a non-linear iterative approach would be both appropriate and effective. The very features of Ecos that make it unique – quasi real-time feedback, solar design days, and parametric analyses – support this approach rather than a more

deterministic linear approach. The following subsections propose a traditional method for design with the heavy support of Ecos. The priority of the design process is to result in a house design that meets all performance objectives while maximizing passivity, robustness, and cost-effectiveness. The tool does not currently directly provide information on costs, but does recognize that passive components tend to be more cost-effective than that active ones and that most upgrades provide diminishing returns.

### **6.3 High-level solar house design methodology**

The high-level design procedure is iterative and starts by noting all objectives and constraints, as shown in Figure 6-2. Following that, non-design parameters are defined; as these are, by definition, supposed to be defined early in the design process. The designer is given three approaches to passive solar design (all of which have their own flow charts): solar design day, parametric analysis, or a hybrid. Following that, the active solar system(s) is/are designed. An iterative approach ensures supports the notion that desired outcome is the optimal combination of passive solar, energy efficiency measures, and active solar. Furthermore, the passive and active elements must be confirmed to be compatible (e.g., roof geometry could affect passive solar performance). Circled numbers or abbreviations in the flowcharts (e.g., ①) refer to auxiliary procedures that usually involve the design of just one parameter and are used on numerous occasions. Two that are involved in the high-level procedure are shown in Figure 6-3. The three subsections that follow contain alternate passive solar approaches.

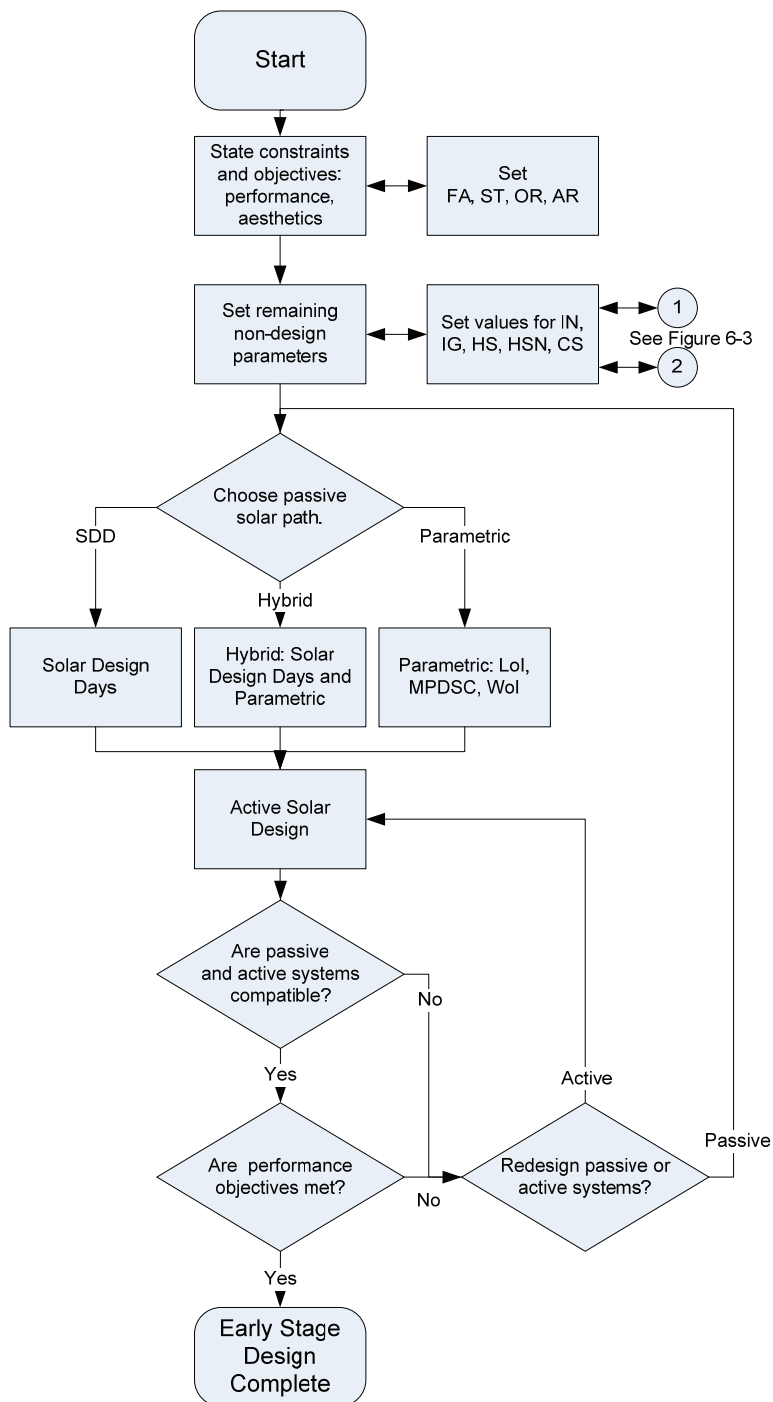


Figure 6-2: High-level design methodology for solar houses

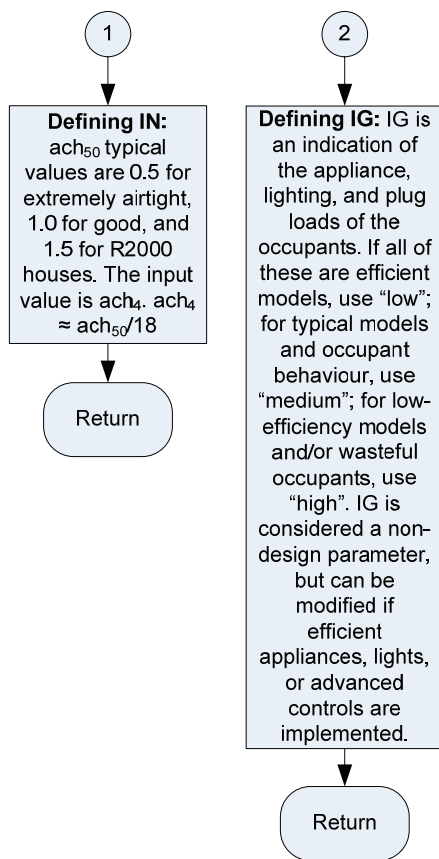


Figure 6-3: Auxiliary procedures for defining IN and IG

## 6.4 Passive solar design: solar design day approach

The solar design day (SDD) approach is best suited for understanding the dynamic behaviour of the house and diagnosing problems such as overheating and peak loads. As described in Chapter 7, SDDs consist of three typical days which are used to identify and understand typical cycles of the house's passive behaviour. The approach is to minimize purchased heating and maximize comfort on the cold sunny day, while using the cold cloudy day to ensure minimal heat loss, and the warm sunny day to ensure that measures for minimizing overheating are in place. The procedure includes a solar design

day approach path, which consists of three procedures for the use of each type of solar design day. Each of those references several auxiliary procedures.

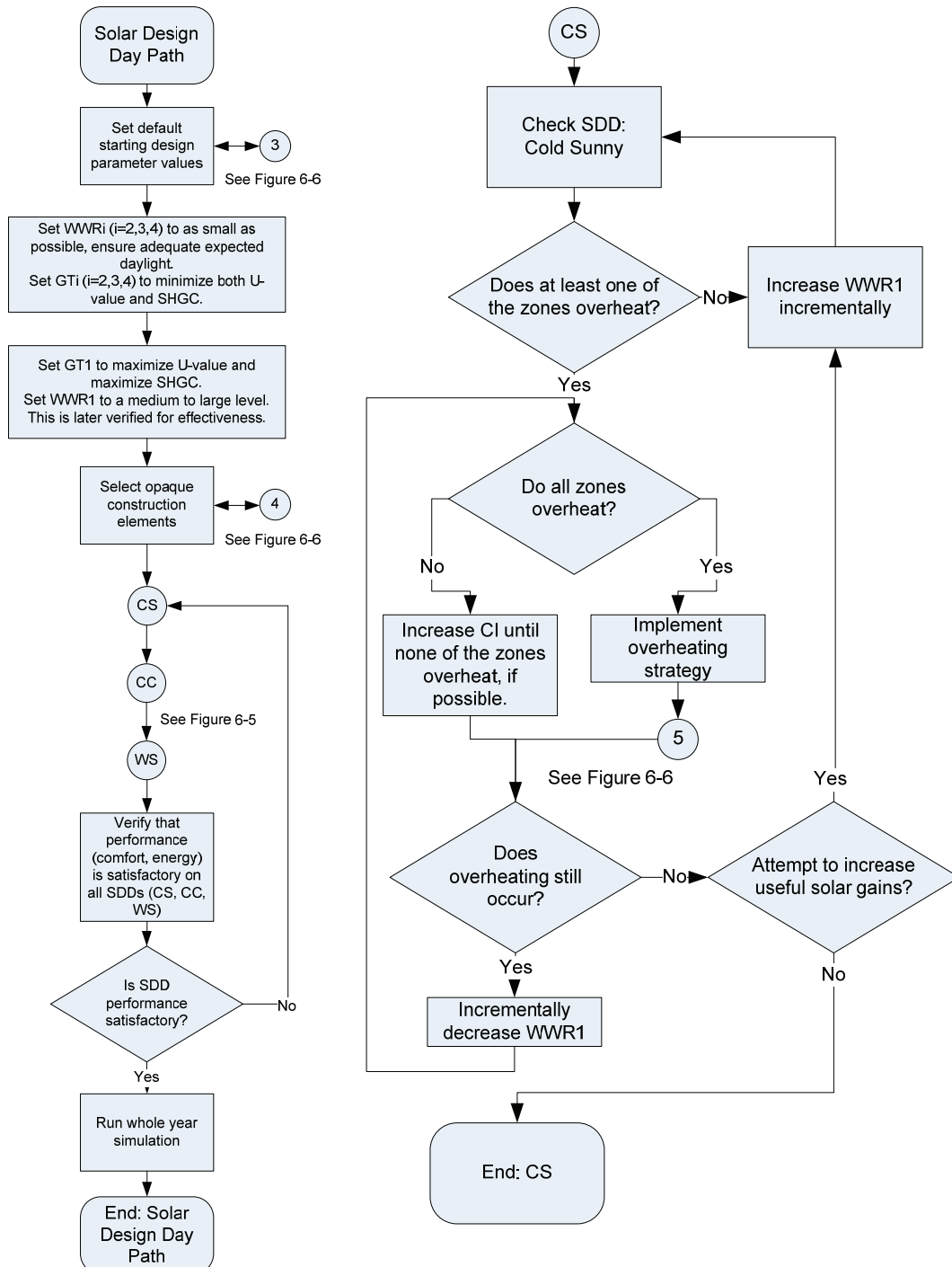


Figure 6-4: Solar design day approach procedure (left) and cold sunny day procedure (right)

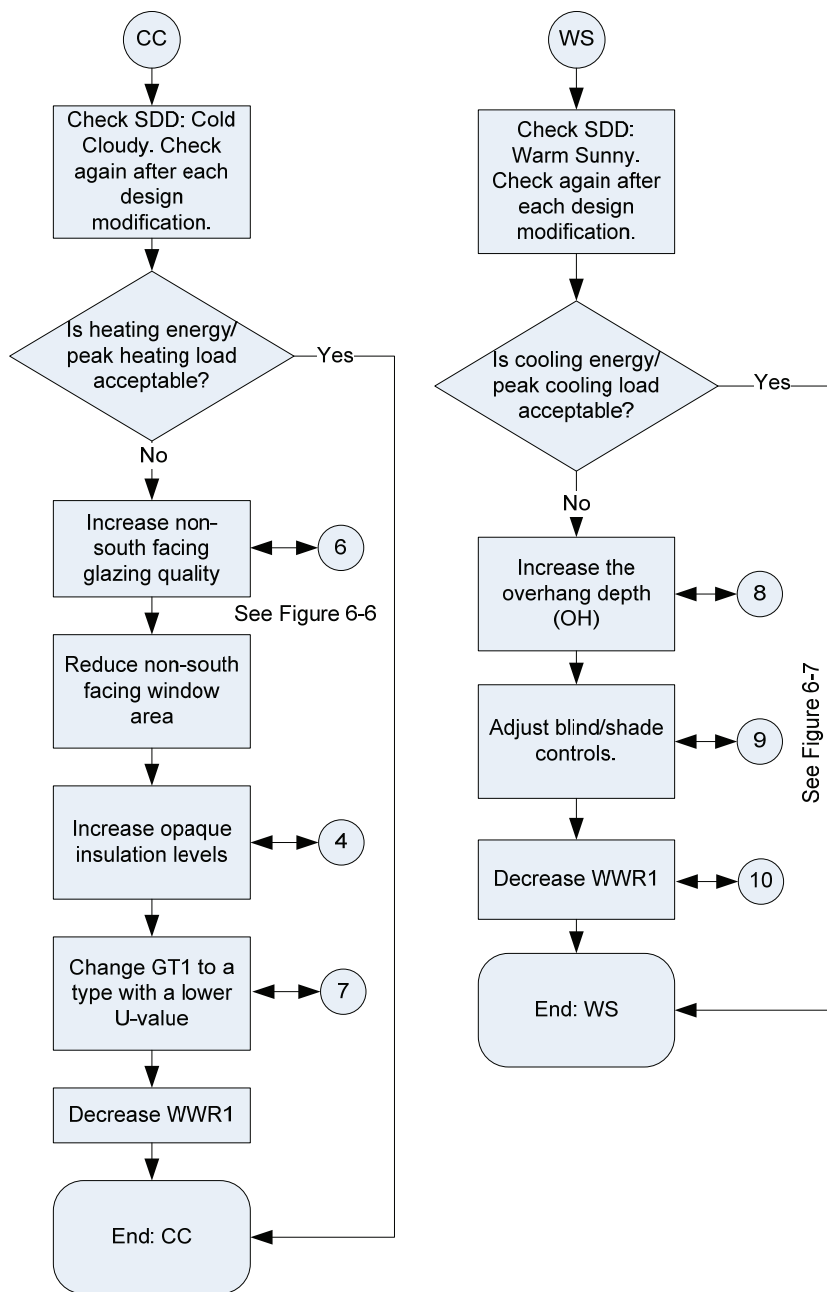


Figure 6-5: Cold cloudy day procedure (left) and warm sunny day procedure (right)

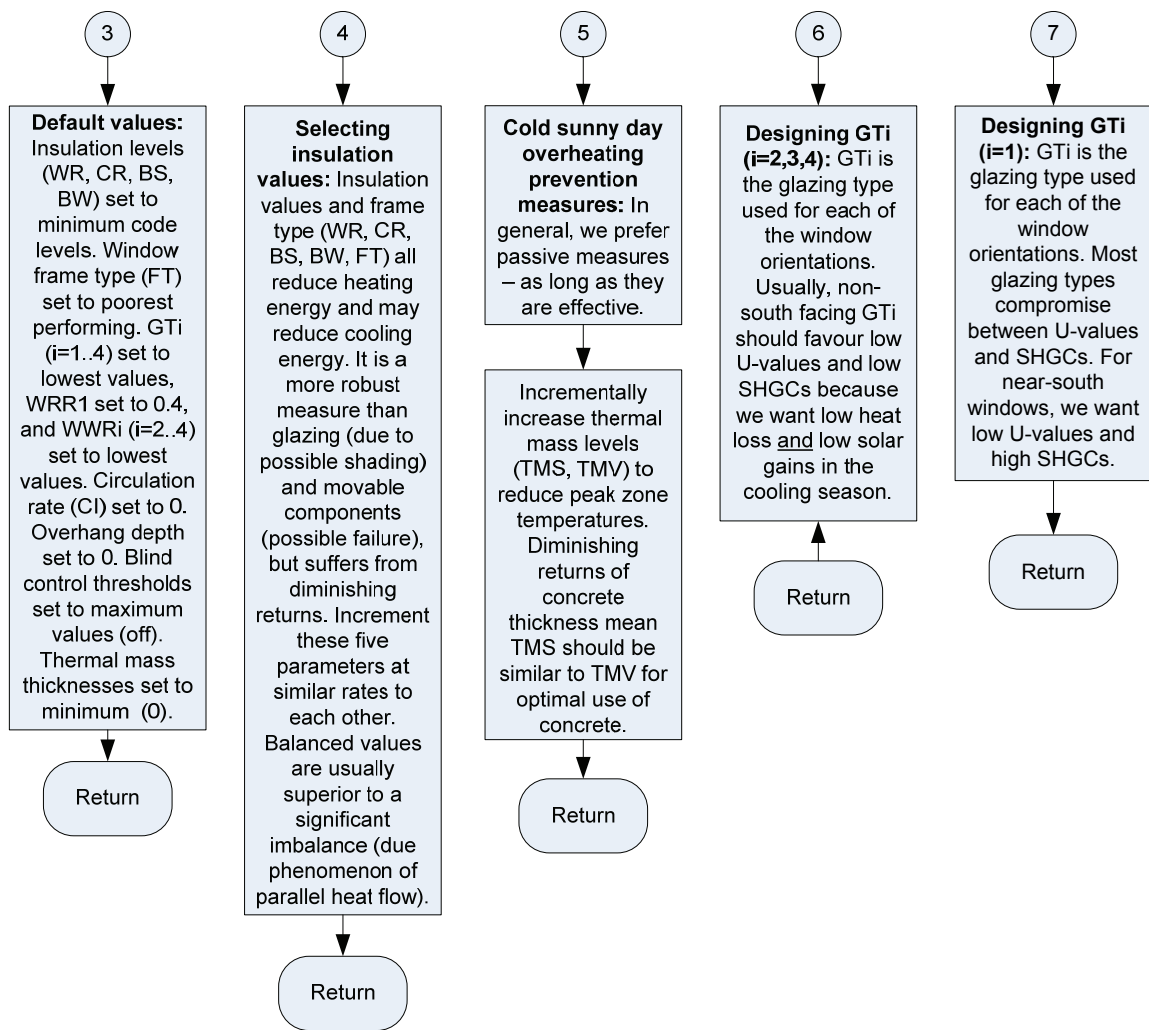


Figure 6-6: Auxiliary procedures 3 through 7.

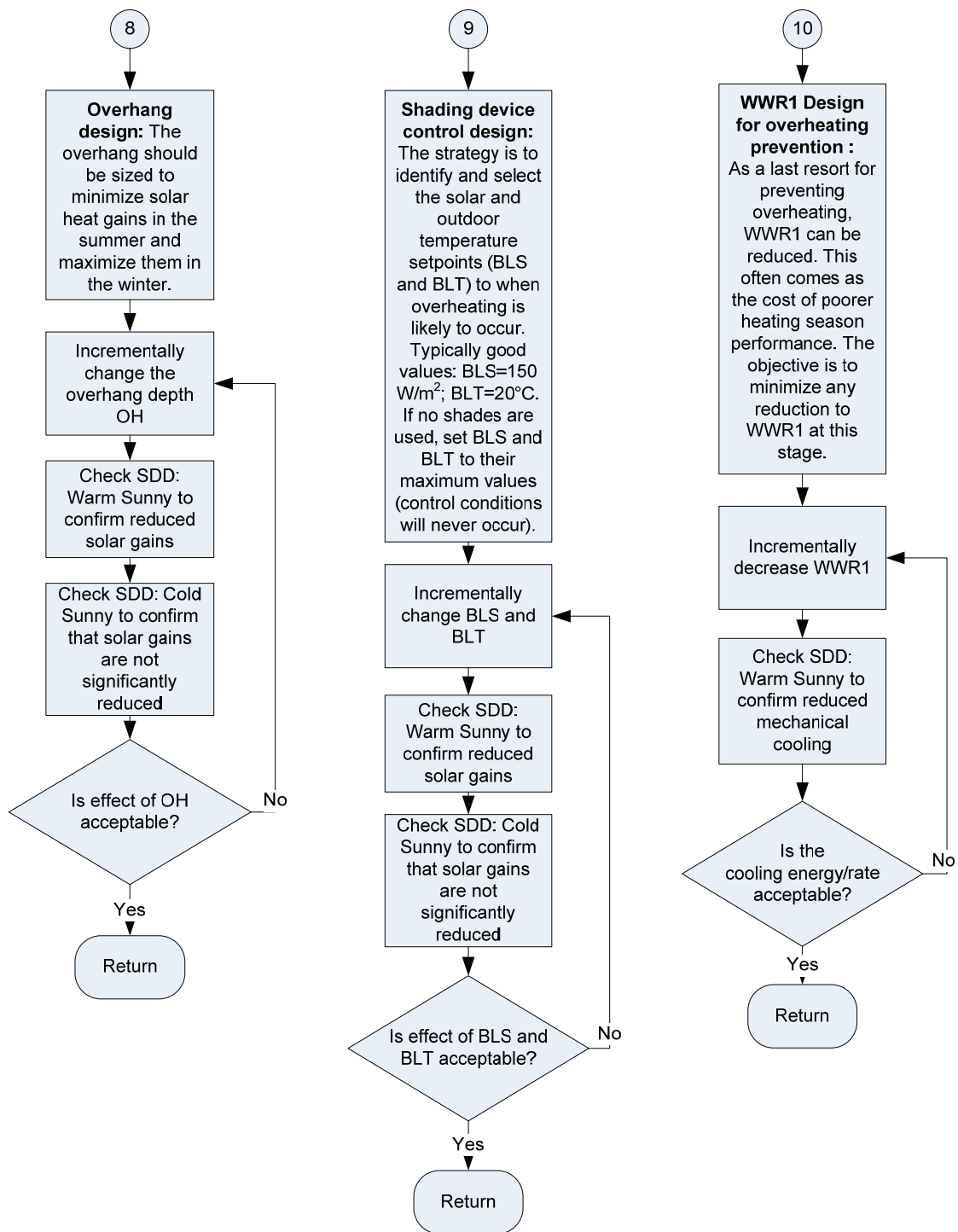


Figure 6-7: Auxiliary procedures 8 through 10.



## **6.5 Passive solar design: parametric analysis approach**

The parametric analysis approach takes advantage of three main features of Ecos: lines of influence (LoI), wheels of interaction (WoI), and multi-parameter decisions support charts (MPDSCs). Compared to the SDD approach for passive solar design, the parametric analysis approach is less linear in nature and therefore requires a strategy to reduce the complex multi-dimensional design space. To do this, the process is broken into four steps that involve first independently selecting the four categories of parameters: robust-passive, non-robust-passive, robust-active, and non-robust-active, for best performance. They are optimized in this order because robust parameters are easier to design and passive parameters define systems that are more reliable. Within each of these four categories, the procedure starts with the parameters that are the most passive and robust. Note that neutrally-robust parameters are included in the robust category. Also note that the reference to “active” is not the same as active solar systems; it merely refers to the fact that the parameters define a system that requires electrical and/or mechanical input to function.

Since some of the design space is highly-interacting, as indicated by the WoI, the procedure requires that all parameters, once optimized using a LoI, are verified to be weakly interacting. If they are not weakly interacting, the procedure requires that the designer loop back and select the optimal set of parameter values using the appropriate MPDSC.

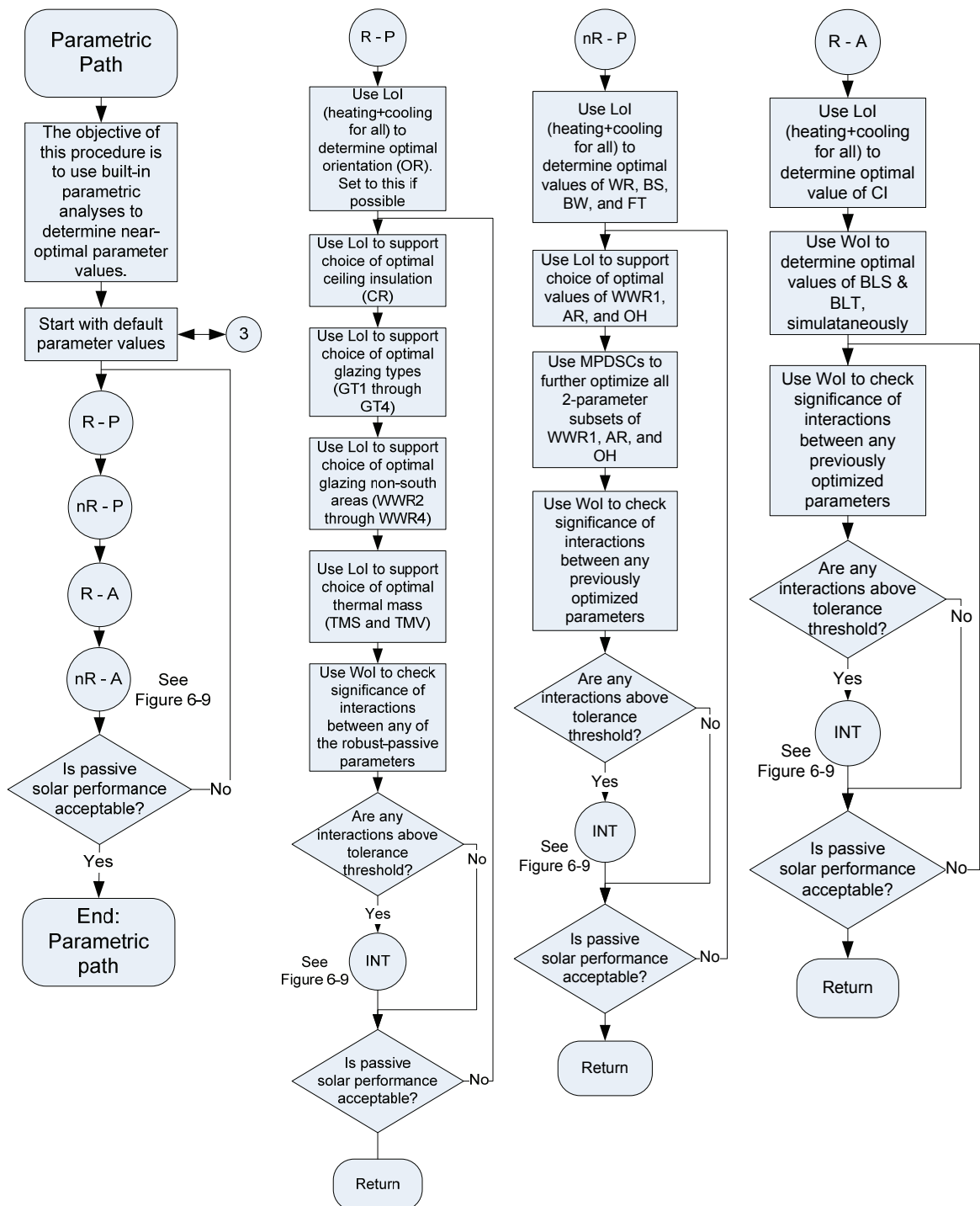


Figure 6-8: Flow charts for the parametric path

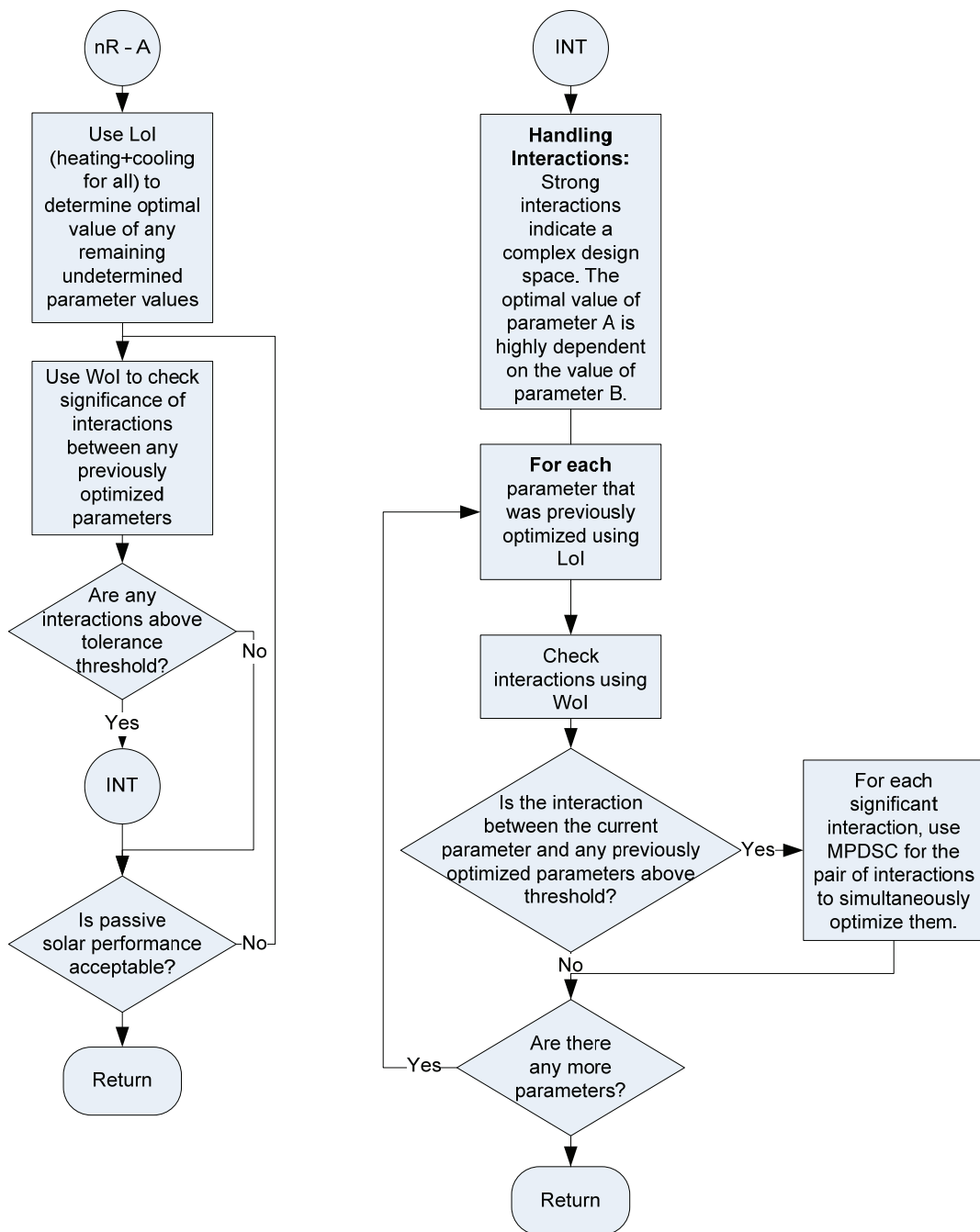


Figure 6-9: Flow charts for the parametric path

## 6.6 Active solar system design

The nature of active solar energy collection for grid-tied houses and without seasonal storage is such that examining the effect of parameter trends on an annual basis is the

best approach. That is to say that the objective here is to maximize annual performance – something that solar design days do not directly do. Furthermore, the active solar systems in Ecos do not affect thermal comfort, meaning that the main objective is energy-based. Thus, the only path provided for designing active solar systems is parametric because the main objective is in maximizing annual performance and the systems (especially PV) are less dynamic.

The main objectives of the procedure are as follows.

1. Select the optimal roof orientation, simultaneously considering both BIPV and SDHW collectors if they are present. Ecos only allows a single active roof area orientation, thus requiring a compromise if conflicting optimal designs occur.
2. Ensure enough roof area or high enough performance collectors are used such that all performance objectives can be met.
3. For BIPV, additional electrical constraints are imposed by modules' array configurations and their compatibility with the inverter.
4. For SHDW, the storage tank volume should be optimized.

Figure 6-10 through Figure 6-12 show the active solar system procedure.

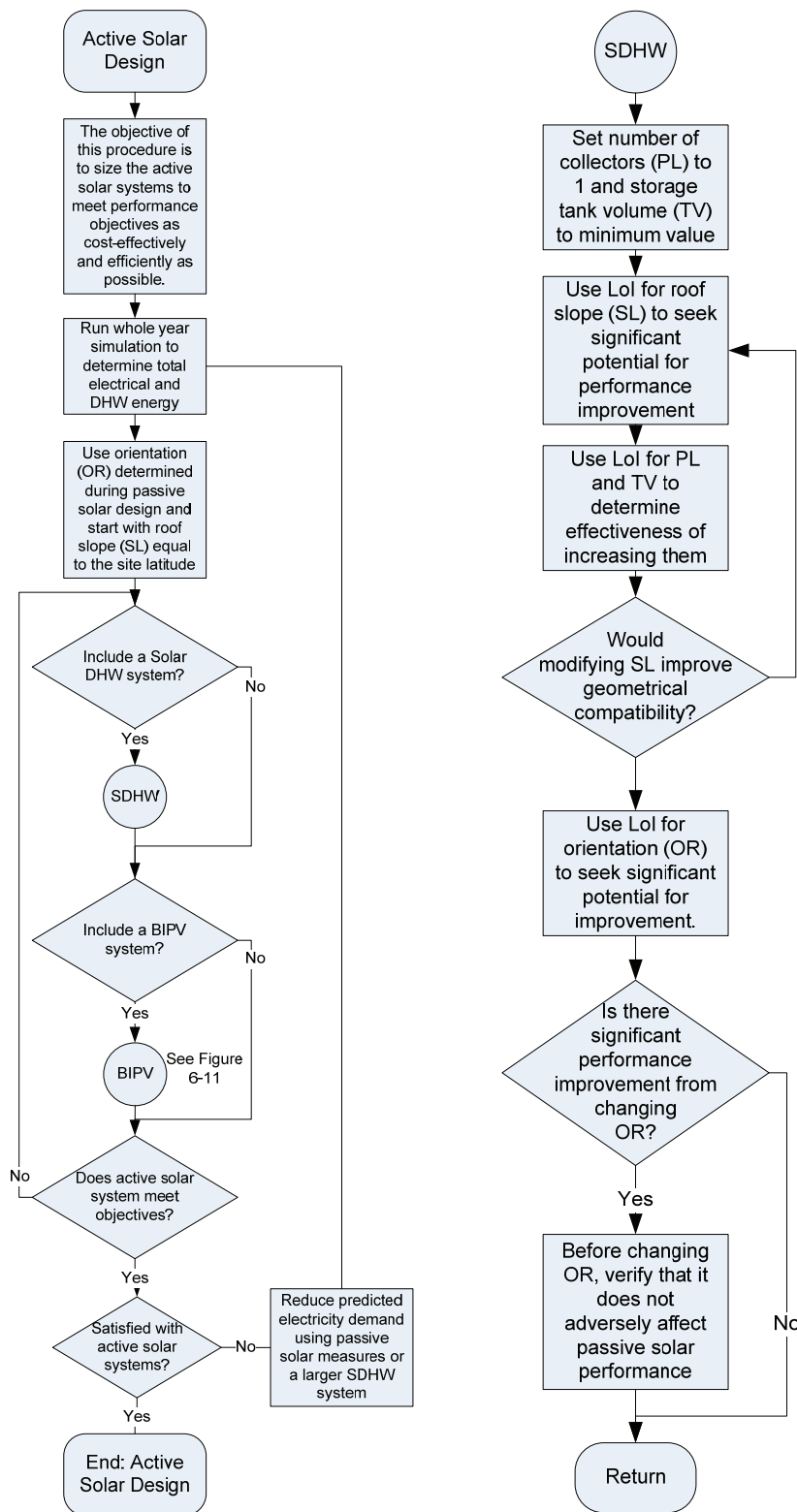


Figure 6-10: Flow charts for active solar system design

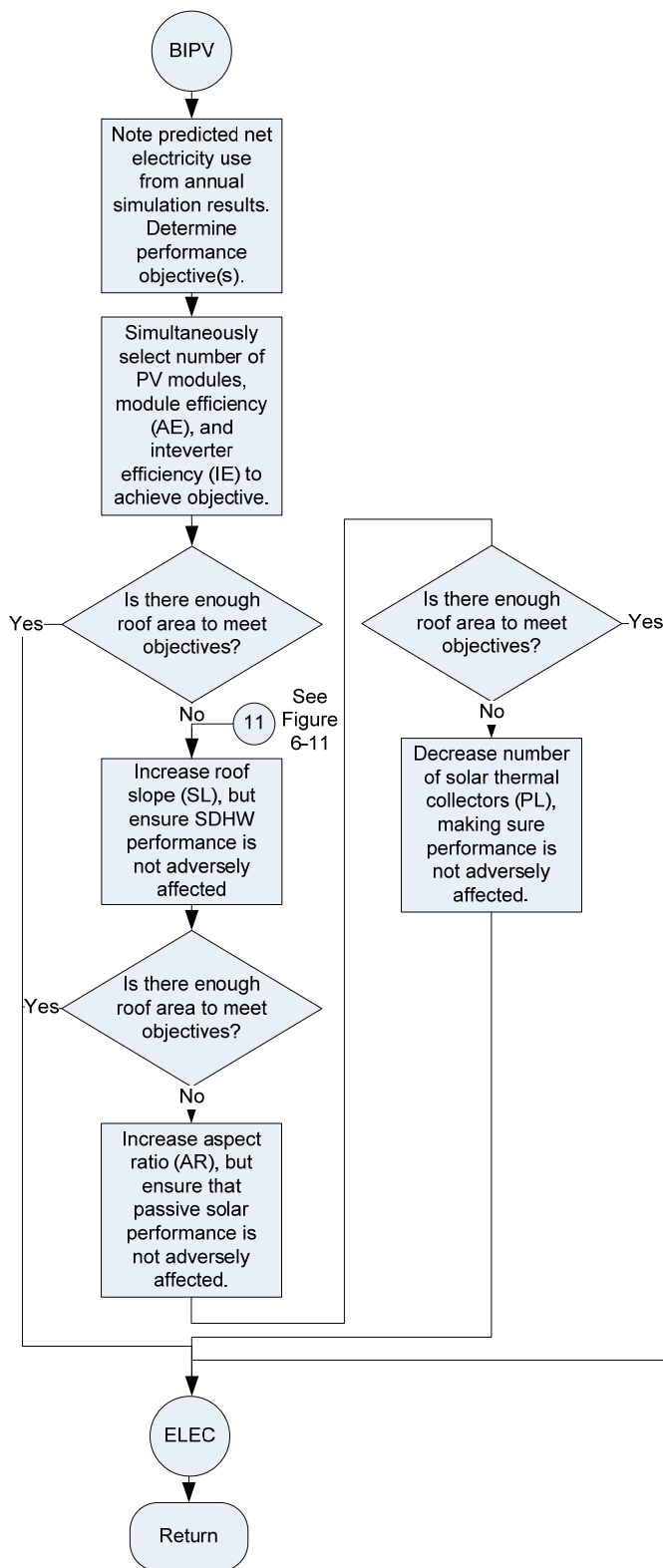


Figure 6-11: Flow charts for active solar system design

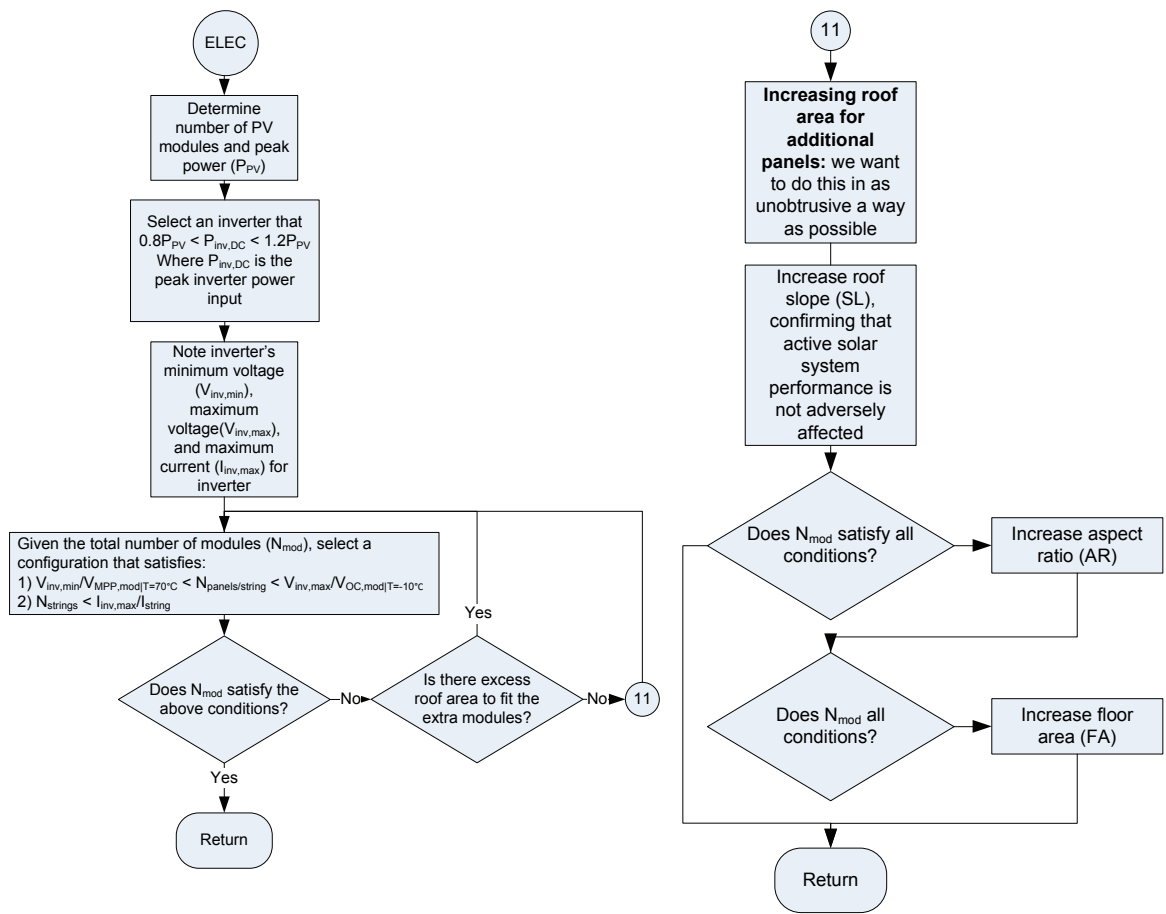


Figure 6-12: Flow charts for active solar system design

## 6.7 Passive solar design: hybrid SDD-parametric approach

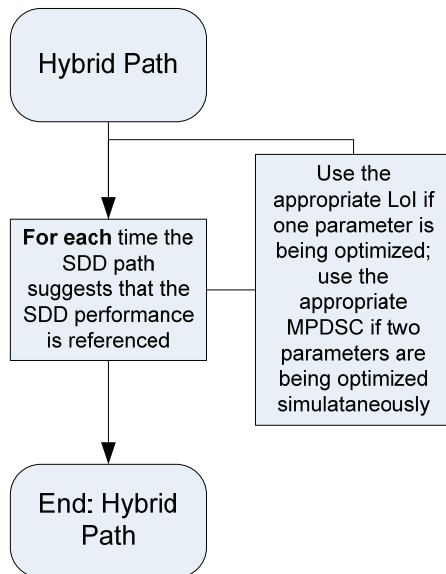


Figure 6-13: Flow chart for hybrid path procedure

## 6.8 Example design exercise

To demonstrate the recommended design procedures that have been outlined, a sample design exercise is shown (Appendix B). A narrative description of the process is accompanied by key screenshots of the Ecos that were used to make informed design decisions. The hybrid approach was taken such that each tool feature was shown at least once. Rather than set absolute objectives, the primary objective was to reduce net energy use as much as possible while considering practical constraints and cost-effectiveness. The final design was predicted to reduce energy use by about one-third and net energy use by half.



## **6.9 Conclusion**

This chapter proposed a design methodology for solar houses. Detailed flow charts are provided to guide the designer to design a high-performance solar house, with the support of Ecos. Parameters are that non-design, passive, and robust are favoured over their counterparts.

## 7 DESIGN TOOL: METHODOLOGY AND IMPLEMENTATION

This chapter explains Ecos in detail and how the previously described work is incorporated. It consists of the requirements of the design tool, the implementation of the model using MATLAB and EnergyPlus, Ecos' features and development, and methods for increasing feedback speed.

### 7.1 Design Tool Requirements

A list of Ecos' requirements is listed below ("shall" indicates that the requirement is mandatory; "should" indicates that the requirement is not mandatory, but noncompliance must be justified). *Ecos...*

1. Shall be able to model the energy performance of both passive and active solar aspects as an integrated system.
2. Shall be intuitive and easy to use.
3. Shall provide guidance towards better solutions.
4. Shall allow whole-year simulations using a validated building energy simulation engine.
5. Shall limit house designs to those that comply with established building standards/codes.
6. Shall prevent physically infeasible or impractical designs.
7. Should allow the same model to be carried through or exported to another tool for detailed design.

8. Should maximize design flexibility.
9. Should provide an understanding of the thermal behaviour of the house.
10. Should allow the early stage design of a solar house on the order of an hour.
11. Should use the language of designers (as opposed to researchers).

## **7.2 Scripting EnergyPlus Input File**

All simulations discussed in this thesis and performed by Ecos use a MATLAB script to map the input parameters to an EnergyPlus input file (idf extension). The script performs the following tasks, in chronological order:

1. Read input values (parameter settings).
2. Read database files from disk, including: materials, constructions, optical properties, parameter data (to ensure inputs are within range), weather data, DHW profile, and occupant load profiles.
3. Do preliminary calculations to map input parameter values to useful quantities (e.g., WWR to window vertices).
4. Create a blank idf file.
5. Write model objects (e.g., schedules, surfaces, zones, controls, and requested outputs) to idf file.
6. Run simulation.
7. Upon completion of simulation, read from output (CSV) file.

An alternative to writing the entire idf file from scratch would have been to merely replace certain values in an existing idf file, much the way GenOpt does (Wetter, 2001). This approach could be seen as more elegant and could potentially save computational time. However, the current approach is considerably more powerful for performing tasks such as creating surfaces and schedules using loops.

A sample section of the script is shown in Figure 13-3. This particular section creates all house surfaces including opaque walls, windows, interzonal partitions, and doors. For each surface, the surface name, construction name (materials), boundary conditions, and vertices are defined. The result is that the tens of building surface objects are written to file with a relatively few number of lines of code.

### **7.3 Ecos Prototype**

The prototype of Ecos is the ultimate implementation of this research. This section describes its requirements, goals, and implementation. A high-level flowchart of the Ecos is shown in Figure 7-1. The basic sequence of events in Ecos is as follows.

1. The user changes an input in the Ecos GUI.
2. After verifying that the input is within the permissible ranges, the inputs are fed to the model where either: runs a one-day simulation for solar design days (SDDs), runs a whole-year simulation if requested by the design management system (DMS), or calls an artificial neural network (ANN).
3. The results of the process in Step 2 are displayed.

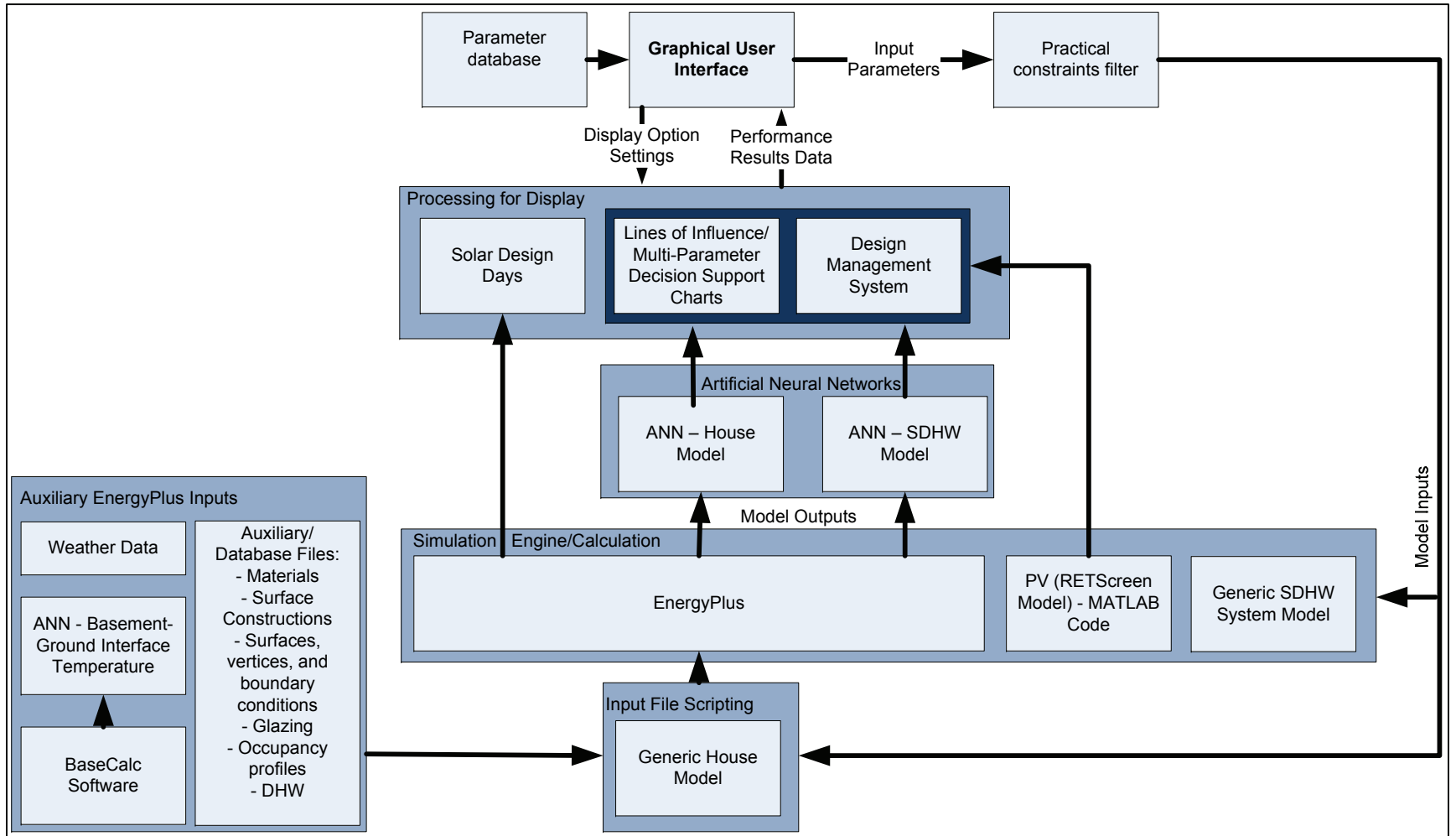


Figure 7-1: High-level flow chart for data flow in Ecos and underlying model

## 7.4 User Inputs

In the development of Ecos, there was a strong desire to accelerate the input process.

The majority of surveyed tools predominantly use text fields for inputting numerical

values. Most tools use drop-down menus for discrete parameters (see Figure 7-2 for

typical user interface (UI) inputs). This offers precision, but resembles a calculator

interface; whereas Ecos is intended to provide an environment for exploratory design.

Therefore, sliders were selected as the main input for input parameters (see Figure 7-3).

	Qty	Gross Area	Net Area
Ext. Walls	4	107.99	93.65
Ext. Ceilings	1	94.98	94.98
Doors	2	3.65	3.65
Windows	4	10.68	
Ext. Floors	0	94.98	
Floor Hdrs	0	0	

m<sup>2</sup> m<sup>2</sup>

Fuel Type: Natural gas  
Tank Type: Conventional tank (pilot)  
Tank Volume: 151.4 L, 33.3 Imp, 40 US gal  
Energy Factor: User specified, 0.554  
Tank Location: Basement

Figure 7-2: Sample of typical tool inputs: text fields (HOT3000)

Non-design parameters

Infiltration 0.05 ach

Internal gains Average

Heating SP 22 C

Figure 7-3: Screenshot of user interface inputs in Ecos

For each parameter, as shown in Figure 7-3, from left to right: there is a checkbox,

parameter label, slider, and dynamic text field and unit label. These elements are

automatically created in the GUI using a *for* loop. The source of the information is a CSV

file which contains information about the parameter name, range, nominal value, and units. These controls for each parameter are described in detail below.

- **Checkbox.** This UI control allows the user to view the current parameter's line of influence (LoI), described later. Upon checking the box, the parameter label changes colour; this color corresponds to the colour of the LoI.
- **Parameter label.** This is simply the name of the parameter as referenced throughout this thesis.
- **Slider.** This is the primary means to input parameter values. For continuous parameters, the slider can be moved in increments of either one-tenth or one-hundredth of the range. The slider can also be moved by 'grabbing' it and releasing it anywhere within the range. For discrete parameters, the slider can only assume  $n$  positions, where  $n$  is the number of allowable discrete parameter values. There are two other ways of changing the slider position: 1) by typing in a value into the dynamic text field (described next), and 2) restoring a previous design with the DMS.
- **Dynamic text field.** This either displays the numerical or text-based value of the current parameter setting. When the corresponding slider is moved, this value updates immediately. A secondary option is to type in the desired value here (numerical parameters only). This option is less desirable because of the extra effort required but is ideal for increasing precision of the input.
- **Parameter unit.** This field stays fixed and informs the user of the unit.

While the parameter inputs are the main form of UI input, there are some instances of drop-down menus, checkboxes, and buttons. Drop-down menus were used for all instances where there are several different display options (e.g., the performance metric selection for the Lol and MPDSC and for the weather conditions (day type) for the SDD). Checkboxes were used if there are two discrete options. For example, the user can use a checkbox to select the metrics for the SDD that they wish to view. Buttons are used sparingly and are used to initiate an event.

Due to the lack of space on the screen, a tabbed system was used. Though there was a preference for all features to be on a single screen, the number of features and inputs made this impractical. The tabs were designed such that all features that are intended to be used in parallel can be seen simultaneously. Because MATLAB does not have a built-in tab UI, tabs were created using buttons. Upon activation of the non-active tab (button), certain features disappear and others appear, creating the same effect as tabs.

## **7.5 Development of Graphical Feedback Methods**

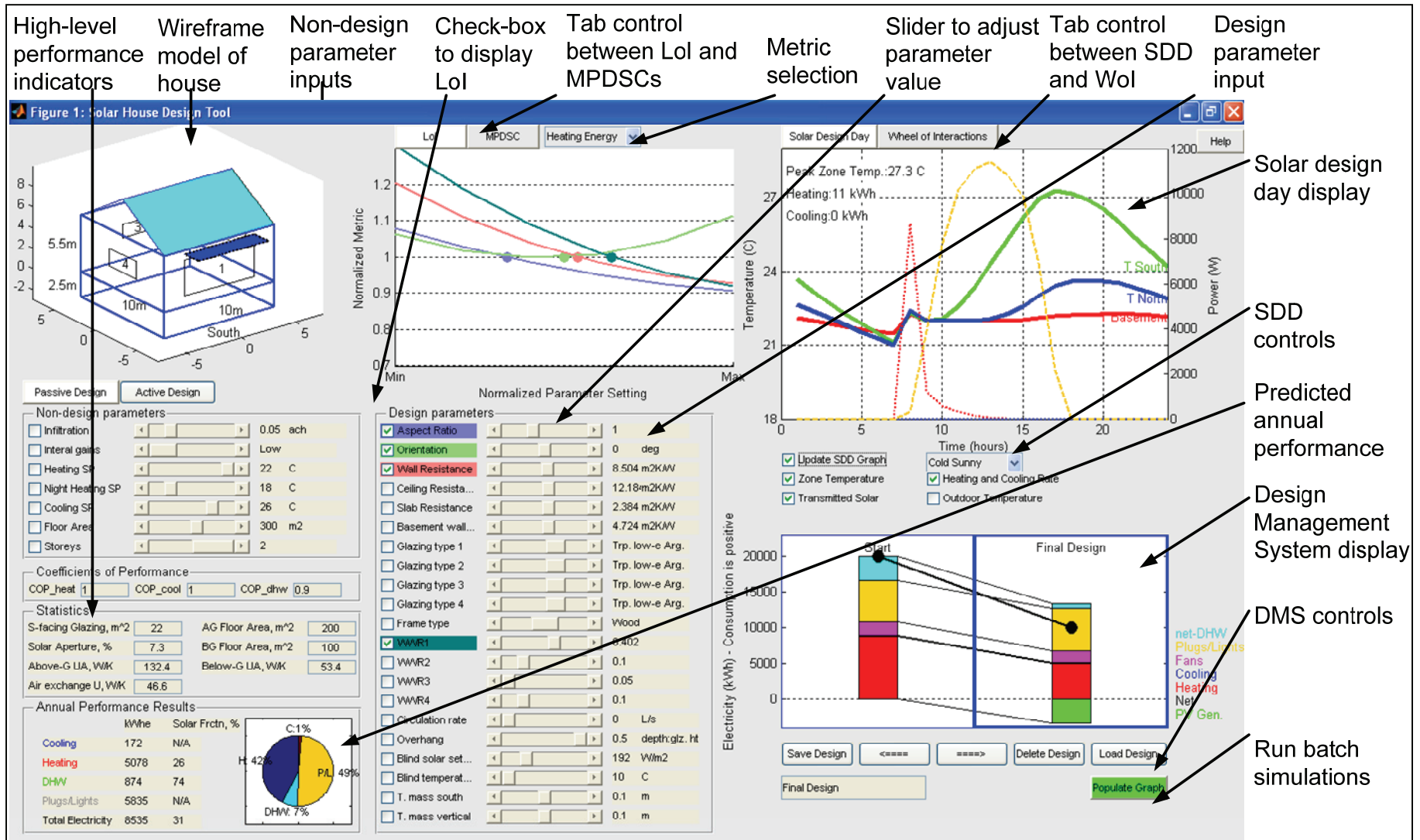
The model described above is merely a foundation for this work. However, it is necessary to develop graphical methods for concisely displaying the performance of the house. It should also answer a lot of questions, such as: Why is the house performing as it is? How can it be improved? And what are the trade-offs between different energy efficiency measures and active solar technologies?



Each of the proposed solutions is intimately tied to the methodology. That is, they complement the methodology in that they offer a comprehensive understanding of the behavior of the design space or house.

Five main methods that display system performance have been developed. They are: solar design days (SDD), lines of influence (LoI), wheel of interactions (WoI), multi-parameter decision support charts (MPDSC), and a design management system (DMS). All of the forms of graphical feedback are intended to support the design process and can be used individually or in parallel. One additional form of feedback – explained in the following subsection – is system and subsystem geometry. This does not require simulation, but is nonetheless critical to supporting design. All of these features are described in the following subsections, including their purpose, use, and implementation.

To introduce the graphical features, two screenshots of Ecos are shown in Figure 7-4 and Figure 7-5. Two screenshots were required since the tabbed control means that some of the screen has two possible modes.



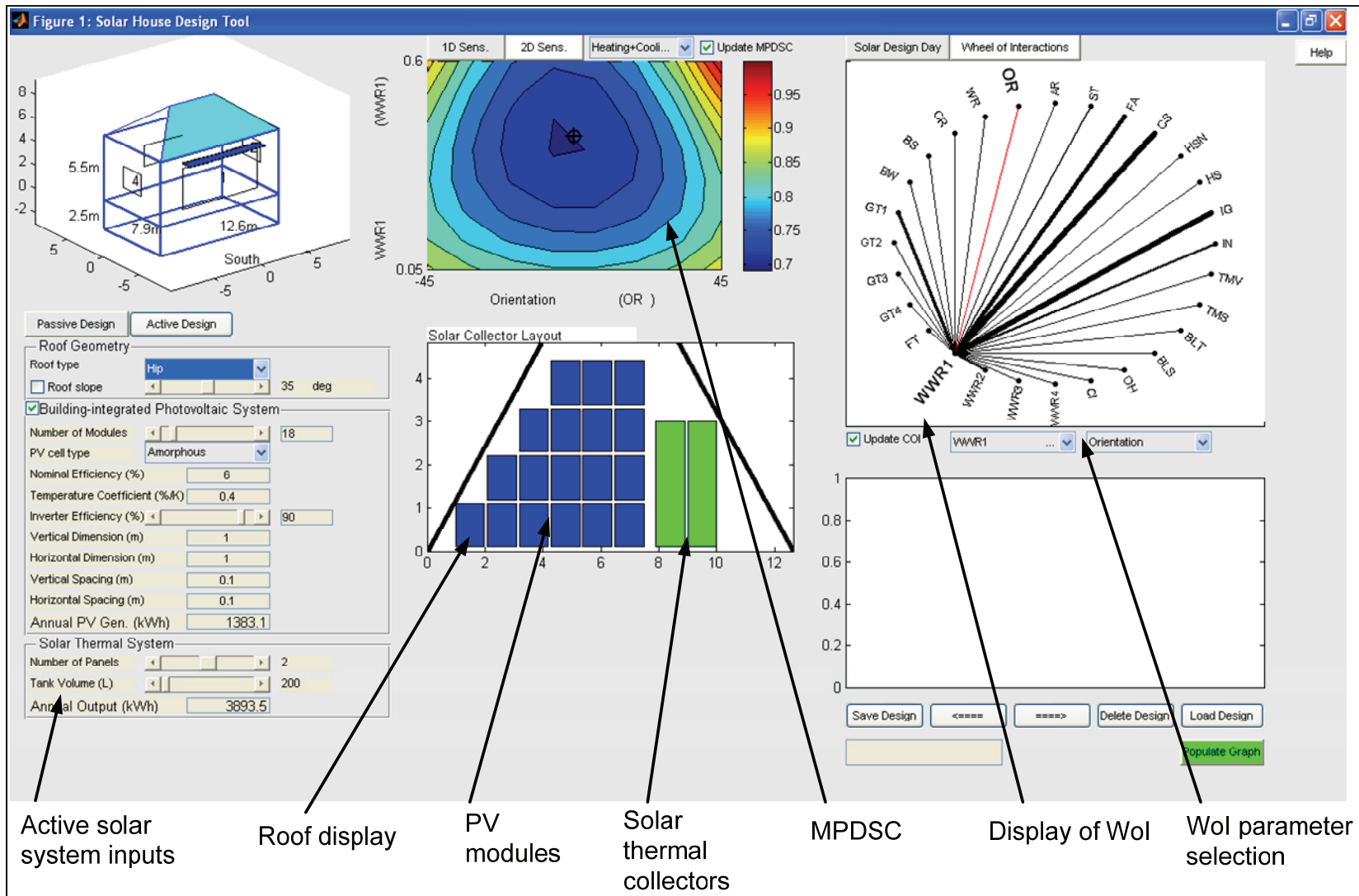


Figure 7-5: Screenshot #2 of Ecos; showing MPDSC and WoI

### 7.5.1 House and component diagrams

The author believes that visually representing major design aspects in Ecos is essential, despite the fact that only about two-thirds of the software tools surveyed have such a feature. Diagrams help the designer ensure that their conceived design is the same as the one being modelled. It also helps ensure geometrical consistency. For instance, the designer must ensure that the window layout is possible, that the overhang does not obstruct doors, and that all of the solar collectors can fit on the roof.

In Ecos, all figures are plotted using lines and planes, using relatively low-level programming. For example, in the wireframe image in Figure 7-6, all windows and edges are plotted by defining each line segment by its endpoints in Cartesian coordinates. Similarly, filled rectangular surfaces are defined by their vertices with Cartesian coordinates. Text is specified by its position and a string. To rotate the wireframe house model, each vertex is multiplied by a three-dimensional rotation matrix, in the form:

$$R_{OR} = \begin{bmatrix} \cos(OR) & -\sin(OR) & 0 \\ \sin(OR) & \cos(OR) & 0 \\ 0 & 0 & 1 \end{bmatrix} \quad (7-1)$$

Note that the Cartesian axes x, y, and z are in the directions South, East, and vertical, respectively. Rotations are only performed about the vertical axis.

EnergyPlus, itself, does not provide any graphical representation, but its files can be viewed in several third party programs such as SketchUp (shown in Figure 7-6) or AutoCAD. The former would be particularly useful if the Ecos user wanted to further develop the model using more complex geometry.

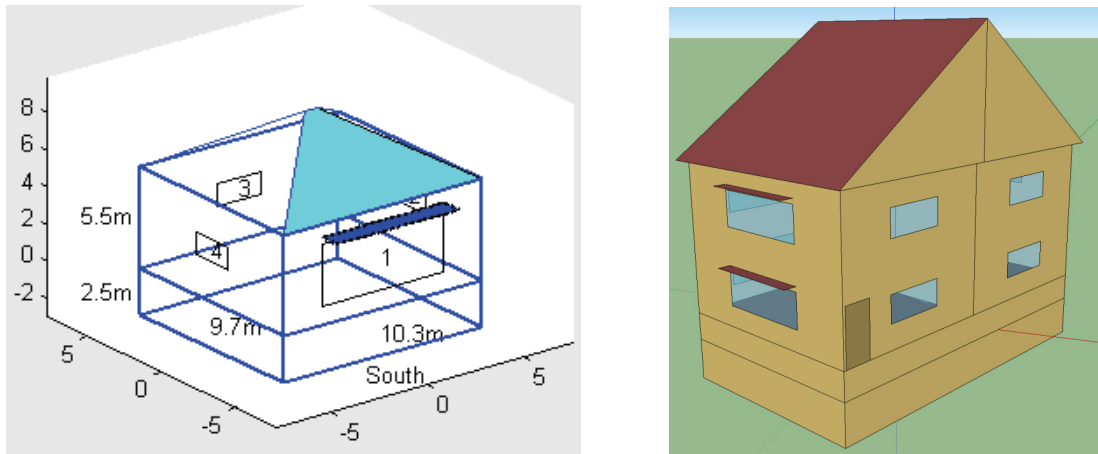


Figure 7-6: Representations of the house: Ecos (left) and SketchUp (right)

To visualize the solar collector layout, a normal view of the roof is provided, as shown in Figure 7-7. The purpose of this feature is not necessarily to perform exact layout of collectors, but rather to ensure that they fit and recognize that it is often not possible to cover an entire roof in collectors.

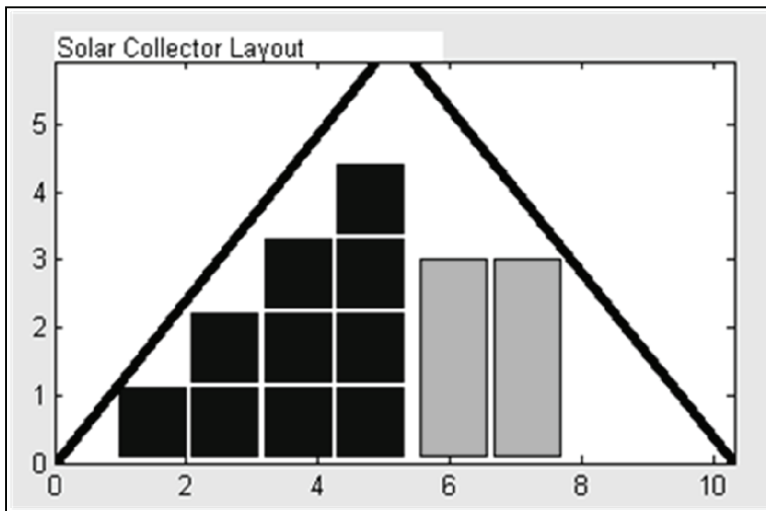


Figure 7-7: Screen shots of house wireframe (left) and normal view of roof with collectors (right)

## 7.5.2 Solar Design Days

Solar design days (SDDs) are used to display the passive performance of the house during key weather conditions, including a cold sunny, cold cloudy, and warm sunny day (O'Brien et al., 2008b). They allow the effect of key design decisions, such as window size, insulation level, and thermal mass quantity, to be identified. Several key performance metrics, including heating load, cooling load, solar gains, and direct gain zone air temperature, are shown in a line graph.

While many programs merely display annual graphs or heating loads, the display of SDDs allows the diagnosis of common passive solar heating problems such as summertime overheating or high nighttime heat loss. It also allows the slow response time that is fundamental to passive solar houses, to be demonstrated. Figure 7-8 shows an example of how SDDs can be used in design.

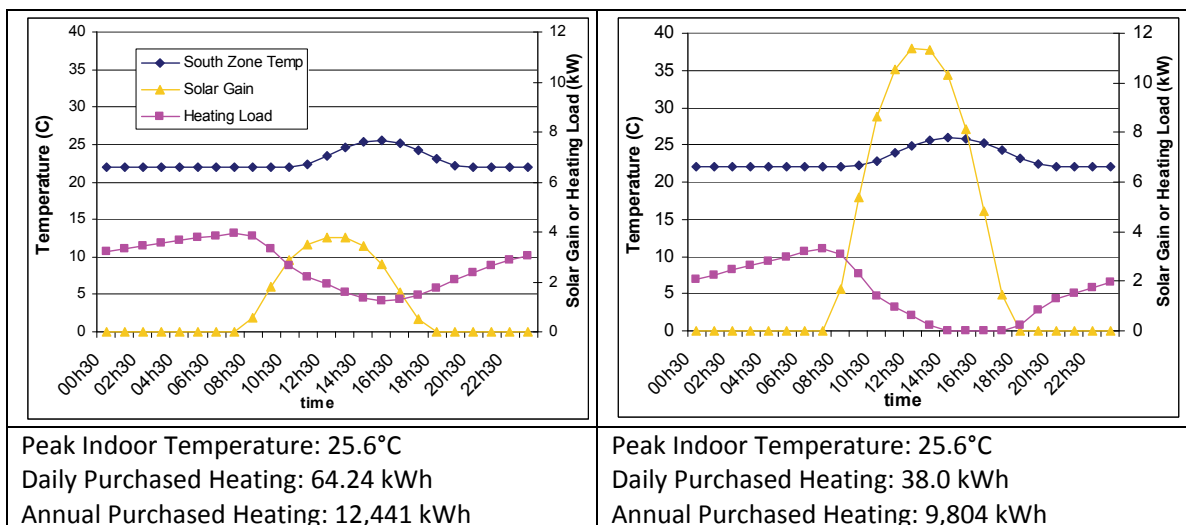


Figure 7-8: Sample SDD graphs (cold sunny day) showing how the design of a house was improved. The design represented on the left has no significant thermal mass and had 15% glazing on the south façade. The design on the right has an 8" concrete slab on the ground floor and 45% glazing on the south façade (O'Brien, 2008a).

SDDs last 24 hours because the heat capacity of passive thermal storage is usually limited to a day. That is, if a cold cloudy day follows a cold sunny day, the thermal mass will normally completely discharge on the second day. Since the solar gains on a sunny day can benefit the next day, SDDs are simulated using at least two consecutive identical days leading up to the day that is studied (until periodic steady state is reached) (i.e., at least three days total). Active solar energy systems, which typically use active storage, can often store heat for several days (depending on the heat capacity and energy use). Thus, a longer response time should be studied. The length of time that performance is displayed should correspond to the time that it takes a fully-charged store to be discharged under normal conditions. The only design period of interest is under cold sunny conditions. The cold cloudy and warm sunny conditions considered for passive performance are of little interest for active solar energy systems, since thermal comfort, space overheating, and heat losses are much less relevant. Since PV systems exhibit minimal transient behaviour, their response is of little interest, and then need not be displayed.

Passive solar design is typically performed with the acceptance that the energy use can be reduced but not eliminated. Thus, a measure of relative performance is the most important aspect. However, SDDs are less suitable for active solar thermal systems, for which absolute performance is needed. SDDs are useful for understanding the thermal behaviour of the house, but offer little explicit design advice. Also, they require some basic knowledge; though they provide education on passive solar heating.

### 7.5.3 Lines of Influence (LoI)

One of the most common approaches to simulation-supported design is to apply parametric analysis to one or more parameters. This is because usually once a model is built, modifying parameters is relatively straightforward.

In the tool, lines of influence are simply a display of curves for performance (one of several metrics) versus the range of one or more parameter values. Examples are shown in Figure 7-9. Early applications of this technique for this work were reported by O'Brien et al (2009a) and Kesik and Stern (2008). LoI provide two valuable pieces of information:

1. The optimal or near-optimal value of a parameter. If the LoI for a particular parameter indicates that an optimum value for it exists, the designer may wish to use this value in the design, assuming it is practical and compatible with other design aspects.
2. The relative sensitivity of a parameter. This is particularly useful when multiple parameters are compared. For instance, if there are multiple methods for obtaining the same desired result, the parameter with the steepest LoI may be the one that for which the desired outcome is easiest to achieve. Furthermore, if a costly upgrade has little bearing on energy performance, there would be little benefit to making that investment.

The metrics that can be plotted as LoI are: heating energy, cooling energy, heating + cooling energy, total energy use, overheating, PV generation, SDHW production, total



renewable production, solar fraction, net energy use, and overheating (all as defined in Chapters 3 and 4). It is up to the Ecos user to select the most appropriate metric.

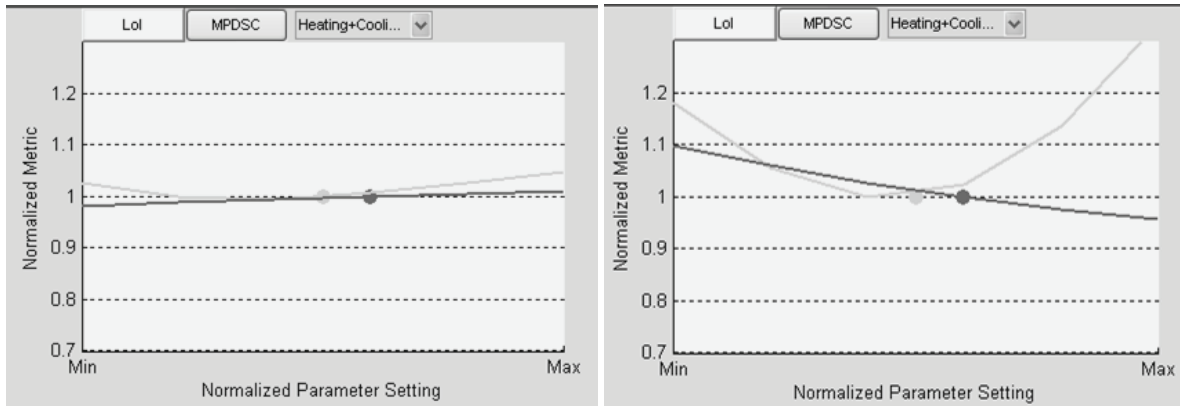


Figure 7-9: Sample Lol overhang depth (near-linear) and house orientation (parabolic); the total annual heating and cooling energy are shown; the left Lol is for a small south-facing window; the right is for a large south-facing window

The Lol are populated with a one-dimensional array of performance data. Continuous parameters use six distinct equally-spaced points while the discrete parameters use a point for each discrete parameter value. All performance data is normalized (i.e., divided by the value at the current settings) as to ensure it can all be plotted on the same set of axes for all different metrics and selected parameters. MATLAB's *plot* function is used to display the corresponding data in the form of a line graph.

As discussed in the previous chapter, designing one parameter at a time without recognizing that there are significant interactions between some subsets of parameters can lead to poor design decisions. For example, Figure 7-9 shows two screenshots of Lol for overhang depth and house orientation. The left screenshot in the figure is for a small south-facing window; the right one is for a large south-facing window. This example

clearly shows how the manipulation of other parameters can affect those being currently displayed. The next form of display – wheel of interactions – addresses this.

#### **7.5.4 Wheel of Interactions (Wol)**

As mentioned in the previous chapter, there is significant value (time savings, better designs) in identifying the strongest parameter interactions. In summary, the designer can independently optimize weakly-interacting parameters; whereas, they should simultaneously design sets of strongly-interacting parameters. Rather than display all major interactions, Ecos only displays all interactions with a single user-selectable parameter (e.g., WWR1 in Figure 7-10). As before, strength of interaction corresponds to line thickness.

A sample survey of tool users suggested that the wheel of interaction only contain the interactions with a single selectable parameter, rather than showing all parameter interactions simultaneously.

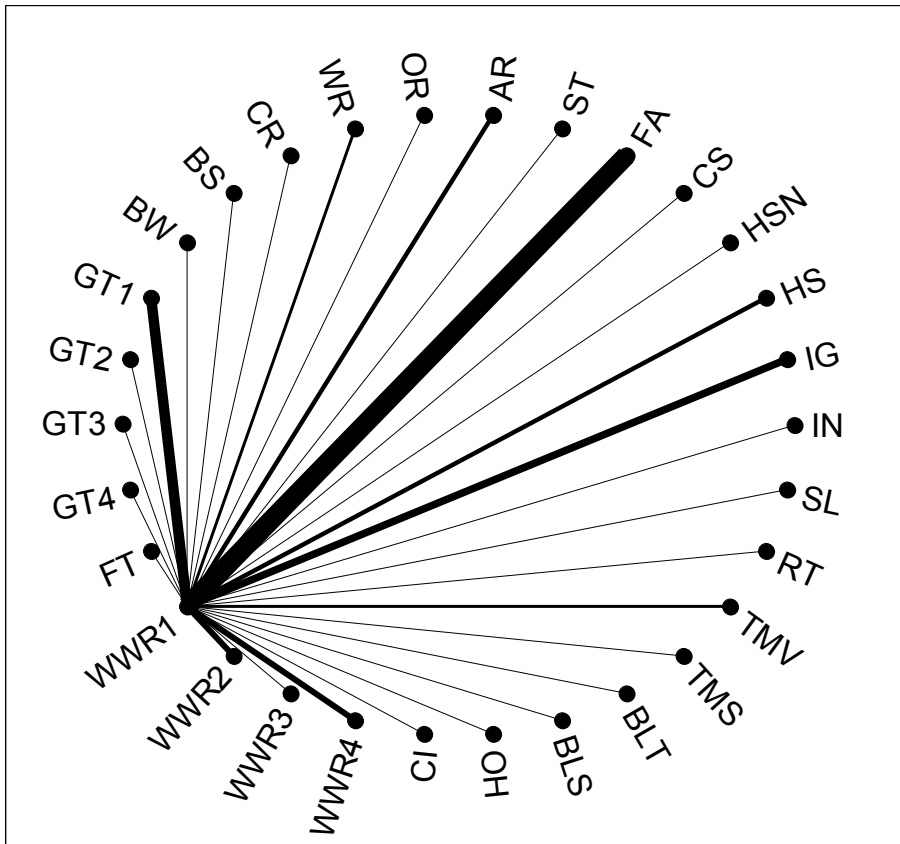


Figure 7-10: Wheel of interactions showing the relative magnitude of interaction between window-to-wall ratio for the near-south facing window and all other parameters. The labels around the outside of the wheel correspond to the abbreviations in the table of parameters.

### 7.5.5 Multi-Parameter Design Support Charts (MPDSC)

In order to visualize the complex interactions between pairs of parameters, the concept of multi-parameter decision support charts (MPDSCs) was created. The user is allowed to select any two parameters, after which the contour plot is promptly updated. The previously-mentioned wheel of interactions should be used as a cue for which pairs of parameters would result in the more complex (interacting) design spaces.

Just as for Lol, the values represented by MPDSCs are normalized – in this case, to the highest value. For instance, if heating energy is being plotted, the entire design space is

represented as using a fraction of the heating energy of the design that uses the most heating energy. It is up to the user to discern whether the current metric should be minimized or maximized (i.e., energy use should be minimized; energy collection should be maximized).

As for Lol, the MPDSC indicates both the optimum design space and the sensitivity. It is also very useful for understanding the relationships between parameters.

MPDSCs are populated by an array of predicted performance data. If a parameter is continuous, 11 equally-spaced points are determined (for a total of  $11^2 = 121$  points). If a parameter is discrete, the number of points is equal to the number of discrete settings. For example, if WWR1 and GT1 are being examined, Ecos populates an array of 11 by 4 distinct designs. 11 was chosen because it provides 10 intervals and because it is a compromise between resolution and computational time. Because the design space is smooth, there is little error introduced by this approach. MATLAB's *contourf* function is used to interpolate between the points.

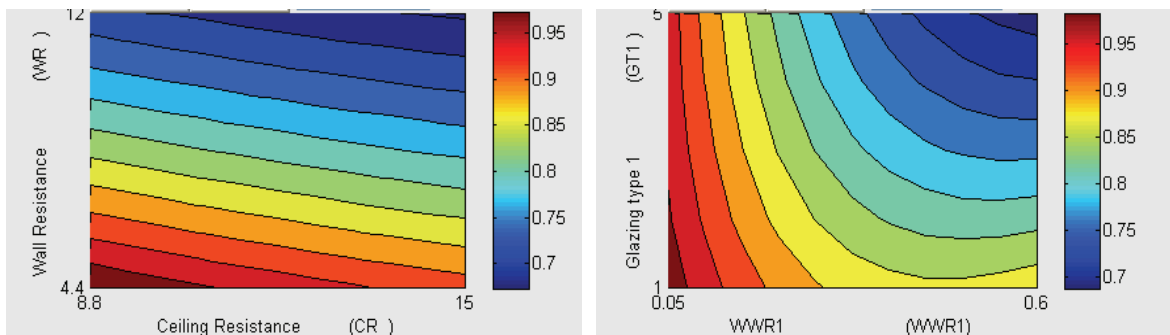


Figure 7-11: Example Lol for heating energy

### **7.5.6 Design Management System (DMS)**

A standard method for design is to establish several alternative design options and compare them. The majority of tools surveyed do not have the facilities to support this activity. While they do allow different designs to be saved; only one can be viewed or modified at a time.

To allow comparative design, a design management system (DMS) was created, illustrated in Figure 7-12. The proposed design management system (DMS) is a standardized method for storing both characteristics of multiple house designs and their performance data and a method for following progress. For instance, multiple paths to a specific energy target or other goals can be followed.

This section begins with a technical description of the DMS implementation and is followed by a design exercise demonstrating its use. The DMS addresses three main needs within Ecos:

1. A visual method of comparing multiple designs for one or more performance metrics;
2. A method for monitoring progress and encouraging goal-setting; and,
3. A standardized method for storing multiple designs and allowing backtracking and retrieval of past designs. Once a design is saved it can be retrieved at any time. Upon loading a design, all parameter settings are set to the stored values. This action cannot be undone.

Theoretically, an infinite number of designs could be saved, although Ecos limits this to 10 for practicality. Any of the saved designs can be over-written.

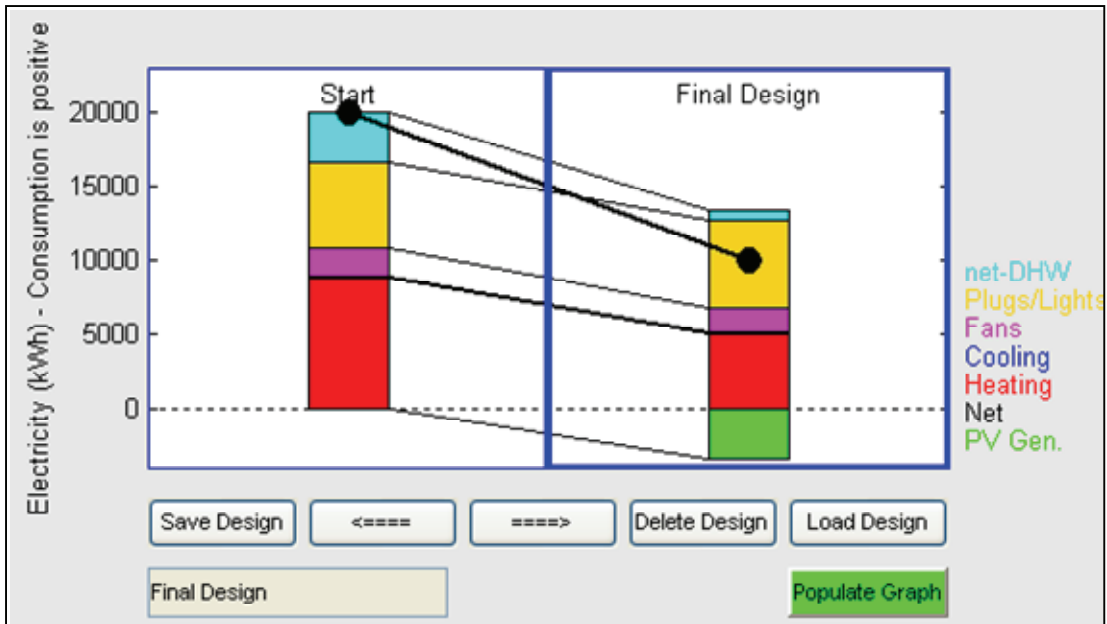


Figure 7-12: Sample screenshot of design management system in use. Like everywhere else in this work, the sign convention is energy consumption is positive and energy generation is negative.

The data structure is shown in Figure 7-13. It is a dynamic array that stores all design parameters and performance data, depending on what has been obtained from the simulation engine. The minimum data for each new design is: the user-defined name and full set of parameter values. The rest of the data is only populated when the user requests it. Between designs, the user can make one or more parameter changes. This allows different strategies – which often involve multiple parameter changes – to be understood in a coupled fashion. The DMS data is stored in comma separated value (CSV) format for easy porting to reports. Furthermore, the model input file is available if

the user wishes to tweak the design using more advanced features that are not available from Ecos.

Design 1	Design 2	Design 3	Design 4	Design 5	
		Higher glazing and thermal mass	Controlled blinds	PV added	← Name
Base Case	Better insulation				← User-defined name
P(1)					← Parameter values
:					
P(n)					
High-level performance metric (1)					← High-level performance metrics
:					
High-level performance metric (n)					
SDD performance(1)					← Solar design day performance
:					
SDD performance (n)					
Whole year performance (1)					← Whole-year performance
:					
Whole year performance (n)					

Figure 7-13: Data structure of DMS


### 7.5.7 GUI event sequences

Programming a fast-responding, “user-friendly” GUI is a non-trivial task. As thoroughly explained in the next subsection, a major objective of Ecos is to provide quasi real-time feedback. As such, the GUI was carefully programmed to provide the users with information as quickly as possible and eliminate downtime.

Normally, the sequence of events for a GUI is: UI input is changed by the user, perform a calculation, an output is provided to the UI. Since Ecos is relatively feature-heavy, the middle step is complex and must be carefully designed to maximize the user’s experience. A typical events sequence is shown in Figure 7-14. It is initiated when a user changes a parameter value – either by slider or dynamic text field. The events that

follow can take between about 0.001 and 5 seconds on a typical desktop computer<sup>9</sup>.

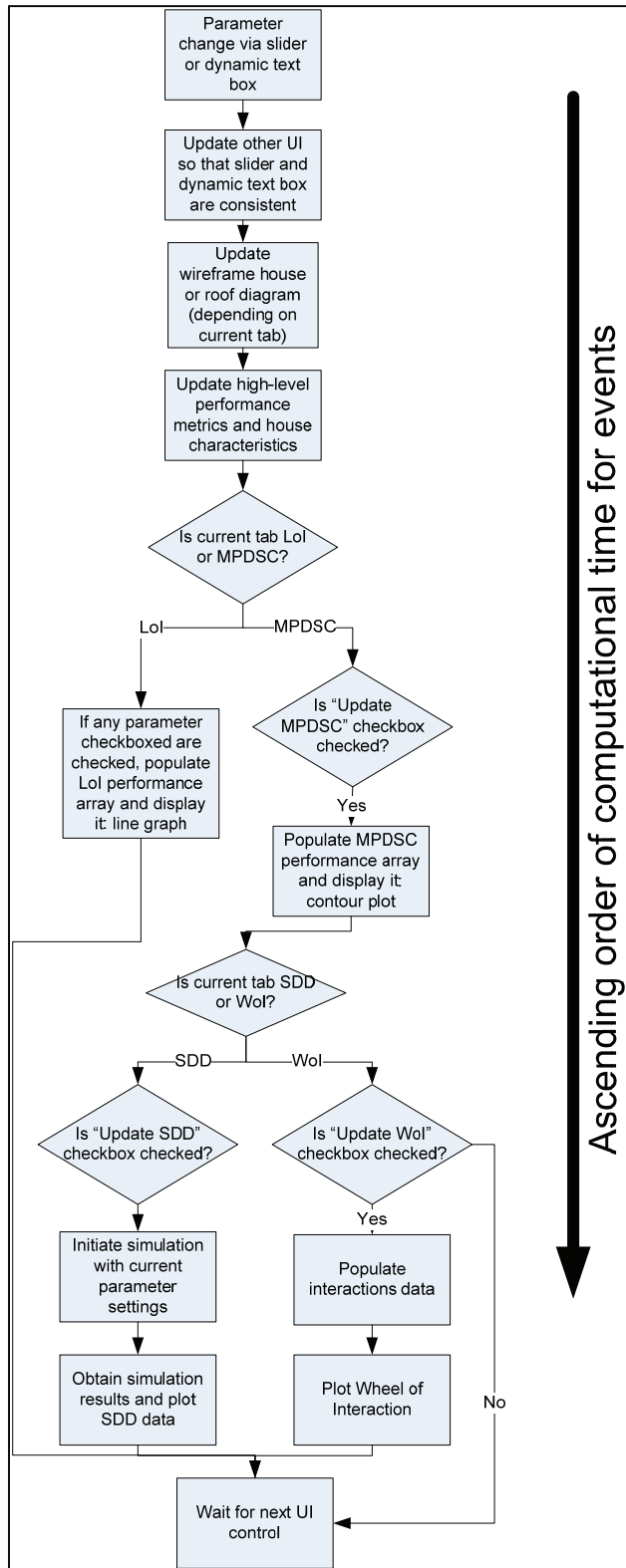
Therefore, the order is carefully selected to display data in order of ascending computational time (i.e., the quickest computations first). In this way, the user is at least presented with some information while they await longer processes. This helps reassure the user that the action they requested is in progress. This is in contrast to most of the surveyed tools which complete all computations before providing any feedback to the user.

Any design tool process that takes longer than about 0.1 second to compute (MPDSC, Wol, SDD, or any other full simulations) can be enabled or disabled by the user, using a checkbox. For the events that are enabled, the cursor is changed to “hourglass mode” (  ) so that the user cannot create a backlog of input events (i.e., one sequence of events must finish before starting the next).

---

<sup>9</sup> The processing times refer to a typical desktop computer and are mainly intended to give the reader a sense of relative durations.





Ascending order of computational time for events

Figure 7-14: GUI events sequence for when the user changes a parameter value.

### **7.5.8 Implementation of Real-Time Feedback**

From the beginning of the development process, a strong desire has been to offer instantaneous performance feedback. That is, graphical feedback display should be updated in real-time (or as close as possible) as parameters are changed. As an interesting aside, two leading experts in the field – Don Greenberg of Computer Graphics at Cornell University and Azam Khan of Autodesk Research - informed the author that the work should proceed with the assumption that the cost of computing (time, money) will be negligible in the future. The following subsection describes how real-time feedback implemented at current technology levels.

For solar design days (SDDs), EnergyPlus can be called at run-time and return a day's simulation data with an acceptably small lag of several seconds, on a typical desktop computer. Naturally, this lag will decrease with the advance of computers. Each time the user adjusts a parameter, the following occurs.

1. The EnergyPlus input file written with the MATLAB script
2. An EnergyPlus building simulation is run for the appropriate day (and up to 25 preceding identical days until quasi steady-state is achieved).
3. The output file is scanned for the information of interest.
4. The information is displayed on the SDD graph.

While simplified models or pre-run simulations could be used to display SDD performance, the use of run-time simulations provides flexibility and accuracy. Overall,

the approach is relatively easy to implement, but presents some lag at run-time. The option to not update the display at every design change is provided for users who find this lag too long.

Since the results of multiple whole-year simulations are required to display MPDSCs, performing simulations at run-time does not meet expectations using contemporary computational power. Two main options to achieve real-time feedback remain: a database of pre-run simulations or a simplified (and computationally fast) model. Given the power and validation of existing simulation engines, such as EnergyPlus, the first option was selected as the most appropriate. Because full factorial (i.e., every possible combination of parameters) design would require an immense number of simulations, regression was explored as a method to reduce the number of required simulations to a manageable number. In full factorial design, all possible design options are explored. If each of the 30 parameters had five possible settings, there would be  $10^{21}$  designs which would take about  $10^{15}$  processor-years with current equipment (based on one minute per whole-year simulation).

The ultimate goal is to be able to accurately predict house performance based on parameter values without performing a simulation at run-time. Furthermore, such predictions should be possible even if that exact set of parameters were never simulated. To determine the feasibility of this, two regression techniques were

explored: non-linear multivariate regression analysis (MRA) and a feed-forward back propagation artificial neural network (ANN).

Both approaches require performing many simulations before applying the regression. To achieve a thorough distribution within the design space, all parameters were randomly set for a large set of “training” simulations. The approach to use randomized inputs is suitable for this situation in which the entire design space is of equal importance. Furthermore, it is relatively simple to implement and has been shown to be effective for the application to building simulation data (see e.g., Hui (1998)).

Validation of the methods can be performed by introducing the regression models to new sets of inputs and comparing the outputs to the simulated outputs. For the implementation below, a set of 10,000 training samples was created. The validation sample size was a further 1,000.

Non-linear multivariate regression is a classical method for predicting an output based on a set of inputs, using a non-linear function. The general form of such a function can be complex and might appear as follows:

$$\hat{y} = \beta_0 + \beta_1 x_1 + \beta_2 x_2 + \beta_3 x_1 x_2 + \beta_4 x_1^2 + \beta_5 x_2^2 + \varepsilon \quad (7-2)$$

Where  $y$  is the predicted output (e.g., heating energy),  $\beta_i$ ,  $x_i$  is one of the inputs (e.g., WWR1), and  $\varepsilon$  is the residual or error. The general form (i.e., number of terms and power of terms) must be manually defined, which can be a considerable effort. Once the form of the Equation is chosen, values for the coefficients  $\beta_i$  are selected to

minimize the error from all training simulations. MATLAB's *nlinfit* function uses the Levenberg-Marquardt algorithm to determine the values of  $\beta_i$  that yield the lowest sum of squared residuals (SSE) (Mathworks Inc., 2008).

An advantage to non-linear multivariate regression is that it is relatively transparent and the coefficients themselves are meaningful indicators. For instance, for the linear terms (e.g.,  $x_1, x_2$ ), the magnitude of the coefficient indicates the significance of the parameter. However, a major disadvantage is that the basic form of the Equation must be provided and requires a certain amount of trial-and-error to achieve good results.

Artificial neural networks (ANNs) are a newer method for regression, but have been used in the field of building performance simulation for a number of applications in which full simulations could not be performed because of time constraints. Examples include: optimization (Magnier et al., 2010), to predict occupant-based loads (Swan et al., 2011), and to predict time-series data of passive solar houses (Kalogirou et al., 2000). Neural networks are best used for approximating complex non-linear systems.

The principle of ANNs is that a network of neurons, each linked by different weights to allow model outputs to be approximated based on inputs. They contain an input layer, at least one hidden layer, and an output layer. Each neuron takes in each of the inputs from the previous layer and uses a function to calculate the neuron output. Much like determining the coefficients in multivariate regression, when an ANN is being trained, the objective is to calculate weights such that the error between the model-predicted

outputs and real outputs is a minimum. The relationship between the inputs and the outputs for each neuron is as follows.

(7-3)

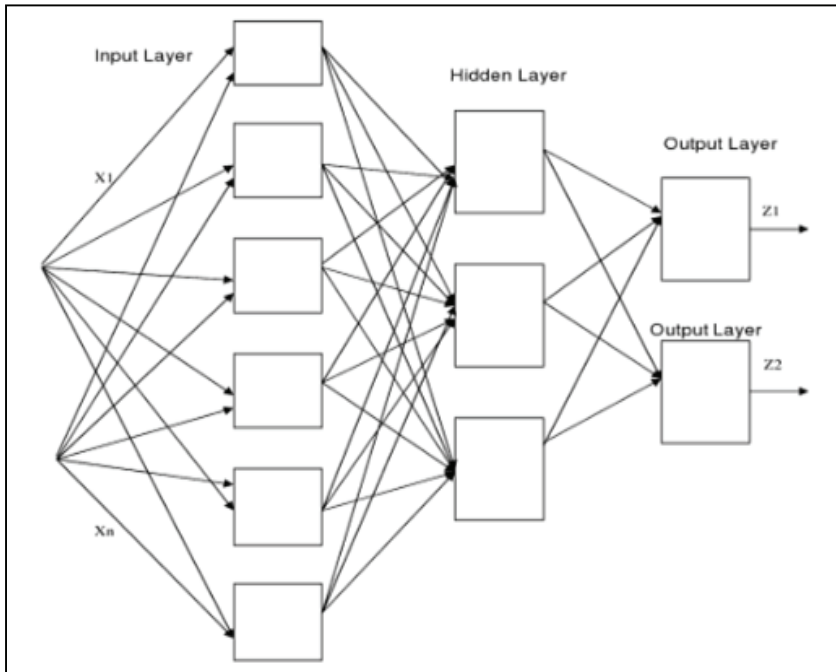


Figure 7-15: ANN structure, showing inputs, the hidden layer, and outputs (taken from Graupe (2007))

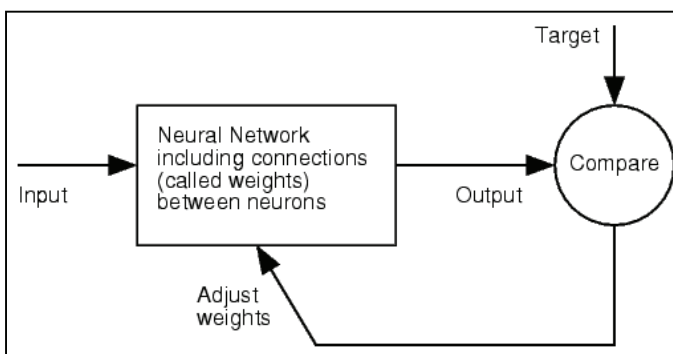


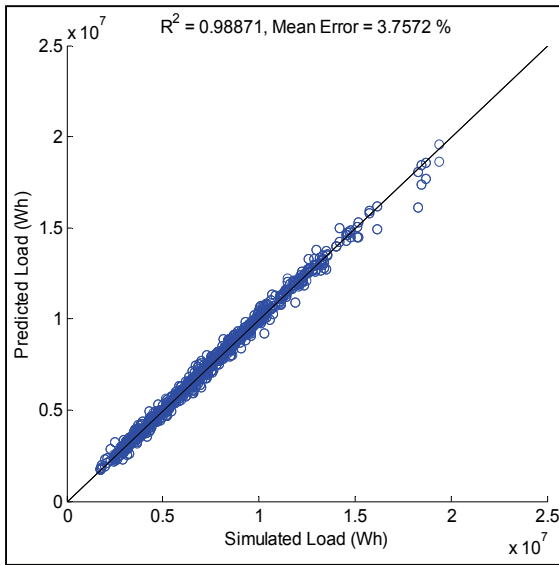
Figure 7-16: Training process for ANNs (Mathworks Inc., 2008)

Unlike multivariate regression, ANNs do not require significant input about Equation form; thus resulting in a much more flexible and adaptive approach. However, ANNs are

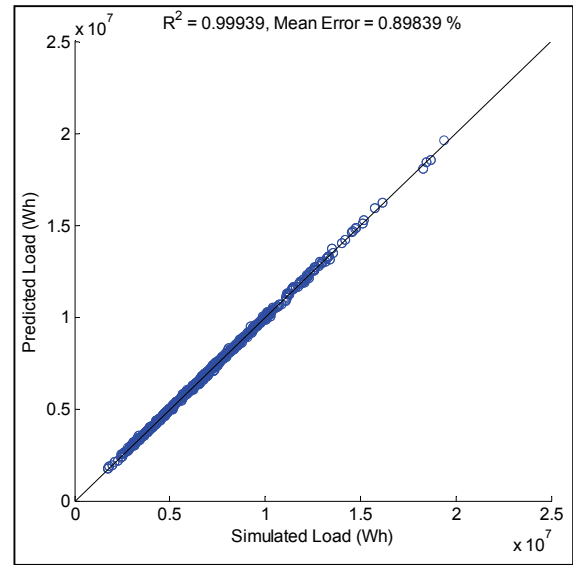
essentially a black-box, providing very little insight into their inner workings. This means that the only means to verify their robustness is to test them using validation samples.

To compare the methods, randomized sampling was used to run simulations and create a database of 10,000 whole year results, based on the parameters that were previously listed, as reported by O'Brien et al (2009c). These simulations represent about 10 days of processing time on a standard desktop computer.

For the multivariate regression, the Equation form was determined iteratively increasing its order. Beyond second-order the results were not found to be significantly more accurate. The ANN uses two hidden layers of 30 nodes. The output of each model is the combined annual heating and cooling load. To compare models for accuracy, MATLAB was used to create the models and validate them against 1000 separate randomized samples. Early results are shown in Figure 7-17. At that point, the model was defined by 12 parameters. These results show that the ANN performs significantly better, in terms of accuracy. Furthermore, it was found that the Equation for the multivariate regression was becoming exponentially longer as the number of parameters increased.



(a) Nonlinear Multivariate Regression Analysis



(b) Artificial Neural Network

*Figure 7-17: Results of the MRA and ANN models*

The validation plots for the current work for the space heating, cooling, and DHW energy are shown in Figure 13-7 through Figure 13-9 in Appendix E. The mean error for the three ANNs is 7.1, 4.7, and 6.5%, respectively. Short of reducing the design space (either number of parameters or parameter ranges), a further increase in accuracy could potentially be achieved by increasing sample size for training the ANN. Note that increasing the number of hidden layers or number of nodes (neurons) in the hidden layer was not found to improve accuracy.



## 8 CASE STUDY: ÉCO TERRA REDESIGN

ÉcoTerra is one of 15 demonstration houses that was selected to be built through a competition conducted under the Canada Mortgage and Housing Corporation (CMHC) Equilibrium Healthy Housing Initiative (CMHC, 2010). The house was prefabricated in a factory in seven modules and assembled on the site in 2007. ÉcoTerra (see Figure 8-1) is a two-story, two-bedroom, single family, detached home located in Eastman, Québec, Canada (45.3° N, -72.3° W) with a basement and single car garage. It has a heated floor area of 211.1 m<sup>2</sup> and a heated volume of 609.1 m<sup>3</sup>. The garage and basement account for an additional 26.6 m<sup>2</sup> and 76.9 m<sup>3</sup>, respectively.



Figure 8-1: A photograph of ÉcoTerra house as seen from the south-west

Its form and fabric were selected for optimal passive solar performance. To supplement heating and cooling in Quebec's heating-dominated climate, a building-integrated

photovoltaic area with thermal recovery (BIPV/T) system was built. The upper south-facing roof section consists of 21 laminate amorphous-silicon (A-Si) modules with an airspace underneath, through which air is drawn and warmed by the absorbed solar radiation. The energy content of this air is used to warm (or cool) a ventilated slab in the basement, preheat domestic hot water, or dry clothes, depending on the current demands. A ground-source heat pump with a COP of about 3.7 is used to supplement the passive and active solar heating. A photograph of the house and timeline of major events are shown in Figure 8-2. A thorough description of EcoTerra’s design details and process and occupied performance data are provided in Appendix E.

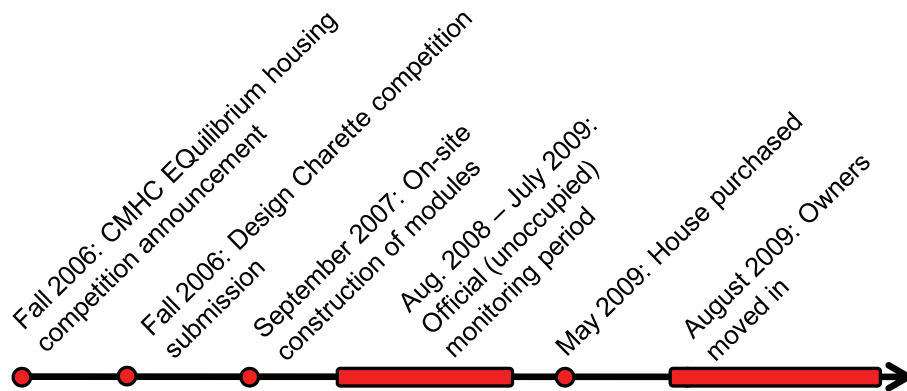


Figure 8-2: Timeline of significant events (taken from (O'Brien et al., 2010c))

## 8.1 Performance model

In order to perform further analysis on ÉcoTerra, a detailed model was created.

EnergyPlus (U.S. Department of Energy (US DOE), 2009), selected for its relative ease of use, extensive features, and interoperability with a variety of other tools, as justified in

Chapter 3. This section describes the modelling that was performed including boundary conditions, form and fabric, operations, renewable energy systems, and results.

### 8.1.1 Boundary conditions

Since ÉcoTerra is about three-quarters of the way from Montreal to Sherbrooke, QC (see Figure 8-3), the model was run for both Montreal and Sherbrooke EPW weather files. A limitation of using an existing weather file is that it does not capture the year-to-year variation in weather. However, the effect is largely reduced by comparing monthly values, for which many of the variations are mostly cancelled out. In ideal circumstances, a high-end local weather station would have collected sub-hourly weather data. The data that was available (from house-mounted sensors) was found to have some major gaps and to be questionable at times – likely due to shading and snow cover.

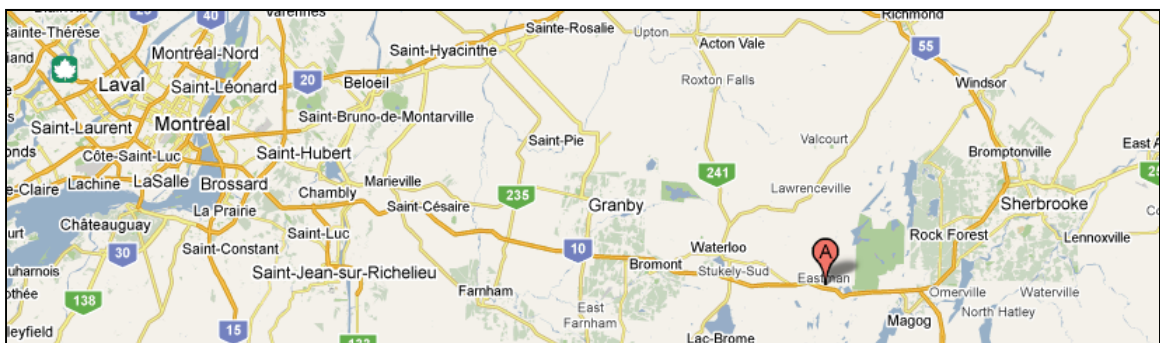


Figure 8-3: Map of area around ÉcoTerra (marked “A”), including nearest EPW format weather file locations: Montreal and Sherbrooke, QC.

### 8.1.2 Form and fabric

The geometry was derived from the architectural drawings and manually input using SketchUp/OpenStudio (U.S. Department of Energy (US DOE), 2009). Ecos was used as a

starting point to establish wall and window constructions, major geometry and operations in the modelling process. However, the model had to be customized to some extent for the following reasons.

- ÉcoTerra has a somewhat complex roof of which part of it is a cathedral ceiling. The generic model assumes a single roof construction with a ventilated roofspace.
- ÉcoTerra's basement is only exposed on the south-facing wall, but the generic model assumes that the top 1 meter of all walls is exposed.
- ÉcoTerra has unusually shaped windows that are largely surrounded in fixed shading devices (overhangs, balconies, awnings), whereas the generic model only has fixed shading devices on the south side of the house.
- Nearly all of the ÉcoTerra's windows are operable and have one or two dividers. This leads to unfavourable thermal performance and was therefore not included in the generic model.
- On the interior, ÉcoTerra has a thermally massive mid-height wall on the first floor. However, the generic model is limited to a consistent wall from floor to ceiling.
- ÉcoTerra's major geometrical features – while being relatively rectangular – deviate from the strictly rectangular generic model. If this were the only limitation, equivalent areas could be determined for a rectangular house

because ÉcoTerra does not suffer from the self-shading that often occurs for irregular geometries.

- The generic model, for a given floor area, only has three internal gains schemes: low, medium, and high. However, given that information about ÉcoTerra’s internal gains is available in higher resolution, it is possible to input this such that this source of uncertainty is eliminated. It is interesting to note that ÉcoTerra’s discretionary electricity use closely matches the “low” scheme.
- ÉcoTerra has a garage, which acts as a buffer zone, slightly reducing heat loss through part of the house’s wall. The generic model does not include a garage.

The house was modelled as four conditioned zones, in an attempt to properly characterize any discomfort resulting from stratification, as shown in Figure 8-4. In addition, a zone was assigned to each of the roof space and to the garage. Six views of the model geometry are shown in Figure 8-5.

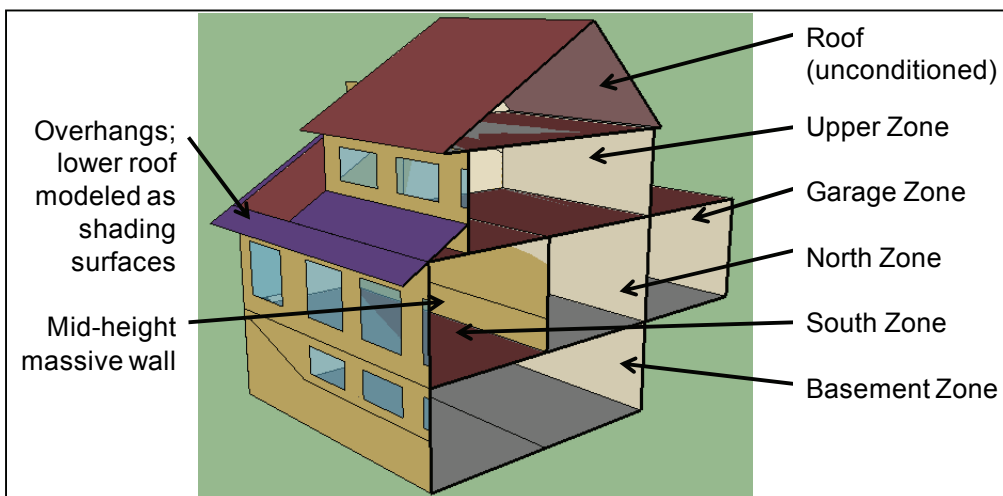


Figure 8-4: Section view of thermal model with zoning scheme

The thermal resistances of the different envelope components are summarized in Table 8-1. Stud wall equivalent thermal resistance values were calculated using the “parallel path” method. Had the studs been metal, a more detailed method would have been required due to the severity of the thermal bridging. Other significant thermal and optical properties are also summarized in Table 8-1.

*Table 8-1: heat transfer characteristics of ÉcoTerra house: opaque constructions, fenestration, infiltration, and ventilation.*

Walls	5.90 m <sup>2</sup> K/W
Cathedral Ceiling	7.83 m <sup>2</sup> K/W
Other Ceiling	8.35 m <sup>2</sup> K/W
Basement Walls	4.01 m <sup>2</sup> K/W
Basement Slab	1.72 m <sup>2</sup> K/W
Door	0.40 m <sup>2</sup> K/W
Frame and Dividers	0.36 m <sup>2</sup> K/W
Triple Glazing	0.85 m <sup>2</sup> K/W; SHGC = 0.53
Double Glazing	0.44 m <sup>2</sup> K/W; SHGC = 0.76
Infiltration Rate	0.043 ach (0.85 @ 50Pa); 8 ach in roof
Ventilation Rate	0.3 ach
HRV Effectiveness	60%

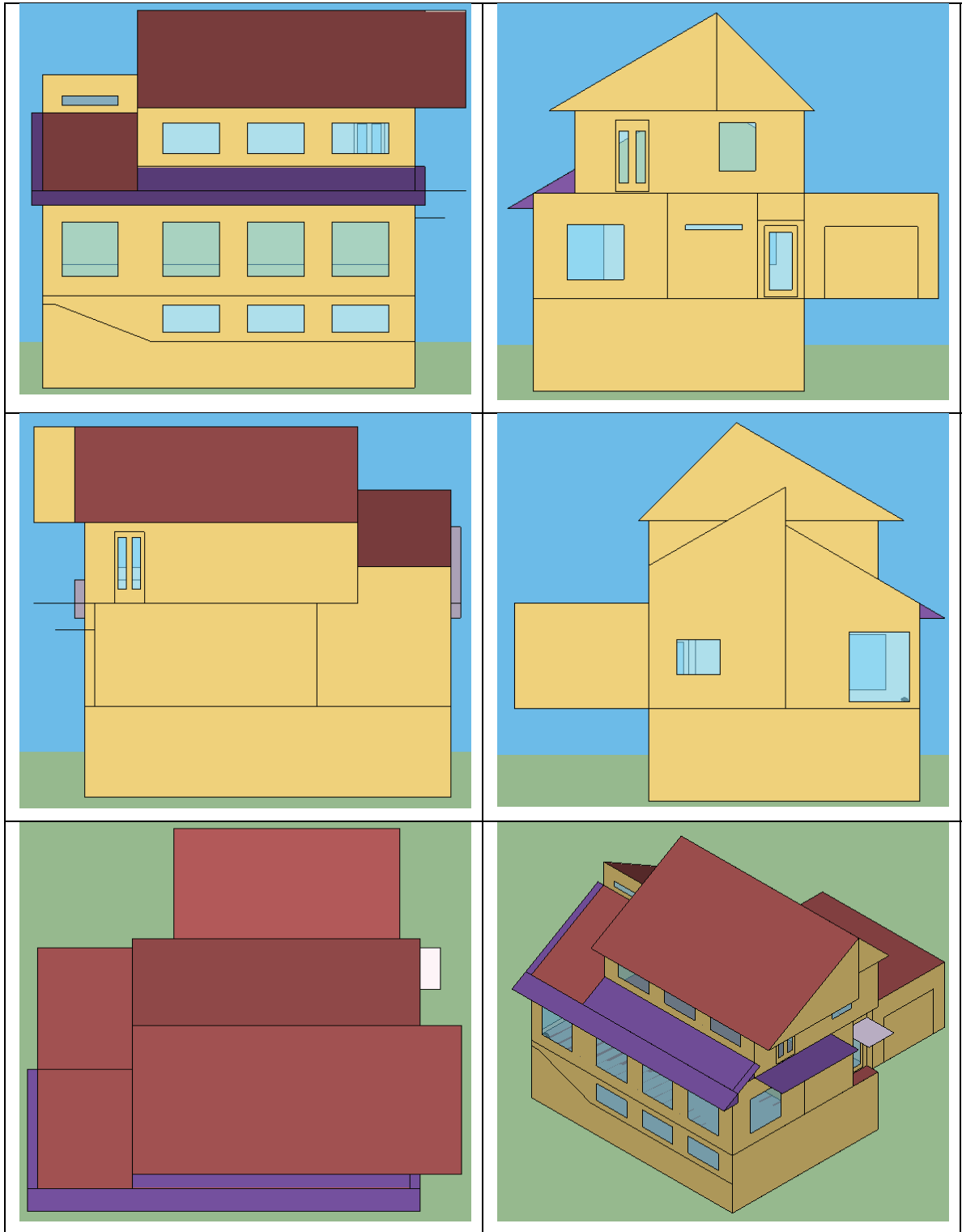


Figure 8-5: Views of model clockwise from top-left: south elevation, east elevation, west elevation, isometric, plan, and north elevation.

### **8.1.3 Operations**

A survey of energy-consuming household objects was performed to determine an appropriate heat gains schedule. Appliance, lighting, and air distribution loads were assumed to be seasonally-invariant. The total internal gains were distributed as per the schedule used for the generic model. Similarly, the same occupant schedule was used but for three adults. The infiltration rate was input based on the measured for the house using a blower door test. The infiltration rate at 50 Pa was measured to be 0.85 ach, which is approximately equivalent to 0.043 ach under typical conditions with a pressure difference of 4 Pa. As in the generic model, this was assigned at a fixed rate and evenly distributed to all zones. Similarly, the 0.3 ach of ventilation was reduced to an effective ventilation rate of 0.12 ach because of the HRV, which is approximately 60% effective. The HRV system was not explicitly modelled.

### **8.1.4 Renewable energy systems**

In adherence with the rest of the model's level of detail, the BIPV was modelled as being thermally coupled to the roof. The 21 UniSolar PVL-136 amorphous silicon modules were modelled using EnergyPlus' one-diode model (as described in Chapter 4). The simple inverter model was used with an assumed operating efficiency of 92%.

Since EnergyPlus does not have a readily-available air-based BIPV/T model, a custom model was created in MATLAB. The limitation to this approach is that the model is decoupled from the main EnergyPlus model (i.e., there is no two-way communication between the models during simulation). However, this approach can be used to assess



the thermal energy availability relative to household thermal energy demand, in an effort to approximate its value.

The model, described in detail by Chen et al (2010b), uses five control volumes, discretized in the direction of airflow. The PV cell and roof surface, bulk air, and insulated surface temperatures are solved simultaneously to determine the outlet air temperature, using the three Equations that follow. This can be related to the energy performance of the BIPV/T system.

$$\text{PV: } I_{\text{solar}} \left( \alpha \frac{A_{\text{PV}}}{A_{\text{roof}}} AE \right) + U_{c,o} (T_o - T_{\text{PV}}) + U_{r,o} (T_{\text{sky}} - T_{\text{PV}}) + U_{c,\text{PV}} (T_{\text{air}}^i - T_{\text{PV}}) + U_r (T_b - T_{\text{PV}}) = 0 \quad (8-1)$$

$$\text{Air: } Q_{\text{af}} (T_{\text{air}}^{i-1} - T_{\text{air}}^i) + U_{c,\text{PV}} (T_{\text{PV}} - T_{\text{air}}^i) + U_{c,b} (T_{\text{back}} - T_{\text{air}}^i) = 0 \quad (8-2)$$

$$\text{Back: } U_a (T_{\text{attic}} - T_{\text{back}}) + U_{c,\text{back}} (T_{\text{air}}^i - T_b) + U_r (T_{\text{PV}} - T_{\text{back}}) = 0 \quad (8-3)$$

These Equations are re-arranged into matrix form so that they can be efficiently solved at each timestep. Since the weather data is hourly, that is the frequency of calculation.

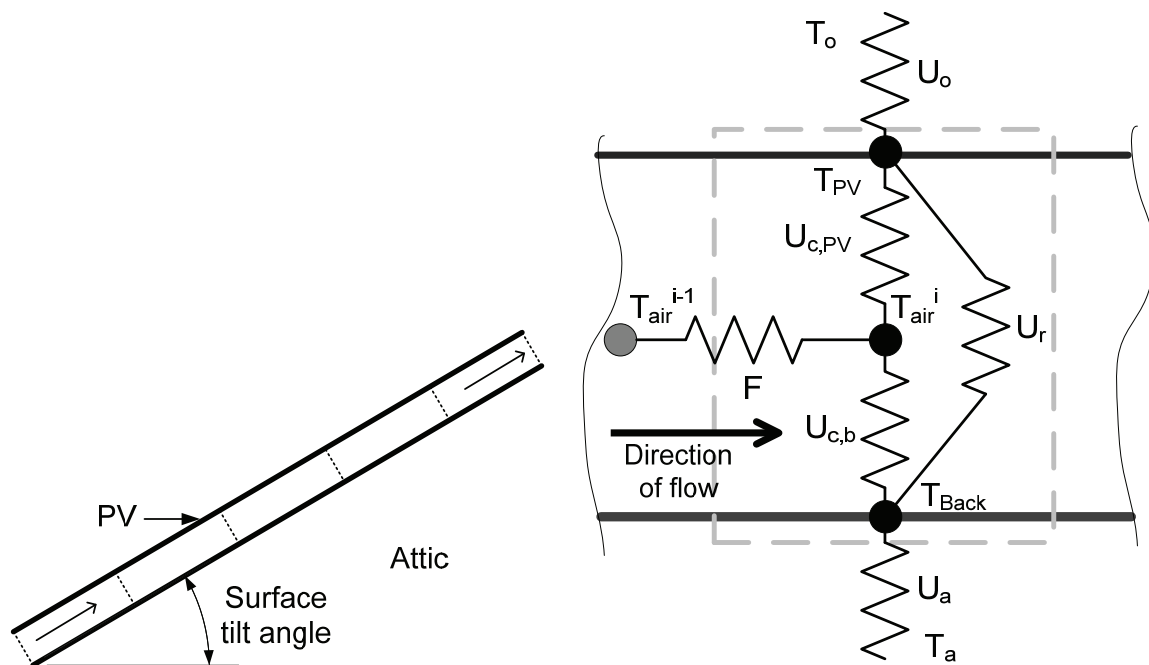


Figure 8-6: Schematic (left) and thermal network of a control volume in the BIPV/T system model (right) (taken from Candanedo L., O'Brien, W., et al (2009))

### 8.1.5 Simulation results

Figure 8-7 shows the measured and simulated heat pump energy consumption. For it, monthly heating and cooling energy were converted to electricity consumption using a COP of 3.7 (as measured to be the annual average for ÉcoTerra's heat pump). Annual results are tabulated in Table 8-2. Interestingly, despite being nearly the same latitude, Montreal and Sherbrooke yield significant different results. Specifically, Montreal is milder, which can be partially accounted for by the urban heat island affect. From here in, Sherbrooke is used for all modelling. The results indicate that the thermal model is accurate and suitable for assessing the building upgrades that are described in the sections that follow.

Unlike for heating which is tightly controlled, the occupants had the option of overriding mechanical cooling by merely switching it off. Consequently, the model over-predicted cooling energy. There was anecdotal evidence from the owners that natural ventilation was used as a means for cooling and increasing air movement. While this was coarsely modelled, other discrepancies could occur from a high-tolerance for high temperatures or significant periods of absence during summer vacation.

Another interesting peculiarity is that the model consistently under-predicts heating energy from January to March and over-predicts heating energy in November and December. Possible explanations are shading from leaves, ground reflectance variability (from snow) or simply, a change in occupant behaviour (e.g., greater internal gains, a changed heating set-point).

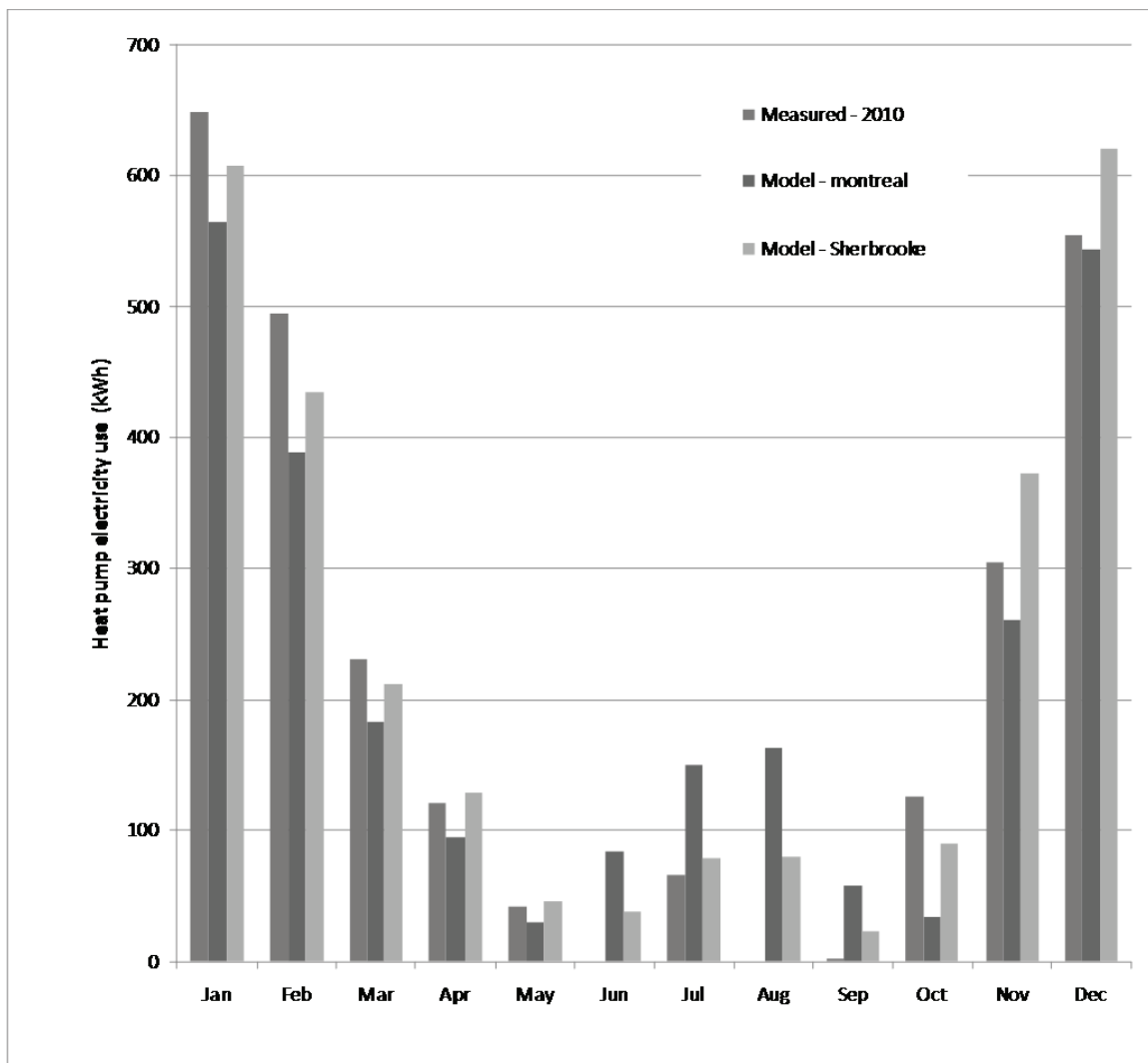


Figure 8-7: Comparison between measured heat pump electricity and modelled values.

Table 8-2: Annual performance results

	Heat Pump Heating
Measured	2,524
Model - Montreal	2,092
Model - Sherbrooke	2,519

## 8.2 Redesign Study

This section outlines the re-design study that was performed. The fundamental question being asked is: how could ÉcoTerra and other similar low-energy houses have been

designed to be closer to achieving net-zero energy status? The EnergyPlus model was used to assess each upgrade for energy performance.

There are three major categories of possible upgrades:

1. Operational changes: existing hardware with changes to control strategies such as setpoints and logic for controls related to solar heat collection and usage/storage;
2. Building envelope changes: either passive or active envelope components to change how the house interacts with the environment; and,
3. Generation: active systems to offset energy use.

For re-design, the operational changes will be considered first because they are non-invasive and have no material costs. Furthermore, they could be implemented in the ÉcoTerra house. The last two options – envelope upgrades and generation – will be considered simultaneously. While envelope improvements are often considered the most cost-effective, they provide diminishing returns unlike PV, for which additional costs increase approximately linearly with output, and for which there are some economies of scale (for auxiliary equipment such as inverters in wiring).

A fourth category of upgrades could be considered a modification to occupant behaviour. Nearly 40% of the electrical loads are related to appliances, lighting, and plug loads. Furthermore, some of the heating and cooling can be attributed to the fact that the occupants have the set points at values other than anticipated during design. For

instance, the daytime heating setpoint is 22.5°C instead of 21°C, resulting in a predicted 10% increase in heating loads, according to the model. However, these social aspects are considered beyond the scope of the current research. Making assumptions that could lead to sacrifices in comfort and convenience would undermine the occupants' values. While the designer cannot predict discretionary energy use to a high degree of certainty, they can inform the occupants about their habits; either informally or through the installation of an "energy dashboard" that provides useful feedback. For example, the authors visited the occupants at their home after several months of occupancy to show a breakdown of energy use. Upon informing the occupants that the electric resistance heater in the garage was using nearly as much energy as the heat pump, they reduced its use to negligible levels. Chetty et al (2008) state real-time feedback of household energy consumption can lead to 10% savings with minimal change in behaviour is achievable. Further grid-side benefits can be achieved through shifting non time-sensitive loads, such as clothes and dish washing.

The analysis of many of the upgrades described are made possible because EnergyPlus is a detailed tool that has a powerful output facility with which many low-level outputs (e.g. nodal temperatures and heat fluxes) are available on the timestep level. Many earlier stage design/simulation tools, such as HOT2000, use standard configurations. However, the creation of the EnergyPlus model took about five days, which is an order of magnitude longer than for the HOT2000 model.

As mentioned, any major savings that can be achieved through changing the controls of the house were explored first. The “equipment” category of energy use is mainly comprised of the distribution fan built into the heat pump. The fan is currently operated at a constant rate, even when fresh air and conditioning requirements are met.

Simulations were run to determine the potential benefit from reducing the fan (when heating and cooling are unneeded) to only operate when the mean air temperature difference between zones exceeds 2°C. The simulation indicates that the fan can be set to low speed for 8% of the year, yielding fan energy savings of about 130 kWh.

Additional savings (460 kWh/year) can be achieved by removing the air cleaner, which can be considered redundant to the air filter in the heat recovery ventilator (HRV), and unnecessary in the rural setting.

In order to assess the best opportunities for improvement to the envelope, the sources of heat loss were predicted for the house during the heating season (see Figure 8-8).

While the window losses account for 21% of total losses, the net energy balance for the windows including solar gains is positive - by about 1000 kWh. Since the house is relatively airtight, there is little benefit to further sealing the envelope. Similarly, the ventilation rate cannot be lowered and the house is already equipped with a HRV. Thus, the opaque envelope and windows represent the only practical potential.

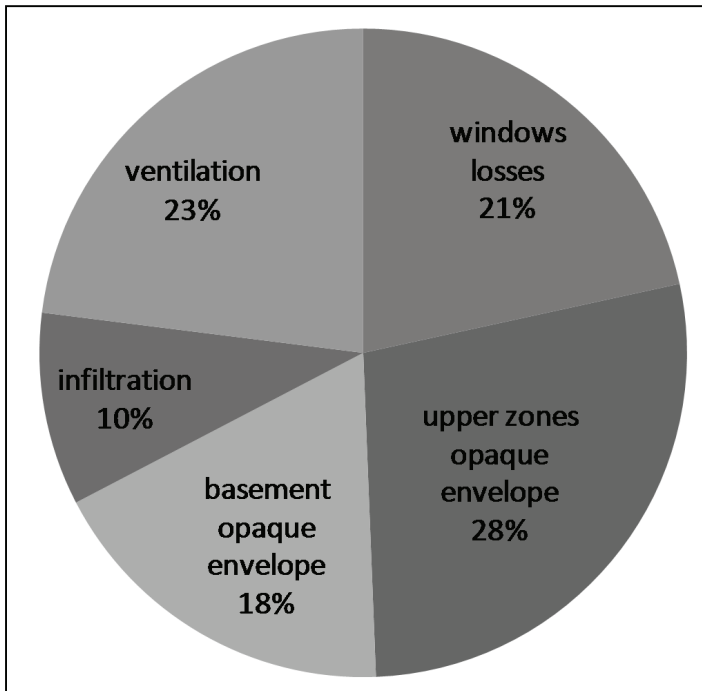


Figure 8-8: Distribution of heat losses

The upside of removing the dividers in the windows was examined. Currently, most of the large south-facing windows are operable and have two dividers in them. This not only increases the conductance of the envelope, it also reduces solar gains. The removal of two-thirds of these (leaving enough operable windows to enable natural ventilation) reduces predicted heating energy by about 12%. The upgrade to better window frames and doors only yields a modest reduction in heating loads and thus they were not changed. As for many aspects of the house, the existing vinyl window frames are high performance.

The addition of intelligent shade control – either manual or automated – was considered. For the cooling season, shades were assumed to be closed during periods when the zone air temperature exceeds 22°C. This is predicted to reduce cooling loads



by about one-third, resulting in 90 kWh of electricity savings. Proper shade control also improves thermal comfort by mitigating overheating and direct beam solar radiation on occupants. The addition of 1 m<sup>2</sup>K/W of insulation on the basement and above-grade walls of the house was found to yield an annual reduction in electricity use of about 150 kWh. This was not considered practical, and thus, the insulation levels were left as is.

The energy implications of each upgrade are quantified in Figure 8-9. With these upgrades, there are few good remaining opportunities to reduce consumption without modifying occupant behaviour. The total predicted energy use was reduced by a mere 7%. This is actually a positive outcome, since it indicates that the designers of ÉcoTerra did not miss any major opportunities. In order to attempt to offset all energy use with renewable energy, the gap should be filled with the supply side.

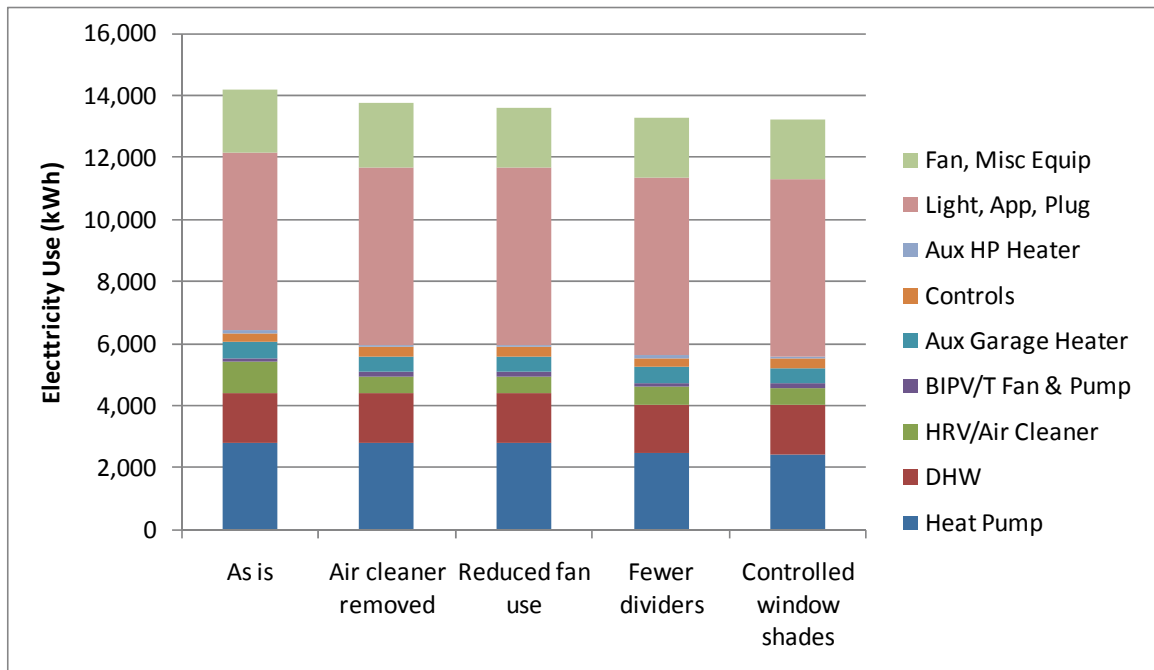


Figure 8-9: Electricity use for successive upgrades

For active solar energy collection, an existing issue that should be considered is snow accumulation on the roof and its negative impact on wintertime generation. For example, the performance in 2010 clearly indicates that the performance in the winter fell short of theoretical performance (Figure 8-10). Thus, the effect of increasing the BIPV/T roof slope to 45° (from 30°) was examined. From experience, this slope has been found to effectively shed snow (Athienitis, 2007). RETScreen (RETScreen International, 2005) indicates that the difference in slope has a negligible effect on annual incident solar radiation of about 1449 kWh/m<sup>2</sup>/year, since both slopes are in the near-optimal range for site's latitude – 45°29' N. Assuming that the base of the south-facing roof remains the same, the additional pitch results in a 22% increase in area for a total surface area of 65.6 m<sup>2</sup>.

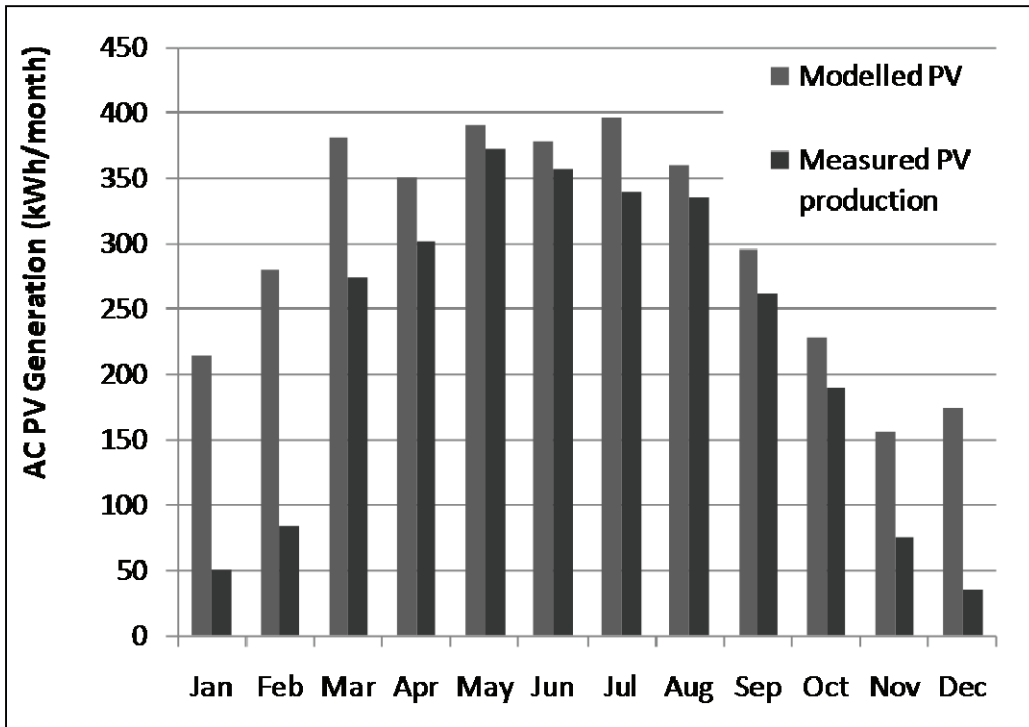


Figure 8-10: Modelled and measured PV performance (for the current design with a 30-degree slope)

Assuming annual electricity use of 13,100 kWh, an inverter efficiency of 92%, shading losses of 8% (as measured for the site), 90% module coverage area (for spaces and edges), a minimum module efficiency of 17.4% is required to achieve net-zero energy.

This level of efficiency is above the range (5-7%) of common amorphous silicon modules, thus poly-silicon or other higher performance modules (such as polycrystalline silicon) are needed. The total capacity of the array must be at least 10.7 kW (or 380% greater than the existing array).

As discussed earlier, timing is critical to BIPV/T performance; the energy is only useful if it is used immediately or stored for future use. Figure 8-11 compares the monthly combined space and DHW heating energy with BIPV/T thermal energy generation. The

air is considered to be useful only if its temperature exceeds 20°C. This is because most of the applications for the heat require this. For instance, in order for heat to be transferred to the ventilated concrete slab, the air temperature must exceed the slab temperature.

Predicted annual performance is similar for both 30 and 45-degree designs. However, in the winter, though performance is low, useful energy output is nearly double for the steeper roof. This is due to the slightly longer (soffit to peak distance) roof and the fact that the roof is oriented better to face the low winter sun.

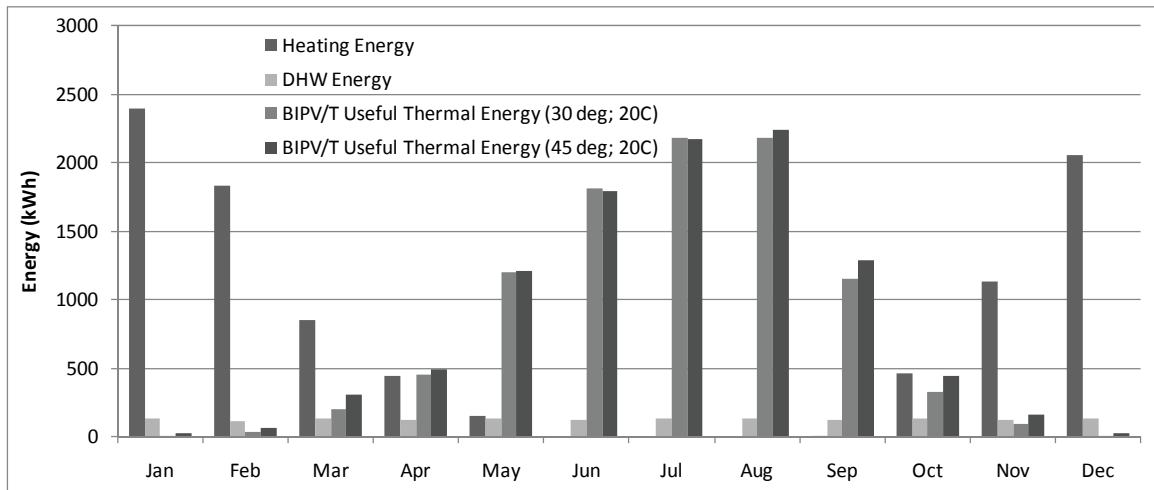


Figure 8-11: Comparison of thermal loads and BIPV/T useful energy output

While total energy output and demand are relatively similar in magnitude over the course of a year, they vary significantly by month and the peaks are about six months out of phase. The most reasonable method to solve this problem is to use seasonal storage, such that the gap is closed. However, the use of a heat pump to upgrade the thermal energy to higher temperatures would be beneficial. For example, this was done

for the Alstonvale House design (Pogharian et al., 2008), since it significantly decreases the outlet temperature threshold above which the energy is in a useful form. For example, the simulations were repeated for a case where this threshold is reduced to 10°C. While there is still a seasonal mismatch between supply and demand, the supply increases significantly – especially in the shoulder seasons and the summer. These results indicate that without the use of a heat pump, effective BIPV/T performance is limited to the warmer months.

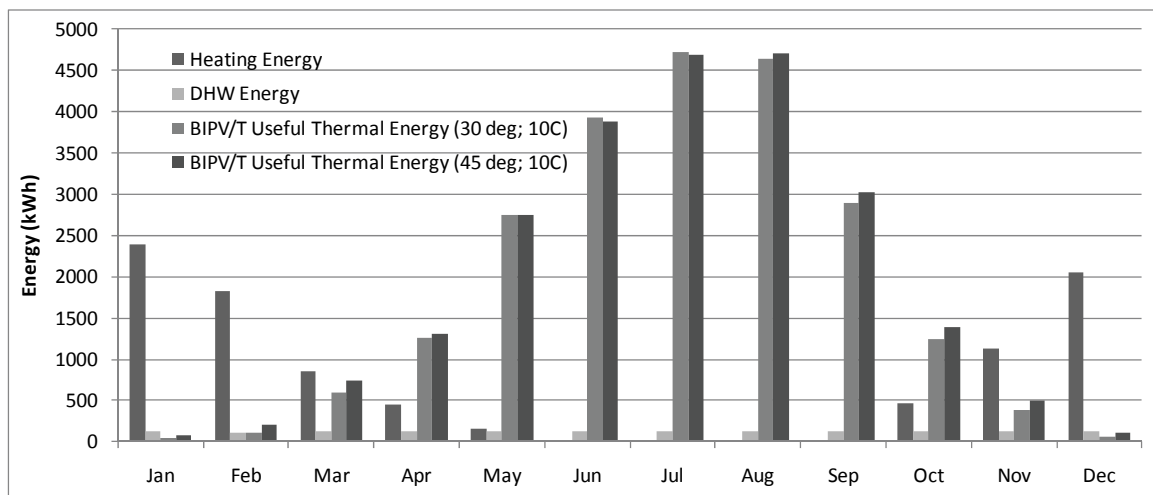


Figure 8-12: Comparison of thermal loads and BIPV/T useful energy output

### 8.3 Conclusions

This chapter examined the design process of a near net-zero energy house, presented measured performance results, and suggested how net-zero energy status could be achieved through some design changes. Simulations showed that only modest electricity savings are possible without taking any extreme measures. Beyond that, additional active building-integrated solar energy generation becomes the most practical upgrade

to achieve net-zero energy. After the design upgrades, discretionary loads account for nearly half of electricity use. For houses for which the envelope heat transfer and passive solar performance have been optimized, the greatest remaining opportunity is to influence occupant behaviour by means of advanced controls, display of resource consumption, and education. This represents a significant and necessary area for further research. Two major trends are expected to aid the movement towards widespread implementation of low-energy houses: 1) the improvement of efficiency and intelligence of appliances and equipment, and 2) the improvement of active solar energy collectors. This means that even a house that is not net-zero energy today may become so as old equipment is replaced with higher performance equipment over its life cycle.

## 9 CONCLUSIONS

Given that the residential sector in Canada accounts for 17% of total energy use and houses have been shown to be able to achieve significant net-energy savings (50 to over 100%) using passive and active solar features, this sector represents an excellent opportunity for a reduction in energy use and the corresponding GHG emissions.

This thesis discusses the development of a generic solar house model in detail. The model was carefully designed to maximize flexibility, simplicity, accuracy, and performance. It includes both passive and active solar components. Many studies were performed to determine the appropriate level of model resolution for the model's subsystems and characteristics, including, but not limited to: windows, interzonal airflow and thermal zoning, thermal mass, shading, infiltration, and BIPV. The two active solar models included in the model are photovoltaic and solar domestic hot water systems.

The model was parameterized such that any of the house designs can be described by 36 parameters. These can be categorized as design and non-design, continuous and discrete. Non-design parameters are those that are normally fixed very early in design because they either describe the service that the house provides (e.g., floor area and number of storeys) or cannot be easily controlled by the designer (e.g., temperature setpoints and infiltration). Design parameters are those that can usually be modified somewhat freely to affect energy performance. Discrete parameters are those that can

accept a finite number of values (e.g., glazing types and number of storeys). Continuous parameters are those that can be set to any value within a range. Where possible, parameters were classified as continuous since this puts less constraint on design.

Many conventional design procedures involve the study and optimization of one design parameter at a time because this reduces the design problem into smaller manageable problems and simplifies analysis. However, there are many instances where this is inappropriate. This thesis carefully examines and quantifies parameter interactions to determine where such decoupling is and is not appropriate. Furthermore, methods for visualizing these interactions were presented. Similarly, certain house subsystems can and cannot be easily decoupled. This thesis identifies these. This information is not limited to informing the designer, but is also manifested in Ecos and underlying model.

With the model and design tool implemented, the next chapter described a design methodology. Using Ecos, a generalized design procedure is proposed. Key elements of it are to start with passive features (insulation, windows, mass) and proceed towards more advanced active features. Furthermore, robust, passive measures are favoured over non-robust, active ones. Throughout the procedure, there are references to the feedback mechanisms in the tool that are most appropriate for any particular aspect of design.

The model is compared to the performance of an occupied and monitored house: ÉcoTerra. It is a near net-zero energy house that features many of the technologies and



aspects contained in the generic model. With the integrated ÉcoTerra house model, various potential design upgrades were examined to determine any possible design improvements. A major conclusion for this study as well as any low-energy houses is that heating and cooling become less significant than plug loads. Beyond good daylighting design, and selecting high-efficiency electric lights and appliances, there is little a designer can do to influence occupant behaviour. Furthermore, often times, the design does not have control over appliance selection – particularly after the original appliances gets replaced. Finally, Jevons' paradox suggests that homeowners may compensate for low total energy costs by being more wasteful for the sake of increasing their comfort. These human factors are not studied beyond anecdotal evidence in this thesis, but are certainly worth exploring.

## 9.1 Major Contributions

The major elements of this research were a generic solar house model, a design tool that includes new methods for performance visualization, a design procedure for solar houses, and application of the model to an existing low-energy solar house. The major contributions of this research are:

1. A **generic solar house model** that uses a balanced approach to maximize flexibility, simplicity, accuracy, and performance. The model includes many passive and active solar elements. Care was taken to select the appropriate level of model resolution and complexity to ensure model accuracy.

2. **A method for quantifying the significance of parameter interactions.** Much of the literature suggests that design be performed by examining just one parameter at a time. However, the current research suggests that this is inappropriate for many pairs of parameters. Equally important, this work demonstrates a method for visualizing and presenting interactions to designers. This element of the research is extended to the interactions between subsystems; though in a qualitative manner.
3. **A prototype solar house design tool – Ecos** - for early stage design that offers the following features:
  - An accurate underlying parameterized model for solar houses, as mentioned above.
  - Five novel methods for visualizing performance or trends over parameter settings, including solar design days, lines of influence, wheels of interactions, multi-parameter decision support charts, and a design management system.
  - Quasi real-time feedback about performance. This is achieved using a combination of the decoupling of models, simplified models, multivariate regression, and trained artificial neural networks.
  - A carefully-constructed graphical user interface that allows single-screen input and output. The inputs user interface controls were selected to be useful in allowing exploratory design.

- The ability to use the house model beyond Ecos by exporting it and modifying in any of the many available EnergyPlus interface tools.
4. A **systematic design procedure** for achieving near-optimal design that is supported by Ecos. The procedure offers three potential paths including: solar design day, parametric, or a hybrid of the two. Furthermore, strategies are ranked by ease of design and implementation, such that the robust and passive measures are implemented first and the non-robust active measures are implemented last. No extensive and complete passive solar house procedure was found in the literature.
  5. **Application** of a solar house model to a case study of an EQUilibrium demonstration house (ÉcoTerra).

## 9.2 Future work

During this research, a number of topics for future work were identified as being valuable, but beyond the current scope. They are listed as follows.

- Occupant behaviour is arguably the single greatest challenge to building energy researchers and modellers. While mathematical and physical models continue to increase to high levels of accuracy, there continues to a lot of uncertainty about how building occupants behave to affect building energy use, despite the fact that lighting and plug loads are beginning to dominate over envelope-based loads. While this has frequently been true in commercial buildings, it is

becoming more significant in high-performance houses. This research clearly identified the importance of occupant-based loads; not only because they affect the total energy use but because in a highly-insulated, well-sealed house, the associated internal gains are well-contained and can lead to overheating. Being able to predict internal gains while designing a house is important. Future work should attempt to build a statistical model that provides useful uncertainty with regards to occupant-based loads. The model should be based on the parameters that a design has control over and not the usual model inputs such as number of adults, since this is unknown in early stage design.

- The current work examined the concept of parameter interactions more deeply than any literature on the topic that was found. However, it would be worthwhile to examine three-way and higher-order interactions. Similarly, methods for visualizing these (which are challenging because computer monitors are limited to two dimensions) would be valuable.
- Inclusion of cost data in modelling capabilities. Construction cost is an unfortunate, but necessarily aspect of low-energy/solar house design. As the tool stands now, a completely naïve user might conclude that excessive PV is a far more effective that good passive solar design as means to meet the design goals. However, this is generally accepted as being considerably less cost effective. Therefore, the inclusion of estimated costs would be a valuable addition to the Ecos; however, this is not trivial. Material and labour costs are

known to vary considerably over time and geographically, making them very dynamic. Furthermore, practical issues become ever more important. For instance, Ecos allows any level of wall insulation, where as practical levels of insulation are more discrete (e.g., 6" or double-stud wall).

- Given that the model is fully parameterized, it is ideally suited for optimization. While Ecos is premised on the fact that designers should be in the loop and input unquantifiable house characteristics such as aesthetics and views, it would be convenient to determine how the current design compares to the mathematically-optimal design.
- The current tool is static with regards to location, included technologies and features, etc. However, it would be valuable to have a method for which users could automate many of the features that were manually performed by the current author, including training the artificial neural network.
- A valuable addition to providing an understanding to the design tool user with regards to house performance would be a Sankey diagram showing all energy flows within the house (example shown in Figure 9-1). This is as difficult to understand as it is to implement within the tool. For example, of the total solar heat gains, some are useful (reduced mechanical heating) others are detrimental (increased mechanical heating). And while daylighting instantaneous, quantifying whether solar gains are beneficial or detrimental is not an instantaneous consideration because solar gains are stored and released

into the space later. Existing tools that state the “useful” solar gains may be kidding themselves regarding the simplicity with which this was calculated. Of the items on this list, the current author hypothesizes that this one would be the most difficult to implement.

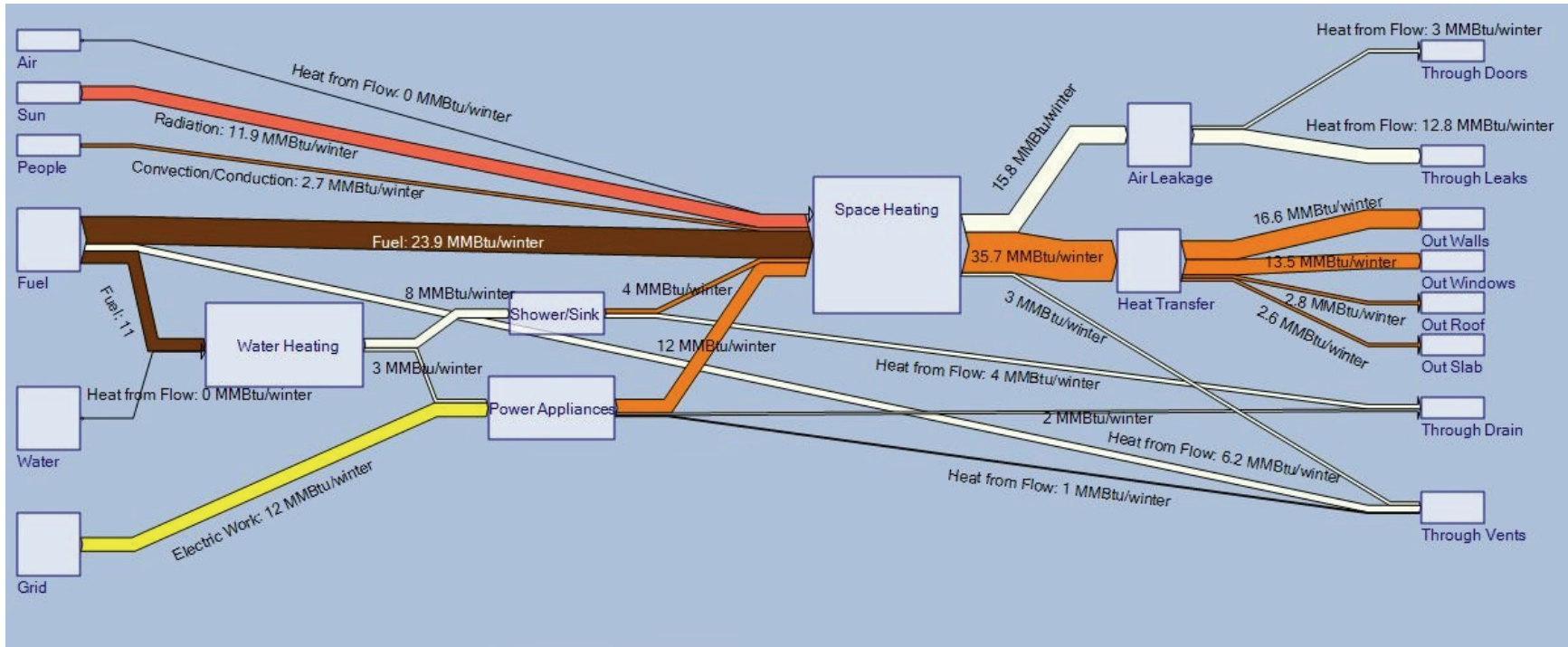


Figure 9-1: Example of Sankey diagram for a house (source:<http://blog.airscapfans.com/wp-content/uploads/2010/08/arron-energy-flow1.jpg>)

- Much the way discretionary loads and embodied energy begin to play a bigger role as heating energy decreases, one must consider the geographical context of the house. O'Brien et al (2010e) demonstrated that the inclusion of transportation energy in the analysis of net energy use actually favours high-density housing, despite the fact that it has lower solar access. Future research and design should put greater emphasis on the impact that the selected building site has on transportation.
- A complex issue arises from the market valuation of solar houses because the solar industry – particularly with regards to buildings – is relatively immature. The average homeowner is likely to sell their house before a typical PV system has reached the end of its life (of about 25 years). Therefore, the homeowner needs to be confident that the investment cost in a PV system will be reflected in the total home's sale price, much the way bathroom and kitchen renovations are valued. Early studies on the topic (e.g., Hoen et al (2011)) have found that most capital costs in PV systems are recovered upon resale and that the premium decreases with the age of the system. However, the houses in the study are too new to provide any data on systems that are approach even half of their expected useful life. Also, the study was performed for California, where the PV market is mature within the North American context.

While it is widely stated by the literature that BIPV achieves the dual purposes of electricity generation and weather protection, thus potentially costing less than the sum



of the two distinct components that achieve these goals, few quantify this benefit. However, the electricity-generating related components dominate the total cost at between 60 (Hagemann, 2004) and 73% (Pagliaro et al., 2010) of the total façade system (which includes: glazing, framing, wiring, etc.). Furthermore, the emphasis is on new construction, but there is a lack of research on replacing BIPV systems (particularly they are often “highly-customized” (Pagliaro et al., 2010) as they approach the end of their useful life. For instance, some questions are: how easily can the old modules be removed? And will products that are compatible with the existing building structure be available?

It is interesting to note that the very fact BIPV is integrated into the house means that moving it would potentially complex and nonsensical since it was custom designed for that particular house. Therefore the original homeowner cannot easily avoid the issue of proper market valuation of BIPV by merely moving it to their next home.

Market evolution towards proper valuation of BIPV at the time of resale will largely occur organically, since the economy is free-market. However, policies can be introduced to home energy performance labeling systems which include the presence of BIPV. Similarly, price premiums for selling PV-generated electricity will increase the valuation of BIPV installations on houses.

## 10 REFERENCES

- Akander, J. (2000). The ORC Method - Effective Modelling of Thermal Performance of Multilayer Building Components. Department of Building Technology. Stockholm, Kungl Tekniska Hogskolan. PhD Thesis: 178.
- Akbari, H., M. Pomerantz and H. Taha (2001). "Cool surfaces and shade trees to reduce energy use and improve air quality in urban areas." *Solar Energy* 70(3): 295-310.
- American Society of Heating Refrigerating and Air Conditioning Engineers (ASHRAE) (2001). Fundamentals: SI Edition. Atlanta, GA, ASHRAE.
- American Society of Heating Refrigeration and Air Conditioning Engineers (ASHRAE) (2001). Fundamentals: SI Edition. Atlanta, GA.
- American Society of Heating Refrigeration and Air Conditioning Engineers (ASHRAE) (2004a). Standard 55 - Thermal environmental conditions for human occupancy. Atlanta, GA.
- American Society of Heating Refrigeration and Air Conditioning Engineers (ASHRAE) (2004b). "ASHRAE Standard, ANSI/ASHRAE Standard 55-2004: thermal environmental conditions for human occupancy."
- American Society of Heating Refrigeration and Air Conditioning Engineers (ASHRAE) (2005). ASHRAE Handbook of Fundamentals:SI Edition. Atlanta, GA.
- Andresen, I. (2008). A multi-criteria decision-making method for solar building design, Norwegian University of Science and Technology, Faculty of Architecture and Fine Art.
- Arasteh, D., S. Selkowitz and J. Wolfe (1989). "The design and testing of a highly insulating glazing system for use with conventional window systems." *Journal of Solar Energy Engineering, Transactions of the ASME* 3.
- Arasteh, D., H. Goudey, J. Huang, C. Kohler and R. Mitchell (2007). Performance Criteria for Residential Zero Energy Windows.
- Architectural Energy Corporation. (2008). "SPOT™: Sensor Position Optimization Tool." from <http://www.archenergy.com/SPOT/>.
- Armstrong, M. M., M. C. Swinton, H. Ribberink, I. Beausoleil-Morrison and J. Millette (2009). "Synthetically derived profiles for representing occupant-driven electric loads in Canadian housing." *Journal of Building Performance Simulation* 2(1): 15-30.
- Athienitis, A. (1985). Application of network methods to thermal analysis of passive solar buildings in the frequency domain. Mechanical Engineering. Waterloo, ON, University of Waterloo. PhD Thesis: 233.
- Athienitis, A. and M. Santamouris (2002). Thermal Analysis and Design of Passive Solar Buildings. London, James & James.
- Athienitis, A., P. Torcellini, et al. (2010). Design, optimization, and modelling issues of net-zero energy solar buildings. EuroSun 2010. Graz, Austria, Sept. 28 - Oct. 1, 2010.
- Athienitis, A. K. and F. Haghghat (1992). Study of the effects of solar radiation on the indoor environment. ASHRAE Transactions. Atlanta, GA, USA.
- Athienitis, A. K. and Y. Chen (2000). "The effect of solar radiation on dynamic thermal performance of floor heating systems." *Solar Energy* 69(3): 229-237.
- Athienitis, A. K., Kesik T., et al. (2006). Development of requirements for a solar building design tool. 1st SBRN and SESCO 31st Joint Conference, Montreal, Aug. 20-24, 2006.

- Athienitis, A. K. (2007). Design of a Solar Home with BIPV-Thermal System and Ground Source Heat Pump. 2nd SBRN and SESCO 32nd Joint Conference, Calgary, AB.
- Augenbroe, G. (2002). "Trends in building simulation." *Building and Environment* 37(8-9): 891-902.
- Balcomb, J. D. (1992). *Passive solar buildings*. Cambridge, MA, The MIT Press.
- Bazjanac, V. (2004). "Building energy performance simulation as part of interoperable software environments." *Building and Environment* 39(8): 879-883.
- Beasley, D. E. and J. A. Clark (1983). "Transient response of a packed bed for thermal energy storage." *International Journal of Heat and Mass Transfer* 27(9): 1659-1669.
- Beausoleil-Morrison, I. (1996). BASECALC™: A Software Tool for Modelling Residential-Foundation Heat Losses. Third Canadian Conference in Computing in Building and Civil Engineering, Concordia University, Montreal Canada.
- Beausoleil-Morrison, I. and G. Mitalas (1997). BASESIMP: A residential foundation heat-loss algorithm for incorporating into whole-building energy-analysis programs. International Building Performance Simulation Association (IBPSA) Conference, Prague, Czech Republic, Sept. 8-10, 1997.
- Belhe, U. and A. Kusiak (1996). "The house of quality in a design process." *International journal of production research* 34(8): 2119-2132.
- Besant, R. W., R. S. Dumont and G. Schoenau (1979). "The Saskatchewan conservation house: Some preliminary performance results." *Energy and Buildings* 2(2): 163-174.
- Boer, K. W. (1974). Solar one - The Delaware solar house and results obtained during the first year of operation. Photovoltaic power generation: Proceedings of the International Conference,, Hamburg, Germany.
- Canada Mortgage and Housing Corporation (CMHC) (1998). Tap the Sun passive solar techniques and home designs, CHMC.
- Canada Mortgage and Housing Corporation (CMHC) (2002) "Sustainable community planning and development: design charrette planning guide." DOI:
- Canada Mortgage and Housing Corporation (CMHC). (2009). "The EQUilibrium™ Sustainable Housing Demonstration Initiative." Retrieved October 17, 2009, from [http://www.cmhc.ca/en/inpr/su/eqho/eqho\\_008.cfm](http://www.cmhc.ca/en/inpr/su/eqho/eqho_008.cfm).
- Canada Mortgage and Housing Corporation (CMHC). (2010). "EQUilibrium™: Healthy Housing for a Healthy Environment." Retrieved June 13, 2010, from [http://www.cmhc-schl.gc.ca/en/co/maho/yohoyohe/yohoyohe\\_001.cfm](http://www.cmhc-schl.gc.ca/en/co/maho/yohoyohe/yohoyohe_001.cfm).
- Candanedo, L. M., W. O'Brien and A. K. Athienitis (2009). Development of an air-based open loop building-integrated photovoltaic/thermal system model. Proceedings of the eleventh international IBPSA Conference, Glasgow, Scotland, July 27-30, 2009.
- CANMET Energy Technology Centre (CETC) (2008). HOT3000, Natural Resources Canada.
- Carmody, J., S. Selkowitz, E. Lee, D. Arasteh and T. Willmert (2004). Window systems for high-performance buildings. New York, WW Norton and Company.
- Charron, R. (2005). A Review of Low and Net-Zero Energy Solar Home Initiatives. NRCan, Natural Resources Canada, Technology and Innovation Program as part of the Climate Change Plan for Canada, CANMET Energy Technology Centre Publication: 1-8.
- Charron, R., A. Athienitis and I. Beausoleil-Morrison (2006a). Tools for the design of zero energy solar homes.

- Charron, R. and A. K. Athienitis (2006b). The use of genetic algorithms for a net-zero energy solar home design optimisation tool. The 23rd Conference on Passive and Low Energy Architecture, Geneva, Switzerland, Sept. 6-8, 2006.
- Charron, R. (2007). Development of a genetic algorithm optimisation tool for the early stage design of low and net-zero energy solar homes. BCEE. Montreal, Concordia University. PhD Thesis: 301.
- Charron, R. (2008) "A review of design processes for low energy solar homes." Open House International 33, 7-16 DOI:
- Charron, R. (2010). EQuilibrium(TM) Demonstrating a Vision for Sustainable Housing in Canada. Presentation to Carleton University.
- Chen, Y., A. K. Athienitis and K. Galal (2010a). "Modeling, design and thermal performance of a BIPV/T system thermally coupled with a ventilated concrete slab in a low energy solar house: Part 1, BIPV/T system and house energy concept." *Solar Energy* 84(11): 1892-1907.
- Chen, Y., K. Galal and A. K. Athienitis (2010b). "Modeling, design and thermal performance of a BIPV/T system thermally coupled with a ventilated concrete slab in a low energy solar house: Part 2, ventilated concrete slab." *Solar Energy* 84(11): 1908-1919.
- Chetty, M., D. Tran and R. Grinter (2008). Getting to green: understanding resource consumption in the home. Proceedings of the 10th international conference on Ubiquitous computing, Seoul, Korea, ACM.
- Chow, T., J. Hand and P. Strachan (2003). "Building-integrated photovoltaic and thermal applications in a subtropical hotel building." *Applied thermal engineering* 23(16): 2035-2049.
- Christensen, C. (2006). BEopt Software for Building Energy Optimization: Features and Capabilities, National Renewable Energy Laboratory.
- Clarke, J. (2001). Energy Simulation in Building Design. Oxford, Butterworth-Heinemann.
- Coley, D. A. and S. Schukat (2002). "Low-energy design: combining computer-based optimisation and human judgment." *Building and Environment* 37(12): 1241-1247.
- Crawley, D. B., J. W. Hand and L. K. Lawrie (1999). Improving the weather information available to simulation programs. *Building Simulation '99*, Kyoto, Japan.
- Crawley, D. B., J. W. Hand, M. Kummert and B. T. Griffith (2008). "Contrasting the capabilities of building energy performance simulation programs." *Building and Environment* 43(4): 661-673.
- Day4 Energy. (2010). "48MC Premium Photovoltaic Modules." Retrieved March 23, 2010, from <http://www.day4energy.com/downloads/Day4-48MC-Specs-051309-EN.pdf>.
- De Meulenaer, V., J. Van der Veken, G. Verbeeck and H. Hens (2005). Comparison of measurements and simulations of a passive house. 9th International Building Performance Simulation Association Conference, Montreal, QC.
- delVall, V., D. Bessette, L. Sopkow, J. Zhou and K. Szymocha (2007). Long-term performance of the phase change materials applied for heat storage. 2nd SBRN and SESCO 32nd Joint Conference, Calgary, Alberta.
- Déqué, F., F. Ollivier and J. J. Roux (2001). "Effect of 2D modelling of thermal bridges on the energy performance of buildings: Numerical application on the Matisse apartment." *Energy and Buildings* 33(6): 583-587.

- Deru, M. and P. Torcellini (2007). "Source energy and emission factors for energy use in buildings." Battelle: National Renewable Energy Laboratory, US Department of Energy.
- Doiron, M., W. O'Brien and A. Athienitis (2011). "Energy Performance, Comfort and Lessons Learned From a Near Net-Zero Energy Solar House." ASHRAE Transactions( Accepted).
- Duffie, J. A. and W. A. Beckman (2006). Solar Engineering of Thermal Processes, Wiley.
- Dumont, R. (2005). Experiences from Low Energy Houses in Canada, Saskatchewan Research Council.
- Elliott, J. F. (1960). "Home generation of power by photovoltaic conversion of solar energy." Journal of Electrical Engineering 79(9).
- Ellis, M. W. and E. H. Mathews (2001). "A new simplified thermal design tool for architects." Building and Environment 36(9): 1009-1021.
- Ellis, M. W. and E. H. Mathews (2002). "Needs and trends in building and HVAC system design tools." Building and Environment 37(5): 461-470.
- Ellis, P. G., P. A. Torcellini and D. B. Crawley (2008). Simulation of energy management systems in EnergyPlus, National Renewable Energy Laboratory.
- Energy Systems Research Unit (ESRU). (2007). "ESP-r." Retrieved September 15, 2009, from <http://www.esru.strath.ac.uk/Programs/ESP-r.htm>.
- EnergyPlus (2009a). EnergyPlus Input/Output Reference.
- EnergyPlus (2009b). EnergyPlus Engineering Reference.
- Evans, D. L. (1981). "Simplified Method for Predicting Photovoltaic Array Output." Solar Energy 27(6): 555-560.
- Fang, X. d. (2000). "A Study of the U-Factor of the Window with a High-Reflectivity Venetian Blind." Solar Energy 68(2): 207-214.
- Fernández-González, A. (2007). "Analysis of the thermal performance and comfort conditions produced by five different passive solar heating strategies in the United States Midwest." Solar Energy 81(5): 581-593.
- Foster, M. and T. Oreszczyn (2001). "Occupant control of passive systems: the use of Venetian blinds." Building and Environment 36(2): 149-155.
- Fraisse, G., K. Johannes, V. Trillat-Berdal and G. Achard (2006). "The use of a heavy internal wall with a ventilated air gap to store solar energy and improve summer comfort in timber frame houses." Energy and Buildings 38(4): 293-302.
- Frei, U. (2003). Solar thermal Collectors, state of the art and further development. ISES Solar World Congress 2003, Gothenburg, Sweden.
- Galloway, T. (2004). Solar House: A Guide for the Solar Designer, Architectural Press.
- Givoni, B. (1991). "Characteristics, design implications, and applicability of passive solar heating systems for buildings." Solar Energy 47(6): 425-435.
- Goetzberger, A., C. Hebling and H. W. Schock (2003). "Photovoltaic materials, history, status and outlook." Materials Science & Engineering R 40(1): 1-46.
- Graupe, D. (2007). Principles of artificial neural networks. Singapore, World Scientific Pub Co Inc.
- Grossman, M. C. (1948). "Occupants of unusual house to be warmed by Sun's heat." Retrieved December 12, 2008, from [http://tech.mit.edu/archives/VOL\\_068/TECH\\_V068\\_S0172\\_P001.pdf](http://tech.mit.edu/archives/VOL_068/TECH_V068_S0172_P001.pdf).
- GSES (2004). Planning and Installing Photovoltaic Systems. London, James & James\Earthscan Publications Ltd.
- GSES (2005). Planning and installing solar thermal systems. London, Earthscan Publications Ltd.

- Hadorn, J.-C., T. Letz and M. Haller (2007) "Method and comparison of advanced storage concepts." Report 4A of Subtask A, IEA Task 32: Advanced storage concepts for solar and low energy buildings, DOI:
- Hagemann, I. B. (2004). "Examples of successful architectural integration of PV: Germany." *Progress in Photovoltaics: Research and Applications* 12(6): 461-470.
- Haltrecht, D., R. Zmeureanu and I. Beausoleil-Morrison (1999). Defining the methodology for the next-generation HOT2000 simulator. Defining the methodology for the next-generation HOT2000 simulator, Defining the methodology for the next-generation HOT2000 simulator.
- Hastings, S. R. (1995). "Myths in passive solar design." *Solar Energy* 55(6): 445-451.
- Hayter, S. J., P. A. Torcellini, R. B. Hayter and R. Judkoff (2001). The energy design process for designing and constructing high-performance buildings. CLIMA 2000. Naples, Italy.
- Henninger, R. H., M. J. Witte and D. B. Crawley (2004). "Analytical and comparative testing of EnergyPlus using IEA HVAC BESTEST E100-E200 test suite." *Energy and Buildings* 36(8): 855-863.
- Hestnes, A., R. Hastings and B. Saxhof (2003). Solar energy houses: strategies, technologies, examples. London, Earthscan/James & James.
- Hoen, B., R. Wiser, P. Cappers and M. Thayer (2011). An Analysis of the Effects of Residential Photovoltaic Energy Systems on Home Sales Prices in California Berkeley, Ca., Lawrence Berkeley National Laboratory.
- Hong, T., S. K. Chou and T. Y. Bong (2000). "Building simulation: an overview of developments and information sources." *Building and Environment* 35(4): 347-361.
- Hottel, H. C. and B. B. Woertz (1942). "The performance of flat-plate solar-heat collectors." *Trans. ASME* 64: 91-104.
- Hottel, H. C. and A. Whillier (1953). "Solar energy collection and its utilization for house heating."
- Hottel, H. C. and A. Whillier (1958). Evaluation of flat-plate solar heat collectors. Conference on the Use of Solar Energy, Tuscon, Arizona.
- Hui, S. C. M. (1998). "Simulation Based Design Tools for Energy Efficient Buildings in Hong Kong".
- Huizenga, C., D. Arasteh, E. Finlayson, R. Mitchell, B. Griffith, C. Kohler and D. Curcija (1999). Therm 2.0: a building component model for steady-state two-dimensional heat transfer.
- Hutcheon, N. B. and G. O. P. Handegord (1995). Building Science for a Cold Climate. Canada, Institute for Research in Construction.
- IEA-SHC Task 23 (2002). Solar low energy buildings and the integrated design process: an introduction.
- IEA SHC Task 40 - ECBCS Annex 52. (2009). "SHC Task 40 - ECBCS Annex 52: Subtasks." Retrieved April 21, 2009, 2009, from <http://www.iea-shc.org/task40/subtask/index.html>.
- Johnson, T. E. (1977). "Lightweight thermal storage for solar heated buildings." *Solar Energy* 19(6): 669-675.
- K. A. Antonopoulos, E. P. K. (2000). "Effect of indoor mass on the time constant and thermal delay of buildings." *International Journal of Energy Research* 24(5): 391-402.
- Kalogirou, S. A. and M. Bojic (2000). "Artificial neural networks for the prediction of the energy consumption of a passive solar building." *Energy* 25(5): 479-491.

- Keoleian, G. A., S. Blanchard and P. Reppe (2000). "Life-cycle energy, costs, and strategies for improving a single-family house." *Journal of Industrial Ecology* 4(2): 135-156.
- Keoleian, G. A. and G. M. D. Lewis (2003). "Modeling the life cycle energy and environmental performance of amorphous silicon BIPV roofing in the US." *Renewable Energy* 28(2): 271-293.
- Kesik, T. and M. Simpson (2002). Thermal performance of attached sunspaces for Canadian houses. eSim, Montreal, QC.
- Kesik, T. and L. Stern (2008). Representation of Performance Indicators for the Conceptual Design of Passive Solar Houses. eSim 2008, The 5th IBPSA-Canada Conference, Quebec City, QC, May 23-25, 2008.
- Kikuchi, E., D. Bristow and C. A. Kennedy (2009). "Evaluation of region-specific residential energy systems for GHG reductions: Case studies in Canadian cities." *Energy Policy* 37(4): 1257-1266.
- La Roche, P. and M. Milne (2004). Automatic Sun Shades, an Experimental Study. American Solar Energy Society 2004, Portland, OR.
- Lawrence Berkeley National Laboratory (LBNL) (2010). Window 6.3 Software. Berkeley, CA.
- Lee, E. S., D. L. DiBartolomeo and S. E. Selkowitz (1998). "Thermal and daylighting performance of an automated venetian blind and lighting system in a full-scale private office." *Energy and buildings* 29(1): 47-63.
- Lomas, K. J. and H. Eppel (1992). "Sensitivity Analysis Techniques for Building Thermal Simulation Programs." *Energy and Buildings* 19(1): 21-44.
- Magnier, L. (2009). Multiobjective optimization of building design using artificial neural network and multiobjective evolutionary algorithms. *BCEE*. Montreal, Concordia University. MASC Thesis: 138.
- Magnier, L. and F. Haghghat (2010). "Multiobjective optimization of building design using TRNSYS simulations, genetic algorithm, and Artificial Neural Network." *Building and Environment* 45(3): 739-746.
- Mason, R., R. Gunst and J. Hess (2003). Statistical design and analysis of experiments: with applications to engineering and science, Wiley-Interscience.
- Massachusetts Institute of Technology (MIT). (2008). "MIT Solar Decathlon Team: History." Retrieved December 12, 2008, from <http://web.mit.edu/solardecathlon/solar1.html>.
- Massachusetts Institute of Technology (MIT). (2008). "MIT Solar Decathlon Team: History." Retrieved December 12, 2008, 2008, from <http://web.mit.edu/solardecathlon/solar1.html>.
- Mathworks Inc. (2008). MATLAB 2008a. Natick, MA.
- Matthiessen, L. F. and P. Morris (2004). Costing green: A comprehensive cost database and budgeting methodology. *Davis Langdon*.
- McKinsey and Company (2007). Reducing US Greenhouse Gas Emissions: How Much at What Cost?, McKinsey and Company.
- Mitchell, R., C. Kohler, D. Arasteh, J. Carmody, C. Huizenga and D. Curcija (2003). THERM 5/WINDOW 5 NFRC simulation manual, LBNL--48255, Ernest Orlando Lawrence Berkeley National Laboratory, Berkeley, CA (US).
- Mottard, J.-M. and A. Fissore (2007). "Thermal simulation of an attached sunspace and its experimental validation." *Solar Energy* 81(3): 305-315.
- National Renewable Energy Laboratory (NREL) (2009). BEopt. Golden, Colorado.



- Natural Resources Canada (NRCan) (2006). Survey of household energy use (SHEU) - detailed statistical report. Office of Energy Efficiency (OEE). Halifax, Nova Scotia, Canada.
- Natural Resources Canada (NRCan) (2008a) "About R-2000." DOI:
- Natural Resources Canada (NRCan) (2008b). Energy use data handbook tables (Canada). Office of Energy Efficiency (OEE).
- Natural Resources Canada (NRCan) (2009). HOT3000: Release Candidate, NRCan. 2009.
- Natural Resources Canada (NRCan). (2010a, July 14, 2010). "Thermostats for Heat Pumps." Retrieved July 18, 2010, 2010, from <http://oee.nrcan.gc.ca/residential/personal/thermostats-controls.cfm?attr=4#zoneControl>.
- Natural Resources Canada (NRCan). (2010b). "Energy Use." Retrieved December 6, 2010, from <http://www.nrcan.gc.ca/eneene/effeff/resuse-eng.php>.
- Natural Resources Canada (NRCan) (2010c). HOT2000. Ottawa, Canada.
- Natural Resources Canada (NRCan): Office of Energy Efficiency (OEE). (2009a). "How a heat recovery ventilator works." Retrieved April 5, 2009, 2009, from <http://oee.nrcan.gc.ca/residential/personal/new-homes/r-2000/standard/how-hrv-works.cfm?attr=4>.
- Natural Resources Canada (NRCan): Office of Energy Efficiency (OEE). (2009b). "Water heaters: energy considerations." Retrieved April 11, 2009, 2009, from <http://oee.nrcan.gc.ca/residential/personal/water-heater-oil-electric.cfm?attr=4>.
- Natural Resources Canada (NRCan): Office of Energy Efficiency (OEE) (2010a). House Energy Audit Database.
- Natural Resources Canada (NRCan): Office of Energy Efficiency (OEE). (2010b). "Heating Equipment and Controls." Retrieved December 5, 2010, from <http://oee.nrcan.gc.ca/residential/personal/heating.cfm?attr=4>.
- Nicol, J. F. and M. A. Humphreys (2002). "Adaptive thermal comfort and sustainable thermal standards for buildings." *Energy & Buildings* 34(6): 563-572.
- Noguchi, M., A. Athienitis, V. Delisle, J. Ayoub and B. Berneche (2008). Net Zero Energy Homes of the Future: A Case Study of the ÉcoTerra. *Renewable Energy Congress*. Glasgow, Scotland.
- O'Brien, W., A. Athienitis and T. Kesik (2008a). Sensitivity Analysis for a Passive Solar House Energy Model. International Solar Energy Society - Asia Pacific (ISES-AP) Conference Sydney, Australia, Nov. 25-27, 2008.
- O'Brien, W., T. Kesik and A. Athienitis (2008b). The use of solar design days in a passive solar house conceptual design tool. 3rd Canadian Solar Buildings Conference, Fredericton, NB, Aug. 20-22, 2008.
- O'Brien, W., A. Athienitis and T. Kesik (2009a). Methodology and development of a solar house design tool. 4th Canadian Solar Buildings Conference, Toronto, ON, June 25-27.
- O'Brien, W., A. Athienitis and T. Kesik (2009b). Roofs as extended solar collectors: practical issues and design methodology. 12th Canadian Conference on Building Science and Technology, Montreal, QC, May 6-8, 2009.
- O'Brien, W., A. Athienitis and T. Kesik (2009c). The development of solar house design tool. 11th International Building Performance Simulation Association (IBPSA) Conference Glasgow, Scotland, July 27-30, 2009.



- O'Brien, W., C. Kennedy, A. Athienitis and T. Kesik (2009d). "The relationship between personal net energy use and the urban density of solar buildings." *Environment and Planning: B*.
- O'Brien, W., A. Athienitis, S. Bucking, M. Doiron and T. Kesik (2010a). A study of design tools and processes through a near net-zero energy house redesign. EuroSun 2010, Graz, Austria.
- O'Brien, W., A. Athienitis and T. Kesik (2010b). "Thermal zoning and interzonal airflow in design of solar houses: a sensitivity analysis." *Journal of Building Performance Simulation* (in press).
- O'Brien, W., A. K. Athienitis, S. Bucking and T. Kesik (2010c). Applying a design methodology for a net-zero energy house to evaluate design processes and tools. EuroSun 2010, Graz, Austria.
- O'Brien, W., K. Kapsis, A. K. Athienitis and T. Kesik (2010d). Methodology for quantifying the performance implications of intelligent shade control in existing buildings in an urban context. *SimBuild 2010*. New York City.
- O'Brien, W., C. Kennedy, A. Athienitis and T. Kesik (2010e). "The relationship between net energy use and the urban density of solar buildings." *Environment and Planning B* 37(6): 1002-1021.
- O'Brien, W., A. Athienitis and T. Kesik (2011a). "Thermal zoning and interzonal airflow in design of solar houses: a sensitivity analysis." *Journal of Building Performance Simulation* (in press).
- O'Brien, W., A. Athienitis and T. Kesik (2011b). "Parametric Analysis to support the integrated design and performance modeling of net-zero energy houses." *ASHRAE Transactions* 117, Part 1.
- Pagliaro, M., R. Ciriminna and G. Palmisano (2010). "BIPV: merging the photovoltaic with the construction industry." *Progress in Photovoltaics: Research and Applications* 18(1): 61-72.
- Parker, D. S. (2009). "Very low energy homes in the United States: Perspectives on performance from measured data." *Energy and Buildings* 41(5): 512-520.
- Pogharian, S., J. Ayoub, J. A. Candanedo and A. K. Athienitis (2008). Getting to a net zero energy lifestyle in Canada: the Alstonvale net zero energy house. 3rd European PV Solar Energy Conference, Valencia, Spain.
- Prazeres, L. and J. A. Clarke (2003). "Communicating building simulation outputs to users." Augenbroe and Hensen, ed. *Building Simulation 3*: 11-14.
- Purdy, J. and I. Beausoleil-Morrison (2001). The Significant Factors in Modeling Residential Buildings. 7th International IBPSA Conference, Rio de Janeiro, Brazil.
- Raeissi, S. and M. Taheri (1998). "Optimum overhang dimensions for energy saving." *Building and Environment* 33(5): 293-302.
- Reed, W. G. and E. B. Gordon (2000). "Integrated design and building process: what research and methodologies are needed?" *Building Research and Information* 28(5-6): 325-337.
- Reinhart, C. and A. Fitz (2006). "Findings from a survey on the current use of daylight simulations in building design." *Energy and Buildings* 38(7): 824-835.
- Reinhart, C. F. and S. Herkel (2000). An Evaluation of Radiance Based Simulations of Annual Indoor Illuminance Distributions due to Daylight. *Building Simulation 1999*. Kyoto, Japan.
- RETScreen International (2005). *Clean Energy Project Analysis*, Ministry of Natural Resources Canada.

- Robinson, D. and F. Haldi (2008). "Model to predict overheating risk based on an electrical capacitor analogy." *Energy & Buildings* 40(7): 1240-1245.
- Saldanha, N. (2010). Towards the assessment of a residential electric storage system: analysis of Canadian residential electricity use and the development of a lithium-ion battery model. *Mechanical Engineering*. Ottawa, Carleton University. MSc Thesis: 134.
- Sander, D. M., S. A. Barakat, C. National Research Council and R. Division of Building (1985). *Mass & Glass: How Much? how Little?*, National Research Council Canada, Division of Building Research.
- Schnieders, J. (2003). CEPHEUS—measurement results from more than 100 dwelling units in passive houses. *Time to Turn Down Energy Demand, European Council for an Energy Efficient Economy*: 340-351.
- Seryak, J. and K. Kissock (2003). Occupancy and behavioral affects on residential energy use. American Solar Energy Society, Portland, OR.
- Shah, J. J., S. V. Kulkarni and N. Vargas-Hernandez (2000). "Evaluation of Idea Generation Methods for Conceptual Design: Effectiveness Metrics and Design of Experiments." *Journal of Mechanical Design* 122(4): 377-384.
- Sherman, M. H. (1987). "Estimation of infiltration from leakage and climate indicators." *Energy and Buildings* 10(1): 81-86.
- Sibbitt, B., T. Onno, D. McClenahan, J. Thornton, A. Brunger, J. Kokko and B. Wong (2007). The Drake Landing solar community project: early results. 2nd SBRN and SESCO 32nd Joint Conference, Calgary, AB.
- Solar Buildings Research Network (SBRN). (2009). "Prototype solar building design synthesis and optimization tool." Retrieved April 21, 2009, 2009, from [http://www.solarbuildings.ca/en/s\\_projects\\_15](http://www.solarbuildings.ca/en/s_projects_15).
- Solar Rating and Certification Corporation (SRCC). (2009). "Directory of SRCC Certified Solar Collector Ratings."
- Spitler, C. and P. E. D. Xiao (2005). "The Residential Heat Balance Method for Heating and Cooling Load Calculations."
- Streicher, W. (2007). Final report of Subtask C "Phase Change Materials" The overview. I. T.-A. s. c. f. s. a. l. e. buildings".
- Swan, L. G. (2010). Residential Sector Energy and GHG Emissions Model for the Assessment of New Technologies. *Mechanical Engineering*. Halifax. NS, Dalhousie University. PhD Thesis: 312.
- Swan, L. G., I. V. Ugarsal and I. Beausoleil-Morrison (2011). "Occupant related household energy consumption in Canada: Estimation using a bottom-up neural-network technique." *Energy and Buildings* 43(2-3): 326-337.
- Taylor, R., C. Pedersen and L. Lawrie (1990). Simultaneous simulation of buildings and mechanical systems in heat balance based energy analysis programs. 3rd International Conference on System Simulation in Buildings, Liege, Belgium.
- Torcellini, P. A. and D. B. Crawley (2006). "Understanding zero-energy buildings." *ASHRAE Journal* 48(9): 62-69.
- Tyagi, V. V. and D. Buddhi (2007). "PCM thermal storage in buildings: A state of art." *Renewable and Sustainable Energy Reviews* 11(6): 1146-1166.
- Tzempelikos, A. and A. K. Athienitis (2007). "The impact of shading design and control on building cooling and lighting demand." *Solar Energy* 81(3): 369-382.

- U.S. Department of Energy (US DOE) (2009). Getting started with EnergyPlus, Department of Energy.
- U.S. Department of Energy: Energy Efficiency and Renewable Energy (EERE). (2008). "Milestone buildings of the 20th century." Retrieved December 12, 2008, from <http://www.artistsdomain.com/dev/eere/web/1940.html>.
- U.S. Department of Energy: Energy Efficiency and Renewable Energy (EERE). (2009). "Air Barriers." Retrieved April 10, 2009, from [http://www.energysavers.gov/your\\_home/insulation\\_airsealing/index.cfm/mytopic=11300](http://www.energysavers.gov/your_home/insulation_airsealing/index.cfm/mytopic=11300).
- Ulrich, K. T. and S. D. Eppinger (1995). Product design and development, McGraw-Hill New York.
- Wall, M. (2006). "Energy-efficient terrace houses in Sweden: Simulations and measurements." *Energy and Buildings* 38(6): 627-634.
- Wang, W., R. Zmeureanu and H. Rivard (2005). "Applying multi-objective genetic algorithms in green building design optimization." *Building and Environment* 40(11): 1512-1525.
- Wang, W., I. Beausoleil-Morrison and J. Reardon (2009). "Evaluation of the Alberta air infiltration model using measurements and inter-model comparisons." *Building and Environment* 44(2): 309-318.
- Warren, P. (1996). Summary of IEA Annex 23 - Multizone Airflow Modelling (COMIS).
- Weiss, W. W. (2003). Solar heating systems for houses: a design handbook for solar combisystems, Earthscan.
- Wetter, M. (2001). GenOpt<sup>®</sup>, "Generic Optimization Program. Building Simulation 2001 Conference, Rio de Janeiro, Brazil.
- Wetter, M. and P. Haves (2008). A Modular Building Controls Virtual Test Bed for the Integrations of Heterogenous Systems. SimBuild 2008. San Francisco, CA.
- Winkelmann, F. C. (2001). Modeling windows in EnergyPlus. Seventh Building Simulation Conference. Rio de Janeiro, Brazil.
- Wittwer, V., C. G. Granqvist and C. Lampert (1994). Optical materials technology for energy efficiency and solar energy conversion XIII. The International Society for Optical Engineering.
- Wright, J. A., H. A. Loosemore and R. Farmani (2002). "Optimization of building thermal design and control by multi-criterion genetic algorithm." *Energy and Buildings* 34(9): 959-972.
- Xu, X., Y. Zhang, K. Lin, H. Di and R. Yang (2005). "Modeling and simulation on the thermal performance of shape-stabilized phase change material floor used in passive solar buildings." *Energy and Buildings* 37(10): 1084-1091.
- York, R. (2006). "Ecological Paradoxes: William Stanley Jevons and the Paperless Office." *Human Ecology Review* 13(2): 143.
- Zhang, D., A. Fung and O. Siddique (2008). Finite element modeling for integrated solid-solid PCM-building material with varying phase change temperatures. 3rd SBRN and SESCI 33rd Joint Conference, Fredericton, NB.
- Zmeureanu, R., P. Fazio, S. DePani and R. Calla (1999). "Development of an energy rating system for existing houses." *Energy and Buildings* 29(2): 107-119.

## Appendix A: Software Tool Survey

The software programs in this survey were selected for being notable. They are either leaders or have some aspects that are particularly suitable for low-energy design and integrated design. These represent a small fraction of all software tools that are available. They are:

1. BEopt
2. ECOTECT
3. Energy-10
4. EnergyPlus
5. ESP-r
6. Green Building Studio (based on DOE-2.1)
7. HEED
8. HOT3000
9. IES-VE
10. MIT Design Advisor
11. TRNSYS
12. DesignBuilder
13. RETScreen

### Summary Chart

The following chart shows how each program fits into the design process. The diagonal line represents the average modeling time for each design stage. While being somewhat subjective, the goal of the chart is to give a sense of the state of available programs on a relative basis.

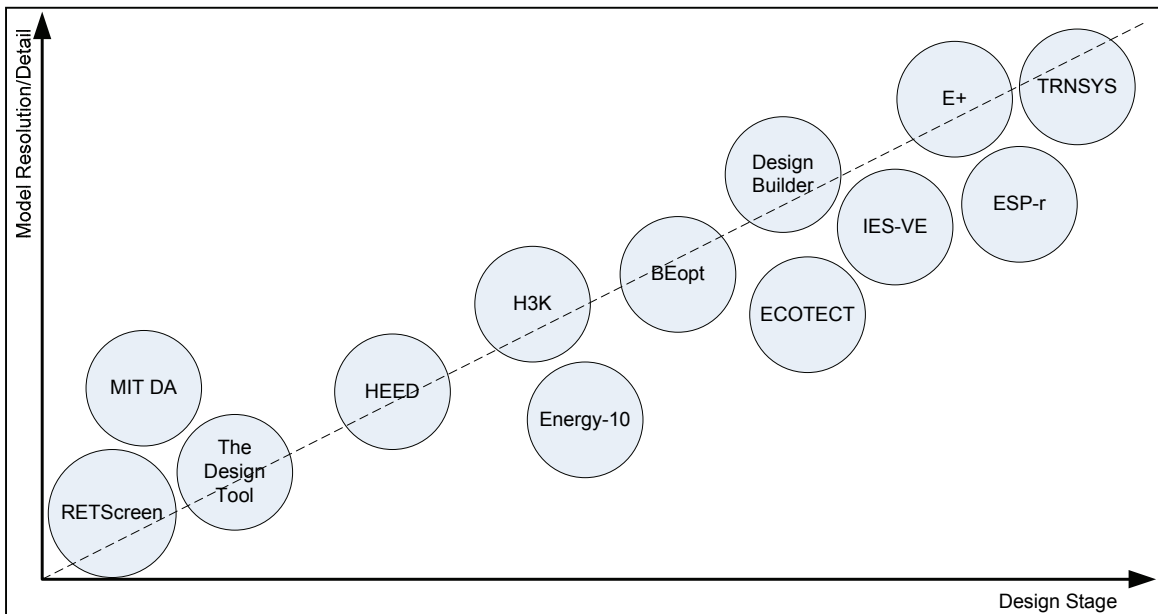


Figure 10-1: The evaluated tools in the resolution-design stage space

Each of the tables below contain a summary of the tool, the applicability to low-energy or net-zero energy building design, and an input and output screenshot.

<b>BEopt</b> ( <a href="http://www.ecotect.com/">http://www.ecotect.com/</a> )	
<b>Summary</b> BEopt is an optimization tool for net-zero energy single detached houses. The user is prompted to input a large number of constraints (if desired), at which point BEopt performs a sequential search to determine the economically optimal set of house designs for any house between the base case and net-zero energy. BEopt interfaces with several different simulation engines. There is a design option within the program, although it offers little guidance to the designer.	
<b>Simulation</b> DOE-2.1 & TRNSYS (eventually, EnergyPlus)	
<b>Key Features/Benefits</b>	
<ul style="list-style-type: none"> <li>• Simple to use</li> <li>• Nifty geometry input interface</li> <li>• Great visualization of the design space (the “BEopt Swish”)</li> <li>• Uses smart sequential search, rather than the evolutionary optimization algorithms that are more common in recent literature</li> </ul>	Design Stage
<b>Limitations</b>	
<ul style="list-style-type: none"> <li>• Optimization can take 4-6 hours (for a population of about 1000 simulations)</li> <li>• There is no practical coupling between the house and the PV. So, for example, the PV array is not limited to the size of the roof. Also, it’s not modelled as building-integrated.</li> </ul>	
<b>Applicability to NZEH</b> In essence, BEopt was created with the intention of designing net-zero energy houses, which makes it unique among the tools in this survey. It can be used to find the optimal mix of energy efficiency measures and energy collectors.	

BEOpt - Building Energy Optimization Tool - prototype-2005-02-18a

File View Case Run Tools Help

Estimated Run Time: 1h 34m  
Estimated Simulations: 1,040

**Building**

- Orientation: 4 3 2 1
- Neighbors: 4 3 2 1
- Total Window Area: 3 2 1

**Envelope**

- Walls: 5 4 3 2 1
- Ceiling: 4 3 2 1
- Foundation: 15 14 13 12 11 10 9 8 7 6 5 4 3 2 1
- Thermal Mass: 4 3 2 1
- Infiltration: 2 1

**Windows & Shading**

- Glass Type: 5 4 3 2 1
- Window Area per Wall: 2 1
- Eaves: 4 3 2 1

**Appliances & Lighting**

- Refrigerator: 2 1
- Dishwasher: 3 2 1
- Clothes Dryer: 2 1
- Clothes Washer: 3 2 1
- Lighting: 4 3 2 1

**Equipment**

- HVAC: 18 17 16 15 14 13 12 11 10 9 8 7 6 5 4 3 2 1
- Water Heater: 6 5 4 3 2 1
- Ducts: 3 2 1

**Renewables**

- Solar DHW: 4 3 2 1

**Include Combinations**

- Glass+Mass: +3

**Exclude Combinations**

**Glass Type**

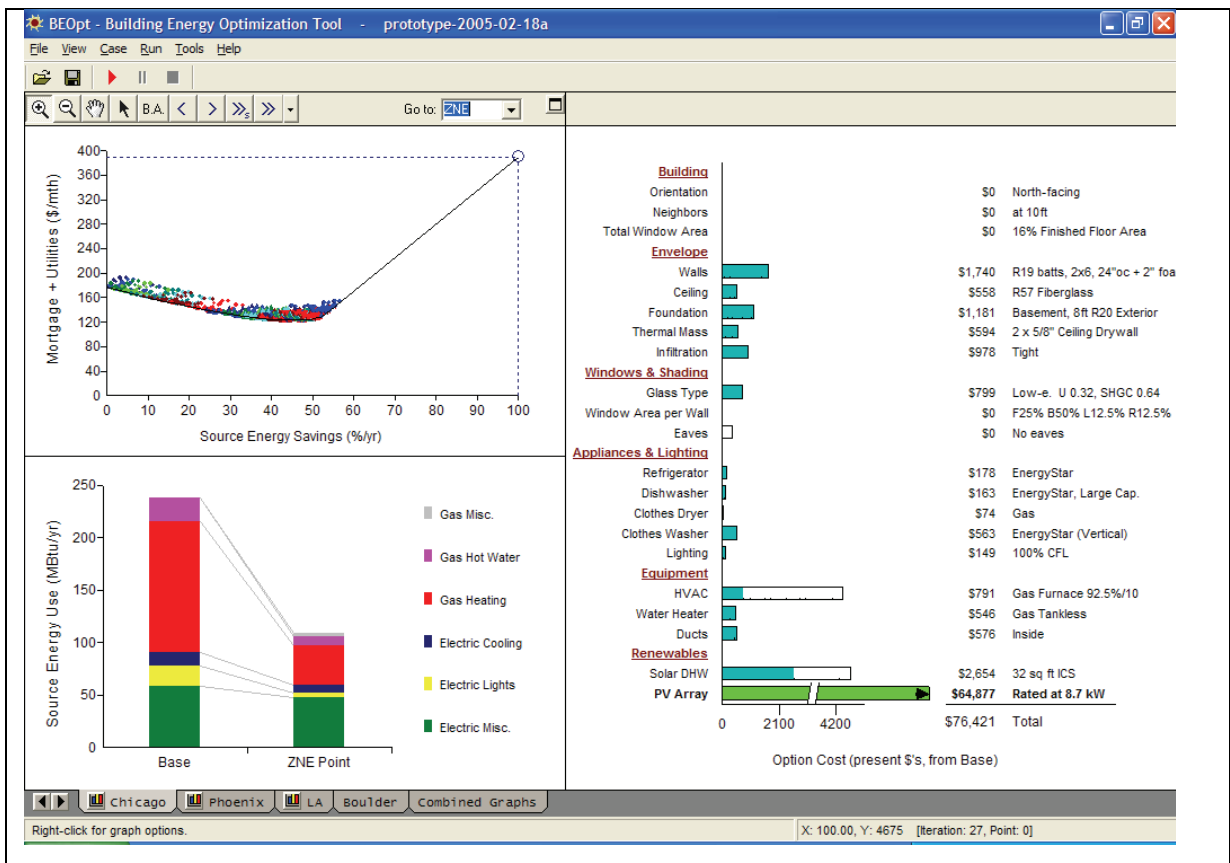
Options: (Select to include in optimization)

Options: (Select to include in optimization)	Unit Cost (\$/sq ft)	Multiplier (sq ft)	Total First Cost	Lifetime (years)	Present Value	Base
Clear. U 0.49, SHGC 0.76	\$21.99	288	\$6,334	30	\$6,334	<input checked="" type="radio"/>
Low-e. U 0.31, SHGC 0.37	\$24.77	288	\$7,133	30	\$7,133	<input type="radio"/>
Low-e. U 0.32, SHGC 0.64	\$24.77	288	\$7,133	30	\$7,133	<input type="radio"/>
Low-e. U 0.30, SHGC 0.44	\$24.77	288	\$7,133	30	\$7,133	<input type="radio"/>
Low-e. U 0.29, SHGC 0.29	\$24.77	288	\$7,133	30	\$7,133	<input type="radio"/>

Category Links: Total Window Area | 16% Finished Floor Area

Category Options

Chicago Phoenix LA Boulder Combined Graphs



## ECOTECT (<http://www.ecotect.com/>)

**Summary** ECOTECT claims to be the first building energy simulation tool that was designed by architects. It uses an AutoCAD-like input for building geometry and specifications. It enables solar, thermal, lighting, acoustic, and cost analyses. ECOTECT is intended to be used for conceptual to detailed design, though its models can be exported to all of the industry-leading simulation engines, such as RADIANCE, ESP-r, and EnergyPlus. ECOTECT's graphical output is among the best in the field. It is particularly useful for visualizing daylighting and solar radiation.

**Simulation engine/calculation method** DOE-2.2

### Key Features/Benefits

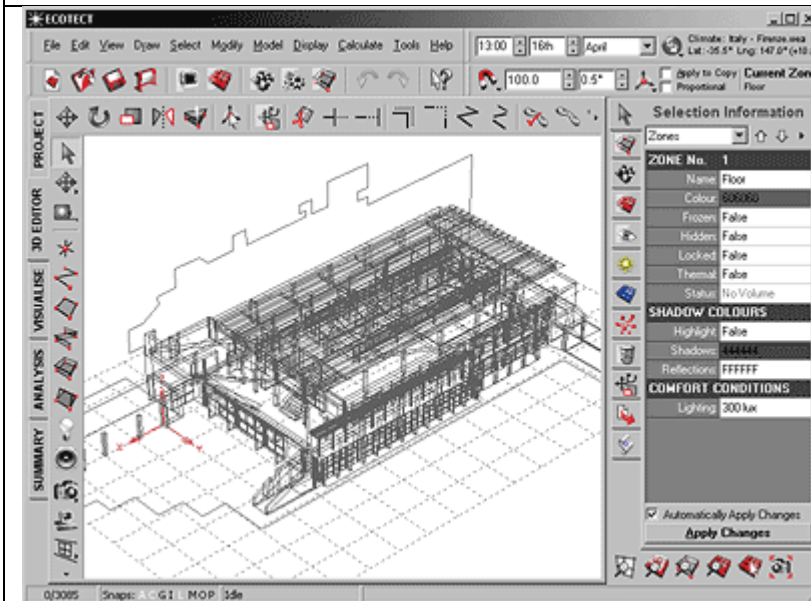
- Industry-leading visualization of daylighting, solar geometry, and shading, that allows the metric of interest to be directly mapped to the surface.
- It is at encouraging an integrated design process
- Has a moderate number of active solar collector models
- Allows photorealistic rendering and animation
- Excellent shading of external obstructions feature through "Right-to-Light" module

## Limitations

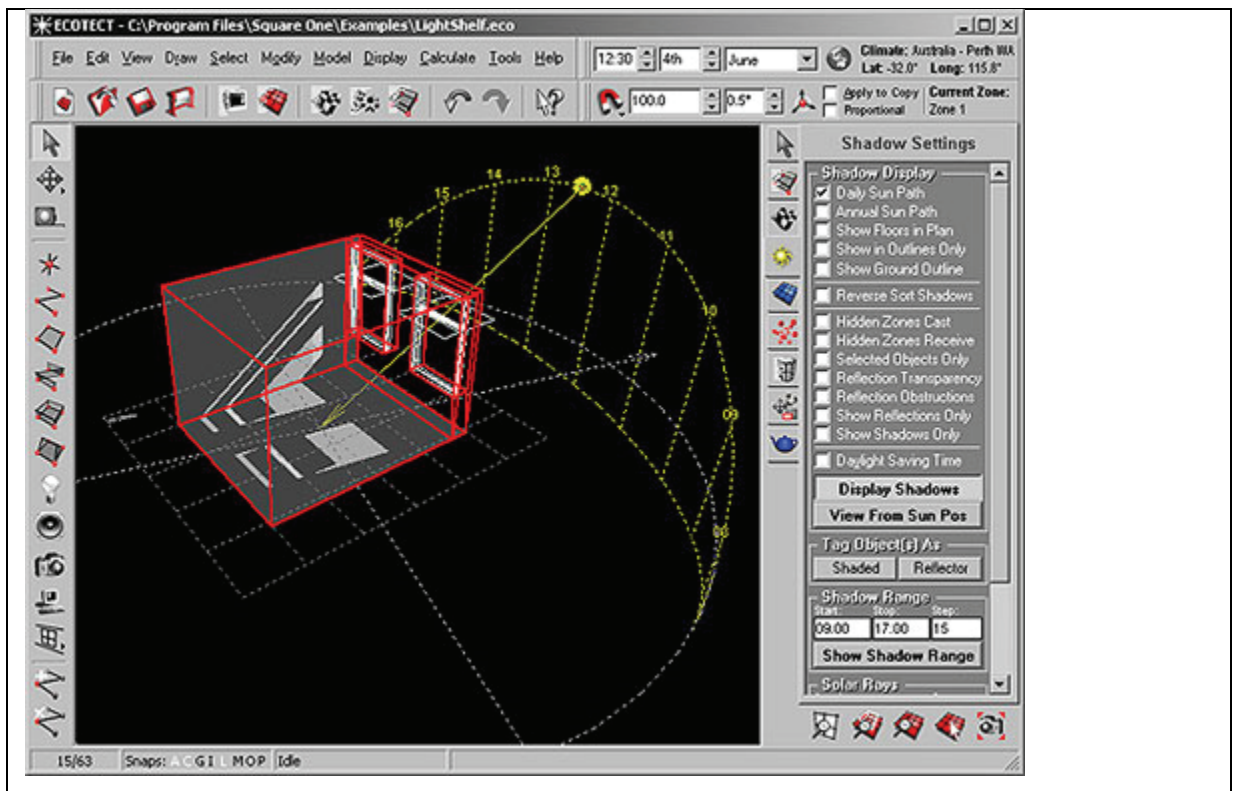
- Thermal calculation method (using DOE-2.2) is not the most accurate method available
- ECOTECT still requires medium to advanced knowledge of building simulation, and risks “garbage in; garbage out”.
- Only models idealized (theoretical) HVAC equipment

## Applicability to NZEH

While ECOTECT’s thermal calculation method lacks accuracy and it cannot explicitly model HVAC or many active solar energy systems, it is ideal for analyzing solar radiation and how it interacts with different configurations. Thus, ECOTECT would be a good tool for establishing the form of a building to maximize solar exposure.







**Energy-10** (<http://www.sbicouncil.org/displaycommon.cfm?an=1&subarticlenbr=112>)

### Summary

Energy-10 is a tool that allows one or two zone buildings that are under 10,000 SF to be modelled and simulated using a proper whole-year simulation in EnergyPlus. While the user interface could use some polishing, it allows numerous energy efficiency and energy production technologies. The level of output data is among the best in the field, with around 40 possible informative graphs. Energy-10 allows upgrades to be systematically applied without manual input. Only two solar collector types are available: PV and DHW.

**Simulation engine/calculation method** EnergyPlus; whole-year or representative days

### Key Features/Benefits

- Can model any building under 10,000 SF (~1000 m<sup>2</sup>)
- Performs detailed simulations without significant input. The default settings allow the simulation to be run. This is a nice feature for first-time users who want to see how things work immediately.
- Inputs are relatively easy.
- Built-in code libraries (e.g., ASHRAE 90.1-2004)
- Simulates both energy and daylighting

- Allows two buildings to be directly compared. Good for benchmarking.
- Large variety of performance graphs for metrics (daylighting, thermal, economics)
- First simulation can be performed within minutes of opening E10; details take time
- Thermal mass can be added to increase passive performance; it is applied to internal walls only as to not affect exterior wall resistance. Option to add furniture to contribute to thermal mass.
- Can simulate the following upgrades: daylighting, glazing, shading, energy efficient lights, insulation, air leakage control, thermal mass, passive solar heating, economizer cycle, high efficiency HVAC, HVAC controls, duct leakage, PV (stand alone and building-integrated), solar domestic hot water.
- “Rank” feature allows all possible upgrades to be simulated independently and compared for effectiveness. While this does not deal with upgrade interactions, it is a great feature that eliminates an otherwise tedious process.
- Explicit model of mechanical systems
- Feature to allow emissions to be calculated
- Some of the reports can be used for LEED processes

#### **Limitations**

- Limited to one or two rectangular zones
- Input detail is probably OK for designers and on the system level, but is insufficient for detailed design. For instance, SDHW system design has only a few inputs and only a single configuration (which is not easily understood)
- Some system parameters are not easy to dig up (e.g., “collector efficiency curve slope”)
- No visualization of the building means that user does not know if the model matches their intended design. Also, it is not clear if there is room for the solar collectors.
- Somewhat primitive and unusual interface. Not too easy to navigate.
- No way to change location (and climate file). Limited cities. Although, E10 does have a utility to convert weather files to E10 format.
- Shading is very limited. No ability to define external solar obstructions.
- Glazing library is limited and little performance data is provided for it.
- No ground source heat pump model.
- No form of feedback guidance, except for analysis of results.
- NO SI units

#### **Applicability to NZEH**

Other than several efficiency measures, the only two energy production systems are PV and SDHW systems. Thus, achieving net zero could be expensive given that PV is required to supplement all energy beyond what the SDHW collector can.

Energy10 Version 1.8 - [Summary Information: Sample]

Energy-10 Summary Page  
 Project: Sample  
 Project Directory: C:\Program Files\Energy-10\Version 1.8\Projects\PROJ1  
 Feb 15, 2009

Description: Reference Case Low-Energy Case  
 Scheme Number: 1 / Saved 2 / Saved  
 Library Name: ASHRAE11B ASHRAE11B  
 Simulation status, Thermal/DL: valid/NA valid/valid  
 Weather file: NEWYORK.ET1 NEWYORK.ET1

Building Zones - Bldg-1

Bldg Title: Reference Case

Building Level Systems: Photovoltaics, Solar Hot Water

Zone	Rotate	Area	Volume	UA	HVAC Class
		m <sup>2</sup>	m <sup>3</sup>	Btu/hF	
Zone 1	0	2000.0	10000.0	97.08	Residential
Zone 2	0	0	0	0	

Photovoltaic System - Bldg-1

System: Building Integrated Stand-Alone

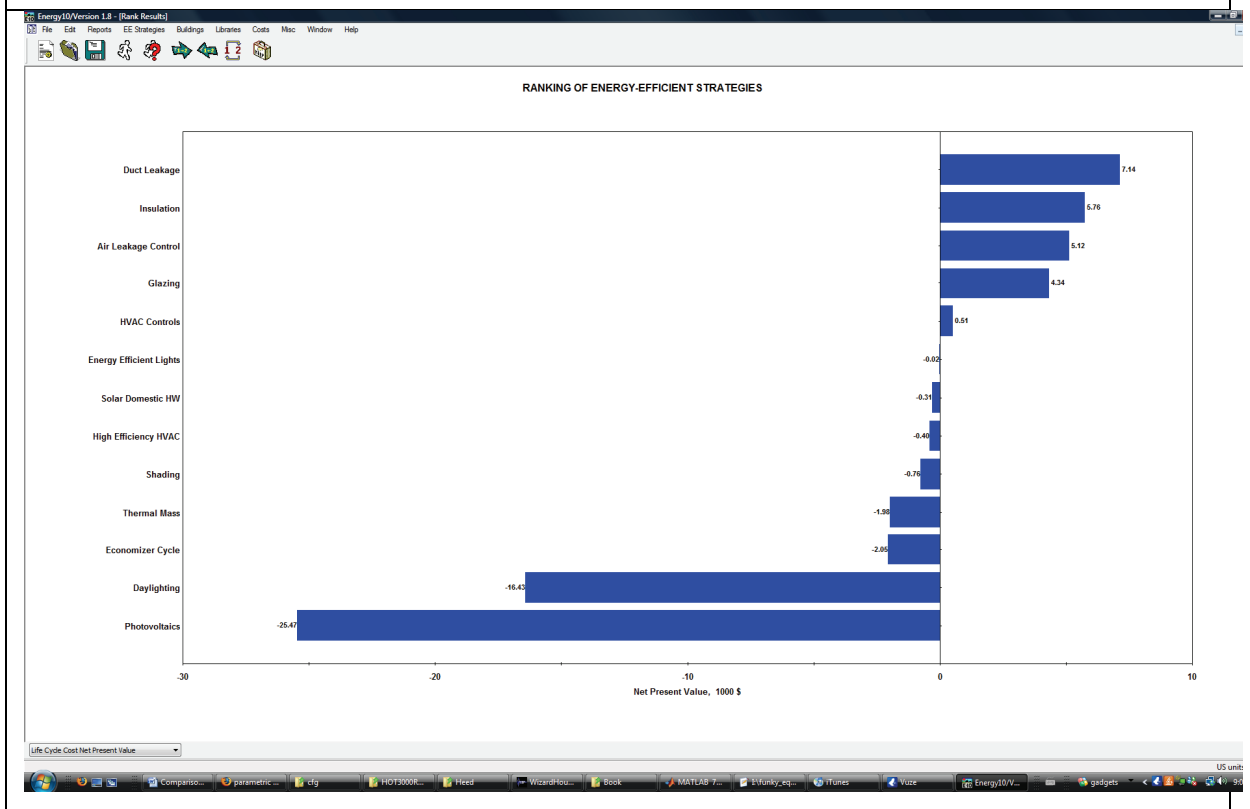
Capacity: 10 kWp  
 Total Area: 0 m<sup>2</sup>  
 System Voltage: 12 VDC  
 Soling Factor: 0.00  
 Derating Factor: 0.00  
 Ground Reference: 0.00  
 Inverter Capacity: 0.0 kWp  
 Apply Status: Unassigned

Results:

Category	Reference Case	Low-Energy Case
Heating/Cooling/Fan-HW, kWh	0/3873/1419	0/2437/557
Hot Water/Other, kWh	0/4764	0/-720
Peak Electric, kW	7.5	3.3
Fuel, kW/Inter/total, kWh	19564/106326/125890	11438/21569/33004
Emissions, CO <sub>2</sub> /SO <sub>2</sub> /NO <sub>x</sub> , lbs	30725/107/65	8183/29/17
Construction Costs	316159	373367
Life-Cycle Cost	968896	386666

Photovoltaics System Summary:

Description: Reference Case Low-Energy Case  
 PV System Definition Status: Undefined Applied  
 Total PV Array Area, ft<sup>2</sup> / m<sup>2</sup>: -- 495 / 46



**EnergyPlus** ([http://apps1.eere.energy.gov/buildings/energyplus/cfm/reg\\_form.cfm](http://apps1.eere.energy.gov/buildings/energyplus/cfm/reg_form.cfm))

**Summary** EnergyPlus emerged from BLAST and DOE-2.1 to become the new generation of simulation engine funded by the USW DOE. Although it's several decades younger than it's simulation engine counterparts – ESP-r and TRNSYS – it has diverse and extensive modeling capabilities. Rather than having a GUI, EnergyPlus merely reads in and outputs ASCII files. However, many commercial GUIs that use EnergyPlus have been created.

**Simulation engine/calculation method** Transfer function method

**Key Features/Benefits**

- Extensive HVAC models
- Weather files from 1250 locations worldwide
- Open-source
- Excellent documentation and industry adoption
- Has a moderate number of active solar energy systems, including PV and basic solar thermal collectors

**Limitations**

- The transfer function method uses linearity assumptions, which results in it being less accurate for thermally massive constructions
- Lack of GUI means that EnergyPlus should either be used by experts or with a commercial GUI

**Applicability to NZEH** EnergyPlus has all of the modeling capabilities required by for the modeling of NZEH buildings. However, it is a simulation engine and not a design tool.

```
Schedule:Compact,
Office Lighting,      !- Name
Fraction,            !- ScheduleType
Through: 12/31,      !- Complex Field #1
For: Weekdays SummerDesignDay, !- Complex Field #2
Until: 05:00, 0.05,  !- Complex Field #4
Until: 07:00, 0.1,   !- Complex Field #6
Until: 08:00, 0.3,   !- Complex Field #8
Until: 17:00, 0.9,   !- Complex Field #10
Until: 18:00, 0.5,   !- Complex Field #12
Until: 20:00, 0.3,   !- Complex Field #14
Until: 22:00, 0.2,   !- Complex Field #16
Until: 23:00, 0.1,   !- Complex Field #18
Until: 24:00, 0.05,  !- Complex Field #20
For: Saturday WinterDesignDay, !- Complex Field #21
Until: 06:00, 0.05,  !- Complex Field #23
Until: 08:00, 0.1,   !- Complex Field #25
Until: 12:00, 0.3,   !- Complex Field #27
Until: 17:00, 0.15,  !- Complex Field #29
Until: 24:00, 0.05,  !- Complex Field #31
```

Date/Time	FULL BUILDING - 1		FULL BUILDING - 1		FULL BUILDING - 1	
	Environment: Outdoor Dry Bulb [C](Hourly)	Zone: Mean Radiant Temperature [C](Hourly)	Zone: Sensible Heating Energy [J](Hourly)	Zone: Sensible Cooling Energy [J](Hourly)	Zone: Temperature [C](Hourly)	Zone: Electricity Facility [J](Hourly)
07/21 01:00:00	22.391625	25.68764762	0	97662314.73	24	4744800
07/21 02:00:00	21.856625	25.4549149	0	84129364.69	24	4744800
07/21 03:00:00	21.3885	25.24914681	0	71930267.53	24	4744800
07/21 04:00:00	21.027375	25.06622736	0	61083933.1	24	4744800
07/21 05:00:00	20.840125	24.90963358	0	52105586.7	24	4744800
07/21 06:00:00	20.93375	24.85181907	0	52272503.21	24	9489600
07/21 07:00:00	21.348375	25.02997175	0	63527348.55	24	9489600
07/21 08:00:00	22.150875	25.31280285	0	91283424.12	24	28468800
07/21 09:00:00	23.381375	25.90704112	0	172113989.1	24	85406400
07/21 10:00:00	24.906125	26.38462879	0	198273461.3	24	85406400
07/21 11:00:00	26.644875	26.80331018	0	221444822.8	24	85406400
07/21 12:00:00	28.397	27.19513693	0	243595599.7	24	85406400
07/21 13:00:00	29.8415	27.54144568	0	256607061.7	24	85406400
07/21 14:00:00	30.858	28.02339571	0	290604364.8	24	85406400
07/21 15:00:00	31.379625	28.42182655	0	313194807.1	24	85406400
07/21 16:00:00	31.299375	28.69170279	0	327942499.8	24	85406400
07/21 17:00:00	30.710875	28.81237708	0	334141157.9	24	85406400
07/21 18:00:00	29.694375	28.54516783	0	282087102.5	24	47448000
07/21 19:00:00	28.383625	28.13719517	0	247592621.4	24	28468800
07/21 20:00:00	26.992625	27.52551031	0	213427454.6	24	28468800
07/21 21:00:00	25.735375	27.03216343	0	180725479.8	24	18979200
07/21 22:00:00	24.62525	26.63681079	0	158994623.3	24	18979200
07/21 23:00:00	23.689	26.27975131	0	133661997.8	24	9489600
07/21 24:00:00	22.96675	25.96718409	0	113489692.4	24	4744800

**ESP-r** (<http://www.esru.strath.ac.uk/Programs/ESP-r.htm>)

**Summary** ESP-r is a low-level open-source simulation engine that includes a project manager (for model input) a building simulator module, and a results viewer. It is very detailed and flexible, at the cost of complexity. Inputting and obtaining results for a model could take from an hour to weeks. It is most suitable for detailed design, once the basic elements are well-defined.

**Simulation engine/calculation method** Implicit Finite Difference; time-step; whole-year

**Key Features/Benefits**

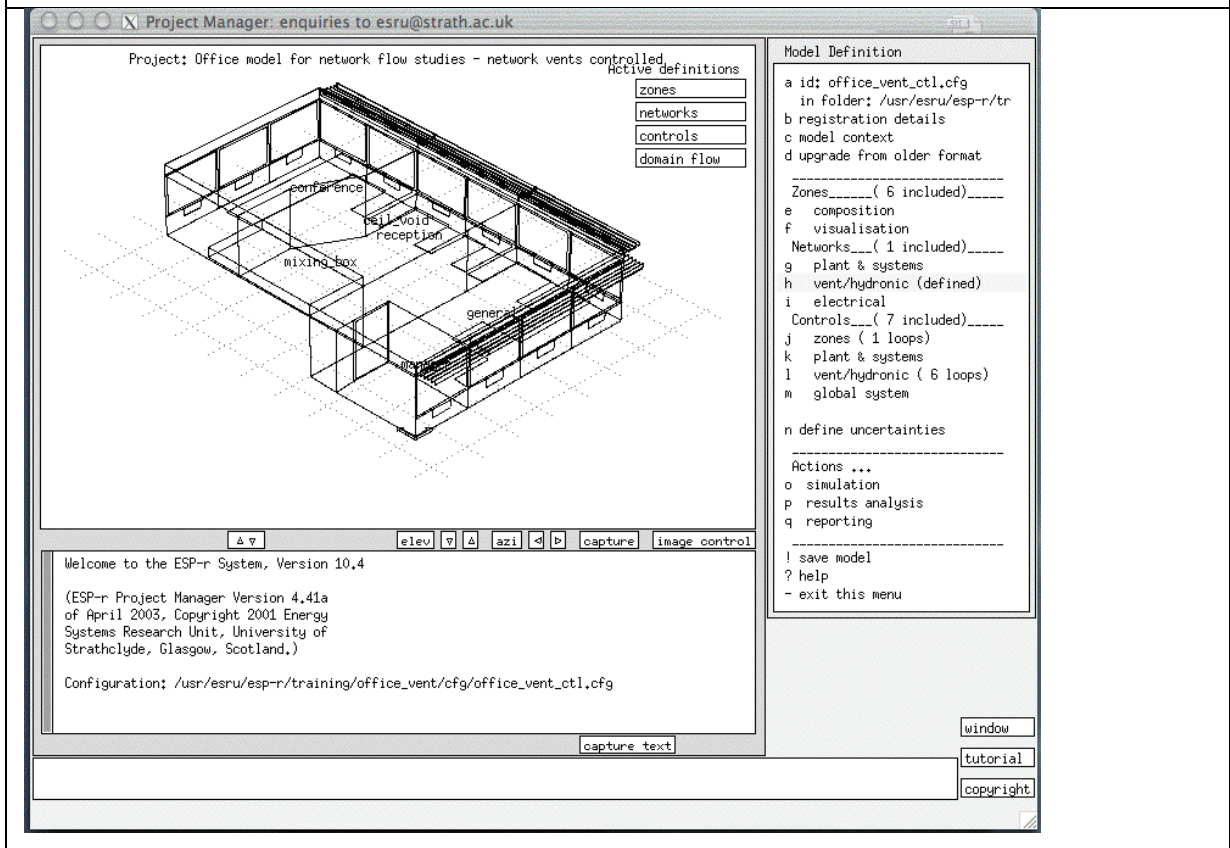
- Has been shown to be very accurate
- Particularly suitable for transient analysis of thermal capacity because of its calculation method
- Custom-built models could
- Explicit definitions of wall constructions; glazing; controls; operations; geometry
- Input files are ASCII-based and can be modified with script for batch runs
- Includes multiple PV and solar thermal, with multiple collector and take models
- Allows either explicit plant models or theoretical loads
- Allows electrical networks
- Can be coupled with RADIANCE for daylighting analysis
- CFD capabilities
- Open-source; allows researchers to modify code or add models

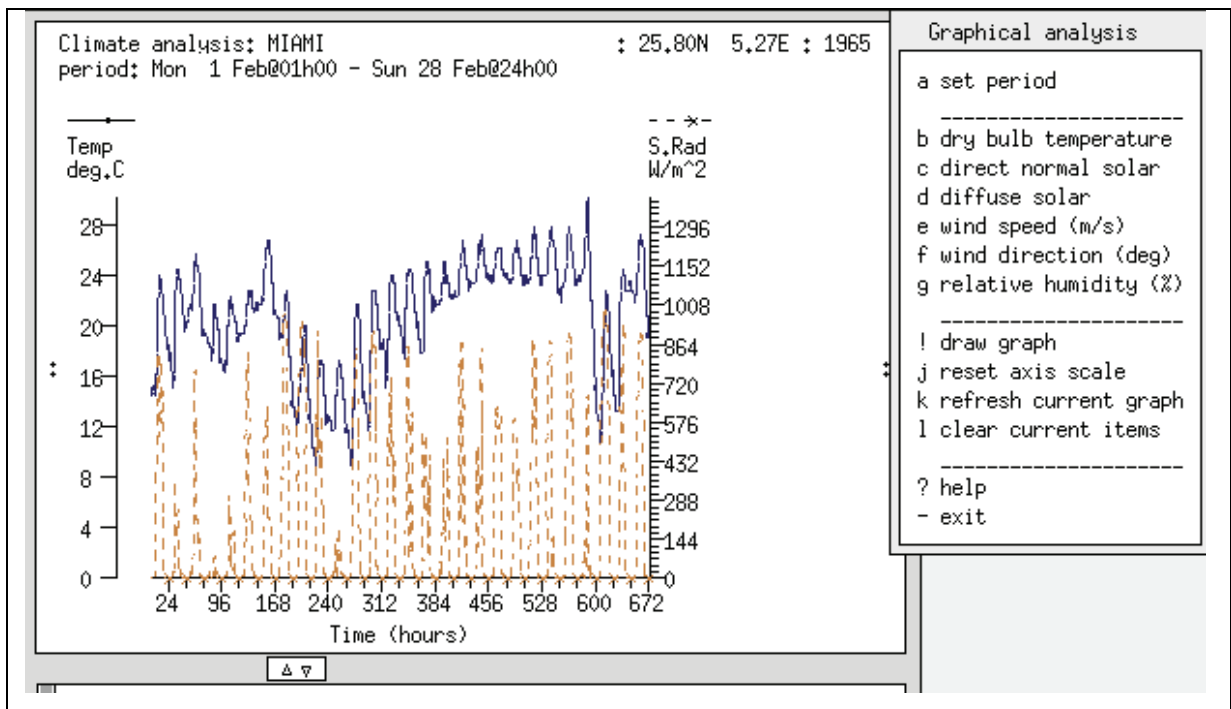
**Limitations**

- User interface is not particularly intuitive and has some bugs
- Export of results is tedious

- Comparison between design concepts is tedious
- While building envelopes are fairly straightforward to input, plants, advanced controls, and solar collectors can be difficult.
- Currently, the glazing definition is approximate (to be improved in near future)
- Best used in a Linux environment, which may not be ideal for some users (though can be installed on Windows and OS X)

**Applicability to NZEH** ESP-r has all modeling features required to build a NZEH building model. It should not be used for the early design stage when performing parametric studies would be tedious. Modeling of plants or solar energy systems requires advanced knowledge of both ESP-r and the system.





**Green Building Studio** (<http://usa.autodesk.com/adsk/servlet/index?siteID=123112&id=11179508>)

**Summary** Green Building Studio (GBS) is an AutoDesk product that allows energy, emissions, and daylighting analyses to be performed on building models.

**Simulation engine/calculation method** DOE-2.2 (default) or EnergyPlus

**Key Features/Benefits**

- Many input processes are automated, eliminating redundant inputs
- Facilitates LEED compliance
- Water use and emissions analyses
- Feature to determine if building is carbon neutral
- Detailed output allows assessment of the source of various loads

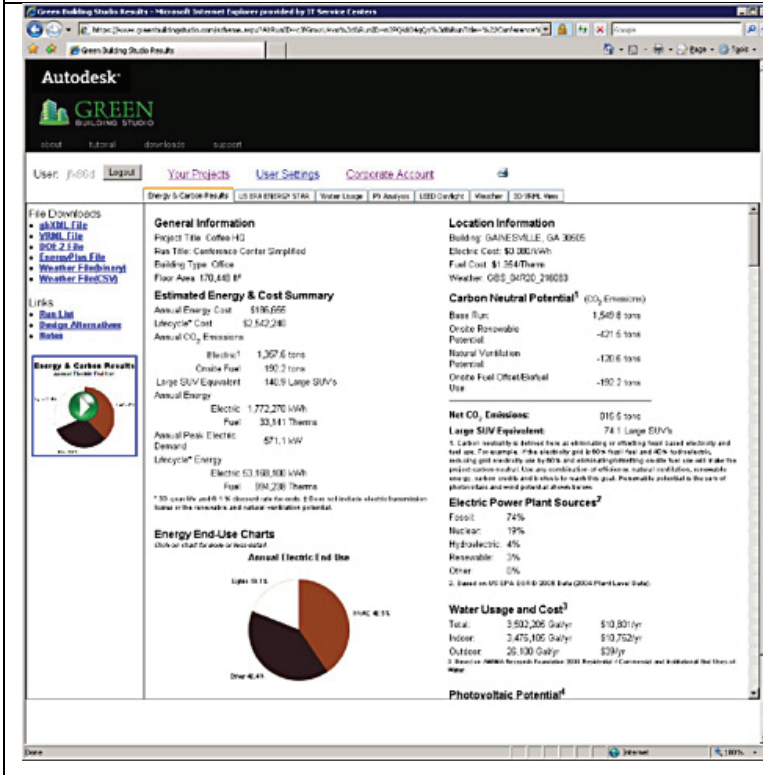
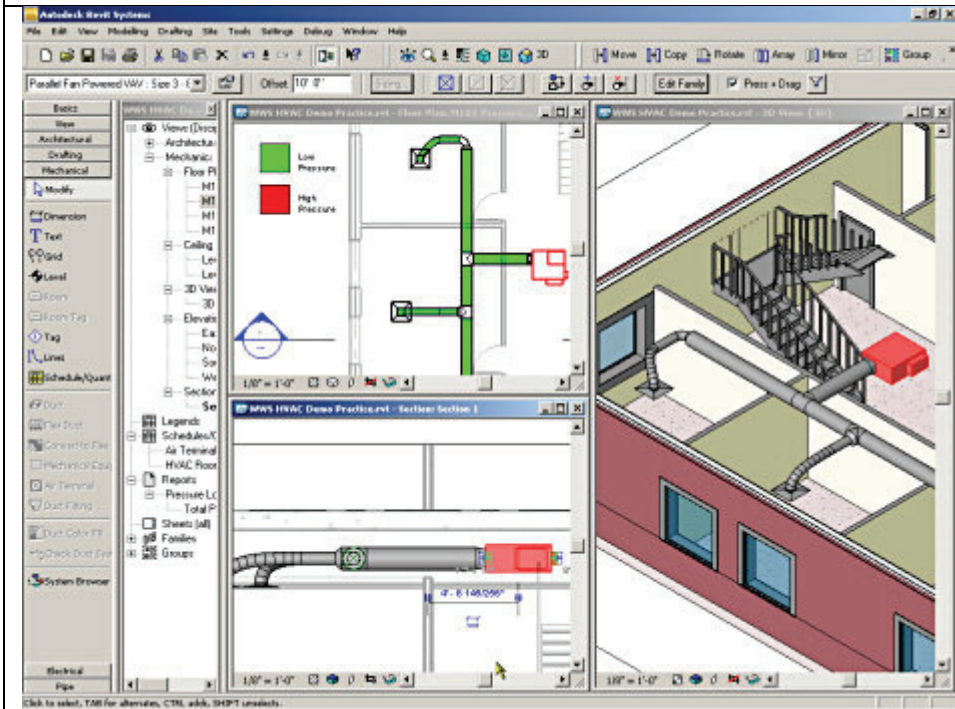
**Limitations**

- Underlying DOE-2.2 models can be complex and cannot necessarily be fine tuned using GBS
- Offers little control over details such as zoning and thermal bridging
- Many energy collection models are high-level and do not allow explicit modeling. For example, solar energy is simply measured as the amount of solar energy incident on building surfaces, rather than by allowing PV to be modelled. Wind energy is handled similarly.

**Applicability to NZEH** GBS is ideal for NZEH building design. However, it should be used towards the beginning of the design process, since many key elements of NZEH buildings, cannot be explicitly

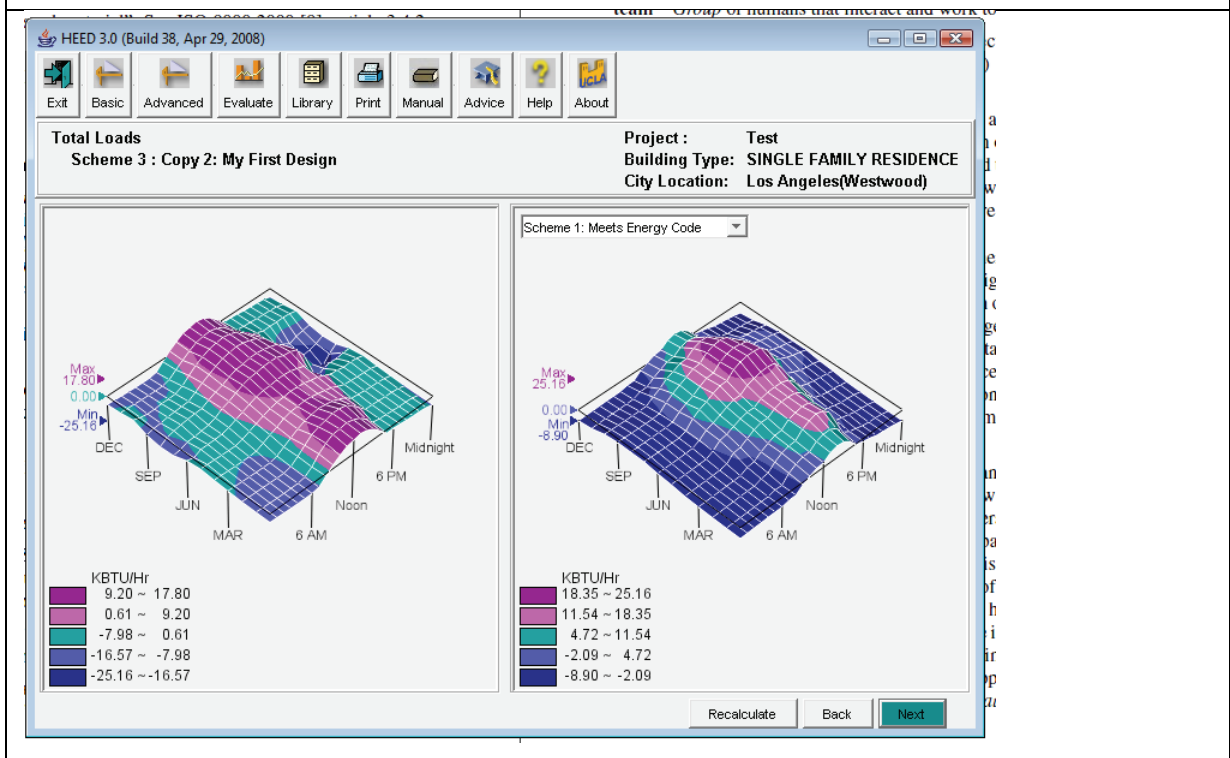
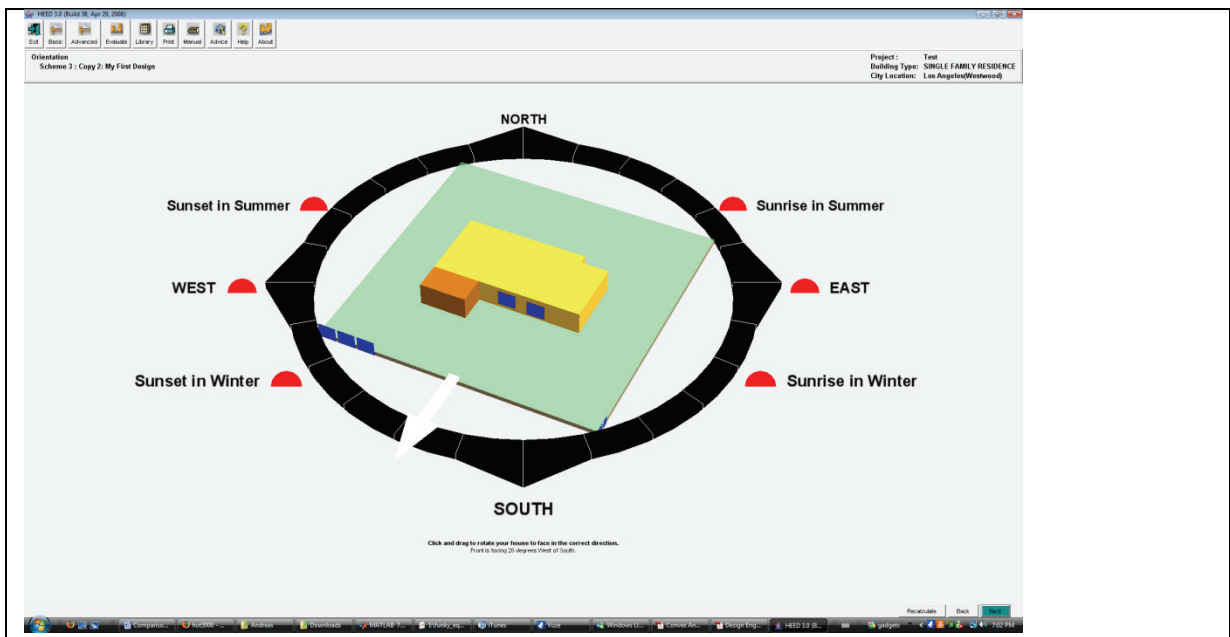


modelled. GBS's reporting, which provides detailed information about carbon neutrality and the cause of heating and cooling loads, is useful for facilitating NZEH building design.





<b>HEED</b> ( <a href="http://mackintosh.aud.ucla.edu/heed/">http://mackintosh.aud.ucla.edu/heed/</a> )
<b>Summary</b> HEED (Home Energy Efficiency Design) allows user to assess the potential benefits to adding upgrades to a baseline house. It considers both energy and GHG emissions. Unlike most tools that were reviewed, it has a strong educational component and very strong visualization of whole-year performance.
<b>Simulation engine/calculation method</b> Solar-5; hourly simulations
<b>Key Features/Benefits</b> <ul style="list-style-type: none"> <li>• Automatically establishes a design that meets code and an energy efficient version</li> <li>• Easy to use footprint editor and window layout</li> <li>• Good visualization of house orientation</li> <li>• Inputs are somewhat limited in choice, but at the advantage of fast input</li> <li>• “Advice” button links to information sources about how to design each element for high performance</li> <li>• Good visualization of typical year-round performance</li> <li>• Good facility for comparing multiple designs</li> <li>• Includes costs and emissions</li> <li>• Feature for external shading: overhangs, side fins</li> <li>• Basic daylighting features</li> </ul>
<b>Limitations</b> <ul style="list-style-type: none"> <li>• Nominally limited to California climates</li> <li>• Single zone</li> <li>• No solar collector models</li> </ul>
<b>Applicability to NZEH</b> While having excellent features for visualization of how the house interacts with the sun, no energy collection models exist. Thus, HEED would have to be used in conjunction with another tool to properly model a NZEH house.



**HOT3000** ([http://canmetenergy-canmetenergie.nrcan-rncan.gc.ca/eng/software\\_tools/hot3000.html](http://canmetenergy-canmetenergie.nrcan-rncan.gc.ca/eng/software_tools/hot3000.html))

**Summary** HOT3000 is a tool intended for energy consultants, students, and researchers. It allows relatively efficient input of common house features. Its object oriented approach to descriptors is well

organized. It has models for BIPV and SDHW collectors. The output is in the form of

**Simulation engine/calculation method** ESP-r; whole-year, hourly time-steps (5 min. for plant)

#### Key Features/Benefits

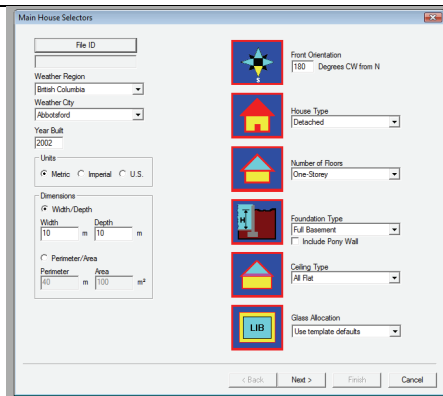
- Wizard feature allows definition of a basic house, which can be simulated immediately.
- Well structured building definition screens (carried over from HOT2000)
- Allows multiple zones
- Good variety of mechanical systems, including GSHP
- While being intended for Canada, it could be used for any location that the climate file is available for
- Model files can be modified within ESP-r
- Good visualization of house geometry with 3D graphics
- Includes a PV model and three SDHW configurations

#### Limitations

- No features to compare multiple designs against each other
- Output report is fairly limited; no graphs, only tabular format
- No form of feedback or guidance, other than summary report

#### Applicability to NZEH

Other than several efficiency measures, the only two energy production systems are PV and SDHW systems. Thus, achieving net zero could be expensive given that PV is required to supplement all energy beyond what the SDHW collector can.



HOT3000 - [Hot3000 Report]

HOT3000  
Natural Resources Canada  
Version 1.0

[Input summary](#) | [Performance summary](#) | [Month-by-month summary](#)

### MONTHLY ZONE ENERGY PROFILE

Month	Average Temperature (°C)	Internal Gains (MJ)	Solar Gains (MJ)	Heating load (MJ)	Supplied heating (MJ)	Cooling load (MJ)	Supplied sensible cooling (MJ)
<b>Zone 01</b>							
Jan	18.3	1,770	98	5,308	3,439	-	-
Feb	18.3	1,599	106	4,470	2,763	-	-
Mar	19.1	1,770	180	3,998	2,213	-	-
Apr	17.1	1,713	196	103	43	-	-
May	20.9	1,770	234	-	-	-	-
Jun	23.6	1,713	239	-	-	-	-
Jul	25.6	1,770	241	-	-	-	-
Aug	26.2	1,770	246	-	-	-	-
Sep	22.2	1,713	208	-	-	-	-
Oct	19.9	1,770	155	2,054	702	-	-
Nov	18.4	1,713	97	4,205	2,408	-	-
Dec	18.3	1,770	71	5,151	3,310	-	-
<b>Annual</b>	<b>20.7</b>	<b>20,842</b>	<b>2,074</b>	<b>25,288</b>	<b>14,878</b>	-	-
<b>Zone 02</b>							
Jan	3.3	-	-	-	-	-	-
Feb	5.4	-	-	-	-	-	-
Mar	11.1	-	-	-	-	-	-
Apr	15.5	-	-	-	-	-	-
May	21.2	-	-	-	-	-	-
Jun	25.6	-	-	-	-	-	-
Jul	27.5	-	-	-	-	-	-
Aug	26.8	-	-	-	-	-	-
Sep	19.6	-	-	-	-	-	-
Oct	13.6	-	-	-	-	-	-
Nov	5.7	-	-	-	-	-	-
Dec	3.6	-	-	-	-	-	-
<b>Annual</b>	<b>15.0</b>	-	-	-	-	-	-
<b>Zone 03</b>							
Jan	17.3	312	-	1,786	1,474	-	-

**IES-VE** (<http://www.iesve.com/content/default.asp?page=home>)

**Summary** IES-VE is a suite of simulation tools that includes analysis for energy, lighting and daylighting, CFD, natural ventilation, mechanical systems, ducting and piping, emissions, and costs. Its 3D modeling capabilities are aimed at designers that are accustomed to AutoCAD-like interfaces.

**Simulation engine/calculation method** Admittance method

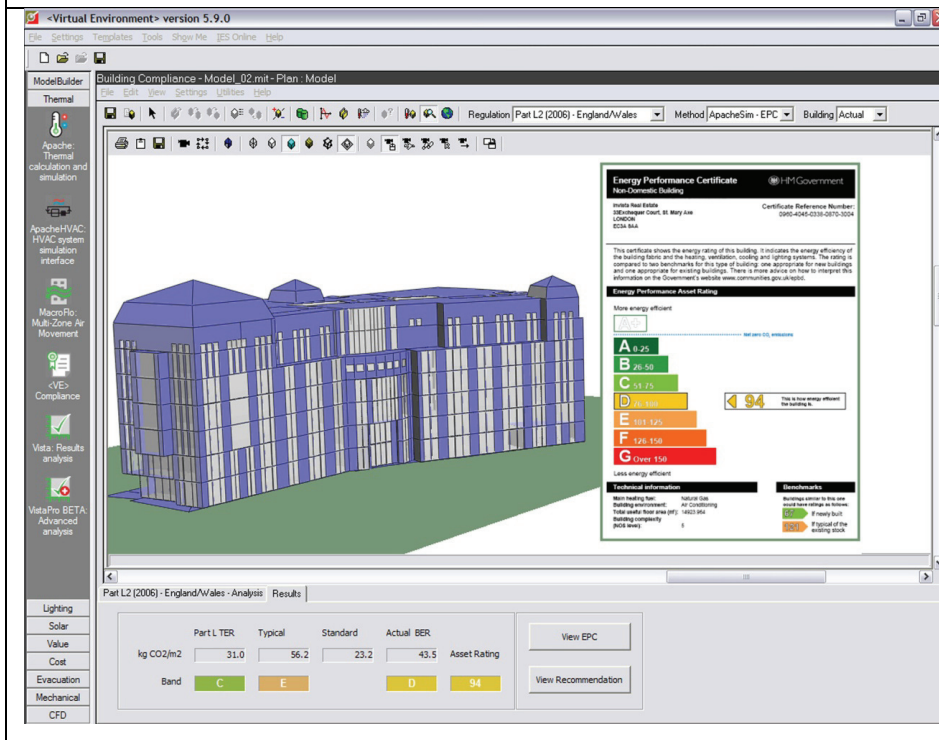
**Key Features/Benefits**

- Multiple daylighting modules allow for a wide range of model complexity
- Integrated model means each aspect of the model is updated each time a change is made.

**Limitations**

- HVAC equipment must be explicitly modelled
- Limited number of active solar collector models

**Applicability to NZEH** While IES-VE provides a number of unique features, it currently doesn't model solar energy collectors – a key component of NZEH buildings. Thus, it can only be used for certain aspects of the building being designed.



**MIT Design Advisor** (<http://designadvisor.mit.edu/design/>)

**Summary** MIT Design Advisor is a web-based tool that allows the design of simple buildings and provides

<p>concise performance information. While having relatively limited inputs, it does have some advanced features such as lighting control, natural ventilation control, a large glazing library, thermal comfort, and venetian blinds (uncontrolled). Up to four designs can be compared in parallel. The tool also features an optimizer that find the optimum based on user-supplied constraints (the feature is not on-line yet).</p>
<p><b>Simulation engine/calculation method</b> A custom-built simplified simulation engine</p>
<p><b>Key Features/Benefits</b></p> <ul style="list-style-type: none"> <li>• Inputs are reduced to a minimum, allowing for rapid input – even from new/inexperienced users</li> <li>• Several advanced features including: lighting control, natural ventilation control, a large glazing library, thermal comfort, and venetian blinds</li> <li>• Large climate database</li> <li>• The tool is web-based and does not require installation</li> <li>• Enables print out of a summary report</li> <li>• LCA for costs, energy, emissions</li> <li>• Radiance-like daylighting display</li> <li>• Allows either single-facade zones or entire floors (with four facades)</li> </ul>
<p><b>Limitations</b></p> <ul style="list-style-type: none"> <li>• Inputs are limited and only suitable for early design stages</li> <li>• No active collector models</li> <li>• Most suitable for commercial buildings; not residential – particularly detached houses</li> </ul>
<p><b>Applicability to NZEH</b> While being a good model for a conceptual design tool, MIT Design Advisor does not have any active solar collector models. It would be most suitably used in conjunction with other software or to determine appropriate insulation, glazing, and mass levels. It would also be good for basic thermal comfort and daylighting analysis.</p>

### Setup: Describe the Building You Wish to Simulate

Getting Started

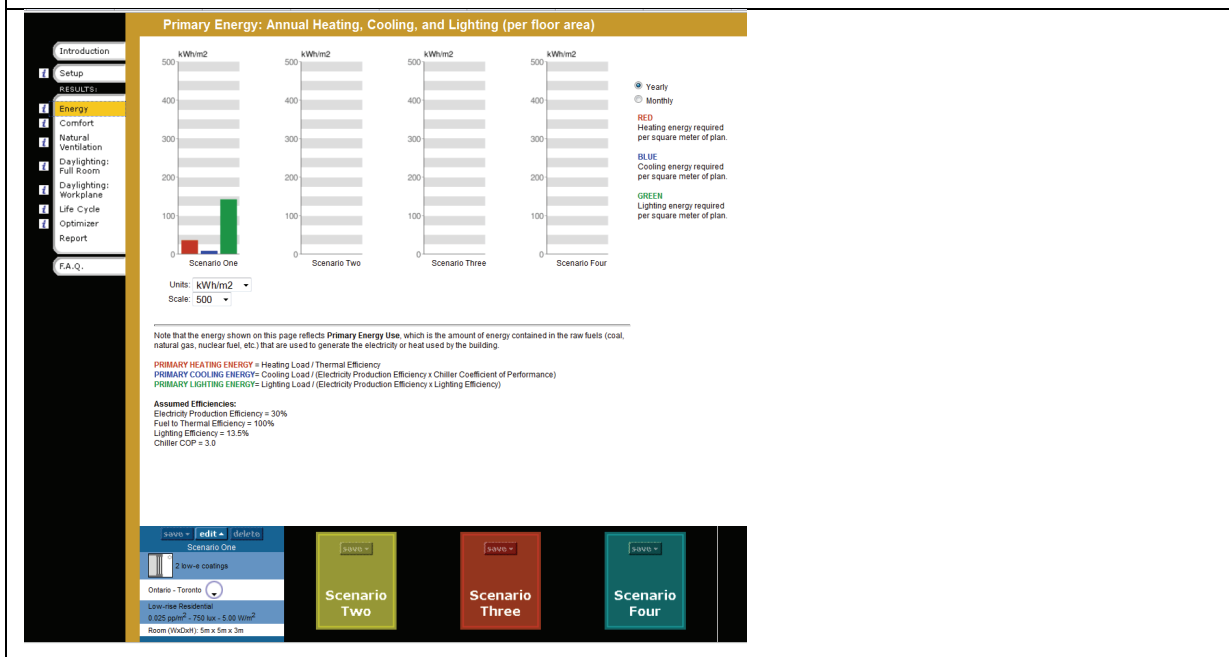
**Building Properties**

- Climate**
  - Region: Canada
  - City: Ontario - Toronto
- Occupancy and Equipment**
  - Occupancy Schedule: 5:00 PM begins, 8:00 AM ends
  - Person-density: 0.025 people per m<sup>2</sup>
  - Lighting: 750 - fine work lux
  - Equipment: 5.0 - office (light) W/m<sup>2</sup>
- Ventilation System**
  - Joint Natural Ventilation Cooling and Mechanical Heating
  - Indoor Air Temperature: Max 26 °C, Min 20 °C
  - Max Relative Humidity: 60 %
  - Ventilation Rate: Fresh Air Rate: filters / sec per person, Air Change Rate: 1 roomfuls per hour
- Thermal Mass**
  - High Mass: exposed concrete slab floor
  - Low Mass: lightweight or obstructed floor
  - Zero Mass
- Building Geometry**
  - Single Zone (1 facade)

**Typical Room Properties**

- Room Dimensions**
  - Width: 5 m
  - Depth: 5 m
  - Height: 3 m
  - Window / Primary Facade Orientation: south
- Window Description**
  - Window Area: 50 % of exterior wall area
  - Select a Window Type: [Visual selection of window types]

Buttons: save, edit, delete, Scenario One, Scenario Two, Scenario Three, Scenario Four

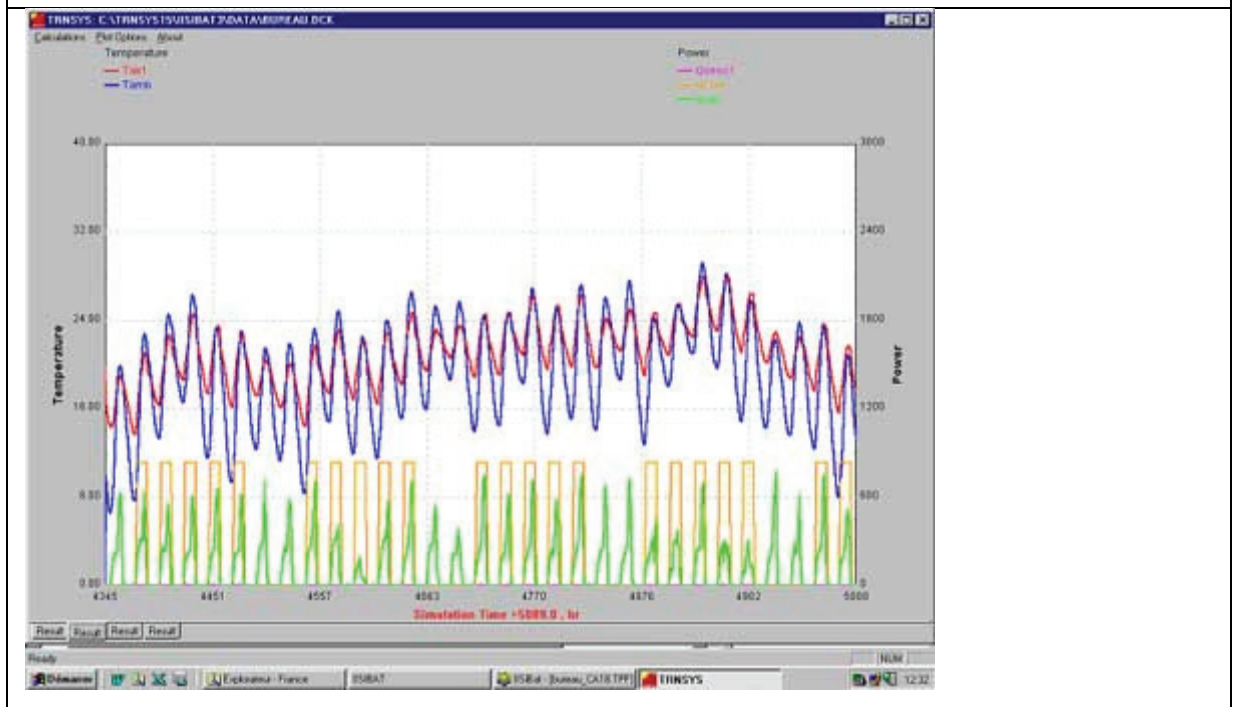
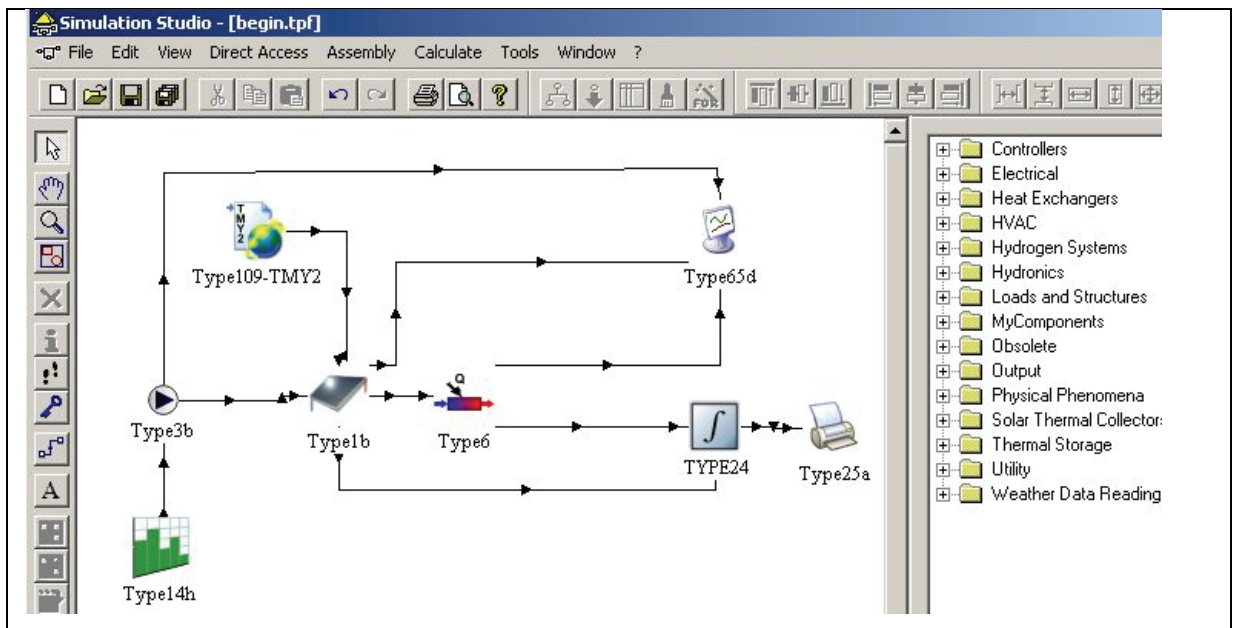


TRNSYS (<http://www.trnsys.com/>)

**Summary** TRNSYS was originally developed for the analysis of solar thermal systems, but can now model a large variety of building features, solar collectors, and other energy systems. It uses modular models that can be connected and reconfigured. This approach provides considerable flexibility and

Simulation engine/calculation method Transfer function method
<p><b>Key Features/Benefits</b></p> <ul style="list-style-type: none"> <li>• Modularity of all components (“types”) is ideal for implementing complex and innovative models.</li> <li>• Modularity allows relatively efficient development of new models. Code can be directly examined within TRNSYS, allowing code to be easily debugged. Also, new components for custom equipment can be programmed.</li> <li>• Components are connected, such that the outputs of one component enter as inputs for another.</li> <li>• TRNSYS arguably has more components (solar collectors, HVAC equipment, storage tanks, etc.) than any other program.</li> <li>• “Equation” type allows output signals to be altered, logically, without requiring users to modify source code.</li> <li>• Overall, TRNSYS has a very intuitive interface.</li> <li>• TRNSYS is designed to interact with a variety of other programs. For instance, input from and output to MATLAB and Excel are possible.</li> </ul>
<p><b>Limitations</b></p> <ul style="list-style-type: none"> <li>• Transfer function method does not accurately handle thermal mass – a fundamental element of passive solar heating</li> <li>• Building model is somewhat limited compared to other simulation engines.</li> <li>• Some component parameters (e.g., for collectors) are difficult to determine for commercial products and are geared towards researchers, rather than practitioners.</li> <li>• The flexibility of configuring components comes at the cost of considerable time to create new models. For instance, a simple solar domestic hot water system requires all tanks, pipes, pumps, etc., to be explicitly modelled.</li> </ul>
<p><b>Applicability to NZEH</b> With its vast collection of renewable energy models, TRNSYS should be considered one of the most important components of NZEH building modeling. However, it is targeted at researchers who have good knowledge of renewable energy systems and building modeling.</p>





**DesignBuilder** ([www.designbuilder.co.uk](http://www.designbuilder.co.uk))

**Summary** DesignBuilder is a prominent front end for EnergyPlus. It has strong geometry capabilities (AutoCAD-like interface) and very efficient methods for inputting building details like internal gains, wall constructions, and schedules. However, like all simplified tools this ease of input comes at the cost of

less control over certain elements of the building.

**Simulation engine/calculation method** Transfer function method, by default

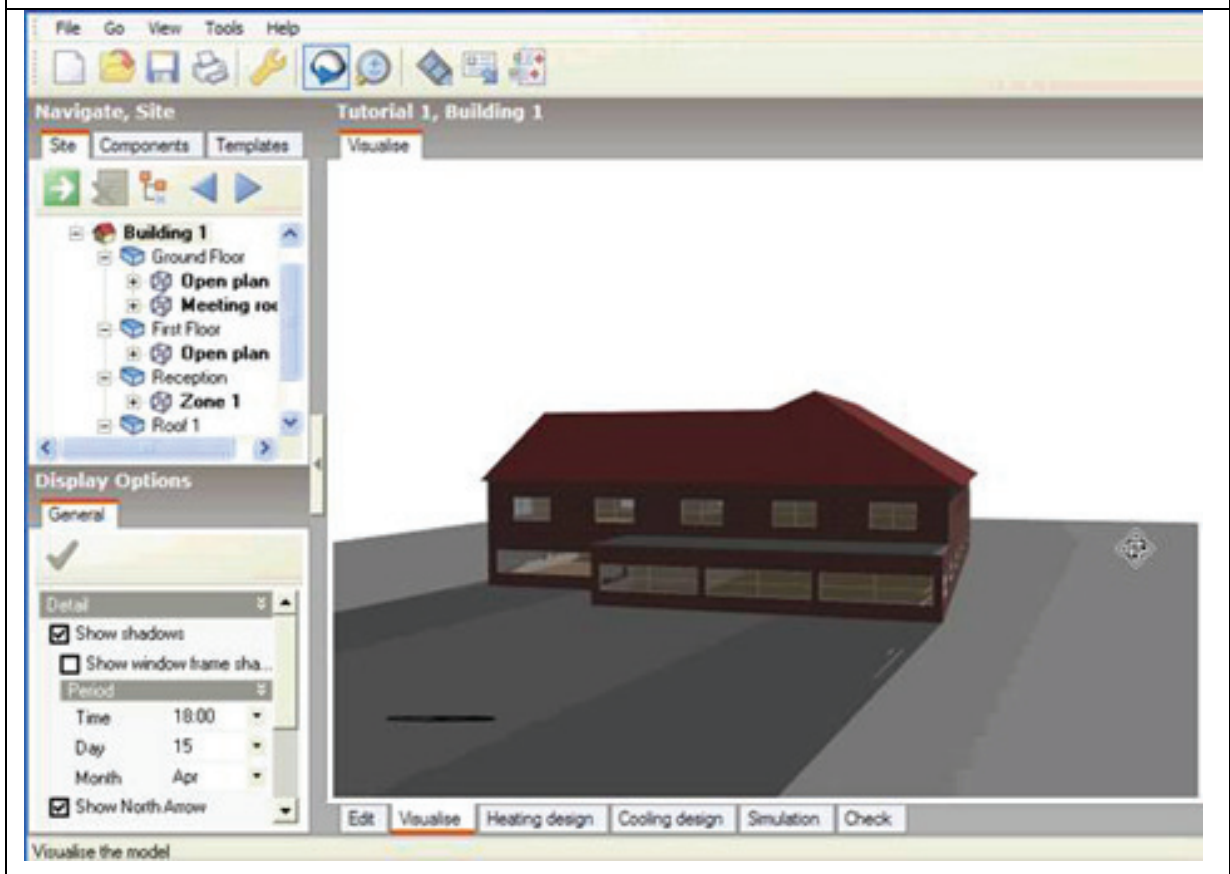
### Key Features/Benefits

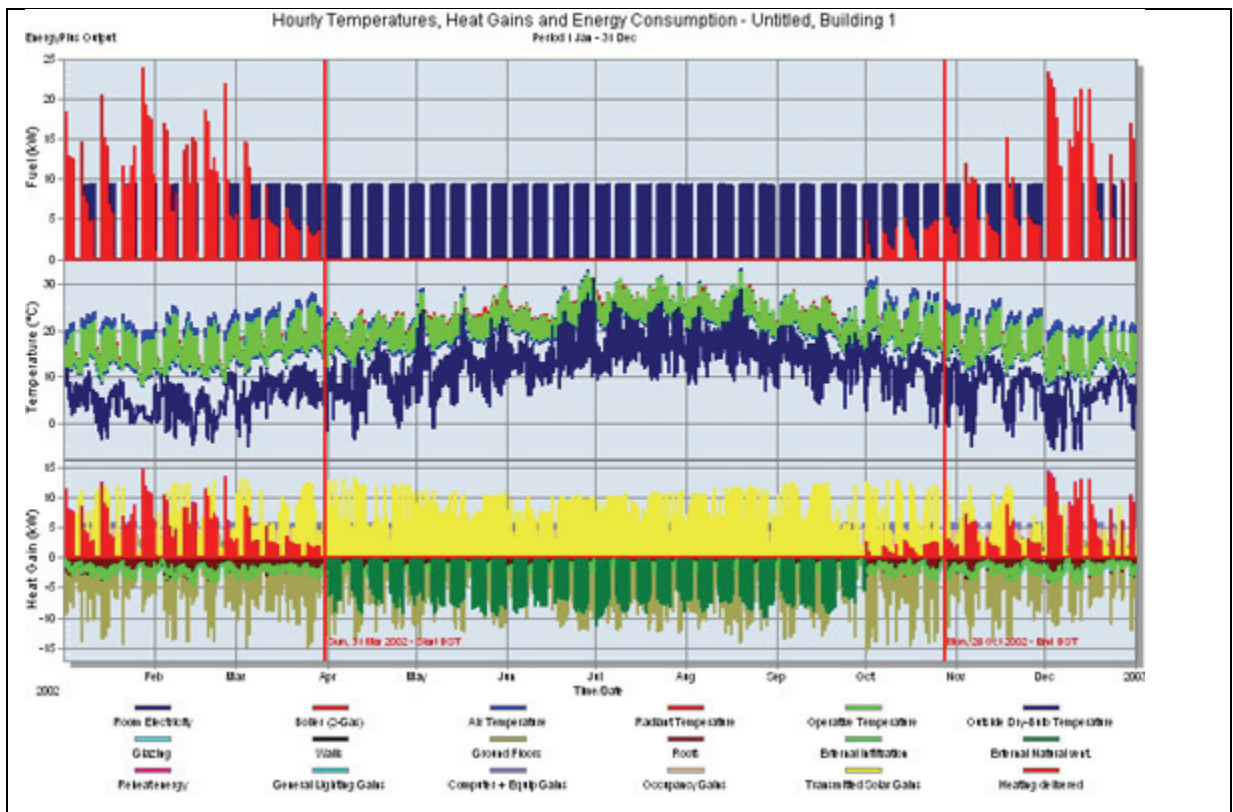
- Based on a prominent simulation engine: EnergyPlus
- Strong geometry input
- Many built-in schedules, controls, wall constructions, etc.
- CFD capabilities
- Detailed natural ventilation model

### Limitations

- Limited HVAC capabilities; the user is forced to manipulate the idf file directly if more complex configurations are modeled.
- Not-backwards compatible with EnergyPlus (i.e., an EnergyPlus model cannot be imported into design builder).

**Applicability to NZEH** DesignBuilder is good for the assessment of passive aspects (form and fabric) and natural ventilation. However, it does not have renewable energy capabilities.





## RETScreen

**Summary** RETScreen is a spreadsheet-based model that is intended to be used for quick analysis and particularly economic feasibility studies for renewable energy systems and energy efficiency measures.

**Simulation engine/calculation method** Depends on the model, but usually very simplified and uses only monthly averages for weather data.

### Key Features/Benefits

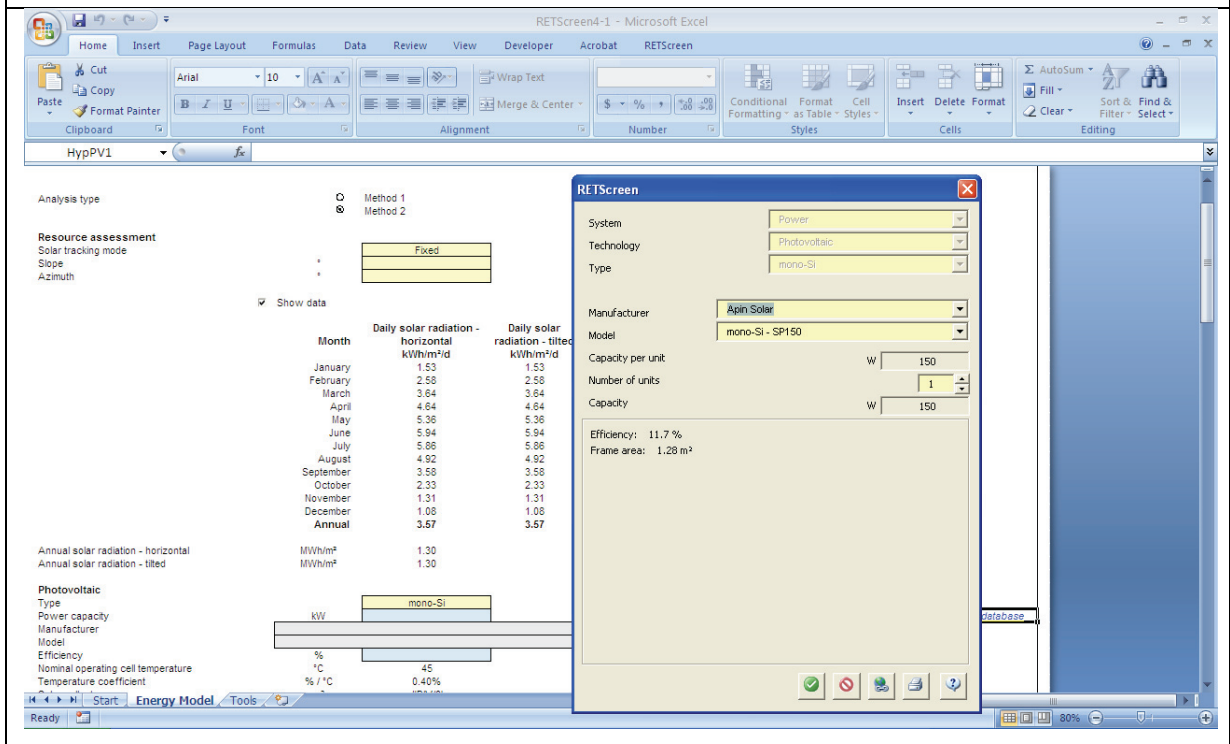
- Minimal inputs
- Instantaneous updating

- Economic feasibility

### Limitations

- Not dynamic and usually based on previously-determined correlations
- Generally, only one system can be examined at a time, thus overlooking possible diminishing returns

**Applicability to NZEH** RETScreen allows one to assess the potential for many different renewable energy and energy efficiency measures. However, this cannot be done in an integrated way. Also, passive solar capabilities are very limited.



## **11 APPENDIX B: DESIGN EXERCISE**

**Step 1** Starting the design with low window areas (WWR1 through WWR4 = 10%), minimal thermal mass, and the minimum allowable insulation values. Furthermore, the occupant behaviour (IG) parameter is set to low, corresponding to energy-conscious occupants.

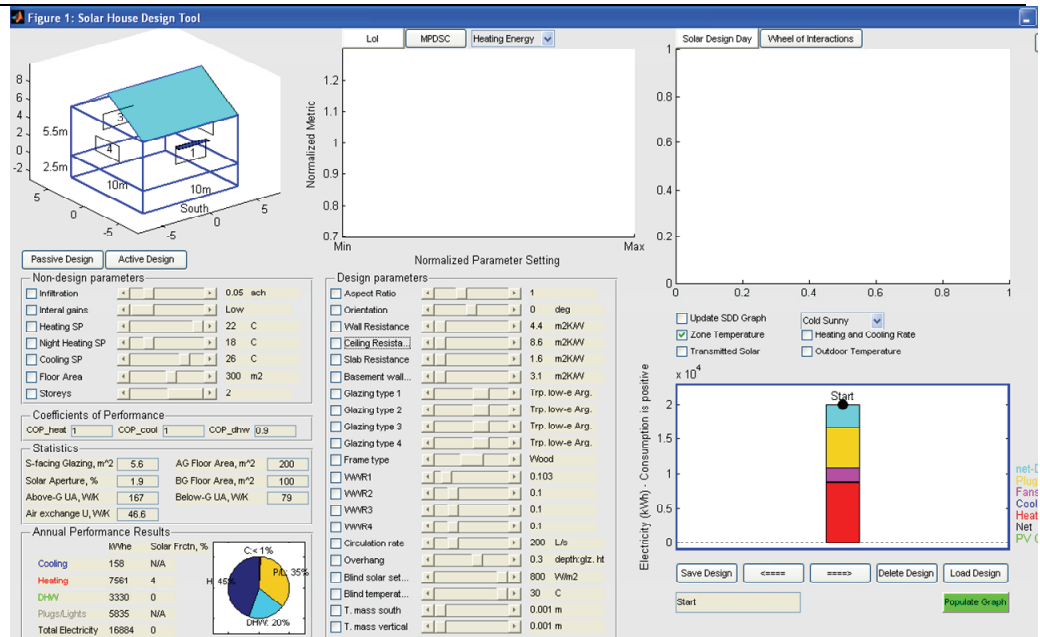
Heating and cooling setpoints were set to typical values. Similarly, infiltration was set to 0.05 ach (at normal conditions), resembling the air tightness of contemporary high-performance houses.

The house is constrained to being two-storey, having a total floor area (including basement) of 300 m<sup>2</sup>, and an aspect ratio of 1.

Note that the coefficients of performance for heating and cooling were left at 1. During design, the first priority will be given to reducing energy use by passive means. A higher COP, appropriate for a ground source heat pump, for instance, may be a practical way to further reducing electricity use.

The whole year simulation was run to assess the breakdown of annual energy use.

The results (in the DMS) show that heating energy is the single biggest use. DHW, plug, and lighting loads are also high, but are not addressed until later in design.



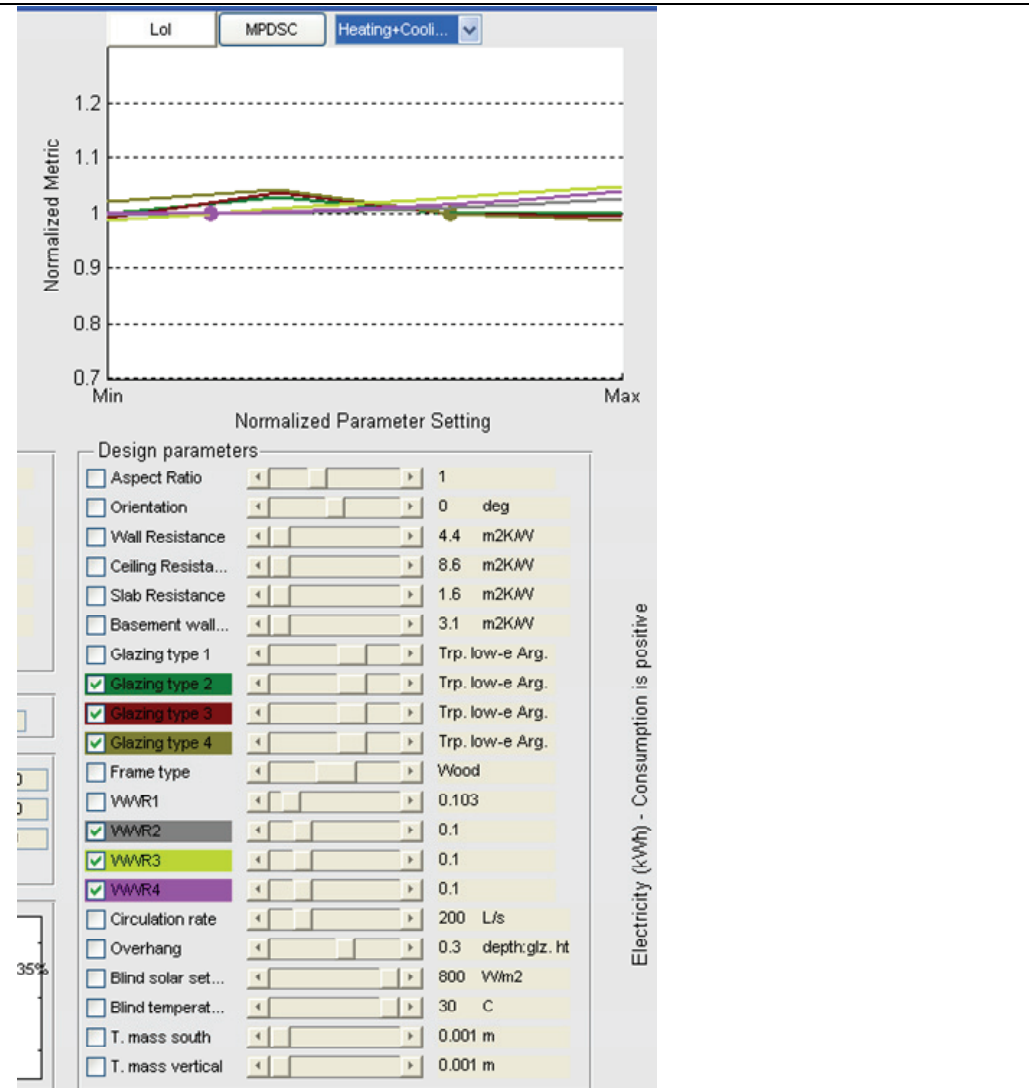


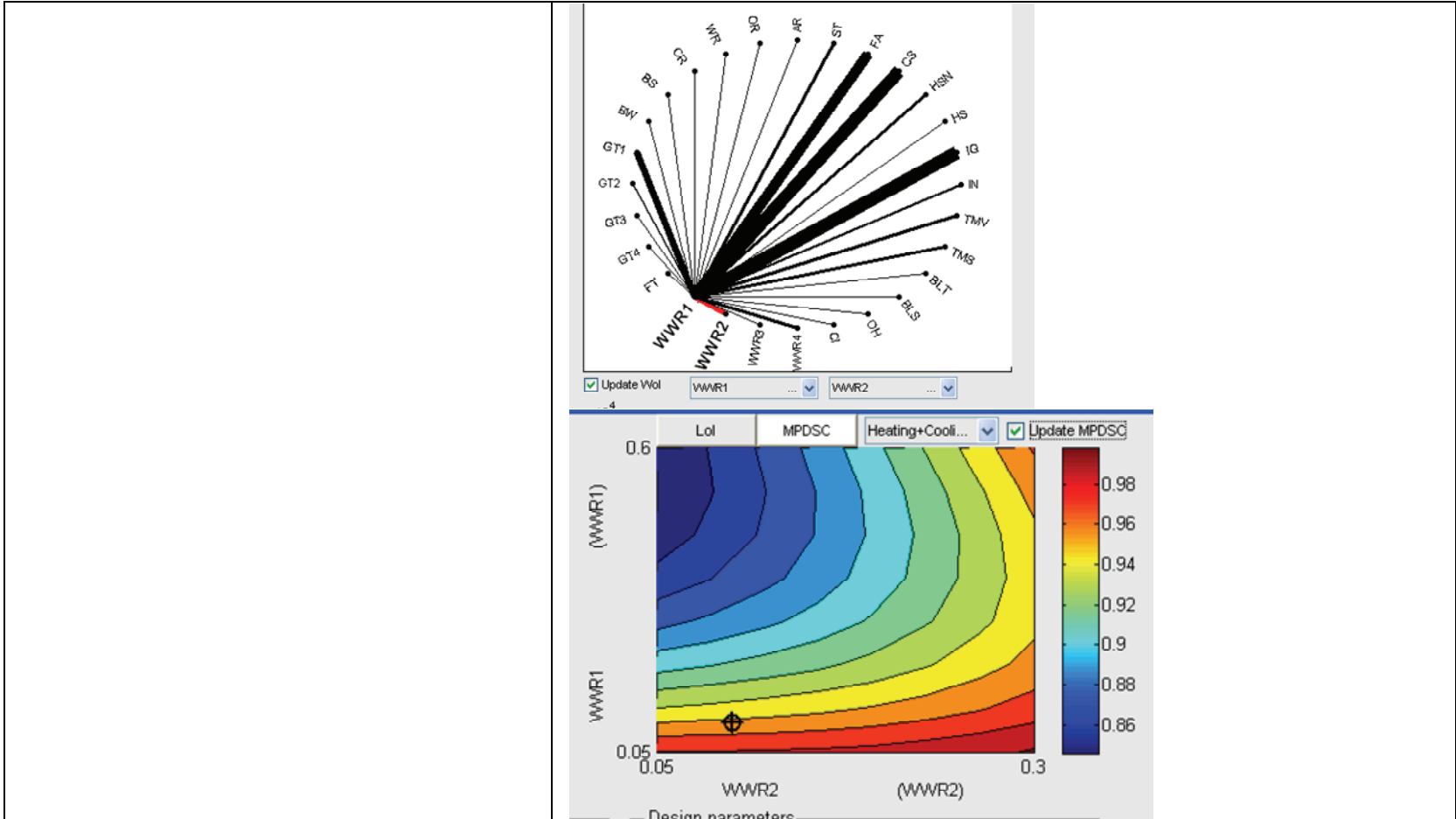
**Step 2** The Lol for the non-south facing window parameters (type and area) indicate that performance is not overly sensitive to them. However, WWR1 is currently only at 10%. A few different methods for understanding the current performance are to either look at the CS SDD or use a Wol to determine if there is a significant interaction between WWR1 and the non-south facing window parameters.

We will use both here to demonstrate their use. First of all, the Wol with WWR1 (at right, below) indicates strong interactions with WWR2 and WWR4. This tells us that we should not necessarily fix those values immediately and revisit them after (if) we change WWR1. The MPDSC for WWR1 and WWR2 shows that as WWR1 or WWR2 increase the optimal value of their counterpart decreases – an important result.

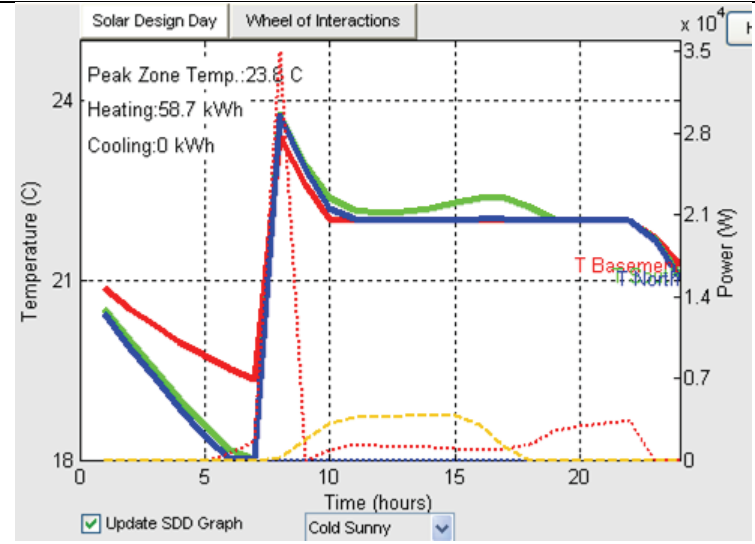
Finally, we use the cold sunny (CS) SDD to understand the dynamics of the house, diagnose problems, and look for opportunities for better performance. The CS SDD (at right, below) indicates relatively high heating energy use, almost no temperature swing and minimal solar gains.

All of the above facts point to the fact that a larger south facing window would be advantageous.

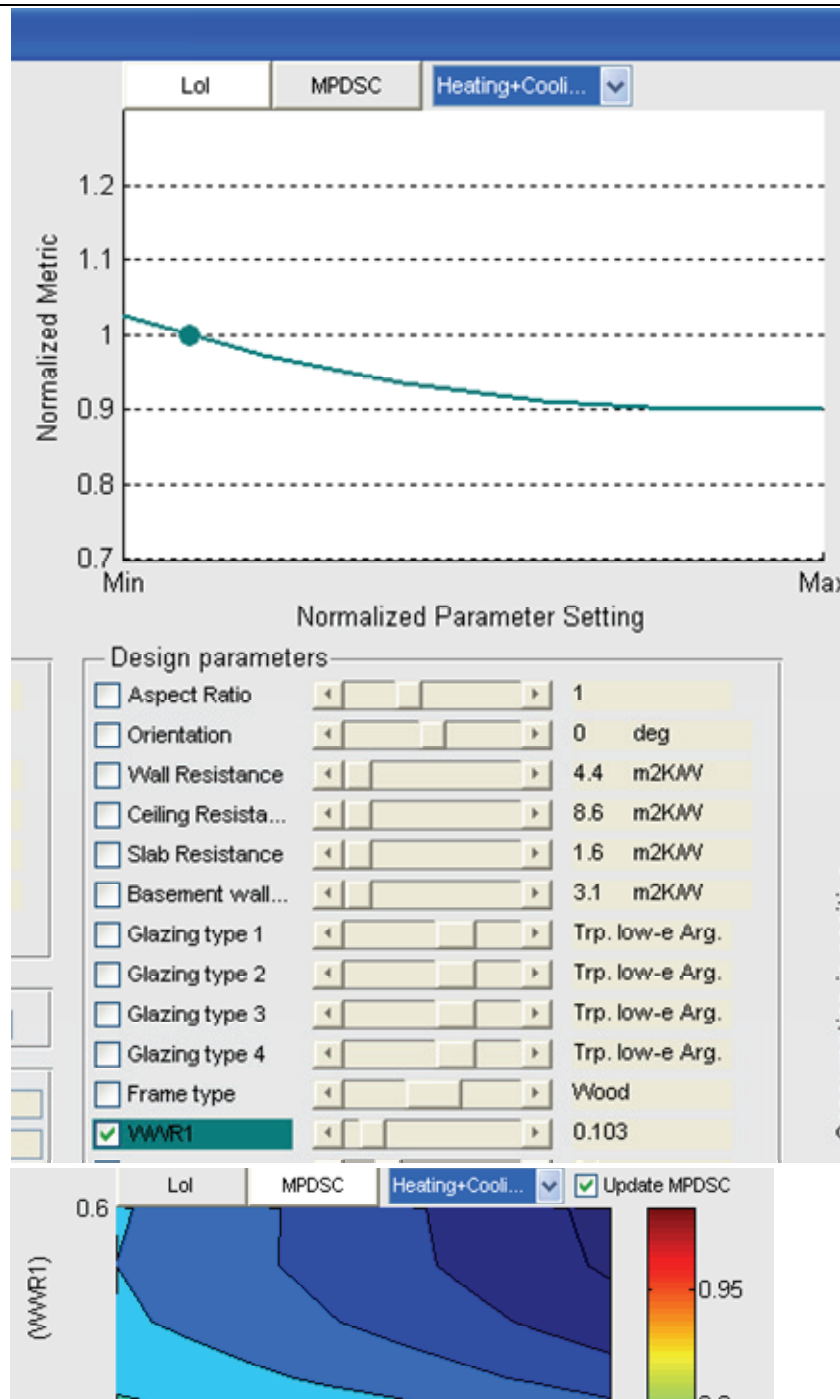








**Step 3** The Lol for WWR1 clearly indicates about 10% upside potential for a larger window. At about 50%, there is no further benefit. Although, this curve will change with the other parameters. As shown by the Wol for WWR1, it strongly interacts with the east and west-facing window parameters, the south-facing glazing type, and the thermal mass parameters. For example, when WWR1 and the thermal mass on the south zone floor are displayed in a MPDSC, the interaction is clear: thermal mass is not beneficial for small windows, but very beneficial for large ones. A similar result occurs for TMV (not shown).

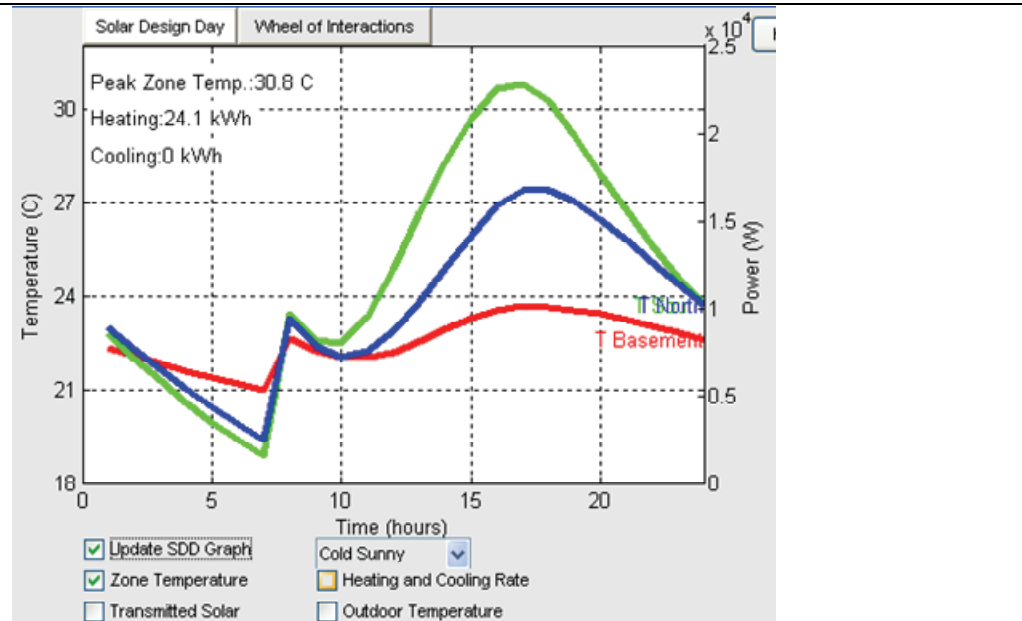


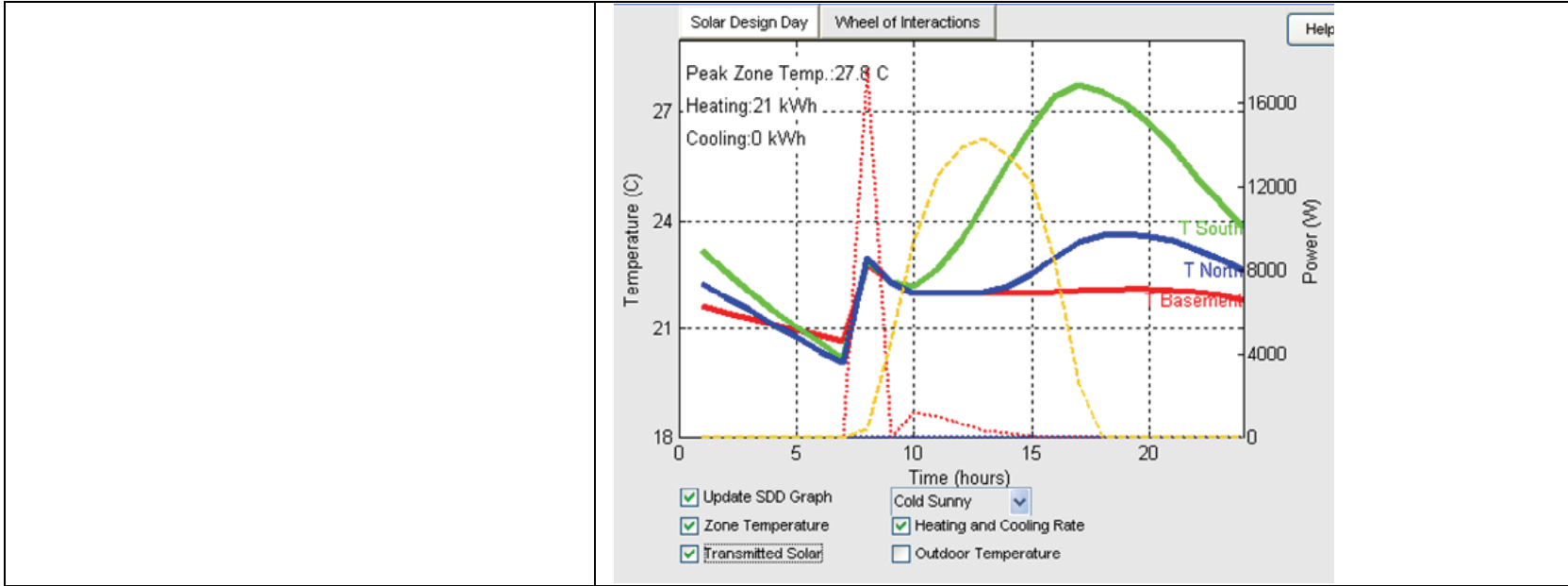
**Step 4** The CS SDD is used to understand the dynamics of the house when WWR1 is increased to 50%

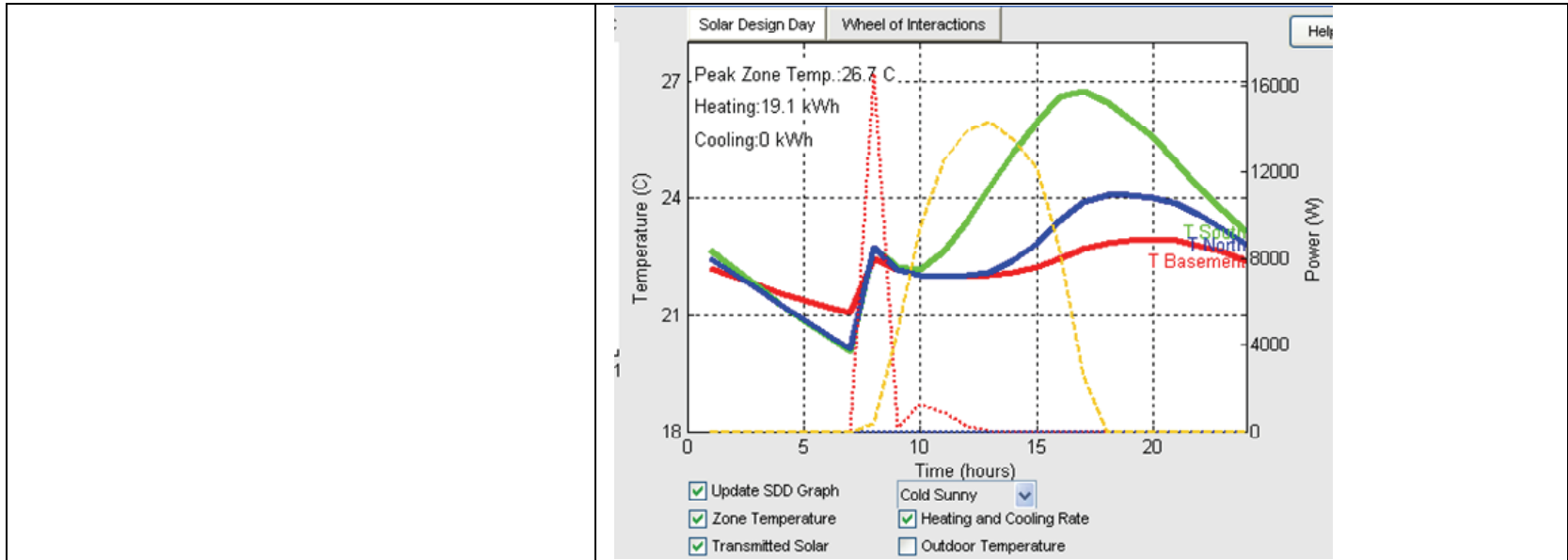
The result indicates fairly severe overheating. Next, the thermal mass parameters are each increased to 10cm. This is a robust and passive measure; making it particularly favourable. The result shows significantly less overheating and a 15% reduction in heating energy.

There is significant stratification between the zones. It would be beneficial to increase interzonal airflow. The airflow rate is increased to 1000 L/s. The resulting CS SDD shows that the peak temperature and heating energy are further reduced.

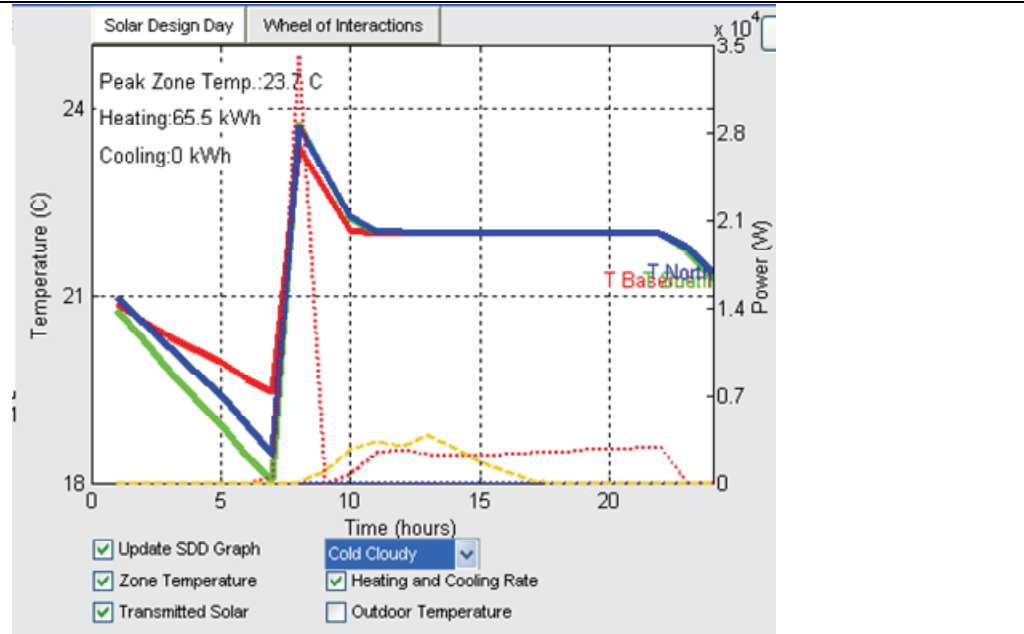
The fact that the passive and robust measures have been partially or fully-exploited and that the south zone still gets quite warm suggests that further increase of WWR1 is unwise.



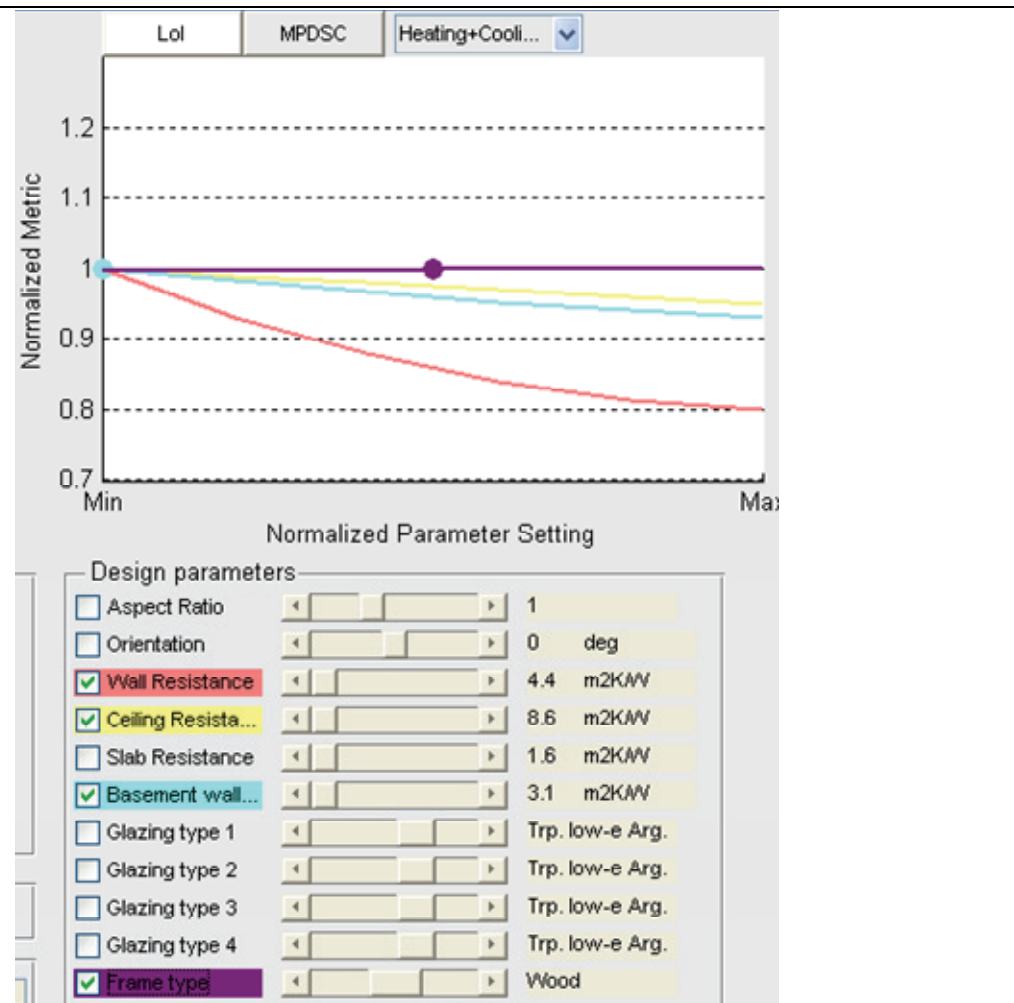


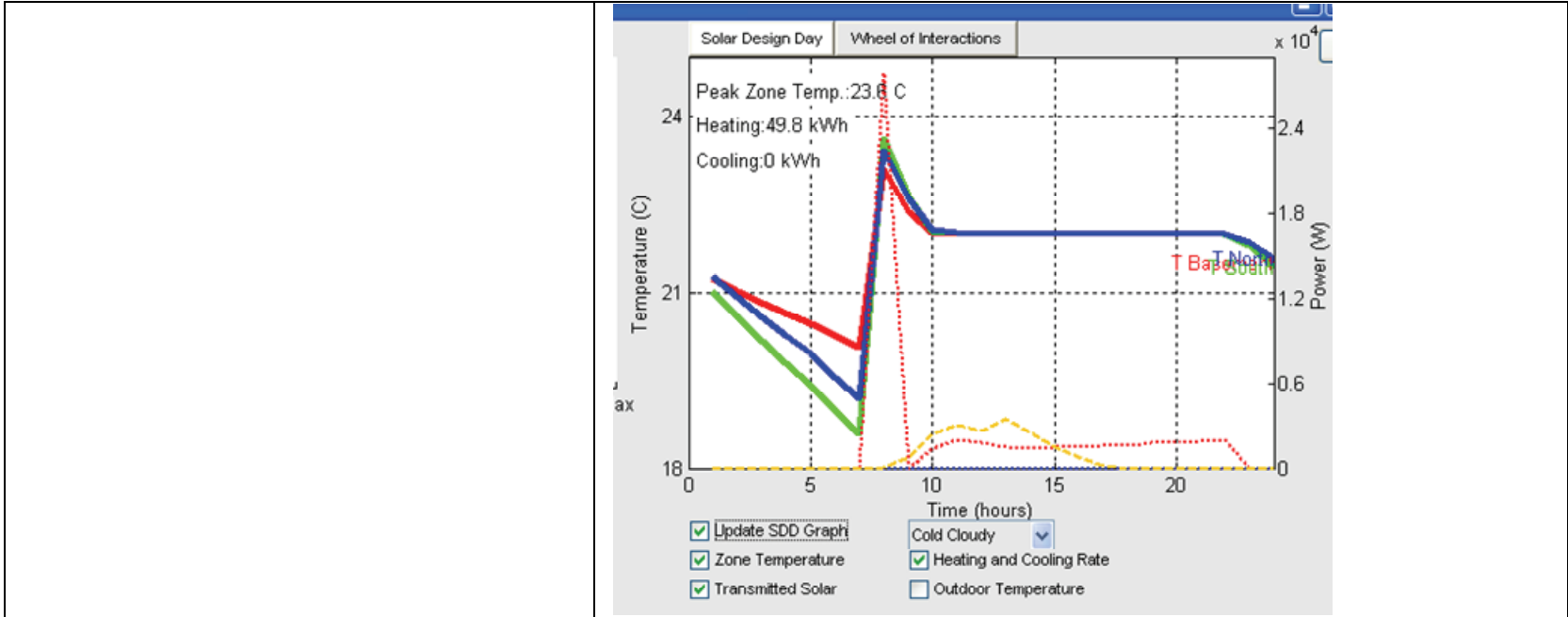


**Step 5** Next, the cold cloudy (CC) SDD in conjunction with the parametric tools are used to examine potential for further reducing the heating energy. The first CC SDD diagram shows the design as is. The heating energy is quite high because of the minimal solar gains. Since we want to avoid decreasing the WWR1, the remaining solutions include increasing the resistivity of the walls. Decreasing non-south facing window areas was previously decided against to ensure ample daylight. Increasing the window performance was also shown to not be significantly advantageous. Thus, we plot the insulation values and window frame type as Lol to determine the best opportunities. The Lol indicate that increasing wall insulation is by far the most beneficial. The frame type (under the current parameter settings) appears to be very insensitive. Since the wall insulation (WR) provides diminishing returns, we will upgrade it to about mid-way. The CS SDD (not shown) indicates that this reduces the heating energy by about 12%. To be more aggressive, the other insulation values are also increased to mid-way. At the cost of also reducing daylighting, the east and west-facing windows are reduced to 5%. (New SDD shown at right). The combined effect of these reduce the heating energy on the CC SDD by 33%. Upgrading the south facing window (GT1) to quad-glazed only reduced heating energy by about 2%, and it comes at the cost of lower solar gains under sunny conditions.



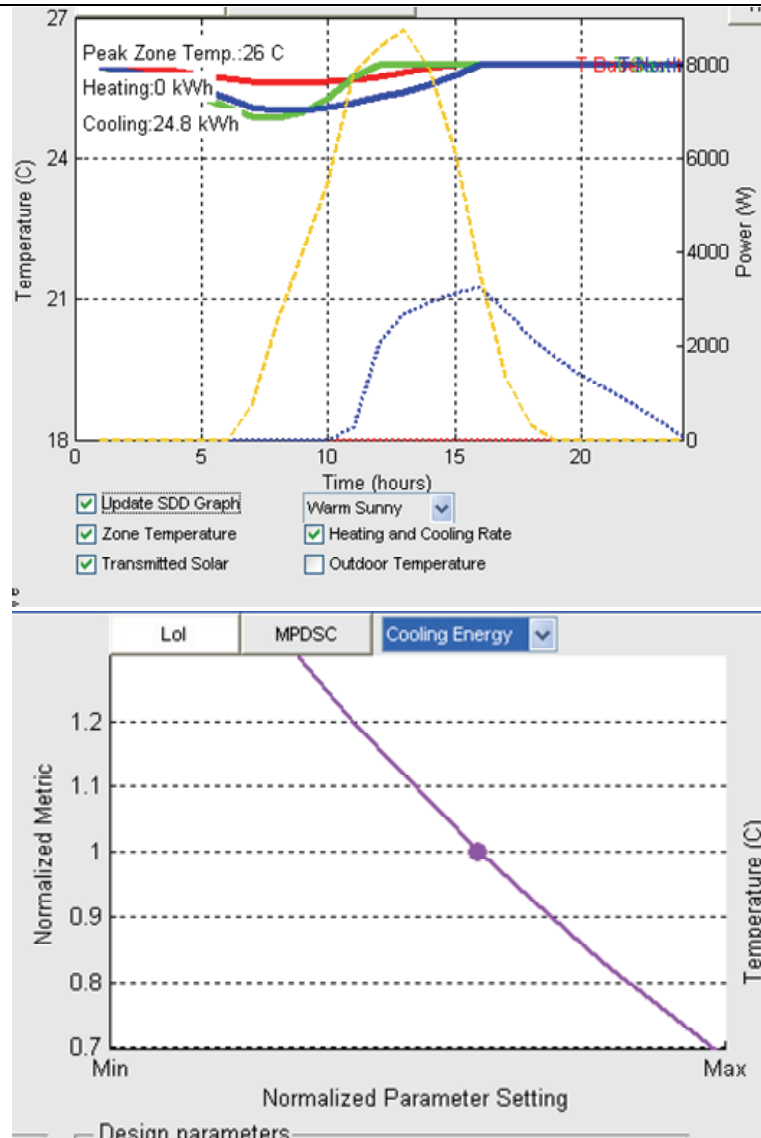
Finally, it is worth verifying that no new strong interactions with WRR1 have appeared after all of the changes; they have not.



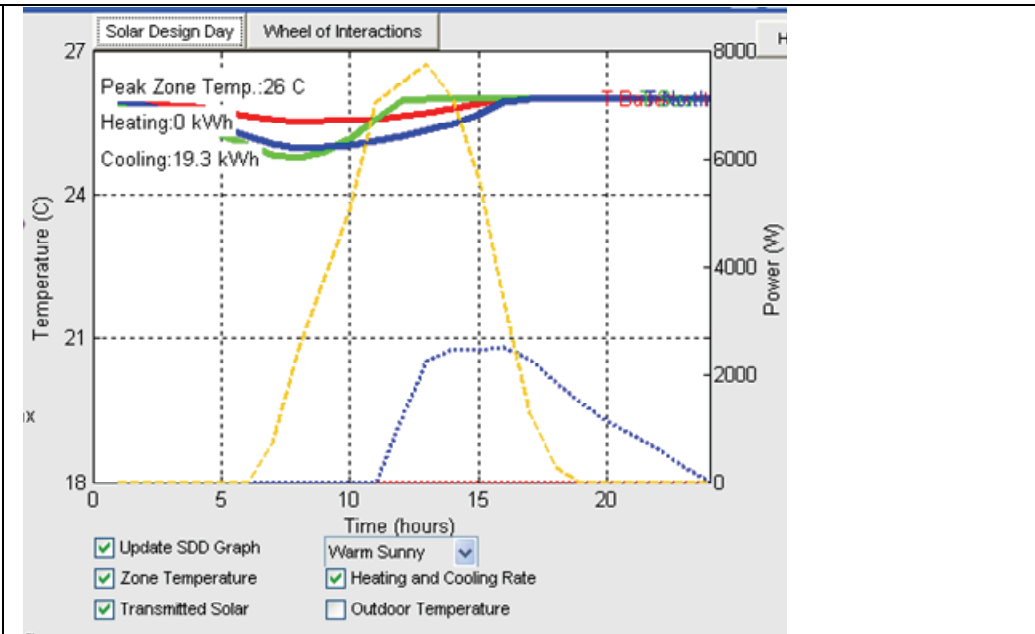


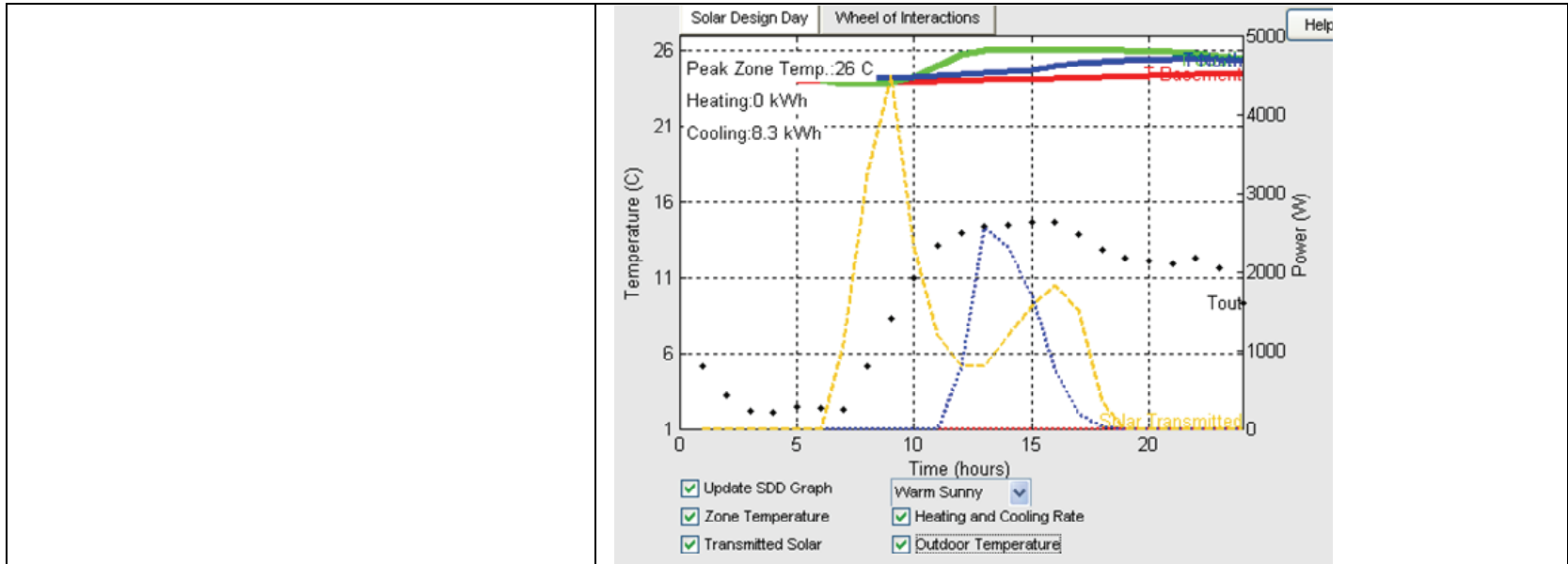


**Step 6** Next, we must ensure that the relatively large south-facing window does not cause major overheating. We shall use the WS SDD to diagnose overheating. As is, the house does admit a significant amount of adverse solar gains. The thermal mass has already been set to 10 cm. The air circulation has already been maximized. The remaining measures (assuming we leave the WWR1 as 50%) are to use the overhang or controlled shading devices. We start with the overhang because it is passive and likely more cost-effective. The Lol for the overhang (cooling energy only) indicates a deeper overhang offers a lot of potential. Refreshing the WS SDD with a maximized overhang reveals a 20% reduction in cooling energy – a respectable amount for such a simple measure. The remaining strategy is to modify the controls for window shades to close under conditions in which we expect the house to overheat. Plotting the outdoor air temperature gives hints about the appropriate value of BLT; we want to close the shades when the outdoor temperature is above 10-15°C because that is when the cooling starts being required. However, we would not want this to occur on a cloudy day, so a value of BLS must be carefully selected to only be triggered on days where some solar gains occur. 200 W/m<sup>2</sup> is considered a reasonable starting point. The CS SDD is checked (not shown) to reveal that the shades are not triggered to close on either of the

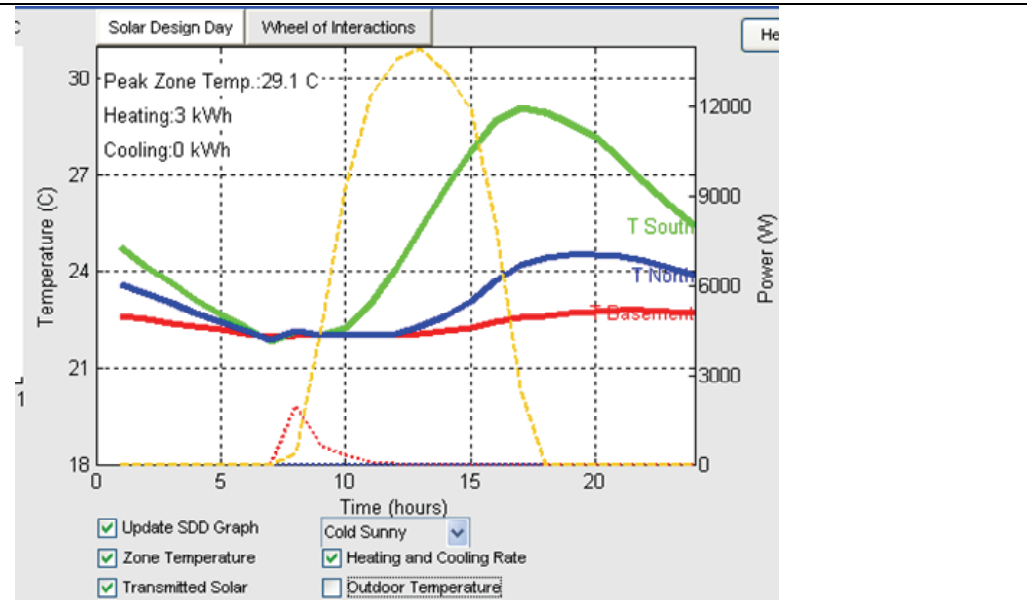


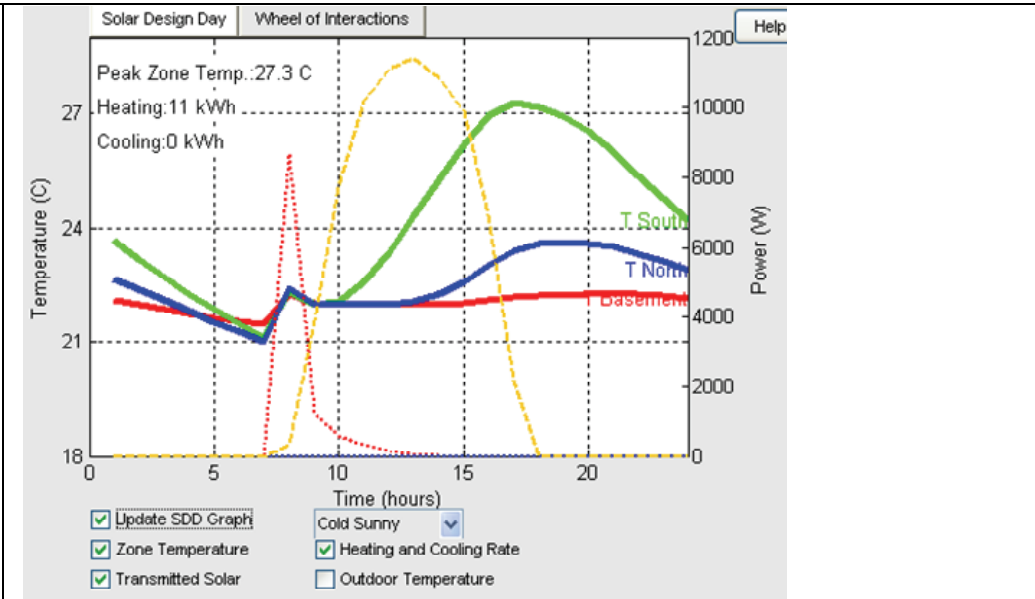
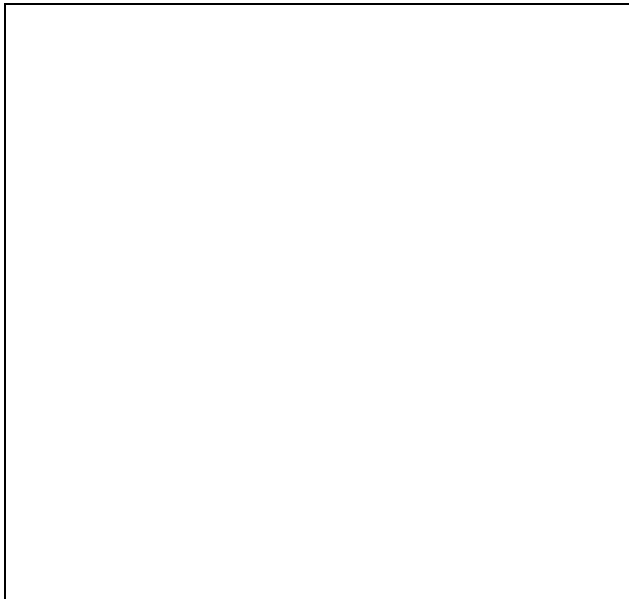
cold SDDs, when we want to maximize solar gains.





**Step 7** Since we have upgraded the envelope, overheating may have become an issue since we last examined the CS SDD. Thus, to complete the passive solar element of the design, we refresh the CS SDD. Unfortunately, the space now reaches a temperature that would normally be deemed too high. The remaining option is to incrementally decrease WWR1. When WWR1 is reduced to 40%, the south zone reaches 27.3°C, but only for a brief period. We will assume that this is acceptable. Unfortunately, this comes at the cost of a higher heating load; though it is still quite low.





**Step 8** Though, further opportunities were demonstrated for potential improvement to passive solar performance, we will move forward to active solar systems because the remaining opportunities may not be cost-effective or practical.

We start with a SDHW system, since the DHW energy was previously shown to be quite high. Incrementally increasing the number of solar thermal panels showed significant diminishing returns and barely any improvement above 2. Similarly, increasing tank size shows diminishing returns; so much so that there was found to be little benefit to having larger than the minimum sized tank (200L). The house is left at its south-

**Roof Geometry**

Roof type: Gable  
 Roof slope: 35 deg

Building-integrated Photovoltaic System

Number of Modules: 0  
 PV cell type: Amorphous  
 Nominal Efficiency (%): 6  
 Temperature Coefficient (%/K): 0.4  
 Inverter Efficiency (%): 90  
 Vertical Dimension (m): 1  
 Horizontal Dimension (m): 1  
 Vertical Spacing (m): 0.1  
 Horizontal Spacing (m): 0.1  
 Annual PV Gen. (kWh): 0

**Solar Thermal System**

Number of Panels: 2  
 Tank Volume (L): 200  
 Annual Output (kWh): 2456

**Solar Collector Layout**

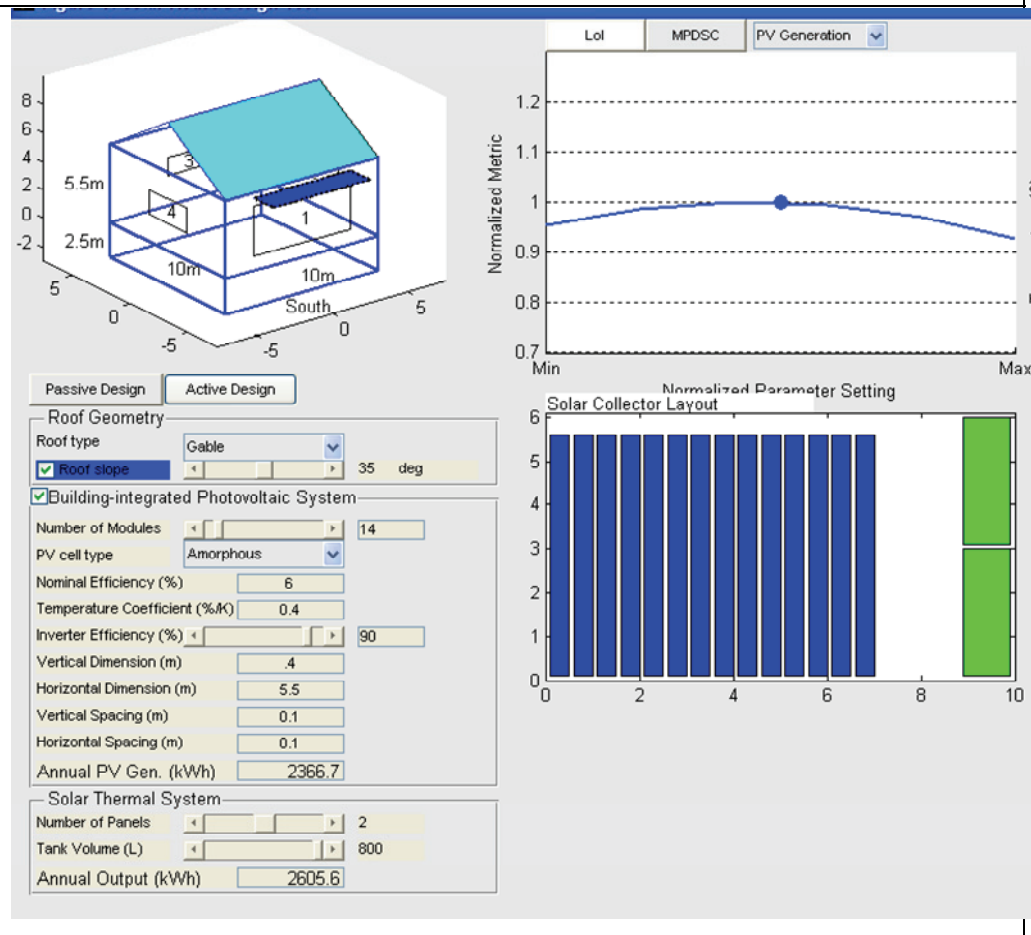
facing orientation. Performance of the SDHW system was found to be relatively insensitive to roof slope and thus it is left at 35°. The solar fraction for SHDW system is 78%.

**Step 9** Since there was not a specific objective imposed on the performance of the PV system, nor was there a net energy objective imposed on the house, we apply common sense and practical consideration to achieve a relatively high performance PV system.

Once a single PV module is installed, the Lol for slope and orientation can be viewed. The Lol for slope indicates that the roof was already in the near optimal range. This gives us the freedom to choose a slope (within reason) that leads to good architectural integration of the PV modules. The electrical constraints must also be considered. The inverter efficiency is given a relatively conservative value of 90% before a specific product is selected.

For this house, UniSolar PL144 PV modules were selected. The Fronius IG3000 was selected as the inverter. Specifications are given (at right, below). The number of modules has to be carefully selected such that all electrical rules are adhered to. An array of all possible configurations shows that only three are electrically possible.

Furthermore only one – with 18 modules – can fit on the current roof. Therefore, that configuration is selected.



Fronius IG	IG 2000	IG 3000	IG 2500-LV
<b>DC Input Data</b>			
Recommend PV power	1500 - 2500 Wp	2500 - 3300 Wp	1800 - 3000 Wp
Max. DC input voltage	500 V	500 V	500 V
Operating DC voltage range	150 - 450 V	150 - 450 V	150 - 450 V
Max. usable DC input current	13.6 A	13.6 A	13.6 A
<b>AC Output Data</b>			
Max. Output power @ 40°C	2000 W	2700 W	2350 W
Nominal AC output voltage	240 V	240 V	208 V
Utility AC voltage range	212 - 264 V (240 V + 10% / -12%)		183 - 227 V
Maximum AC current	8.35 A	11.25 A	11.25 A
Max. utility back feed current	0.0 A	0.0 A	0.0 A
Operating frequency range	59.3 - 60.5 Hz (60 Hz nom)		
Total Harmonic Distortion THD	<5%		
Power Factor (cos phi)	1		
<b>General Data</b>			
Max. Efficiency	95.2%	95.2%	94.4%
Consumption in stand-by	< 0.15 W (night)		
Consumption during operation	7 W		
Enclosure	NEMA 3R		

### Electrical Specifications

#### STC

(Standard Test Conditions)  
(1000 W/m<sup>2</sup>, AM 1.5, 25 °C Cell Temperature)

Maximum Power ( $P_{max}$ ): 144 W  
Voltage at Pmax ( $V_{mp}$ ): 33.0 V  
Current at Pmax ( $I_{mp}$ ): 4.36 A  
Short-circuit Current ( $I_{sc}$ ): 5.3 A  
Open-circuit Voltage ( $V_{oc}$ ): 46.2 V  
Maximum Series Fuse Rating: 8 A

#### Temperature Coefficients

(at AM 1.5, 1000 W/m<sup>2</sup> irradiance)

Temperature Coefficient (TC) of  $I_{sc}$ : 0.001/°K (0.10%/°C)  
Temperature Coefficient (TC) of  $V_{oc}$ : -0.0038/°K (-0.38%/°C)  
Temperature Coefficient (TC) of  $P_{max}$ : -0.0021/°K (-0.21%/°C)  
Temperature Coefficient (TC) of  $I_{mp}$ : 0.001/°K (0.10%/°C)  
Temperature Coefficient (TC) of  $V_{mp}$ : -0.0031/°K (-0.31%/°C)  
 $y = y_{reference} \cdot [1 + TC \cdot (T - T_{reference})]$

#### NOCT

(Nominal Operating Cell Temperature)  
(800 W/m<sup>2</sup>, AM 1.5, 1 m/sec. wind)

Maximum Power ( $P_{max}$ ): 111 W  
Voltage at Pmax ( $V_{mp}$ ): 30.8 V  
Current at Pmax ( $I_{mp}$ ): 3.6 A  
Short-circuit Current ( $I_{sc}$ ): 4.3 A  
Open-circuit Voltage ( $V_{oc}$ ): 42.2 V  
NOCT: 46 °C

<b>PV</b>		
Pmod	144	W
Vmpp	33	V
Voc	46.2	A
Imod	4.36	A
<b>Inverter</b>		
Power	2500 - 3300	W
Vmin	150	V
Vmax	450	V
Imax	13.6	A



		Modules/string									
		1	2	3	4	5	6	7	8	9	10
Strings	1	0	0	0	0	0	0	0	0	0	0
	2	0	0	0	0	0	0	0	0	1	0
	3	0	0	0	0	0	1	1	0	0	0
	4	0	0	0	0	0	0	0	0	0	0
	5	0	0	0	0	0	0	0	0	0	0
	6	0	0	0	0	0	0	0	0	0	0
	7	0	0	0	0	0	0	0	0	0	0
	8	0	0	0	0	0	0	0	0	0	0
	9	0	0	0	0	0	0	0	0	0	0
	10	0	0	0	0	0	0	0	0	0	0

Passive Design  Active Design

**Roof Geometry**

Roof type:

Roof slope:  deg

Building-integrated Photovoltaic System

Number of Modules:

PV cell type:

Nominal Efficiency (%):

Temperature Coefficient (%/K):

Inverter Efficiency (%):

Vertical Dimension (m):

Horizontal Dimension (m):

Vertical Spacing (m):

Horizontal Spacing (m):

Annual PV Gen. (kWh):

**Solar Thermal System**

Number of Panels:

Tank Volume (L):

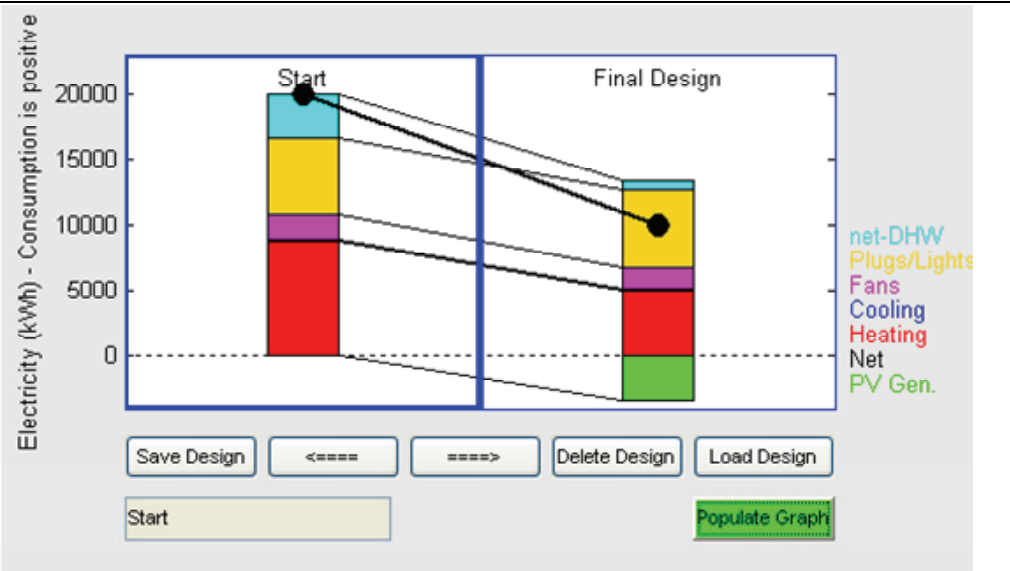
Annual Output (kWh):

Normalized Parameter Setting

Solar Collector Layout

Module Index	Normalized Value
1	5.5
2	5.5
3	5.5
4	5.5
5	5.5
6	5.5
7	5.5
8	5.5
9	5.5
10	3.0
11	2.0

**Step 10** After the design is finalized, we rerun the whole year simulation using the DMS facility. The result shows that major savings were achieved in heating energy and DHW energy, though cooling energy and the fan energy increased slightly. The net energy was nearly halved.



## 12 APPENDIX C: WINDOW HEAT BALANCE STUDY

Significant information can be obtained from calculating the heat balance of a window since passive solar heating is premised on the fact that windows have a net heat gain during the heating season<sup>10</sup>. The instantaneous net heat gain through a window can be calculated using Equation C-1. Note that the U-value and SHGC can be either for glazing sections alone or entire windows. The latter is more appropriate for gauging real performance.

$$Q = I \cdot \text{SHGC} - (T_{\text{in}} - T_{\text{out}})U \quad (\text{C-1})$$

To determine seasonal net energy through a window, Equation C-1 can be integrated over a period of time. O'Brien et al (2010c) found an appropriate balance temperature (temperature at which no heating or cooling is required in a house) to be 12°C for passive solar houses, such as the ÉcoTerra house. Using this value, the heating and cooling degree hours for Toronto are shown in Figure 12-1. For this study, the heating season is assumed to last from November to April, inclusive; the cooling season is assumed to last from June to August, inclusive. May, September, and October are shoulder periods in which both heating and cooling energy are both very low. The indoor temperature was assumed to be 21°C for all analyses.

---

<sup>10</sup> Technically, glazing should only be expected to have a higher heating season net heat gain than the opaque walls, because even highly-insulated walls have some heat loss.

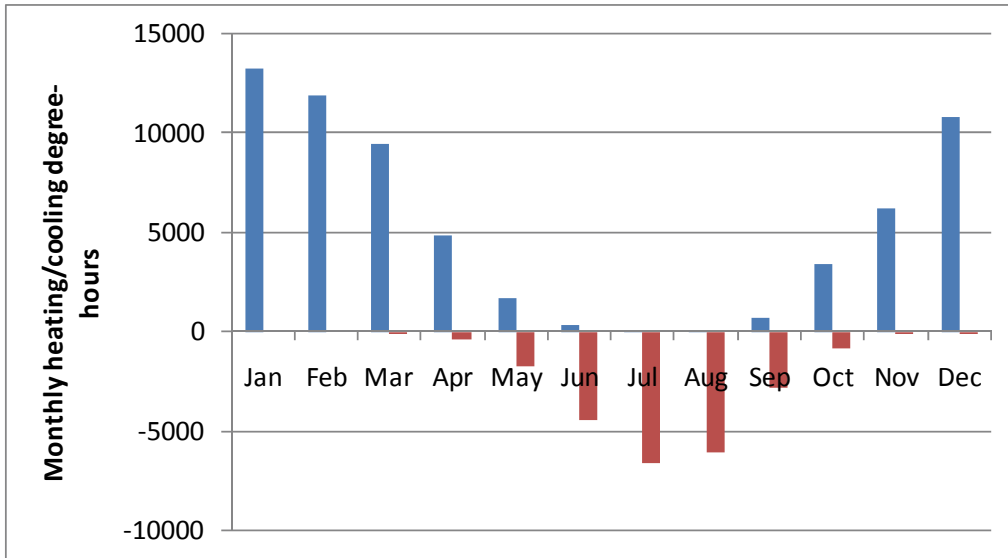


Figure 12-1: heating and cooling degree-hours for Toronto with a balance point of 12°C

The monthly incident solar radiation on vertical surfaces in all directions in Toronto is shown in Figure 12-2. This graph clearly illustrates the mechanics of passive solar heating: solar radiation on the near-south facing surfaces peaks in winter months and actually dips in the summer months. However, note that September violates this and April nearly violates this. This is the cause of shoulder period overheating in passive solar houses.

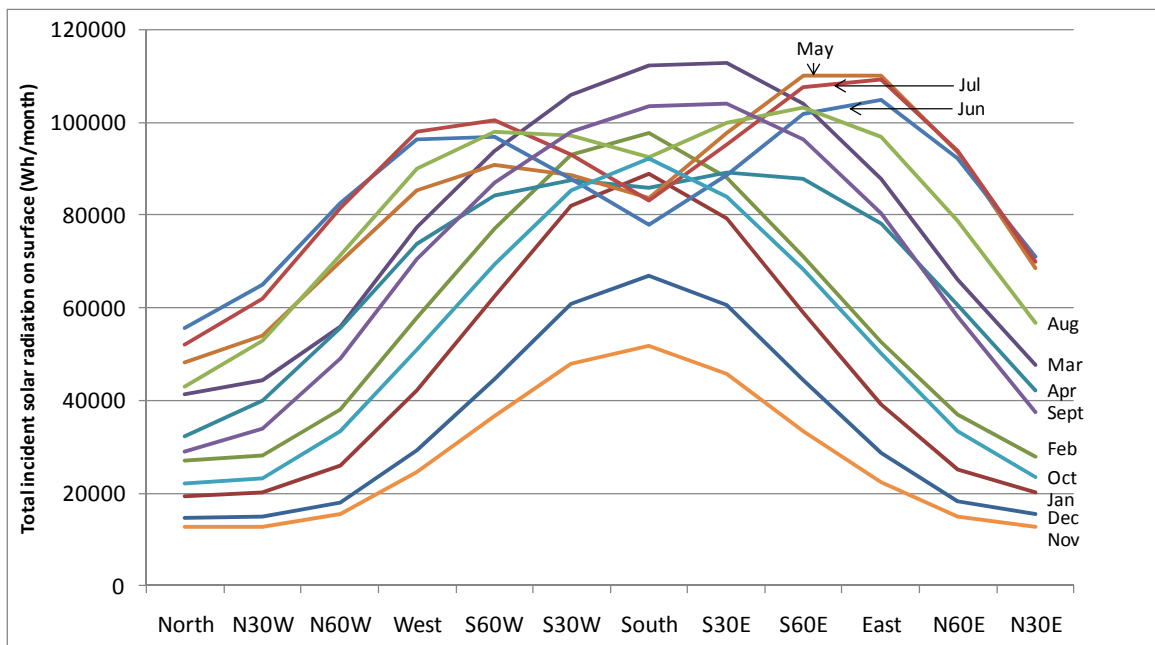


Figure 12-2: Monthly incident solar radiation on vertical surfaces in 30-degree increments

Figure 12-3 shows the total solar radiation incident on vertical surfaces of all orientations differentiated by the heating and cooling seasons. It clearly indicates that south-facing surfaces receive the most solar radiation in the heating season relative to that in the cooling season. This graph does not show the complete picture because, as mentioned, net heat transfer through windows is based on both solar radiation and temperature difference.

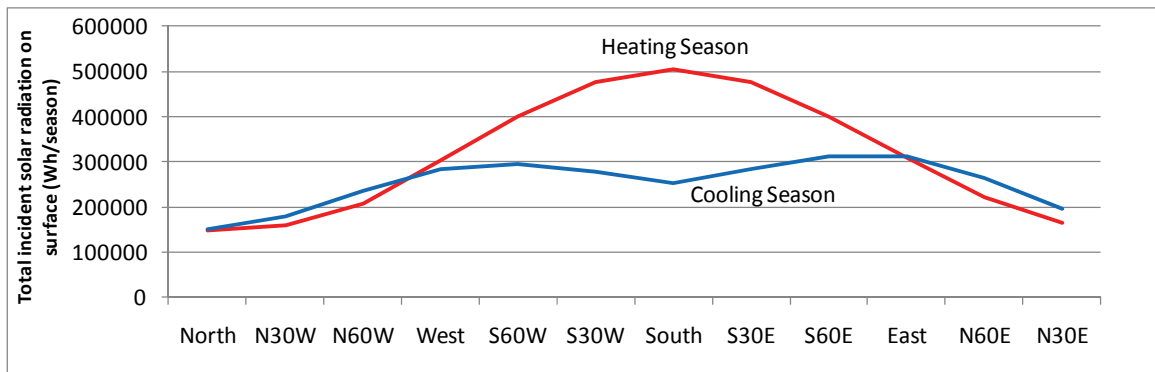


Figure 12-3: Total solar radiation incident on surfaces during the heating and cooling seasons

Combining the solar and temperature data, one can approximate the heat balance for a window during the heating and cooling seasons. The following figures show the net heat gain (or loss when negative) during the heating season in Toronto for a wide range of SHGCs and U-values. Also, the locations of several common glazing types are shown – both with and without a wooden frame. The windows are assumed to be 1.2 by 1.5 m, measured from the outside of the frame. The results are premised on the fact that unwanted solar heat gains are rejected during the non-heating season. Furthermore, it is assumed that all heating season solar heat gains are useful. Thus, the net heat gain values represent the maximum possible reduction of purchased heating.

Since the ultimate choice in sizing windows is between window and opaque insulated wall, window performance should be compared to wall performance. That is, it is more appropriate to use the heat loss of an opaque wall than 0 heat loss. Thus, in each of the figures, the heat loss during the heating season for walls that are RSI-4.4 and RSI-8.8. These walls sections lose about 20 and 10 kWh/m<sup>2</sup>/heating season, respectively.

The results indicate that all window types, oriented south-ward, except for single glazing, have positive net heat gains during the heating season. The triple-glazed, low-e, argon-filled window actually performs better than the quad-glazed window. This suggests that the additional cost of quad-glazing is not justified, as also concluded by Charron (2007). For all other orientations, at least two of the window types have net

heat losses. For the north orientation, only the quad-glazing, without a frame has a net heat gain, though it is marginal.

These graphs assist in selecting the optimal glazing type, which is usually not the best U-value or SHGC individually, but rather the best combination. Furthermore, the effect of the frame and window orientation is evident. However, this cannot replace the utility of a whole-year simulation, which identifies usefulness of solar gains, thermal comfort, cooling repercussions, and shading strategies.

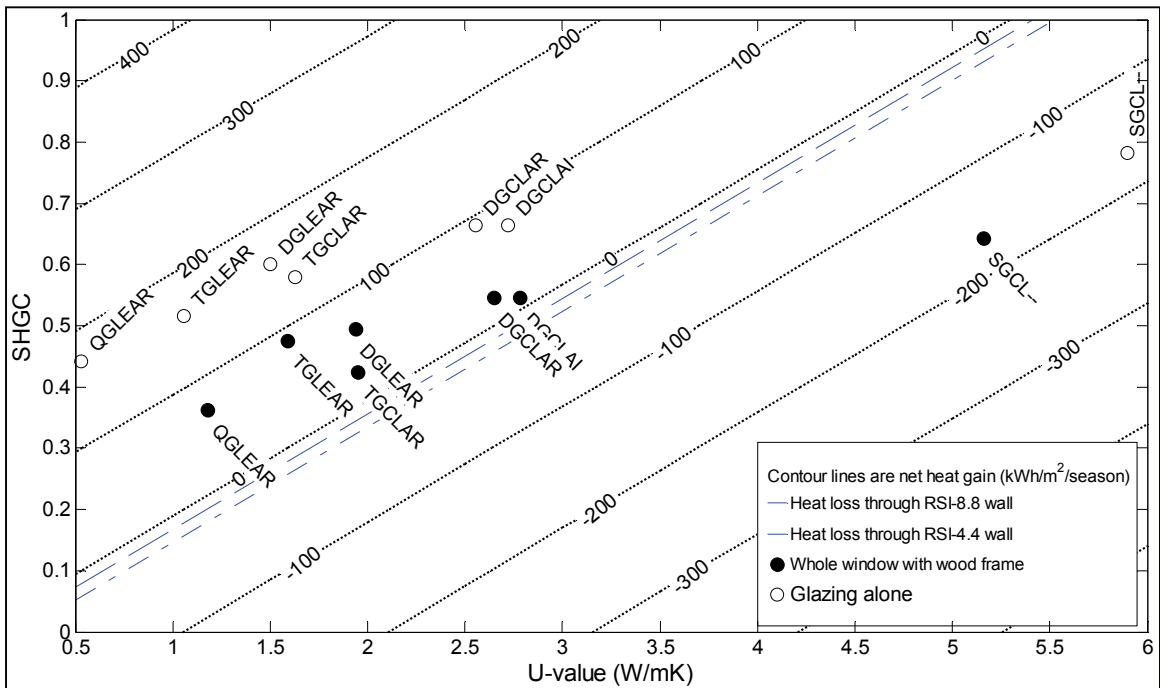


Figure 12-4: Net heat gain during heating season for South-facing windows

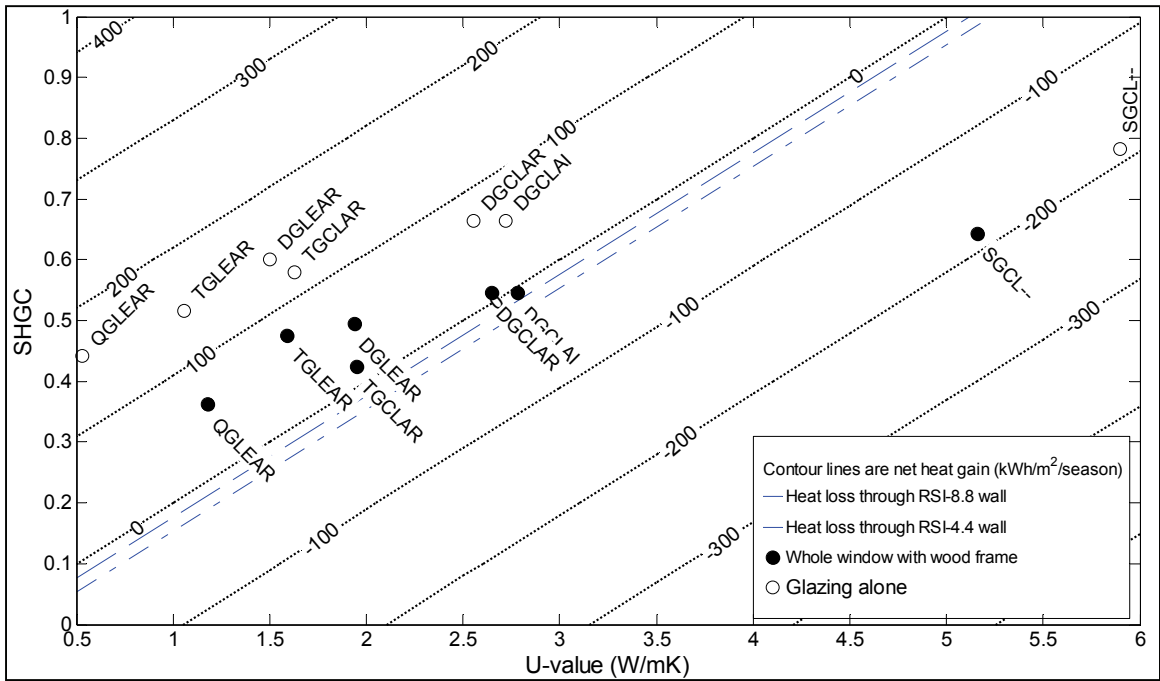


Figure 12-5: Net heat gain during heating season for S30E

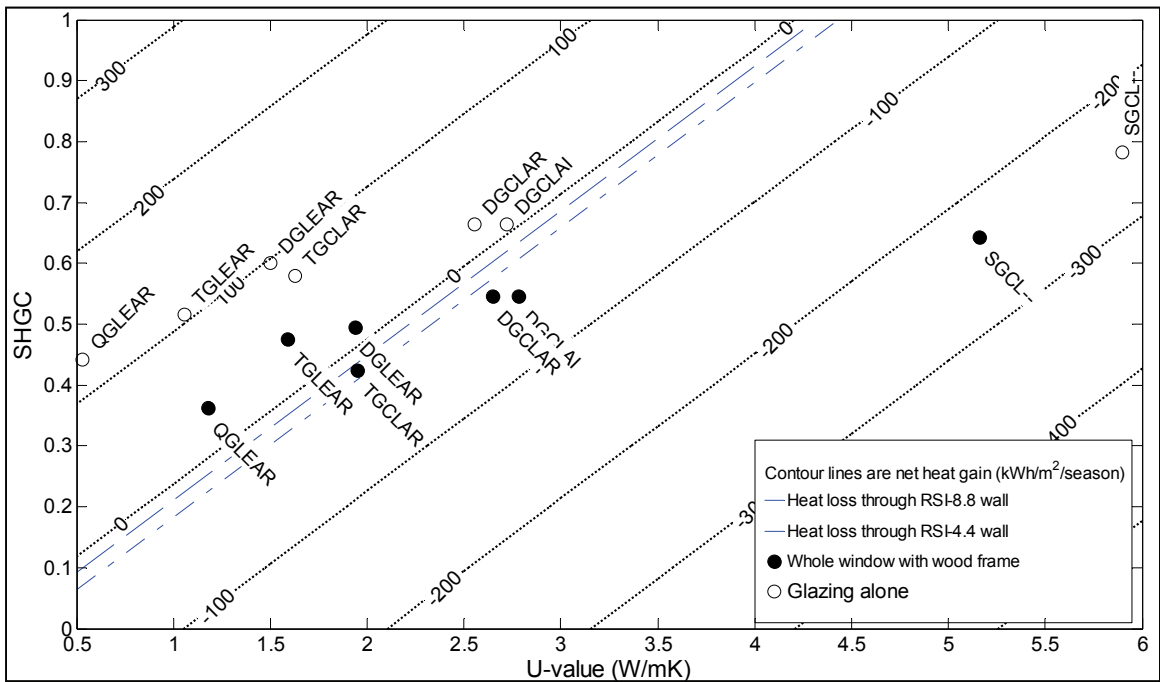


Figure 12-6: Net heat gain during heating season for S60E



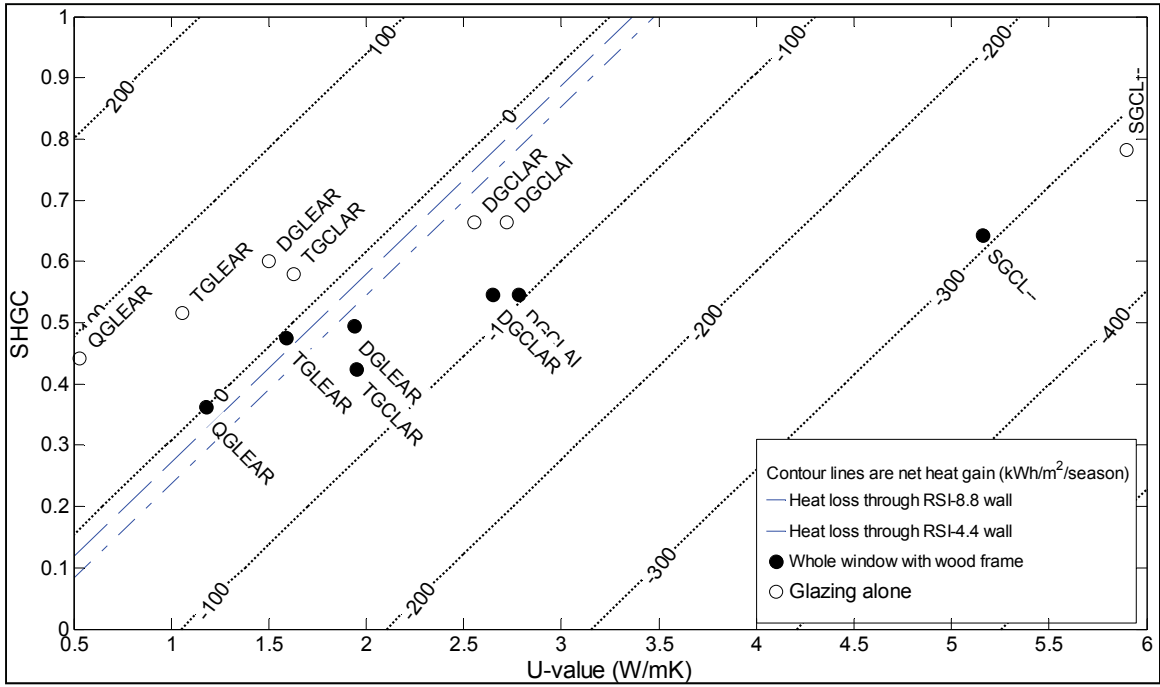


Figure 12-7: Net heat gain during heating season for East

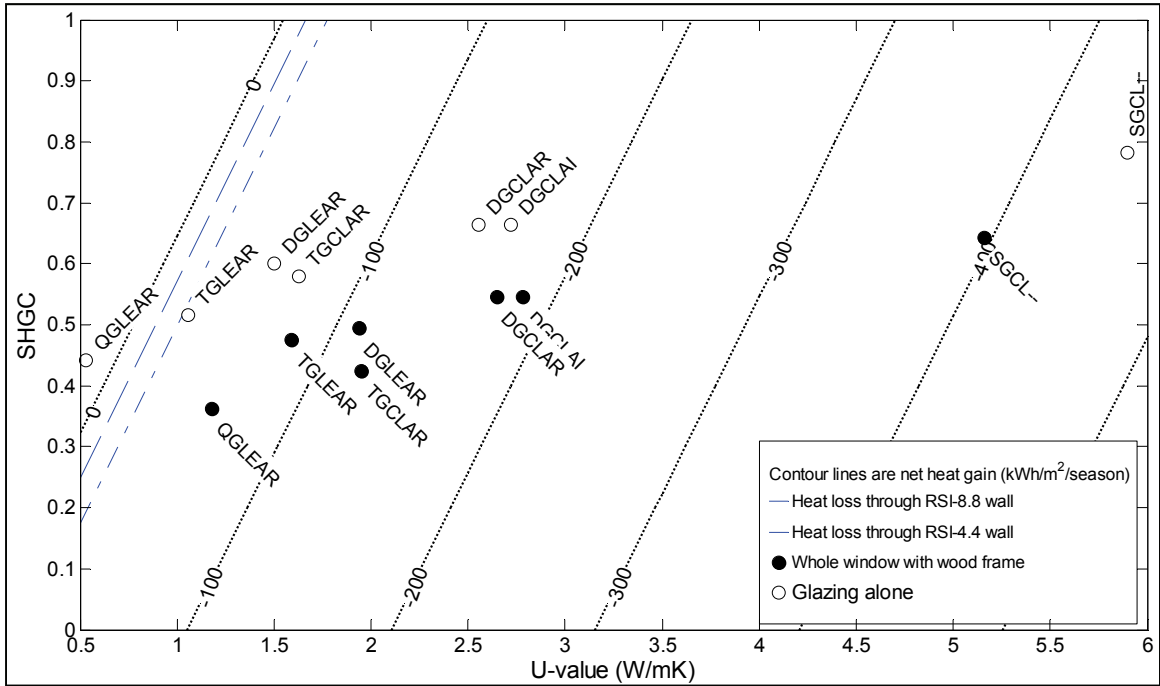


Figure 12-8: Net heat gain during heating season for North-facing windows

## 13 APPENDIX D: EXTENDED CALCULATIONS AND CODE

### 13.1 Detailed PV model calculations

The weather data used and reported by RETScreen International (2005) and shown in

Table 13-1.

*Table 13-1: Toronto Weather data from RETScreen*

<b>Month</b>	<b>Days/month</b>	<b>Horizontal solar radiation, Wh/m<sup>2</sup></b>	<b>Mean air temperature (°C)</b>
Jan	31	1440	-7.1
Feb	28	2220	-6.2
Mar	31	3360	-0.8
Apr	30	4500	6.3
May	31	5470	12.4
Jun	30	6000	17.4
Jul	31	6140	20.5
Aug	31	5140	19.5
Sep	30	3750	15.2
Oct	31	2470	8.9
Nov	30	1310	3.1
Dec	31	1000	-3.2

Duffie and Beckman (2006) suggest which day should be used to represent the month, although it falls on roughly the 15<sup>th</sup> day of the month. For each month, the mean solar declination, hour angle at sunrise/sunset, sunrise/sunset time, and extraterrestrial solar radiation are found with the following Equations.

$$\delta = 23.45^\circ \left( 2\pi \frac{284 + n}{365} \right) \quad (D-1)$$

$$\cos \omega_s = -\tan \psi \tan \delta \quad (D-2)$$

$$t_{\text{sunset}} = \omega_s / 15 \quad (D-3)$$

$$H_0 = \frac{86400 G_{sc}}{\pi} \left( 1 + 0.033 \left( 2\pi \frac{n}{365} \right) \right) (\cos \psi \cos \delta \sin \omega_s + \omega_s \sin \psi \sin \delta) \quad (D-4)$$

A clearness index for each month is defined as the actual amount of horizontal solar radiation as a fraction of the extraterrestrial solar radiation. This value is typically 0.3 to 0.6 for Canadian locations and is found with the following Equation.

$$\overline{K_T} = \frac{\overline{H}}{\overline{H_0}} \quad (D-5)$$

The Erbs et al. correlation is used to determine the ratio of diffuse to total solar radiation based on the monthly clearness index only (Duffie and Beckman, 2006). The ratio depends on whether the sunset hour angle is less than or greater than  $81.4^\circ$  as follows.

$$\frac{\overline{H_d}}{\overline{H}} = 1.391 - 3.560 \overline{K_T} + 4.189 \overline{K_T}^2 - 2.137 \overline{K_T}^3 \quad (D-6)$$

$$\frac{\overline{H_d}}{\overline{H}} = 1.311 - 3.022\overline{K_T} + 3.427\overline{K_T}^2 - 1.821\overline{K_T}^3 \quad (\text{D-7})$$

The hourly distribution of the total solar radiation is found with the following Equation.

$$r_t = \frac{\pi}{24} (a + b \cos \omega) \frac{\cos \omega - \cos \omega_s}{\sin \omega_s - \omega_s \cos \omega_s} \quad (\text{D-8})$$

$$a = 0.409 + 0.5016 \sin \left( \omega_s - \frac{\pi}{3} \right) \quad (\text{D-9})$$

$$b = 0.6609 + 0.4767 \sin \left( \omega_s - \frac{\pi}{3} \right) \quad (\text{D-10})$$

Similarly, the hourly diffuse portion of the solar radiation is found with the following Equation.

$$r_d = \frac{\pi}{24} \frac{\cos \omega - \cos \omega_s}{\sin \omega_s - \omega_s \cos \omega_s} \quad (\text{D-11})$$

It follows that the total horizontal, diffuse, and beam solar radiation are found by:

$$H = r_t \overline{H} \quad (\text{D-12})$$

$$H_d = r_d \overline{H_d} \quad (\text{D-13})$$

$$H_b = H - H_d \quad (\text{D-14})$$

The total solar radiation on the surface is the sum of the beam, diffuse, and ground-reflected solar radiation.

$$H_t = H_b R_b + H_d \left( \frac{1 + \cos\beta}{2} \right) + H\rho \left( \frac{1 - \cos\beta}{2} \right) \quad (\text{D-15})$$

From the average monthly weather data, hourly levels of diffuse and beam radiation are determined for the average day of each month. Since the incidence angle of solar beam radiation can be determined using geometrical relationships, the total amount of incident solar radiation on the PV panel for each hour of the average day of each month can be derived. To model the effect that snow has on ground reflectance (denoted  $\rho$ ), albedo is assumed to be 0.2 for months with average ambient temperatures of above 0°C, 0.7 for below -5°C, and interpolated for months in between.

The average module efficiency is determined by:

$$\eta_p = \eta_r [1 - \text{TC}(T_c - T_r)] \quad (\text{D-16})$$

Evans (1981) established an Equation to determine average solar cell temperature from local monthly ambient temperature and clearness index only, meaning that simultaneous Equations do not have to be solved. The average monthly operating temperature is calculated by:

$$T_c - T_a = (219 + 832\overline{K_T}) \frac{\text{NOCT} - 20}{800} \quad (\text{D-17})$$

The energy delivered by the PV array and to the house, respectively, are found by:

$$E_p = S(\text{AE})\overline{H_T} \quad (\text{D-18})$$

$$E_{grid} = E_p(IE)(1 - \lambda_{losses}) \quad (D-19)$$

The inverter efficiency ( $IE$ ) is modelled as being constant and is one of the BIPV system inputs. Miscellaneous losses, such as those from wiring, are assumed to be a constant 2%.

The accumulation of snow on solar collectors can have a detrimental effect on performance; affecting more than the covered area alone because the panel's current tends to be based on the worst-performing cell (GSES, 2004). Snow shedding can be promoted by increasing the roof slope, using smooth materials, and eliminating any construction details that create dams (e.g., eaves troughs). For the Montreal climate, experience has shown that slopes of at least 30° and preferably 40° are desirable. A major weakness of existing research is that no generalized relationships have been established for predicting snow shedding from BIPV. As shown by Figure 13-1 (right), snow shedding is unpredictable even under apparently identical conditions. For Ecos, if the designer chooses a shallower slope than 40°, annual performance can be approximated by assuming electricity generation varies linearly from zero if the roof is flat to nominal if the roof is sloped at 40°, for months when the average ambient temperature is below -5°C. The effect is shown in Figure 13-1 (left). The model uses this relationship. It is hoped that future experimental research will provide more accurate relationships for a variety of configurations, climates, and geometries. However, it is

best to merely use a sufficiently high slope that snow accumulation is an infrequent event.

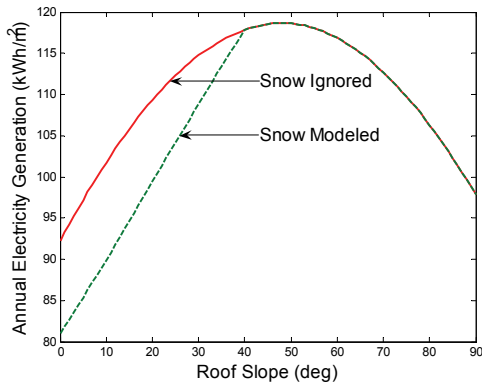


Figure 13-1: Modeling the effect of snow on annual performance (left); a photograph of ÉcoTerra after snowfall (right).

For this research, the algorithm was implemented in a MATLAB program. This allowed batch runs, sensitivity analysis, optimization, and a quantification of runtime to be performed. The total runtime was found to be about three milliseconds for a whole-year performance prediction. This is expected to be suitable for the implementation for Ecos, where quasi real-time feedback is desired. The equivalent runtime in TRNSYS and EnergyPlus was about 2 and 30 seconds, respectively.

A sensitivity analysis (first presented at the National Building Envelope Council Canada (NBEC) Conference 2009 (O'Brien et al., 2009b)) was performed to examine the effects of some of the critical model assumptions including ground reflectance, cell temperature, and the temperature coefficient. Two metrics were explored: optimal panel orientation and predicted electricity output. Of the two, the optimal panel orientation is considered to be much more critical. For grid-tied systems, slightly under

or over-predicted performance will lead to a difference of a few tens of dollars in annual utility bills – a value that is trivial relative the system’s capital cost. However, a sub-optimal orientation cannot be rectified after construction and will lead to a system that can never perform at its full potential.

For the sensitivity analysis, the model used to predict performance for roof slopes of 0 to 90° and azimuths from -90 to 90° in 1° increments in Ottawa. The PV was a 1 m<sup>2</sup> panel with a nominal efficiency of 7% and a temperature coefficient of 0.2%/K; typical for amorphous silicon panels.

As expected, the model showed that a south-facing roof is optimal for all sloped roofs, and is thus, not shown. The results are shown in Table 13-2. The last column represents the consequence of making incorrect assumptions (assuming the nominal assumptions are correct) and using the optimal slope. For example, if the ground reflectance is assumed 0.7 year-round, the optimal slope is 50 degrees. However, if this assumption is found to be incorrect (and the nominal assumptions correct), the optimal slope is 39 degrees. Under nominal conditions, the 50 degree slope performs 1.2% worse than the optimal slope. Higher ground reflectance assumptions lead to a higher optimal slope because this captures more reflected solar radiation (i.e., the view factor between the roof and ground is higher).

The sensitivity analysis shows that performance is relatively insensitive to the assumptions explored, with a maximum variation of about 8%. The performance is very



insensitive to roof slope in the near-optimal range. Even the more extreme assumptions do not misguide the designer significantly. This suggests that designers need only ensure the slope is within 10 to 15 degrees of optimal while ensuring architectural constraints are met. The same applies to the roof azimuth.

*Table 13-2: Summary of sensitivity analysis*

	Average Annual Output (kWh)	Change in Average Output	Optimal Slope (degrees)	Potential Consequence of assumption (%)
Nominal	96.76	-	39	-
$\rho = 0.2$ year-round	95.26	-1.6%	37	-0.036%
$\rho = 0.5$ year-round	100.5	3.9%	44	-0.171%
$\rho = 0.7$ year-round	104.0	7.5%	50	-1.234%
$\rho_{\text{no\_snow}} = 0.2;$ $\rho_{\text{snow}} = 0.9$	97.07	0.3%	40	-0.018%
Cell temp.: + 10°C	94.43	-2.4%	39	0.000%
Cell temp.: + 20°C	92.89	-4.0%	38	-0.009%
Cell temp.: + 20°C and $\beta = 0.4\%/K$	88.68	-8.4%	39	0.000%

### 13.2 Whole envelope conductance

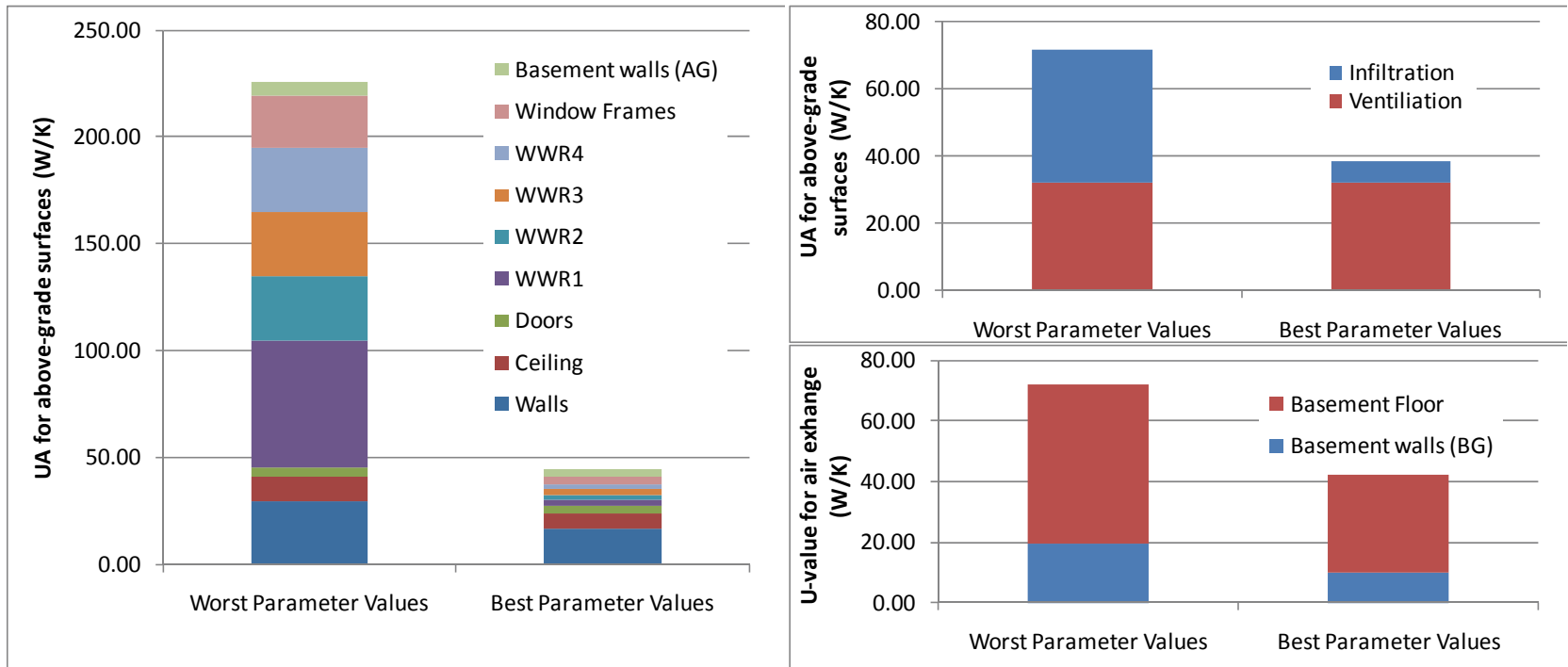


Figure 13-2: Example heat loss values for (clockwise, starting with left): the above-grade envelope, below-grade envelope, and air exchange. Note that “Worst parameter values” refers to all parameters being set to the values that cause the highest heat loss. Similarly, “Best parameter values” refers to all parameters being set to the values that cause the lowest heat loss.

## 13.3 Sample MATLAB Code

```

for s=1:NO_S
    if SOPAQUE(s)==1
        fprintf(fid,'\n');
        fprintf(fid,'BuildingSurface:Detailed,\n');
        fprintf(fid,' %s,          !- Name\n',char(SNAME(s,:)));
        fprintf(fid,' %s,          !- Surface Type\n',char(STYPE(s,:)));
        fprintf(fid,' %s,          !- Construction Name\n',char(SCONS(s,:))); %eg. exterior roof
        fprintf(fid,' %s,          !- Zone Name\n',char(SZONE(s,:)));
        if strcmp(char(SEXPOSURE(s,:)),'Ground')==1 && DO_BASEMENT==1 %if basement calcs were done and current surface is in basement
            fprintf(fid,' OtherSideCoefficients,      !- Outside Boundary Condition\n');
            fprintf(fid,' CalculatedGroundContact,      !- Outside Boundary Condition Object\n');
        else
            fprintf(fid,' %s,          !- Outside Boundary Condition\n',char(SEXPOSURE(s,:)));
            fprintf(fid,' %s,          !- Outside Boundary Condition Object\n',char(SOTHER(s,:)));
        end
        if strcmp(char(SEXPOSURE(s,:)),'Outdoors')==1
            fprintf(fid,' SunExposed,          !- Sun Exposure\n');
            fprintf(fid,' WindExposed,          !- Wind Exposure\n');
        else
            fprintf(fid,' NoSun,          !- Sun Exposure\n');
            fprintf(fid,' NoWind,          !- Wind Exposure\n');
        end
        fprintf(fid,' autocalculate,          !- View Factor to Ground\n');
        fprintf(fid,' autocalculate,          !- Number of Vertices\n');
        v=1;
        NO_V=sum(isfinite(SVERTICES(s,:))');
        for v=1:NO_V
            fprintf(fid,' %0.5f,          !- Vertex %i X-coordinate (m)\n',V(SVERTICES(s,v),1),SVERTICES(s,v));
            fprintf(fid,' %0.5f,          !- Vertex %i Y-coordinate (m)\n',V(SVERTICES(s,v),2),SVERTICES(s,v));
            if v==NO_V
                fprintf(fid,' %0.5f,          !- Vertex %i Z-coordinate (m)\n',V(SVERTICES(s,v),3),SVERTICES(s,v));
            else
                fprintf(fid,' %0.5f;          !- Vertex %i Z-coordinate (m)\n',V(SVERTICES(s,v),3),SVERTICES(s,v));
            end
        end
    elseif SOPAQUE(s) == 2 && WIN_NO<=ST*6+2 %second condition prevents 2nd floor windows if there's only 1 storey.
        fprintf(fid,'\n');
        fprintf(fid,' FenestrationSurface:Detailed,\n');
        fprintf(fid,' %s,          !- Name\n',char(SNAME(s,:)));
        fprintf(fid,' %s,          !- Surface Type\n',char(STYPE(s,:)));
        fprintf(fid,' %s,          !- Construction Name\n',char(SCONS(s,:))); %eg. exterior roof
        fprintf(fid,' %s,          !- Building Surface Name\n',char(SOTHER(s,:)));
        fprintf(fid,' %s,          !- Outside Boundary Condition Object\n', '');
        fprintf(fid,' autocalculate,          !- View Factor to Ground\n');
        if WIN_NO==3 || WIN_NO==9 %put shades on south-facing windows
            fprintf(fid,' Shading Control,          !- Shading Control Name\n');
        else
            fprintf(fid,' ,          !- Shading Control Name\n');
        end
        %else
        if WIN_NO >2 %its a window
            fprintf(fid,' %s Frame,          !- Frame and Divider Name\n',char(FrameType(FT,:)));
            %fprintf(fid,' ,          !- Frame and Divider Name\n'); %NO FRAME FOR TESTING
        else %its a door
            fprintf(fid,' ,          !- Frame and Divider Name\n'); %NO FRAME FOR TESTING
        end
        if WIN_NO==1
            fprintf(fid,' 1,          !- Multiplier\n');
        else
            fprintf(fid,' 1,          !- Multiplier\n');
        end
        fprintf(fid,' autocalculate,          !- Number of Vertices\n');
        NO_V=sum(isfinite(SVERTICES(s,:))');
        for v=1:NO_V
            fprintf(fid,' %0.5f,          !- Vertex %i X-coordinate (m)\n',V(SVERTICES(s,v),1),SVERTICES(s,v));
            fprintf(fid,' %0.5f,          !- Vertex %i Y-coordinate (m)\n',V(SVERTICES(s,v),2),SVERTICES(s,v));
            if v==NO_V
                fprintf(fid,' %0.5f,          !- Vertex %i Z-coordinate (m)\n',V(SVERTICES(s,v),3),SVERTICES(s,v));
            else
                fprintf(fid,' %0.5f;          !- Vertex %i Z-coordinate (m)\n',V(SVERTICES(s,v),3),SVERTICES(s,v));
            end
        end
        end
        WIN_NO=WIN_NO+1;
    end
end
end

```

Figure 13-3: Sample MATLAB script to create the building surface objects in the idf file

### 13.4 Solar domestic hot water system modeling

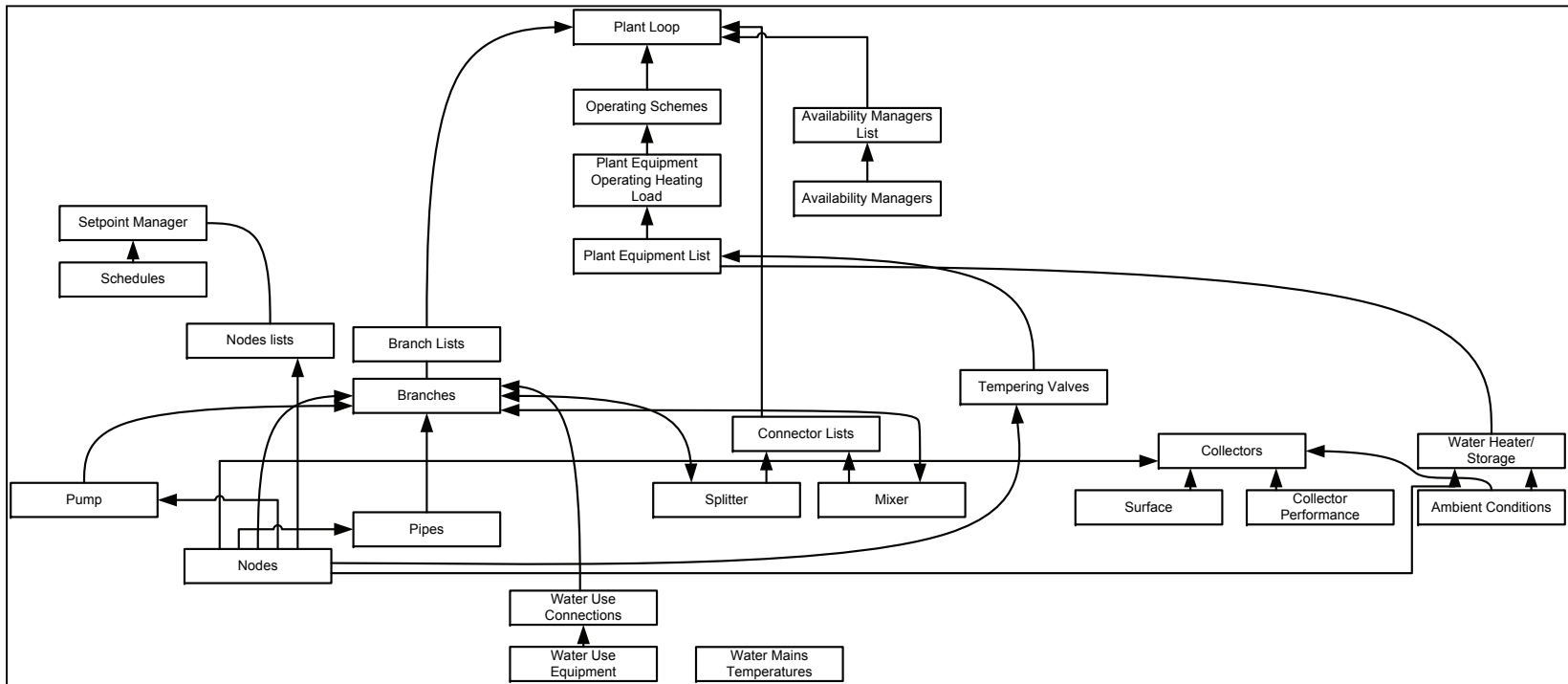


Figure 13-4: Hierarchy of EnergyPlus components/objects that are part of the SDHW system. Arrows indicate the direction of referencing of components (e.g., the water use connections object references the water use equipment object)



Figure 13-5: EnergyPlus schematic of SDHW system (note: purpose of this figure is merely to show the limitations of EnergyPlus output; not to see individual components)

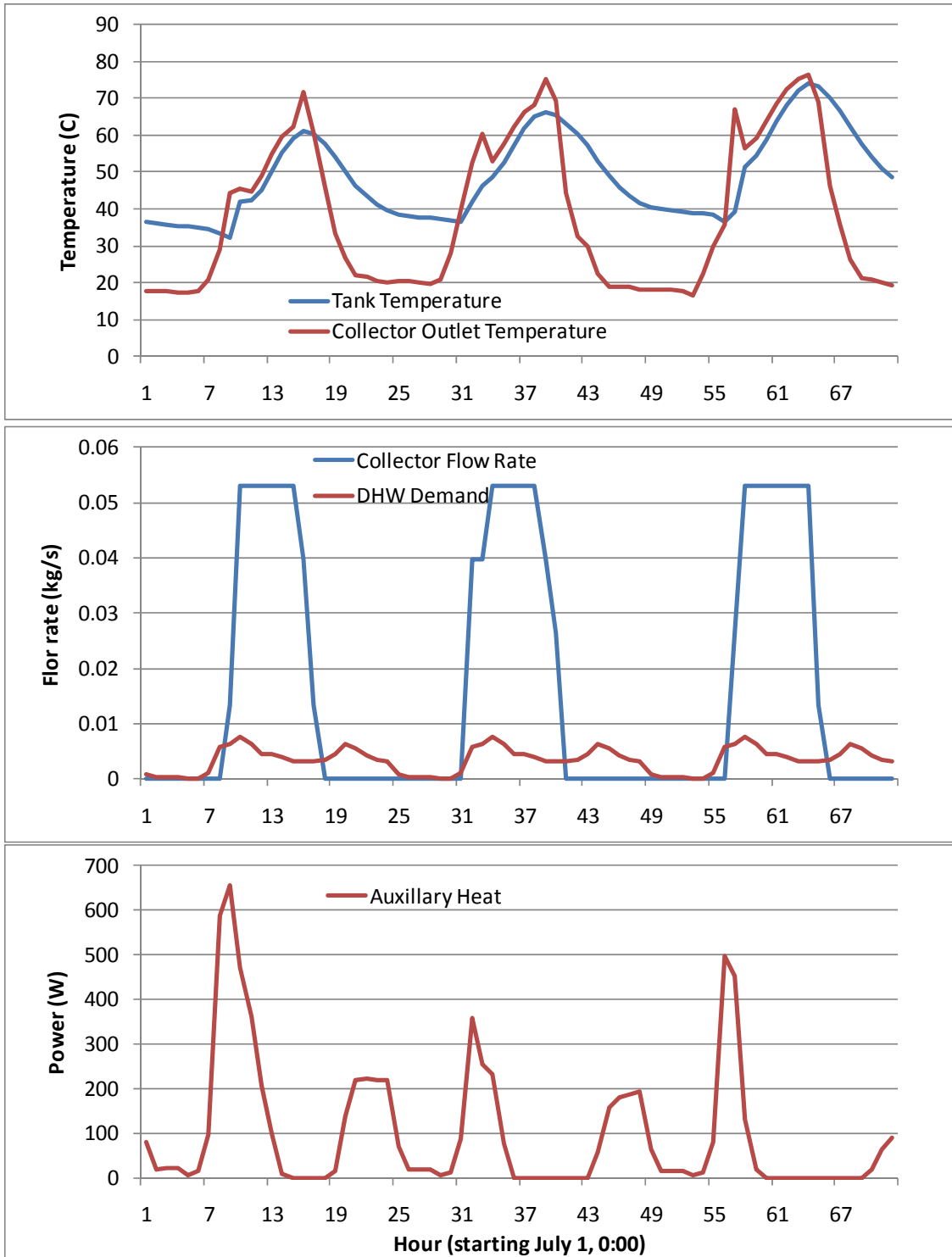


Figure 13-6: SHDW system sample performance

## 13.5 ANN Results

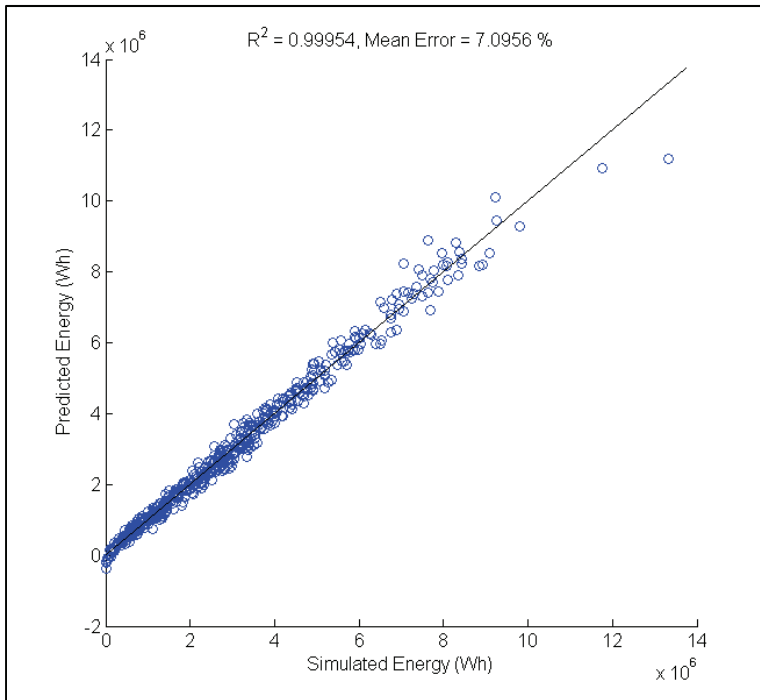


Figure 13-7: Validation plot for annual heating energy

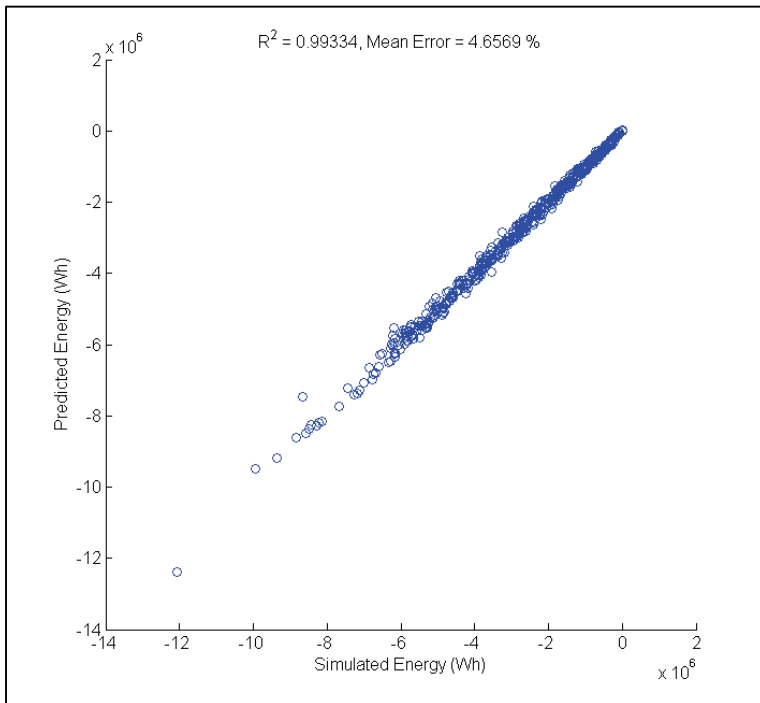


Figure 13-8: Validation plot for annual cooling energy

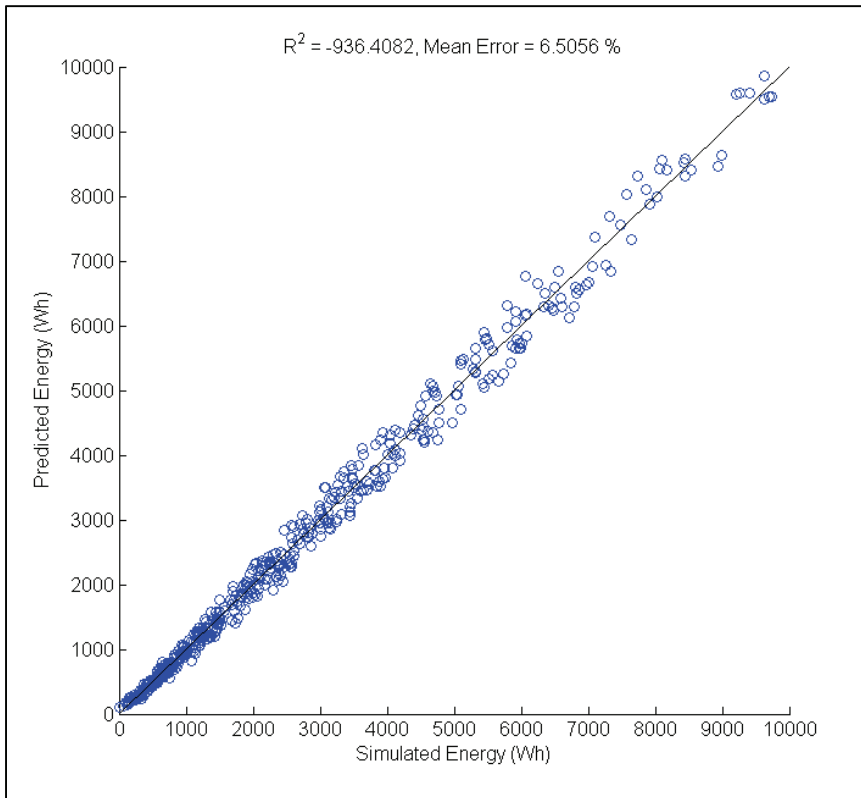


Figure 13-9: Validation plot for annual DHW energy



## 14 APPENDIX E: ÉCO TERRA BACKGROUND INFORMATION

### 14.1 The Design and Construction

ÉcoTerra's building envelope was designed according to passive solar design principles. It has a south facing width-to-depth ratio of 1.38, an overall window-to-wall-area ratio of 15.2% (42% for the south façade) which is equivalent to a solar aperture (south-facing window area-to-total floor area ratio excluding the garage) of 9.1%. The windows are triple-glazed, low-e coated, and argon-filled.

There is significant thermal mass integrated into the basement and main levels of the house. The basement floor is divided into northern and southern halves. The northern part has a standard concrete slab with a thickness of 75 mm, while the southern part has 100 mm of concrete cast over steel decking to form a ventilated slab. There is a 250 mm thick concrete dividing wall between the basement's main areas (in the east-west direction) and it extends 900 mm up into the first floor of the living space. There is a 150 mm concrete slab on the floor in the south zone.

After construction, the air-tightness of the house was measured using a blower-door test to be 0.85 at 50 Pa. The predicted infiltration rate was predicted to be 0.5 ach during design, but as stated in Chapter 3, this is unpredictable.

The house was equipped with new appliances, many of which are EnergyStar, including the fridge, dishwasher, and clothes washer. While compact fluorescent bulbs were

installed in all light fixtures upon sale of the house, the owners installed about two dozen additional light bulbs – most of which are halogen.

ÉcoTerra's building-integrated photovoltaic/thermal (BIPV/T) system is designed to increase the overall solar energy collected (by collecting both electrical and thermal energy) and is integrated into the building itself, forming the outer layer of the metal roof (on the south top side).



*Figure 14-1: Photographs of the underside of the BIPV/T roof (left) and the ventilated slab before the concrete is poured on the decking (right)*

While the heat recovery system of the BIPV/T roof is operating, air is drawn through openings along the under-side of the soffit of the roof and through channels on the underside of the roof surface by a variable speed fan. This air is convectively heated as it travels under the metal roof layer and is drawn through an insulated manifold and duct into the mechanical room of the house in the basement to be used. The outer surface of the roof is covered by amorphous silicon PV panels which convert the incident solar radiation into electricity. Since the PV panels are about 6% efficient at converting the energy into electricity, much of the remainder can be recovered by the air passing

below their surface. Figure 14-2 shows a system schematic of ÉcoTerra (Chen et al. 2010)

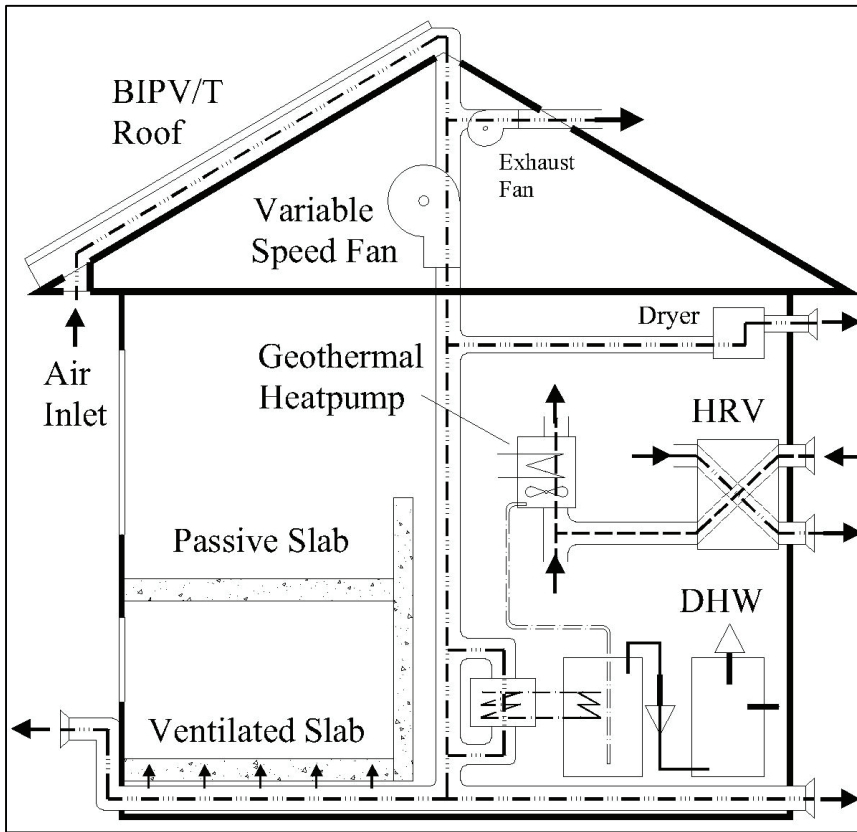


Figure 14-2: ÉcoTerra system schematic (Chen et al. 2010)

The energy balance of the roof is as follows.

$$\alpha IA = E_{PV} + E_{Thermal} + E_0 \quad (E-1)$$

where  $\alpha$  is the mean solar absorptance of the BIPV/T roof,  $I$  is the incident solar radiation,  $A$  is the roof area,  $E_{PV}$  is the rate of electrical energy generation,  $E_{Thermal}$  is the rate of thermal energy collection, and  $E_0$  is the rate of energy that is lost to the

surroundings. For instance, for the current roof under sunny conditions at about solar noon, it is possible to have  $1000 \text{ W/m}^2$  of solar incident solar radiation, of which nearly 6% (3 kW) can be converted to electrical energy and about 20% (12 kW) can be converted to thermal energy.

The integrated nature of this system means that the surface on which the PV is installed serves the dual purposes of being an energy collector (for electricity and heat) and protecting the house from weather, as standard roofs do. This integration saved on cost and allows the modules to be virtually undetectable by the house's neighbours.

The electrical energy produced by the PV is used on-site and the excess is sold to the electrical utility, while the thermal energy must be used on-site – either immediately or stored for later use. The heated air can be used to preheat the domestic hot water (DHW), assist in drying clothes, heat the ventilated concrete slab (VCS) in the basement, or any combination of these. The usefulness of the thermal portion is highly-dependent on the house's ability to utilize it immediately or store it until it can be utilized.

The slab is a structural element of the house (the basement floor), but also has corrugated metal decking embedded in its bottom, which forms air channels. Heated air from the BIPV/T roof is passed through these channels, thereby actively heating the slab. The energy stored in the significant thermal mass of the floor is then discharged passively into the space in a delayed manner, offsetting the heating load when passive solar gains are unavailable. To put the advantage of this strategy into context, it is

important to remember that the house meets most heating loads on a sunny day from passive solar gains alone. If the heat from the roof were immediately added to the space, overheating would almost certainly occur.

The controls for selecting where the heated air from the BIPV/T roof is used were designed to minimize purchased energy use. As a first priority, if the air is warmer than 15°C, has a relative humidity of under 50%, and the occupants wish to dry their clothes, it is used for this purpose. Otherwise, it is used to heat the colder of the DHW or VCS (during the heating season only). The controls require that the air leaving the BIPV/T roof be at least 5°C warmer than the DHW tank or 3°C warmer than the VCS for the system to operate; otherwise, the fan energy use may not be justified. A temperature drop of 2-4°C has been measured between the outlet of the roof and the location of use.

## **14.2 The Design Process**

This section provides a brief summary of the design process that was applied to ÉcoTerra in 2006. The purpose of assessing this in detail is that it provided a list of needs for Ecos.

### **14.2.1 Design Objectives**

The objectives of the house design were to achieve near net-zero energy consumption, while maintaining a healthy and comfortable indoor environment (good thermal comfort, air quality and daylighting) and low water use, as specified by the competition

requirements (CMHC, 2010). An additional goal of the design team was to emphasize building integration of solar technologies and thermal storage. Furthermore, the designers aimed to make the house affordable, with a minimal premium to similarly-sized Canadian houses. Since the house is manufactured, there is an opportunity for mass-producing the house, thereby facilitating adoption of net-zero energy home design concepts and systems. One of the purposes of this paper is to identify potential improvements to the design and disseminate this information to homebuilders.

#### **14.2.2 Design team and design process**

The design team was composed of a team of about ten experts and led by an architect-engineer team. The complete list of members and a summary of the design process are shown in Figure 14-3. The design process started with Dr. Athienitis proposing some rules of thumb for passive solar design, including form (e.g., aspect ratio of about 1.2 to 1.3 and two storeys), window area, thermal mass location and quantity, and shading. The architect, Masa Noguchi, used these to establish a sketch design for presentation at the design charrette. The design charrette consisted of a two-day intensive meeting that included all of the design team members. A decision was made that the house would combine three main technologies:

1. direct gain passive solar design coupled with a highly-insulated and airtight building envelope,

2. a BIPV/T systems as the main active thermal-electric generation system coupled with a floor integrated active charge/passive release thermal storage, and;
3. a geothermal heat pump with vertically-drilled wells, connected to a forced air system as the main HVAC system of the house.

It is interesting to note that the roof design changed significantly after the design charrette. Its slope was reduced from 45 to 30 degrees - to allow it to be prefabricated and transported to the site and to ensure that the modules extend the entire length of the roof for better building integration - a decision that is relatively inconsequential to theoretical electrical generation, but proved to result in some snow accumulation and reduced useful thermal energy collection.

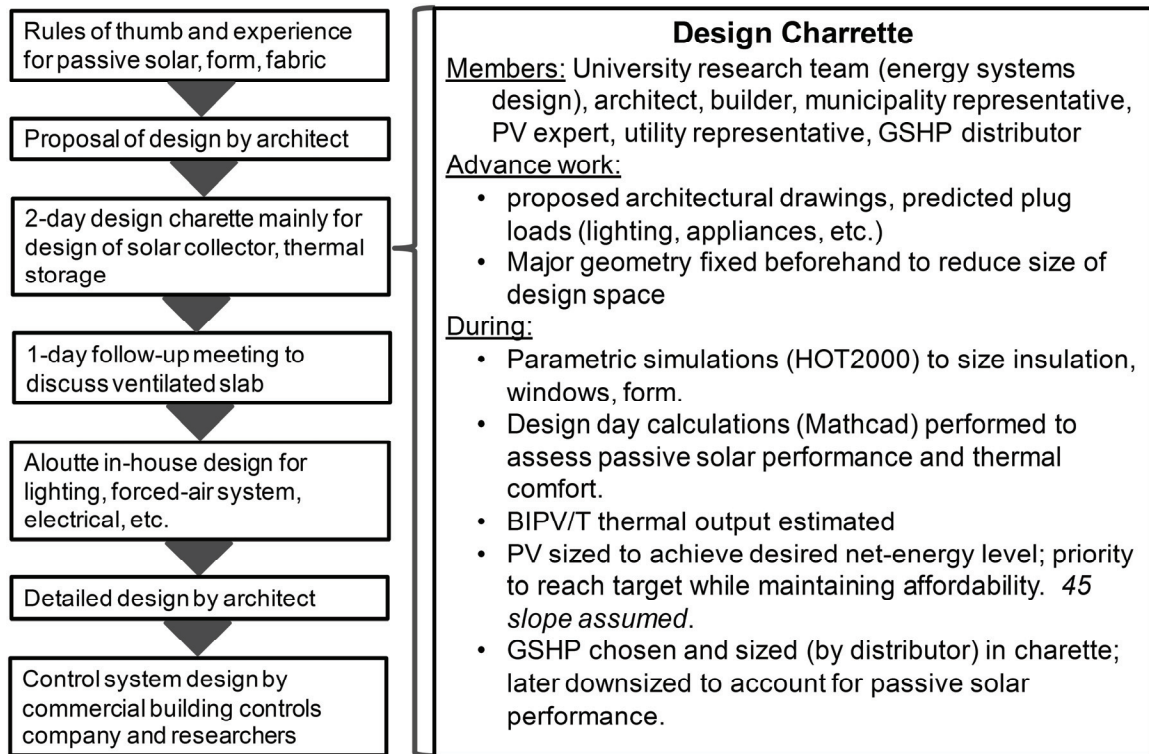


Figure 14-3: Design process outline (taken from (Doiron et al., 2011))

### 14.2.3 Use of design and analysis tools

The design competition required the use of HOT2000 (NRCan, 2010c) and RETScreen (RETScreen International, 2005) for predicting performance, as a minimum. The former was used to determine the household energy consumption, while the latter was used to determine the predicted output of renewable energy systems (PV in this case).

HOT2000 uses a bin method and is intended to assess the performance and possible retrofits of detached houses. Its features are aimed at Canadian homes and the associated construction practices (e.g. wood frame) and technologies (e.g., HVAC systems). HOT2000's calculation method makes it less suitable for assessing dynamic behaviour – something that is fundamental for passive solar performance assessment.



Also, its lowest reporting frequency for output is monthly, meaning that hourly comfort metrics, which are fundamental to informed passive solar design, are unavailable. To supplement this, the design team used customized software (Chen et al., 2010a; Chen et al., 2010b). The custom software uses the explicit finite difference method for spatial and temporal discretization, so that short timesteps could be used and the benefit of thermal mass could be accurately assessed. Rather than performing whole-year simulations, the emphasis was on characterizing performance for a cold sunny day, which is typical of the region's winters. This practice is similar to what Ecos facilitates. Regardless of HOT2000's limitations, it was useful in estimating annual performance – an essential element of predicting the net energy consumption (or production) of the house in a standardized way.

One of the common methods used for deciding on key elements of ÉcoTerra design was parametric analysis. For example, Figure 14-4 and Figure 14-5 show results that were presented at the design charrette to support the decision to not “super-insulate” the house. It clearly indicates that increasing wall insulation from 8 to 10-RSI only has about half the impact of increasing it from 6 to 8-RSI.

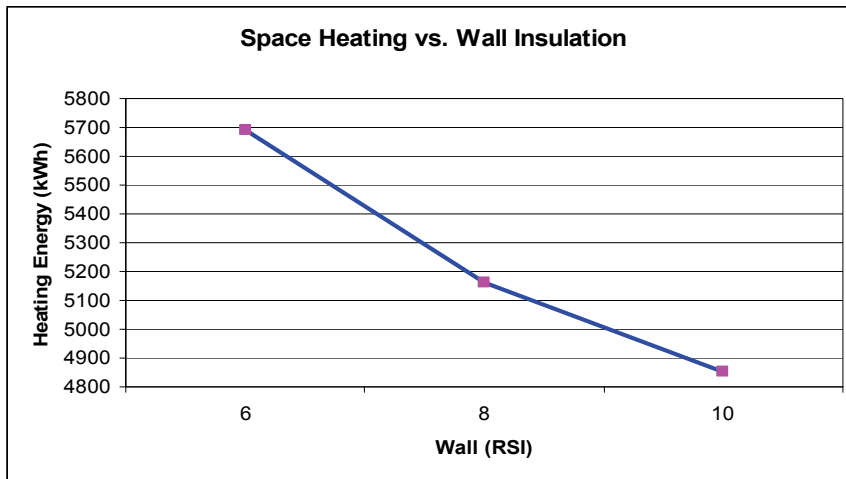


Figure 14-4: Results of parametric analysis that was used to decide on the optimal insulation level in the walls.

Roof		Wall		Under Basement Slab	
RSI	Heat Loss [MJ]	RSI	Heat Loss [MJ]	RSI	Heat Loss [MJ]
5.5	6784	4.0	22524	0.5	13821
7.1	5381	5.3	16986	1.3	13314
8.4	4631	6.3	14337	2.6	12702
9.1	4294	7.6	11879		
9.5	4104				

RSI value is the effective value.  
Heat loss is the annual value. 1kWh = 3.6MJ

Figure 14-5: Sample results from parametric analysis for roof, wall, and basement slab insulation

It should be noted that the next generation of HOT2000 – HOT3000 – uses dynamic simulations by means of a finite difference method, which will improve characterization of passive solar performance (NRCAN, 2009).

RETScreen (RETScreen International, 2005) is a spreadsheet-based tool for assessing the energy performance and economic feasibility of many building upgrades and renewable

energy projects. Its role in the design of ÉcoTerra was to predict the performance of the PV element of the proposed BIPV/T roof. The tool's simplicity allowed the effect of many design options (such as slope, orientation, and technology) to be explored very quickly. However, the model is steady-state and only intended for stand-alone (non building-integrated) PV installations. This means that the effect of heat transfer to the roof is neglected. Furthermore, thermal coupling with the thermal energy collection aspect of the roof was not possible. Finally, the RETScreen model does not consider snow accumulation in its model, a factor that proved to be significant (O'Brien et al., 2009b).

To assess the combined performance of the thermal and electrical aspects of the BIPV/T roof, a custom program was built, similar to the one for assessing the house's passive solar performance. The results of this analysis were used to make design changes and ultimately to predict the net-energy consumption of the house (Chen et al., 2010b).

The wall constructions are detailed in Figure 14-6.

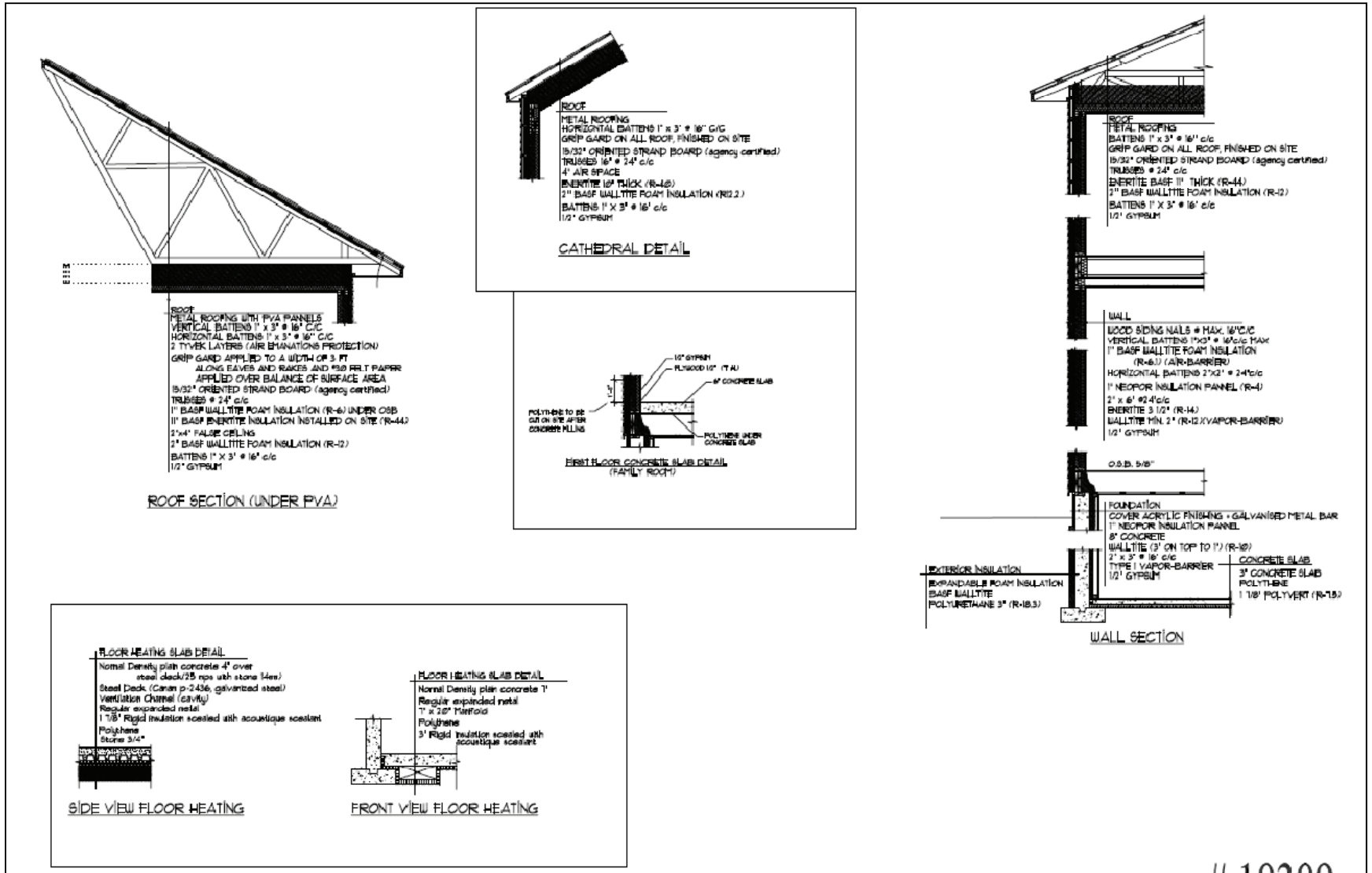


Figure 14-6: Construction details of the EcoTerra house

#### **14.2.4 Assessment of the design process**

Upon interviewing several design team members, several notable conclusions were drawn. They stated that the main (two-day) design charrette was very effective, that the collaboration between the large group of experts exceeded expectations, and that the work that was completed in advance was essential to a productive group design session. However, improved communication between the designers and builder teams regarding some of the more innovative aspects of the house, such as the ductwork linking the BIPV/T roof to the sites of demand was desirable. Also, the use of design tools was somewhat fragmented, since at least four separate models were used. It would have been preferable to use a single tool, so that proper thermal couplings between house components could be assessed (O'Brien et al., 2009c), but such a tool that is available for the early design stage is not currently available. This is difficult when new technologies, such as the BIPV/T roof linked to a ventilated slab, are being modelled.

#### **14.3 Measured performance**

ÉcoTerra's zone temperatures and energy consumption have been monitored by over 150 sensors since construction. The data is collected automatically and stored in a central database from which it is queried for the various, ongoing analyses that are being performed on the house. The major categories of electricity use that are measured are: PV generation, the heat pump, DHW, and total electricity use. The data were disaggregated using knowledge of power draw and by using pattern recognition on

the total power draw, as explained by Doiron et al (2011). The results are shown in Figure 14-7 and Figure 14-8. Some interesting observations from the data are as follows.

- Total heating electricity (space heating and DHW) are only about one-third of the total. This is in contrast to the existing housing stock, for which this fraction is closer to 80%. Three major reasons for this are the decreasingly important impact of heating as envelopes become higher in quality, the strong passive solar component, and the fact that a heat pump was used, reducing the space heating and cooling energy by a factor of about 3.7.
- The HRV and air cleaner use a significant amount of electricity. Future analysis to determine the effectiveness of the HRV over no heat recovery would be worthwhile, in the context of a highly-efficient building envelope and a high-performance heating system.
- The “discretionary” loads (lights, appliances, plug loads) account for over one-third of the total energy use, yet this was given a disproportionate level of attention relative to other aspects of the design. While new high-efficiency appliances were selected, the potential for real-time display of data in an effort to impact occupant behaviour was not examined.

The heat pump electricity consumption for both heating and cooling are combined. For the purpose of the analysis that follows, it is assumed that only heating or cooling

occurs in any given month and that therefore, there is a modest amount of cooling in July and heating is used for the months other than June through August.

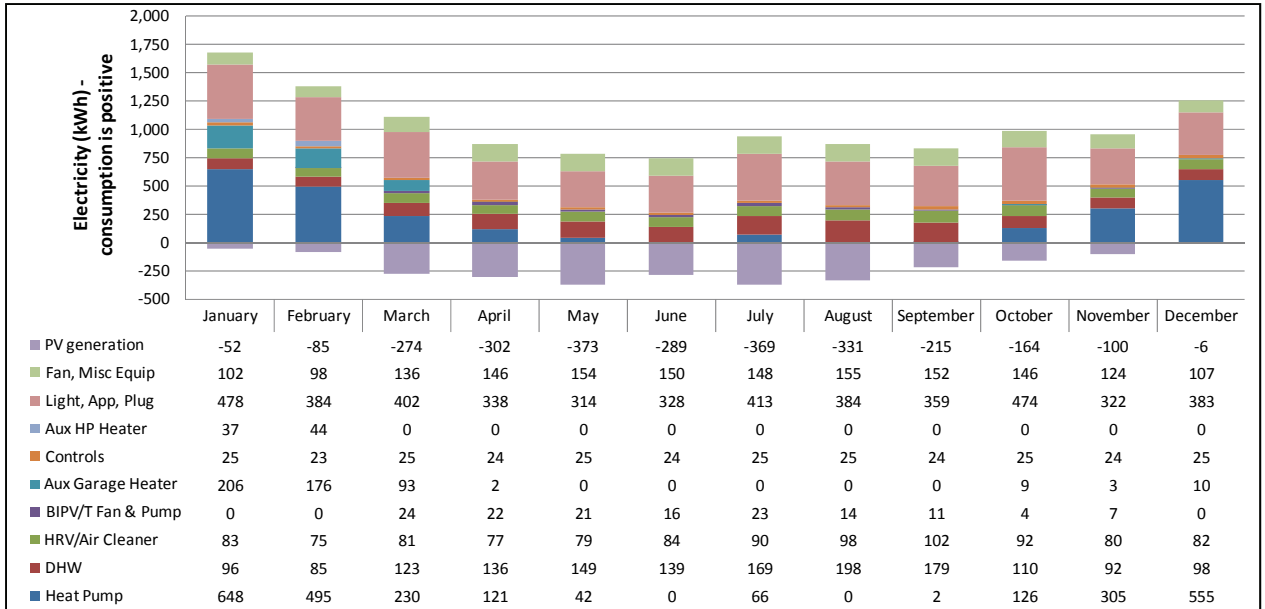


Figure 14-7: EcoTerra's monthly energy use in 2010 (values in kWh)

The total annual energy use breakdown is shown in Figure 14-8.

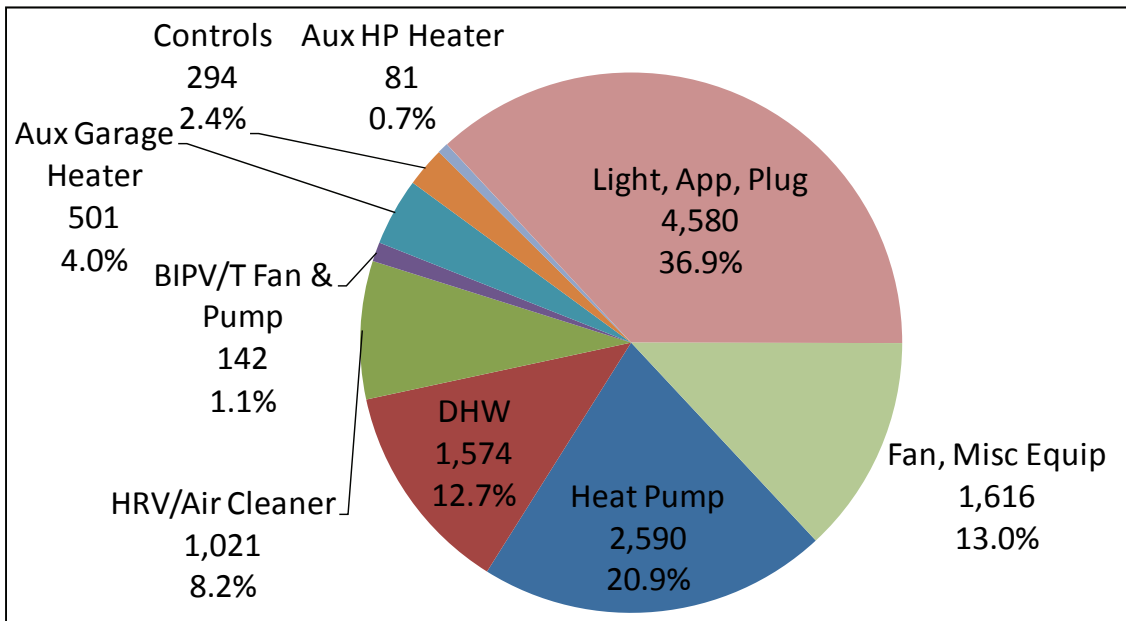


Figure 14-8: Annual breakdown of electricity use in EcoTerra house (values in kWh)

At least as useful as annual performance results, short-term high-resolution electricity use and supply profiles provide information about a house's characteristics. Figure 14-9 shows the house's performance on a typical sunny shoulder season day. Particularly notable is that there are several large spikes in electricity draw – particularly early in the morning when the heating setpoint increases, and then throughout the rest of the day for DHW and appliances.



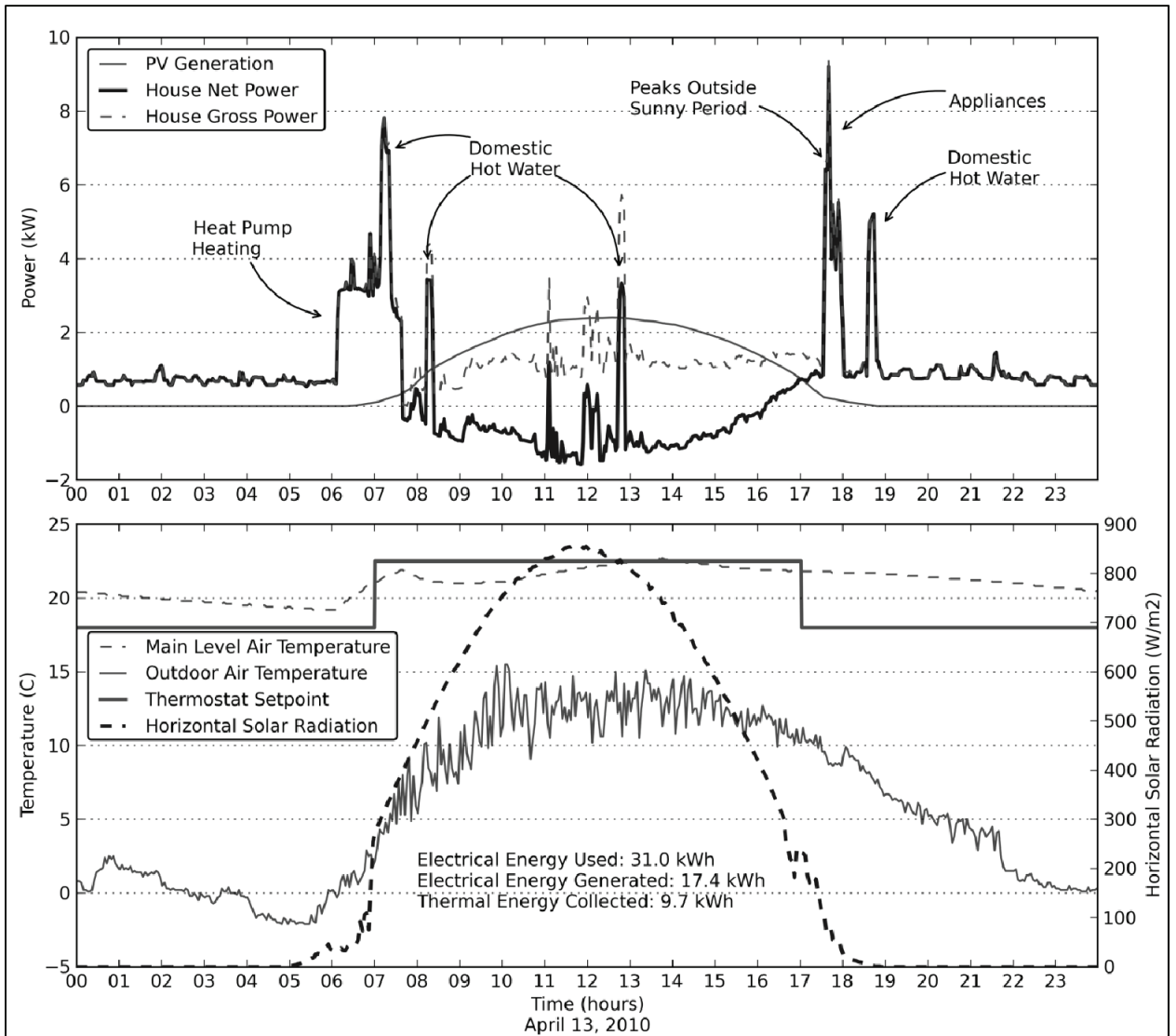


Figure 14-9: Daily power draw, generation, and indoor temperature profiles (taken from Doiron et al (2011))

## 14.4 Lessons learned

One of the most useful outcomes demonstration projects such as ÉcoTerra comes from reflecting on the design process and the performance of the house. These details cannot be obtained from any simulations or design exercises. The major lessons learned are described in this subsection.

There is an interesting trade-off between thermal performance and daylighting in any building. For ÉcoTerra, in the interest of minimizing north-facing glazing, which barely contributes any solar gains in the heating season, daylight availability was sacrificed. However, this unintentionally led to the owners installing about 24 additional light bulbs to brighten the space. With increasingly high performance windows, perhaps future designs should provide a greater emphasis on daylighting even at the cost of thermal performance.

As is often seen for thermally massive floors, the ÉcoTerra owners placed large shag carpets over the slate floor, rendering the thermal mass significantly less effective. Their motivation could be aesthetic, acoustical, or for thermal comfort. The latter two considerations could be resolved by design. If the issue is acoustic, sound absorbing panels or furniture could be strategically positioned. If the issue is cold feet from the highly-conductive floor, two solutions are to use: 1) radiant floor heating instead of forced-air to increase the floor temperature or 2) the other room surfaces (i.e., walls, ceiling) for thermal mass while ensuring the floor is reflective but not highly-conductive.

The auxiliary heater, before intervention, was being triggered on a daily basis when the setpoint increased from 18 to 22.5°C each morning. This is simply because the controls caused this if immediate heating loads could not be met by the heat pump alone.

However, this heat comes at a cost that is 3-4 times greater than from the heat pump.

To resolve this, the controls were tweaked. As a result, the space does not reach the

daytime setpoint as quickly. Another method for reducing energy use would be to delay the setpoint increase until after some solar gains have occurred (around 10AM) such that the space is warmed for free. The suitability of this approach depends on the lifestyle of the occupants.

As can be expected, the rooms of the house are not being used exactly as planned. The most extreme instance of this is that the garage was converted into a workshop. To warm the space, the owners installed a 5 kW electric resistance heater. For the few months that this went undetected by the Concordia team, this heater was using one-third of the electricity that was used to heat the entire house. This is despite the fact that the garage represents a mere 10% of the floor area of the house and was never heated to the temperatures of the rest of the house. If the space must be heated, it would be favourable to either heat it with the central heat pump, or more interestingly, be heated with the BIPV/T roof. Since the BIPV/T outlet air is often less than 15°C, it would still be of use in the garage (due to adaptive comfort and the fact that a coat may be worn) despite not being useful in the house.

As previously addressed, the shallow roof slope resulted in poorer than expected BIPV/T performance. A solution to overcome this (for future houses) would be to build the roof on-site to remove the constraint from module transportation. Alternatively, a heater could be used to act as a catalyst in melting snow. More complex approaches could be to route exhaust ventilation air through the BIPV/T air space or to use have a small

steeper solar collector that is used to melt snow. While all of these solutions come at some cost (energy, equipment), it may be worthwhile considering that measured wintertime PV generation was only at a fraction of the potential.

Despite the high resolution of monitoring equipment for certain aspects of the house performance – particularly the innovative technologies – it would have been ideal to sub-meter many of the electricity-consumers, including lights, appliances, the HRV and air cleaner, and the other fans. A total of two-thirds of the electricity use is measured only in aggregate form, leaving some uncertainty as to exact final use. As a result, detailed studies such as understanding the electric lighting use and its relationship with occupancy and daylight availability cannot be performed. Another aspect of monitoring that could be improved is to have a single data acquisition system recording all data. In the current configuration, the heat pump is being monitored separately at a different sampling frequency and at a significant delay to the other measurements. Such issues represented a significant challenge for the data analyst, Matt Doiron.